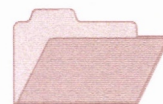




**CRCLEME**

Cooperative Research Centre for  
Landscape Evolution & Mineral Exploration



**OPEN FILE  
REPORT  
SERIES**



**CSIRO**  
EXPLORATION  
AND MINING



Australian Mineral Industries Research Association Limited ACN 004 448 266

# **GEOCHEMICAL EXPLORATION IN COMPLEX LATERITIC ENVIRONMENTS OF THE YILGARN CRATON, WESTERN AUSTRALIA**

## **P240A Final Report Volume I**

*R.R. Anand, R.E. Smith, C. Phang, J.E. Wildman,  
I.D.M. Robertson and T.J. Munday*

**CRC LEME OPEN FILE REPORT 58**

**November 1998**

(CSIRO Division of Exploration Geoscience Report 442R, December 1993.  
Second impression 1998)

CRC LEME is an unincorporated joint venture between The Australian National University, University of Canberra, Australian Geological Survey Organisation and CSIRO Exploration and Mining, established and supported under the Australian Government's Cooperative Research Centres Program.



# **GEOCHEMICAL EXPLORATION IN COMPLEX LATERITIC ENVIRONMENTS OF THE YILGARN CRATON, WESTERN AUSTRALIA**

## **P240A Final Report Volume 1**

*R.R. Anand, R.E. Smith, C. Phang, J.E. Wildman,  
I.D.M. Robertson and T.J. Munday*

**CRC LEME OPEN FILE REPORT 58**

November 1998

(CSIRO Division of Exploration Geoscience Report 442R, December 1993.  
Second impression 1998)

© CSIRO 1993



## RESEARCH ARISING FROM CSIRO/AMIRA REGOLITH GEOCHEMISTRY PROJECTS 1987-1993

In 1987, CSIRO commenced a series of multi-client research projects in regolith geology and geochemistry which were sponsored by companies in the Australian mining industry, through the Australian Mineral Industries Research Association Limited (AMIRA). The initial research program, "Exploration for concealed gold deposits, Yilgarn Block, Western Australia" (1987-1993) had the aim of developing improved geological, geochemical and geophysical methods for mineral exploration that would facilitate the location of blind, buried or deeply weathered gold deposits. The program included the following projects:

**P240: Laterite geochemistry for detecting concealed mineral deposits (1987-1991).** Leader: Dr R.E. Smith.  
Its scope was development of methods for sampling and interpretation of multi-element laterite geochemistry data and application of multi-element techniques to gold and polymetallic mineral exploration in weathered terrain. The project emphasised viewing laterite geochemical dispersion patterns in their regolith-landform context at local and district scales. It was supported by 30 companies.

**P241: Gold and associated elements in the regolith - dispersion processes and implications for exploration (1987-1991).** Leader: Dr C.R.M. Butt.

The project investigated the distribution of ore and indicator elements in the regolith. It included studies of the mineralogical and geochemical characteristics of weathered ore deposits and wall rocks, and the chemical controls on element dispersion and concentration during regolith evolution. This was to increase the effectiveness of geochemical exploration in weathered terrain through improved understanding of weathering processes. It was supported by 26 companies.

These projects represented "an opportunity for the mineral industry to participate in a multi-disciplinary program of geoscience research aimed at developing new geological, geochemical and geophysical methods for exploration in deeply weathered Archaean terrains". This initiative recognised the unique opportunities, created by exploration and open-cut mining, to conduct detailed studies of the weathered zone, with particular emphasis on the near-surface expression of gold mineralisation. The skills of existing and specially recruited research staff from the Floreat Park and North Ryde laboratories (of the then Divisions of Minerals and Geochemistry, and Mineral Physics and Mineralogy, subsequently Exploration Geoscience and later Exploration and Mining) were integrated to form a task force with expertise in geology, mineralogy, geochemistry and geophysics. Several staff participated in more than one project. Following completion of the original projects, two continuation projects were developed.

**P240A: Geochemical exploration in complex lateritic environments of the Yilgarn Craton, Western Australia (1991-1993).** Leaders: Drs R.E. Smith and R.R. Anand.

The approach of viewing geochemical dispersion within a well-controlled and well-understood regolith-landform and bedrock framework at detailed and district scales continued. In this extension, focus was particularly on areas of transported cover and on more complex lateritic environments typified by the Kalgoorlie regional study. This was supported by 17 companies.

**P241A: Gold and associated elements in the regolith - dispersion processes and implications for exploration.** Leader: Dr. C.R.M. Butt.

The significance of gold mobilisation under present-day conditions, particularly the important relationship with pedogenic carbonate, was investigated further. In addition, attention was focussed on the recognition of primary lithologies from their weathered equivalents. This project was supported by 14 companies.

Although the confidentiality periods of the research reports have expired, the last in December 1994, they have not been made public until now. Publishing the reports through the CRC LEME Report Series is seen as an appropriate means of doing this. By making available the results of the research and the authors' interpretations, it is hoped that the reports will provide source data for future research and be useful for teaching. CRC LEME acknowledges the Australian Mineral Industries Research Association and CSIRO Division of Exploration and Mining for authorisation to publish these reports. It is intended that publication of the reports will be a substantial additional factor in transferring technology to aid the Australian Mineral Industry.

This report (CRC LEME Open File Report 58) is a First revision (second printing) of CSIRO, Division of Exploration Geoscience Restricted Report 442R, first issued in 1993, which formed part of the CSIRO/AMIRA Project P240A.

### Copies of this publication can be obtained from:

The Publication Officer, c/- CRC LEME, CSIRO Exploration and Mining, PMB, Wembley, WA 6014, Australia. Information on other publications in this series may be obtained from the above or from <http://leme.anu.edu.au/>

### Cataloguing-in-Publication:

Geochemical exploration in complex lateritic environments of the Yilgarn Craton, Western Australia. Final Report.

ISBN 0 642 28237 4 v1, v2: 0 642 28264 1 v3: 0 642 28271 4 v4: 0 642 28276 5 set: 0 642 28282 X

1. Geochemical prospecting 2. Laterite 3. Gold - Western Australia 4. Geochemistry.

I. Anand, R.R. II. Title

CRC LEME Open File Report 58.

ISSN 1329-4768

## **PREFACE TO THE SECOND IMPRESSION**

**R. E. Smith and R.R. Anand, 1st October 1998.**

This final report is one of two companion volumes (CRC LEME Open File Reports 50 and 58) which bring together the results of the CSIRO-AMIRA projects 'Laterite Geochemistry' and its extension 'Yilgarn Lateritic Environments' which, in total, ran from July 1987 to December 1993.

These summary and final reports synthesise 25 reports and three field guides which cover the project components, including multidisciplinary studies of several 'type' districts, across the Yilgarn Craton of Western Australia and many geochemical dispersion studies about concealed gold deposits.

Although the main focus of the project concentrated on gold exploration, the knowledge, regolith mapping methods, regolith stratigraphy, models and evolution are applicable to exploration for a wide range of commodities (including base metals, rare metals and diamonds) and the geochemical data are comprehensively multi-element.

In this second impression (second printing), the senior authors made the decision to produce the two reports as they were except for the correction of a small number of typographical errors, minor omissions and some additional acknowledgments.

We direct readers' attention to the following correlation of terms used for regolith-landform regimes developed in later work:

### **This Report**

*Residual regime*

As defined in Section 2.4.3,  
page 12, Open File Report 50

equivalent to:

### **Terminology used in 1994 onwards**

*Relict regime*

Anand and Smith (1993)

### **Comment on use of regolith-landform regimes**

The first step is to make an objective map of the regolith-landform units present in an area, with little or no genetic bias. Such a factual map forms the basis of derivative or interpretative maps based on genetic grouping of the regolith and associated geomorphic features. It should also be pointed out that ferruginous materials have formed both in *in-situ* and transported materials. Laterite residuum, formed by residual enrichment in the weathering of parent rocks, is included with the relict regime. Iron cemented sands and gravels (ferricretes) are different because there is no direct genetic relationship between these ferricretes and the underlying bedrocks. Therefore, they are included with the depositional regime.

Although focus of the research presented here is on the Yilgarn Craton of Western Australia and its periphery, the research findings have wider application. Sponsors have used the research findings in other parts of Australia (Northern Territory and Queensland) and in appropriate terrain overseas, including western Africa, southern Asia and South America. However, having said this, we stress the importance of carrying out systematic research, including orientation studies, in each of these more distant areas.

We hope the approaches we have found helpful in the Yilgarn, translated generically, will be a guide to approaches that can be used in other lateritic terrains around the world.

### **Reference:**

Anand, R.R. and Smith, R.E. (1993). Regolith distribution, stratigraphy and evolution of the Yilgarn Craton. In: P.R. Williams and J. A. Haldane (Compilers), An International Conference on Crustal Evolution, Metallogeny and Exploration of the Eastern Goldfields. Kalgoorlie 1993. Australian Geological Survey Record 1993/54. pp187-193.



## **Addresses and affiliations of authors**

**Dr R.R. Anand**

CSIRO Exploration and Mining  
Private Bag, P.O. Wembley  
WA 6014, Australia

**Mr J.E. Wildman**

CSIRO Exploration and Mining  
Private Bag, P.O. Wembley  
WA 6014, Australia

**Dr R.E. Smith**

CSIRO Exploration and Mining  
Private Bag, P.O. Wembley  
WA 6014, Australia

**Dr I.D.M. Robertson**

CSIRO Exploration and Mining  
Private Bag, P.O. Wembley  
WA 6014, Australia

**Mr C. Phang**

CSIRO Exploration and Mining  
Private Bag, P.O. Wembley  
WA 6014, Australia

**Dr T.J. Munday**

CSIRO Exploration and Mining  
Private Bag, P.O. Wembley  
WA 6014, Australia

## EXECUTIVE SUMMARY

The objectives of this two-year extension project were to develop and improve methods of finding mineral deposits (particularly gold and base metals) in lateritic environments of the Yilgarn Craton, using geochemistry within a sound regolith-landform framework. The project focussed on more complex lateritic environments than its precursor, by including a study of the Kalgoorlie region and areas of transported cover overlying variably truncated laterite profiles elsewhere. The multidisciplinary project team augmented its skills in remote sensing and regolith mapping through collaboration with the newly-formed Co-operative Research Centre in Australian Mineral Exploration Technologies.

### *The Kalgoorlie region*

A regolith-landform framework for the Kalgoorlie region was established over an area of 10,000 km<sup>2</sup>. Landscapes were shown to be characterised by extensive stripping of upland areas, very shallow to deep weathering, patchy development of lateritic residuum and extensive occurrence of calcareous and acid, red clays, which commonly contain ferruginous granules. Erosional stripping of the upper, more weathered, parts of the regolith, appear to be important factors, coupled with the distribution of mafic and ultramafic rocks, influencing the gross distribution of carbonates in the regolith. Results were then compared and contrasted with other parts of the Yilgarn Craton.

### *Orientation studies*

Eight additional geochemical orientation studies were completed and set within their district-scale regolith-landform setting. In the Kalgoorlie region these were: Ora Banda (Matt Dam), Kanowna Belle and Wombola; and elsewhere: Boddington, Mt. McClure, Lawlers (Waroonga and Genesis), Bottle Creek, Golden Grove, Beasley Creek and Lights of Israel. All are Au deposits except Golden Grove, a Cu-Zn-Au volcanic-hosted massive sulphide deposit.

### *Systematising regolith-landform mapping units*

A framework for classification of regolith-landform mapping units was established which links landforms with regolith stratigraphy. Most regolith-landform mapping units so far encountered in the Yilgarn are accommodated and can be compared with each other. An accompanying atlas aids recognition of regolith units being mapped or sampled.

### *Developments in new sample media*

Several new sample media were demonstrated to have application in exploration, particularly where lateritic residuum is missing. These include ferruginous saprolite, iron segregations, ferruginous mottles in upper saprolite, ferruginous granules in soils (including soils on transported overburden) and ferruginous mottles in cover sequences.

*Ferruginous granules in soil.* It was shown at Kanowna Belle, that near-surface ferruginous granules hold trace element indicators (As, Sb, Au) of the Au deposit forming a broad (>400 m wide) anomaly in the thin, transported cover overlying the deeply leached, partly truncated profile. These granules are a distinctive sample medium, quite separate from lateritic nodules. Their use holds considerable promise in exploration for Au and base metals in areas of deeply leached, partly truncated profiles, with or without the presence of transported cover, situations which are common in the Kalgoorlie region.

*Ferruginous saprolite.* At Matt Dam, ferruginous saprolite gave a strong multi-element anomaly (Au, As, W) over the deeply leached, partly truncated profile and the concealed Au mineralisation are similar to Lawlers. Ferruginous saprolite is common, in both the Kalgoorlie and Leonora-Wiluna regions, and forms a useful sampling medium for reconnaissance. It is a useful medium for target definition by sampling at surface or by drilling through sedimentary cover.

*Ferruginous mottles in cover sediments.* It was shown by the research at the Kanowna deep leads and the Matt Dam prospect that such ferruginous mottles in the vicinity of concealed Au deposits can carry anomalous As, Sb, W, and Au, apparently generated through hydromorphic dispersion (As, Sb, and Au) during weathering after sediment deposition.

### *Dispersion models and exploration procedures*

Regolith and geochemical dispersion findings have been integrated into new exploration models for the following settings: (i) full lateritic profile, high seasonal rainfall, no surficial cover (based on Boddington); (ii) full lateritic profile, semi-arid to arid climate, little or no cover (based on Golden Grove,



## *Executive Summary*

VHMS Cu-Zn; Mt. Gibson, Bottle Creek and Beasley Creek). Updated models were generated for: (iii) buried, complete profile, arid terrain (based on Mt. McClure and Waroonga), (iv) buried, partly truncated profile, arid terrain (based on Kanowna Belle, Matt Dam, Kanowna deep leads, Bottle Creek, Boags, Mt. McClure, Waroonga and Genesis).

Systematic differences in the distribution of Au between the high and low rainfall areas were revealed by the Boddington orientation study, in comparison with the Mt. McClure and Lawlers Au orientations. The surface depletion of Au in the upper ferruginous part of the profile at Boddington is opposite to that found at Mt. McClure and Lawlers. However, despite surface depletion of Au at Boddington, Sn, W, Mo, and As are strongly anomalous throughout the profile.

### *Transfer of research findings to the industry*

Research findings were transferred to sponsors through production of research reports, review meetings, workshops and a field trip. Research projects for nine Bachelors Degree Honours students, in regolith geology, geochemistry or geophysics, were an integral part of project strategy, providing an additional, effective mechanism of experience transfer to industry.

---000---

## PROJECT LEADERS' PREFACE

R.E. Smith and R.R. Anand, 30 November 1993

This project, AMIRA P240A, with the shortened title *Yilgarn Lateritic Environments*, was a two-year extension of its precursor, AMIRA P240 (*Laterite Geochemistry*). The term for this extension was from 1 July 1991 to 30 June 1993. Writing of this final report and completion of other project reports continued until 31 December 1993.

Sponsorship was by the 17 companies listed in Table 1. The project was collaborative with the Co-operative Research Centre for Australian Mineral Exploration Technologies (CRCAMET), which financially supported part of the research through its Regolith Characterisation Program. An integral part of the collaboration was participation by the Australian Geological Survey (AGSO) and the Geological Survey of Western Australia (GSWA).

Collaboration was extended through participation by Bachelor-level Honours students from several universities: Curtin University of Technology, School of Applied Geology (three students), Department of Exploration Geophysics (three students); University of Western Australia, Geology Department (two students); and University of Tasmania (1 student). Four of the Honours projects received extra funding from the respective tenement holders.

Staff and collaborators who have contributed to the project are listed in Table 2. The list of research support staff includes those from the CSIRO Division of Exploration Geoscience research support services.

External funding for *Yilgarn Lateritic Environments* is summarised in Table 3. It is satisfying to note that the total external funding (\$749K) marginally exceeded the total sought (\$743K) in the original proposal. However, this was the result of finding alternative funding sources to fill a significant shortfall in AMIRA-sourced funds. The AMIRA-sourced funds of \$513K represent 32% of the total project costs. The CSIRO Division of Exploration Geoscience (now Division of Exploration and Mining), together with GSWA and AGSO, have provided a further \$850K funding in salaries, overheads and operating funds, representing 53% of the total project costs. Other funding from industry constituted the remaining 15%.

The substantial sponsorship from CRCAMET and industry, the collaboration of these sponsors, as well as the collaboration through CRCAMET and universities, enabled the interdisciplinary team, which was established during the precursor project, to continue unimpeded. Without this support and collaboration, including enhanced interaction with the *Dispersion Processes Project* (AMIRA P241A, led by Dr C.R.M. Butt), the advances in knowledge of regolith relationships, regolith evolution, geochemical dispersion and exploration methods would not have been possible.

Expertise in exploring lateritic terrain continued to be improved, building upon findings of the precursor project. In this extension, focus was particularly on areas of transported cover and on more complex lateritic environments typified by the Kalgoorlie regional study.

Research findings were readily taken up by sponsors and further ore deposit discoveries were made where the concepts, methods and knowledge arising from the research directly contributed to the discoveries. The most notable discoveries during the course of this extension project are the Bronzewing Au deposits by Great Central Mines in areas of transported cover in the northern part of the Eastern Goldfields Province.



*Preface*

Table 1. Sponsors and collaborating organisations for AMIRA Project P240A, *Yilgarn Lateritic Environments*.

**SPONSORS:**

- Australian Consolidated Minerals
- Analabs (in kind)
- BHP Limited
- Billiton Australia
- Centaur Mining/Great Central Mines
- CRA Exploration
- Croesus Mining
- Geochemex Australia
- Geopeko
- Geoscan
- Homestake
- Newcrest Mining Limited
- Pancontinental Mining
- Placer Pacific
- Poseidon
- RGC Exploration
- Western Mining Corporation Ltd

**COLLABORATING ORGANISATIONS:**

- Australian Geological Survey Organisation (AGSO)
- Geological Survey of Western Australia (GSWA)
- Curtin University of Technology
- University of Western Australia
- University of Tasmania

**Table 2. List of Project Personnel.**

<p><i>Project Staff</i>  <i>CSIRO Floreat Park Laboratories, WA</i>  R.E. Smith (Project Leader)  R.R. Anand (Co-Leader)  H.M. Churchward (joint CSIRO-AGSO appointee)  I.D.M. Robertson  D.J. Gray  C. Phang  J.E. Wildman  T.J. Munday (joint Curtin-CSIRO appointee)</p>	<p><i>Collaborators</i>  J.R. Gozzard, Geological Survey of Western Australia  M.A. Craig, Australian Geological Survey Organisation, Canberra  K. Smith, Curtin University of Technology, School of Information and Library Studies  V.C. Wilson, Curtin University of Technology, Department of Exploration Geophysics</p>
<p><i>Research Support Staff contributing to the Project:</i>  R. Bilz  J.F. Crabb  M.K. Hart  C. Harris  A. Howe  W. Maxwell *  J. Porter  B.W. Robinson  C.R. Steel  A. Vartesi  M. Cheeseman  G. Hitchen  J. Wilson *</p> <p>* Provided the main laboratory support.</p>	<p><i>Visiting Scientist:</i>  R.J. Gilkes, Soils Group, Department of Agriculture, University of Western Australia</p> <p><i>Honours Students:</i>  R. Twomey, Department of Geology and Geophysics, University of Western Australia  A. Williamson, Department of Geology and Geophysics, University of Western Australia  M.P. Nelson, Department of Exploration Geophysics, Curtin University of Technology  K.A. Mayes, Department of Exploration Geophysics, Curtin University of Technology  R. Wills, School of Applied Geology, Curtin University of Technology  M.R. Dell, Geology Department, University of Tasmania  A.D. Von Perger, School of Applied Geology, Curtin University of Technology  G.P. Cant, Department of Exploration Geophysics, Curtin University of Technology  J.D. King, School of Applied Geology, Curtin University of Technology</p>



*Preface*

Table 3. Summary of funding for the Yilgarn Lateritic Environments Project, P240A, 1 July 1991 to 31 December 1993.

	\$
<b>1. External funding</b>	
Total funds for P240A to AMIRA (includes AMIRA administrative fees).	513,000
Sponsorship in kind.	14,000
Sponsor support for two B.Sc. Honours studies.	20,000
Additional in-kind support for four Honours projects.	10,000
Curtin-CSIRO research grant in support of Honours activities and university supervisors (Curtin contribution to funding listed.)	3,000
CRCAMET funding for regolith characterisation activities 1992/93.	50,000
CRCAMET funding for regolith characterisation and regolith models first half of 1993/94.	92,000
Funding for staff travel to conferences, workshops etc.	20,000
Other activities, including sale of reports, workshops for sponsors, consultations to sponsors.	27,000
<b>Sub-total</b>	
Funding from sources external to CSIRO	<b>749,000</b>
<b>2. Internal funding</b>	
Funding for salaries, overheads and operating from CSIRO, GSWA and AGSO, (estimate)	<b>852,000</b>
<b>3. Total project costs (approximate)</b>	<b><u>1,601,000</u></b>

# TABLE OF CONTENTS

## Volume I

<b>EXECUTIVE SUMMARY</b>	iii
<b>PROJECT LEADER'S PREFACE</b>	v
<b>TABLE OF CONTENTS</b>	ix
<b>1.0 INTRODUCTION</b>	
1.1 Exploration Issues Addressed	1
1.2 Background	1
1.3 Scope	1
1.4 Objectives and Strategy	1
1.5 Expected Benefits	5
1.6 Purpose of this Report	6
<b>2.0 UPDATE OF DEFINITIONS</b>	
2.1 Introduction	7
2.2 Definitions	7
<b>3.0 REGOLITH AND LANDFORM EVOLUTION IN THE KALGOORLIE REGION</b>	
3.1 Introduction	11
3.2 Regional geology and geomorphology	11
3.3 Regional trends of regolith distribution and stratigraphy	15
3.4 Regolith characteristics	20
3.5 Regolith evolution and implications in exploration	24
<b>4.0 ORIENTATION STUDIES IN THE KALGOORLIE REGION</b>	
4.1 Introduction	33
4.2 Ora Banda district (including the Matt Dam prospect)	34
4.3 Kanowna Belle district	63
4.4 Wombola district	87
<b>5.0 ORIENTATION STUDIES OUTSIDE THE KALGOORLIE REGION</b>	
5.1 Introduction	101
5.2 Boddington district	102
5.3 Mount McClure district	136
5.4 Waroonga and Genesis Au deposits, Lawlers district	157
5.5 Bottle Creek deposits	177
5.6 Golden Grove Cu-Zn-Au VHMS deposits	192
5.7 Beasley Creek and Lights of Israel	205
5.8 Madoonga	213
<b>6.0 CLASSIFICATION OF REGOLITH-LANDFORM MAPPING UNITS</b>	
6.1 Introduction	233
6.2 Regolith-landform mapping	233
6.3 Guide for use	233
6.4 Classification tables	234
6.5 Atlas of regolith-landform mapping units	234
6.6 Glossary	234
<b>7.0 COMPARATIVE STUDIES OF REGOLITH EVOLUTION AND GEOCHEMICAL DISPERSION</b>	
7.1 Introduction	241
7.2 Regolith Evolution - Darling Range, Leonora-Wiluna and Kalgoorlie regions	241
7.3 Geochemical dispersion - Darling Range, Leonora-Wiluna and Kalgoorlie regions	245
7.4 Implications in exploration	250

## *Table of contents*

<b>8.0</b>	<b>DATA INTERPRETATIONAL METHODS</b>	
8.1	Introduction	251
8.2	Some comparisons between data sets	251
8.3	Data interpretation practical	254
<b>9.0</b>	<b>GEOCHEMICAL DISPERSION MODELS AND EXPLORATION PROCEDURES</b>	
9.1	Introduction	261
9.2	Full lateritic profile, high seasonal rainfall, no surficial cover	261
9.3	Full lateritic profile, semi-arid to arid climate, little or no surficial cover	264
9.4	Full lateritic profile, semi-arid to arid climate, transported cover	268
9.5	Partly truncated profile, semi-arid to arid, transported cover	274
<b>10.0</b>	<b>OUTLOOK</b>	
10.1	General	277
10.2	Yilgarn transported overburden, AMIRA P409	277
10.3	Teaching and training	277
10.4	Developments in regolith mapping technologies	277
10.5	Regolith characterisation and the CRCAMET	277
10.6	Developments in GIS and 3D visualisation	277
10.7	North Queensland regolith, AMIRA Project P417	278
<b>11.0</b>	<b>CONCLUSIONS</b>	
11.1	Reconciling project outcomes with objectives and expected benefits	279
11.2	Transfer of research findings to sponsors	282
11.3	Final comment	283
<b>12.0</b>	<b>ACKNOWLEDGEMENTS</b>	285
<b>13.0</b>	<b>REFERENCES</b>	287
<b>14.0</b>	<b>APPENDICES</b>	
Appendix Ia	List of reports issued by the precursor project (P240)	293
Appendix Ib	List of reports issued by this project (P240A)	295
Appendix II	List of reports issued to tenement holders	295
Appendix III	Meetings held with sponsors	296
Appendix IV	List of Bachelors Degree Honours Theses	297
Appendix V	Regolith-landform map, Kalgoorlie region, 1:250,000	map tube
Appendix VI	Regolith-landform map, Ora Banda district	map tube
Appendix VII	Regolith-landform map, Kanowna Belle district	map tube
Appendix VIII	Regolith-landform map, Wombola district	map tube
Appendix IX	Regolith-landform map, Mt. McClure district	map tube

### **Volume II** (Appendix X)

<b>DATA AND PLOTS FROM:</b>	1
Matt Dam	1
Kanowna Belle	69

### **Volume III** (Appendix X - cont'd)

<b>DATA AND PLOTS FROM:</b>	1
Wombola Dam	1
Mt McClure	60
Golden Grove	120

Appendix XI Data from the orientation studies

diskette

## 1.0 INTRODUCTION

### 1.1 Exploration issues addressed

The presence of a thick regolith is recognised as a major impediment to mineral exploration in the Yilgarn Craton and adjacent regions, as well as in many other parts of Australia. The processes of deep chemical weathering, erosion and sedimentation have served to conceal ore deposits in the underlying rocks, such that their geological, geochemical and geophysical expression in the regolith is greatly altered, weakened or buried. As a result, exploration of difficult regolith environments has tended to be expensive and therefore either very selective or high-risk.

However, the same processes that have led to development of a thick regolith have also formed geochemical dispersion haloes and related dispersion patterns. Some of these dispersion patterns, although weak, can greatly enlarge target size. Examples of enlarged geochemical haloes in lateritic residuum were well documented in the precursor *Laterite Geochemistry Project* (AMIRA P240; Report 236R, Smith *et al.*, 1992).

### 1.2 Background

This two-year continuation of the *Laterite Geochemistry Project* capitalised upon the experience, information, and knowledge already established by the research group. The approach of viewing geochemical dispersion within a well-controlled and well-understood regolith-landform and bedrock framework, at both detailed and district scales, continued. This approach has general significance to exploration for a wide range of commodities, in addition to Au, which has been the main focus of this project, and is applicable to most geochemical sampling media.

### 1.3 Scope

This extended project has developed exploration methods through understanding lateritic regolith environments, regolith evolution and dispersion processes by tackling progressively more complex lateritic environments. This has included recognising geochemical haloes in lateritic residuum buried beneath transported cover. Focus also extended to the concept of using associated ferruginous materials in the upper saprolite where laterite residuum is missing because of erosion, for example. Soils formed from saprolite and from alluvial cover were also investigated. The components of this research are shown in Table 1.1.

The Project has as its core methods of sampling, analysis and interpretation in exploration geochemistry using lateritic materials, particularly lateritic residuum and associated ferruginous materials, whether they be at surface or buried beneath cover.

Considerable emphasis has been on translating research findings into practical exploration procedures and on facilitating the uptake of new methods by sponsors through workshops and visiting field study areas.

### 1.4 Objectives and strategy

*The overall objective of the Yilgarn Lateritic Environments Project has been to continue to develop and improve methods for finding mineral deposits in complex lateritic environments of the Yilgarn Craton, using geochemistry integrated within a sound regolith-landform framework.*

#### *Specific objectives:*

- (i) To expand the knowledge base of the physical and chemical processes and patterns of dispersion from concealed mineral deposits within complex lateritic environments.
- (ii) To establish a framework of reference for classification of Yilgarn regolith-landform mapping units for the purposes of exploration geochemistry.
- (iii) To provide examples of comparative testing of alternative methods for interpretation of multivariate geochemical data using the well-controlled data sets from the orientation studies.
- (iv) To provide some well-controlled data sets from partly truncated, buried weathering profiles in carefully chosen orientation situations, with emphasis on ferruginous material and saprolite and soils.
- (v) To continue to integrate the research findings into progressively more effective exploration methods and to carry out feasibility tests of promising procedures.
- (vi) To improve the criteria for identification of regolith units in drill spoil and for distinguishing between residual and transported regolith materials.

- (vii) To characterise iron oxides in surficial materials so as to establish their surficial environments of formation and the nature of the underlying bedrock.

Table 1.1 The main research components of the Yilgarn Lateritic Environments Project, 1991-1993

---

♦	<b>Regolith evolution in the Kalgoorlie Region</b>
♦	<b>Orientation studies within the Kalgoorlie Region</b>
•	Wombola
•	Ora Banda
•	Kanowna Belle
♦	<b>Orientation studies outside the Kalgoorlie Region</b>
•	Lawlers
•	Boddington*
•	Bottle Creek* i
•	Mt. McClure
•	Lights of Israel i
•	Golden Grove
•	Madoonga
♦	<b>Classification of regolith-landform mapping units</b>
♦	<b>Data interpretational methods</b>
♦	<b>Integration, dispersion models and exploration procedures</b>
♦	<b>Experience transfer</b>

---

\* Continues from Project P240 (Laterite Geochemistry)

i Interfaces with Project P241A (Dispersion Processes)

---

The approach of first establishing the regolith-landform relationships of an area, at local and district scales, then establishing and interpreting geochemical dispersion within this framework, was continued. This approach has general application in exploration geochemistry (and geophysics) and has been referred to as landscape geochemistry particularly in the Russian and Canadian literature (Perel'man, 1972; and Fortescue, 1975, 1992).

The focus of the project remained the Yilgarn Craton and orientation studies continued to be foundations to the project. These were expanded to include those shown in Fig. 1.1. Part of the strategy was to develop Bachelor-level Honours projects within the research and thesis areas are shown in Fig. 1.2. Orientation studies completed during this extension, and its precursor, are shown in Fig. 1.3, arranged in terms of regolith setting and annual rainfall. Within the Yilgarn Craton, an important part of the strategy was generating an understanding of regolith-landform evolution for a 10,000 km<sup>2</sup> region about Kalgoorlie, Fig. 1.1. This region provides strong contrasts with other studies in the project and its precursor.

Although the main focus of the project concentrated on Au exploration, the knowledge, regolith mapping methods, regolith stratigraphy, models and evolution are applicable to exploration for a wide range of commodities and the geochemical data are comprehensively multi-element. Orientation work also included new data generated from archived samples from the Golden Grove base metal sulphide orientation study (Smith and Perdrix, 1983).

Although focus is on the Yilgarn Craton of WA and its periphery, the research findings have wider application. Sponsors have used the research in other parts of Australia (NT and Qld) and in appropriate terrain overseas, including western Africa, southeast Asia and South America.



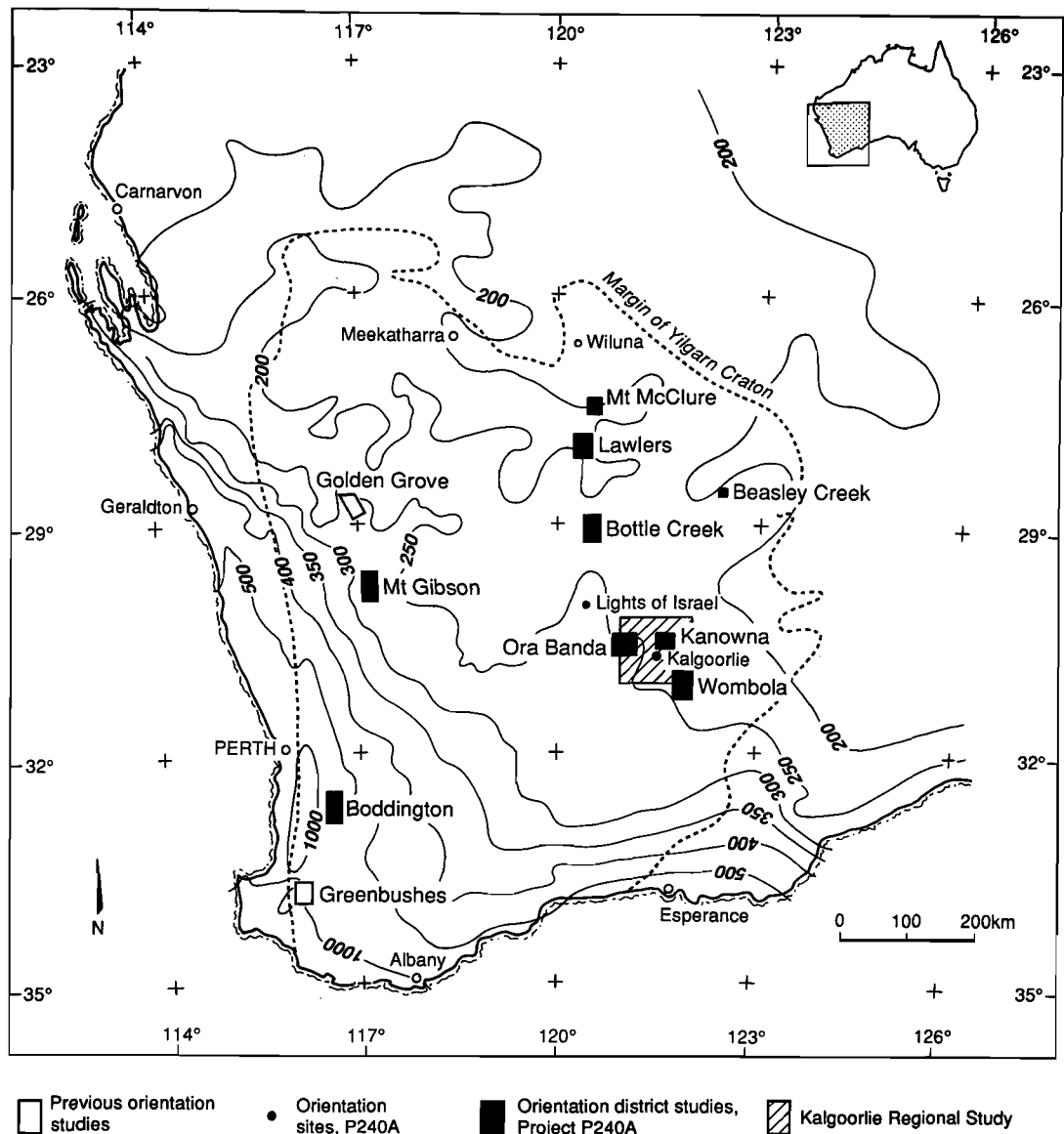


Fig. 1.1 Map showing the locations of orientation studies from this extension project. Bottle Creek, Beasley Creek and Lights of Israel were collaborative studies involving Project P241, Weathering Processes. Isohyets show the average annual rainfall in millimetres.

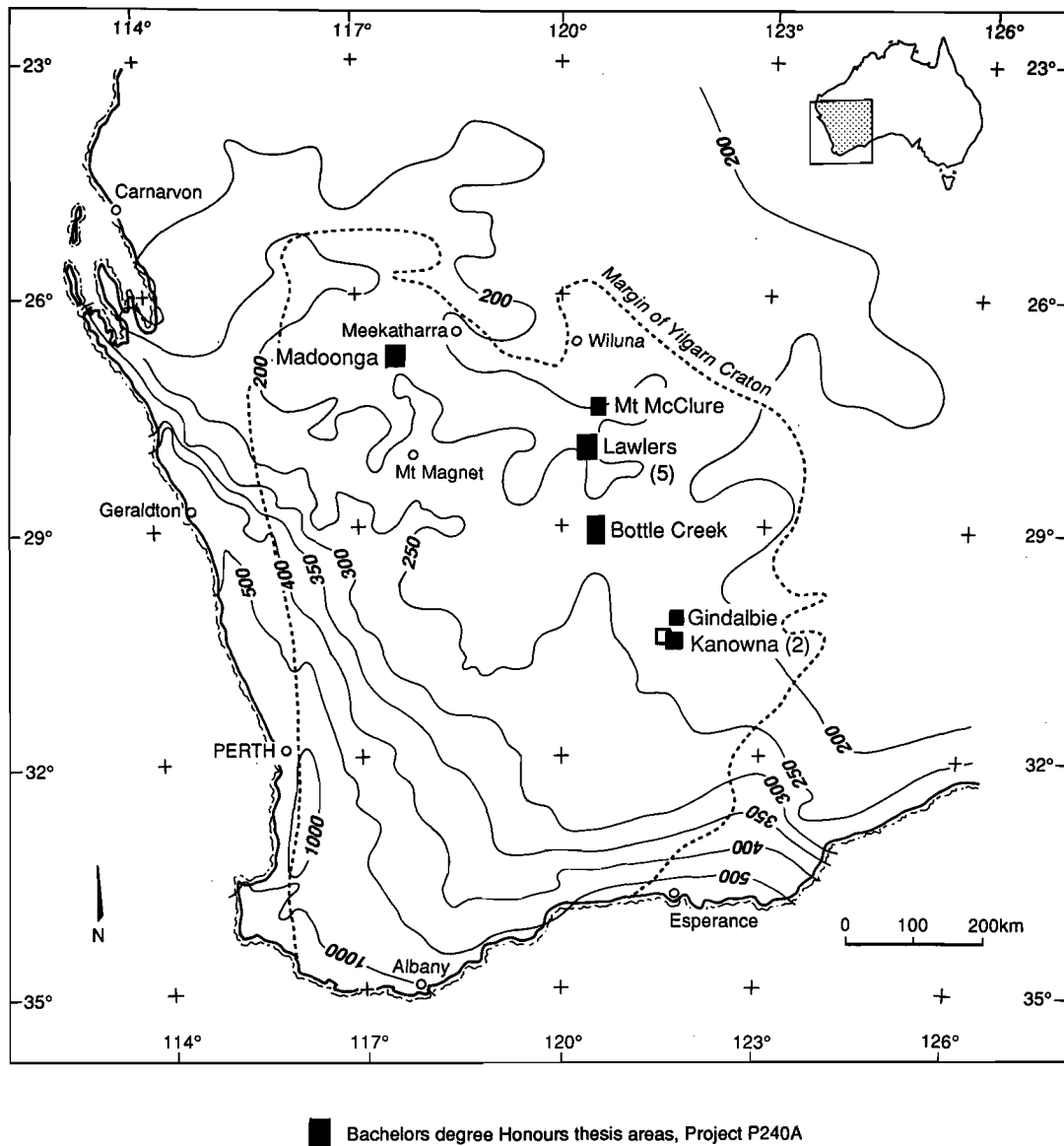


Fig. 1.2 Map showing the distribution of Bachelors degree Honours theses carried out within this extension project.

**Fig. 1.3** Orientation studies carried out by the Laterite Geochemistry Group arranged according to average annual rainfall and showing the status of lateritic residuum. Orientation studies are located in Figs. 1.2 and 1.3. ***Bold italics*** show orientation studies presented in this report.

At commencement of this extension project, its precursor had already resulted in a quantum advance in the use of laterite geochemistry for mineral exploration (summarised in Report 236R, Smith *et al.*, 1992). It was anticipated that developments would continue and result in:

- Improved understanding of some of the more complex regolith situations of the Yilgarn Craton, condensed into a series of exploration models;
- Generations of further orientation data sets within well-controlled regolith-landform frameworks (a crucial part of system development for data interpretation).
- Expansion of field criteria for recognising units of the regolith stratigraphy from drill spoil.
- Expansion of the volume Terminology, Classification and Atlas of laterite and associated regolith materials - which provides a common language.
- Recommendations on some alternative weathered sample media where lateritic residuum is absent.
- Worked-through examples of multivariate manipulations of target and background orientation data sets, as part of an integrated exploration system.
- A classification and terminology scheme for regolith-landform mapping units to facilitate correlation, comparison and contrasts across the Yilgarn Craton.
- Transfer of research experience to sponsors via comprehensive research reports, a series of review meetings, workshops and field trips.
- Continued integration, synthesis of research findings and development of exploration models.
- Feasibility tests for exploration.

**1.6 Purpose of this report**

This report provides a summary and synthesis of the research findings of this extension project. It is a companion volume to Report 236R, the Summary Report to the precursor project. This report cross-references individual reports and provides links with other research, including the AMIRA Dispersion Processes Project (P241A). The report also provides an outlook on future direction of research and exploration. Research has been presented to sponsors through periodic sponsors' meetings, in brief quarterly and semi-annual reports and in workshops and field trips. These activities and reports are listed in Appendices I to IV.

## 2.0 UPDATE OF DEFINITIONS

### 2.1 Introduction

This section updates definitions of some of the main terms used in the project. Terms used to describe regolith units of the weathering profile were given in detail in *Terminology and classification of laterites and associated ferruginous materials* (Anand *et al.*, August 1989) and in the Summary Report 236R for project P240 (Smith *et al.*, 1992).

For the purposes of geochemical exploration two major families of ferruginous regolith materials were recognised and described in Section 6.3 of Report 236R. This subdivision is retained with some amplification, Fig. 2.1. The main change is use of the term *non-lateritic family* to include other non-lateritic ferruginous materials in addition to the iron segregations originally described.

### 2.2 Definitions

Updated definitions are arranged alphabetically:

#### Clasts

Clast is used here as a general term for fragments of a rock or hardened regolith material, particularly in the granule, pebble or cobble size range. It includes fragments of ferruginous saprolite, hardened mottles, ferruginous lithic fragments, iron segregations, lateritic nodules and pisoliths.

#### Collapsed Ferruginous Saprolite

Ferruginous saprolite may form a continuous blanket, as the upper zone of the saprolite, and can be overlain by collapsed ferruginous saprolite, where soft, soluble, less ferruginous material has been removed by leaching, causing the structure to collapse.

#### Ferruginous Lithic Fragments

Lithic fragments enriched in Fe-oxides. These are generally yellowish brown through reddish brown to black, and commonly have relict textures. Some may have a matt surface, others glossy, generally referred to as varnish. Ferruginous, lithic fragments are derived from the ferruginisation of the lower part of the saprolite, saprock and bedrock.

#### Ferruginous Saprolite

Ferruginous saprolite is firm to hard, massive to mottled, and is dominated by goethite and kaolinite. It is formed by infusion of clay-rich saprolite with goethite. Fragments of ferruginous saprolite are yellowish-brown to reddish-brown, non-magnetic and may have incipient nodular structure or accretionary coatings on surfaces and voids.

#### Lateritic Family of Ferruginous Materials

The lateritic family of ferruginous materials consists of lateritic residuum (lateritic gravel consisting of nodules and/or pisoliths, and lateritic duricrust) and transitional types (ferruginous mottles and ferruginous saprolite).

They are yellowish brown to dark reddish brown and largely consist of kaolinite, hematite, goethite and maghemite. The original rock texture may be partly preserved or completely destroyed.

The lateritic family results from ferruginisation and residual accumulation of Fe in the upper lateritic profile.

#### Lithic Family of Regolith Materials

The lithic family includes materials which contain very little or no Fe and are derived from the lower part of a weathering profile. Generally the fabric of the rock is preserved in these materials which include saprolite, saprock and fragments derived from them.

#### Lithic Nodules and Pisoliths

Lithic nodules are Fe and Al accumulations in which the original structure of the parent rock can be seen. These nodules are developed by fragmentation and ferruginisation of saprolite. Their formation is initiated in saprolite, eventually accumulating in lateritic residuum through ground surface reduction. Some of the Fe required for ferruginisation may have been derived from patches of sulphides and ferromagnesian minerals.



**Mega-mottles**

Mega-mottles are brown to reddish brown, irregular Fe accumulations (up to several metres across) commonly containing smaller (< 10 mm) ferruginous granules. The mottles have a dull, earthy lustre and have gradational to abrupt boundaries with surrounding, bleached clays. They may develop in a wide range of weathering settings but are typical features of palaeochannel environments. Mega-mottles in the Kalgoorlie region have been described by Ollier *et al.* (1988).

**Mottled Saprolite**

This is similar to ferruginous saprolite but is incipiently or strongly mottled.

**Non-lateritic Family of Ferruginous Materials**

The non-lateritic family includes iron segregations, ferruginous lithic fragments and ferruginous granules. The term non-lateritic family has been introduced to broaden categories beyond those covered within the group of iron segregation types. Figure 2.1 shows the revised categories and families.

The very diverse non-lateritic family results from ferruginisation and has developed predominantly within saprolite. Its members are not confined to a single unit of regolith stratigraphy.

**Non-lithic nodules and pisoliths**

These nodules are generally formed high in the mottled zone or ferruginous saprolite and result from pedogenic activity in the vadose zone. Non-lithic nodules and pisoliths are formed by leaching, migration and accumulation of Fe in voids or the clay matrix. This is not a singular event, but involves multiple Fe leaching and precipitation and leads to mottles. With further mobilisation and concentration of Fe, mottles and incipient nodules evolve into true nodules and thence into pisoliths.

**Silcrete**

Strongly silicified, indurated regolith components, commonly having a conchoidal fracture and a vitreous lustre. Silcretes represent complete or near-complete silicification of a precursor regolith horizon by infilling of voids and replacement of matrix with silica. The fabric and mineralogical composition of silcretes may reflect those of the parent regolith and, hence, if residual, the underlying lithology.

**Transported Overburden**

General term referring to material of exotic or redistributed origin such as alluvium, colluvium and aeolium that blanket fresh or weathered bedrock. It may be friable or partially or wholly consolidated, cemented by Fe-oxides, silica, carbonates, gypsum or clays.

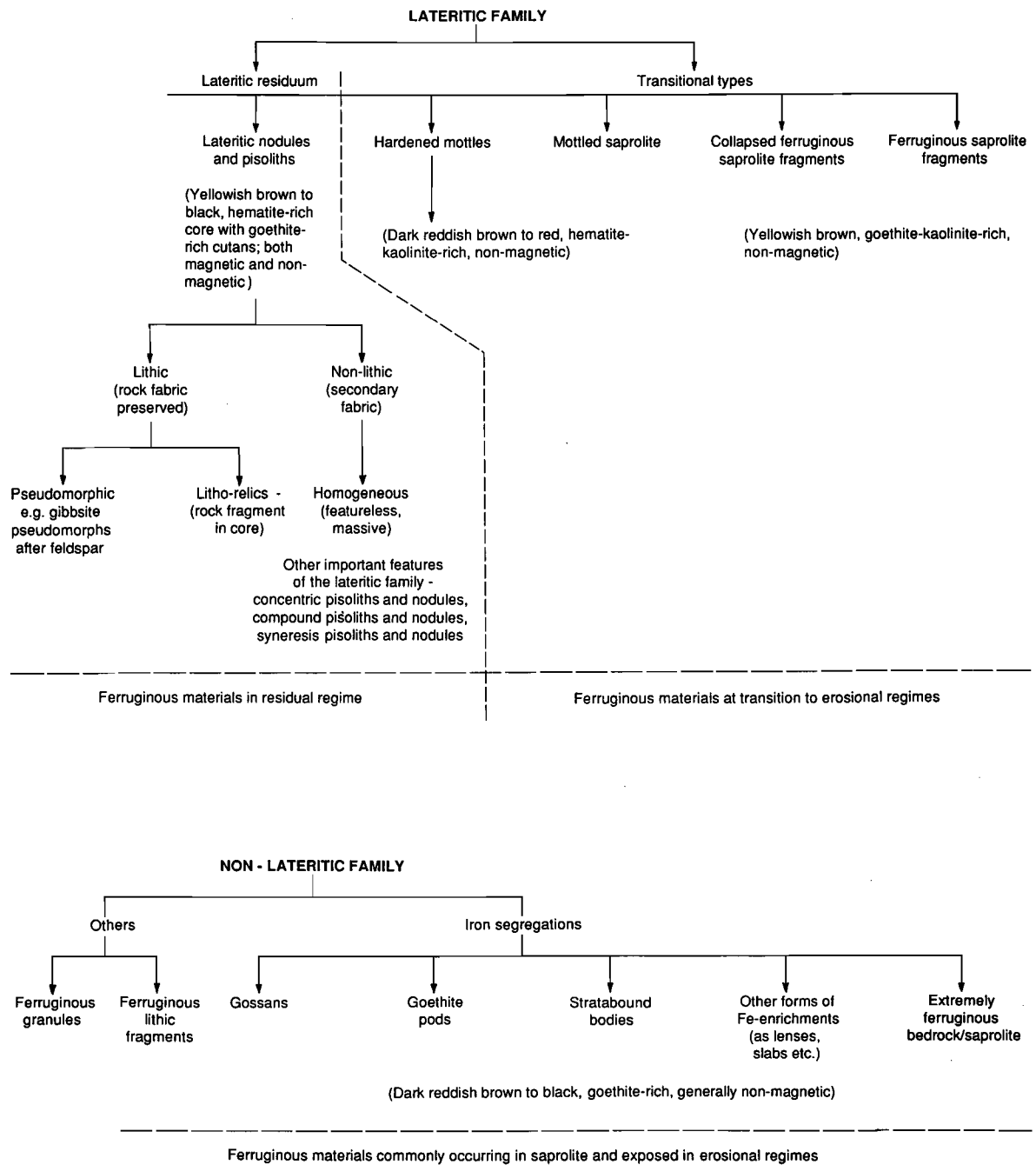


Fig. 2.1 Subdivisions of common ferruginous regolith materials. As shown in this figure, mottled saprolite and ferruginous saprolite belong to a transitional subdivision within the lateritic family, as distinct from lateritic residuum. It is important to maintain this distinction in assigning codes to samples for entry into geochemical databases.



### 3.0 REGOLITH AND LANDFORM EVOLUTION IN THE KALGOORLIE REGION

#### 3.1 Introduction

The purpose of this section is to describe those aspects of the evolution of regolith and landscape that are important to mineral exploration in the Kalgoorlie region. This region is an integral part of the array of weathering terrains in the Yilgarn Craton. Thus, in common with other terrains, deep weathering is widespread. However, details of weathering, including laterite formation and modification since development by erosion, deposition and secondary enrichment is significantly different from other areas of the Yilgarn such as the Leonora-Wiluna region. Consequently, the Kalgoorlie region requires use of different sampling media compared to the Leonora-Wiluna region.

#### 3.2 Regional geology and geomorphology

The climate of the Kalgoorlie region is semi-arid, with a Mediterranean (winter rainfall maximum) tendency; hot summers alternate with cool to mild winters. The vegetation is a mosaic of predominantly eucalypt woodlands, tending to open with a saltbush and bluebush understorey on the more calcareous soils.

The Kalgoorlie region covers a number of geological provinces and major structural elements. Granite-greenstones of the Kalgoorlie region form the southern part of the Eastern Goldfields Province in the Yilgarn Craton of Western Australia. The greenstones, which host rich deposits of Ni and Au, comprise metamorphosed mafic volcanic and intrusive rocks, felsic volcanic rocks and sedimentary rocks which crop out in highly deformed linear belts intruded by, and separated by, variably deformed and metamorphosed granitoids. In the Kalgoorlie region, systematic regional mapping at 1:100,000 scale by the Geological Survey of Western Australia (GSWA), has delineated a number of structural and stratigraphic domains with similar geological histories (Swager *et al.*, 1990). These are: the Kalgoorlie, Callion, Norseman, Kurnalpi and Menzies Terranes.

The Kalgoorlie Terrane is sub-divided into four major domains (Coolgardie, Ora Banda, Kambalda, Boorara) and two smaller domains (Bullabulling, Parker), Fig. 3.1. The domains are separated by shear zones that include dismembered and attenuated elements of the stratigraphy. Despite these structural breaks, a similar regional stratigraphic succession (with some variations) and a common deformation history are recognised throughout. The Callion and Norseman Terranes lack significant komatiite and contain extensive BIF units, the latter have not been found in the Kalgoorlie Terrane. The Kurnalpi Terrane contains komatiite but is dominated to the east by mafic and felsic to intermediate volcanic rocks.

The Kalgoorlie region (Fig. 3.2) is characterised by gently undulating, subdued relief broken by greenstone strike ridges, granite mounds and low breakaways. It lies within the Salinaland Division of Jutson (1950). The region has an eastward-flowing integrated trunk drainage system, underlain by well-developed palaeochannels. Surface flow in the main drainages is very sporadic and the trunk drainages incorporate salt lakes. Landforms largely reflect the underlying geology. Thus the greenstone belts, which generally trend north-northwest, are associated with a series of strike ridges, low hills and broken slopes rising above the general level of the gently undulating landscape. The terrain decreases in altitude away from greenstone ridges towards broad, colluvium filled valleys. The Kalgoorlie region ranges in elevation from 320 to 480 m (Fig. 3.2). Numerous playa lakes occupy the lower areas.

Some drainages have extensively dissected a zone peripheral to the playas and discontinuous breakaways are associated with both greenstone and granite terrain.

The Kalgoorlie region is here subdivided into seven broad regolith-landform modules: *upland areas with hills, stripped plains, greenstone sandplains, granite sandplains, broad alluvial floors, playas and associated dunes, and palaeochannels* (Fig. 3.3).

Upland areas comprise broad crests, and long gentle slopes including backslopes of breakaways and gently sloping plains that forms a downslope continuum with backslopes. The high hills, generally flanked by steep slopes, rise above the relics of lateritised surface and expose fresh bedrock. Ferruginous granules commonly occur in the areas of low hills.

Stripped plains that are peripheral to playa systems have active drainages. These plains are occupied by calcareous soils, containing abundant carbonate nodules. The soils overlie bedrock or saprolite with little ferruginous lag.

Greenstone sandplains are associated with playas and are characterised by sandy soils with a quartz lag. At depth, calcareous soils can occur. A zone of clayey alluvium, of varying thicknesses (3-10 m), occurs beneath the soils.

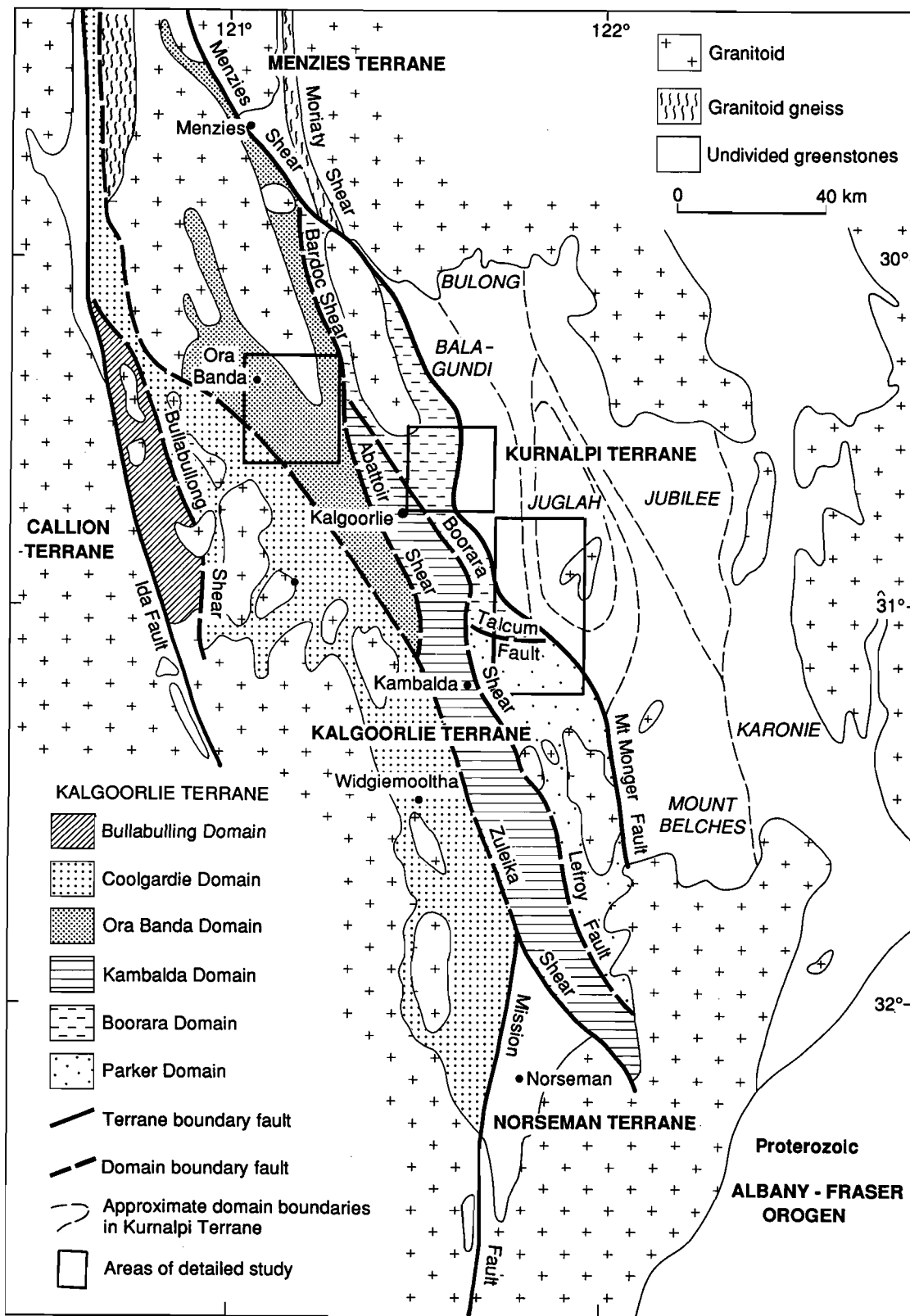


Fig. 3.1 Map of the Kalgoorlie Terrane and its six constituent structural-stratigraphic domains (after Swager *et al.*, 1990). Detailed areas of study in this project are also shown.



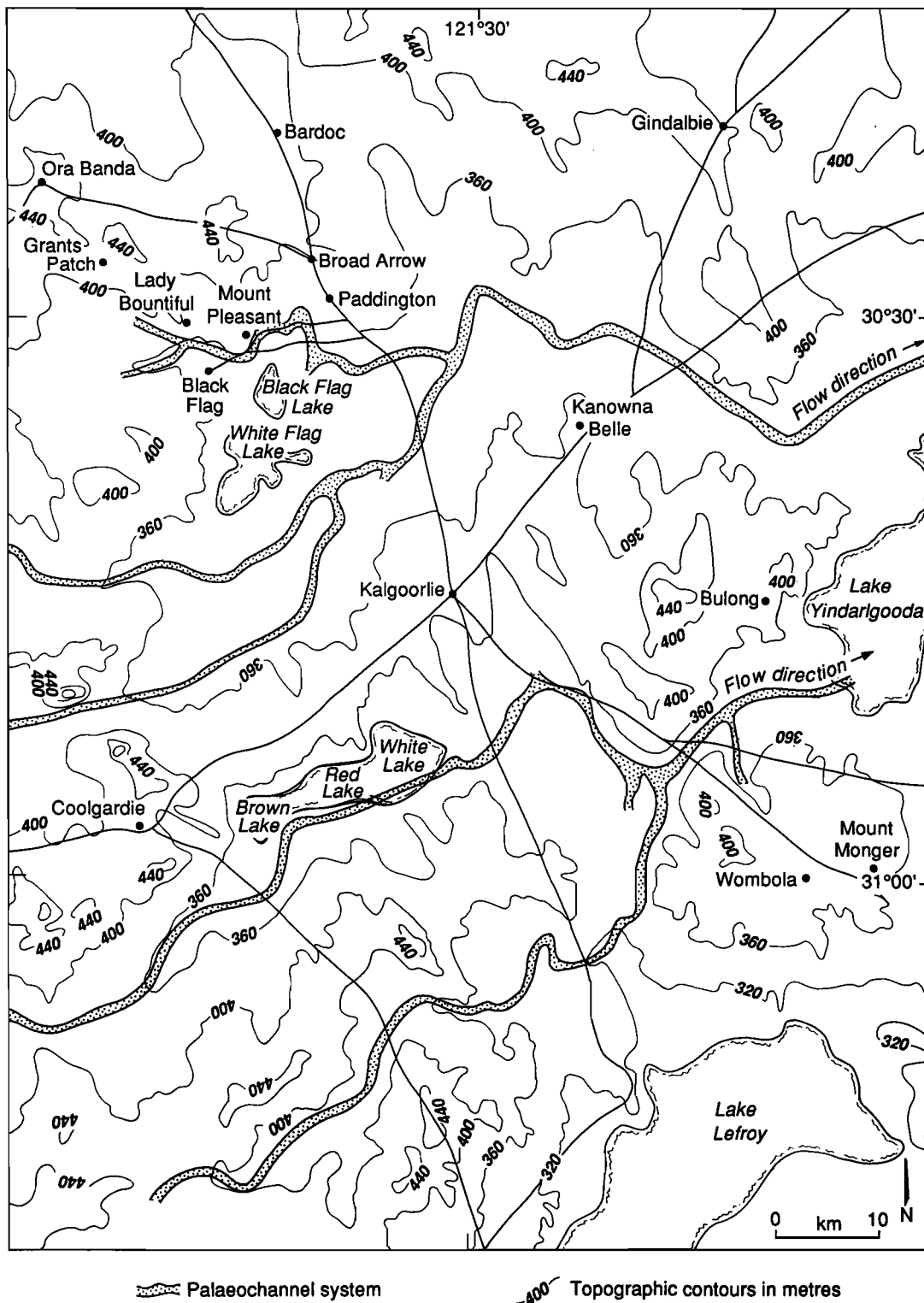


Fig. 3.2 Map showing the topographic setting of the Kalgoorlie region. The palaeochannel information is taken from Commander *et al.* (1992).

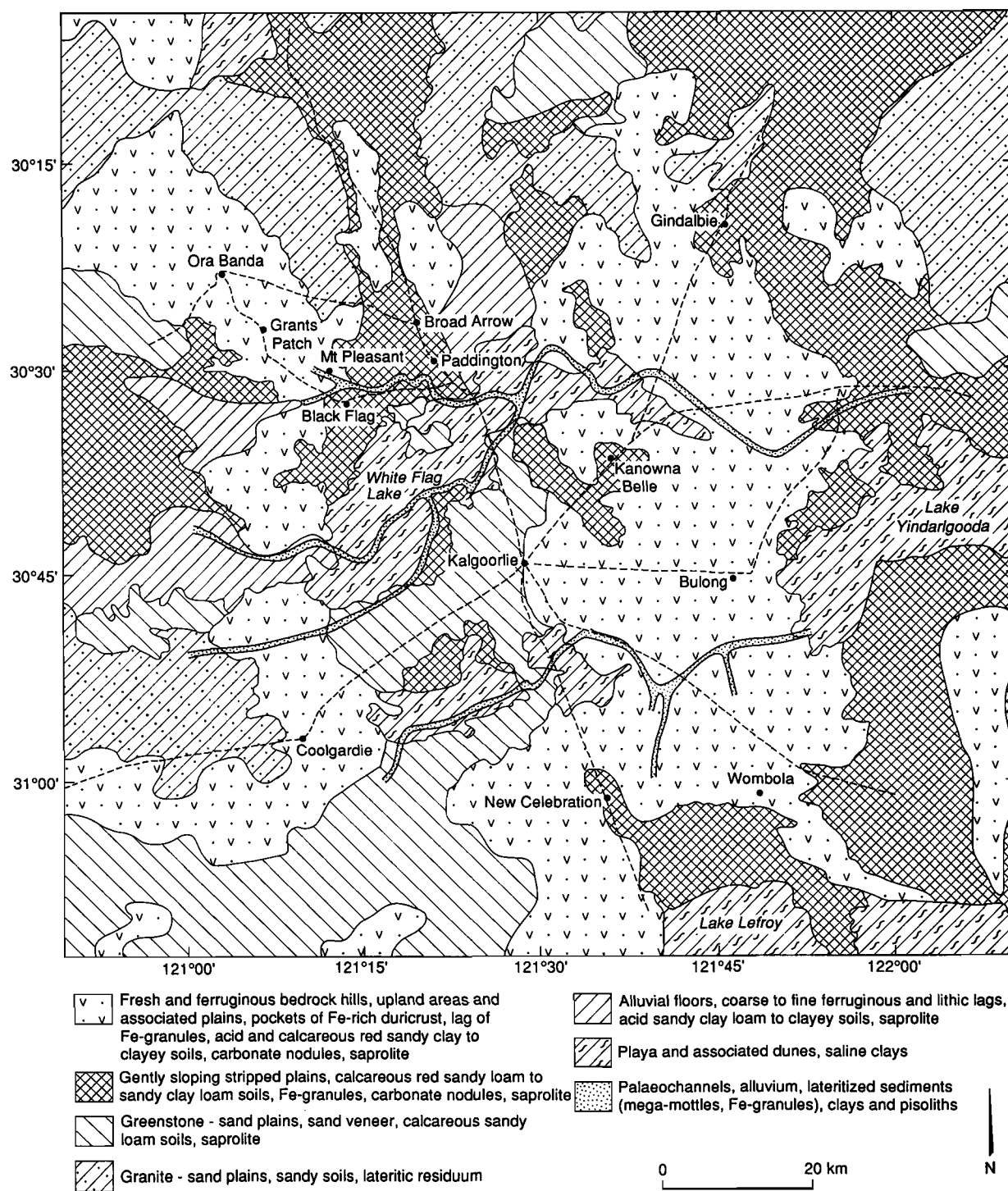


Fig. 3.3 Generalised regolith-landform modules of the Kalgoorlie region and its environs.

Within sandplains overlying granitic bedrock, lateritic profiles are developed on a freely draining surface of low relief. Typically, here, a layer of yellow, non-calcareous sand overlies a layer of lateritic pisoliths and nodules. However, pockets of pedogenic carbonates can occur.

Alluvial valley floors have clearly defined but minor channels. Red brown to light brown clays occur extensively and are generally overlain by a coarse to fine ferruginous and lithic lag. Ferruginous granules are commonly present in these soils. Alluvium, of varying thicknesses (up to 10 m) including lacustrine clays, underlies the calcareous clays.

Playas are characterised by saline, dark to pale brown, fine clays and muds. The saline clays can be underlain by varying thicknesses of lacustrine clays which, in turn, overlie saprolite or bedrock. In places bedrock or saprolite occurs close to the surface. Gypsiferous and quartz-rich clayey sands border the salt lakes and playa system.

Clay deposits, within which mega-mottles have developed are characteristic of the edges of salt lakes and these can also occur as low rises within the lakes. The mega-mottles are dark brown, ferruginous patches, up to a metre across. Many have an abrupt boundary with the surrounding clay material (Ollier *et al.*, 1988).

### 3.3 Regional trends of regolith distribution and stratigraphy

The regolith-landform map (scale 1:250,000) for the Kalgoorlie region, generated by this project, accompanies Volume 2 of this report as Appendix V. This map was produced in collaboration with AGSO (Craig and Anand, 1993). A summary of the map in terms of *erosional*, *residual* and *depositional regimes* is shown in Fig. 3.4. This map is based upon 1:50,000 scale mapping of the Kanowna-Belle, Ora Banda and Wombola districts. The regolith stratigraphy for the Kalgoorlie region is summarised in Fig. 3.5 and profiles typical of crests, low hills, plains and palaeochannels are shown in Fig. 3.6. Variations in regolith in the Kalgoorlie region can be explained in terms of erosional and depositional regimes that modified a relatively stable, weathered landscape, scattered remnants of which form residual regimes.

*Residual regimes*, by definition, are characterised by preservation of lateritic residuum; these areas are limited in extent in the Kalgoorlie region. Such areas occupy crests and subdued topographic highs.

Iron rich duricrusts ( $>70\%$   $\text{Fe}_2\text{O}_3$ ) and brown duricrusts ( $<50\%$   $\text{Fe}_2\text{O}_3$ ) generally occur as large slabs and blocks on small broad convex crests of low rises. A mixed lag of lateritic nodules, pisoliths and ferruginous saprolite fragments occurs over a shallow (10-30 cm) reddish brown, sandy, clay loam to clay soil. The duricrust and lateritic nodules are commonly infused with carbonates which are clearly visible where the lag-covered surface is slightly disturbed. The thickness of duricrust ranges from 0.5 to 2 m and is underlain either by ferruginous saprock or ferruginous saprolite or by deep saprolites. The weathered profiles are generally shallow and range in thickness from 0.5 to 20 m but may exceed 50 m.

In the *erosional regimes* there has been varying degrees of truncation of the weathering profile; generally the lateritic residuum has been completely removed, exposing the mottled zone, ferruginous saprolite, saprolite or fresh bedrock or these may be concealed beneath soils, or beneath locally-derived colluvium. These areas comprise backslopes, hills, breakaways, pediments and erosional plains.

Backslopes that extend from the crests are mantled by a lag of yellowish brown to black nodules, ferruginous saprolite and ferruginous lithic fragments. This lag is coarse upslope, on the fringes of the duricrust-capped crests, becoming finer downslope. Lag on the upper slopes also contain an appreciable amount of fragments of Fe-rich duricrust. The soils are acidic, sandy clay to sandy clay loams over a weakly to strongly developed hardpan at about 15 cm depth, although carbonates generally appear within 20 cm of the surface. The soils contain moderate to large amounts of  $<1$  mm quartz, particularly between a depth of 0-50 cm (Fig. 3.7). The carbonates may continue to a depth of about 1 m which may then merge with acid red clays. Saprolite or bedrock generally appear below 2 or 3 m. In addition, there are scattered pockets of cracking red clay (overlying bedrock) which have a finely patterned micro-relief (gilgai).

The high hills, generally flanked by steep slopes, rise above the relics of lateritised surface and expose fresh bedrock. Some shallow ( $<50$  cm), stony, calcareous soils occur. On steep slopes scattered outcrops and cobbles of saprock on the upper slopes outcrop through a shallow, stony, sandy clay to sandy clay loam with powdery and nodular carbonates.

Low hills are characterised by both fresh and ferruginous bedrock and saprock. Soil formation is quite common on low hills. Typically these gently undulating hills have well-developed calcareous red sandy clay loam soils which can be underlain by acid red clay. The total thickness of soils vary from

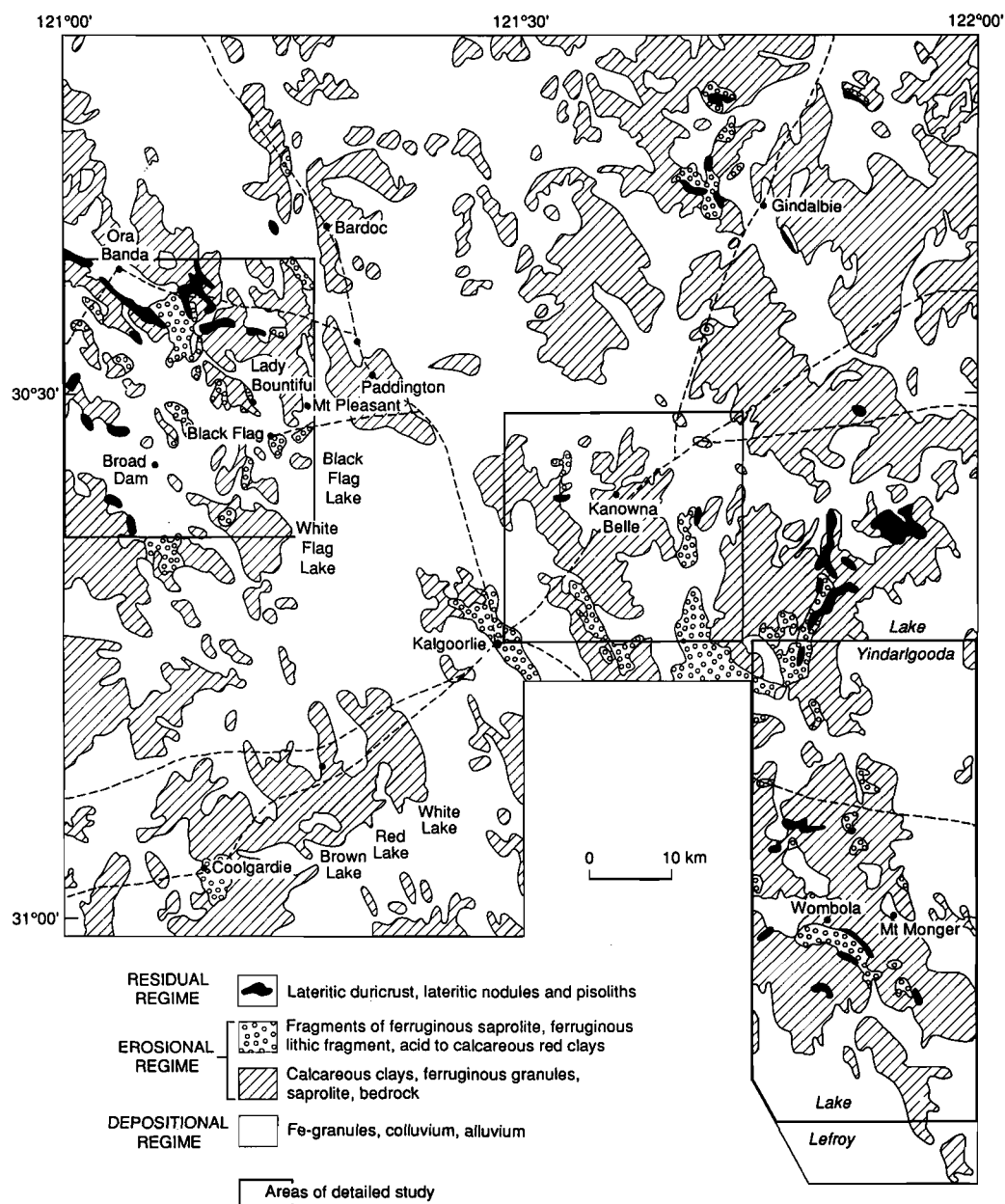


Fig. 3.4 General regional patterns of the regolith for the Kalgoorlie region studied in this report.

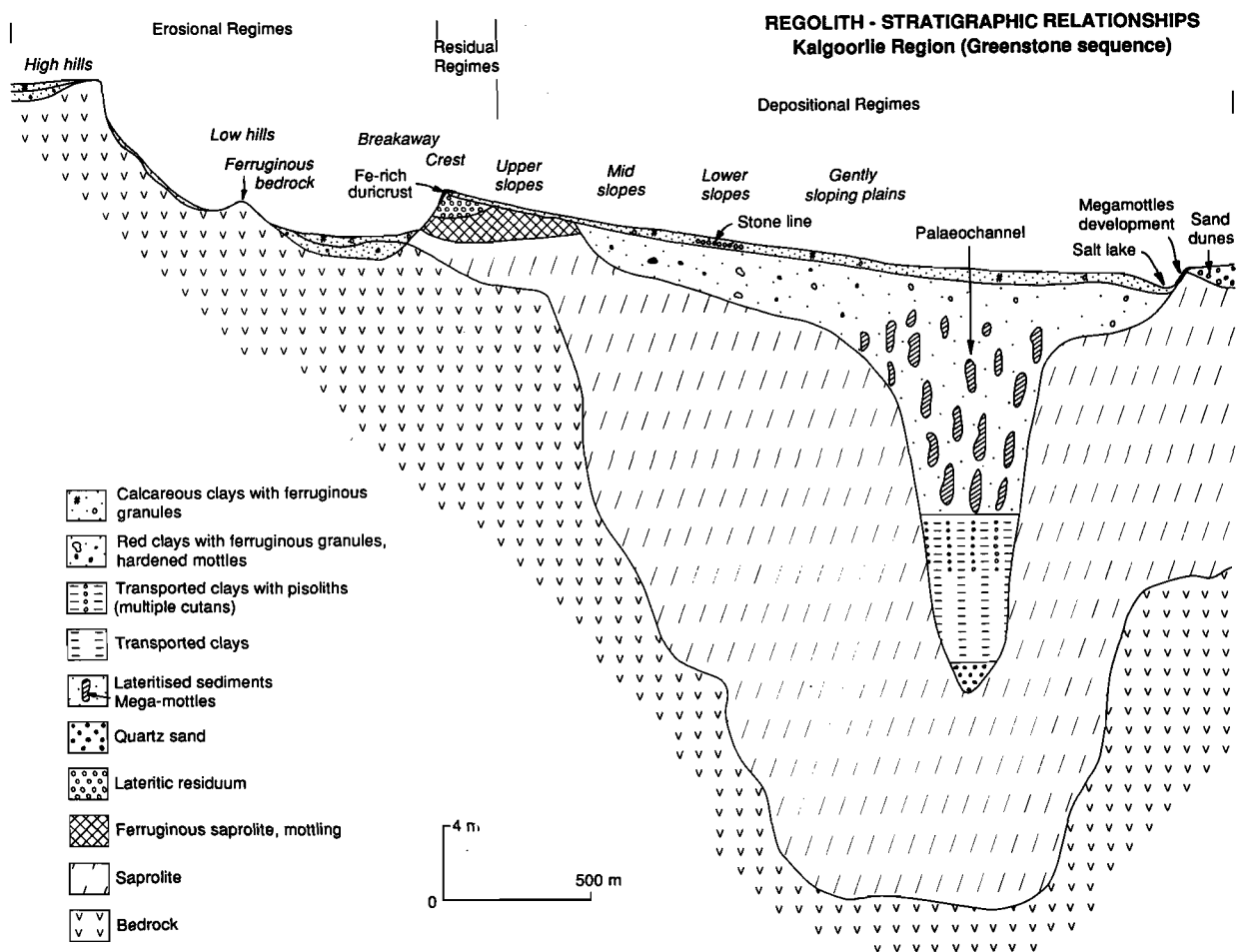


Fig. 3.5 Schematic cross section for the Kalgoorlie region showing regolith stratigraphy and landforms.

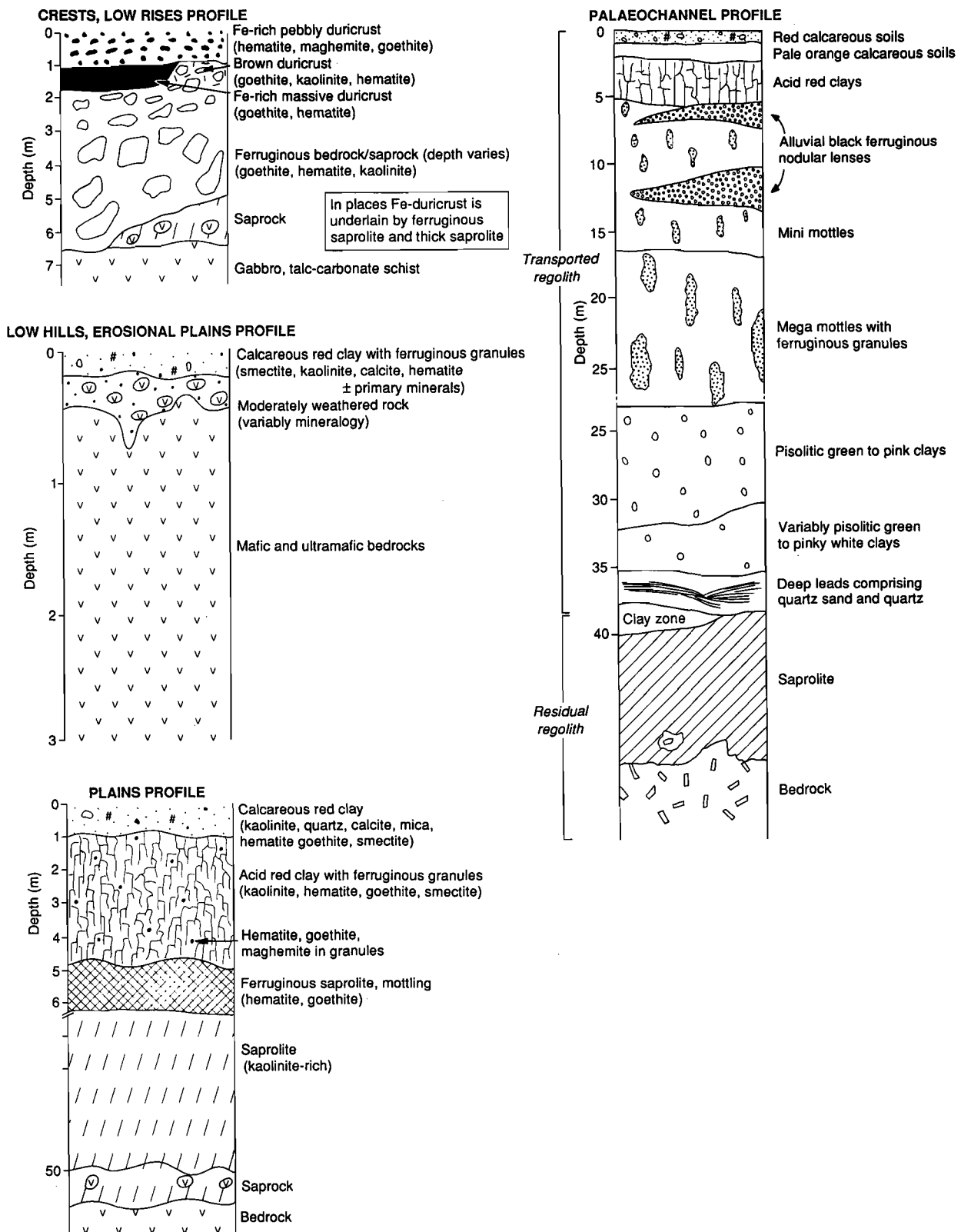


Fig. 3.6 Regolith profiles typical of crests, low hills, plains and palaeochannel environments in the Kalgoorlie region.



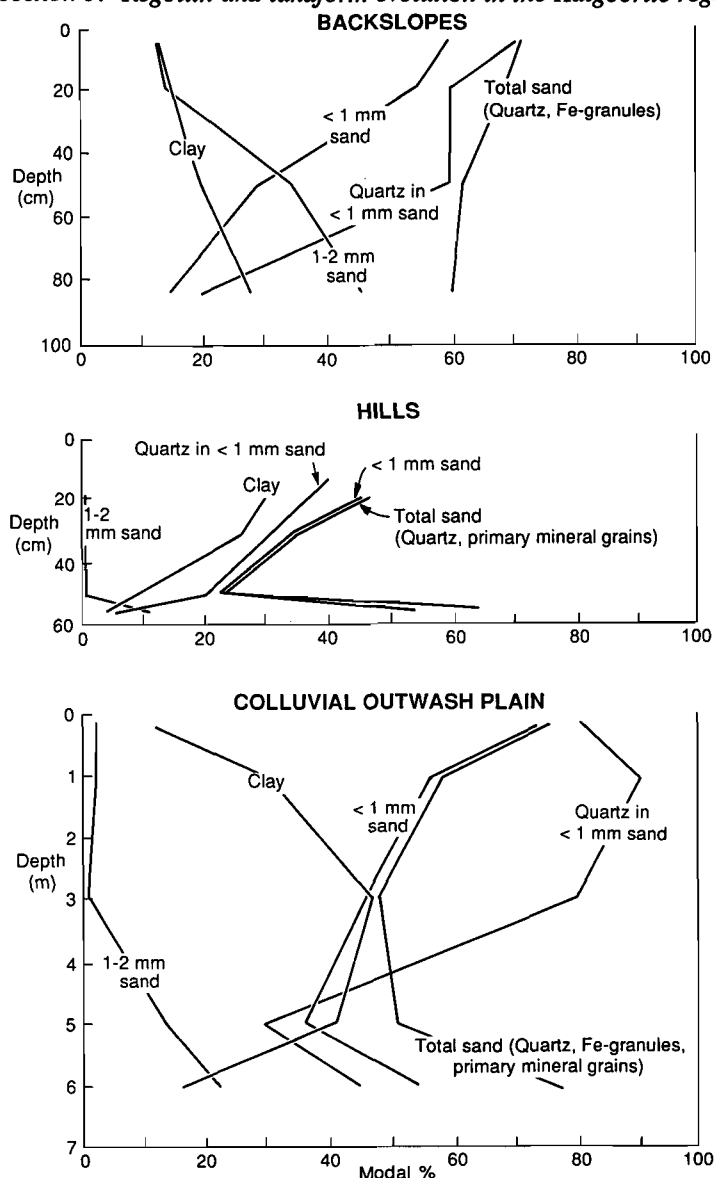


Fig. 3.7 Distribution of total sand, clay and quartz in vertical profiles from backslopes, hills and colluvial outwash plains, Kalgoorlie region.

30 cm to 100 cm and black ferruginous granules are common. Bedrock or saprolite forms a general substrate.

*Depositional regimes* comprise gentle, sloping, colluvial and alluvial plains and salinas. The transported regolith of the depositional regimes can have been derived locally or, in other cases, distally, and the thickness can reach tens of metres. Here also, pockets of the deeply weathered profile can form discontinuous substrates.

Gently sloping plains, that form a downslope continuum with backslopes, are extensively mantled by fine black ferruginous lag and this generally overlies acid red sandy clay loam with mildly developed hardpan at a depth of 30 cm. Calcium carbonate in several forms (powdery, nodular, stringers) occurs within 15-100 cm depth. The calcareous soils are extensively underlain by a 2-5 m thick zone of plastic uniform red clays. Ferruginous granules and mottles are commonly present in the soils.

Palaeochannels are known to generally occur in the lower parts of the landscape beneath the playas and salinas. They are characterised by substantial thicknesses of alluvium which has buried the channels cut into saprolite. Development of a mega-mottled clay zone and spherical pisoliths in underlying grey kaolinitic clays are typical of palaeochannels in the Kalgoorlie region. Profiles within these generally comprise 20 to 50 cm of red to brown calcareous clay soils with polymictic lag of abundant black ferruginous granules, and lithic fragments. The soils overlie plastic, red clays of varying thicknesses. The plastic clays commonly contain black, ferruginous granules. The clast components observed within the unit commonly occur as horizontally elongate lenses. Bleaching and pseudomottle development within the basal Fe-rich clays of the unit marks the transition into the mega-mottled zone.

The mega-mottled zone is characterised by increased bleaching and development of evenly-spaced irregular, hematite-goethite-rich, 10 cm to several metres long mottles or septa (Fig. 3.8A). Abundant ferruginous granules may occur within the mottles. Both mottles and ferruginous granules appear to have formed in the sediments. The creamy white, bleached clays become more prominent with increasing depth and may develop an elongate, columnar cracking structure exposing root systems, commonly sheathed by Fe-rich accumulations. The transition from the mega-mottled zone to the underlying pisolitic clay is marked by a gradual decrease of ferruginous mottles until the clays are totally bleached.

The pisolitic clay horizon is characterised by sub- to well-rounded pisoliths with greenish brown to grey cutans, in a matrix of pink-whitish to grey clays with minor detrital quartz (Fig. 3.8B). The underlying unit of angular to sub-angular, quartz-rich, alluvial sediments forms the deep leads. Saprolite forms the lowest unit of the weathering profile.

Residual regimes occupy less than 5% of the mapped area, whereas erosional and depositional regimes account for about 90%.

### 3.4 Regolith characteristics

#### 3.4.1 Ferruginous materials

A wide variety of ferruginous materials occur in the Kalgoorlie region. They occur as crusts, lag and as gravel components in soil, colluvium and alluvium. Research has shown that important patterns of geochemical dispersion from mineral deposits can be preferentially contained or preserved within many of these ferruginous materials. Consequently, understanding their internal and external characteristics, their mineralogy, chemistry and evolution is very relevant to geophysical and geochemical exploration methods. This section presents their salient features and seeks to clarify the relationships between some of the main types of ferruginous materials. Their evolutionary pathways are then summarised.

For the purpose of geochemical exploration, several types of ferruginous materials are recognised, based upon their mesoscopic and chemical characteristics as well as their position in the regolith stratigraphy, and in the regolith-landform framework as well as their chemical characteristics. The materials considered are Fe-rich black duricrusts, brown duricrusts, yellowish brown nodules, ferruginous granules and mega-mottles.

#### *Fe-rich black duricrusts*

The Fe-rich duricrusts are hard, ferruginous crusts, reaching several metres in thickness and comprise several secondary structures (nodular, pisolitic). They are sporadically distributed throughout the Kalgoorlie region. The outer surfaces of these duricrusts may have a pebbly appearance. These duricrusts occur at surface and are typically 0.5-2 m thick. They are largely pedogenic in origin formed as part of lateritisation and result from the weathering of Fe-rich mafic and ultramafic rocks.

In detail, these duricrusts comprise dark reddish brown to reddish black nodules and pisoliths set in a fine grained, sparse, reddish brown matrix (Fig. 3.8C). In slices, the ratio of nodules to matrix ranges from 60:40 to 80:20; most samples examined having a ratio close to 80:20. The boundary between nodules and matrix is generally not well defined and nodules show weak or no development of mesoscopic cutans. There are small vermiform voids, to 3 mm in diameter in the matrix, generally lined with yellow goethite. In places, the matrix is porous and white; cryptocrystalline silica occupies some of the small voids. Many of the nodules of the duricrust contain lithorelics. The centres of the nodules may show pseudomorphs after primary minerals (Fig. 3.9A,B) but much of the nodule fabric appears to have been destroyed by massive to slightly porous Fe-oxides. In polished sections of some samples, pseudomorphed wood fragments are conspicuous and occur in a finely crystalline matrix of hematite and goethite. In the nodules, many pieces of wood are replaced by Fe-oxides so completely that, in polished sections, cell structure can readily be seen (Fig. 3.9C,D). Similar cell structures have been observed in the oolitic Fe-rich duricrusts of the Lawlers district (Anand *et al.*, 1991) and at Ora Banda, occurring as low outcrops on peridotites (Butt *et al.*, 1992).

Hematite, goethite and maghemite are the major minerals present in the Fe-rich duricrusts. Kaolinite is either absent or present only in small amounts. Small amounts of talc and chromite are generally present in ultramafic-derived duricrusts. Nodules and pisoliths are generally magnetic because of the presence of maghemite which may occur around the margins or within the cores of nodules and pisoliths.

The chemical compositions of duricrusts derived from gabbro and talc-carbonate schists is given in Table 3.1. There is no significant difference in major element compositions between the duricrusts derived from the weathering of gabbro and talc-carbonate schist. These are characterised by high



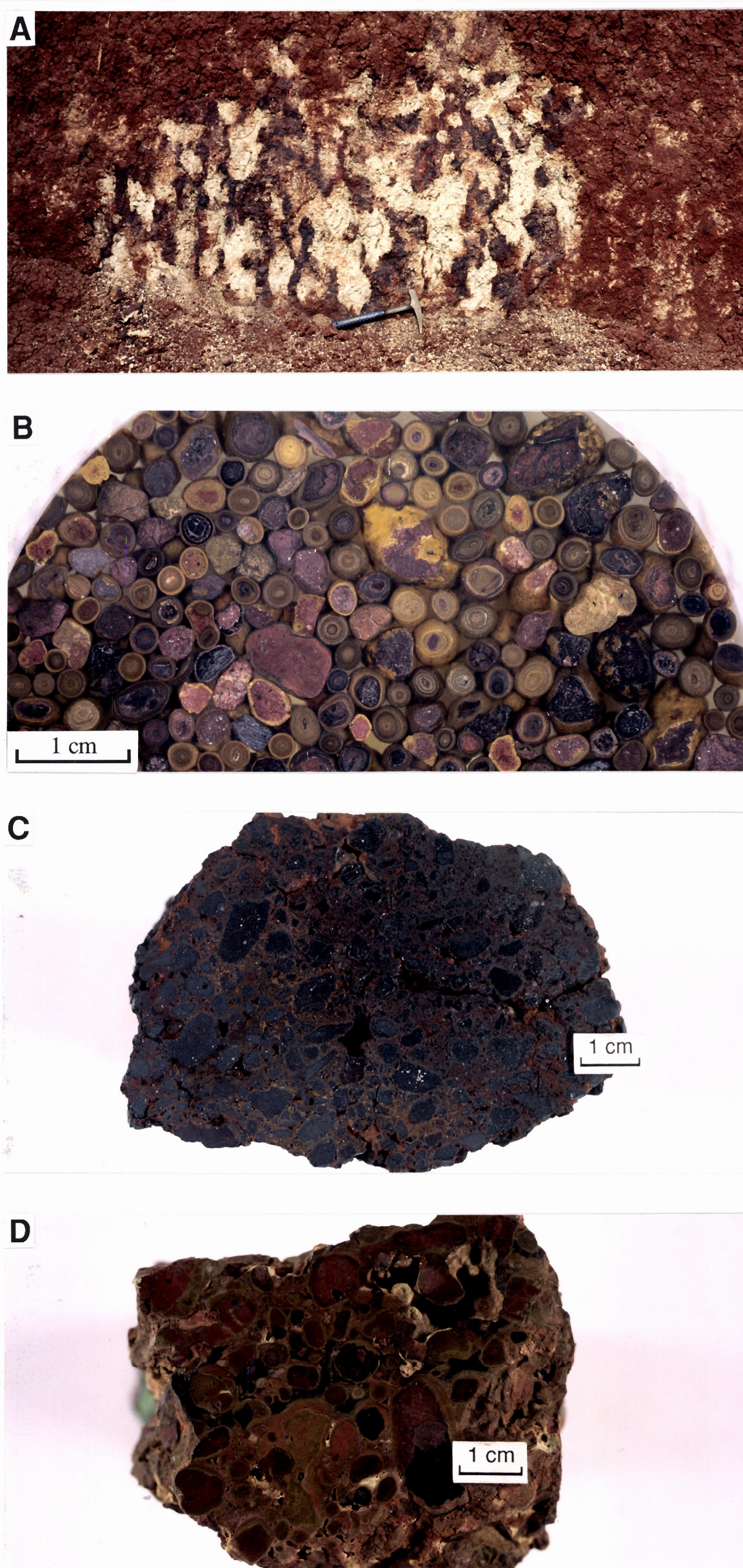


Fig: 3.8 Some examples of the ferruginous materials from the Kalgoorlie region. (A) Mega-mottles in a palaeochannel profile, (B) Pisoliths in a palaeochannel profile, (C) Black, Fe-rich nodular duricrust, (D) Pisolitic-nodular duricrust (low in Fe).





concentrations of  $\text{Fe}_2\text{O}_3$  (>70%  $\text{Fe}_2\text{O}_3$ ) and very low concentrations of  $\text{SiO}_2$  and  $\text{Al}_2\text{O}_3$ . However, the distribution of the trace elements is controlled by the nature of the bedrock. The duricrusts formed from the weathering of talc-carbonate schist show high values of Cr, Ni, and Co whereas these elements are much lower in duricrusts derived from the weathering of gabbro.

#### *Brown duricrusts and loose lateritic nodules*

These are weathering crusts composed of goethite, hematite, and kaolinite (Fig. 3.8D). Irregular, vermiform voids (2-10 mm) are generally lined with pale yellow-brown goethite and kaolinite. Some of these are filled with clay, having an incipient pisolitic structure. A sandy clay matrix (30-60 vol%) is generally yellowish brown to dark red and is predominantly kaolinite, goethite and quartz. Nodules and pisoliths are red to reddish brown and generally have goethite-kaolinite rich cutans. In polished sections, the central parts of nodules may show relict fabrics. The duricrusts are comparatively rich in kaolinite and goethite but poor in hematite. They are relatively low in  $\text{Fe}_2\text{O}_3$  (<50%  $\text{Fe}_2\text{O}_3$ ) and higher in  $\text{Al}_2\text{O}_3$  and  $\text{SiO}_2$ . The compositions of these duricrusts generally reflect the underlying lithologies.

#### *Ferruginous granules*

Ferruginous granules occur in soil or as lag. They are black, sub- to well-rounded and vary in size from 0.5 to 10 mm in diameter. Typically, the granules have an earthy to silvery sub-metallic lustre and a few have a thin, earthy cutan. Both magnetic and non-magnetic granules occur.

The granules largely consist of hematite and maghemite, with variable quantities of goethite, kaolinite and quartz. The quartz occurs as angular to well-rounded grains commonly incorporated into the structure or forming the nucleus. Numerous black pits and voids are present within the granules, highlighting relict fabrics such as fossilised cellulose or providing pathways that have initiated partial or total hematite replacement of clays.

Petrographic examination reveals several types of internal fabrics. The non-magnetic granules show progressive replacement of clays by hematite forming essentially massive granules. The internal parts of some granules show preservation of relict rock fabrics and pseudomorphs after rock-forming minerals. Some granules contain ferruginised cellulose fragments, showing the intricate preservation of individual cell walls now totally replaced by hematite. A large proportion of the granules have a concentric outer shell developed around a nucleus. Quartz fragments are commonly incorporated into the concentric bands, indicating multiple periods of development. These granules are comprised mainly of  $\text{Fe}_2\text{O}_3$  (>70%),  $\text{SiO}_2$  (10-15%) and  $\text{Al}_2\text{O}_3$  (2-7%).

#### *Mega-mottles*

The mega-mottles are brown to reddish brown, irregular Fe accumulations (up to several metres across) containing smaller (<10 mm) sub-angular metallic granules. The mottles have a dull, earthy lustre and a gradational to abrupt boundary with the surrounding bleached clays. Root systems, surrounded by a sheath of bleached clays, are common and show a close spatial relationship to zones of Fe accumulation. The bleaching extends down cracks in some instances, and also down root channels. Mega-mottles are characterised by kaolinite, hematite and quartz.

#### *Silicon-Aluminium-Iron relationships in ferruginous materials*

The Si-Al-Fe relationships of the Fe-rich duricrusts, brown duricrusts and loose brown nodules, and ferruginous granules are shown in the ternary diagram (Fig. 3.10). The compositional fields of Fe-rich duricrusts and ferruginous granules are similar. The Fe-rich duricrusts have a relatively restricted compositional range and there is a tendency for a higher concentration of Fe in the Fe-rich duricrusts relative to ferruginous granules. Brown duricrusts and nodules have a wide compositional range reflecting variation in the Al and Si contents.

#### *Soils*

The major regolith units of the deep weathered profile form distinctive soil parent materials, either where exposed *in situ* or as transported sediments. The soil patterns depend partly on the degree of stripping of the weathered mantle, on the bedrock lithology and on the spread of weathering and erosional products across the various slope elements. The following soil sequences in greenstone terrain in the Kalgoorlie region illustrate these relationships.

Gravelly soils occur on areas dominated by duricrust. These are generally brown to reddish brown, friable sandy loams to sandy clay loams. Soils are up to 30 cm thick and are generally residual, being derived from the weathering of lateritic duricrust. The dominant gravel component of these soils is lateritic nodules and pisoliths. The soils largely consist of kaolinite, quartz and goethite.

Calcareous red clay to sandy clay and shallow stony soils occupy the erosional areas. These soils show a close association with weathered or sub-cropping mafic and ultramafic rocks and appear to result from *in situ* weathering of bedrock. The gravel fraction is dominated by 1 to 5 mm shiny, black, ferruginous granules and lithorelics. Lateritic nodules and pisoliths are typically absent. The calcareous, red earths are dominated by kaolinite, calcite, smectite and mixed layer minerals with small amounts of goethite, hematite, quartz and dolomite.

Soils, in the depositional regimes, are generally calcareous clays to sandy clay loams developed in colluvium and alluvium. The most common substrate to the calcareous red clay is non-calcareous, dark red brown clays which generally merge with mafic or ultramafic saprolite at a depth of 2 to 5 m. These soils are generally plastic, uniformly Fe-stained and may contain ferruginous granules.

### 3.5 Regolith evolution and implications in exploration

The regolith-landform relationships and regolith stratigraphies indicate a polyphase, multi-process history. Many of the regolith types resulting from this complex array of processes, have a distinctive pattern. In the Kalgoorlie region, the processes of regolith evolution, particularly deep weathering, laterite formation and modification of the deeply weathered regolith in response to the change from a humid to an arid climate are markedly different from those of the Leonora-Wiluna region. These are shown in Fig. 3.11 and are discussed below. The main implications in exploration of these findings are listed in Table 3.2.

#### 3.5.1 Lateritic weathering processes

In the Kalgoorlie region, the effects of past weathering is widespread as shown by deep kaolinisation of basement rock. However, lateritic residuum is limited in extent. It may be that the lateritic residuum had never developed over large areas in the mapped region. Rather, duricrust, red soils and mottled zones may have developed in specific sites in response to bedrock geology and local environments. This is in contrast to the Leonora-Wiluna region, for example, where lateritic residuum formed an almost continuous blanket deposit. Indeed, buried residual laterite profiles are also widespread beneath an overlay of colluvium and alluvium (Anand *et al.*, 1991).

Weathered profiles are thinner and less continuous in the upland areas. The profiles are comparatively thicker in valleys and plains, where profile thickness generally exceed 50 m. Ferruginisation is much less common in these areas. The formation of deep saprolite is favoured on stable, subdued land surfaces (Mabbutt, 1980). Variation in the depth of weathering tend to be controlled by the nature of bedrock and may give little evidence of the form and position of any associated originating land surfaces.

#### *Fe-rich duricrusts*

Genesis of the Fe-rich duricrusts observed in the Kalgoorlie region are explained by two different mechanisms. Firstly, lateritic processes have produced the Fe-rich duricrusts by *in situ* weathering of mafic and ultramafic rocks, resulting in a relative accumulation of Fe. Secondly, Fe-rich duricrusts have been produced by absolute accumulation of Fe in valley floors, followed by relief inversion in response to drainage incision. Examples of the latter category are rare. These two mechanisms are now discussed.

#### *In situ weathering*

The general preservation of Fe-rich duricrusts over mafic (*e.g.* gabbro, basalt) and ultramafic rocks (*e.g.* talc-carbonate schist, peridotite) suggests that these duricrusts appear to be closely associated with the weathering of Fe-rich lithologies or lithologies with a high Fe:Al ratio. These duricrusts are formed by the intense infusion of Fe into saprock without forming a thick saprolite. Weathering of the Fe-rich mafic and ultramafic rocks has produced shallow profiles which consist of rock, saprock, ferruginous saprock, ferruginous saprolite and Fe-rich duricrust. These horizons tend to merge one with another. Deep clay-rich saprolites are not common beneath these duricrusts. Primary minerals weather into secondary products which in turn transformed into new products, amongst which hematite, goethite and maghemite are the most abundant. It appears that kaolinite, formed from the weathering of primary minerals, may have been replaced by Fe-oxides by epigenetic reactions suggested by Didier (1983).



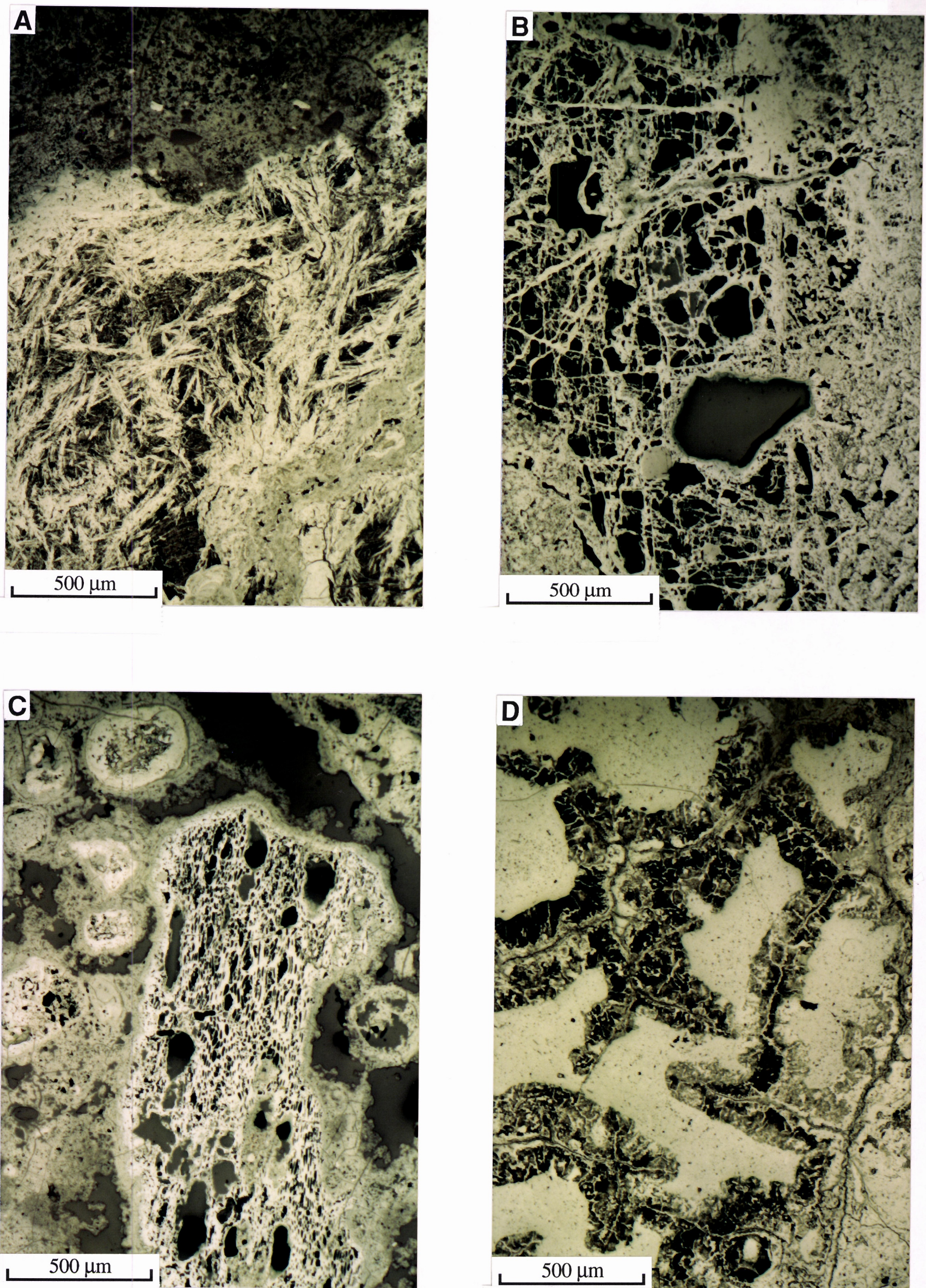


Fig. 3.9 Photomicrographs of polished sections of part of nodules in the Fe-rich nodular duricrusts in the Kalgoorlie region. (A) Hematite pseudomorphs after actinolite, (B) hematite pseudomorphs after olivine, (C) ferruginised wood fragments within a hematite-rich matrix and (D) ferruginised leaf (?) in a hematite-rich matrix.







**Table 3.1:** A comparison of the characteristics of Fe-rich duricrusts developed from gabbro and talc-carbonate schist. Arithmetic means are shown.

	Parent gabbro/basalt N=3	Fe-rich duricrusts developed from gabbro/basalt N=3	Parent talc-carbonate schist N=5	Fe-rich duricrusts developed from talc-carbonate schist N=5
SiO <sub>2</sub> %	47.9	4.9	53.9	7.8
Al <sub>2</sub> O <sub>3</sub> %	16.2	7.5	4.3	7.6
Fe <sub>2</sub> O <sub>3</sub> %	7.3	74.4	13.4	73.1
MgO%	8.86	0.11	16.90	0.14
CaO%	14.40	0.16	0.30	0.12
Na <sub>2</sub> O%	1.25	0.01	0.11	0.01
K <sub>2</sub> O%	0.09	-	-	-
TiO <sub>2</sub> %	0.48	4.22	0.27	2.01
LOI%	2.47	6.21	9.92	6.59
Mn ppm	983	339	330	411
Cr ppm	289	831	3370	18760
V ppm	178	2125	79	802
Cu ppm	76	42	26	25
Zn ppm	40	15	58	30
Ni ppm	136	48	2160	566
Co ppm	37	38	185	149
As ppm	6	12	10	16
Mo ppm	3	9	1	6

- below detection limit

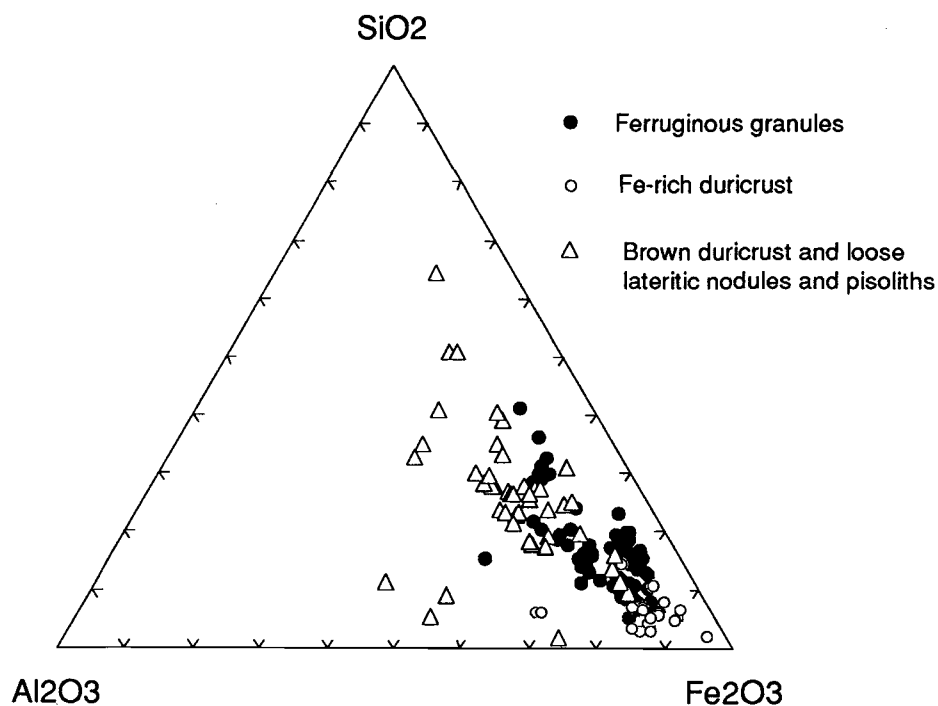


**Fig. 3.10** Triangular diagram showing compositions of ferruginous materials from the Kalgoorlie region, in terms of SiO<sub>2</sub>, Al<sub>2</sub>O<sub>3</sub> and Fe<sub>2</sub>O<sub>3</sub>.

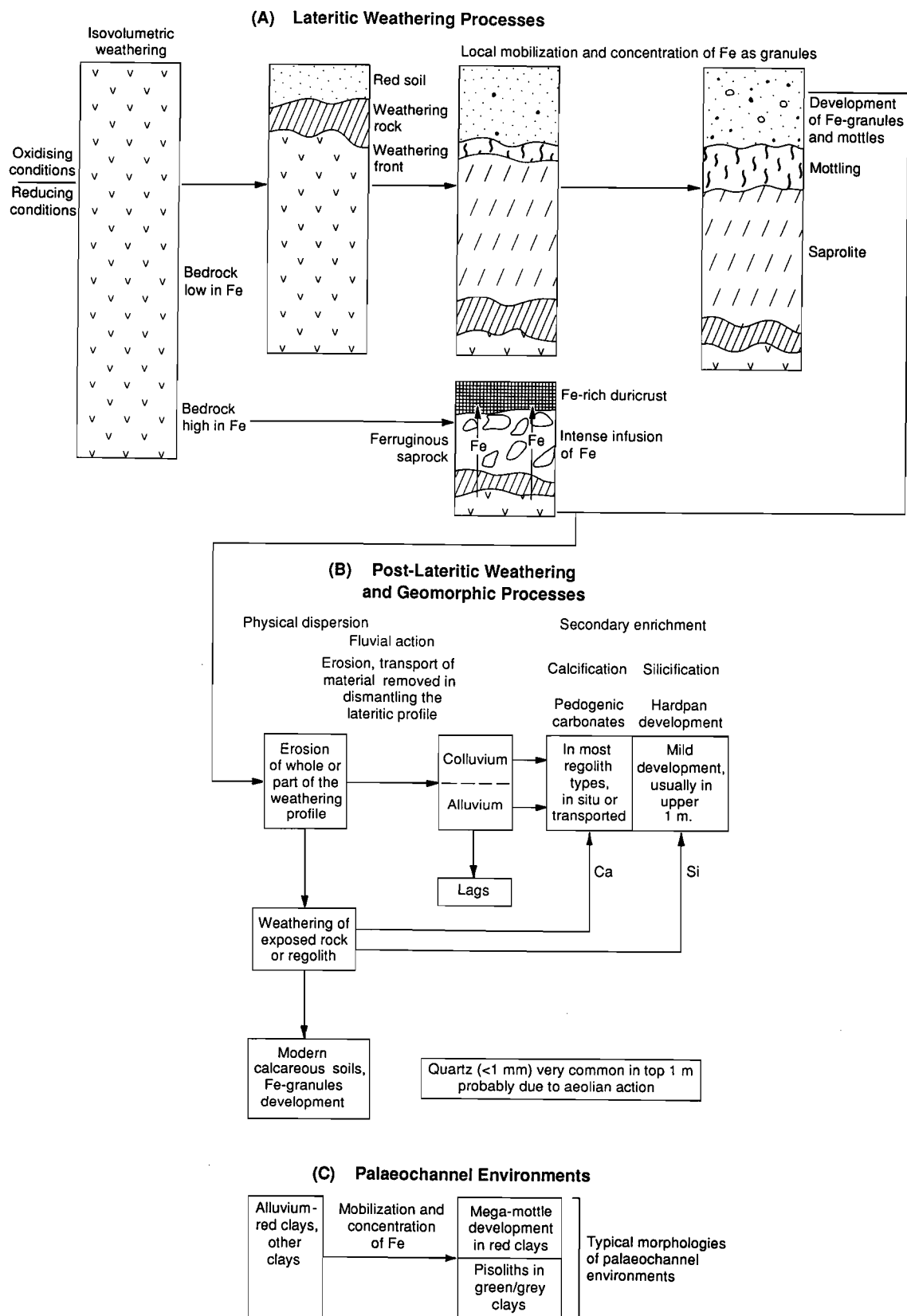


Fig. 3.11 Schematic diagram showing an inferred genetic relationship between the major regolith types in the Kalgoorlie region.

The geochemical data suggest that these Fe-rich duricrusts have a geochemical affinity with mafic and ultramafic bedrocks. The concentration of Cr, Co and Ni can be used to discriminate the duricrusts derived from the weathering of mafic and ultramafic rocks. Those rich in Cr, Ni and Co are derived from the weathering of ultramafic rocks, whereas those containing relatively-lower levels of these elements are likely to have a mafic origin.

#### Relief inversion

Field relationships and petrographic data of some duricrust samples (*e.g.* 2 km south of Ora Banda) suggest that duricrusts on low hills are remnants of what was once an ancient lower surface or depression, into which sediments accumulated. South of Ora Banda, 1 m thick Fe-rich duricrust has developed on surficial sediments which are underlain by lenses of coarse to fine pisoliths (Fig. 3.12). This is underlain by ferruginous saprolite and clay-rich horizon consisting of boulders of Fe-rich duricrusts and lenses of polymictic gravels. In some cases, the duricrust rests directly on fresh bedrock. The depressions are seen as favoured sites for the precipitation of Fe-oxides from groundwater. In this regard, these low hills and their duricrusts could be an expression of a complex series of erosional, aggradation, and weathering events (Anand *et al.*, 1991; and Butt *et al.*, 1992). Relief inversion may have occurred and duricrust covered depressions may have become hills and ridges. Examples of relief inversion have been provided in the literature, some including laterites which occur as long sinuous ridges and may have formed as valley laterites (Goudie, 1973; Ollier *et al.*, 1988).

Iron may have been derived by weathering processes from ancient upland positions and transported laterally to valley floors. The dissolved ferrous iron is subsequently precipitated and oxidised or oxidised and precipitated. In general, goethite and hematite form where oxidation precedes hydrolysis. When hydrolysis and precipitation occur before oxidation, lepidocrocite and maghemite may occur (Taylor and Schwertmann, 1974). These possible processes would result in the formation of Fe-rich duricrust. The valley floors, capped with Fe-rich duricrust, would be the most indurated, and thus the most resistant to erosion. The softer, upland and valley side materials would be more susceptible to erosion, leaving the former valleys as low ridges and hills.

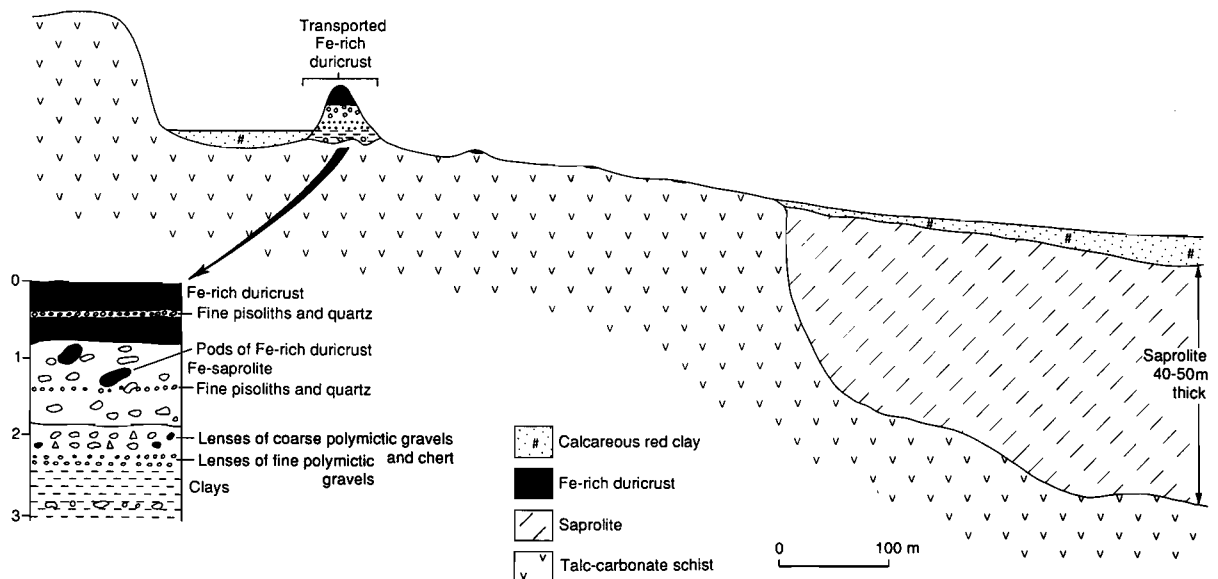


Fig. 3.12 The development of Fe-rich duricrust by absolute accumulation of Fe together with relief inversion (see explanation in text).

Anand *et al.* (1991) and Butt *et al.* (1992) suggested that pisoliths and nodules for certain of the Fe-rich duricrusts accumulated in local valley floors, possibly swampy drainages and ponds, during humid conditions, where they were cemented in place. With a subsequent climatic change to aridity, these materials hardened more than surrounding lateritic materials and erosion produced local landscape inversion. Similarities were noted with the Channel Iron Deposits (Ramanaidou *et al.*, 1991) of the Hamersley Province.

#### *Red soils and ferruginous granules*

Red soils are very common on the greenstones. Detailed investigations show that these red soils are derived from the weathering of underlying bedrock and may have even once completely blanketed the land surface.

The non-calcareous nature and very low level of smectite in these soils suggest that they have formed under generally mild to warm conditions, free drainage, and sub-humid to humid climates with alternating wet and dry periods. These are the conditions necessary for leaching of bases and the formation of kaolinitic clays that are acidic and unsaturated with bases. Some Fe released on weathering has been mobilised and segregated as granules and mottles. Granules which show the preservation of rock fabrics are formed by the ferruginisation of the saprolite or saprock.

#### *3.5.2 Post-lateritic weathering*

Figure 3.11 depicts the effects of post-lateritic weathering upon areas where erosion has removed the red soils or laterite. Whilst the underlying lithologies are best exposed in the erosional area, even the broad smooth crests and backslopes frequently show mild to strong stripping. The regolith types contain useful traces of underlying lithologies.

#### *Modern calcareous soils and carbonates*

After erosion, weathering of bedrock and saprolite continues to produce calcareous red clays. These soils are much more immature based upon the presence of fresh, primary minerals and recognisable pseudomorphs after primary minerals. Smectites in these soils are the product of the weathering of mafic and ultramafic lithologies during the arid climate in which they now occur. In arid climates, pedogenic processes, such as the loss of bases, are decreased due to reduced leaching.

Carbonates are generally redistributed into massive, nodular or laminar calcrete. Erosion and stripping of the upper, more weathered, parts of the regolith, appear to be important factors influencing the gross distribution of carbonates coupled with the distribution of mafic and ultramafic rocks. Weathering of mafic and ultramafic bedrocks provides Ca and Mg-rich solutions that infuse the upper parts of the regolith.

The carbonates in the depositional areas appear to be largely dependent on the occurrence of basement highs on mafic lithologies. These latter are associated with an irregular weathering front, protruding through the more weathered parts of the regolith. Upon weathering, these could be a source of Ca-rich solutions that would infuse the upper parts of the regolith. Alternatively, the carbonates may have been derived by lateral transportation and redeposition of weathered fragments of calcrete derived from the erosional areas which are then dissolved and precipitated at the top of the profile.

Calcareous clays contain varying amounts of fine quartz, particularly in top 1 m which appears to be aeolian in origin. This has been probably re-worked by colluvial processes and affected by chemical leaching and precipitation.

**Table 3.2** The implications in exploration listed against the research findings, Kalgoorlie region.

Research Findings	Implications in Exploration
<ul style="list-style-type: none"> <li>• Regolith-stratigraphic relationships were mapped on regional scale (1:250,000); erosional and depositional regimes are dominant. Residual regimes, comprising lateritic duricrust and lateritic nodules and pisoliths, are sporadically distributed. In the depositional areas, lateritic residuum is absent beneath the red clays but ferruginous granules are commonly developed in soils.</li> <li>• Hardpan is mildly developed in colluvium. Pedogenic carbonates are more abundant in the erosional regimes than in the depositional regimes.</li> <li>• Regional scale regolith-stratigraphic relationships were established.</li> <li>• Top 50 cm of soils may contain significant amounts of aeolian quartz.</li> <li>• The development of a mega-mottled zone and pisoliths in kaolinite-rich clays are typical features of palaeochannel environments.</li> </ul>	<ul style="list-style-type: none"> <li>- Appropriate exploration methods can be chosen according to regolith-landform mapping units or regime and regolith stratigraphy.</li> <li>- Ferruginous saprolite, ferruginous granules in soils, mottles in sediments and calcareous soils are alternative sample media in situations where lateritic residuum is absent, Section 9.</li> <li>- Establishes the framework for understanding dispersion models</li> <li>- Provides control for interpretation of Landsat TM for regolith mapping.</li> <li>- Avoid sampling top soil.</li> <li>- Presence of mega-mottles and pisoliths may aid in identifying palaeochannels in drill spoil.</li> </ul>



## 4.0 ORIENTATION STUDIES IN THE KALGOORLIE REGION

### 4.1 Introduction

The Kalgoorlie region was chosen because of the known mineral deposits it contains, the possibility of future major discoveries, and because of the complexities of regolith environments which pose considerable difficulties and challenges to exploration and research. The initial objective of the Kalgoorlie regional study was to establish a sound regolith-landform framework for research on geochemical dispersion. Regolith-landform units were mapped, the regolith stratigraphy established, and the regolith units characterised petrographically, mineralogically and geochemically. These findings were then synthesised at district and regional scales to form the basis for interpreting geochemical data.

Three orientation districts (Kanowna, Ora Banda - Matt Dam, Wombola) were selected for detailed regolith-stratigraphic and geochemical studies (Fig. 4.1). These districts were chosen as they represent examples of geological-geomorphological-regolith associations that are common in the Kalgoorlie region. In each case, geochemical dispersion from concealed Au deposits has been studied by understanding the regolith-stratigraphic relationships both near the ore deposits and distant from them. This information led to the development of regolith-landform dispersion models.

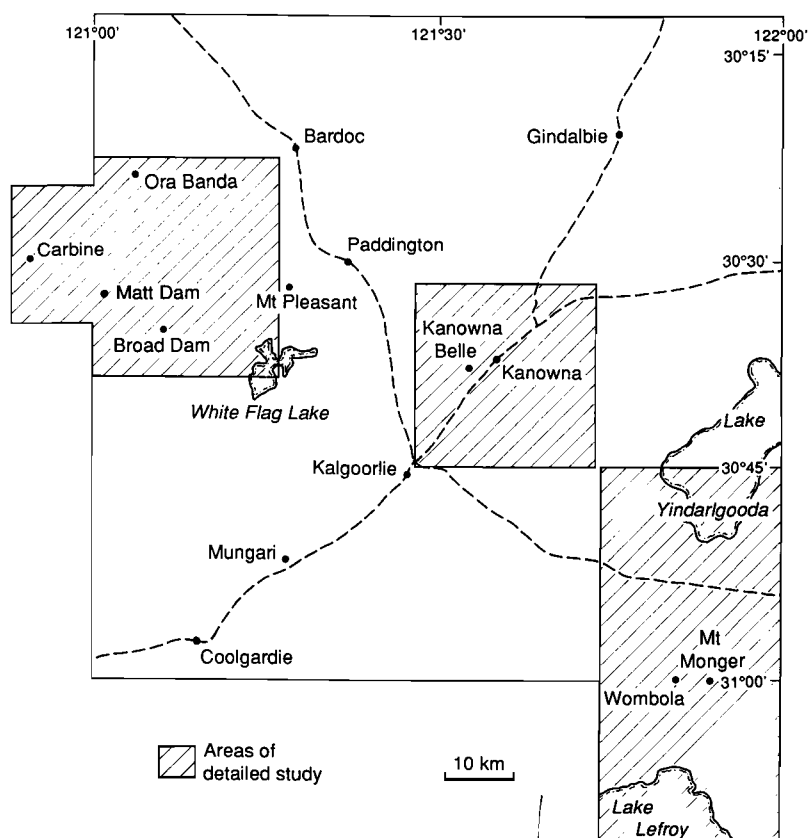


Fig. 4.1 Map showing the borders of the Kalgoorlie regional study and the component orientation districts within it.

## 4.2 Ora Banda district (including the Matt Dam prospect)

### 4.2.1 The Ora Banda district

#### Location

The Ora Banda district is centred 50 km northwest of Kalgoorlie. It has an area of 1,100 km<sup>2</sup> and spans parts of the Bardoc, Kalgoorlie, Davyhurst and Dunnsville 1:100,000 map sheets.

#### Regional and local geology

The Ora Banda district comprises dominantly mafic and ultramafic rocks, separated by a parallel, thin belt of felsic to intermediate volcaniclastic sedimentary rocks, conglomerate and sandstone. Intrusions of granitoid are found mainly in the northwestern part of the district.

The Ora Banda Au lodes are located in basalts of the Kalgoorlie greenstone belt. The Siberia Komatiite which is the oldest in the sequence, is a succession of ultramafic flows and serpentinites capped by high Mg basalts (Fig. 4.2). A thin sequence of siltstone, shale and quartz porphyry separates these basalts from the overlying tholeiites, which host the Ora Banda Au deposits (Harrison *et al.*, 1990). The greenstone sequence has undergone regional deformation and metamorphism, resulting in widespread modification and obliteration of primary igneous and depositional textures (Swager, 1990). The felsic volcaniclastic rocks are mainly fine- to medium-grained felsic fragmental rocks and schists and are deeply weathered. Exposure is poor. The sedimentary rocks are mainly quartz-rich siltstone, sandstone and polymictic conglomerate, containing ellipsoidal clasts of granitoid, banded iron-formations and greenstone lithologies.

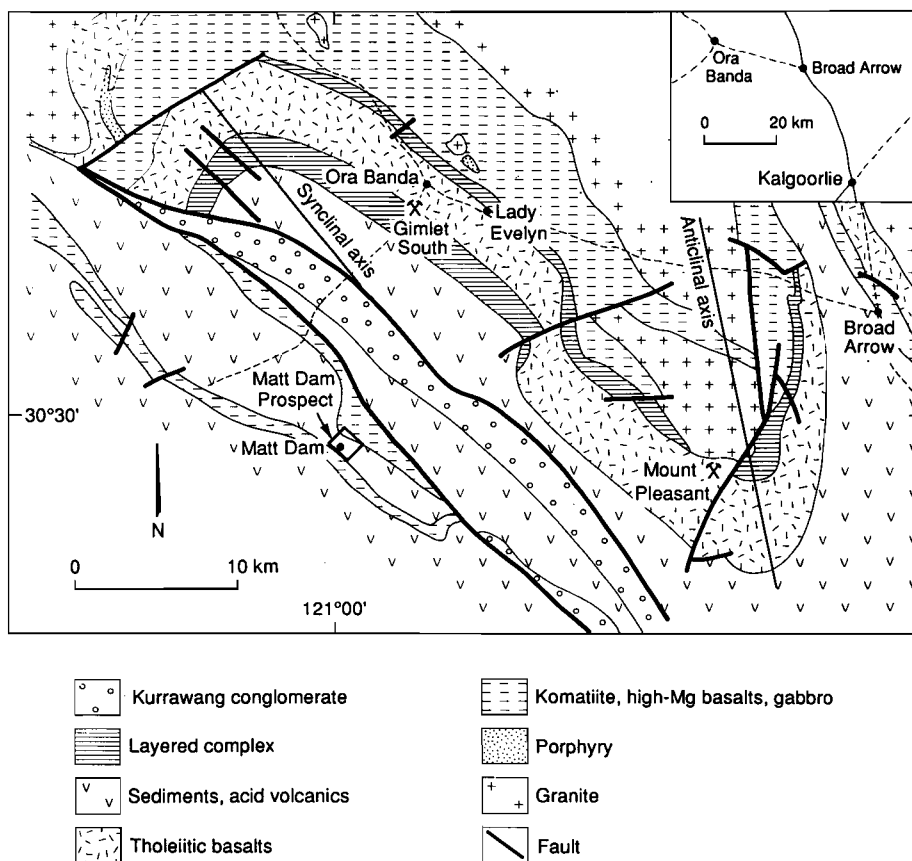


Fig. 4.2 Regional geology of the Ora Banda district (after Harrison *et al.*, 1990).



### *Geomorphology and drainage*

The Ora Banda district lies mostly between 360 m and 440 m above sea level (see Fig. 3.2). It is gently undulating and is punctuated by low hills and ridges of mafic rocks. In the north, the area is dissected by many channels and the general drainage trends northwest towards salt lakes such as Lake Owen and Lake Goongarrie. South of the Ora Banda - Broad Arrow road, drainage flows south towards other salt lake systems.

#### *4.2.2 Regolith-stratigraphic relationships*

##### *Regolith distribution*

The surface distribution of regolith-landform units for the Ora Banda district is shown in Appendix VI. This map was produced in collaboration with GSWA (J.R. Gozzard). The map was produced by interpretation of 1:50,000 aerial photographs substantiated by ground traverses. The air photo patterns are largely related to gross changes in vegetation, soil type and local relief along with some features of rock and regolith outcrop. Detailed observations were made at a number of type locations, identified during reconnaissance. This resulted in detailed regolith-stratigraphic relationships for the north part of the Ora Banda and Cawse Find - Lady Evelyn areas (Figs. 4.3 and 4.4).

Using the terms residual, erosional and deposition regimes, after Anand *et al.*, (1989), the Ora Banda district is mantled by about 10% of residual regime. This regime is characterised by a lateritic duricrust 1-2 m thick overlying, in places, ferruginous saprolite or saprock and is sporadically distributed over the district. The lateritic duricrusts are found on crests and are closely associated with breakaways.

The erosional regime, which covers about 30% of the area, is shown as erosional mapping units E1, E3, E6, E7 and E8. Unit E1 is closely associated with the residual regime in that the fragments of duricrust and nodules, resulting from the dismantling of the lateritic duricrust, and ferruginous saprolite are scattered over the surface, especially along backslopes. There has been a mechanical sorting of the lateritic fragments, with the finer lag at the base of the slope. Unit E3 comprises breakaway scarps and pediments. The breakaway scarp exposes the lateritic profile, usually a mantle of lateritic duricrust overlying ferruginous saprolite or saprock. The lateritic debris from this breakaway is deposited as colluvium on the pediments. The transition between the pediment and the backing scarp is generally abrupt, due to the escarpment being capped by resistant lateritic duricrust. At the pediment, the soils are thicker, hardpanised just below the surface and enriched with Si, Mn and carbonates. Underlying this is bedrock. Units E6-E8 characterise mafic and ultramafic outcrops, with E6 comprising exposed bedrocks of low hills, E7 for exposed ferruginous bedrock and E8 outcrops related to high hills.

The depositional regime covers about 60% of the district, with mapping unit D4 dominant. Unit D4 forms gently sloping alluvial floors, with a lag of fine, ferruginous granules. The soils tend to be richer in clay loam and have carbonate coatings. Other minor depositional units include sheetwash colluvium (Unit D2), colluvium/alluvium on gently sloping plains (Unit D3), broad alluvial floors (Unit D5), saline clays and muds in playas (Unit D6) and calcareous sand dunes associated with swales (Unit D8).

##### *Traverses at North Ora Banda (mafic bedrock) and Cawse Find (ultramafic bedrock)*

Two traverses were selected to compare the regolith characteristics developed from mafic and ultramafic bedrocks (shown on Figs 4.3, 4.4). One transect measuring 1 km in length, is situated north of Ora Banda across mafic gabbro. The other is of 850 m length over the ultramafics at Cawse Find - Lady Evelyn. Changes in regolith stratigraphy and soil types along the traverses are shown in Figs 4.5 and 4.6 and are discussed below.

Over the mafic gabbro lithology, the residual regime is characterised by about 2 m of lateritic duricrust overlying ferruginous saprolite. A thin (5-15 cm) layer of gravelly, dark red, clay loam soil with a lag of lateritic nodules and pisoliths and ferruginous saprolite fragments, mantle the residual regime.

In the erosional regimes, the high hills, flanked by steep slopes, rise above the relics of lateritised surface and expose fresh bedrock. Some shallow soils occur. The soil profile consists of a horizon of 10-20 cm of acid red clay sandwiching about 20 cm of calcareous red clay with the saprock. On steeper slopes, scattered outcrops and cobbles of saprock on the upper slopes outcrop through a shallow, stony, sandy clay loam with powdery to nodular carbonates. The soils are immature, with similar mineralogical and geochemical characteristics to the bedrock. These soils contain weathered rock fragments and pedogenic calcite released by the weathering of calcic plagioclase of the gabbro.

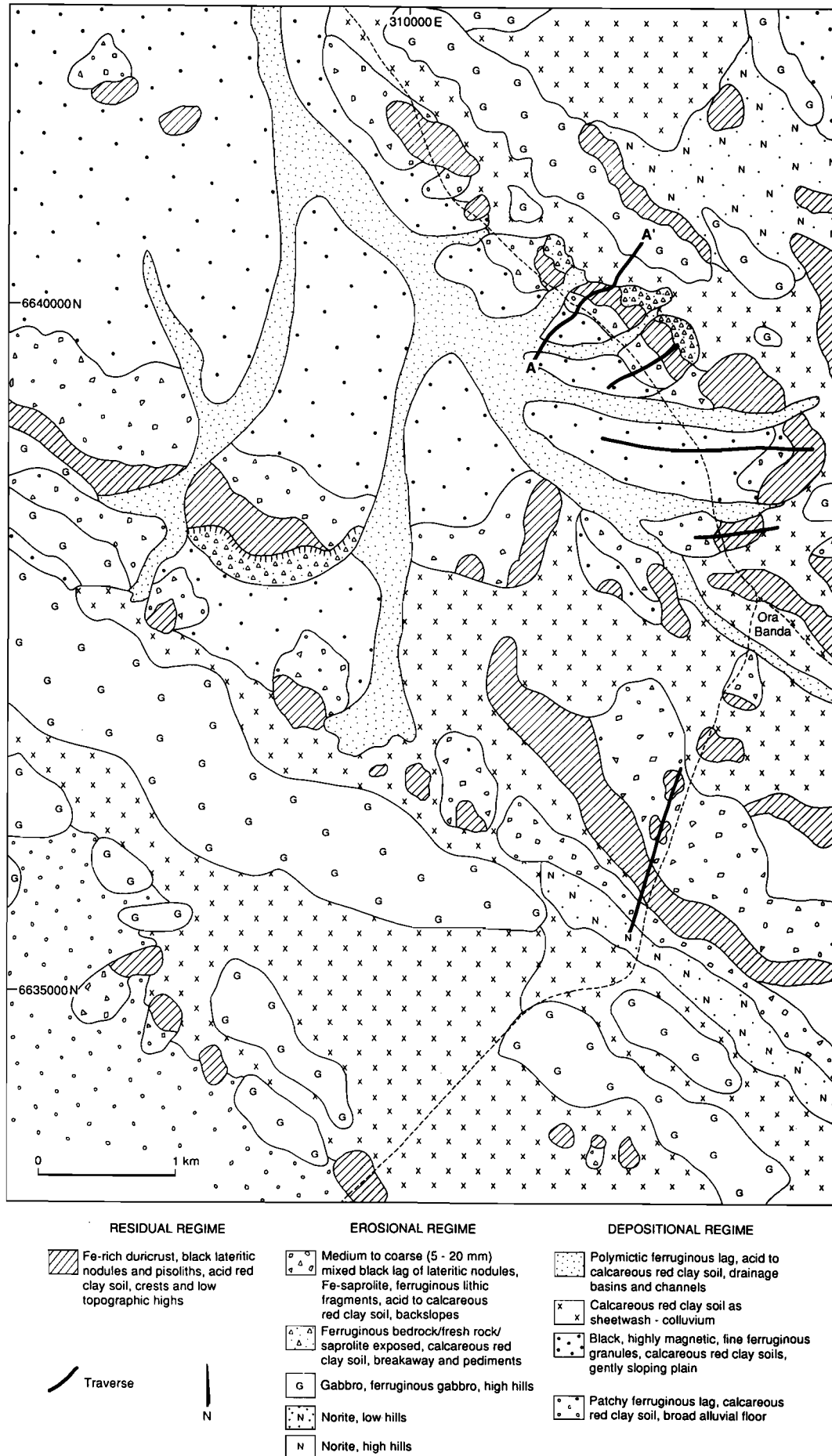


Fig. 4.3 Detailed map of the regolith in part of the Ora Banda district.

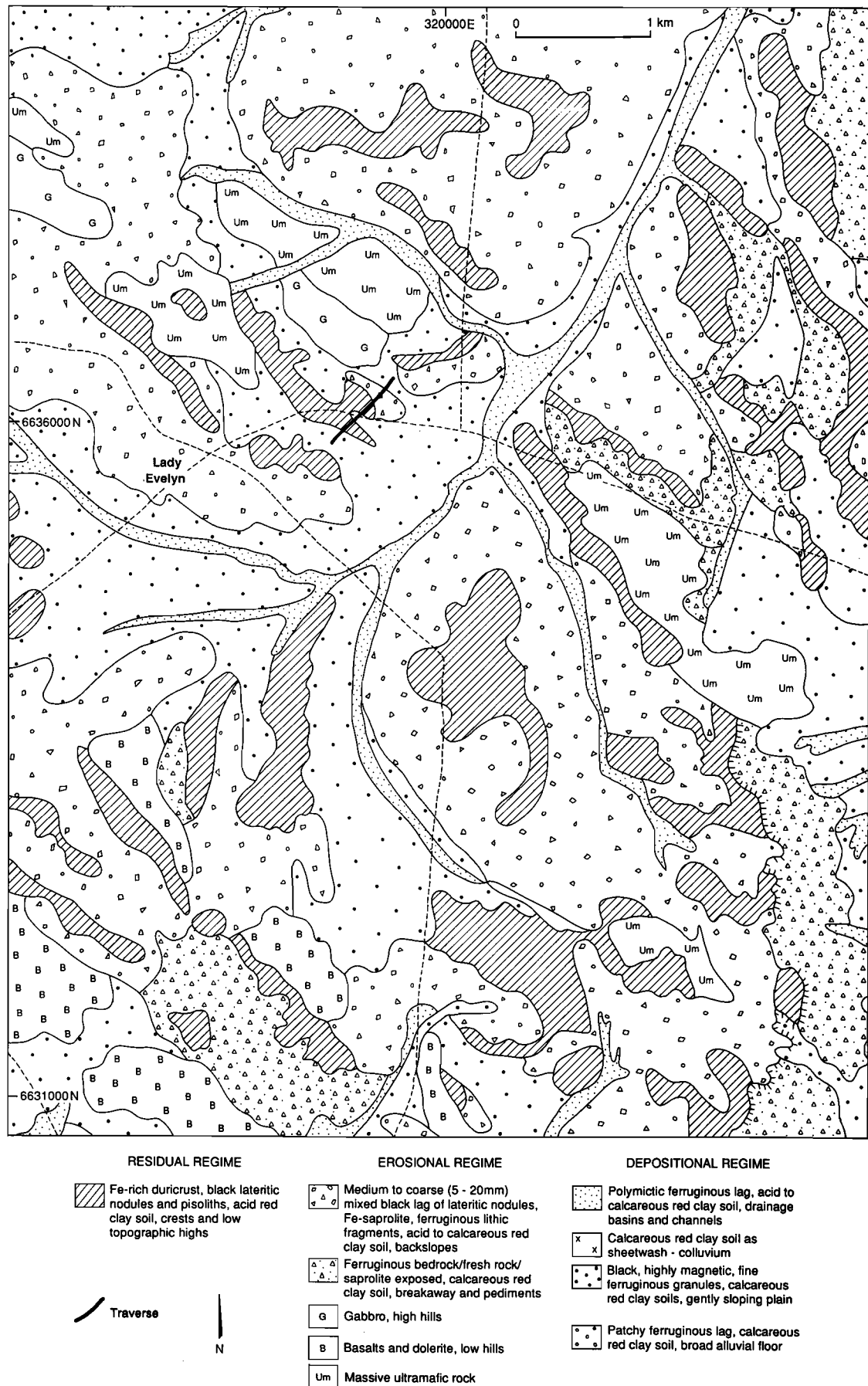


Fig. 4.4 Detailed map of the regolith in the Cawse Find - Lady Evelyn area, Ora Banda district.

In the depositional regime, particularly along long gentle slopes, the soil is a dark gravelly red sandy loam 20-30 cm thick overlying 1 m of weakly developed hardpanised colluvium, with silica cementation and Mn staining. This hardpan in turn overlies 2-3 m of acid red clay over saprolite. In areas near to valleys, smectitic clay is dominant.

Where the bedrock is ultramafic, the residual regime has a nodular duricrust about 1 m thick, overlying saprock or bedrock. There is a sharp contact between the duricrust and the underlying bedrock. However, there appears to be no sedimentary structures in the duricrust horizon to suggest a transported unit. This duricrust contains subrounded and subangular, hematite-rich nodules in a very small quantity of matrix. A thin cover of acid, dark reddish brown sandy loam, about 15 cm deep, with strong development of brown nodules, mantles the duricrust.

The backslopes that trend down from the crests are mantled with a lag of lateritic nodules and ferruginous saprolite fragments. The lag was derived from the breakdown of lateritic duricrust upslope. The backslopes (mid and lower slopes) are highly stripped as is indicated by a shallow soil (20 cm) directly underlain by bedrock. Talc and kaolinite are the dominant clay minerals, with some amphibole. The saprock beneath the soil consists mainly of smectite, talc, kaolinite and some amphibole.

At the pediment, the soil is thicker and is underlain by about 50 cm of hardpanised colluvium containing Mn, Si and carbonates. Beneath the hardpanised colluvium is saprock. The depositional regime is depicted by a lag of black ferruginous granules, pebbles and hard, brown nodules. Dark, reddish-brown, sandy, clay loam overlies the hardpanised soils containing Mn, Si, smectite and some talc.

#### *Geochemistry*

Tables 4.1 and 4.2 compare the chemical compositions of regoliths developed over the two lithologies. The geochemical data of the two types of weathered and altered bedrock show the gabbro has greater  $\text{Al}_2\text{O}_3$ , CaO,  $\text{Na}_2\text{O}$ ,  $\text{K}_2\text{O}$ , Mn, V, Cu, and Ga contents compared to the talc schist. The weathered gabbro contains calcium-bearing minerals, plagioclase feldspar and amphibolitised pyroxene. The higher  $\text{Al}_2\text{O}_3$  content is attributed to the feldspars and there is possibly some substitution of Al with the Ga. The talc schist of the ultramafics contains talc and serpentine (Mg-bearing minerals). It is relatively richer in Fe, Mg, Cr, Ni, Co and Ba compared with the gabbro. The geochemical composition of the regolith reflects the underlying lithology. The primary difference between these two lithologies, based on the geochemical signature of the regolith, is in Cr and Ni, with higher values indicating ultramafics.

The soils developed over the bedrock show relatively higher Ca and Mg. For very immature soils, where there is constant movement of weathered products downslope as alluvium or colluvium, these soils tend to closely resemble the bedrock in mineralogy and geochemistry as they contain more weathered lithic fragments. Over the gabbro, the soil developed over bedrock is highly calcareous. Conversely, soil over the ultramafic shows high magnesium, reflecting that of Mg-rich bedrock.

The soil developed over colluvium is primarily controlled by the combination of the colluvium and its topographic position. The colluvium can be either the weathering products of lateritic duricrust or rock outcrop, or a mixture of both. In general, the soil developed over colluvium tends to have higher Si and Mn associated with hardpanisation. An upper value of 1070 ppm Mn in the ultramafics comes from soils developed in pediments.

In both lithologies, mobilisation of the Fe from the weathered rocks supplies Fe-oxides in the lateritic residuum and concentrates Cr, V, and Cu in this residuum.

## NORTH OF ORA BANDA TRAVERSE

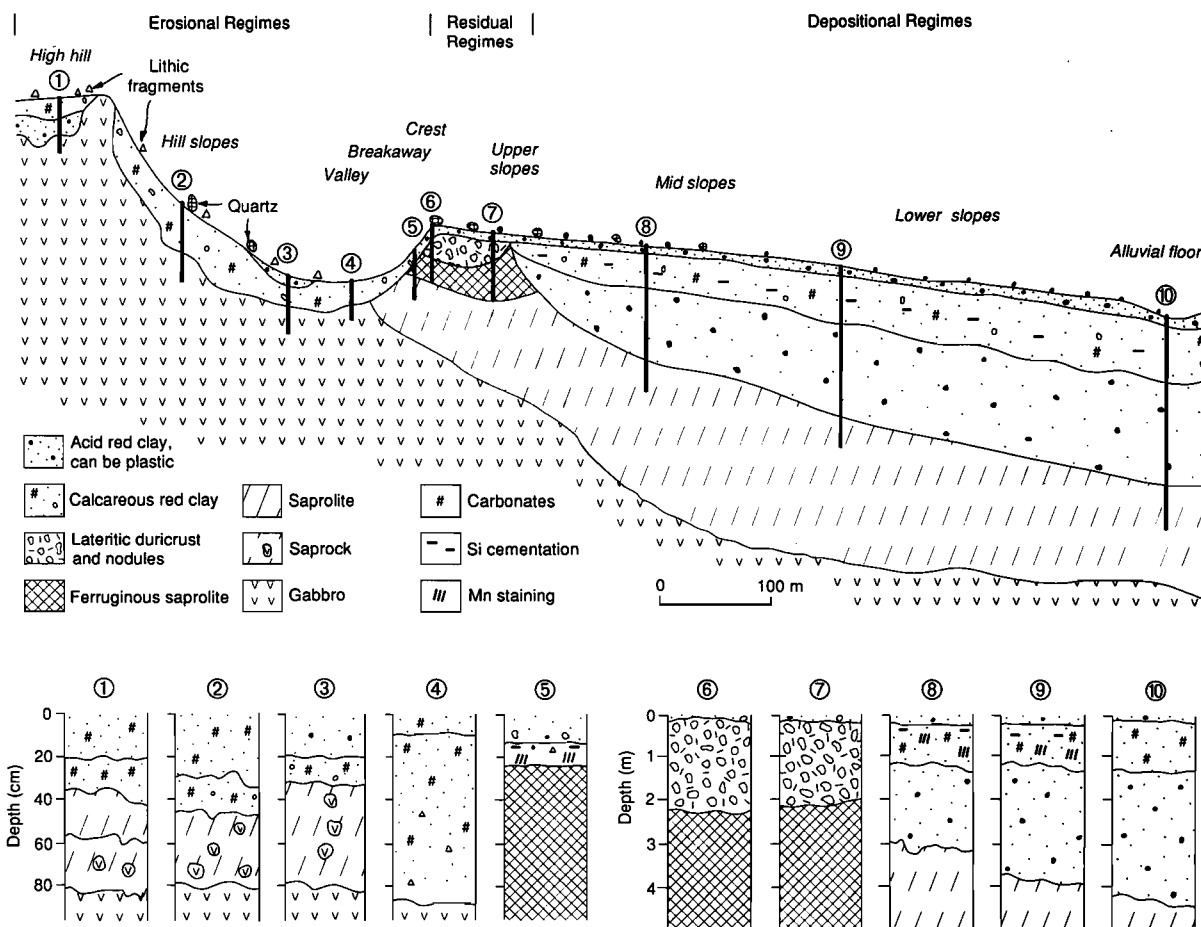


Fig. 4.5 Schematic representation of the regolith stratigraphy and landforms over mafic bedrock, Ora Banda district.

## CAWSE FIND - LADY EVELYN TRAVERSE

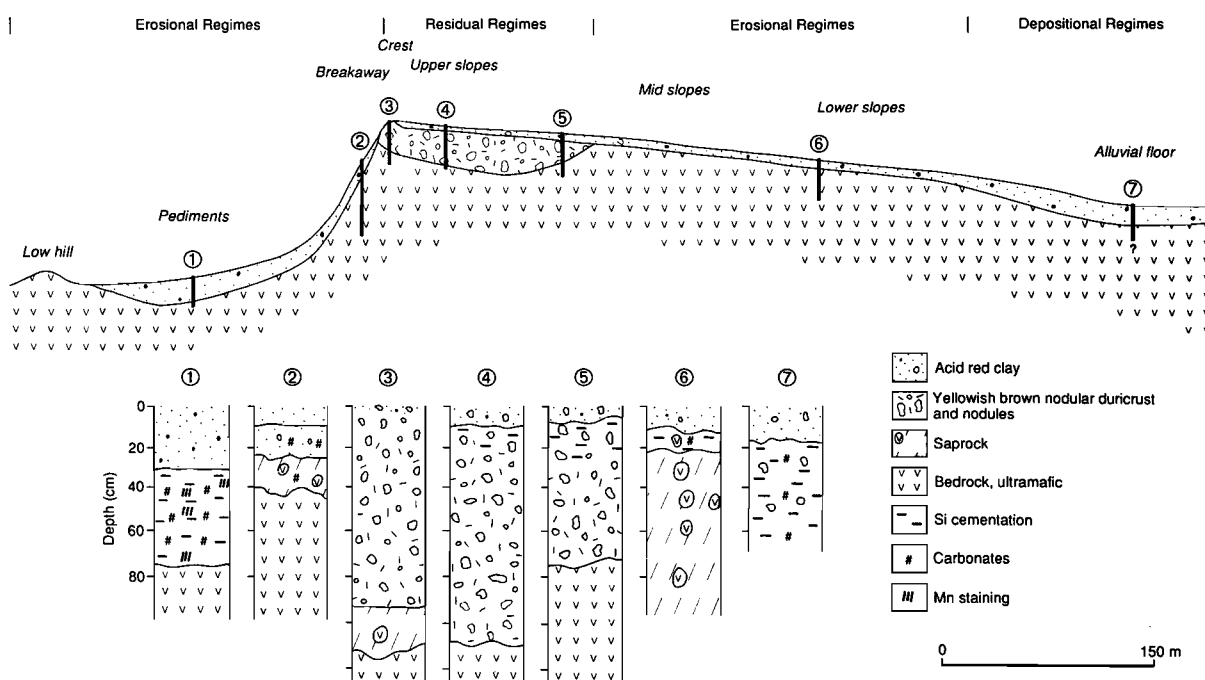


Fig. 4.6 Schematic representation of the regolith stratigraphy and landforms over ultramafic bedrock, Ora Banda district.

Table 4.1 Regolith characteristics over mafic bedrock (gabbro).

Range of values are shown.

ELEMENT	Gabbro n=2	Soils on bedrock n=3	Soils on colluvium n=2	Soils on laterite n=2	Laterite n=2
SiO <sub>2</sub> %	47.7-47.8	42.6-57.0	54.7-59.3	57.5-59.0	19.9-20.3
Al <sub>2</sub> O <sub>3</sub> %	15.4-17.7	8.5-12.3	11.7	12.2-13.9	17.6-18.7
Fe <sub>2</sub> O <sub>3</sub> %	6.8-7.2	4.6-9.1	19.9-24.1	15.6-18.6	46.9-50.4
MgO %	8.4-9.8	3.4-5.8	0.4	0.5	0.04-0.09
CaO %	14.3-14.4	3.6-15.3	0.25	0.3-0.5	0.05-0.06
Na <sub>2</sub> O %	1.08-1.17	0.31-0.81	0.45	0.46	0.01-0.02
K <sub>2</sub> O %	0.26-0.3	0.59-1.23	0.18	0.19	<0.05
TiO <sub>2</sub> %	0.51-.59	0.39-0.95	1.04-1.14	1	1.20-1.92
LOI %	2.6	11.5-20.2	6.3	6.6-8.6	9.8-13.3
Mn ppm	949-995	297-780	356-410	285-422	74-113
Cr ppm	108-307	330-572	901-910	810-993	810-1280
V ppm	184-185	126-184	389-515	257-332	838-840
Cu ppm	70-124	60-92	38	36-48	149-328
Pb ppm	<5	5-6	12	11-16	7-14
Zn ppm	40	29-61	38	36-40	80-100
Ni ppm	123-170	91-126	112	111-122	39-133
Co ppm	36	22-34	19-22	19-22	7-8
As ppm	5-6	5-8	6-15	5-12	13-184
Sb ppm	<2	<2	<2	<2	<2
Bi ppm	<2	<2	<2	<2	<2
Mo ppm	<2	<2	<2	3	<2
Ag ppm	0.23	0.21-0.40	0.47-0.52	0.45-0.53	0.57-0.61
Sn ppm	<2	2	2-4	2	2-4
Ge ppm	<2	<2	<2	<2	2-3
Ga ppm	12	9-15	21	21-23	32
W ppm	<3	8-268	6-16	6	3-5
Ba ppm	56-75	89-169	119-179	129-143	14-29
Zr ppm	10-15	74-108	149-220	206-229	60-131
Nb ppm	<3	3-5	8-11	6-10	3
Se ppm	<3	<3	3	<3	4-8
Be ppm	<1	1-3	1-2	1	1
Au ppb	5-20	10-26	14-36	55-140	750-4760

Table 4.2 Regolith characteristics over ultramafic bedrock (talc schist).  
Range of values are shown.

ELEMENT	Talc schist n=1	Soils on bedrock n=2	Soils on colluvium n=2	Soils on laterite n=3	Laterite n=2
SiO <sub>2</sub> %	52.9	46.2-52.7	45.6-62.0	48.6-51.3	15.2-15.6
Al <sub>2</sub> O <sub>3</sub> %	6.4	8.4-11.4	9.0-14.3	11.2-18.8	17.6-18.0
Fe <sub>2</sub> O <sub>3</sub> %	10.2	13.2-23.6	10.1-25.0	18.8-28.1	51.2-53.5
MgO %	17.6	1.1-15	1.4-6.5	0.4-0.8	0.1
CaO %	0.4	0.4-1.3	0.4-0.9	0.2-0.6	0.1
Na <sub>2</sub> O %	0.1	0.27-0.39	0.55-0.65	0.35-0.43	0.02
K <sub>2</sub> O %	<0.05	0.16-0.47	0.17-0.48	0.11-0.16	<0.05
TiO <sub>2</sub> %	0.4	0.3-1.0	0.5-0.9	0.7-1.2	0.6
LOI %	11.1	8.7-14.8	9.4-14.1	8.4-12.0	11.7-14.8
Mn ppm	171	265-427	384-1070	247-423	181-210
Cr ppm	2590	2600-5130	1750-4280	3180-4540	5480-5870
V ppm	82	153-352	127-382	268-440	360-374
Cu ppm	25	38-90	41-56	36-68	80-87
Pb ppm	<5	<5	5-14	7-12	<5
Zn ppm	51	41-52	42-50	27-41	26-30
Ni ppm	1740	604-1190	642-765	341-699	650-672
Co ppm	103	53-98	49-69	30-58	43-47
As ppm	7	5-12	5-8	4-14	9-19
Sb ppm	<2	<2	<2	<2	<2
Bi ppm	<2	<2	<2	<2	<2
Mo ppm	<2	<2	<2	<2	<2
Ag ppm	0.38	0.13-0.29	0.24-0.39	0.29-0.52	0.57-0.72
Sn ppm	<2	<2	2-5	<2-3	<2
Ge ppm	1	<2	<2	<2	<2
Ga ppm	6	11-17	11-25	17-27	13-16
W ppm	<3	3-4	3-4	<3-5	<3
Ba ppm	188	78-138	104-144	100-121	20-22
Zr ppm	8	39-176	111-152	140-173	66-68
Nb ppm	<3	3-8	5-8	5-7	<3
Se ppm	2	<2-3	<2	<2-3	4
Be ppm	<1	<1	<1	<1	1
Au ppb	2	4-23	3-11	4-45	9-14

### 4.2.3 Matt Dam prospect

#### Location and geology

Matt Dam is a Au prospect held by Newcrest, 15 km west-south west of Ora Banda and 4 km from the Au operations at Zuleika (see Fig. 4.2). The regional geology of the area has been described by Harrison *et al.*, 1990. Primary mineralisation is hosted by northwest trending high magnesium basalts and komatiites with bands of intermediate to felsic tuffs and sediments (Fig. 4.7). Structural complexity is indicated by interlayering of sediments, shales and ultramafics within the tuffaceous zone (see Figs 4.12-4.18). Minor old workings, indicated by shallow pits, dry blowings and a shaft are found in the area.

#### Previous work

Gold mineralisation was found by Newcrest during a RAB drilling program on a grid of 200 m by 80 m. Five metre bottom-of-hole composite samples were analysed for Au and As. This was followed up with a soil survey using one metre auger holes on a 200 m by 50 m grid. This survey outlined a 3 km-wide northwest trending anomaly of over 30 ppb Au.

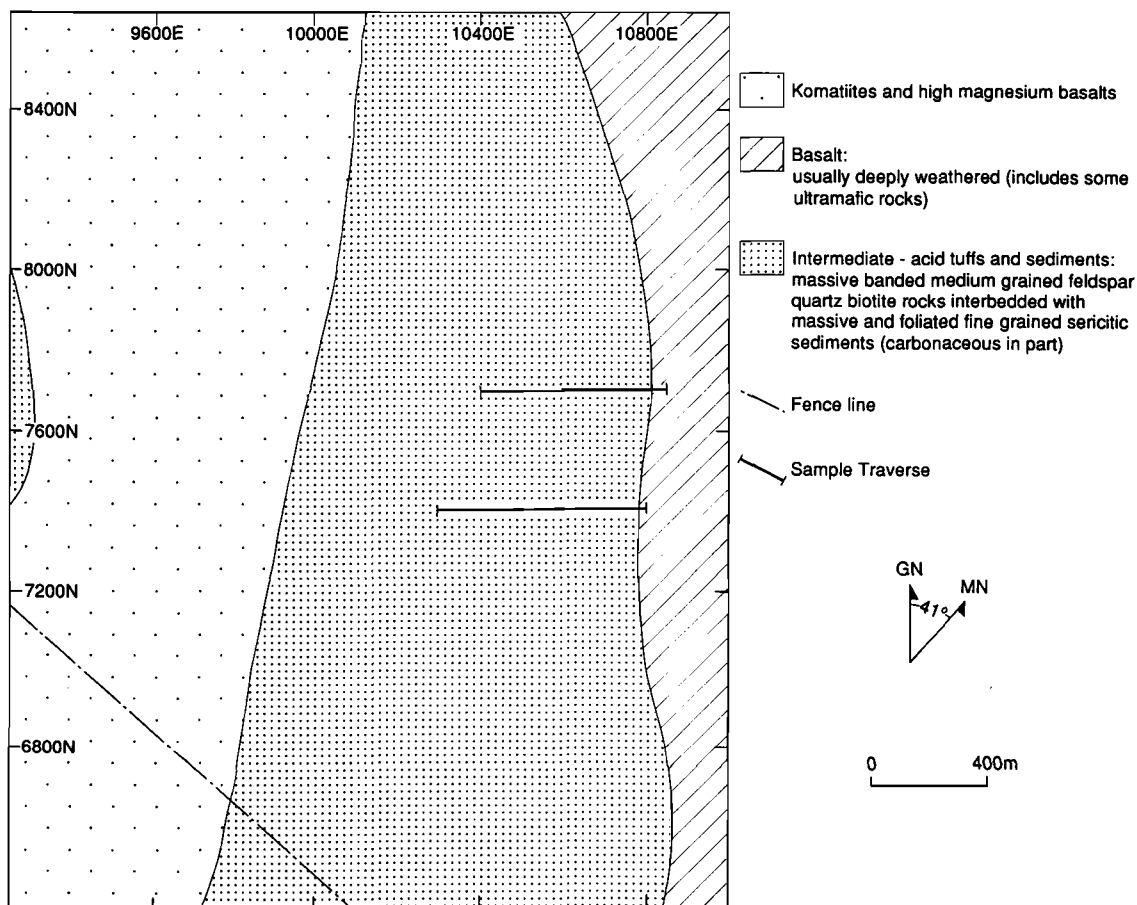
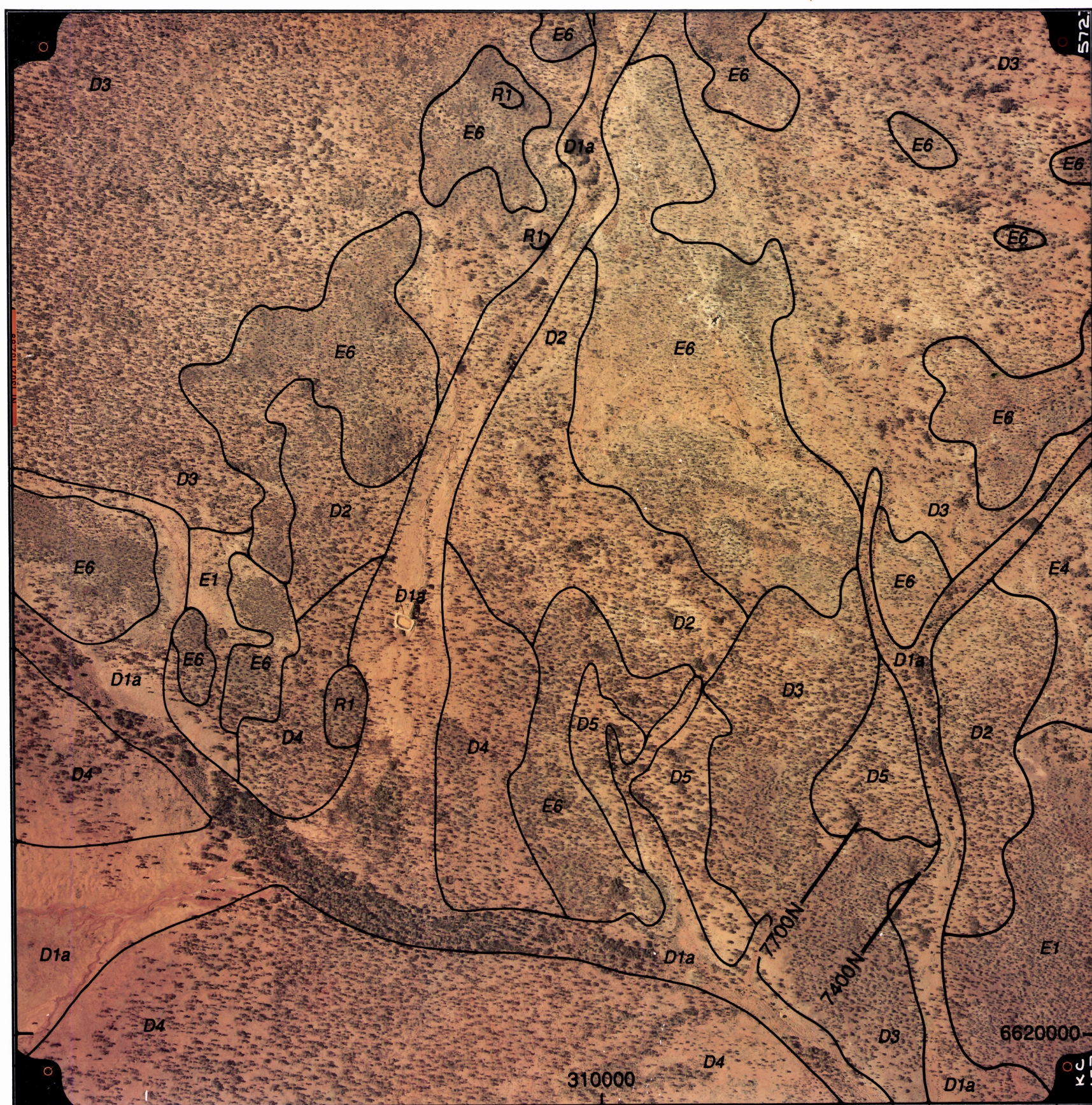


Fig. 4.7 Detailed bedrock geology in the Matt Dam area, Ora Banda district.



**RESIDUAL REGIME**

- R1 Lateritic duricrusts, lateritic pisoliths and nodules-crests and low topographic highs

**EROSIONAL REGIME**

- E1 Fragments of ferruginous saprolite and ferruginous lithic fragments - backslopes  
 E4 Saprolite, black ferruginous granules and quartz - erosional plains  
 E6 Bedrock-low hills

**DEPOSITIONAL REGIME**

- D1a Acid red clay soil with polymictic ferruginous lag within major drainage basins and channels  
 D2 Calcareous soils as sheetwash - colluvium  
 D3 Black, ferruginous granules, non-calcareous red clays at surface, carbonates at 10-20 cm - gently sloping plain  
 D4 Black, ferruginous granules, acid to calcareous red clay soils, colluvium/alluvium - gently sloping alluvial floor  
 D5 Acid to calcareous soils - broad alluvial floor

— Traverse

N

0 1 km

Approximate scale due to distortion from aerial photography

Fig. 4.8 Map showing the surface distribution of regolith-landform units and vegetation as an overlay to the colour air photograph, Matt Dam prospect, Ora Banda district (Kevron Aerial Surveys, photo 8/5723, 9.3.82) published with permission of Centaur Mining & Exploration Ltd.





#### 4.2.4 Objectives

The objective of the Matt Dam study was a concise orientation geochemical dispersion study over the prospect, which was concealed by transported cover. This was to be done by developing a stratigraphic model of the regolith and integrating it with a multi-element geochemical program.

Specific objectives:-

1. To map the distribution of regolith materials at surface and in drill spoil to produce a regolith-stratigraphic model for the area.
2. To analyse the size distributions of various regolith units and relate them to the regolith-landform settings.
3. To delineate the multi-element dispersion patterns along two sampled lines over the Matt Dam prospect.
4. To define the most appropriate sampling media and methods for geochemical exploration in the Matt Dam regolith environments.

#### 4.2.5 Regolith-stratigraphic relationships

##### *Regolith distribution*

The surface distribution of regolith units in the Matt Dam area is shown in Fig. 4.8, as an overlay to a colour airphoto. The Matt Dam prospect, and its immediate surroundings, are characterised by a broadly undulating, variably truncated lateritic, terrain dominated by both saprolitic to fresh bedrock and broad colluvial and alluvial plains. Residual regimes, containing lateritic duricrust and lateritic pisoliths and nodules, are sporadically distributed within the study area and are restricted to gentle topographic highs, which occupy less than 5% of the area. The erosional regimes are dominated by shallow, residual, calcareous soil and a lag of Fe-saprolite and Fe-lithic fragments with outcrops of bedrock and saprolite. The depositional regimes are mantled by a friable, acid to calcareous, red, sandy, clay soil with abundant lag of black ferruginous granules. These regolith relationships are similar to those observed in other parts of the Kalgoorlie region.

##### *Regolith stratigraphy-Matt Dam Prospect (Lines 7400 mN and 7700 mN)*

The Matt Dam prospect is located partly within a depositional and partly within an erosional regime. The regolith stratigraphy was established from RAB drill spoil and is shown for the two lines which were studied (Fig. 4.9). In erosional regimes, the surface is mantled by a coarse, irregular, yellowish brown to reddish brown, residual lag of ferruginous saprolite (Fig. 4.10A). The pale, orange, calcareous, sandy, clay soils form a 0 to 50 cm thick mantle, containing ferruginous saprolite fragments. The carbonates occur as coatings on, and as nodules within, the clay (Fig. 4.10B). The calcrete nodules are composed of irregular, pinkish nodules, varying from 1 to 5 cm in diameter which show evidence of having partially- to completely replaced ferruginous saprolite fragments and hardened mottles (Fig. 4.10C). A zone of saprolite occurs at depths generally greater than 0.5 m.

A black lag of ferruginous granules mantles the depositional regimes (Fig. 4.10D,E). Fragments comprising this lag are generally less than 10 mm in diameter and range from subrounded to irregular; the more platy fragments are generally lithic. In the depositional regimes, calcareous soils are up to 1 m thick and contain varying amounts of carbonate nodules and ferruginous granules. The carbonate nodules vary between dense, homogeneous calcrete and a thin calcareous coating on soil fragments containing ferruginous granules. The ferruginous granules at the boundary of the red soils and the calcareous soils are commonly coated with a thin carbonate skin.

This stratigraphy of regolith units along line 7400 mN indicates a channel approximately 16 m deep centred over 10450 mE with a white, kaolinite-rich, bleached clay zone extending to 25 m under the channel (Fig. 4.9). The channel is infilled with clays that have been weathered since deposition. The transported regolith consists of calcareous clays, acid red clays and smectite-rich puggy grey clays with coarse, hardened mottles and fine, ferruginous granules. Mottles and ferruginous granules are developed in the sediments. Towards the surface, the mottles decrease and the granules become more abundant. Underlying this unit is a residual, white, bleached clay zone, which merges at depth with saprolite. The saprolite forms a broad zone, 30 to 50 m thick.

The stratigraphy of line 7700 mN is more complex. It has several zones of transported clays with a mottled zone dipping into the residual saprolite (Fig. 4.9). This reflects underlying interbedded tuffs, dolerites, ultramafics and shales which dip near vertically to the east. Zones of white, bleached, clays are again evident under transported clays containing hardened mottles. There is a lag of fine, ferruginous granules over the traverse except from 10450 to 10500 mN where it is missing.

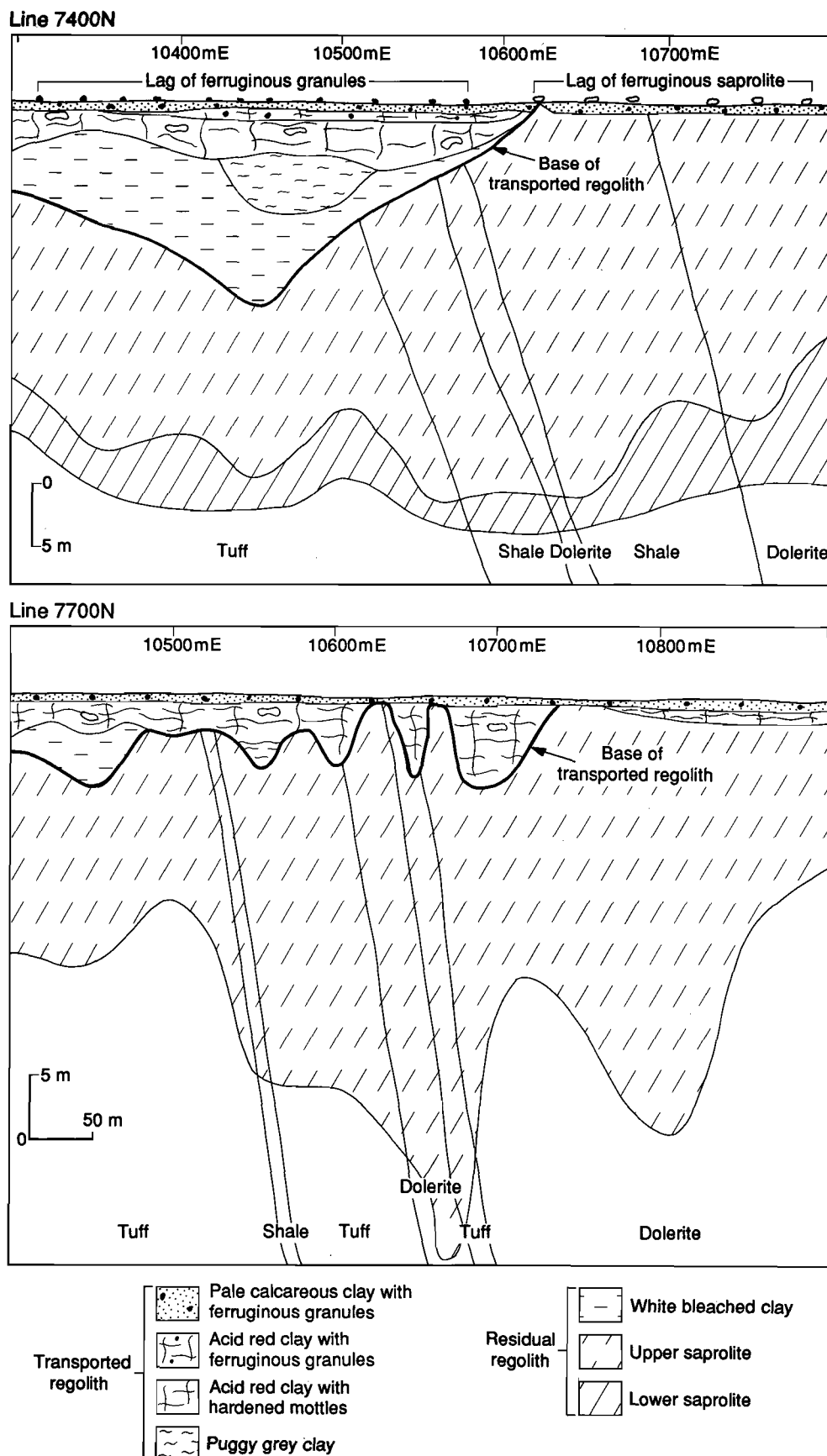


**Fig. 4.9** Diagrammatic cross sections showing the regolith stratigraphy for lines 7400N and 7700 mN, Matt Dam prospect, Ora Banda district.



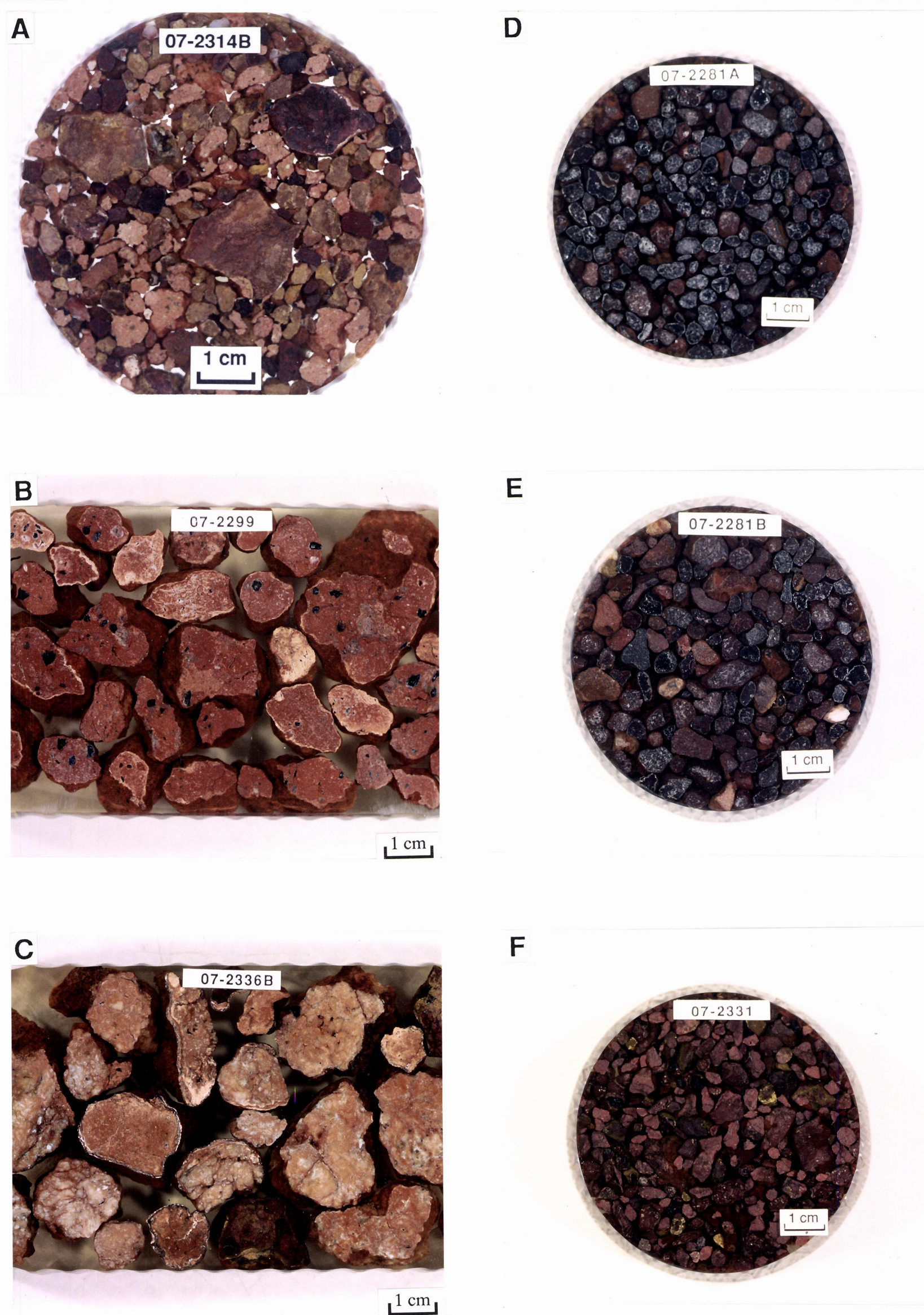


Fig: 4.10 Matt Dam sample types. (A) ferruginous saprolite with carbonate nodules, (B) calcareous coatings on hardened soil fragments, (C) carbonate nodules and ferruginous saprolite fragments, (D,E) magnetic and non-magnetic ferruginous lag in the depositional regime and (F) red clay and ferruginous mottles from the depositional regime.





#### 4.2.6 Geochemical Dispersion

##### Sampling

The study area has a range of lag types and surface densities which vary along the two lines sampled. Representative lag samples (approx. 1 kg) were brushed from the surface and sieved into 1-2, 2-4, 4-10, 10-20 and >20 mm fractions. Each was then separated into magnetic and non-magnetic fractions using a permanent magnet. Soil samples were taken from 15 to 20 cm depth to avoid contamination from aeolian materials. These soils were later split into less than 75  $\mu\text{m}$ , 75  $\mu\text{m}$  to 710  $\mu\text{m}$  and 710 to 2000  $\mu\text{m}$  fractions by wet sieving. The intermediate size fraction 75  $\mu\text{m}$  to 710  $\mu\text{m}$  was not analysed as inspection showed it dominantly consists of quartz. The <75  $\mu\text{m}$  fraction is dominated by kaolinite and calcite whereas the 710-2000  $\mu\text{m}$  fraction consists largely of goethite and hematite. Samples of hardened mottles were taken from RAB drill spoil at depths of between 1.5 and 4.5 m. The number of samples analysed from each unit are as follows:

Magnetic lag	N = 20,
Non-magnetic lag	N = 20,
Mottles developed in sediments	N = 26,
<75 $\mu\text{m}$ soils	N = 26; and
Carbonate nodules in sediments	N = 6.

Table 4.3 Mineralogical comparisons of regolith materials at Matt Dam.

Mineralogy of regolith materials in a depositional area.

7400N,10300E	HEMATITE	GOETHITE	MAGHEMITE	KAOLINITE	QUARTZ	CALCITE	DOLOMITE
MAGNETIC LAG	XXXXX		XXXX	X	X		
NON-MAGNETIC LAG	XXXXX	X		XX	XX		
<75 $\mu$ SOIL	X	X		XX	XXXXX	XXXXX	
710-2000 SOIL	XXX	X	XX	X	XX	X	
MOTTLES IN SEDIMENTS	XXXX	X	XX	X	XX		

Mineralogy of regolith materials in an erosional area over dolerite.

7400N,10750E	HEMATITE	GOETHITE	MAGHEMITE	KAOLINITE	QUARTZ	CALCITE	DOLOMITE
MAGNETIC LAG	XX		XXXXX	X	X		
NON-MAGNETIC LAG	XX	XX		XX	XX	X	
<75 $\mu$ SOIL				XX	X	XXXX	
710-2000 SOIL	X	X		XX	XX	XX	

Mineralogy of regolith materials in an erosional area over ultramafic bedrock.

7700N,10650E	HEMATITE	GOETHITE	MAGHEMITE	KAOLINITE	QUARTZ	CALCITE	DOLOMITE
MAGNETIC LAG	XXX	X	XXXXX	X	XX		
NON-MAGNETIC LAG	XX			X	XXX	X	X
<75 $\mu$ SOIL				X	XXXXX	XXXXX	XX
710-2000 SOIL		X		X	XXXX	XX	XXXXX
MOTTLES	X	XXXX		XXXX	XX		X
CARBONATE NODULE		X		X	XXX	X	XXXXX

*Lags*

As discussed above, the nature of lag gravels is related to the regolith substrate. The coarse (> 10 mm), yellowish brown lag of ferruginous saprolite tends to dominate erosional areas to the east, whereas black, fine, ferruginous granules (< 8 mm) dominate the depositional area over the channel. In the erosional areas, non-magnetic (ferruginous saprolite) lag makes up about 80% of the lag gravel (Fig. 4.11). By contrast, magnetic and non-magnetic components are present almost in equal proportions in the depositional area (Fig. 4.11). It appears that ferruginous granules are formed by a combination of several pathways, including mobilisation and segregation of Fe in soils and ferruginisation of saprolite or bedrock fragments. Similar observations were made for the ferruginous granules in the red clays at the Kanowna Belle Au deposit (see Section 4.3). These lags may have been concentrated at the surface by a variety of processes, including deflation, removal of matrix and the burrowing action of termites, ants etc.

The relative abundances of hematite, goethite, maghemite, kaolinite, quartz, calcite and dolomite in different sample media are given in Table 4.3. Magnetic, ferruginous granules consisted mostly of hematite and maghemite, with small amounts of kaolinite and quartz. Goethite was absent or present in trace amounts. The non-magnetic ferruginous granules consist mostly of hematite and quartz, with small amounts of kaolinite and goethite. Fragments of ferruginous saprolite are characterised by hematite, goethite and quartz.

*Mottles in sediments*

These mottles are irregular to sub-rounded, yellowish brown to reddish brown and range in size from 5 to 15 mm. They are dominated by hematite, goethite and quartz.

*Soils*

The soil samples, collected over the 7400 mN transect, also reflected their erosional or depositional environments. The soil over ferruginous saprolite in the erosional area was shallow (0 to 50 cm) and calcareous, containing fragments of ferruginous saprolite. Pedogenic carbonates are formed from weathering of underlying mafic saprolite. By contrast, the soil over the channel was relatively deep (0.5 to 2 m) and is derived from colluvial processes. The origin of carbonates in the depositional areas may have involved lateral transportation and redeposition of weathered fragments of calcrete, which were then dissolved and precipitated at the top of the profile.

*Dispersion of Au and ore-related elements in ferruginous granules, mottles in sediments and soils*

The sample fractions chosen were analysed for a suite of elements by methods consistent with the CSIRO geochemical database for the P240 and P240A projects (See page 45, Report 20R, and page 18, Report 27R).

The analytical data for all sample types are tabulated in Appendix X. Plots of the two lines for most elements are also included in Appendix X with summary statistics, histograms and plots of interelement correlation coefficients for all sample types. The figures and tables included in this section are summaries and examples. Summary statistics (Table 4.4) give an overview of the geochemical data.

*Line 7400 mN*

This line is partly on a depositional area, over a channel (10,300 to 10,620 mE) and partly on an erosional area, where ferruginous saprolite outcrops patchily (10,620 to 10,800 mE). The major element component of the lag responds to the subsurface materials with SiO<sub>2</sub> and Al<sub>2</sub>O<sub>3</sub> increasing over saprolite and Fe responding to the ferruginous materials accumulated in the channel. Magnesium, Ca and Na peak over a dolerite unit at 10650-10750 mE.

There are two Au peaks in the line, one at 10500 mE, in a depositional area, over mineralisation at 15 m depth, and one at 10700 mE in an erosional area, over mineralisation at 35 m depth. The distributions of Au and trace element associations in different sample types are quite different in the two cases. A summary of the major geochemical differences at these locations is shown in Table 4.5 and a complete set of line diagrams are included in Appendix X.



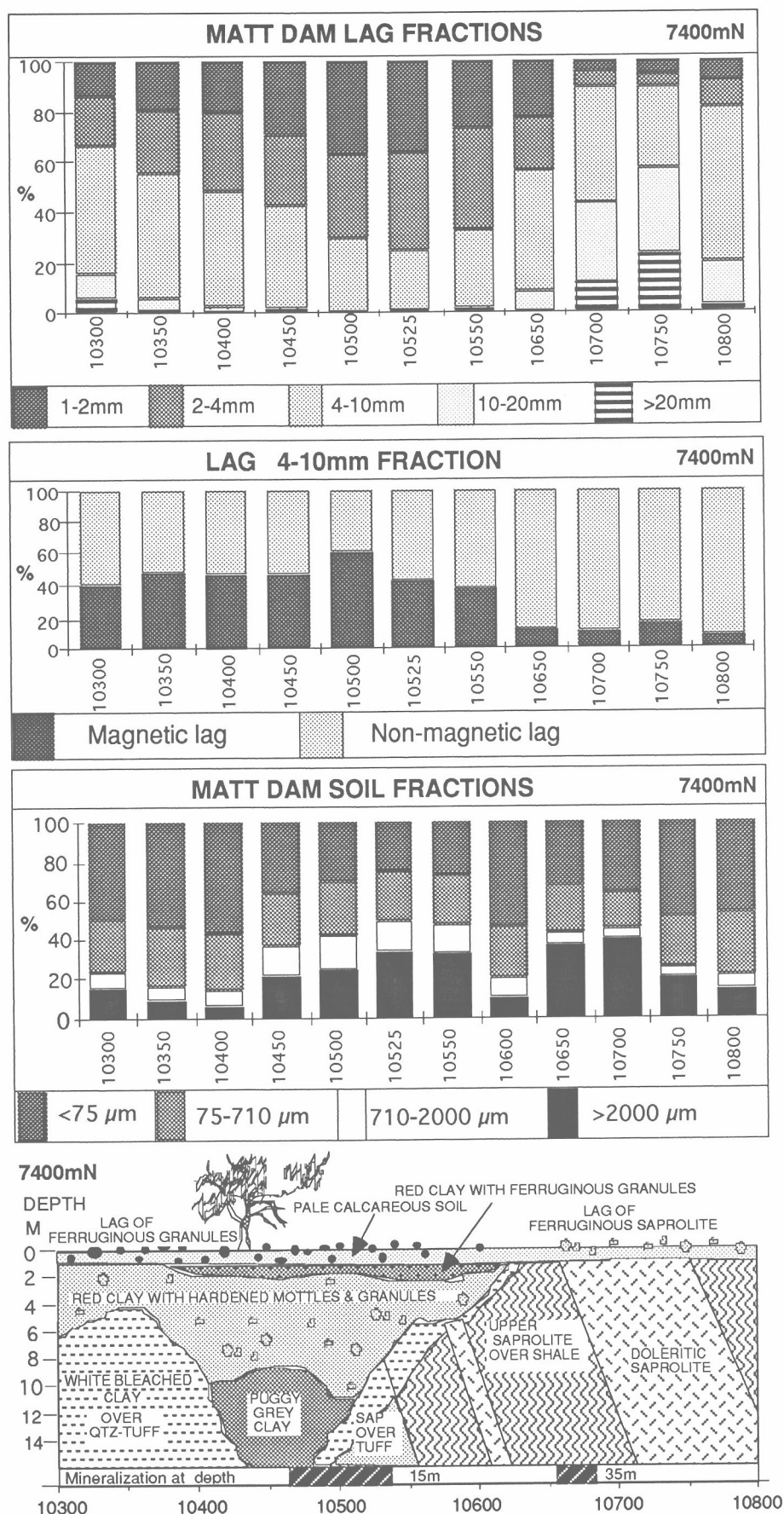


Fig. 4.11 Distribution of size fractions in soil and lag, Matt Dam prospect, Ora Banda district.

Table 4.4 Some summary statistics on element concentrations in samples from the Matt Dam prospect.

	Ferruginous saprolite N=20					Ferruginous granules N=20					Mottles in sediments N=26				
	Mean	Std Dev	Min	Max	Median	Mean	Std Dev	Min	Max	Median	Mean	Std Dev	Min	Max	Median
SiO <sub>2</sub> %	24.4	9.2	9.6	50.9	22.0	10.1	4.5	5.8	22.0	8.5	25.8	11.3	9.0	59.0	23.2
Al <sub>2</sub> O <sub>3</sub> %	14.0	2.4	10.6	19.9	13.7	9.7	1.7	7.4	14.2	9.8	13.3	2.9	8.5	19.5	13.4
Fe <sub>2</sub> O <sub>3</sub> %	48.2	10.0	25.7	69.9	50.5	71.8	7.8	58.0	80.9	72.0	49.2	13.4	22.1	75.3	48.3
MgO%	0.71	0.63	0.21	3.05	0.59	0.51	0.76	0.13	3.39	0.21	0.38	0.26	0.12	1.09	0.29
CaO%	1.52	1.44	0.11	5.05	1.06	0.86	1.38	0.13	5.61	0.30	0.25	0.32	0.02	1.17	0.07
Na <sub>2</sub> O%	0.21	0.15	0.00	0.48	0.16	0.07	0.03	0.00	0.10	0.07	0.15	0.05	0.06	0.27	0.15
K <sub>2</sub> O%	0.12	0.09	0.02	0.39	0.09	0.03	0.01	0.02	0.05	0.03	0.12	0.26	0.02	1.25	0.055
TiO <sub>2</sub> %	0.66	0.24	0.40	1.34	0.60	0.78	0.19	0.49	1.11	0.72	1.36	0.32	0.77	2.41	1.385
LOI%	8.6	3.0	4.8	14.0	7.5	4.4	2.3	2.2	10.5	4.0	9.37	2.72	4.28	14.8	10.145
TOT%	98.4	0.5	97.4	99.5	98.4	98.3	0.4	97.6	99.3	98.2	99.9	0.3	99.1	100.4	100.0
Mn ppm	1401	692	530	3160	1230	722	378	257	1820	652	206	229	32	970	131
Cr ppm	1899	664	805	2960	2080	5088	1565	2140	7470	5390	2618	1410	986	5760	2175
V ppm	887	172	538	1270	873	1352	108	1090	1490	1375	978	270	436	1480	1010
Cu ppm	110	38	36	175	119	53	14	34	78	50	55	25	26	143	48
Pb ppm	14	7	1	28	12	26	8	15	41	24	13	8	1	31	11
Zn ppm	38	14	15	65	36	16	9	2	30	19	18	34	2	176	8
Ni ppm	161	69	67	295	143	162	52	98	255	153	122	43	31	231	132
Co ppm	17	6	8	28	17	15	9	6	35	12	15	10	2	57	15
As ppm	553	254	269	1177	489	281	118	178	534	235	294	200	74	952	238
Sb ppm	6.6	1.8	3.0	10.0	7.0	10.1	1.4	7.0	13.0	10.0	7.6	2.9	2.0	13.0	7.0
Bi ppm	0.4	0.2	0.3	1.0	0.3	0.7	0.6	0.3	2.0	0.3	0.8	0.6	0.3	2.0	0.3
Mo ppm	0.6	0.6	0.3	2.0	0.3	1.1	0.8	0.3	3.0	1.0	1.7	1.5	0.3	7.0	1.0
Ag ppm	0.2	0.1	0.1	0.5	0.2	0.4	0.1	0.3	0.7	0.4	0.5	0.2	0.0	1.0	0.4
Sn ppm	2	1	0.33	4	2	3	2	0.33	6	3	2	1	0.33	6	2
Ge ppm	1	1	0.33	5	0.33	0.46	0.28	0.33	1	0.33	1	1	0.33	5	1
Ga ppm	32	10	21	61	31	38	5	31	49	37	32	7	19	51	31
W ppm	15	17	0.33	60	8	7	4	0.33	16	7	7	6	0.33	35	6
Ba ppm	315	243	50	879	242	119	105	46	464	93	313	420	31	1550	117
Zr ppm	92	34	60	159	79	120	25	89	165	113	119	41	52	192	115
Nb ppm	4	2	1	8	3	4	2	0.33	8	4	4	2	0.33	9	5
Se ppm	2	2	0.33	9	2	4	2	0.33	7	4	7	4	1	19	7
Au ppb	6	17	2	76	2	7	10	2	39	2	15	40	2	206	2
Ce ppm	18	7	8	33	15	28	8	12	42	29	11	10	2	39	9

	<75µm Soils N=26					710-2000µm Soils N=26					Carbonate nodules N=6				
	Mean	Std Dev	Min	Max	Median	Mean	Std Dev	Min	Max	Median	Mean	Std Dev	Min	Max	Median
SiO <sub>2</sub> %	39.7	5.5	26.3	51.1	39.0	24.5	9.8	9.6	45.2	23.6	17.4	5.8	12.7	27.5	16.0
Al <sub>2</sub> O <sub>3</sub> %	15.0	3.3	7.1	21.0	14.8	11.3	2.2	8.4	15.3	11.5	9.2	4.1	4.8	14.8	8.8
Fe <sub>2</sub> O <sub>3</sub> %	7.3	1.8	3.5	10.9	6.7	46.3	18.5	12.6	74.4	45.1	24.3	15.1	7.6	44.7	23.8
MgO%	2.90	1.17	1.23	6.45	2.61	1.46	1.73	0.24	7.75	0.80	6.25	5.34	0.71	12.90	5.96
CaO%	11.24	5.49	0.49	23.80	12.15	3.99	4.37	0.27	13.70	2.16	15.32	8.67	5.34	27.20	15.25
Na <sub>2</sub> O%	0.48	0.31	0.14	1.27	0.40	0.09	0.04	0.03	0.18	0.10	0.13	0.08	0.07	0.28	0.11
K <sub>2</sub> O%	0.88	0.20	0.47	1.48	0.86	0.17	0.13	0.02	0.50	0.11	0.07	0.05	0.02	0.13	0.08
TiO <sub>2</sub> %	1.25	0.26	0.65	2.13	1.23	1.24	0.31	0.64	1.96	1.24	0.63	0.24	0.42	0.95	0.54
LOI%	21.1	4.0	12.9	30.2	21.8	10.8	6.1	3.7	24.5	9.0	26.1	9.8	15.5	36.3	26.5
TOT%	99.8	0.4	98.6	100.3	99.9	99.8	0.3	99.0	100.4	99.8	99.4	0.5	98.6	99.9	99.6
Mn ppm	621	313	233	1360	584	675	295	313	1280	551	300	378	59	1050	176
Cr ppm	538	113	308	838	531	2567	1499	695	5410	1975	1229	665	646	2330	1007
V ppm	133	30	87	194	125	904	351	204	1380	916	446	295	139	881	383
Cu ppm	55	11	39	82	53	77	23	45	157	69	82	57	18	166	88
Pb ppm	7	3	1	15	7	26	13	7	54	23	7	4	3	11	7
Zn ppm	50	15	23	90	46	30	15	15	90	24	25	24	10	73	16
Ni ppm	131	42	57	236	122	144	42	77	213	136	113	81	37	217	89
Co ppm	20	6	10	34	20	17	4	10	23	18	12	6	7	23	9
As ppm	42	20	19	103	36	286	125	185	765	239	363	386	27	1048	298
Sb ppm	1.1	0.8	0.33	3.0	1.0	6.1	3.2	1.0	12.0	6.0	3.0	1.5	1.0	5.0	3.0
Bi ppm	0.4	0.2	0.33	1.0	0.33	0.5	0.4	0.33	2	0.33	0.33	0.00	0.33	0.33	0.33
Mo ppm	1.2	0.6	0.33	3.0	1.0	0.33	0.00	0.33	0.33	0.33	0.33	0.00	0.33	0.33	0.33
Ag ppm	0.4	0.2	0.03	0.9	0.38	0.4	0.2	0.03	0.88	0.4	0.2	0.3	0.03	0.6	0.1
Sn ppm	2	1	0.33	4	1	1	1	0.33	4	1	1	1	0.33	2	1
Ge ppm	1	0	0.33	2	1	2	2	0.33	5	1	1	0.3	0.33	1	0.33
Ga ppm	17	4	7	25	16	28	8	12	45	30	16	7	7	24	15
W ppm	5	2	1	9	5	10	9	2	41	9	1	1	0.33	3	1
Ba ppm	206	49	127	321	206	169	106	64	513	133	89	60	24	201	84
Zr ppm	170	29	93	247	174	108	27	68	158	109	54	10	38	65	55
Nb ppm	8	2	5	12	7	3	2	0.33	8	3	1	1	0.33	3	1
Se ppm	1	1	0.33	3	1	3	2	0.33	9	3	2	2	0.33	4	1
Au ppb	168	226	31	1010	81	27	28	2	99	15	73	47	19	160	62
Ce ppm	38	15	14	75	35	35	13	14	64	35	8	4	4	13	8

Table 4.5 Comparison of anomalies from depositional and erosional areas, Matt Dam prospect.

7400mN	Depositional area 10450mE		
	Calcareous <75 $\mu$ soil	Non-magnetic lag of mixed ferruginous granules and quartz	Magnetic lag of mixed ferruginous granules
Au ppb	1010	20	39
As ppm	27	258	212
W ppm	1	7	9

7400mN	Erosional area 10700mE		
	Calcareous <75 $\mu$ soil	Non-magnetic lag of ferruginous saprolite	Magnetic lag of mixed ferruginous saprolite and ferruginous granules.
Au ppb	182	76	<5
As ppm	103	1177	674
W ppm	8	54	60

In the depositional regime the Au anomaly over mineralisation at 10500 mE is strongest in the <75  $\mu$ m soils (1010 ppb) with the 710-2000  $\mu$ m soil showing 34 ppb and 39 ppb in the magnetic, ferruginous granules (Figs. 4.12, 4.13). The high concentrations are in transported soil which could suggest a distant source of Au. Mineralisation in the area has high As and W (from Newcrest) which are not expressed in the <75  $\mu$ m soil in the depositional area but are present in the <75  $\mu$ m soil from the erosional area. If the materials were derived from the erosion of an upland area they would have an As and W anomaly consistent with their Au content. This suggests a chemical process which concentrates Au in the <75  $\mu$ m calcareous soils and separates the other elements associated with mineralisation from the Au.

The second Au peak is much lower (182 ppb in <75  $\mu$ m soil) at 10700 mE which is in an erosional area with a lag of ferruginous saprolite. This anomaly shows an element association consistent with a saprolitic geochemical halo of the mineralisation with Au in the ferruginous saprolite lag. Arsenic and W are very strongly anomalous in the lags of ferruginous saprolite and soils in contrast to the anomaly in the depositional area.

Plots of Au, As, W and Ce over the 7400 mN line (Fig. 4.12, 4.13) show that the strong Au peak over the channel is quite discrete from the multi-element peak in the erosional area, indicating subdued interaction of physical or chemical processes. The conclusion that can be drawn is that the Au has been concentrated in the calcareous soil over mineralisation after the main depositional event, since the Au is concentrated strongly in the near surface calcareous layer and not deeper in the channel profile. Similar observations were made by Butt *et al.*, 1991 and 1993, who established the close association between Au and pedogenic carbonate overlying concealed Au deposits.

Over the whole area, the magnetic and non-magnetic black Fe-rich granules and mottles show a broad anomaly in As, W, Ce, Sb and Pb (Figs 4.12, 4.13). The 710-2000  $\mu$ m fraction, dominated by very fine, ferruginous granules, also shows broad anomalies in As, Ce and W. The abundances of these elements are significantly greater than background concentrations and are associated with Au mineralisation. This distribution is consistent with scavenging by Fe<sub>2</sub>O<sub>3</sub> and mobility away from mineralisation. Arsenic appears to have a higher mobility and sufficiently high concentration to produce a broad anomaly plus a peak over mineralisation, whereas W is immobile and only is anomalous over mineralisation in residual or erosional areas.

Over the whole line Cr, V, Sb and Ga follow the Fe<sub>2</sub>O<sub>3</sub> concentration with no significant association with the Au anomalies. Manganese, Cu, Zn, Co, As, W and Ba all increase over the doleritic saprolite. Copper and Pb are not as well correlated with the Au anomalies as As and W. Cerium is present in significant concentrations in both soils and ferruginous granules. Ranges vary from 14 to 64 ppm for soils and from 9 to 42 ppm in lag.

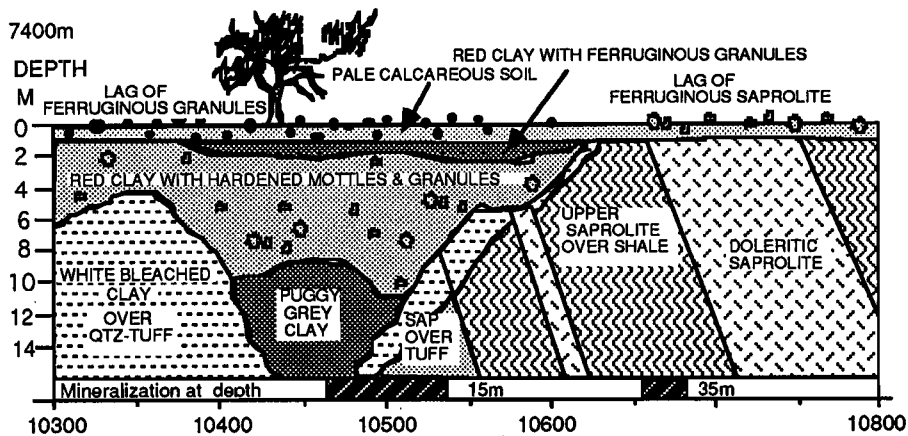
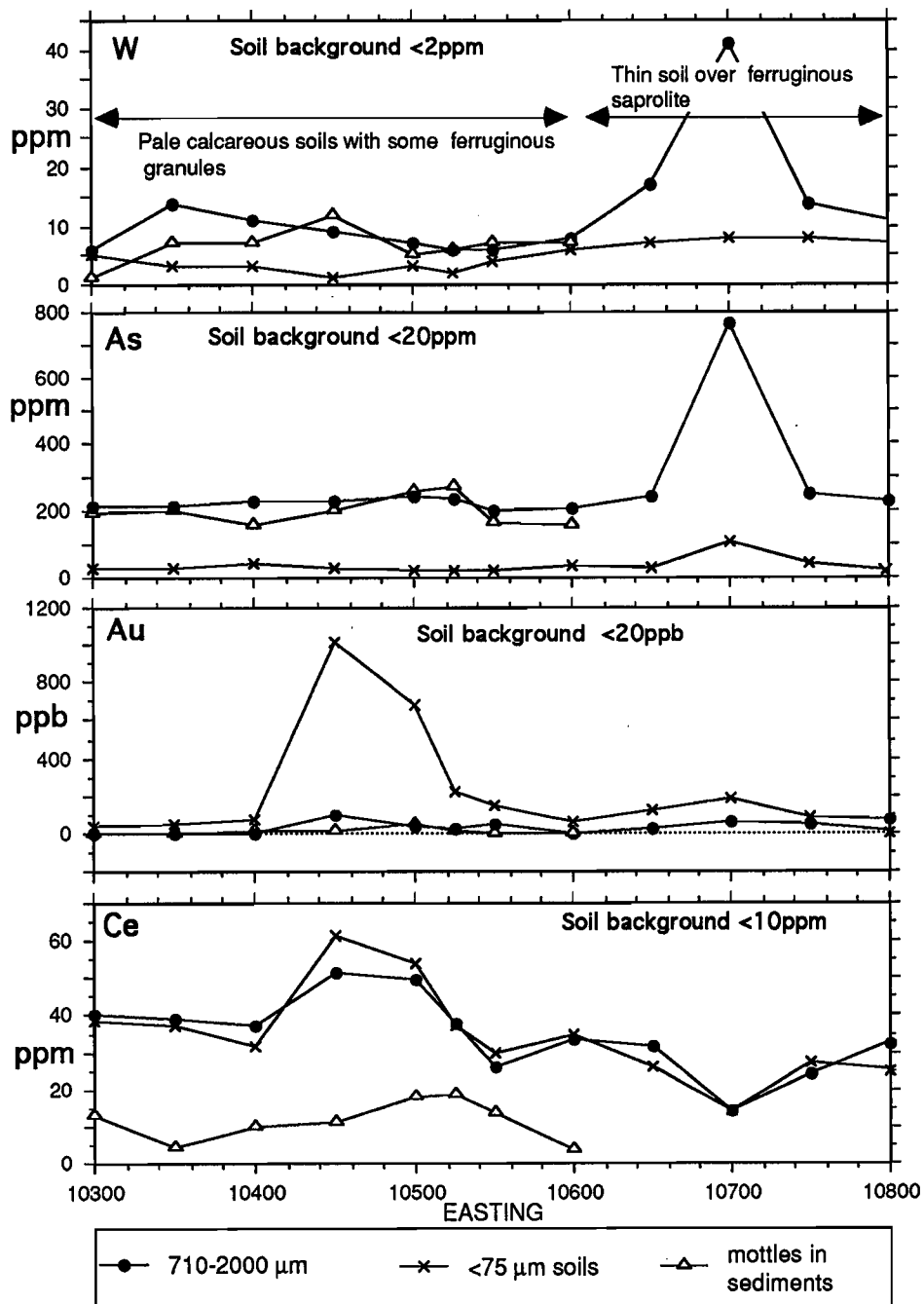


Fig. 4.12 Traverse along line 7400 mN showing the distribution of W, As, Au and Ce in soils and mottles developed in sediments, Matt Dam prospect, Ora Banda district.

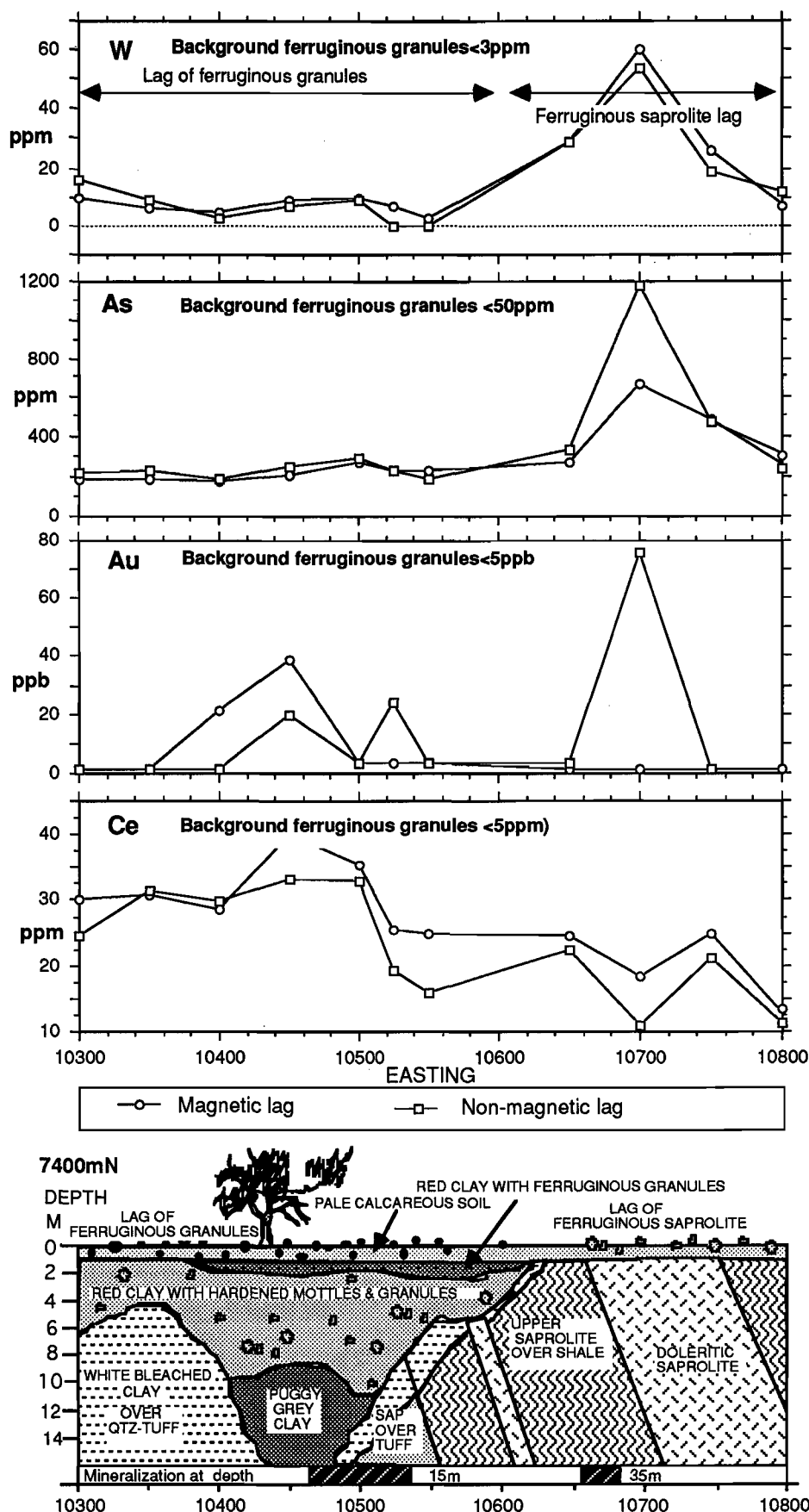


Fig. 4.13 Traverse along line 7400 mN showing the distribution of W, As, Au and Ce in magnetic and non-magnetic lags, Matt Dam prospect, Ora Banda district.

*Line 7700 mN*

This line is more complex than 7400 mN, with the depth of weathering varying with basement rock type and the depositional channel areas not as clearly defined (Figs. 4.14, 4.15). The trace element signature of the steeply dipping bedrock also affects the interpretation of the element associations with mineralisation. The W on this line appears to be related to the doleritic saprolite rather than to the mineralisation. However, the mineralisation is depicted by a multi-element geochemical halo within both the ferruginous granules and mottles. The granules and mottles are anomalous in As and W.

The  $\text{SiO}_2$  and  $\text{Fe}_2\text{O}_3$  in the  $<75\ \mu\text{m}$  soils stay constant over the traverse but the  $\text{Al}_2\text{O}_3$  is displaced by CaO and MgO where saprolite comes close to the surface at 10650 mN. Potassium follows the same pattern to  $\text{Al}_2\text{O}_3$ .

The trace elements Mn, As, Cu and Ni reach maxima where the saprolite is closest to the surface but Au reaches a maximum in samples directly above mineralisation at 10550 mE. The Au maximum is stronger over weak mineralisation (0.74 ppm at 20 m) than over stronger mineralisation (8.13 ppm at 40 m). The Au peak is again in the  $<75\ \mu\text{m}$  soils and the Mn, As, Cu and Ni peaks are in ferruginous lags and soil displaced 100 mE from the Au peak over the ferruginous saprolite.

*4.2.7 Sample type comparisons*

The geochemistry of the five sample types collected over the two traverses was compared using descriptive statistics, frequency distribution and inter-element correlations (Appendix X).

The distribution of major elements is shown in ternary plots (Fig. 4.16). The  $<75\ \mu\text{m}$  soils are the most siliceous sample type with a restricted sample composition in the low  $\text{Fe}_2\text{O}_3$  area of the plot. The coarser soil fraction (710–2000  $\mu\text{m}$ ) and the lag have a larger range of  $\text{SiO}_2$  and  $\text{Fe}_2\text{O}_3$ , reflecting their position in erosional, saprolitic areas or in transported red soils and ferruginous granules. The  $\text{Al}_2\text{O}_3$ , MgO, CaO ternary plot shows that mottles have relatively high  $\text{Al}_2\text{O}_3$  and low CaO contents while the  $<75\ \mu\text{m}$  soils have high CaO. The six calcareous nodule samples have a large range because one group of three are homogeneous calcrete and the others are coatings of calcite on ferruginous material derived from soil or saprolite.

*Lag*

Both the magnetic and non-magnetic fractions consist mainly of  $\text{Fe}_2\text{O}_3$ . The magnetic fraction has a higher mean (65.4%)  $\text{Fe}_2\text{O}_3$  than the non-magnetic (54.5%). In the histograms, both fractions show a trimodal distribution of  $\text{Fe}_2\text{O}_3$  concentrations which relate to sample type (Fig. 4.17). The magnetic and non-magnetic lag formed from weathering of the ferruginous saprolite have low  $\text{Fe}_2\text{O}_3$  and high concentrations of As and W. In contrast, the black magnetic and non-magnetic, ferruginous granules have high iron and low As and W relative to lag derived from the ferruginous saprolite. This suggests that the abundances of elements are determined by the sample type. There are no significant differences in the abundances of As and W between the two fractions. It therefore can be concluded that both lag fractions relate to the underlying material.

The correlation coefficients (Table 4.6) show the expected strong association of  $\text{Fe}_2\text{O}_3$  with Cr, V and Pb in the Fe-rich materials. However, some elements reflect the genesis of the lag rather than a straight correlation with  $\text{Fe}_2\text{O}_3$ . Strong negative correlations of  $\text{Fe}_2\text{O}_3$  with As and W can be attributed to the three populations described in the previous paragraph. Copper, Co and Ba also have negative correlations with iron and trimodal frequency distributions. The three populations also give an unexpected positive correlation between Mn and As which are both high in the saprolitic lag.

*Soils*

The  $<75\ \mu\text{m}$  soils contain clays and fine carbonates and the 710–2000  $\mu\text{m}$  soils contain small ferruginous granules, quartz and fragments of ferruginous saprolite. The smaller size fraction ( $<75\ \mu\text{m}$ ) samples all have less than 18%  $\text{Fe}_2\text{O}_3$  while the larger size fraction (710–2000  $\mu\text{m}$ ) has between 10 and 74%  $\text{Fe}_2\text{O}_3$ . The  $<75\ \mu\text{m}$  fraction has more  $\text{SiO}_2$ ,  $\text{Al}_2\text{O}_3$ , MgO, CaO and  $\text{K}_2\text{O}$  and has higher concentrations of those elements associated with carbonates and kaolinite (Co, Ba and Zn). The coarse soil has two populations with some high calcium samples which stand out from the Fe-rich group and give the LOI histogram a bimodal distribution. While the fine fraction has a normal distribution. Gold is significantly higher in the  $<75\ \mu\text{m}$  soils with the lowest value 30.8 ppb and mean of 168 ppb.

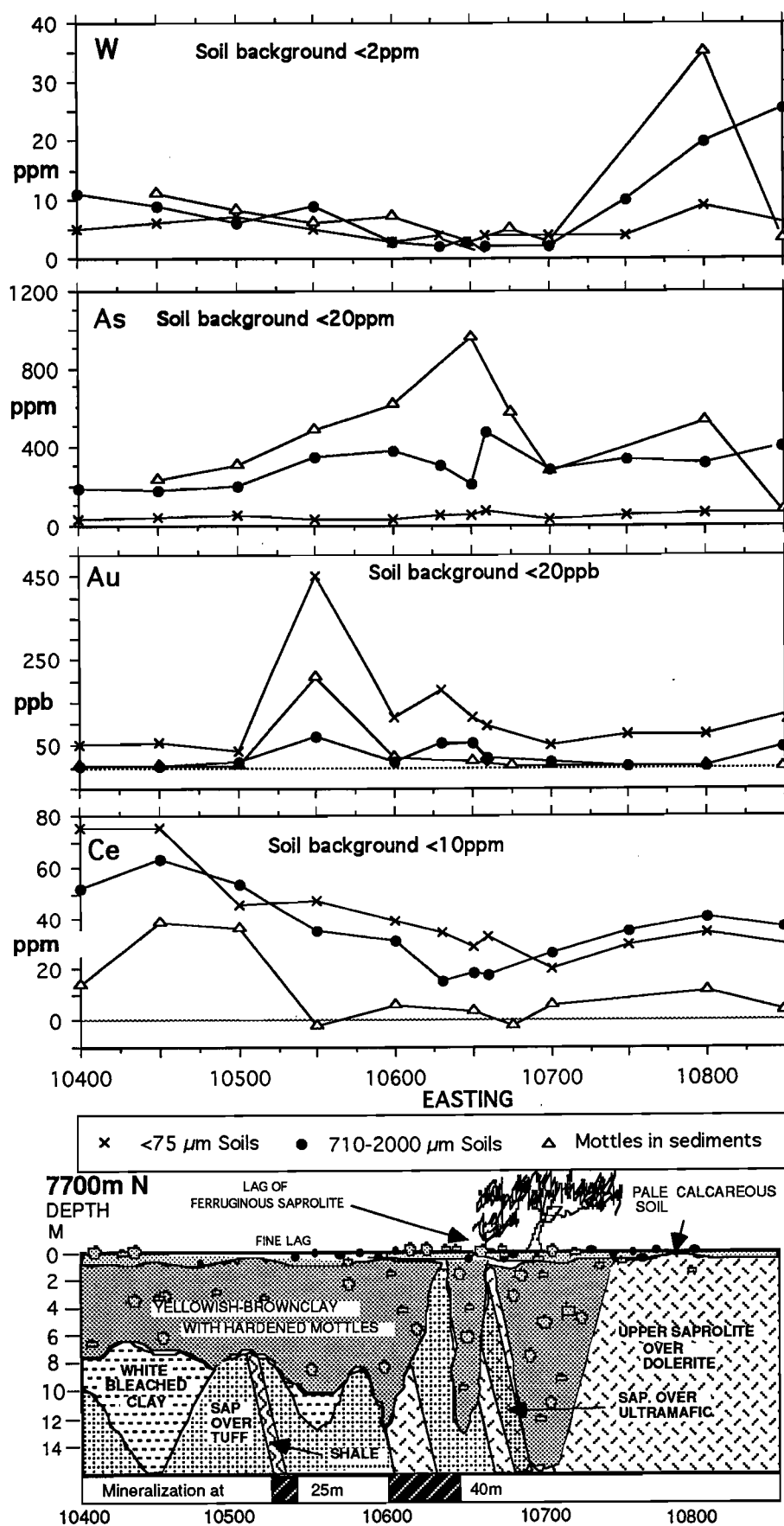


Fig. 4.14 Traverse along line 7700 mN showing the distribution of W, As, Au and Ce in soils and mottles developed in sediments, Matt Dam prospect, Ora Banda district.

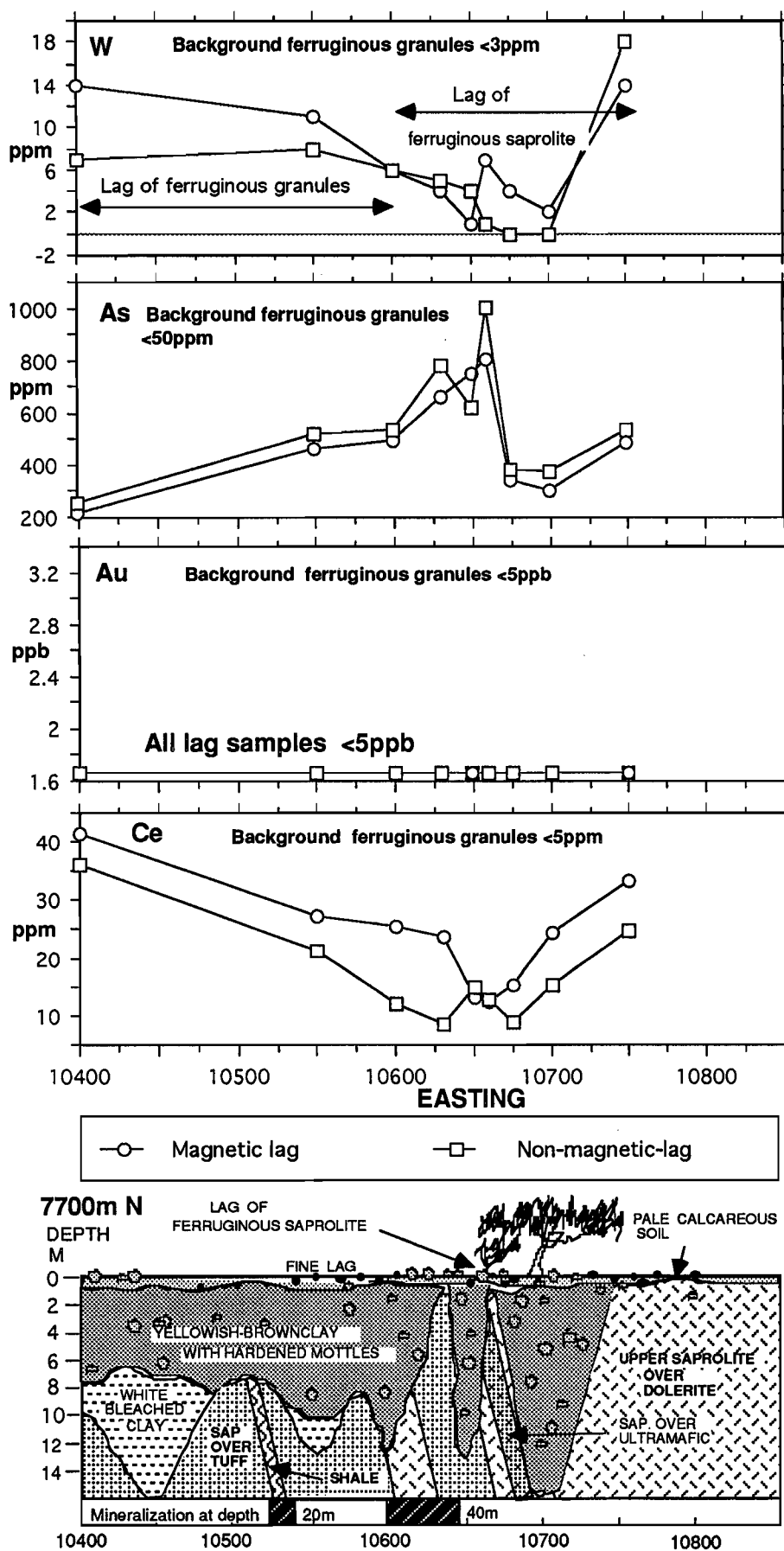


Fig. 4.15 Traverse along line 7700 mN showing the distribution of W, As, Au and Ce in magnetic and non-magnetic lags, Matt Dam prospect, Ora Banda district.



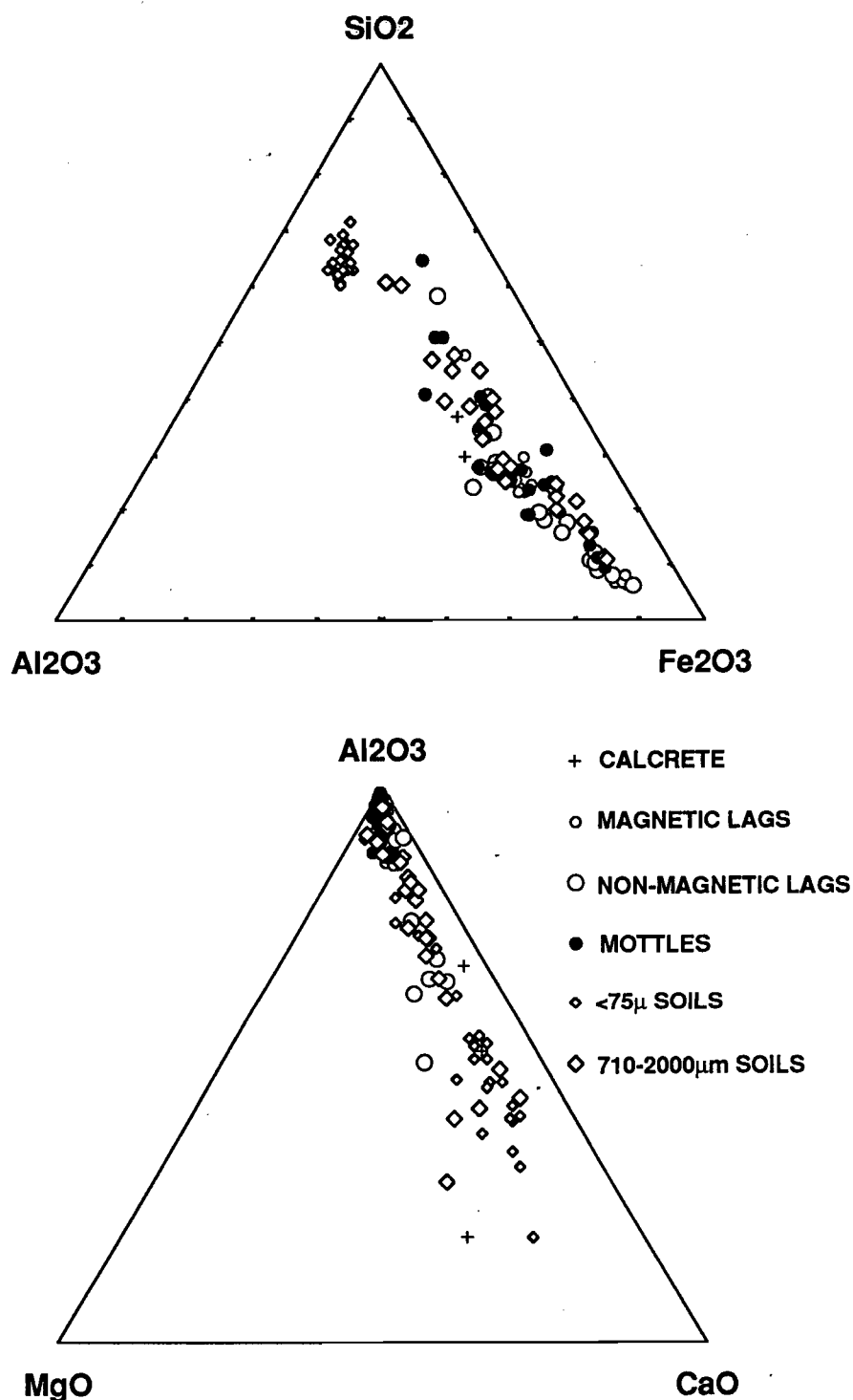


Fig. 4.16 Triangular diagrams showing compositions of soils, carbonate nodules and magnetic and non-magnetic lags in terms of  $\text{SiO}_2$ ,  $\text{Al}_2\text{O}_3$  and  $\text{Fe}_2\text{O}_3$ , Matt Dam prospect, Ora Banda district.

All previous investigations have shown strong negative  $\text{Fe}_2\text{O}_3$  to  $\text{SiO}_2$  correlations, similar to those in the lag and mottles (Table 4.6). The positive correlation shown for the <75 µm soil arises from the parallel displacement or replacement of iron and silica by calcium carbonate. The <75 µm soils show good correlations between  $\text{K}_2\text{O}$  and Zn, and Zr and Nb, indicating the role of micas in their elemental distribution.

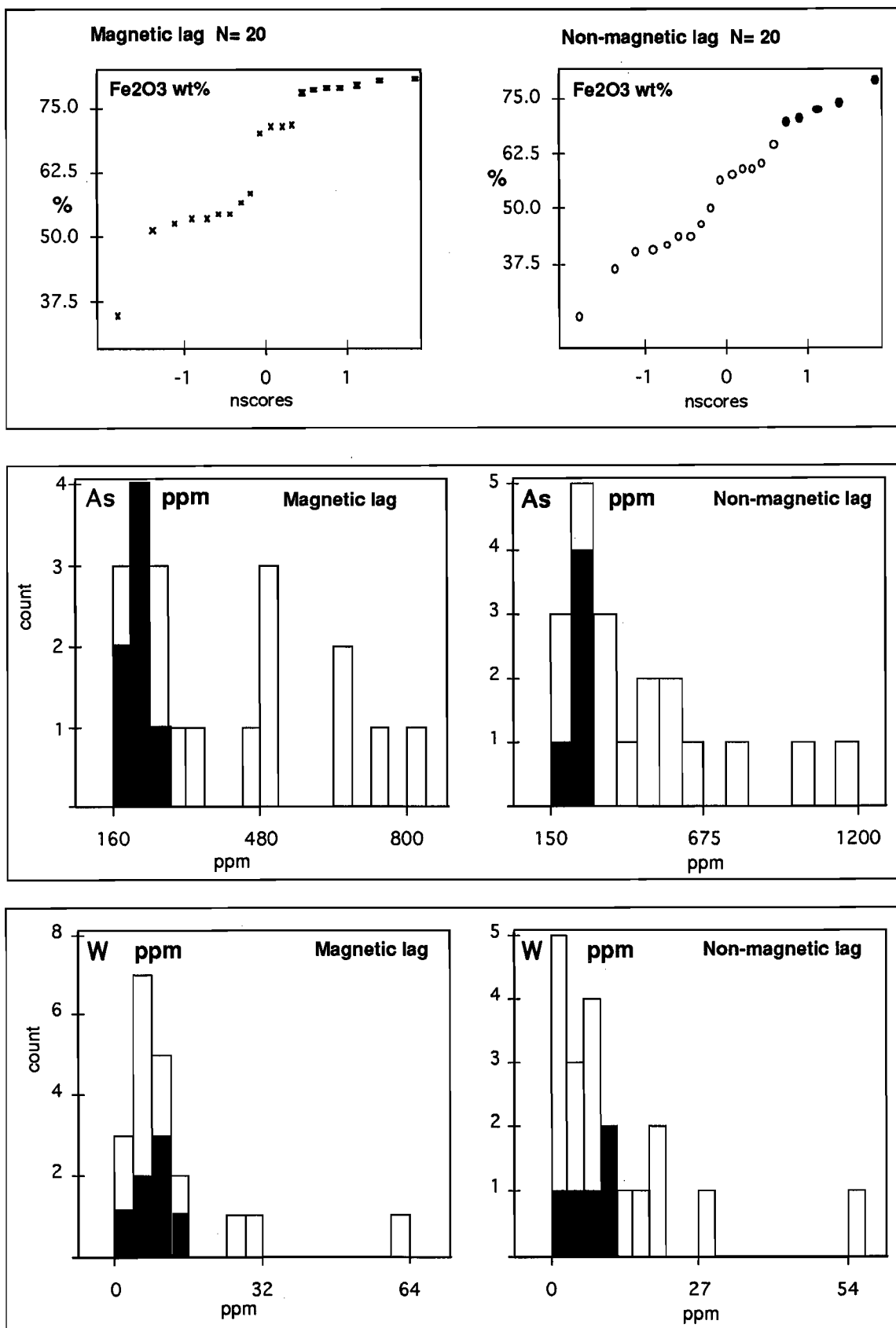


Fig. 4.17 Comparisons between magnetic and non-magnetic lag, Matt Dam prospect, Ora Banda district. The high-iron groups in the magnetic and non-magnetic lags (highlighted in the normal probability plots) have low As and W (highlighted in the histograms).

Table 4.6 Inter-element correlations, Matt Dam prospect.

	Magnetic lags N=20	Non-magnetic lags N=20	<75 $\mu$ soil N=26	710-2000 $\mu$ soil N=26	mottles in sediments N=26
Fe <sub>2</sub> O <sub>3</sub> /Cr	0.837	0.909	0.646	0.923	0.825
Fe <sub>2</sub> O <sub>3</sub> /V	0.926	0.938	0.912	0.975	0.859
Fe <sub>2</sub> O <sub>3</sub> /As	-0.625	-0.581	0.177	-0.518	-0.111
Mn/As	0.615	0.416	0.186	-0.048	0.073
Fe <sub>2</sub> O <sub>3</sub> /Pb	0.597	0.639	0.741	0.917	0.567
K <sub>2</sub> O/Zn	0.575	0.473	0.874	0.334	0.907
Zr/Nb	0.139	0.226	0.597	0.225	0.445
SiO <sub>2</sub> /Fe <sub>2</sub> O <sub>3</sub>	-0.972	-0.900	0.789	-0.788	-0.911

### Mottles

The mottles generally behave geochemically intermediate between the lags and the soils, having a range of Fe-oxide and clay contents but having the lowest levels of carbonates, Mn, Cr and Zn. The elements significantly higher in the mottles are Ti, Ba and Se.

### 4.2.8 Implications in exploration

The main research findings and their implications in exploration are listed in Table 4.7 and the geochemical dispersion model is shown in Fig. 4.18.

The erosional and depositional regimes constrain the distribution of geochemically anomalous sampling media and dispersion processes. Thus sampling must take account of the possible origin of the sample media and regolith-stratigraphic relationships. This is essential to allow correct decisions on appropriate sampling media. Lag of ferruginous saprolite is an excellent sampling medium. A marginal improvement may be gained by using the non-magnetic fraction of the Fe-saprolite. Apart from Au, anomalies in As and W comprise the useful multi-element signature of the Matt Dam prospect.

Black, ferruginous granules and mottles in sediments that mantle the depositional areas show broader anomalies in As, Sb and W related to the underlying mineralisation. Thus these media have considerable significance in exploration.

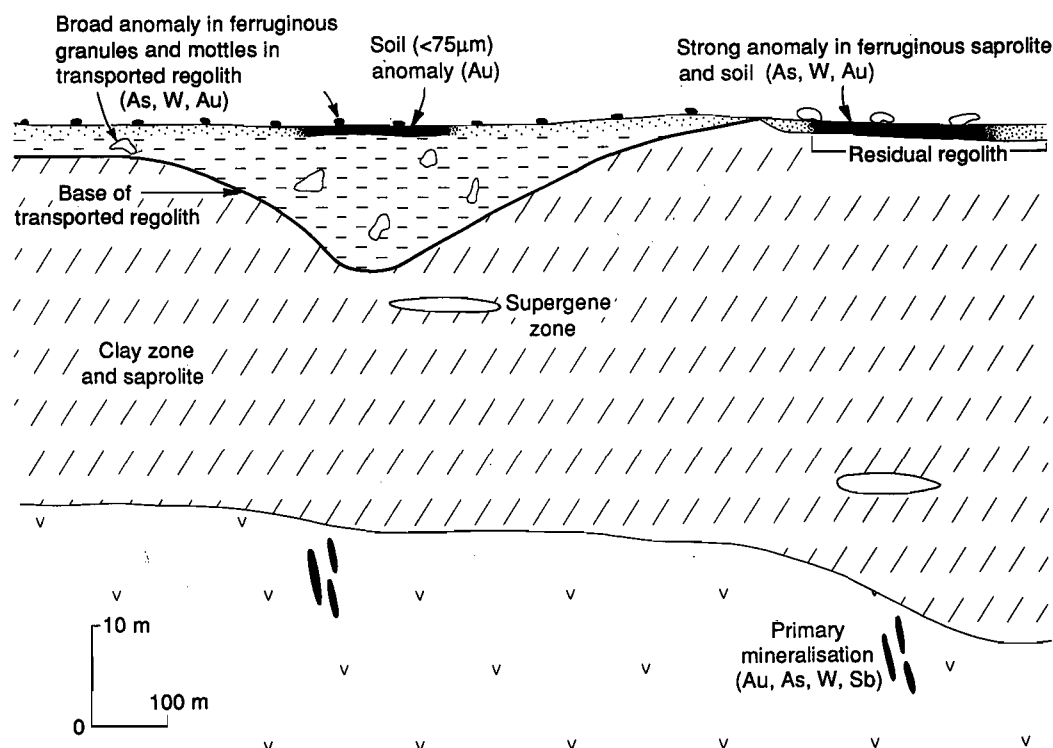


Fig. 4.18 Geochemical dispersion model of the Matt Dam orientation area, Ora Banda district.

Table 4.7 The implications in exploration listed against the research findings for the Matt Dam prospect, Ora Banda district.

Research Findings	Implications for Exploration
<ul style="list-style-type: none"> <li>• The area studied contains mainly erosional regimes with a thin soil over ferruginous saprolite and depositional regimes with up to 15m of colluvium and alluvium.</li> <li>• At Matt Dam, ferruginous saprolite gave best multi-element (As, W and Au) anomalies. Ferruginous granules and mottles in sediments gave broader but weaker As, W, and Au anomalies.</li> <li>• The strongest gold anomaly (1010 ppb) is in the &lt;75 µm fraction of the calcareous soils directly above mineralisation.</li> <li>• Geochemical data sets were established for several sampling media.</li> </ul>	<ul style="list-style-type: none"> <li>- Mapping of the regolith-landform regimes will provide a framework for interpreting the observed anomaly distribution.</li> <li>- Ferruginous saprolite, ferruginous granules and mottles are suitable geochemical sampling media for the Matt Dam area.</li> <li>- The accumulation of gold in calcareous soils may be used as an indication of mineralisation at Matt Dam.</li> <li>- Provides well controlled reference data for use in multivariate interpretation procedures.</li> </ul>

### 4.3 Kanowna Belle district

#### 4.3.1 Introduction

##### Location

The Kanowna Belle Au deposit, jointly held by Geopeko and Delta Gold, is located some 18 km northeast of Kalgoorlie. The district chosen for study (Fig. 4.19), typical of the Kalgoorlie region, covers an area of some 600 km<sup>2</sup>.

##### Regional and local geology

The Kanowna district lies on the eastern margin of the Kalgoorlie Terrane within the Eastern Goldfields Province. It forms part of a belt of north-northwest trending metamorphosed ultramafic, mafic, sedimentary and felsic volcanic and intrusive rocks of the Norseman-Wiluna Belt (Figs 3.1 and 4.19). The Kanowna Belle deposit is contained within a package of northeast trending, south-dipping, predominantly intermediate to felsic, volcanic-derived tuffaceous mass flow units and breccias.

The Kanowna Belle sequence has distinct hanging wall and footwall rock types, generally separated by the Fitzroy Fault. The footwall sequence is mostly a polymictic conglomerate and the hangingwall sequence consists of felsic angular rudites with sporadic pebble-to-boulder beds and mafic flows (Fig. 4.20). The feldspar-phyric to aphyric Kanowna Belle Porphyry, ranging from less than 10 m to 80 m in thickness, appears to intrude along a pre-existing shear zone cut by the Fitzroy fault, which transgresses the porphyry at an acute angle (Thomson and Peachey, 1993).

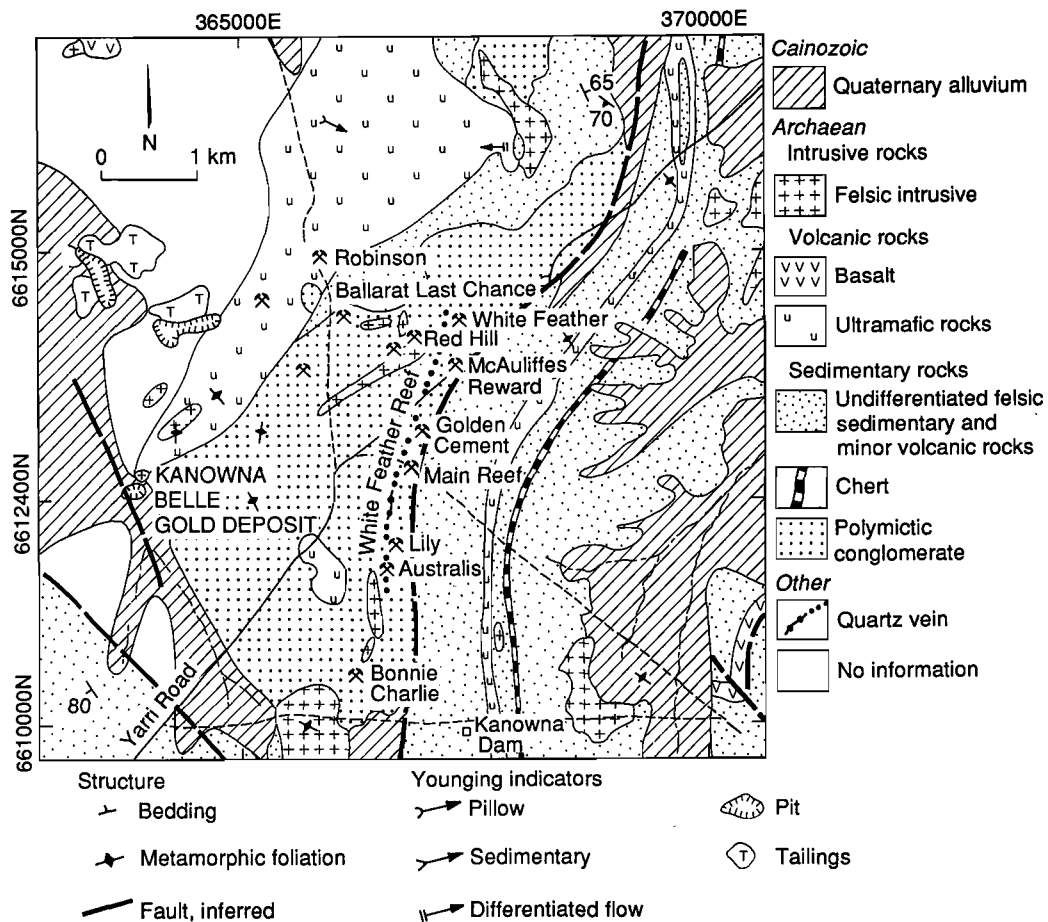


Fig. 4.19 Schematic geology and gold deposit location map of the Kanowna district (after Ross, 1993).

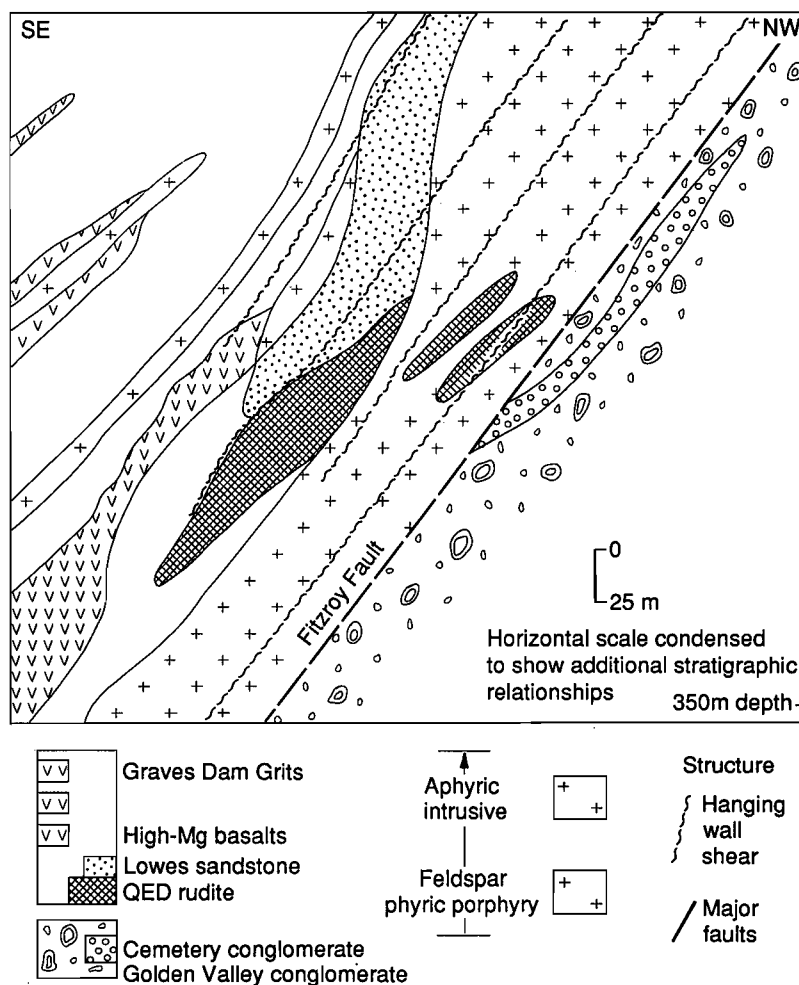


Fig. 4.20 Schematic cross section and mine stratigraphy of the Kanowna Belle Gold Mine (after Ross, 1993).

#### *The Kanowna Belle Au deposit*

The Kanowna Belle deposit is surrounded by an asymmetric alteration envelope consisting of three principal zones; a peripheral chlorite-calcite zone, a thick sericite-carbonate-pyrite-fuchsite zone and an inner quartz-albite-pyrite zone, closely associated with ore-grade mineralisation.

The main orebody at Kanowna Belle is the Lowes Shoot, a tabular, mostly porphyry-hosted body, which strikes from 350 m to 500 m and is 5 to 50 m thick and which remains open below a vertical depth of 800 m (Thomson and Peachey, 1993). The Lowes Shoot shows a close spatial relationship to the Fitzroy Fault, generally lying above it in the upper parts of the deposit and below it at depth. Smaller mineralised bodies occur in the Hilder Shoot, the Troy Shoot and in shoots developed in the hanging wall to the upper part of the Lowes Shoot.

Supergene gold mineralisation is significant at Kanowna Belle, with a well-developed sub-horizontal mineralised horizon, as defined by gold values greater than 0.1 ppm, occurring at depths of 35 m to 45 m below surface as a series of lenses between 1 m and 4 m thick at the base of the saprolite. This mineralisation extends laterally for up to 200 m from the margins of the primary mineralisation and thus presents a larger target for exploration (Thomson and Peachey, 1993). Very small pods of shallow supergene mineralisation, generally less than 20 m in length, are developed at depths of 5 m to 12 m, within or at the base of a silcrete horizon. Gold concentrations in the saprolite outside of these supergene enrichments are low, generally less than 104 ppb.

The total resources at Kanowna Belle is 15 million tonnes at 5.3g/t Au to a depth of 650 m (Thomson and Peachey (1993)).

#### *Geomorphology and drainage*

The Kanowna district lies on the eastern margin of the Salt Lake or Salinaland physiographic division of Jutson (1950) and incorporates part of the Lake Yindarlgooda drainage system. The district forms a broadly undulating terrain between 320 and 420 m above sea level, with isolated belts of low hills and ridges providing local relief. More detailed relief variations are observed within breakaway country, resulting from differential stripping processes, and within the sand and gypsum dune country bordering the salt lakes and playas.

The elevated ridges and hills (areas above 400 m) are generally restricted to the south, southeast and central regions of the study area and give way to gently sloping pediments to the north.

Several 10 to 30 km long, shallowly incised drainage systems lead into the sandplain playas and salt lakes in the north of the study area. These are prominent on air photos (Fig. 4.21). The breakaways generally occur in the headwaters of these drainage systems or on isolated, low, topographic rises on the boundaries of the sandplains.

#### *Thesis produced:*

The orientation district included a Bachelor-level Honours study of regolith relationships and geochemical dispersion from the Kanowna Belle deposit by M.R. Dell (1992, University of Tasmania).

#### *4.3.2 Objectives*

The objectives of the Kanowna Belle study were to provide a regolith-landform framework for the district and, within this, to carry out multi-element, orientation geochemical dispersion studies about the concealed Kanowna Belle and nearby deep lead Au deposits.

Specific objectives were:

1. To establish regolith-landform relationships over the district surrounding the Kanowna Belle Au deposit.
2. To delineate multi-element geochemical dispersion patterns in the soils overlying the Kanowna Belle deposit as well as in ferruginous granules developed in the soils.
3. To carry out a concise, multi-element, geochemical dispersion and regolith stratigraphic study within palaeochannel environments of the nearby deep lead deposits (particularly the NLP9 Pit).
4. To establish the origin of mega-mottles and ferruginous granules in the regolith.

#### *4.3.3 Regolith-stratigraphic relationships*

##### *Regolith distribution*

A framework of regolith distribution and stratigraphy was established for the district surrounding the Kanowna Belle Au deposit, as a basis for geochemical dispersion studies. Two regolith maps were produced which resulted from the interpretation of aerial photographs and Landsat images substantiated by extensive field work (Figs 4.21, 4.22 and Appendix VII). These include (a) a detailed regolith map at 1:25,000 scale for the Kanowna district and (b) district-scale map at 1:50,000 scale over an area of approximately 600 km<sup>2</sup> surrounding the detailed study.

The district is characterised by a broadly undulating, variably truncated, lateritic terrain, dominated by both saprolitic to fresh mafic and felsic bedrock, and broad colluvial and alluvial plains. The regolith-landform relationships can be explained in terms of the *residual*, *erosional* and *depositional regimes* (defined in Section 3.3 in this report and Section 2.4.3 in Report 236R). Residual regimes, containing lateritic duricrust, lateritic nodules and pisoliths are sporadically distributed within the study area, and are restricted to small crests which occupy less than 5% of the area. Backslopes are stripped and are characterised by the fragments of ferruginous saprolite and ferruginous lithic fragments. This contrasts with the Lawlers, Mt. McClure, Mt. Gibson and Bottle Creek orientation districts where complete or near-complete lateritic profiles are preserved on the backslopes.

In the Kanowna district, lateritic duricrust commonly overlies a well developed ferruginous saprolite or mottled zone which, in turn, overlies leached saprolite. This is exposed along the truncated profile of breakaways. Lateritic duricrust is strongly developed (in terms of thickness) over the mafic and ultramafic units and is weakly developed above the granitoid and felsic lithologies. This difference is due to the amounts of Fe available during the duricrust formation being considerably greater in mafic rocks than in felsic rocks. Replacement of the kaolinite-goethite-rich matrix by carbonate in the lateritic duricrust is common, with the carbonate penetrating to depths of more than 1.5 metres.

In the erosional regimes, deeper units of the weathered profile, and, in places, unweathered bedrock, are exposed. The units of the erosional regimes are dominated by a shallow, residual calcareous soil and a lag of ferruginous lithic fragments, ferruginous granules and vein quartz, with outcrops of ferruginous bedrock and saprolite. Seven regolith-landform mapping units were mapped in the erosional regimes (regolith map, Appendix VII).

Eight major units form the dominant depositional regimes which comprise over 50% of the study area. The most extensive depositional regimes are mantled by a friable, acid to calcareous, red to orange, sandy clay soil with an abundant lag of black ferruginous granules, and lesser detrital vein quartz, lateritic gravels and lithic fragments. Extensive salt lake and playa systems are characterised by the saline, dark to pale brown fine clays and muds. Gypsiferous and quartz-rich clayey sands border the salt lakes and playa systems.

#### *Regolith stratigraphy, Kanowna-Belle Deposit (Lines 8550 mE, 8810 mE)*

The Kanowna-Belle deposit is located within a major northward-flowing drainage basin, Fig. 4.21. The pale orange, calcareous, sandy clay soils form a 20 to 100 cm thick mantle containing common black ferruginous granules (Fig. 4.23). Carbonates occur as coatings on, and as soft aggregates within, the clay. The 2 to 5 m of acid red clays underlying the calcareous soils, show a decreased to non-existent carbonate content within the top 30 cm of the unit. This acid red clay also contains abundant, black, ferruginous granules. The thickness of the acid red clays increases northwards over 1-2 km. A mottled zone occurs at depths generally greater than 2 m. A zone of silcrete, 1 m to 8 m thick and preferentially developed from the weathering of grits and feldspar porphyry, marks the base of the mottled zone above bleached saprolite. The silcrete, here, is a strongly silicified, indurated saprolite, commonly with a conchoidal fracture and a vitreous lustre. It appears to represent complete silicification of saprolite by the filling of available voids with silica. Primary quartz crystals and bedrock fabrics can be observed within the silcrete and assist in determining the parent material. Saprolitic clays form a 20-50 m thick weathered mantle above the bedrock. A thin (2 m) mineralised supergene blanket occurs within the lower saprolite (Peachey, 1991).

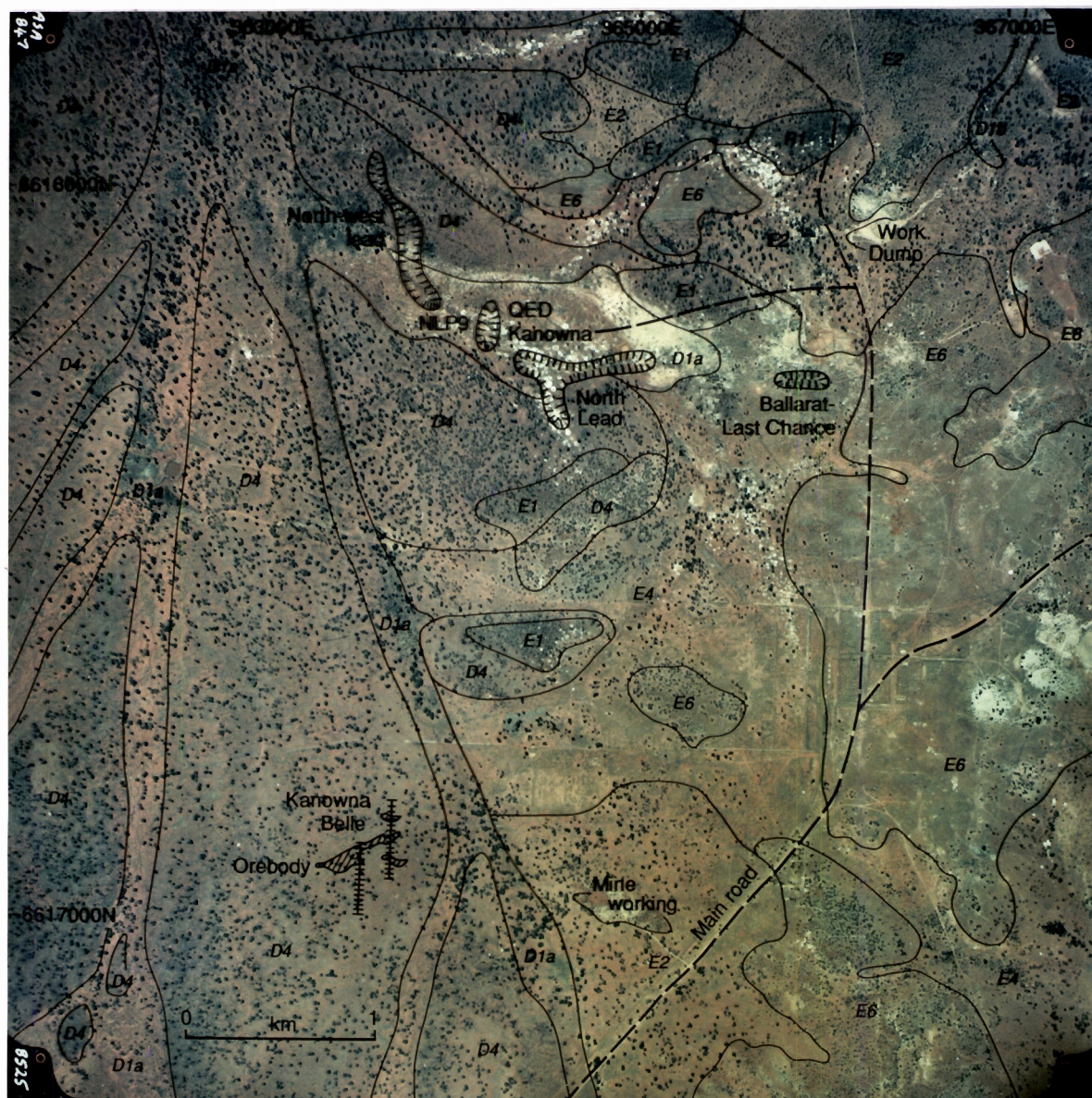
#### *Regolith stratigraphy - palaeochannel environments of the NLP9 Pit*

The NLP9 Pit was chosen as a site at which to examine the morphological, mineralogical and geochemical characteristics of a weathering profile typical of palaeochannel environments. The pit provided an opportunity to study the characteristics and development of regolith units within the weathering profile and the inter-relationships between units.

The stratigraphic sequence of regolith units within the NLP9 pit is summarised in Fig. 4.24. The uppermost unit consists of 20 to 40 cm of red to brown calcareous soil overlain by a medium to fine polymictic lag comprising abundant ferruginous gravels, vein quartz and lithic fragments. The soils lie above a 1 to 4 m thick horizon of pale orange, calcareous soil. The unit consists of multiple lenses of bedded and graded alluvial deposits which have cut channels in the underlying clays. An acid red clay unit forms a sharp but irregular lower boundary with the overlying calcareous alluvials. The 2 to 5 m thick red clay contains small, magnetic, sub-angular to rounded, black, ferruginous granules, fine, lithic fragments, detrital quartz and vein quartz. The clasts observed within the unit occur as horizontally elongate lenses up to 20 m wide. Root systems penetrate the unit and show an intimate relationship with Fe-accumulations. Bleaching and incipient mottles develop within the basal Fe-rich clays and mark the transition into the mottled zone.

The mega-mottled zone is characterised by increased bleaching and development of evenly-spaced irregular, hematite and goethite-rich, 10 to 25 cm long mottles or septa (Fig. 4.24). Mega-mottles are conspicuous within the transported overburden. Two zones are recognised within the mottled zone, the mini-mottled (4-8 m thick) and mega-mottled zones (6-10 m), the boundary between the units is marked by a large shrinkage crack within the clays. Magnetic, black, ferruginous granules are abundant in the mottled zone. The transition from the mottled zone to the underlying pisolithic clay unit is marked by gradual decrease of mottles until the clays are totally bleached.



**RELICT REGIME**

- R1 Lateritic duricrusts, lateritic pisoliths and nodules, crests and low topographic highs

**EROSIONAL REGIME**

- E1 Lag of hardened mottles and ferruginous saprolite, backslopes
- E2 Calcareous clay soils over mottled zone, ferruginous granules, gently sloping terrain
- E4 Saprolite, black ferruginous granules and quartz, erosional plains
- E6 Bedrock, low hills
- E8 Bedrock, high hills

**DEPOSITIONAL REGIME**

- D1a Acid red clay soils with polymictic ferruginous lag within major drainage basins and channels
- D1b Acid red clays with common black polymictic ferruginous lag within minor drainage basins and channels
- D4 Red clay soils with black ferruginous granules over saprolite, alluvial floors

N

Figure 4.21. Map showing the surface distribution of regolith-landform units and vegetation, overlay to colour air photograph 3/8525, 20.3.85, Kanowna Belle Au deposit, Kevron Aerial Surveys, published with permission of North Ltd.



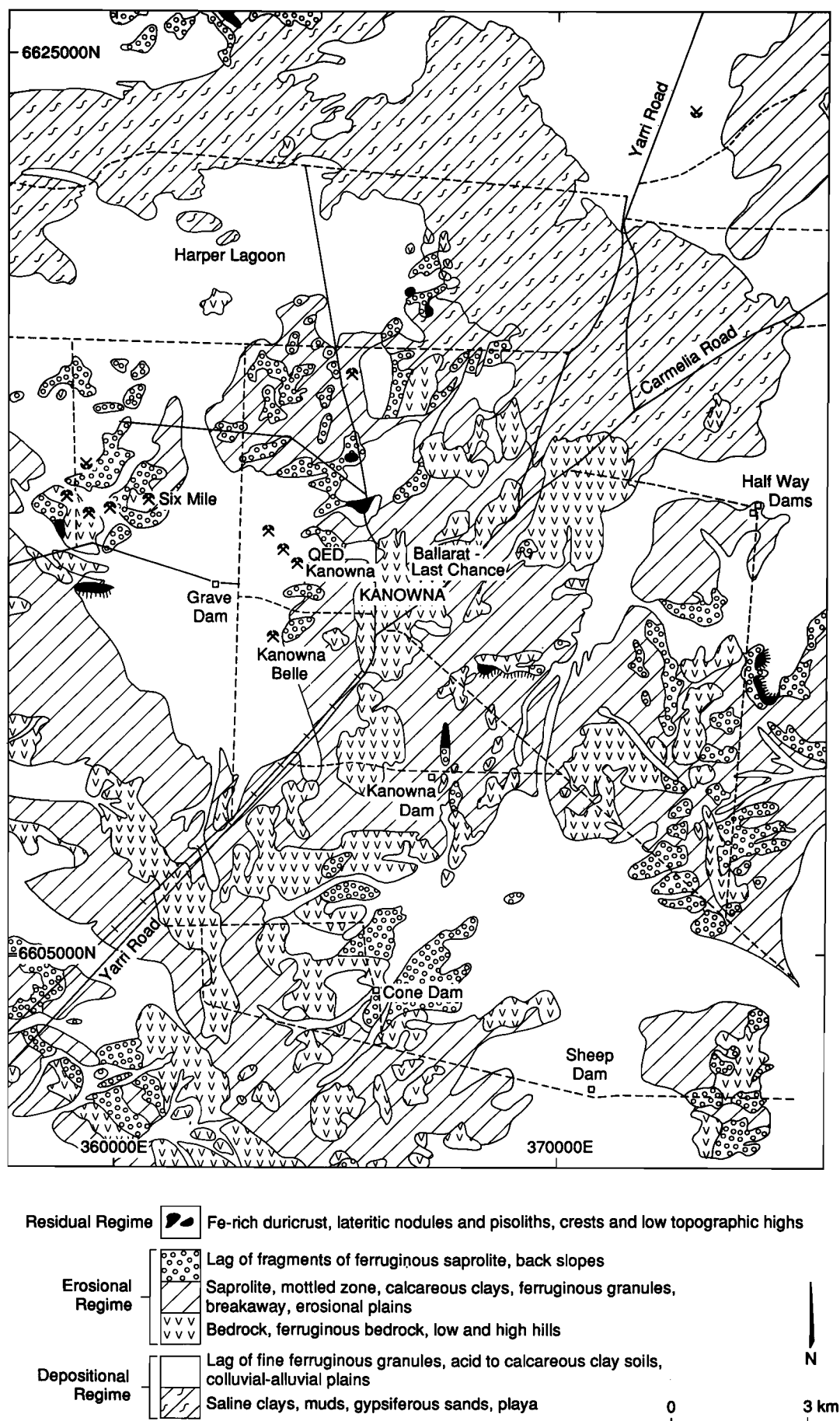


Fig. 4.22 Simplified regolith map of the Kanowna district.

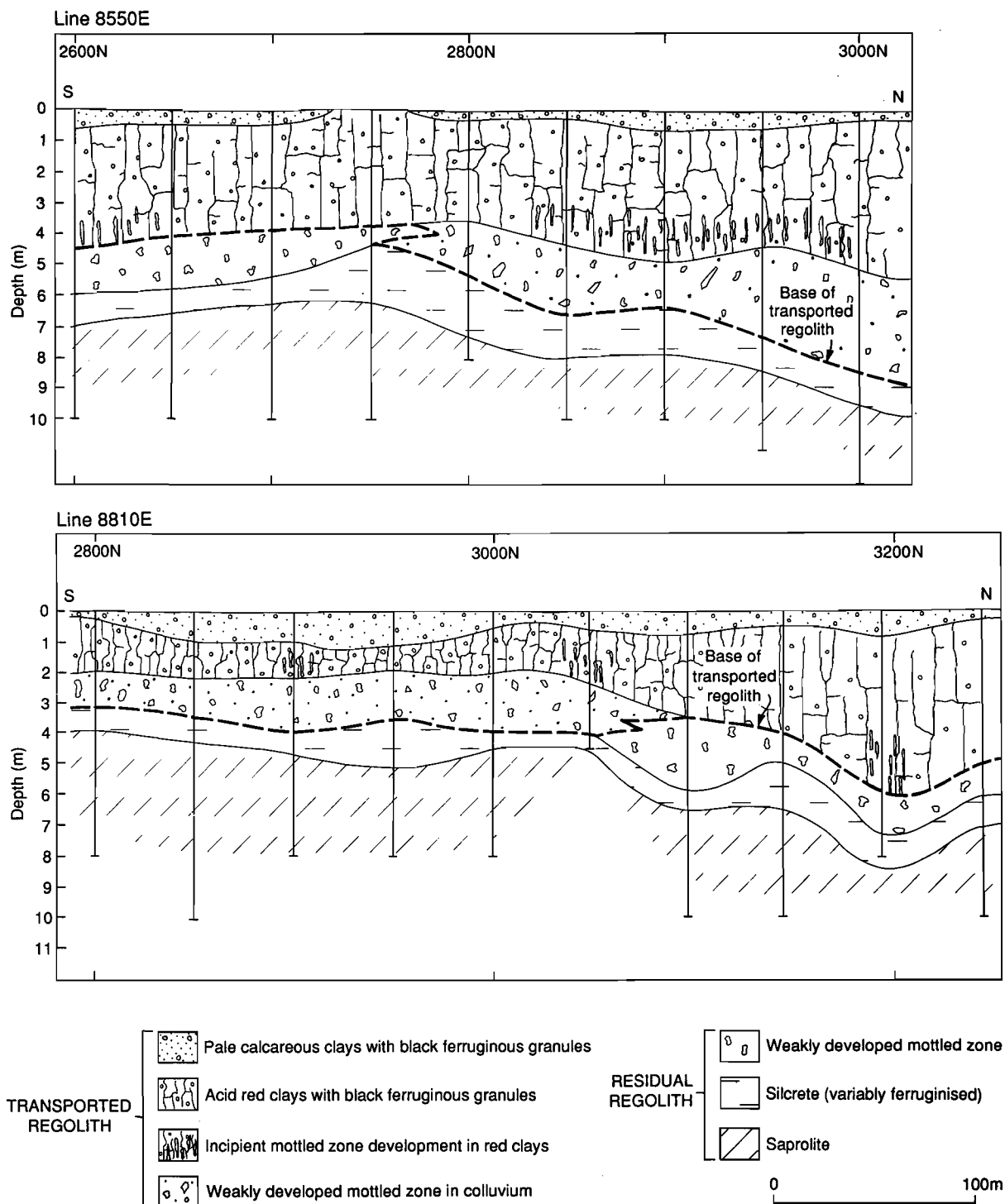


Fig. 4.23 Cross sections showing the regolith stratigraphy for lines 8550 mE and 8810 mE, overlying the Kanowna Belle Au deposit. The lines are located on Fig. 4.28.



The pisolitic clay horizon, 4 to 6 m thick, is characterised by sub- to well-rounded pisoliths, with greenish-brown to grey cutans, in a matrix of pale-pink through to grey clays with minor detrital quartz. Pisoliths are typical of the palaeochannel profiles in the Kalgoorlie region.

The underlying deep leads comprise angular to sub-angular, bipyramidal, quartz-rich alluvial sediments. Bedding and grading within the basal units of the deep leads are enhanced by fine, black organic-rich material forming bands along with the gravels.

Saprolite forms the lowest unit of the weathering profile with variably green, orange to white clays overlying bedrock.

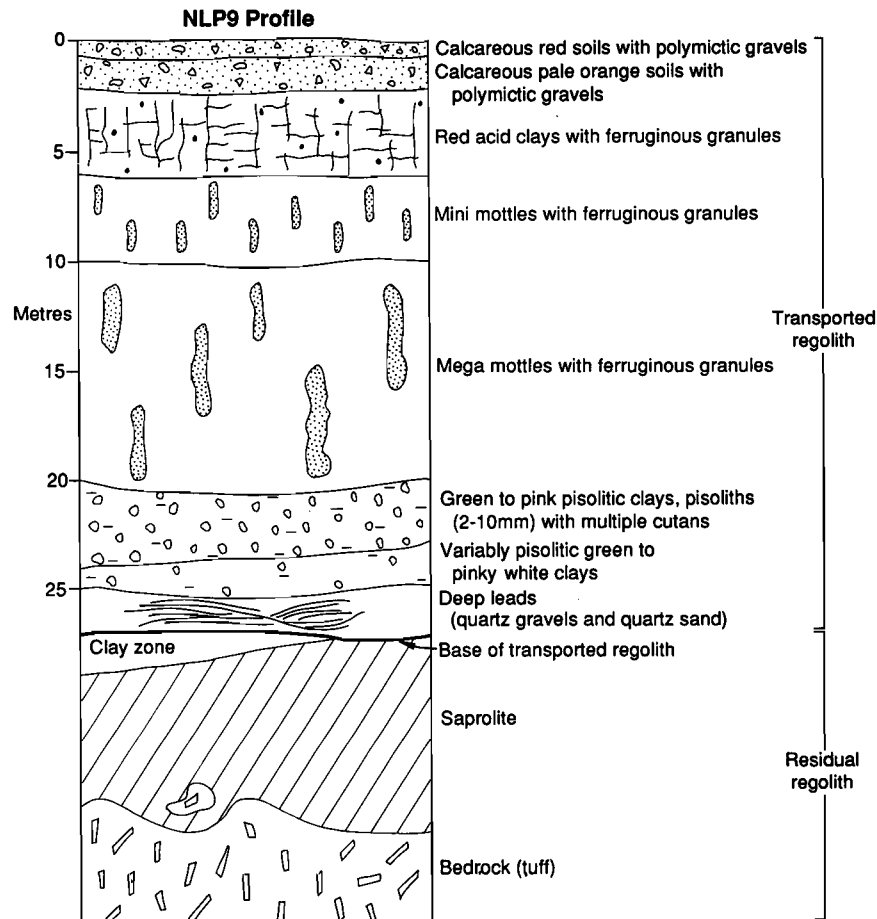


Fig. 4.24 Regolith section through the palaeochannel at NLP 9 pit, Kanowna district.

#### 4.3.4 Development of ferruginous granules

Granules, extracted from the bulk soil samples, are remarkably uniform, occurring as black, hematite-maghemite rich, sub- to well-rounded granules <0.2 to 15 mm in size (Fig. 4.25A). Typically the granules have an earthy to sub-metallic lustre and some thin earthy, clay cutans are developed around rare spherical granules.

Petrographic examination of granules indicated that they have formed by a combination of pathways (Fig. 4.26). Textural variations have enabled recognition of the four major granule groups outlined below:

1. *Granules developed within the soils:* These are textureless granules formed by the replacement of clays by hematite. Polished sections of these granules show brown, ferruginous clays pervasively replaced, along cracks and voids by hematite (Fig. 4.25B,C).

2. *Granules derived from ferruginisation of mineralised bedrock or saprolite fragments:* these granules are identified by preservation of relict rock fabrics and pseudomorphs after rock-forming minerals preserved within the interiors of the granules (Fig. 4.25D,E,F). Figure 8E shows numerous hematite pseudomorphs after carbonate rhombs within the granules taken from the soils above the orebody.
3. *Ferruginised cellulose:* some of the granules represent ferruginised cellulose fragments, which are clearly identifiable by the intricate preservation of individual cell walls now totally replaced by hematite. The cellulose fragments may represent vestiges of penetrative root systems which show a close spatial relationship to areas of granule development within the clays and mottled zones. The cavities generated by root penetration may, upon death of the roots, provide voids within which Fe-oxides may be precipitated, with the hematite selectively replacing dead cellulose.
4. *Concentrically zoned granules:* these granules have a cutan developed around a nucleus of the cellulose, quartz, clays, and saprolite fragments. Quartz fragments are commonly incorporated into the concentric bands indicating multiple periods of development.

#### 4.3.5 Regolith-landform model

Generalised regolith-stratigraphic relationships for the Kanowna district are shown in Fig. 4.27. This figure is based on the district-scale regolith-landform assessment throughout and a detailed study at the Kanowna Belle and NLP9 pits. The regolith-landform relationships and regolith stratigraphies indicate a polyphase, multi-process history. The wide range of regolith units developed within the Kanowna Belle district reflects the highly variable bedrock geology described above.

#### 4.3.6 Geochemical dispersion in ferruginous granules and soils - Kanowna Belle

The main aim of this study was to assess the use of soils and ferruginous granules, which are common in the soils, as sampling media for exploration geochemistry.

A total of 175 samples were collected at 1 m intervals from two traverses (Fig. 4.28). From these, 75 were selected for analysis, of which 38 were ferruginous granules separated from bulk soil samples from depths of 0-1 m and 2-3 m. Ferruginous granules occur throughout the soil but were chosen for separation from these two depths. The black ferruginous granules were removed from the bulk soil by wet sieving. A total of 37 whole soil samples, comprising calcareous (0-1 m) and acid (2-3 m) red clay soils, were also analysed.

#### Geochemistry

The granules from both depths (0-1, 2-3m) are comprised mainly of  $\text{Fe}_2\text{O}_3$  (68.6-78.8%),  $\text{SiO}_2$  (10.0-22.3%), and  $\text{Al}_2\text{O}_3$  (5.1-7.8%) which, when combined, account for 95% of the total granule composition (Tables 4.8, 4.9 and Fig. 4.29). Abundances of these elements are very similar for the ferruginous granules from both depths. These elements occur mainly as hematite, maghemite and quartz. The soils contain higher concentrations of  $\text{SiO}_2$  (38.7-67.7%) and  $\text{Al}_2\text{O}_3$  (5.6-17.7%), relative to the ferruginous granules, principally occurring in quartz and clay minerals (kaolinite and smectite).

The results are tabulated and plotted in Appendix X together with histograms of the elements for the ferruginous granules and soils. Element associations were investigated using correlation matrices and binary plots (Appendix X). Summary statistics for ferruginous granules and soils are given in Tables 4.8 and 4.9.

The alkaline earth elements, Ca and Mg, are strongly concentrated in the top 1 m of the regolith. Mean concentrations of Ca and Mg differ significantly between the top soil (CaO 7.41%, MgO 1.34%) and sub-surface soil (CaO 0.28%, MgO 0.85%). Calcium and Mg contents are very low in the ferruginous granules. They occur predominantly as calcite, gypsum and dolomite with minor quantities in smectite and inter-stratified clay minerals. Calcium is strongly correlated with Mg.

The  $\text{K}_2\text{O}$  content of the ferruginous granules is low compared to that of the soils. The amount of  $\text{K}_2\text{O}$  is more concentrated in the top-soil than in sub-surface soil. Potassium concentrations range from 0.31% to 1.07% in soils, occurring as muscovite and illite.



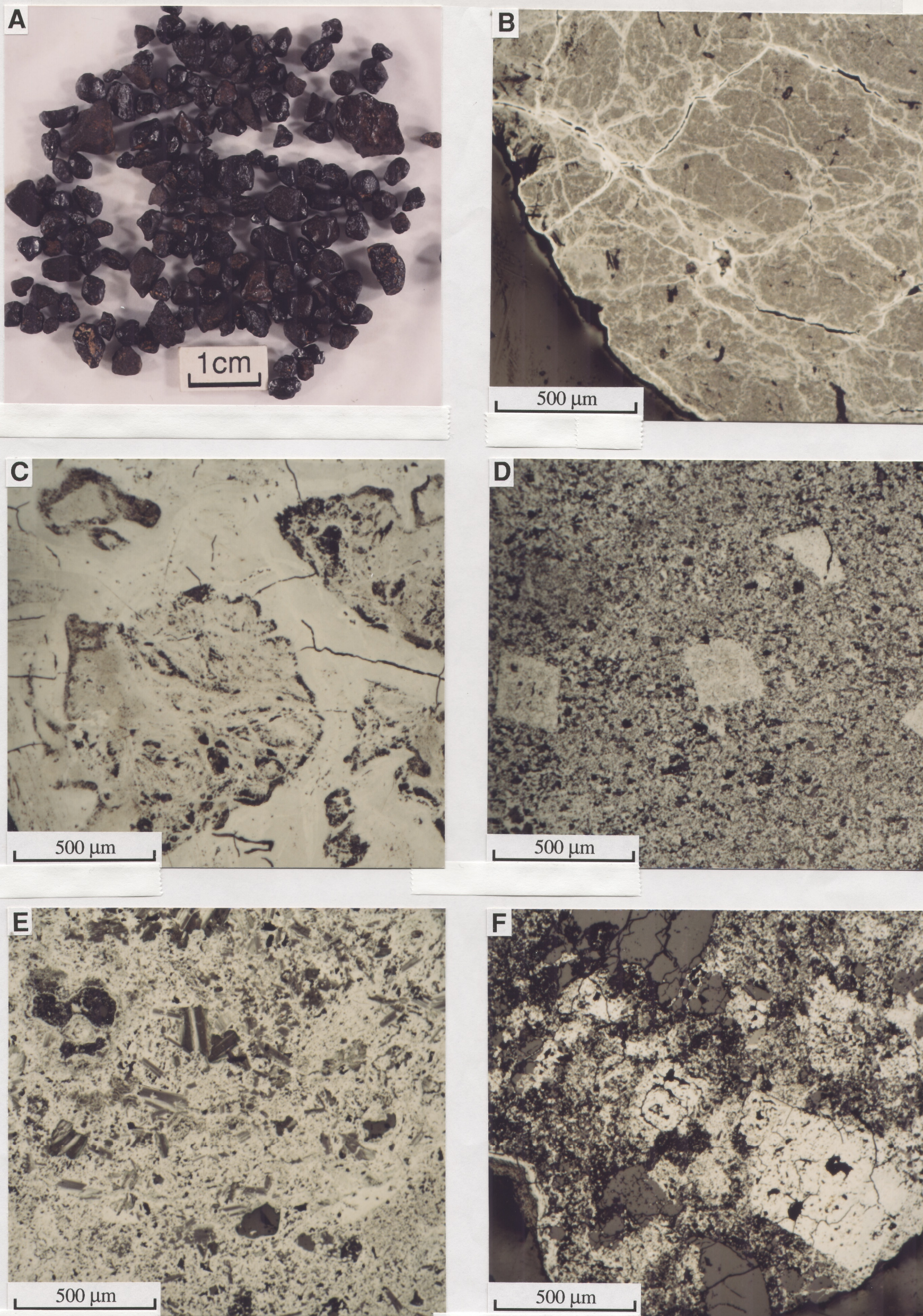


Fig. 4.25 Ferruginous granules and their petrographic characteristics, Kanowna Belle. (A) Black ferruginous-granules separated from red clays, (B) photomicrograph of polished section of a granule showing infusion of Fe along cracks, (C) photomicrograph of polished section of a granule showing complete replacement of clays by hematite, (D) hematite pseudomorphs after carbonate rhombs within a ferruginous granule, (E) goethite pseudomorph after mica, and (F) cubic hematite pseudomorphs possibly after pyrite within a massive hematite-rich matrix.







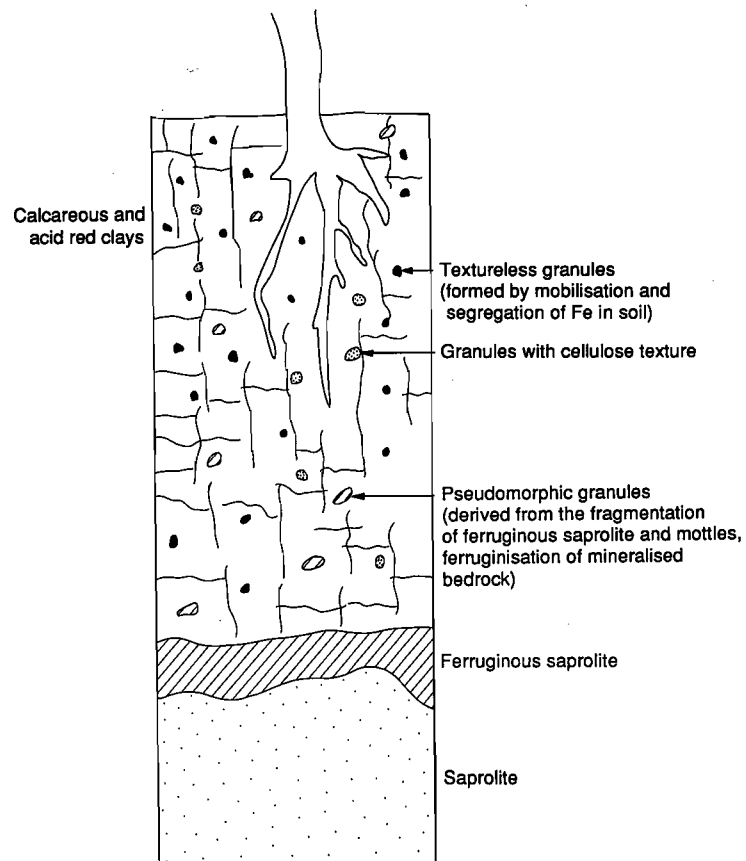


Fig. 4.26 Types of ferruginous granules and their possible origins within the upper part of a regolith profile, Kanowna district.

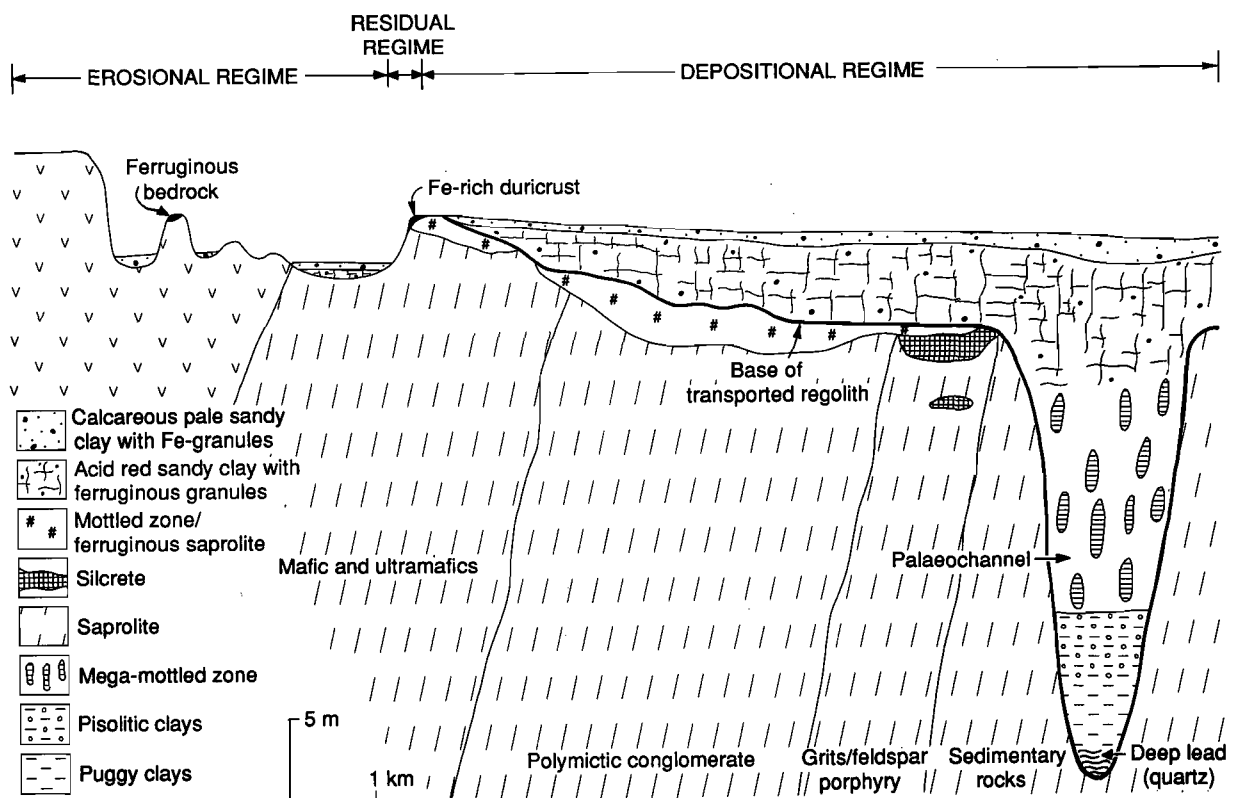


Fig. 4.27 Regolith model of the Kanowna Belle area.

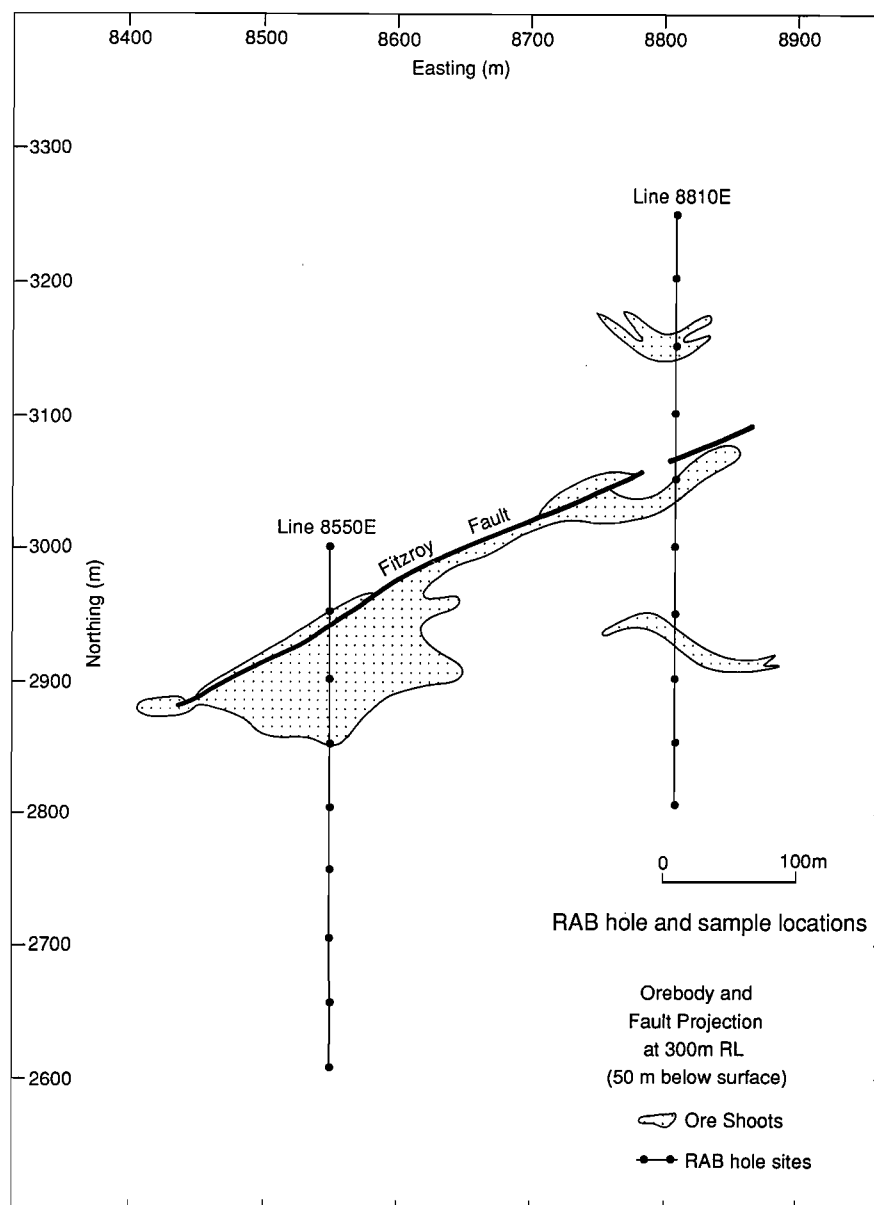


Fig. 4.28 Location of the main ore-shoots and sampling lines, Kanowna Belle Au deposit. Northings and eastings are for the local mine grid.

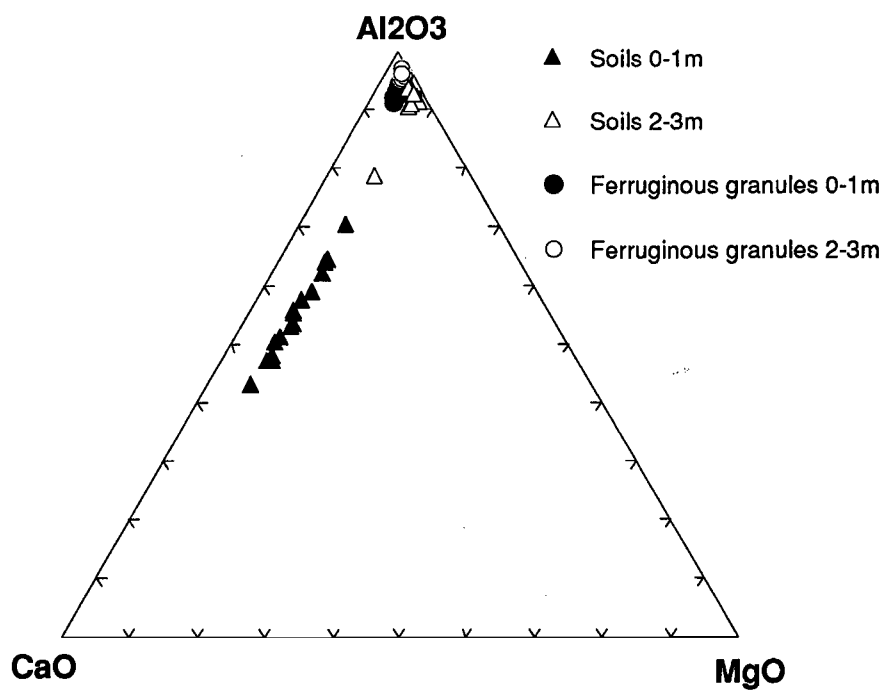
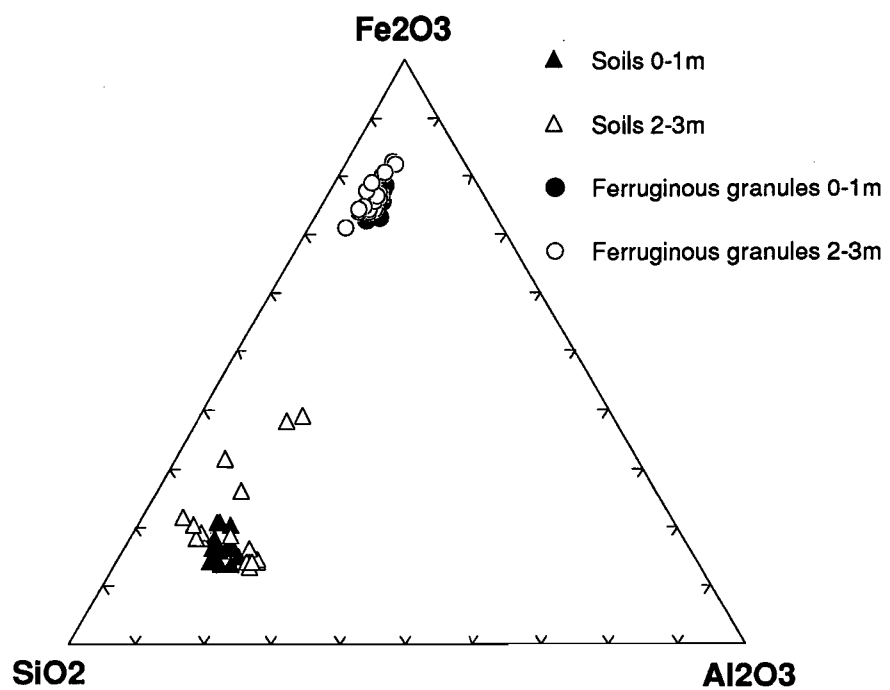


Fig. 4.29 Triangular diagrams showing compositions of soils and ferruginous granules in terms of  $\text{SiO}_2$ ,  $\text{Al}_2\text{O}_3$ ,  $\text{Fe}_2\text{O}_3$ ,  $\text{CaO}$  and  $\text{MgO}$ , Kanowna Belle Au deposit.

Table 4.8: Some summary statistics on element concentrations in bulk soils, Kanowna Belle

ELEMENT	BULK SOILS									
	0-1m					2-3m				
	Mean	Std. Dev.	Minimum	Maximum	Median	Mean	Std. Dev.	Minimum	Maximum	Median
SiO <sub>2</sub> %	50.9	2.4	45.9	55.7	51.2	57.4	7.1	38.9	67.7	57.1
Al <sub>2</sub> O <sub>3</sub> %	10.7	1.3	9.2	14.3	10.5	13.1	4.2	5.6	17.7	13.3
Fe <sub>2</sub> O <sub>3</sub> %	12.3	2.1	9.9	17.4	11.9	17.8	7.5	11.1	34.4	16.6
MgO %	1.34	0.13	1.11	1.58	1.34	0.85	0.26	0.32	1.23	0.92
CaO %	7.41	1.67	4.62	10.80	7.49	0.28	0.51	0.07	2.32	0.14
Na <sub>2</sub> O %	0.50	0.17	0.21	0.96	0.47	0.77	0.28	0.31	1.16	0.70
K <sub>2</sub> O %	0.87	0.13	0.64	1.07	0.87	0.66	0.21	0.31	1.05	0.69
TiO <sub>2</sub> %	0.59	0.06	0.51	0.72	0.59	0.79	0.12	0.55	1.04	0.81
LOI %	13.6	1.3	9.7	15.4	13.8	7.4	2.2	4.0	10.1	8.8
TOTAL	98.18	1.75	94.70	99.84	98.91	98.99	0.55	97.10	99.56	99.08
Mn ppm	445	41	353	507	447	156	21	126	201	150
Cr ppm	538	95	441	731	521	902	650	489	2850	728
V ppm	173	29	142	236	167	203	91	120	403	175
Cu ppm	41	3	36	46	41	32	6	20	41	32
Pb ppm	13	2	10	20	13	9	4	2	19	8
Zn ppm	43	4	36	50	43	34	13	15	52	33
Ni ppm	113	10	100	134	113	102	39	46	210	100
Co ppm	18	3	14	25	17	10	4	5	25	9
As ppm	29	10	18	49	26	64	65	21	238	48
Sb ppm	5.0	2.7	0.7	12.0	5.0	9.8	11.1	2.0	39.0	6.0
Bi ppm	0.7	0.3	0.7	2.0	0.7	0.9	0.7	0.7	3.0	0.7
Mo ppm	1.0	0.6	0.7	2.0	0.7	2.0	1.0	0.7	4.0	2.0
Ag ppm	0.7	0.0	0.7	0.7	0.7	0.5	0.2	0.2	0.9	0.4
Sn ppm	1.0	0.7	0.7	3.0	0.7	2.3	1.0	1.0	4.0	2.0
Ge ppm	0.7	0.0	0.7	0.7	0.7	0.9	0.5	0.7	2.0	0.7
Ga ppm	15.6	1.2	14.0	19.0	15.0	22.0	2.7	18.0	28.0	22.0
W ppm	3.0	1.6	0.7	5.0	3.5	4.8	1.5	2.0	7.0	5.0
Ba ppm	390	98	234	571	362	533	193	321	878	435
Zr ppm	123	11	106	142	122	164	21	117	209	165
Nb ppm	6.3	1.7	3.0	9.0	6.5	8.8	2.5	5.0	14.0	9.0
Se ppm	nd	nd	nd	nd	nd	3.3	1.5	1.0	7.0	3.0
Be ppm	1.0	0.0	1.0	1.0	1.0	0.7	0.4	0.3	1.0	0.7
Au ppb	90	70	17	232	76	11	15	1	57	5
Ce ppm	40	7	30	55	37	nd	nd	nd	nd	nd

Table 4.9: Some summary statistics on element concentrations in ferruginous granules separated from soils, Kanowna Belle.

ELEMENT	FERRUGINOUS GRANULES									
	0-1m					2-3m				
	Mean	Std. Dev.	Minimum	Maximum	Median	Mean	Std. Dev.	Minimum	Maximum	Median
SiO <sub>2</sub> %	15.2	1.2	13.1	18.6	15.0	15.6	3.0	10.0	22.2	16.0
Al <sub>2</sub> O <sub>3</sub> %	7.4	0.6	6.3	8.7	7.3	6.4	0.9	5.1	7.6	6.7
Fe <sub>2</sub> O <sub>3</sub> %	72.2	1.6	69.1	75.0	72.6	72.8	2.9	68.6	78.8	72.1
MgO %	0.25	0.02	0.20	0.28	0.24	0.15	0.03	0.12	0.21	0.14
CaO %	0.26	0.06	0.16	0.39	0.26	0.08	0.02	0.05	0.13	0.08
Na <sub>2</sub> O %	0.10	0.02	0.07	0.14	0.10	0.08	0.01	0.06	0.11	0.08
K <sub>2</sub> O %	0.37	0.05	0.27	0.46	0.37	0.23	0.09	0.05	0.36	0.22
TiO <sub>2</sub> %	0.76	0.03	0.70	0.80	0.75	0.76	0.05	0.67	0.90	0.76
LOI %	2.9	0.1	2.7	3.2	2.8	3.1	0.4	2.5	3.8	3.2
TOTAL	99.36	0.36	98.61	99.73	99.42	99.18	0.45	98.14	99.68	99.32
Mn ppm	1001	138	765	1270	1000	490	151	181	774	502
Cr ppm	3163	187	2850	3560	3140	3746	1102	2860	6920	3570
V ppm	979	58	871	1080	985	1025	61	890	1140	1010
Cu ppm	64	6	57	77	62	40	10	27	59	38
Pb ppm	69	4	61	74	70	60	5	53	67	59
Zn ppm	43	7	32	59	43	20	8	8	34	19
Ni ppm	221	25	179	264	218	177	37	112	253	182
Co ppm	16	2	12	19	16	14	3	9	23	13
As ppm	241	34	201	321	238	292	79	201	485	290
Sb ppm	37.9	2.6	34.0	42.0	38.0	42.7	8.7	32.0	67.0	42.0
Bi ppm	1.3	1.0	0.7	4.0	0.7	1.2	0.8	0.7	3.0	0.7
Mo ppm	1.6	1.1	0.7	4.0	0.7	3.1	1.5	0.7	6.0	2.5
Ag ppm	0.7	0.0	0.7	0.7	0.7	0.7	0.0	0.7	0.7	0.7
Sn ppm	6.1	2.7	0.7	9.0	6.0	5.9	2.8	0.7	9.0	7.0
Ge ppm	0.8	0.5	0.7	3.0	0.7	0.7	0.0	0.7	0.7	0.7
Ga ppm	33.2	2.1	29.0	39.0	33.0	32.2	2.7	28.0	37.0	32.5
W ppm	2.4	1.7	0.0	6.0	3.0	3.1	2.8	0.7	8.0	1.8
Ba ppm	1379	361	812	2120	1300	1476	510	840	2560	1370
Zr ppm	167	6	158	179	167	161	9	136	176	164
Nb ppm	3.7	1.8	0.7	6.0	4.0	4.1	2.4	0.7	8.0	5.0
Se ppm	4.8	2.1	0.7	9.0	5.0	11.2	2.8	7.0	18.0	11.0
Be ppm	1.0	0.0	1.0	1.0	1.0	1.0	0.2	0.3	1.0	1.0
Au ppb	38	45	2	147	22	7	16	2	71	2
Ce ppm	29	6	17	38	29	5	5	1	22	4

Mineralisation is indicated by a multi-element geochemical halo within both the ferruginous granules and the soils (Figs 4.30-4.33). The granules are anomalous in Au, Sb, As, and Ce (Figs 4.31, 4.33). High values of Au coincide with the elevated Sb and As. The mean values of As, Sb, Au and Ce in granules collected across the Kanowna Belle orebody are considerably elevated relative to granules collected away from the known mineralisation (Table 4.10).

Gold is most concentrated in soil samples with the average surface soil expression (90 ppb) consistently 10-20 ppb above the concentrations obtained from the ferruginous granules extracted from the same soils. Gold concentrations in the top metre range from 17 to 232 ppb and are commonly in excess of 60 ppb (Figs 4.30, 4.32). There is a considerable decrease in Au abundances in the soil samples collected from 2 to 3 m. The observed peak Au concentrations within the surface calcareous soils conform well with the sub-surface position of the major ore shoots. This observation is consistent with previous findings in the Southern Yilgarn Craton (Butt *et al.*, 1991; Anand *et al.*, 1991), in which a close correlation has been identified between Au and pedogenic carbonates.

In the traverses across Kanowna Belle, the near surface (0-1m) ferruginous granules mimic the bulk soil pattern for Au (Figs 4.31, 4.33). Gold concentrations in ferruginous granules range from 2 to 147 ppb. The granules separated from the 2-3 m soil sample contain lesser amounts of Au. A high 75 ppb peak for Au in the granules separated from an acid red clay (2-3 m depth) is observed at 3200N, 8810E. However, the peak may be due to particulate gold.

Arsenic and Sb are notably enriched in the granules in the area above and surrounding the orebody, with respective concentrations on average of 4 and 7 times greater than those in the bulk soils. Mean concentrations of As and Sb are similar for the ferruginous granules separated from the top soil (As 241 ppm, Sb 38 ppm) and sub-surface soil (As 292 ppm, Sb 43 ppm). These abundances are significantly greater than known background levels (As <40 ppm, Sb <1 ppm, Table 4.10) and are associated with Au mineralisation.

Cerium is present in significant concentrations both in soil and in the ferruginous granules and is strongly correlated with Ca. It ranges from 7 to 37 ppm in soils and 17 to 38 ppm in ferruginous granules.

The ferruginous granules are enriched in TiO<sub>2</sub>, Mn, Cr, V, Cu, Pb, Ni, Mo, Ba, Ga and Zr relative to the bulk soils. By contrast, the soils contain higher concentrations of Ce, Zn, Co and Nb. Barium concentrations are highly elevated in both the soils (500 ppm) and the granules (1500 ppm) when compared to regional data, but are more elevated in the ferruginous granules with concentrations commonly exceeding 2000 ppm (Tables 4.8, 4.9). Chromium, V, As, Sb, and Ba show very close associations with Fe. These elements probably substitute for, or are absorbed on to Fe-oxides such as hematite and maghemite. Strong correlations exist between Cu-K-Mg, and Zn-Mg-K which suggest that these elements are associated with clays such as smectite and illite.

Both Cr and V show intimate association with Fe, As, Sb and Ba within the soils. Surprisingly, this close association is not mimicked by the ferruginous granules with Cr in the soils being most closely associated with As, Sb, and Fe whereas V shows no real association with any element except Ba.

#### *Palaeochannel environments - NLP9 Pit*

The deep-leads occur within alluvial palaeochannels, with the gold occurring in a basal clayey grit and in shallower clay horizons. In the latter case, supergene processes are interpreted to have re-deposited gold derived from the alluvial mineralisation.

The objective for the study at the NLP9 Pit was to determine whether there is a surface or near-surface geochemical expression of the palaeochannel-related Au deposit. Samples of the major regolith units were analysed for Au and a range of minor and trace elements with distributions plotted against depth (Fig. 4.34). The regolith stratigraphy of the profile is discussed in section 3.4.3.

Gold is concentrated significantly within the calcareous soils, within the mega-mottle zone and is present in very small concentrations in other regolith units. Gold reaches 250 ppb in the mega-mottled zone. The processes of enrichment of Au in mega-mottles and calcareous soils are not fully understood (Lintern and Butt, 1993). The processes may involve chemical transport of dissolved Au deep in the regolith by diffusion, capillarity, evapotranspiration, cycling by deep-rooted plants, and accumulation in the soil evaporite horizon.

Chromium, V, Cu and Zn are concentrated in the Fe-rich mottles. Aluminium shows increased concentrations towards the base of the clay-rich zones above the deep lead unit. The pisolitic clay horizon shows enrichment in Fe, Ni, Cr, V, Cu, Pb, Zn, As, Sb and Ba. Cerium, W, Zr, Mn, Ti and Co are concentrated within quartz-rich deep leads present at the base of the profile, overlying residual saprolite.

## Kanowna Belle geochemical sampling line 8810E - Soils

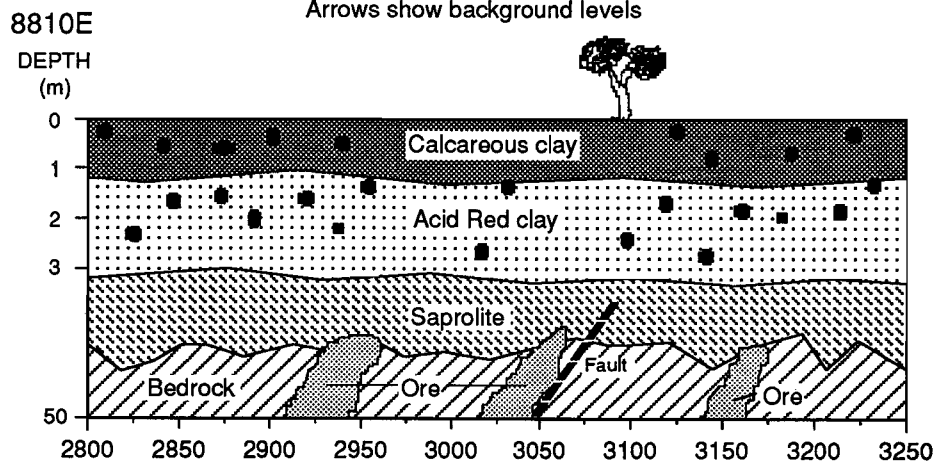
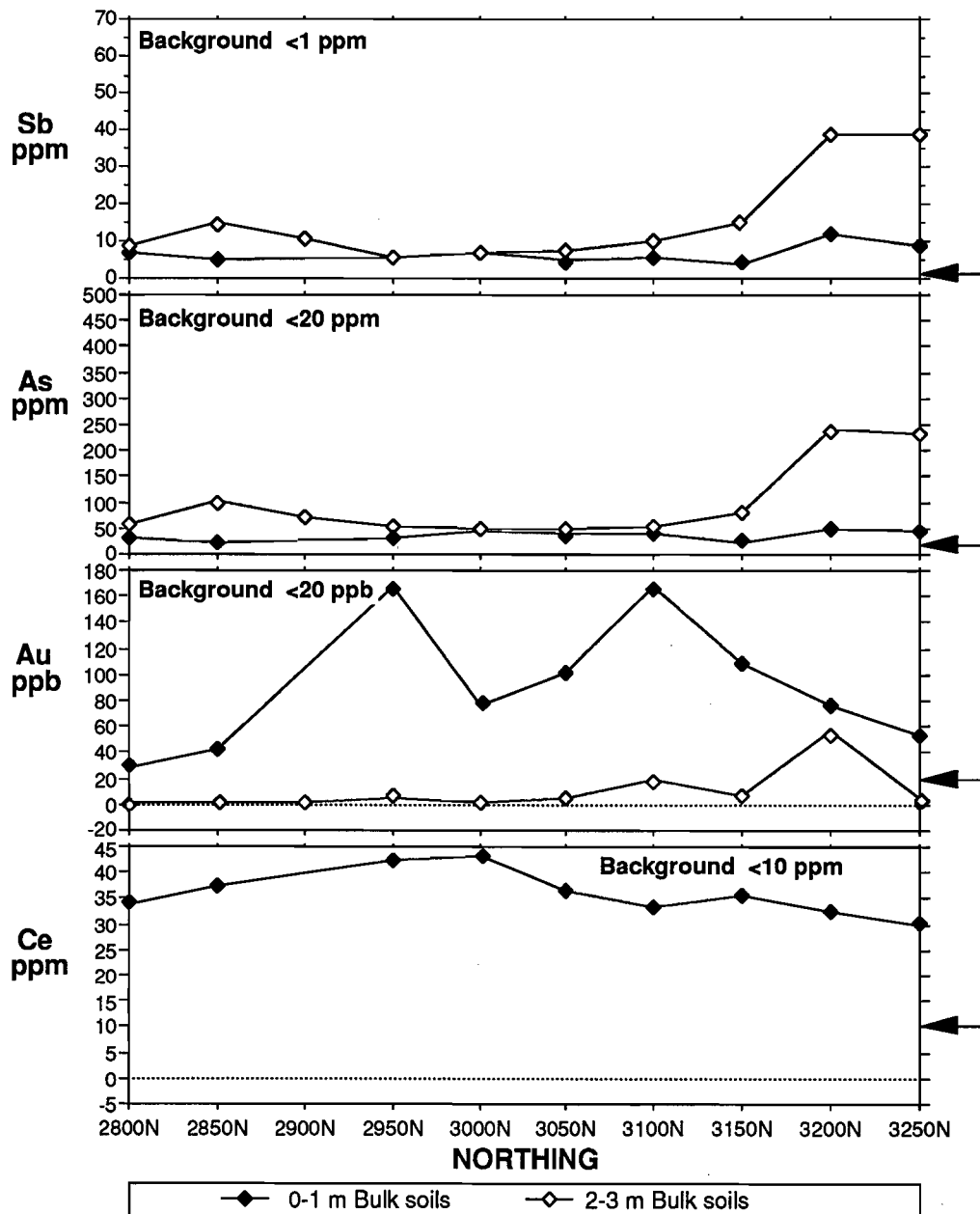


Fig. 4.30 Traverse along line 8810 mE showing the distribution of Sb, As, Au and Ce in soils, Kanowna Belle Au deposit.

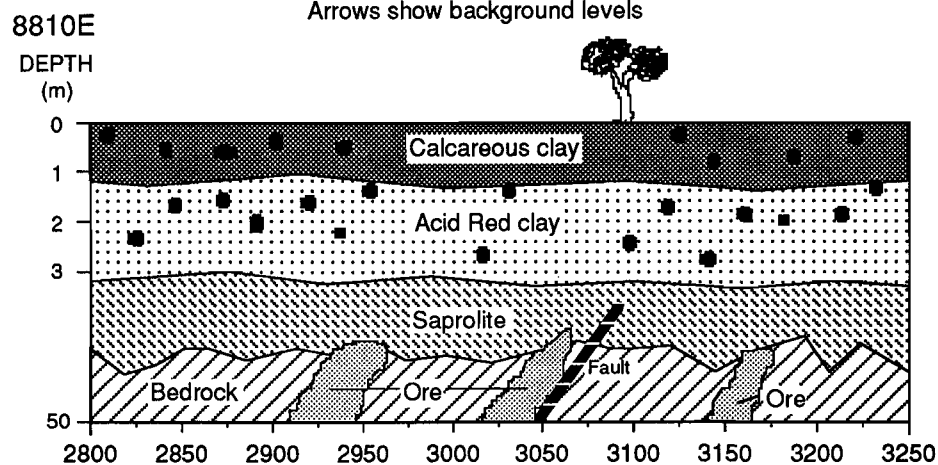
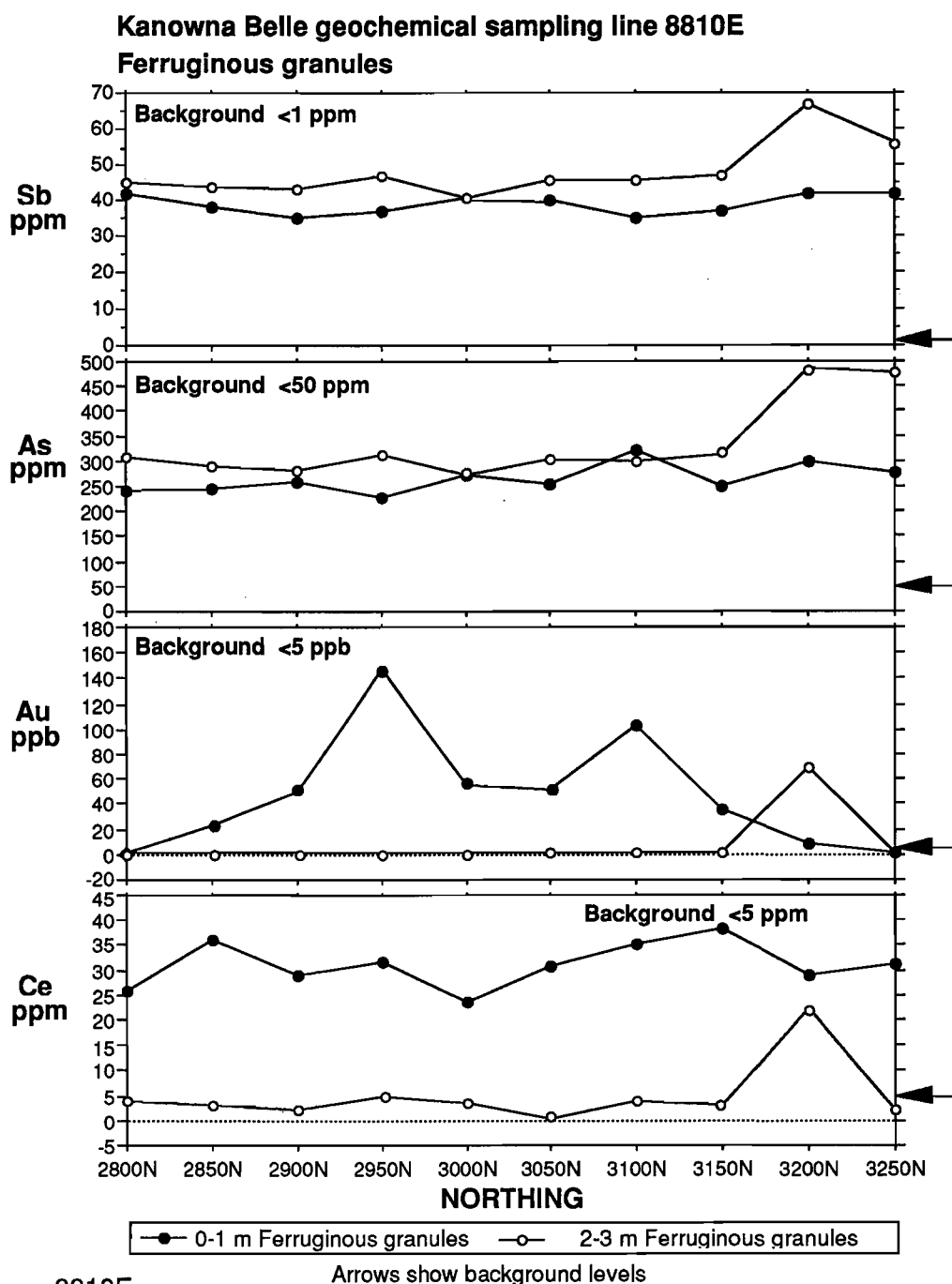


Fig. 4.31 Traverse along line 8810 mE showing the distribution of Sb, As, Au and Ce in ferruginous granules, Kanowna Belle Au deposit.

## Kanowna Belle geochemical sampling line 8550E - Soils

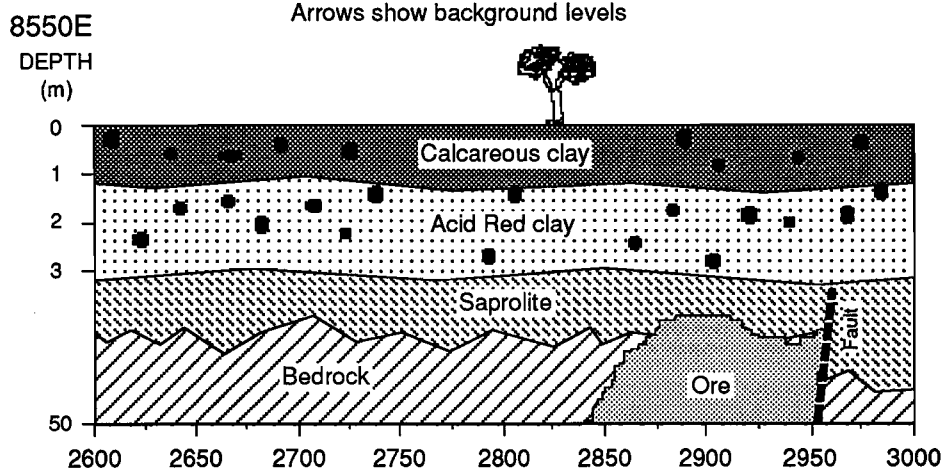
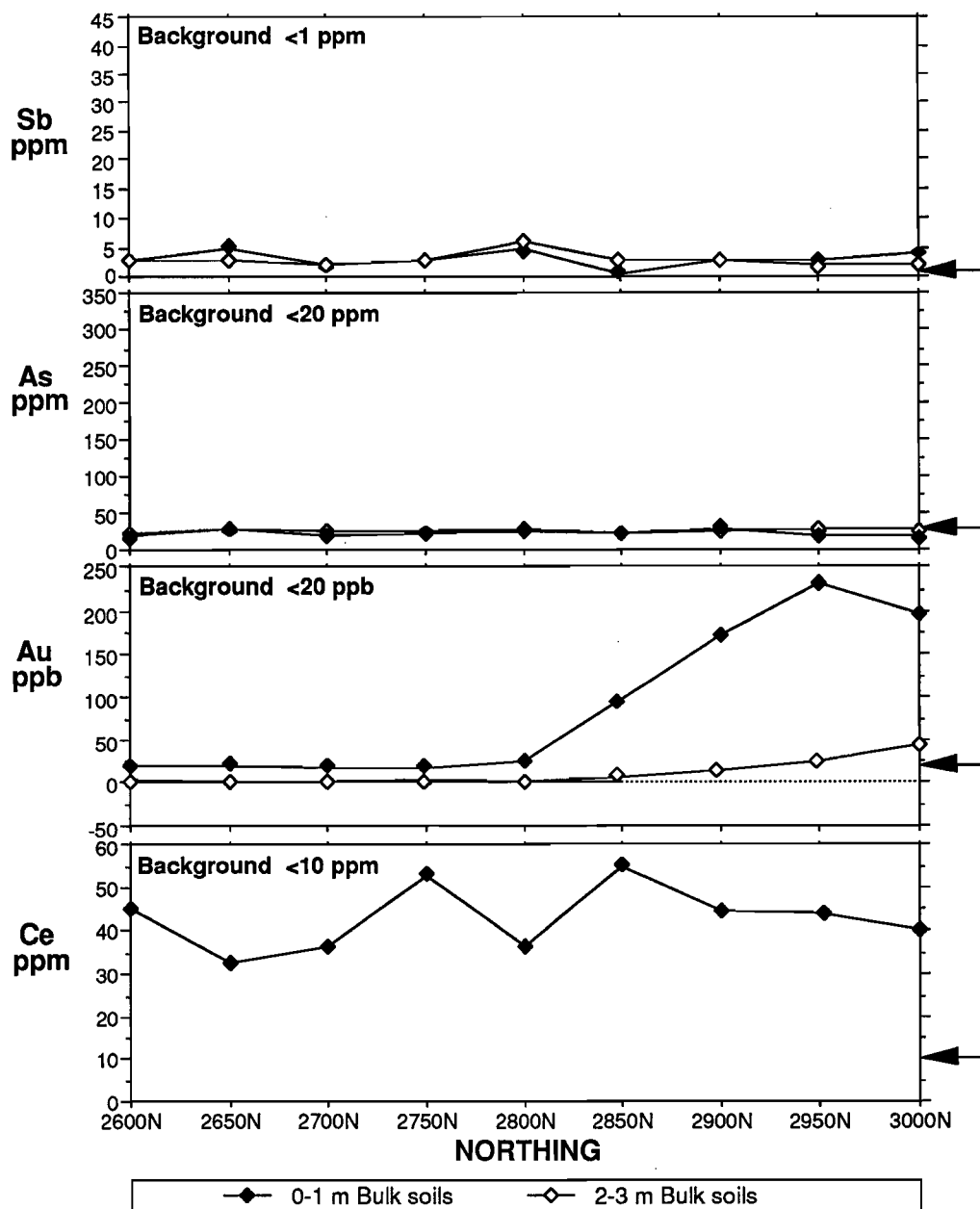


Fig. 4.32 Traverse along line 8550 mE showing the distribution of Sb, As, Au and Ce in soils, Kanowna Belle Au deposit.



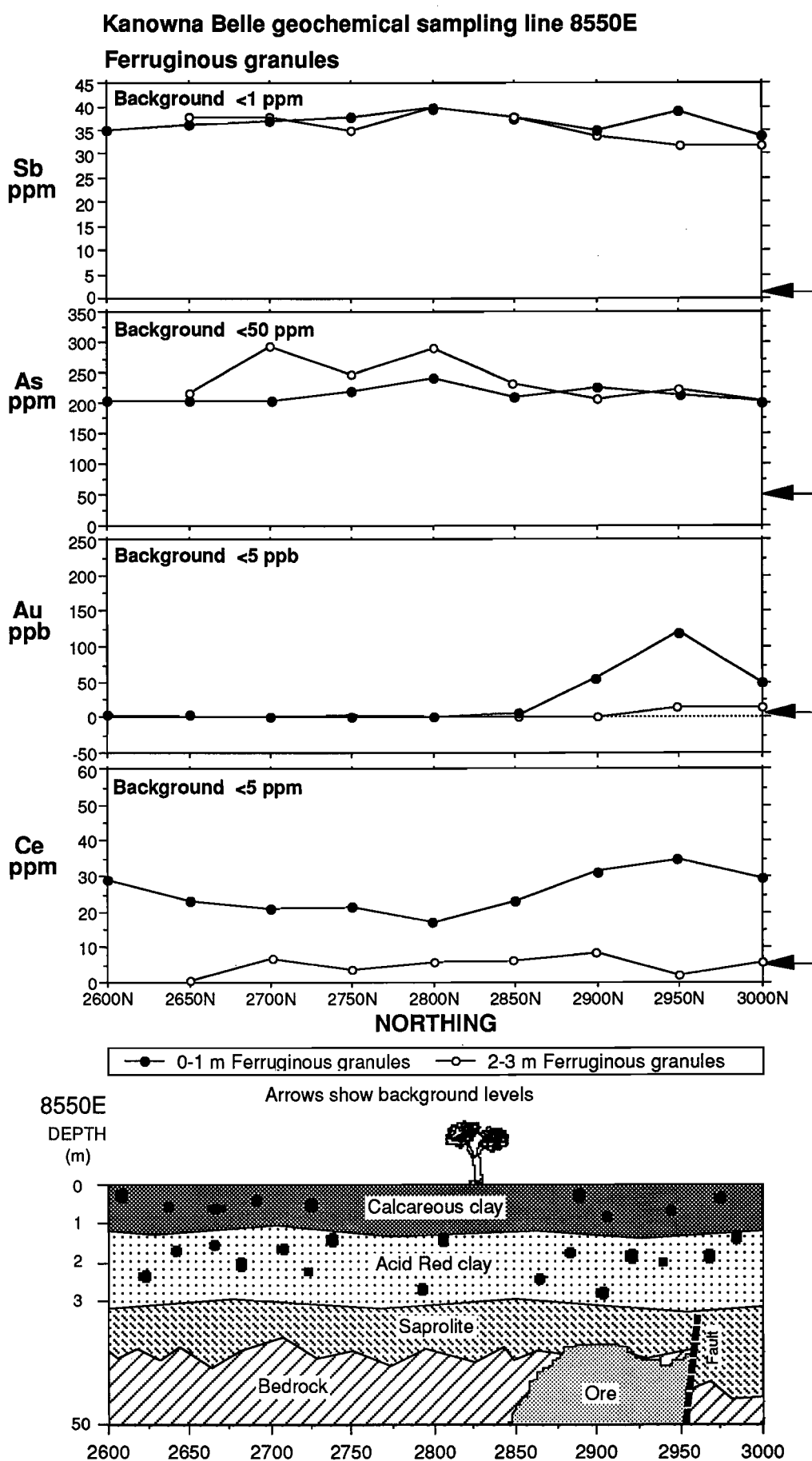


Fig. 4.33 Traverse along line 8550 mE showing the distribution of Sb, As, Au and Ce in ferruginous granules, Kanowna Belle Au deposit.

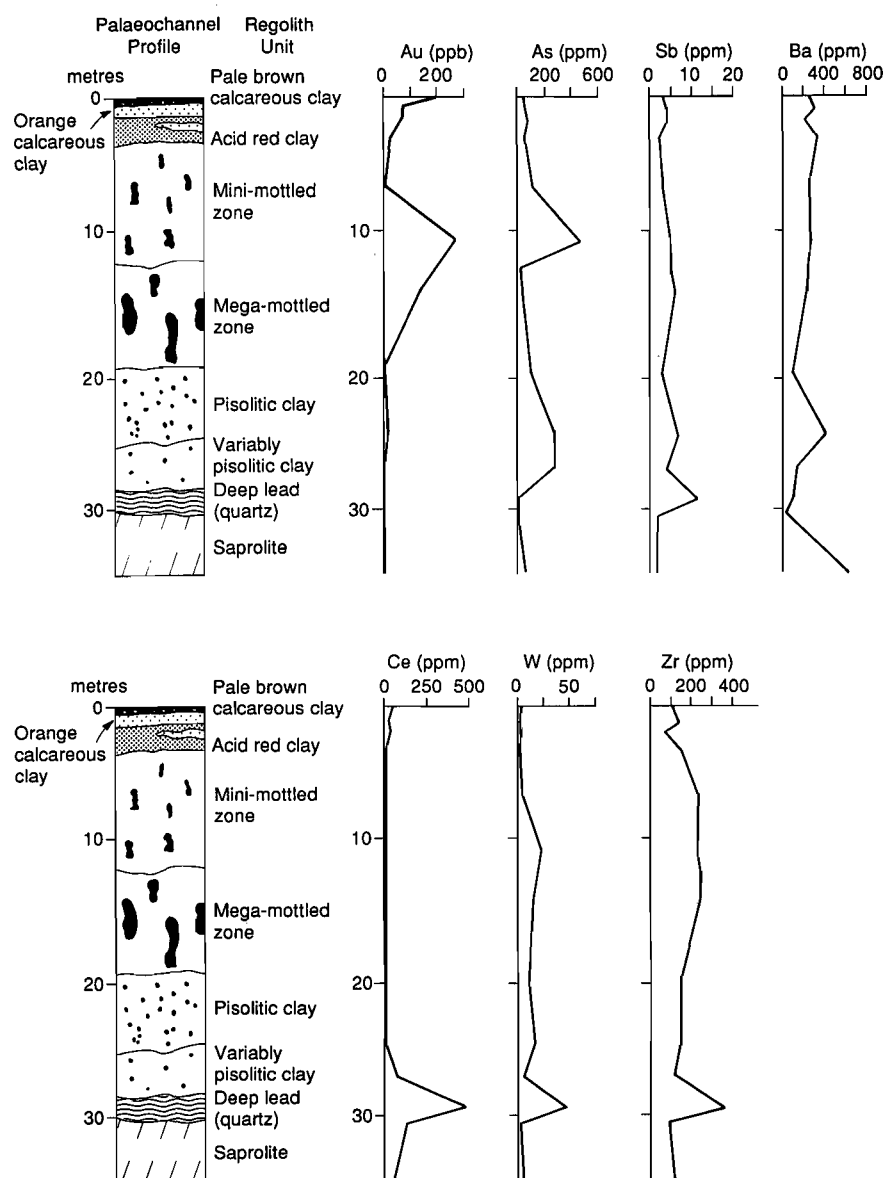


Fig. 4.34 Geochemical variations within the regolith units of the NLP 9 Pit, Kanowna.

These elements are contained in heavy minerals (zircon, scheelite) which were concentrated by the alluvial processes in the bed load of the deep lead systems. Aluminium and Fe are noticeably depleted within this zone due to the absence of a clay matrix. High Ba and Zn concentrations within the saprolite may be due to elevated levels in the bedrock.

#### 4.3.7 Implications in exploration

The red clays forming the top 2 to 6 m of the regolith overlying the Kanowna Belle deposit are transported. These red clays are underlain by residual saprolite which is up to 50 m thick, with the deepest development overlying the Fitzroy Fault. Ferruginous granules commonly occur in the soils and are formed by a combination of pathways. The soils show anomalous Au with weak As and Sb. By contrast, the ferruginous granules in the red clays are markedly anomalous in As, Sb and Au (relative to appropriate backgrounds) and the multi-element anomaly is broader and stronger (forming a larger target) in ferruginous granules than shown by soil geochemistry. Below this surface expression, there is a depleted or leached zone to depths of 50 m. The research shows that the Kanowna Belle deposit, concealed beneath 50 m of barren saprolite, has a significant multi-element surface geochemical expression.

The results from this study have substantial potential for application in the extensive deep saprolitic erosional and depositional regimes of the Kalgoorlie region. The main research findings and their implications in exploration for the Kanowna Belle research are listed in Table 4.11. A geochemical dispersion model is shown in Fig. 4.35.

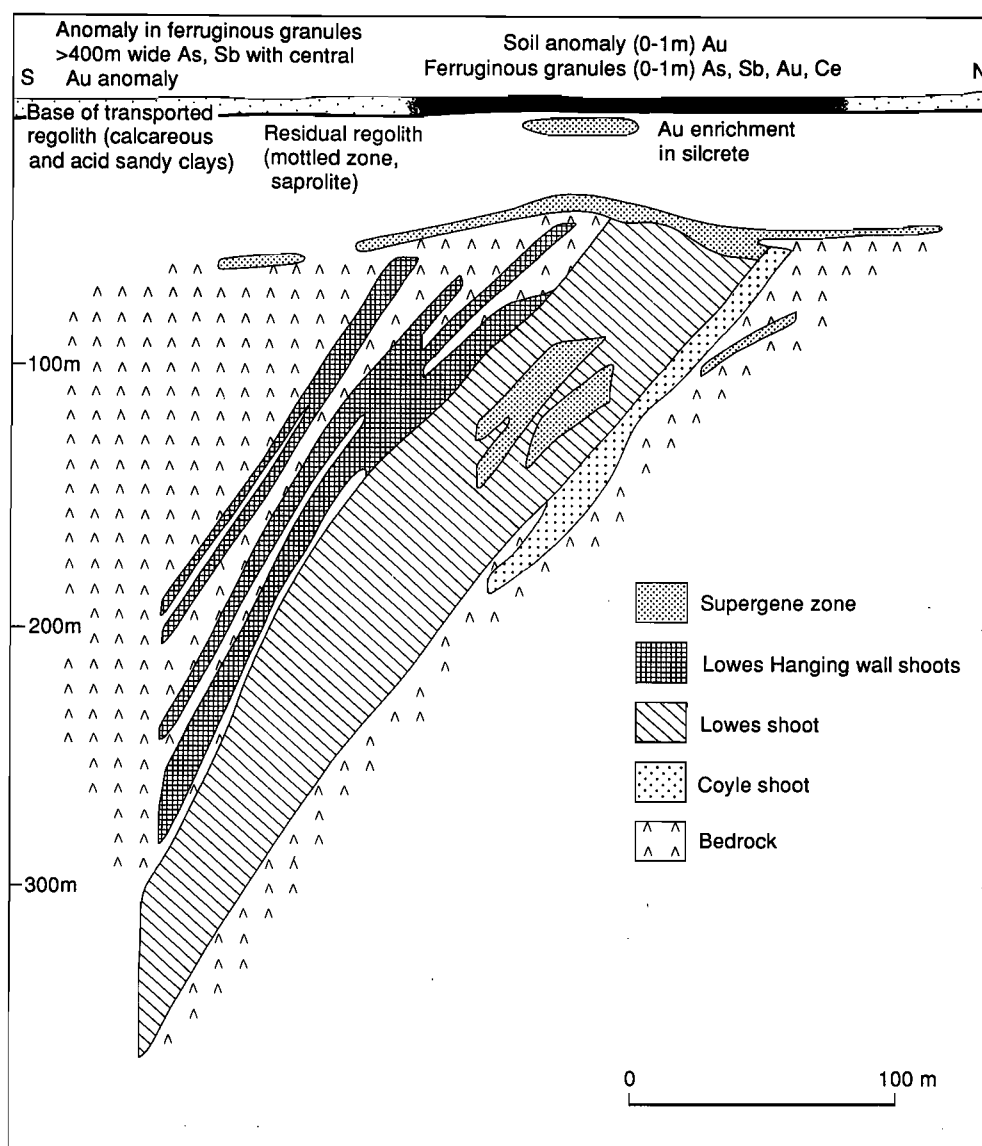


Fig. 4.35 Geochemical dispersion model of the Kanowna Belle orientation area.

**Table 4.10** Mean abundances of some elements in ferruginous granules separated from soils - from the Kanowna Belle, Wombola and Ora Banda orientation studies in the Kalgoorlie Region.

Element	Target, Kanowna Belle N=19	Background, Wombola N=3	Background, Ora Banda N=2
SiO <sub>2</sub> %	15.2	10.1	13.9
Al <sub>2</sub> O <sub>3</sub> %	7.4	9.8	13.3
Fe <sub>2</sub> O <sub>3</sub> %	72.2	70.6	62.6
As ppm	241	31	38
Sb ppm	38	<1	<1
Ba ppm	1427	207	180
Au ppb	38	<5	<5

**Table 4.11** The implications in exploration listed against the research findings, Kanowna Belle orientation study.

Research Findings	Implications in Exploration
<ul style="list-style-type: none"> <li>Regolith-landform relationships were mapped on district and local scale; erosional and depositional regimes are dominant. Residual regimes comprising lateritic duricrust and lateritic nodules and pisoliths are sporadically distributed. In the depositional areas, lateritic residuum is absent beneath the red clays but ferruginous granules are commonly developed in soils. Ferruginous granules in soils are developed by several pathways.</li> <li>District scale regolith-stratigraphic relationships were established.</li> <li>At Kanowna Belle, both calcareous soils and ferruginous granules show Au anomalies. However, multi-element anomaly (As and Sb) is broader and stronger in ferruginous granules than in the soils.</li> <li>The development of mega-mottled clay zone and pisoliths in grey clays are typical features of palaeochannel environments.</li> <li>In the palaeochannel environments (NLP9), anomalous concentrations of Au occur in mega-mottles and calcareous soils directly overlying the buried mineralisation.</li> <li>Geochemical data sets were established for ferruginous granules and soils.</li> <li>Well-documented project material has been generated.</li> </ul>	<ul style="list-style-type: none"> <li>Appropriate exploration methods can be chosen according to regolith-landform mapping units or regime and regolith stratigraphy.</li> <li>Established framework for the interpretation of geochemical data.</li> <li>Provides control for interpretation of Landsat TM for regolith mapping.</li> <li>Ferruginous granules and calcareous soils are effective media for sampling: Calcareous soils: Au halo over deposit Ferruginous granules: As, Sb, Au broad, strong, halo greater than 400 m across</li> <li>Presence of mega-mottles and pisoliths may aid in identifying palaeochannels in drill spoils.</li> <li>Mega-mottles and calcareous soils show promises for sampling in channel environments.</li> <li>Provides well-controlled reference data for use in multivariate interpretation procedures.</li> <li>Provides material for educational training of explorationists.</li> </ul>

#### 4.4 Wombola District

##### 4.4.1 Introduction

###### Location

The Wombola district lies in the East Coolgardie Gold Field, some 50 km south-east of Kalgoorlie. It covers about 1400 km<sup>2</sup>, spanning the southwestern boundary of Kurnalpi (SH 51-6) and northwestern boundary of Widgiemooltha (SH 51-10) 1:250,000 map sheets. It is accessible by the Bulong-Curtin road in the north and the Mt. Monger road towards the south.

###### Regional and local geology

The Wombola district lies in the Archaean granite-greenstone terrane. It is dominated by the Gindalbie terrane which consists of lower unit of felsic volcanic rocks (rhyolite-dacite, plus some basalt-andesite) overlain by a strongly deformed ultramafic-mafic sequence (Ahmat *et al.*, 1993). This ultramafic-mafic sequence is predominantly a thick sequence of serpentinised peridotite with subordinate gabbro, pyroxenite, felsic volcanic-volcaniclastic rocks and high-Mg basalt.

The geology of the Wombola prospect (Croesus Mining NL) area consists of a thin belt of amphibolite, dolerite, shale, black shale and porphyry intrusions as shown in Fig. 4.36.

###### Geomorphology and drainage

The Wombola district is characterised by low, rounded hills which grade gently into broad alluvial floors and salt lakes (such as Lake Yindarlgooda in the northwest and Lake Lefroy in the south). The arcuate shapes of the present salt lakes are a consequence of climatic changes to the present semi-arid conditions which led to the alluviation along the old courses and to the formation of present disjointed series of lakes. Boreholes penetrating the salt lake sediments show depths of unconsolidated material, indicating the salt lakes are a recent physiographic feature (Williams, 1970). A thin belt of hills generally oriented northwesterly, characterises the central Wombola district. These hills control the northwesterly direction of the main drainage channels.

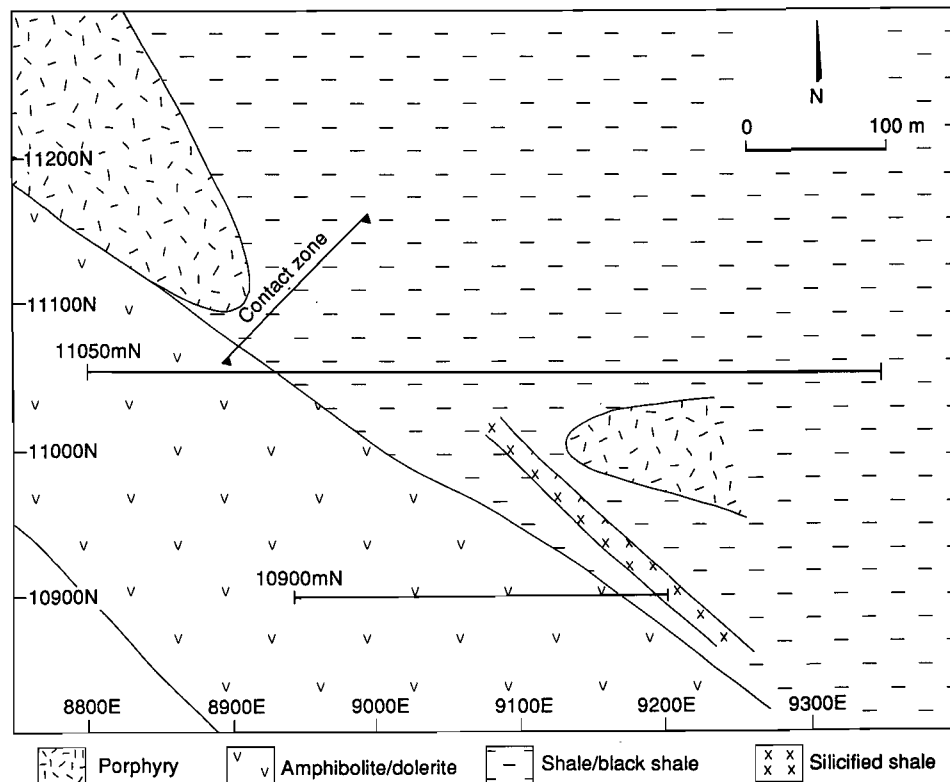


Fig. 4.36 Detailed geology of the Wombola Gold Prospect.

#### 4.4.2 Objectives

The objectives of the Wombola study were to provide a regolith-landform framework for the district and, within this, to complete a concise multi-element orientation geochemical dispersion studies about Wombola prospect. The specific objectives were:

1. To establish the regolith-stratigraphic relationships over the district surrounding the Wombola Au prospect.
2. To mineralogically and geochemically characterise the regolith developed from the weathering of felsic and ultramafic bedrocks.
3. To delineate multi-element dispersion patterns in the soils, mottles and ferruginous pebbles.

#### 4.4.3 Regolith-stratigraphic relationships

##### *Regolith distribution*

As a basis for geochemical dispersion studies, a framework of regolith distribution and stratigraphy was established for the district surrounding the Wombola Prospect. A regolith-landform map for Wombola, at 1:50,000 scale was produced, covering an area of 1100 Km<sup>2</sup> which is based upon interpretation of 1:50,000 air photographs, Landsat images and extensive field work (Appendix VIII). A detailed regolith map at 1:25,000 scale for the Wombola prospect is shown in Fig. 4.37. The regolith landform relationships in the district can be interpreted as *residual*, *erosional* and *depositional regimes* as described by Anand *et al.*, March (1989).

The residual regime is characterised by a lateritic residuum of Fe-rich nodular duricrust with a lateritic lag of nodules merging down to hardened mottles and saprolite. It is found commonly associated with crests, in places, appearing as isolated pedestals above the surrounding exposed saprolite on erosional plains. The residual regime occurs as pockets around the southwestern part and constitutes about 5% of the district.

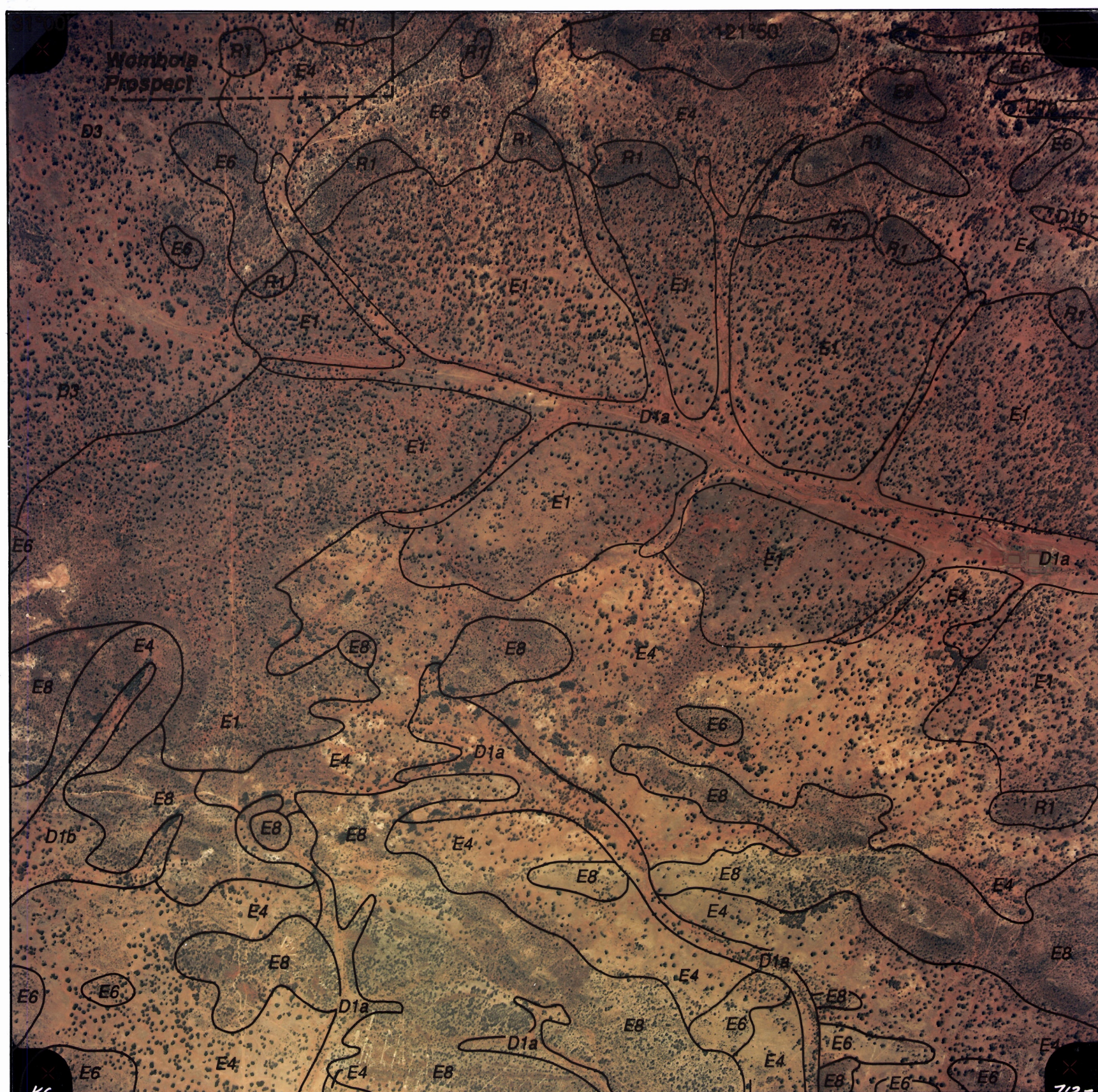
The erosional regime is extensive, covering about 45% of the district and spans the north-western and central portions. This includes areas of breakaways, low and high hills, where erosion has truncated the regolith to ferruginous saprolite, saprolite or bedrock. Commonly, this erosional regime is covered by patchy, locally derived sediments or is concealed beneath calcareous soils.

Within the erosional regime, four mapping units were delineated, E1, E4, E6 and E8. Unit E1 generally lies topographically near the residual regime and is typified by a long, gentle backslope, mantled by fragments of ferruginous saprolite, ferruginous lithic fragments, black nodules and pisoliths. The lag is coarse upslope, on the fringes of the duricrust and becomes finer downslope. The soils are acid sandy clay loam, although carbonates generally occur within 20 cm of the surface. Some areas covered by Unit E1 are characterised by semiparallel blocks caused by interfingering of channels into the backslopes. In addition, there are scattered pockets of cracking red clay, which have a finely patterned micro-relief (gilgai).

Unit E4 is characterised by exposed saprolite along erosional plains, mantled by black, ferruginous granules and quartz. The outcrops of mainly mafic and ultramafic rocks, forming low hills and ridges, are delineated as map units E6 and E8 respectively. Soil is quite common on the low hills. Typically, these undulating hills have a calcareous, sandy, clay-loam soil which can be underlain by acid red clay.

The depositional regime, which covers 50% of the district, acts as a reservoir for colluvium and alluvium derived by erosion of upland lateritic profiles. Towards the eastern portion of the district, in the depositional regime, a few isolated felsic outcrops are found. Buried, truncated, lateritic profiles are common beneath the transported overburden. The depositional regime comprises major mapping units, such as D3 (is typical of this district) and mapping units associated with the lake environment, or D6-D8, around Lake Yindarlgooda in the north and Lake Lefroy in the south. The sediments have both local and distal origins and the lags are commonly polymictic. Unit D3 is quite extensive, especially in the eastern part of the district, and consists of black ferruginous granules with acid clays at surface and calcareous clays with carbonates at 10-20 cm depth along gently sloping plains. Essentially, Unit D6 includes saline clays and muds. Unit D7 is gypsiferous sand and Unit D8 is calcareous sandy soil as dunes. All are within the lake environment.



**RESIDUAL REGIME**

**R1** Lateritic duricrusts, lateritic pisoliths and nodules, crests and low topographic highs

**EROSIONAL REGIME**

**E1** Fragments of ferruginous saprolite and ferruginous lithic fragments - backslopes

**E4** Saprolite, black ferruginous granules and quartz - erosional plains

**E6** Bedrock, low hills

**E8** Bedrock, high hills

**DEPOSITIONAL REGIME**

**D1a** Acid red clay soil with polymictic ferruginous lag within major drainage basins and channels

**D1b** Acid red clay soil with polymictic ferruginous lag within minor drainage basins and channels

**D3** Black, ferruginous granules, non-calcareous red clays at surface, carbonates at 10-20 cm - gently sloping plain

N

0 1 km

Approximate scale due to distortion from aerial photography

Fig: 4.37 Map showing the surface distribution of regolith-landform units and vegetation for the Wombola district as an overlay to a colour air photograph (Kevron Aerial Surveys, photo 1/7137, 5.4.1988), Wombola, published with permission of Croesus Mining NL.







*Regolith stratigraphy and regolith characteristics*

A generalised regolith-stratigraphic model for the Wombola District, summarising the regolith stratigraphy of three dominant regimes, is shown in Fig. 4.38. The residual regime is characterised by a cap of Fe-rich, nodular duricrust (0.5-1 m thick) over 20 cm of calcareous, pale, red soil with carbonate nodules. This is underlain by about 1.5 m of calcified, hardened mottles, nodules and hardened mottles grading into saprolite. In places, the weathering profiles are very shallow and the duricrust is underlain by ferruginous saprock.

Figure 4.39 shows a vertical 1 m profile depth on a crest. It illustrates the regolith stratigraphy over a mafic lithology in the residual regime. The profile shows a gradation of slightly calcareous, reddish soil with abundant hematitic, ferruginous granules and pebbles with 67.5% Fe<sub>2</sub>O<sub>3</sub> to calcareous soils with carbonate nodules, reflected by a higher CaO content of 9.1% in the soil (<2 mm fraction) and 16.2% in nodules (>2 mm fraction) to yellowish red soil over hardened mottles. The yellowish red colour of the soil over the hardened mottles is due to colouring by goethite, which is commonly more abundant in the hardened mottles and deeper subsurface layers. Some feldspars and mica are found in the soil associated with lithic fragments.

Figure 4.40 shows two regolith profiles over low hills in the erosional regime, one developed over a felsic lithology (silicified black shale) and the other over ultramafic (talc schist) lithology. The geochemical data only show the soils (< 2 mm fraction) over the weathered bedrocks. The soils are the products of direct breakdown of the underlying parent material and, consequently, contain both primary and secondary minerals. The ultramafic bedrock contains 51.0% SiO<sub>2</sub>, 7.9% Al<sub>2</sub>O<sub>3</sub>, 11.6% Fe<sub>2</sub>O<sub>3</sub>, 19.5% MgO, 2630 ppm Cr and 114 ppm Cu with dominant talc, chlorite and dolomite. The silicified black shale contains 72.2% SiO<sub>2</sub>, 14.2% Al<sub>2</sub>O<sub>3</sub>, 2.9% Fe<sub>2</sub>O<sub>3</sub>, 0.11% MgO, 22 ppm Cr and 46 ppm Cu dominated by quartz, kaolinite, feldspar, mica and iron oxides. The bedrocks are not entirely fresh because they contain kaolinite and smectite. Correspondingly higher concentrations of Fe<sub>2</sub>O<sub>3</sub>, MgO, Cr and Cu are found in the soils over the ultramafics than over the black shale. The soils of both profiles consistently reflect the mineralogy of the weathered bedrock.

*Wombola Prospect (Lines 10900 mN and 11050 mN, Fig. 4.36)*

The depositional regime is represented by the two transect lines in the Wombola Prospect area. The Wombola prospect is in a colluvial outwash plain (Fig. 4.41). The buried, residual regolith overlies a heterogeneous amphibolite or dolerite and a silicified black shale lithology. The regolith stratigraphy, as in Fig. 4.41, consists of a mantle of fine to coarse, ferruginous granules, pebbles, quartz and carbonate nodules, which overlies 1 m of calcareous red soil with gravels and carbonate nodules. This, in turn, overlies 2 m to 4 m of transported red clay with gravel. Below this is a buried, truncated, lateritic profile, with lenses of transported, loose pisoliths overlying 2 m to 8 m of mottled zone. Bleached saprolite lies beneath this mottled zone.

*4.4.4 Geochemical dispersion in the regolith*

A total of 55 samples were collected along two transects 10900 mN (8950-9200 mE) and 11050 mN (8800-9300 mE). Sampling was at an interval of 50 m along these transects. A total of 16 samples, each of ferruginous pebbles and calcareous soil (0-1 m), 8 samples of loose pisoliths separated from the red soil matrix and 15 samples of hardened mottles from the *in situ* mottled zone, spread across the two lines, were analysed. The depth at which the pisoliths or hardened mottles were collected varied considerably with their depth of occurrence. The 4-10 mm ferruginous pebbles were used for geochemical analyses as they represent the dominant fraction in all sampling points. The calcareous soil, ferruginous pebbles and pisoliths are transported whereas mottles are developed *in situ*. As most of the sampling was on line 11050 mN, it will be discussed in detail.

*Geochemistry*

The geochemical analyses are plotted to show individual elemental concentration of various sampling media along the transects and selected correlation plots between elements as shown in Appendix X. Summary statistics for ferruginous pebbles, calcareous soil, loose pisoliths and hardened mottles are given in Tables 4.12 and 4.13.

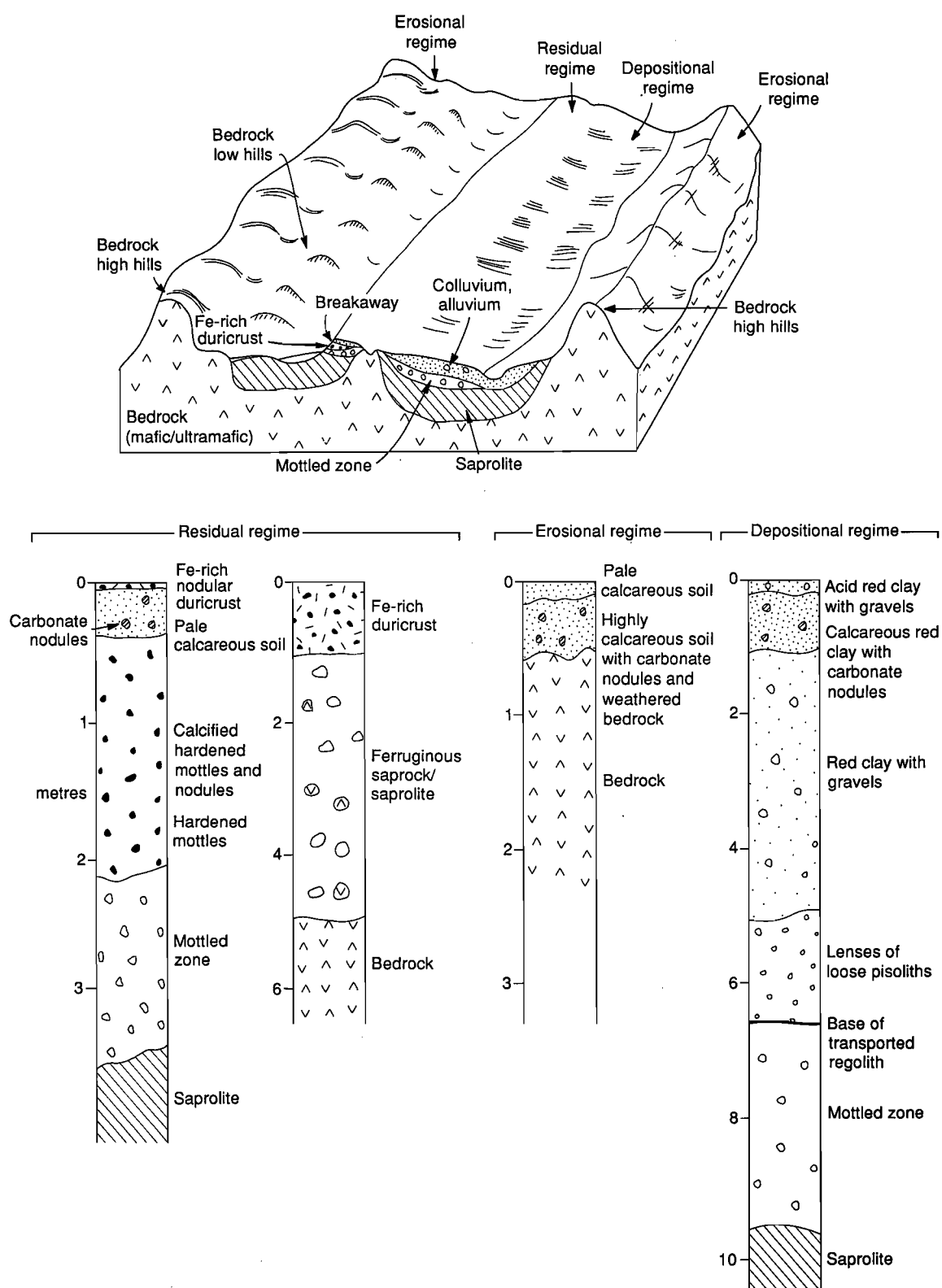


Fig. 4.38 Generalised regolith-landform model for the Wombola district, columns show units of the regolith stratigraphy.

## Residual Regime - Crest, Wombola

Description	Regolith stratigraphy	Mineralogy	%					ppm	
			SiO <sub>2</sub>	Al <sub>2</sub> O <sub>3</sub>	Fe <sub>2</sub> O <sub>3</sub>	CaO	MgO	Cr	Cu
Slightly calcareous reddish brown sandy clay with black ferruginous granules and pebbles	0	H, Q, K, Go, Ma, M (>2mm)	13.8	10.8	67.5	0.10	0.09	987	89
		Q, H, Ma, K, Go, F (<2mm)	52.4	11.3	24.3	0.42	0.49	951	52
Calcareous red sandy clay with carbonate nodules and few ferruginous lithic fragments	#	Ca, Q, H, Go, M, F (>2mm)	19.0	9.3	29.2	16.20	1.54	549	70
		Q, Ca, K, Go, H, F, M (<2mm)	42.4	11.4	15.5	9.10	1.75	551	50
Calcareous yellowish red sandy/loamy sand with strong brown hardened mottles and few ferruginous lithic fragments	50cm	Q, Go, H, K, M (>2mm)	26.8	13.1	45.8	0.63	0.52	825	171
		Q, Go, K, H, Ca, F, M, Sm (<2mm)	37.6	16.7	23.3	3.19	1.21	392	98
Strong brown hardened mottles with few ferruginous lithic fragments	100cm	Go, K, H, Q, M, (>2mm)	22.8	13.1	50.3	0.3	0.41	889	252
		<div> <div>Ca: Calcite</div> <div>F: Feldspar</div> <div>Go: Goethite</div> <div>H: Hematite</div> <div>K: Kaolinite</div> <div>Ma: Maghemite</div> <div>M: Mica</div> <div>Q: Quartz</div> <div>Sm: Smectite</div> </div>							

Fig. 4.39 Vertical profile showing the regolith stratigraphy, mineralogy and chemical composition of the regolith units for the residual regime, Wombola district.

A ternary plot of the major oxides SiO<sub>2</sub>, Al<sub>2</sub>O<sub>3</sub> and Fe<sub>2</sub>O<sub>3</sub>, is shown in Fig. 4.42 and discriminates the two sampling media. One group constitutes the ferruginous pebbles and loose pisoliths which is high in Fe<sub>2</sub>O<sub>3</sub> and low in SiO<sub>2</sub>. The other group constitutes the calcareous soil and hardened mottles with high SiO<sub>2</sub> and low Fe<sub>2</sub>O<sub>3</sub>. From Tables 4.12 and 4.13, Fe<sub>2</sub>O<sub>3</sub> is concentrated the highest in ferruginous pebbles (51.2%) followed by the loose pisoliths (41.8%) whereas the calcareous soils (21.6%) and the hardened mottles (20.4%) are comparable. The SiO<sub>2</sub> concentration for calcareous soil (41.6%) and hardened mottles (46.3%) are higher compared to ferruginous pebbles (25.5%) and loose pisoliths (24.4%). Silica is present mainly as quartz and in the calcareous soils, quartz is dominant in the <1 mm fraction. The SiO<sub>2</sub> concentration in the hardened mottles reflects the underlying lithology, in which SiO<sub>2</sub> is more abundant over the silicified black shale.

Iron is present mainly as hematite with some maghemite in ferruginous pebbles and calcareous soil. It is mainly as goethite, with some hematite, in the loose pisoliths and hardened mottles. Hematite and maghemite in the calcareous soils are mainly attributed to the finer, ferruginous granules. Aluminium is largely in Kaolinite.

Calcium and Mg are most abundant in the calcareous soil and occur as calcite and dolomite. The presence of carbonates on the surface soil indicates insufficient rainfall to leach the carbonates deeper into the profile. Potassium (0.57%) is highest in the calcareous soil and may be contained in the feldspars which were detected by XRD diffraction.

The highest concentration of Au is 440 ppb over the mineralisation in the calcareous soil which coincides with an increase in Ca and Mg (Figs 4.43, 4.44). The Au peak within the surface calcareous soil conforms well with the underlying mineralisation. This correlation of high Au with high CaO has been previously observed in the southern Yilgarn Craton (Butt *et al.*, 1991; Anand *et al.*, 1991; Lintern and Butt, 1993). Gold is consistently concentrated in the calcareous soils with a median of 135 ppb compared to ferruginous pebbles (34 ppb), loose pisoliths (9 ppb) and hardened mottles (9 ppb).

## Erosional Regime - Lowhill (felsic lithology) Wombola

Description	Regolith stratigraphy	Mineralogy	%					ppm	
			SiO <sub>2</sub>	Al <sub>2</sub> O <sub>3</sub>	Fe <sub>2</sub> O <sub>3</sub>	CaO	MgO	Cr	Cu
Slightly calcareous dark reddish brown clay with vein quartz and some black ferruginous granules	0	Q, K, F, H, Ma, Ca, Sm	64.3	12.7	7.3	0.68	1.28	478	55
Strongly calcareous red clay with vein quartz and some black ferruginous granules		Q, Ca, K, F, H, Go, Ma, Sm	57.0	13.5	6.8	5.08	1.70	477	58
Weathered silicified black shale	1 m	Q, K, F, M, H, Ma, Go	72.2	14.2	2.9	0.05	0.11	22	46
Quartz vein									
	2 m								

Ca: Calcite      K: Kaolinite  
 F: Feldspar    Ma: Maghemite  
 Go: Goethite    M: Mica  
 H: Hematite    Q: Quartz  
                     Sm: Smectite

## Erosional Regime - Lowhill (ultramafic lithology) Wombola

Description	Regolith stratigraphy	Mineralogy	%					ppm	
			SiO <sub>2</sub>	Al <sub>2</sub> O <sub>3</sub>	Fe <sub>2</sub> O <sub>3</sub>	CaO	MgO	Cr	Cu
Calcareous dark reddish brown sandy clay loam, ferruginous granules and lithic fragments		Q, Ta, Ca, Ch, Do, H, Am, F	48.6	6.4	9.8	6.43	11.30	1730	57
Calcareous reddish brown loam and lithic fragments		Q, Ta, Do, Ch, Ca, H, F, Sm, K	40.4	5.8	7.9	11.10	11.90	1430	58
Weathered talc schist	1 m	Ta, Ch, Q, Do, Go, Sm, K	51.0	7.9	11.6	0.09	19.50	2630	114
	2 m								

Ca: Calcite      K: Kaolinite  
 Ch: Chlorite    Q: Quartz  
 Do: Dolomite    Sm: Smectite  
 F: Feldspar    Tc: Talc  
 Go: Goethite  
 H: Hematite

Fig. 4.40 Vertical profiles showing the regolith stratigraphy, mineralogy and chemical composition of the regolith units for the erosional regime, Wombola district.

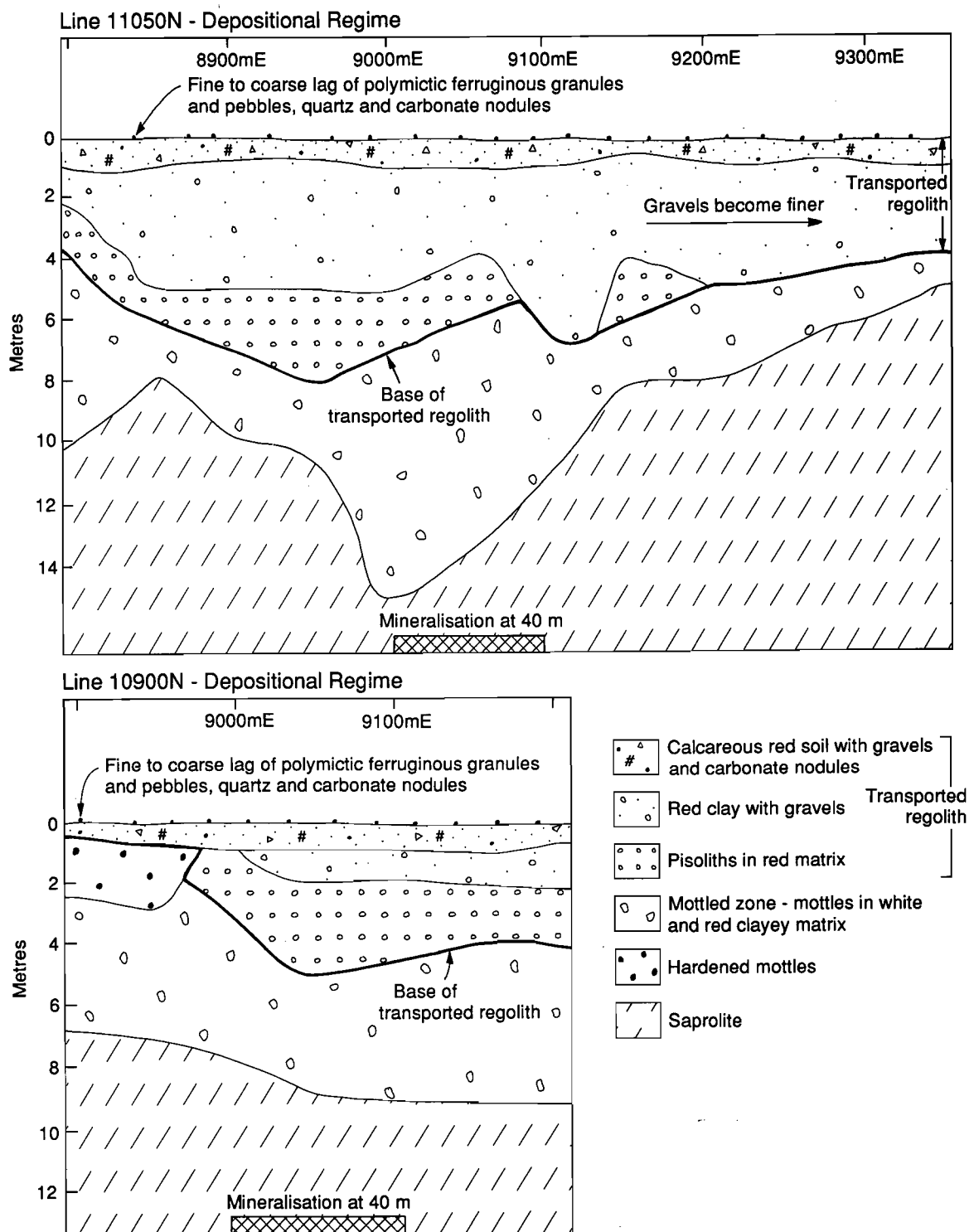


Fig. 4.41 Cross section showing the regolith stratigraphy for lines 11050 mN and 10900 mN, Wombola district.

Table 4.12: Summary statistics on element concentration in lag of ferruginous pebbles and calcareous red soils

ELEMENT	Lag of Fe pebbles n=16					Calcareous Red Soils n=16				
	Mean	Std. Dev.	Min	Max	Median	Mean	Std. Dev.	Min	Max	Median
SiO <sub>2</sub> %	25.6	6.4	16.9	38.8	25.6	39.6	11.0	20.2	54.3	41.7
Al <sub>2</sub> O <sub>3</sub> %	13.2	2.5	9.8	17.6	12.8	15.3	2.6	10.5	19.4	15.8
Fe <sub>2</sub> O <sub>3</sub> %	50.8	3.6	43.7	58.6	51.2	22.7	7.5	12.3	36.6	21.7
MgO %	0.26	0.19	0.07	0.83	0.22	2.15	1.50	0.85	5.87	1.63
CaO %	0.83	0.90	0.11	2.94	0.46	4.13	3.05	0.82	10.46	2.95
Na <sub>2</sub> O %	0.03	0.01	0.02	0.05	0.03	0.33	0.08	0.19	0.49	0.32
K <sub>2</sub> O %	0.06	0.03	0.02	0.09	0.07	0.53	0.25	0.12	0.91	0.57
TiO <sub>2</sub> %	1.20	0.17	0.91	1.59	1.19	0.94	0.11	0.75	1.12	0.96
LOI %	5.91	1.39	3.83	8.24	6.05	13.62	3.11	9.63	19.38	12.72
TOTAL %	97.89	1.14	95.77	99.17	98.13	99.26	1.41	95.50	101.80	99.65
Mn ppm	1514	753	307	2540	1620	473	202	110	800	445
Cr ppm	422	103	288	609	386	431	77	293	570	428
V ppm	1112	139	866	1380	1090	494	183	249	874	465
Cu ppm	114	11	88	138	116	71	15	55	122	68
Pb ppm	19.0	3.3	14.0	26.0	19.0	14.4	4.7	1.7	21.0	15.5
Zn ppm	29.9	7.6	19.0	49.0	28.5	40.3	18.8	10.0	69.0	46.0
Ni ppm	94	20	47	116	103	91	24	38	124	99
Co ppm	17.3	4.1	10.0	24.0	17.0	19.6	6.3	11.0	36.0	18.0
As ppm	15.9	5.0	5.0	24.0	16.0	9.4	4.4	1.7	17.0	9.5
Sb ppm	1.0	0.7	0.7	3.0	0.7	1.1	0.7	0.7	3.0	0.7
Bi ppm	3.4	2.0	0.7	8.0	2.5	0.8	0.5	0.7	2.0	0.7
Mo ppm	0.7	0.0	0.7	0.7	0.7	1.0	0.7	0.7	3.0	0.7
Ag ppm	0.7	0.0	0.7	0.7	0.7	0.6	0.2	0.2	0.9	0.6
Sn ppm	1.9	1.2	0.7	4.0	2.0	1.3	0.8	0.7	3.0	0.7
Ge ppm	0.7	0.0	0.7	0.7	0.7	0.7	0.0	0.7	0.7	0.7
Ga ppm	34	5	27	44	34	25	4	17	32	25
W ppm	8.5	1.9	5.0	12.0	8.0	3.1	2.2	1.0	6.0	3.0
Ba ppm	121	48	43	188	126	275	77	165	463	250
Zr ppm	125	23	100	181	121	146	21	104	174	145
Nb ppm	4.3	1.7	1.0	7.0	4.0	5.9	2.7	3.0	10.0	5.0
Se ppm	2.6	1.3	1.0	4.0	3.0	4.0	3.1	1.0	10.0	3.5
Be ppm	0.8	0.3	0.3	1.0	1.0	1.1	0.3	1.0	2.0	1.0
Au ppb	152	228	3	791	34	235	296	57	1230	135

Table 4.13: Summary statistics on element concentration in loose pisoliths and hardened mottles

ELEMENT	Loose Pisoliths n=8					Hardened Mottles n=15				
	Mean	Std. Dev.	Min	Max	Median	Mean	Std. Dev.	Min	Max	Median
SiO <sub>2</sub> %	24.2	2.9	19.6	29.1	24.4	45.7	13.6	21.5	64.9	46.3
Al <sub>2</sub> O <sub>3</sub> %	18.8	2.8	13.5	23.6	19.0	16.6	3.3	11.8	25.5	16.8
Fe <sub>2</sub> O <sub>3</sub> %	41.1	4.6	30.9	45.9	41.9	24.6	13.1	4.1	48.6	20.4
MgO %	0.09	0.04	0.05	0.18	0.08	0.20	0.13	0.05	0.57	0.21
CaO %	0.09	0.05	0.03	0.16	0.10	0.11	0.10	0.03	0.35	0.08
Na <sub>2</sub> O %	0.05	0.05	0.02	0.18	0.03	0.11	0.08	0.02	0.36	0.09
K <sub>2</sub> O %	0.03	0.02	0.02	0.07	0.02	0.31	0.37	0.02	1.29	0.13
TiO <sub>2</sub> %	1.03	0.32	0.55	1.53	1.03	0.96	0.34	0.43	1.55	0.99
LOI %	13.01	1.32	11.30	15.10	12.85	10.16	1.41	8.63	12.80	9.79
TOTAL %	98.28	1.32	95.87	99.74	98.46	98.71	1.28	95.82	99.94	99.23
Mn ppm	148	58	67	218	168	315	222	47	734	282
Cr ppm	336	119	216	530	329	249	124	89	535	233
V ppm	856	309	376	1420	777	578	424	84	1810	535
Cu ppm	146	39	77	201	146	89	61	21	214	70
Pb ppm	6.0	4.7	1.7	12.0	4.8	1.7	0.0	1.7	1.7	1.7
Zn ppm	23.6	16.7	9.0	50.0	17.5	41.9	23.2	14.0	105.0	39.0
Ni ppm	49	30	11	98	50	35	18	2	74	32
Co ppm	16.0	7.9	6.0	30.0	15.5	10.0	4.0	1.7	17.0	10.0
As ppm	10.4	9.1	1.7	26.0	8.5	9.8	12.5	1.7	50.0	7.0
Sb ppm	1.0	0.6	0.7	2.0	0.7	0.7	0.0	0.7	0.7	0.7
Bi ppm	1.9	1.1	0.7	3.0	2.0	1.6	1.7	0.7	7.0	0.7
Mo ppm	0.7	0.0	0.7	0.7	0.7	0.7	0.3	0.7	2.0	0.7
Ag ppm	0.7	0.0	0.7	0.7	0.7	0.7	0.0	0.7	0.7	0.7
Sn ppm	1.8	0.8	0.7	3.0	2.0	2.4	1.6	0.7	7.0	2.0
Ge ppm	0.8	0.5	0.7	2.0	0.7	0.7	0.3	0.7	2.0	0.7
Ga ppm	37	7	29	52	37	26	4	20	34	25
W ppm	3.9	2.4	1.0	7.0	3.5	1.7	1.8	1.0	7.0	1.0
Ba ppm	35	20	8	75	35	201	224	23	821	96
Zr ppm	106	22	82	138	108	104	24	64	152	101
Nb ppm	3.3	2.2	1.0	6.0	3.0	3.9	1.7	1.0	6.0	5.0
Se ppm	4.6	2.8	1.0	9.0	5.5	2.3	2.5	1.0	10.0	1.0
Be ppm	0.3	0.0	0.3	0.3	0.3	0.4	0.2	0.3	1.0	0.3
Au ppb	162	302	3	805	9	17	26	3	98	9

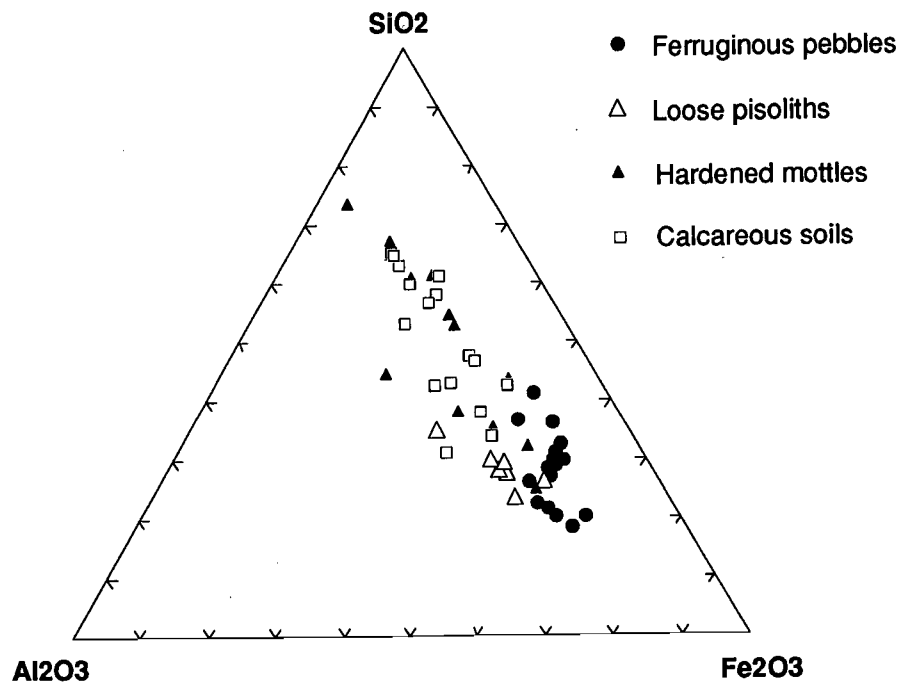


Fig. 4.42 Triangular diagram showing compositions of calcareous soils and ferruginous materials in terms of  $\text{SiO}_2$ ,  $\text{Al}_2\text{O}_3$  and  $\text{Fe}_2\text{O}_3$ , Wombola orientation study.

The range of Zn values in hardened mottles along line 11050 mN is from 10 ppm to 105 ppm (the latter being one sample) and the median (29 ppm) is high compared with the median (16 ppm) of lateritic samples in the AGE database (2434 samples).

As and Sn in hardened mottles show median values of 16 ppm and 2 ppm with individual peaks of 50 ppm and 7 ppm respectively. It is not clear whether or not the range of values shown in Fig. 4.43 are background variations. The median values of Zn, As and Sn are (28.5, 16.0, 2.0 ppm) for ferruginous lag, (6.0, 9.5, 0.7 ppm) for calcareous soils, (17.5, 8.5, 2.0 ppm) for loose pisoliths and (9.0, 7.0, 2.0 ppm) for hardened mottles.

Manganese, normally associated with Fe, is strongly enriched in the ferruginous pebbles with a median value of 1620 ppm. The ferruginous pebbles are also enriched in  $\text{TiO}_2$  (1.19%), V (1090 ppm), Pb (19 ppm), Ni (102 ppm), W (8 ppm) relative to the other sampling media.

The calcareous soil show elevated concentration of Cr (428 ppm), Co (18 ppm), Ba (250 ppm) and Zr (144 ppm). The K-feldspars could be the carriers of Ba in the soils.

Copper (146 ppm) and Ga (37 ppm) are concentrated in the loose pisoliths. The relatively high Cu concentration could reflect the underlying dolerite and amphibolites. As very little information is available on various bedrock chemistry, a cursory look at the geochemical data on the hardened mottles of the buried residual lateritic profile may indicate implicitly the bedrock geochemical signature. The geochemistry of the hardened mottles tends to fluctuate across the transect, possibly reflecting changes in the underlying lithology. On the western part of the transect, there is higher Fe, V, Cu and Cr in the mottles possibly associated with the mafic lithology of dolerite/amphibolite, whereas  $\text{SiO}_2$  is higher in the mottles from the silicified black shale.



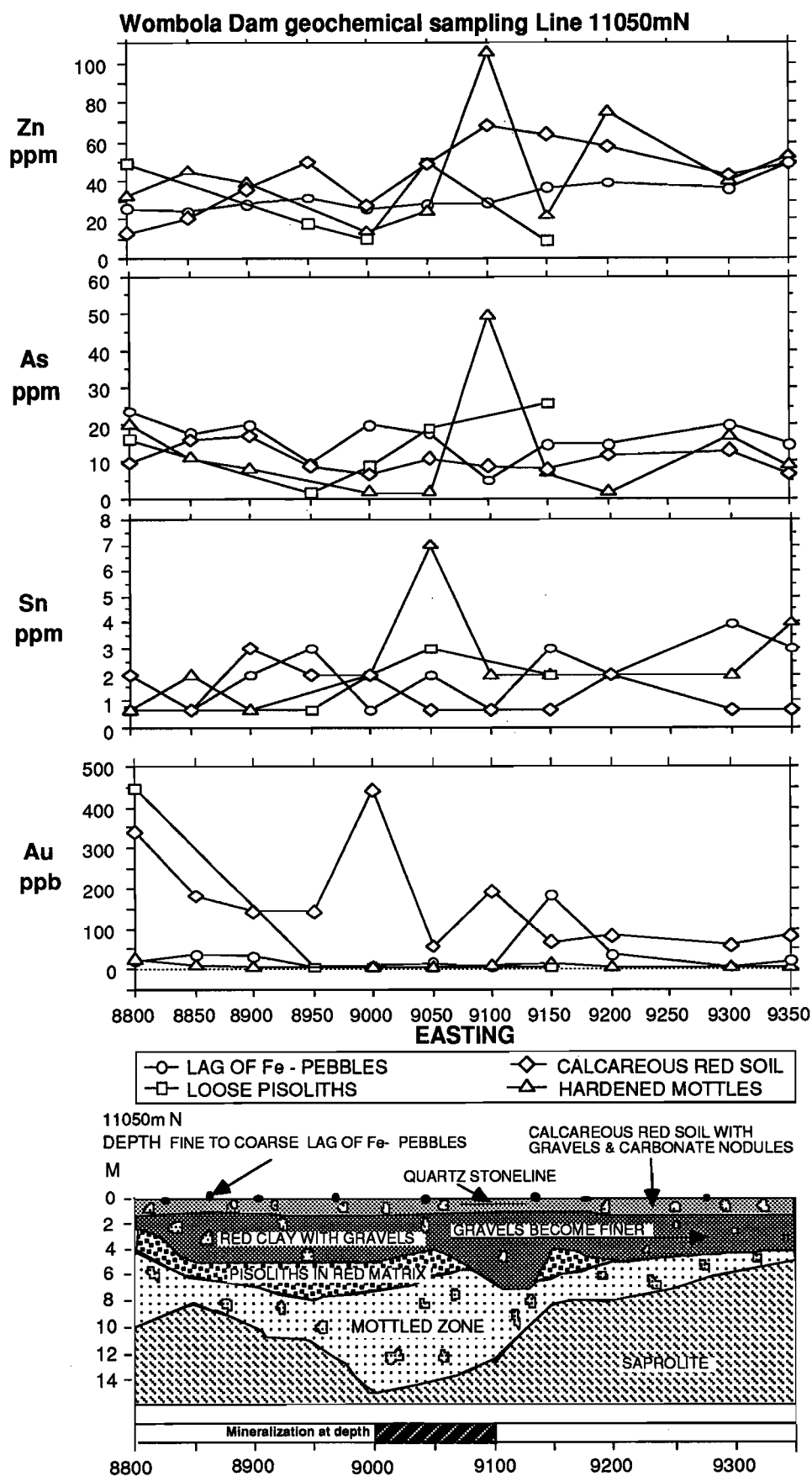


Fig. 4.43 Traverse along line 11050 mN showing the distribution of Zn, As, Sn and Au in soils and ferruginous materials, Wombola orientation study.

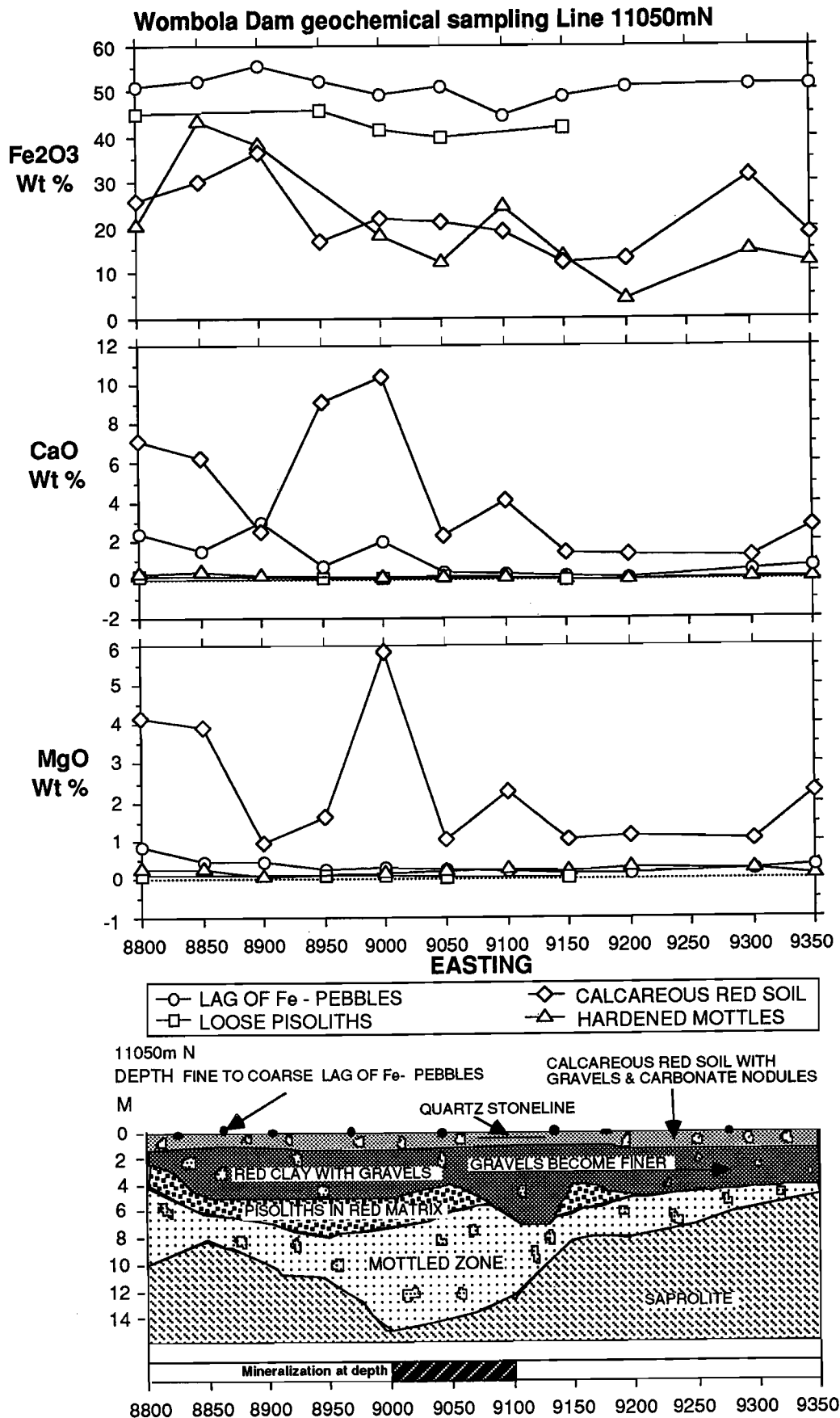


Fig. 4.44 Traverse along line 11050 mN showing the distribution of Fe<sub>2</sub>O<sub>3</sub>, CaO and MgO in soils and ferruginous materials, Wombola orientation study.

#### 4.4.5 Implications in exploration

At the Wombola prospect, ferruginous pebbles and pisoliths are transported and do not show the multi-element geochemical expression of mineralisation. This emphasises the importance of understanding the regolith-stratigraphic relationships and the processes of development and origin of these ferruginous materials. In a depositional regime, where there is a thick, transported overburden lying on partially dismantled lateritic profile, using the appropriate sampling media requires prior knowledge of whether the media are residual or transported.

The calcareous soils in the colluvium/alluvium show a very strong Au anomaly (440 ppb) over mineralisation.

The main research findings and their implications in exploration of the Wombola district are listed in Table 4.14.

Table 4.14. The implications in exploration listed against the research findings, Wombola orientation study.

Research Findings	Implications in Exploration
<ul style="list-style-type: none"> <li>Regolith-stratigraphic relationships were mapped on district and local scale, with erosional and depositional regimes dominant. The residual, erosional and depositional regimes comprise 5%, 45% and 50% respectively of the district.</li> </ul>	<ul style="list-style-type: none"> <li>Knowledge of the regolith-stratigraphic relationships helps in deciding which appropriate exploration method to use.</li> </ul>
<ul style="list-style-type: none"> <li>District scale regolith-stratigraphic relationships were established for Wombola.</li> </ul>	<ul style="list-style-type: none"> <li>Establishes framework for exploration geochemistry.</li> </ul>
<ul style="list-style-type: none"> <li>At Wombola, the calcareous soils show Au anomaly. Hardened mottles may show enhanced concentration of Zn, As, and Sn related to mineralisation.</li> </ul>	<ul style="list-style-type: none"> <li>Provides control for interpretation of satellite imagery for regolith mapping.</li> </ul>
<ul style="list-style-type: none"> <li>Well documented project material has been generated.</li> </ul>	<ul style="list-style-type: none"> <li>Calcareous soils are effective sampling media, hardened mottles possibly.</li> </ul>
	<ul style="list-style-type: none"> <li>Provides material for education training of explorationists.</li> </ul>

## 5.0 ORIENTATION STUDIES OUTSIDE THE KALGOORLIE REGION

### 5.1 Introduction

The purpose of the orientation studies outside the Kalgoorlie region was to add to the Craton-wide research by providing case studies of geochemical dispersion from selected parts of the Yilgarn, each within a well-established regolith framework. Emphasis in many of these studies was on linking detailed regolith-stratigraphic relationships with district-scale perspectives, an approach which had been particularly worthwhile in providing foundations for the precursor project. The orientation studies represent a range of important regolith, geomorphic and climatic settings and expanded those presented in Report 236R.

The district-scale studies have been important for other work in the project. In this extension, they were a prerequisite to establishing a classification of regolith-landform mapping units, a topic that was viewed as a priority by sponsors. It has been presented as Report 440R and is summarised in Section 6.

The Boddington study, described fully in Report 246R, is summarised below. This study had not cleared confidentiality in time for inclusion in the Summary Report 236R. The Bottle Creek study was continued during the extension project. It includes a Bachelors Degree Honours project (R. Wills, Curtin University) and a stage of reconciling orientation research with the original exploration geochemistry carried out by the Electrolytic Zinc Co.

Research in the Lawlers orientation district included an Honours project (R.F. Twomey, UWA) focussed on the regolith relationships and geochemical dispersion at the Waroonga and Genesis Au deposits as well as two Honours projects reconciling exploration geophysics with regolith relationships (K.A. Mayes and M.J. Nelson, Curtin University).

An orientation district centred on the Mt. McClure mining areas was included to exemplify areas where thick, transported cover overlies complete and partly truncated laterite profiles as well as concealed bedrock Au deposits. An Honours project was included (A. Williamson, UWA).

Orientation, particularly on soil and lag geochemistry at Lights of Israel south of the Menzies line (Butt *et al.*, 1977) has provided a comparison with the previous Beasley Creek study in an arid area north of the Menzies line; both were studies jointly with AMIRA Project P241A *Dispersion Processes*.

New orientation information was generated on archived CSIRO samples from the Gossan Hill and blind Scuddles VHMS districts at Golden Grove as well as the area in between these two deposits. The Golden Grove area was the focus of the first laterite geochemical orientation research carried out by CSIRO, in the 1970s. The new phase of research was designed to test the application of analytical developments which, since then, have lowered the limits of detection considerably, particularly for Au, Sb and Bi. Another aim was to review the anomalous ferruginous materials at Golden Grove (gossans and lateritic residuum) after some 15 years of accumulated knowledge in lateritic environments.

The Madoonga district, which also included an Honours study (A.D. Von Perger, Curtin University) has been the focus for establishing and testing technologies for regolith mapping, particularly reconciling experimental treatment of Landsat TM multispectral remote sensing data with field relationships.

## 5.2 Boddington district

### 5.2.1 Introduction

#### *Previous work*

The Boddington Au deposits, which are distributed along 5 km of strike length, are located mainly within the saprolitic part of the lateritic mantle and were formed by supergene enrichment during weathering of a Cu-Au porphyry system (Monti, 1987, Symons, *et al.*, 1990). This research at Boddington provides an orientation study of geochemical dispersion in a relatively-high rainfall part of the Yilgarn and it also allows comparison with the orientation studies in the semi-arid and arid areas.

The first significant event for Au and base metals exploration in the region was recognition of the relatively-small greenstone belt by Wilde (1976). A geochemical prospecting programme, seeking Au, Cu, and Zn mineralisation in the Saddleback greenstone belt, instituted by the Geological Survey of Western Australia followed. This led to the discovery, in 1979, of an area of anomalous Au, As, Cu, Pb, Mo, and Zn (Davy, 1979).

In 1980, Reynolds Australia Mines Pty. Ltd. commenced an exploration programme in the area for commodities other than bauxite (El-Ansary, 1980). Surface laterite sampling, followed by systematic reassaying of bauxite drill samples, led to the discovery of the Boddington Au deposit (60 million tonnes of lateritic ore at 1.6 g/t Au, (Symons *et al.*, 1990) with a total resource of some 118 t Au (Roth and Symons, 1990). The mine, commissioned in August 1987, produced 7,166 kg of Au during the first year of operation (Symons *et al.*, 1990).

A study of the mineralogy and geochemistry of four drill holes and geochemical patterns in the lateritic profile at the Boddington Au deposit has been carried out by Davy and El-Ansary (1986) while information on primary mineralisation is given by Symons *et al.* (1988).

#### *Location*

The Boddington Au deposit occurs within the northern part of the Saddleback greenstone belt, which is centred at 32°50'S and 116°57'E, approximately 100 km south-south-east of Perth (Fig. 5.1).

#### *Climate and vegetation*

The climate of the area is Mediterranean with warm, dry summers and mild, wet winters with mean maximum temperatures ranging between 12 and 28°C. Rainfall is estimated at 810 mm per annum and most of the rain falls regularly during the cool winter months from May to September. The dominant vegetation is sclerophyll forest. Varying proportions of *Eucalyptus marginata* and *Eucalyptus calophylla* form the upper storey on the ridge crest and slopes.

#### *Regional geology and mineralisation*

The Saddleback greenstone belt (Wilde, 1976), varies from 5 to 12 km wide and extends 43 km in a north-northwest direction from Mt Saddleback to Mt Wells. It is a steeply-dipping sequence which contains metamorphosed (greenschist to lower amphibolite) sedimentary, felsic, and mafic volcanic and pyroclastic rocks, which have been extensively faulted (Fig. 5.1). The greenstone sequence, known as the Saddleback Group, is subdivided into the Hotham, Wells, and Marradong Formations. The granite-greenstone contacts are generally considered to be faulted, although intrusive contacts have been established in the southwestern part of the belt (Wilde and Low, 1980) and to the east of the Boddington Au deposit.

Geochronological studies by Wilde and Pidgeon (1986) date the volcanics at 2.65-2.67 MA, indicating a similar age to greenstones from the Eastern Goldfields Province. The entire area has been intruded by post-mineralisation doleritic rocks, which are now largely amphibolite, though relict primary fabrics and minerals occur in places.

Bedrock in the Boddington Au mining area consists of felsic andesite, passing to mafic andesite to the east and schist to the west. Mineralisation has been found mainly in the andesitic and dacitic rocks, some of which are intrusives; the sequence is traversed by dykes of dolerite, diorite and some of ultramafic mineralogy.

Low-grade Au mineralisation forms a semi-continuous blanket, hosted within the laterite, the bauxite-zone, and the uppermost clay zone of the lateritic profile (Symons *et al.*, 1988). This style of Au mineralisation constitutes 30% of the total contained Au within the oxidised profile, with the remaining 70% hosted within the lower clay and lower saprolite zones. Gold distribution is relatively homogeneous. Clay-hosted Au mineralisation exhibits highly-variable grades and poor lateral continuity. Thin, primary quartz veins are commonly well mineralised. Clays adjacent to quartz veins (particularly in footwall locations) are commonly Fe stained and contain anomalously high concentrations of Au. Secondary,

shallowly-dipping, Fe-oxide-rich horizons also contain anomalous but erratic Au concentrations. In addition, kaolinitic clays, with little or no quartz or ferruginisation, can be well mineralised.

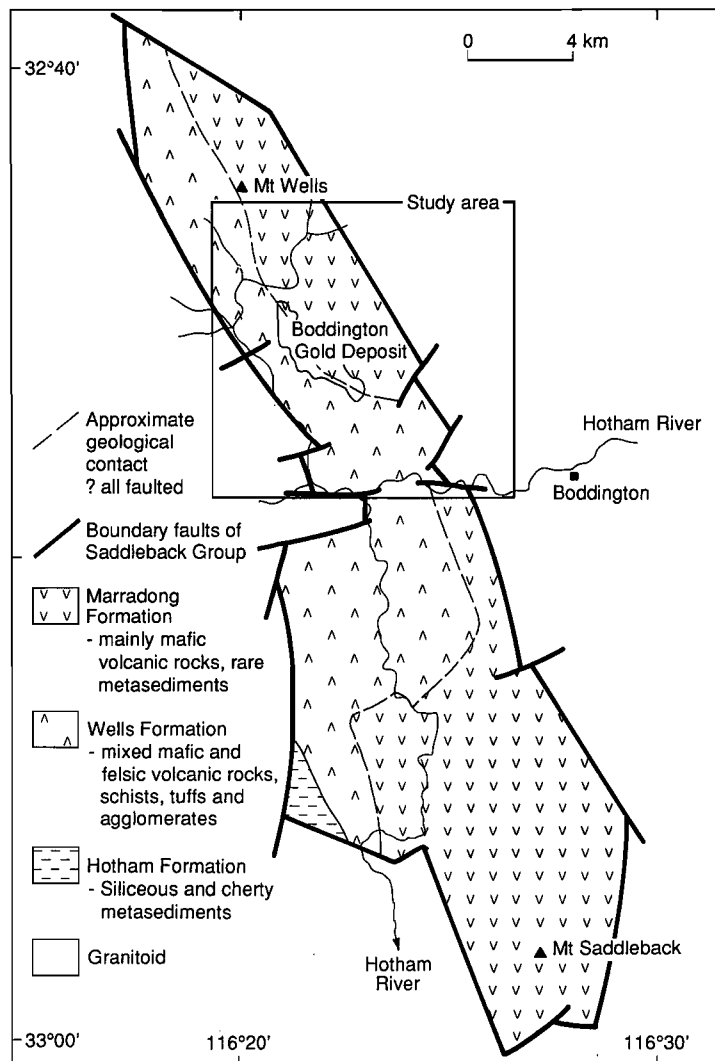


Fig. 5.1 Generalised bedrock-geological map of the Saddleback greenstone belt (after Wilde and Low, 1980).

### Geomorphology

The Boddington area is situated towards the western edge of the Darling Plateau, a physiographic feature of south Western Australia. This area is incised by drainage from the Darling Plateau with the Hotham River forming the major divide. Tributaries of this system grade up to the adjacent undulating plateau surface that forms the principal drainage divide. Thus, the local tributaries may terminate as broadly concave features forming the swales of these undulations. In this location, the plateau has relief of some 50 m, forming a shallow valley floor adjacent to smooth broadly-convex crest (Fig. 5.2). The latter forms a general skyline at 330 to 360 m above sea level while the floors of the major valley are some 60 m below. More distinct summits, such as Mt. Wells and Mt. Saddleback rise above the plateau at 547 and 575 m respectively above sea level.





### 5.2.2 Objectives of the Boddington district study

The broad objectives of the Boddington study were to provide a well-understood, regolith-landform framework over the district and, within this, to investigate the multi-element, geochemical dispersions about the concealed Au deposits.

Specific objectives were:

1. To establish regolith-landform relationships;
  - to establish the regolith stratigraphy;
  - to characterise regolith units; and
  - to generate a model of regolith-landform evolution.
2. To elucidate the origin and mode of formation of lateritic pisoliths and nodules;
3. To compare the geochemistry, petrology, and mineralogy of regolith units developed on the intermediate and felsic rocks.
4. To document the variation in abundances of ore-associated elements, including Au.
5. To investigate element-mineral associations.
6. To produce a multi-element orientation geochemistry data base.

### Report produced:

Regolith-landform evolution and geochemical dispersion - Report 246R (submitted to the tenement holders, Boddington Gold Mines, November 1992, report scheduled for distribution to sponsors March 1994).

### 5.2.3 Regolith-landform evolution

#### Typical profile

An understanding of the nature, distribution and origin of regolith units of the Boddington area over a 11.5 x 11.5 km area is discussed in this section. Figure 5.3 shows a typical laterite profile for the Boddington area. In the Darling Range bauxitic laterites, an increase in  $Al_2O_3$  has taken place in the upper parts of some profiles to the extent that gibbsite occurs in the lateritic residuum and the mottled zone. The mottled zone is dominant and is locally referred to as the bauxite zone or B-zone by the bauxite mining company. The principal regolith units are described below.

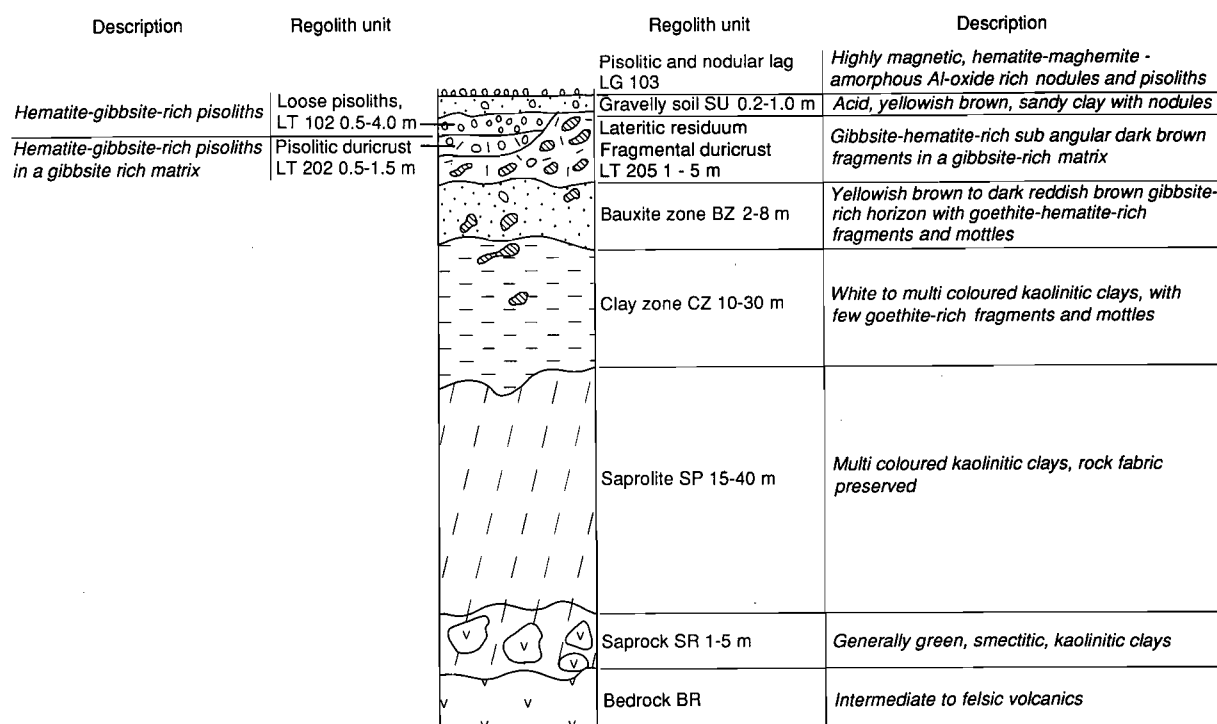


Fig. 5.3 Typical weathering profile in the Boddington gold mining area.

### *Saprolite and clay zone*

The saprolite is 25-70 m thick and ranges from white to multicoloured kaolinitic clays with mottles, commonly overprinted by liesegang rings. Goethite staining is common around the areas of multicoloured clays. Microscopic examination of thin sections of upper saprolite from Profile 1 shows areas that are made up of a mosaic of kaolinite and gibbsite crystals, a few hundred  $\mu\text{m}$  to a few  $\mu\text{m}$  in size, passing into goethite-kaolinite-rich areas.

### *Bauxite zone*

The bauxite zone is about 4 m thick. It is an earthy, porous, friable to firm, yellowish-brown to dark reddish-brown mass, rich in gibbsite which underlies the lateritic duricrust. It contains fragments, incipient nodules and, in places, is mottled. Voids of up to 10 cm in diameter are common and are generally partially filled by coatings of gibbsite. Relict rock fragments and pseudomorphs after feldspars are common in this horizon. These pseudomorphs are micro-crystalline aggregates of gibbsite after feldspar in an isotopic groundmass of Fe-oxide (goethite, hematite) impregnated gibbsite.

### *Lateritic residuum*

The lateritic residuum characterises the residual regime in Fig. 5.4. Lateritic residuum is typically 2-3 m thick, includes two horizons, an unconsolidated pisolitic horizon (upper) and the duricrust (lower), each of which exhibit several morphologies. Two duricrust morphologies are recognised, viz fragmental and pisolitic. Fragmental duricrust is characterised by subangular to angular, dark brown to red, gibbsite- and hematite-rich fragments of various dimensions ranging from a few mm to more than 3 cm. Fragments up to 10 cm in diameter may be present. The fragments are cemented by various amounts of a fine-grained, yellowish-red to strong brown, gibbsitic matrix. Pseudomorphs after primary minerals are common in the fragments. In some areas of fragments, the pseudomorphs have mostly disappeared, leaving a spongy mass in which loose sand sized quartz grains may occur.

In general appearance, the pisolitic-nodular duricrust is darker and less porous than the fragmental duricrust and contains black hematite-maghemite-rich pisoliths and nodules up to 25 mm in diameter.

### *Soils*

The soils forming the upper part of profiles are a clayey sand. Within a depth of 30-40 cm, lateritic gravels often exceed 75% of the total soil mass. Except for a dark surface soil due to the accumulation of organic matter, these soils show no pedogenic horizons. The soils range from yellowish-brown to light yellowish-brown and become paler with depth.

### *Pisolitic and nodular lag*

The nodules and pisoliths are irregular to rounded, dark-reddish brown to black, highly magnetic, and are normally between 5 and 20 mm in diameter. Pisoliths with multiple cutans are rare. Some nodules may show lithic remnants in their nucleus.

### *Regolith distribution*

Figure 5.4 shows the distribution of regolith-landform mapping units for the Boddington area. The map, at a scale of 1:50,000, shows areas dominated by lateritic residuum, separated by various erosional and depositional units.

### *Residual regime*

These are areas dominated by lateritic duricrust and a thick mantle of lateritic gravels. They comprise gently-undulating lateritic uplands and associated minor valleys. Duricrust outcrops are covered by a thin veneer of lateritic gravels on the crests and upper slopes. The lateritic gravels become thicker downslope in shallow depressions and the upper parts of these can be cemented.

### *Erosional regime*

As mapped in this study, the erosional regime comprises areas in which there has been extensive removal of the lateritic residuum. Areas of erosional regime range from smooth gentle to moderate ( $5-12^\circ$ ) slopes. These are mantled by colluvium, containing a mixture of lateritic gravels and overlie various saprolitic clays at depths of 0.5 to 1.5 m. On steeper slopes ( $>12^\circ$ ), stripping of the weathered mantle has been more effective and fresh rock is exposed.

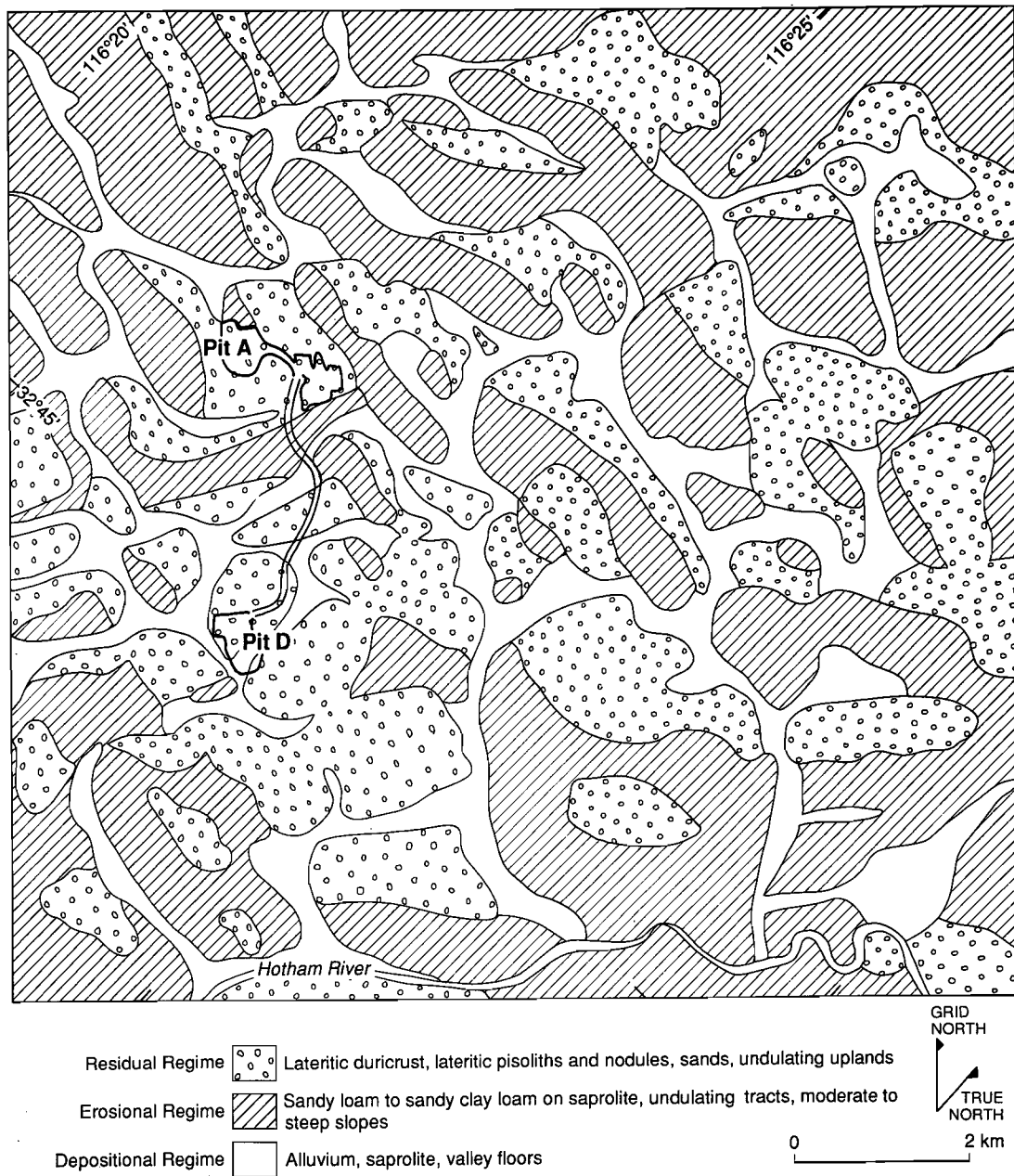


Fig. 5.4 Map showing the surface distribution of regolith-landform regimes for the Boddington district.

### Depositional regime

The depositional regime comprises valley floors. It has a gradient of about 1:250 and is seldom more than 1 km wide. The lower colluvial slopes grade into the valley floor and it is, in places, difficult to distinguish between these two units. On the valley floor, the dominant soils are yellow earths, the texture of the surface horizon ranges from sand to sandy clay loam.

### Regolith stratigraphy

The open pit mining operations have exposed the regolith stratigraphy extensively at Boddington. Pit A, located adjacent to a minor valley, contrasts with Pit D, which is part of an undulating lateritic upland surface. The general trends in the regolith stratigraphy and morphology of the lateritic residuum from crest to lower slopes is shown in Fig. 5.5. Yellowish-brown, sandy gravels overlying fragmental duricrust, extend from the ridge crest to the upper slopes. Fragmental duricrust crops out or is overlain by 20-50 cm thick, yellowish-brown, sandy gravels. Sandy gravels increase in thickness to more than 1 m on mid slope and lower slope positions, where they overlie various forms of lateritic duricrust, including loosely-packed pisolitic duricrust; these, in turn, overlie the bauxite zone and/or the clay zone. Fragmental duricrust is not generally developed on lower slopes. On lower slopes, a bauxite zone 3-4 m thick underlies the thick mantle of pisoliths which can sometimes reach a thickness of 4 m. The bauxite zone commonly overlies multicoloured saprolite derived from andesite. The saprolite merges into underlying parent rock through a zone of the saprock. The depth of weathering is variable, commonly extending to more than 30 m.

The absence of pisolitic duricrust on the crests and upper slopes suggests that this unit has been truncated. Such a profile could be typical of the upper slopes of the Boddington gold mining area, where the duricrust is known to be thin (Symons *et al.*, 1988).

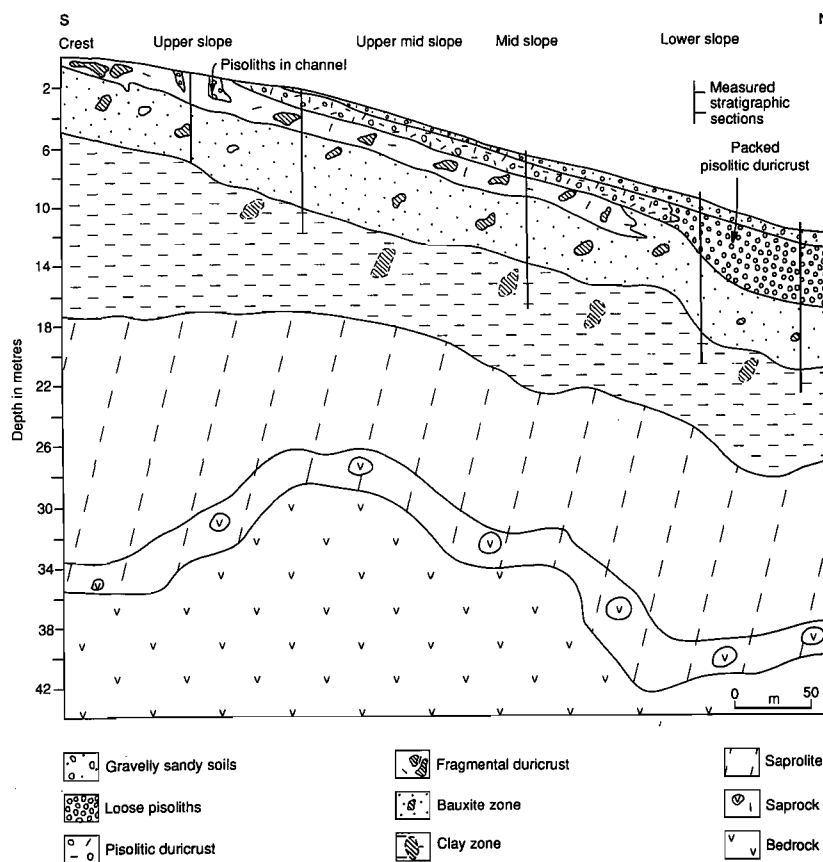


Fig. 5.5 Cross section for Pit A showing the general trends in the regolith stratigraphy and morphology of the lateritic residuum, following a sequence from crest to lower slopes, Boddington.

#### 5.2.4 Geochemical dispersion in regolith

##### *Introduction*

This study is based on geochemical data for a set of 284 samples. These were taken from the surface as well as from vertical sections across the geochemical anomaly. Samples of specific regolith units within vertical profiles generally consisted of a 1.5-kg grab sample. Locations of samples are shown in Fig. 5.2. Many of the systematic surface samples were collected for the study by Boddington Gold Mines. The results are presented in three sections:

- (a) data from drill holes and costeans (vertical profiles);
- (b) geochemical dispersion in pisolitic and nodular lag; and
- (c) all samples grouped into six categories of sample type.

##### *Weathering profiles developed from andesite and dolerite –*

##### *Drill Holes WBC15, 16, 21, 26, and Costean 2*

This section discusses the geochemistry and mineralogy of the weathering profiles sampled from four diamond drill holes (WBC 15, 16, 21, 26, locations shown in Fig. 5.2) through felsic andesite and one from the costean in weathered dolerite. The purpose of these profiles was to examine the variations in geochemistry (with depth) of the regolith units. This was done to establish the weathering behaviour of different elements, to gain knowledge of how the geochemistry and mineralogy of deeply-weathered regolith relates to the underlying bedrock; and to determine the utility of various regolith materials as geochemical sampling media.

##### *Mineralogical composition*

The mineralogical compositions for the andesite profile (WBC15), related to detailed logging, are shown in Fig 5.6. The bedrocks in these profiles contain feldspars, quartz, biotite, amphiboles, and chlorite. The bedrocks are not entirely fresh because they contain kaolinite and smectite. Minor minerals, include ilmenite and sphene. In andesite profiles, plagioclase, amphiboles, and biotite have disappeared within 2 m of the bedrock and have altered to a mixture of smectite, kaolinite, and goethite. Primary minerals were not detected in middle and upper saprolite, indicating complete weathering to secondary minerals.

Moving downward through the andesite profiles, the major change from lateritic residuum to saprolite is characterised by a decrease of gibbsite; only small amounts of this mineral is present in the saprolite. Gibbsite also decreases appreciably in the top of the lateritic residuum (loose pisoliths) where amorphous Al-oxide becomes the major Al mineral. In the dolerite profile, gibbsite is present almost throughout the profile, but it is relatively-less abundant than in andesite profiles. Gibbsite in the lower horizons of dolerite profiles is the result of weathering of plagioclase directly to gibbsite (Anand and Gilkes, 1984).

Kaolinite, as expected, was most abundant in the middle saprolite and it was much less common at the top and at the bottom of the profile.

The bauxite zone is characterised by replacement of kaolinite by gibbsite, and with the appearance of hematite. Iron-oxides and oxyhydroxides generally increase in abundance upwards. Goethite is present at a greater depth than hematite, which is probably due to its formation as an initial alteration product of ferromagnesian minerals. Hematite and goethite are relatively more abundant in the dolerite profile than in andesite profiles. Maghemite, boehmite, and corundum (not shown) occur only in surface or near-surface horizons (loose pisoliths and pisolitic duricrust). These minerals are absent in fragmental duricrust and in the underlying horizons.

Quartz decreases in abundance upwards. The relative decrease in the abundance of quartz in the upper horizons may be due to dissolution during weathering or to dilution by introduced Fe and Al minerals from overlying soil horizons. Small amounts of muscovite are present in the bauxite zone, the clay zone, and the upper saprolite. However, muscovite is not present in the bedrock of WBC15 and 21. Its appearance in significant quantity in the clay zone and bauxite zone may be attributed to dyke-like muscovite-rich rock similar to others seen elsewhere in the Boddington area. Over dolerite anatase, a weathering product of ilmenite is an important secondary mineral.

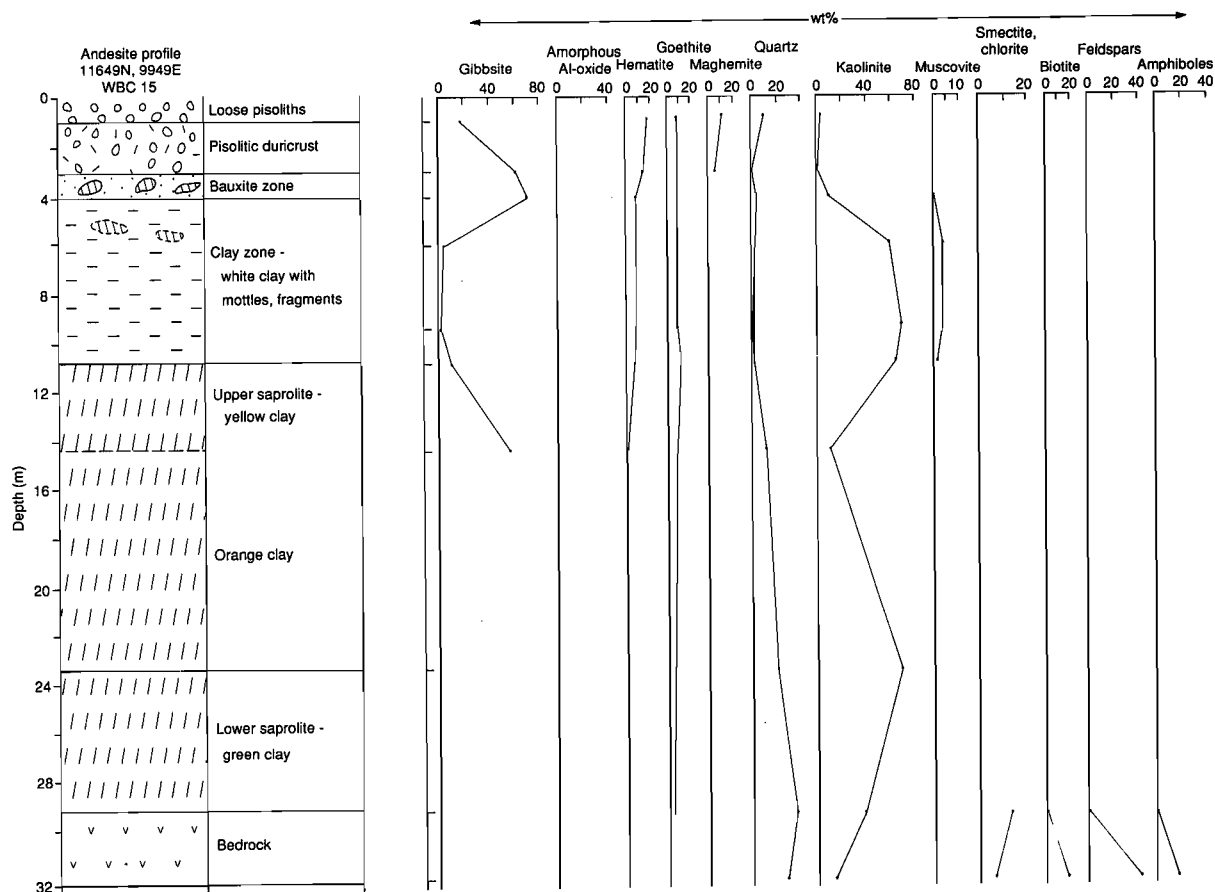


Fig. 5.6 Regolith stratigraphy and distribution of dominant minerals in the andesite profile, WBC 15, Boddington gold mining area.

### Geochemistry

The chemical compositions of bedrock, saprolite (lower, upper), clay zone, bauxite zone, lateritic duricrust and loose pisoliths for andesite and dolerite profiles are given in Table 5.1, and the distributions of selected elements are compared in Fig. 5.7. Chemical data for fresh dolerite were taken from Monti (1987). Aluminium and  $\text{Fe}_2\text{O}_3$  are by far the most abundant constituents with each being greater than 40% in loose pisoliths and pisolitic duricrust. These are enriched throughout the weathered profile compared to the bedrock. These elements are largely residual products of deep chemical weathering, occurring as goethite, hematite, and maghemite or as gibbsite, amorphous Al-oxide and kaolinite. Each is strongly enriched in the upper saprolite and overlying horizons, by factors of two or more, due to residual concentration concomitant with the leaching of other elements. The highest concentration of  $\text{Fe}_2\text{O}_3$  occurs in pisolitic duricrusts and loose pisoliths and is relatively greater in the doleritic profile than in andesitic profiles. The Fe content of dolerite is greater than that for felsic andesite (17.5-21.5%  $\text{Fe}_2\text{O}_3$  compared with 4.8-8.5%  $\text{Fe}_2\text{O}_3$ ). Iron retention or enrichment during lateritisation results in the laterites derived from dolerite being far more ferruginous than the felsic andesite-derived laterite. The concentrations of these elements correspond well with their mineralogy.

Little  $\text{SiO}_2$  remains in the bauxite zone and overlying horizons, with only about 1.7% in the loose pisoliths, relative to an initial content of 57.8% in andesite and 12.4% in saprolite. Silica occurs mostly as quartz and kaolinite.

The minor oxides,  $\text{Na}_2\text{O}$ ,  $\text{K}_2\text{O}$ ,  $\text{CaO}$ , and  $\text{MgO}$ , are strongly depleted in saprolite and the overlying horizons. Of these, Ca, Mg and Na in particular, are all strongly leached at the onset of weathering and almost totally depleted from the upper saprolite, lateritic duricrust and loose pisoliths. Calcium oxide,  $\text{MgO}$ , and  $\text{Na}_2\text{O}$  concentrations are low (0.01-0.06%) in the middle and upper saprolite, bauxite zone and lateritic duricrust. Titanium gradually increases upwards through the profiles and is mainly present as anatase and unweathered ilmenite.



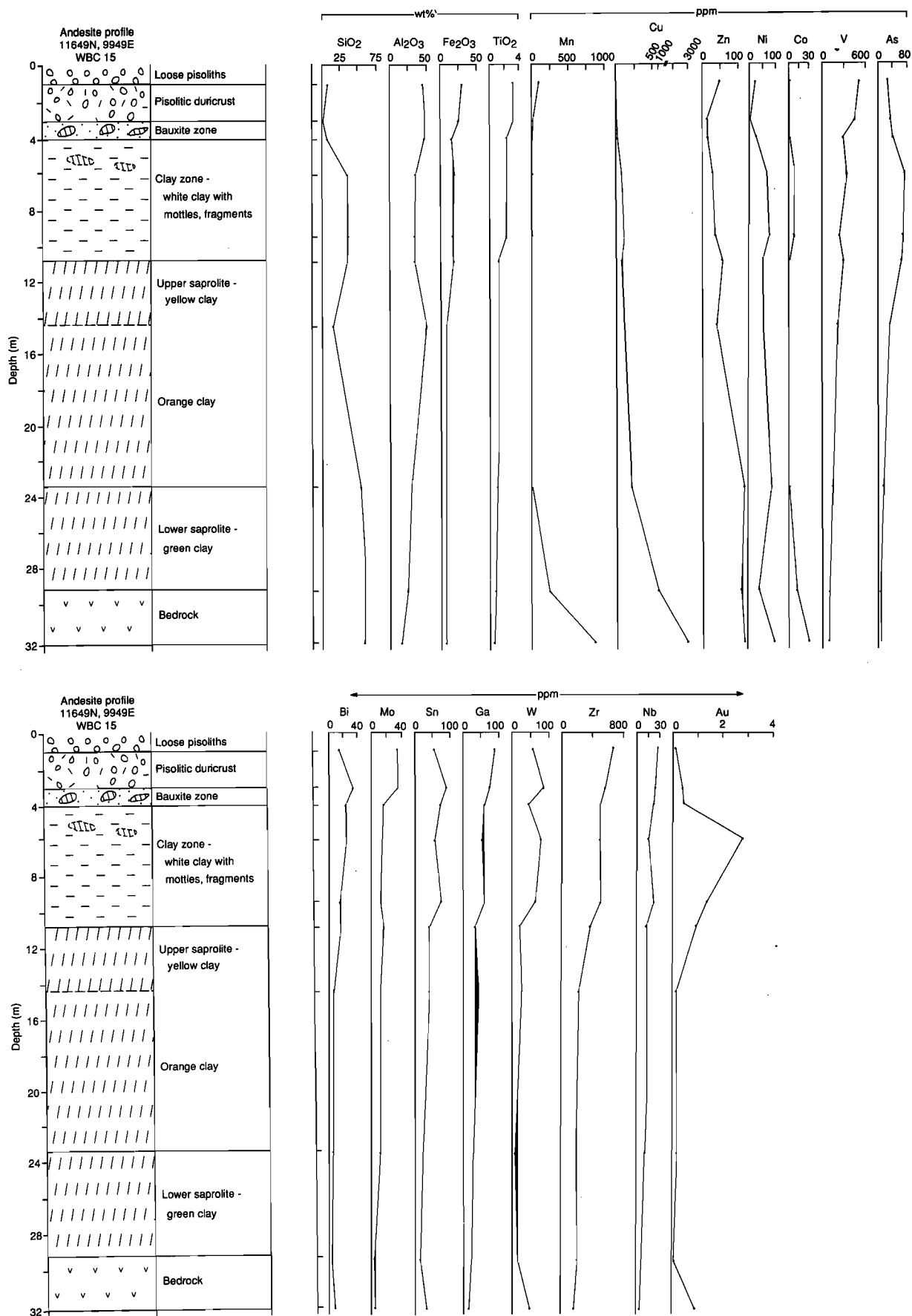


Fig. 5.7 Vertical distribution of some major, minor and trace elements in the andesite profile, WBC 15, Boddington gold mining area.

TABLE 5.1. Summary of the Chemical Composition of the Various Regolith Units Over Andesite and Dolerite Bedrocks

	Andesite Profiles							Dolerite Profiles					
	Bedrock	Lower Saprolite	Middle Saprolite	Upper Saprolite	Bauxite Zone	Lateritic Duricrust	Loose Pisoliths	Bedrock*	Lower Saprolite	Upper Saprolite	Bauxite Zone	Lateritic Duricrust	Loose Pisoliths
No. of Samples	4	7	5	9	2	4	3	NA	5	2	3	3	1
Wt %													
SiO2	57.8-69.7	51.8-72.7	17.5-62.5	12.4-68.0	4.5-8.1	1.7-7.9	1.5-10.9	NA	2.1-50.5	6.2-25.2	1.1-4.7	0.9-3.0	8.3
Al2O3	13.37-17.5	15.70-29.09	8.76-47.98	8.05-33.25	47.22-49.30	38.91-50.63	45.34-49.87	10.00-15.10	28.71-38.16	27.20-30.22	30.41-32.49	23.42-42.69	39.10
Fe2O3	4.86-8.48	4.70-7.05	1.36-11.41	1.37-43.47	15.01-17.30	16.16-32.03	31.46-36.04	17.50-21.50	9.62-33.60	32.03-40.47	37.75-43.61	27.03-53.77	38.90
MgO	1.38-3.68	0.05-1.16	0.02-0.13	0.03-0.11	0.03-0.04	0.01-0.06	0.02-0.07	1.90-4.00	0.03-0.06	0.01-0.03	0.01	0.01-0.03	0.05
CaO	3.03-6.48	0.02-0.91	0.01-0.04	0.02-0.05	0.02	0.02-0.03	0.04-0.09	2.30-7.30	0.02-0.04	0.01-0.02	0.02	0.02-0.04	0.08
Na2O	1.81-3.94	0.04-0.43	0.03-0.11	0.03-0.11	0.01-0.03	0.01-0.03	0.03-0.05	1.20-2.80	0.07-0.47	0.01-0.03	0.01-0.05	0.01-0.03	0.03
K2O	1.42-2.75	0.14-1.45	0.40-0.71	0.10-0.67	0.10-0.18	<0.06-0.4	<0.06-0.12	0.50-1.00	<0.06-0.24	<0.06	<0.06	<0.06-0.19	0.20
TiO2	0.48-0.72	0.52-0.93	0.25-1.67	0.25-4.09	2.25-2.59	2.37-3.90	2.57-3.32	2.20-2.30	1.22-2.80	2.40-3.00	2.47-2.92	1.68-2.74	3.57
LOI	0.87-2.52	5.03-11.40	6.14-24.10	5.78-13.50	26.10-26.60	18.20-27.10	9.43-10.60	NA	12.10-24.00	13.50-20.70	22.20-22.40	18.30-26.40	9.78
ppm													
Mn	305-865	15-1788	4-50	2-306	5-15	11-99	84-113	775-1675	7-123	127-134	92-103	19-95	137
Cr	16-126	16-182	16-325	16-734	340-490	251-408	354-408	16-25	89-267	127-129	177-217	113-220	424
V	66-91	72-126	89-208	71-744	283-369	361-699	513-699	591-910	163-688	737-806	760-917	169-821	669
Cu	92-4850	191-6740	107-125193	76-3310	36-66	16-308	2-14	117-314	104-222	112-263	98-124	41-279	11
Pb	2-8	<2-14	<2-8	<2-20	<2	<2-14	18-20	<2	<2-6	<2-3	3-6	2-6	23
Zn	52-118	36-119	11-35	13-116	11-13	8-18	32-49	96-198	12-18	13-22	10-13	11-12	14
Ni	35-91	27-139	12-77	15-114	<4	<4	<4-17	25-65	<4-48	<4-27	<4	<4	12
Co	13-28	<4-127	<4-8	<4-15	<4	<4	<4	27-56	<4-9	6	<4	<4-6	6
As	<2-44	<2-62	4-48	9-183	40-109	47-123	35-206	<10	8-58	13-32	51-116	26-76	82
Sb	<2	<2	<2	<2-5	<2	<2-4	<2	<5	<2-3	<2	<2-4	<2-3	<2
Bi	<2-9	<2-10	<2-20	2-26	13-25	8-35	7-12	NA	<2	<2	<2	<2	4
Mo	2-8	2-56	4-39	11-87	14-15	34-88	33-46	<5-5	1-10	<1-4	<1-9	4-11	30
Ag	<0.1-9	<0.1-9	<0.1-233	<0.1	<0.1	<0.1	<0.1	<10	<0.1	<0.1	<0.1	<0.1	<0.1
Sn	15-46	10-26	3-50	14-70	18-72	17-84	7-52	<5	<2-4	<2-4	<2-6	2-4	16
Ge	<2	<2-3	<2-3	<2-5	<2	<2	<2	NA	<2-4	<2	<2	<2	<2
Ga	15-20	17-26	2-42	10-83	59-80	68-93	83-87	NA	22-45	36-44	47-52	42-46	93
W	<4-43	6-61	5-55	14-79	17-43	41-85	7-52	<10-20	<4-21	<4	5-6	<4-6	19
Ba	138-577	56-638	27-624	31-195	30-75	13-109	25-41	83-116	8-92	<5	<5	<5-64	64
Zr	37-109	65-181	65-301	48-689	462-497	420-564	470-700	120-143	106-208	149-174	161-228	241-424	542
Nb	<2-5	<2-10	<2-17	4-24	21-22	17-26	16-28	8-12	6-14	6-7	10-13	11-14	29
Se	<2-26	<2-4	<2-79	<2-15	<2-4	<2-3	<2	NA	2-4	2-4	4-8	3-9	<2
Au	0.29-1.19	0.01-1.53	0.17-5.15	0.54-12	0.56-9.10	0.05-1.01	0.02-0.11	<0.01-0.06	0.02-0.20	0.06	0.42-0.81	0.43-5.02	0.06

\* Taken from Monti (1987).

NA = Not available

The elements Mn, Cu, Zn, Co and Ni are considered together because they have many similarities in chemical behaviour in the weathering environment. The chemical patterns of these elements are not consistent from profile to profile for andesite profiles. Manganese, Cu, Ni and Co, for example, are enriched in the lower saprolite of WBC21, but are leached from the lower saprolite of WBC15. However, these elements are strongly leached from the middle saprolite and the overlying horizons in all the profiles. There is a general decrease in Zn and Ni up through the profiles, although there is a near-surface increase in these components. There is also a surface and near-surface increased concentration of Mn and Co.

Vanadium, Cr, As, Bi, Sn, Ga, W, Zr, Nb and Pb are concentrated up the profiles particularly in the upper saprolite, bauxite zone, and lateritic duricrust. However, the concentrations of W, Sn, and Bi are decreased in the pisolitic duricrust and loose pisoliths relative to the underlying fragmental duricrust and bauxite zone. These elements follow more or less the pattern for  $\text{Fe}_2\text{O}_3$ , which suggests that they are associated with Fe-oxides and oxyhydroxides. Some of the elements are retained in primary minerals which are resistant to weathering, such as zircon (Zr, Nb), ilmenite (Cr, V), and sphene (Nb).

There is a gradual increase of Mo up through the profiles. Gallium behaves similarly to Al, as it can substitute for Al in gibbsite and  $\text{Fe}^{3+}$  in goethite.

The Ba contents are maintained throughout the profiles and Ba is reduced only in lateritic duricrust. The concentrations of Ba are generally slightly enriched in the saprolite compared to the bedrock. High concentrations of Ba are closely related to K concentrations.

Gold is detectable in the pisolitic duricrust and loose pisoliths, but the contents are very low compared to the underlying horizons. Gold is strongly concentrated in the bauxite zone and upper clay zone of all the profiles and it decreases sharply from the bauxite zone to loose pisoliths. Exploration work conducted by Reynolds over the Boddington Au deposit shows that the highest and most continuous Au values in the laterite profile occur over mineralised bedrock. However, Au tends to be concentrated at three subhorizontal levels within the profile, namely the lower part of the bauxite zone (Level 1), middle saprolite (Level 2), and lower saprolite (Level 3) (Symons *et al.*, 1988). The three levels are generally separated by barren or weakly-mineralised saprolitic clays. In terms of mineral exploration, Au is showing weak anomalies associated with high As, Mo, Bi, Sn, and W in loose pisoliths and lateritic duricrust.

In the dolerite profile, severe leaching of many major and trace elements occurs at the bedrock-saprolite interface. The trends in element behaviour in andesite and dolerite profiles are very similar, with minor differences due to the contrasting chemistry and mineralogy of the host rock. Gold is not enriched in the clay zone and upper saprolite overlying barren dolerite. However, significant amounts of Au are in the bauxite zone and lateritic duricrust which probably have been laterally transported into these.

The presence of W and Sn in all regolith units of the profiles developed from andesite and its absence from the dolerite profile indicates a relative lack of mobility and lateral transport. However, there is a small surface concentration in loose pisoliths, probably because of residual enrichment.

#### *Geochemical dispersion in pisolitic and nodular lag*

The geochemical patterns are based on 146 sample sites of loose nodules and pisoliths. The sampling pattern may be broken into two parts, namely, that over the Pit A and its surroundings and, that from Pit D. Bedrock relationships for the corresponding areas are shown in Figs. 5.8 and 5.10. Surface samples were collected at 100 m intervals and a radius of 5 to 10 m at each site. The lateritic pisoliths and nodules were generally in the size range of 5 to 15 mm and have a 1-2 mm thick goethite-gibbsite-rich cutan around dark reddish brown to black cores. These lag gravels are highly magnetic and are dominated by hematite, maghemite, amorphous Al-oxides with small amounts of goethite, gibbsite, corundum, and boehmite.

The lag gravels are dominated by  $\text{Al}_2\text{O}_3$  (mean 44%) and  $\text{Fe}_2\text{O}_3$  (mean 40%) with lesser amounts of  $\text{SiO}_2$  (mean 5%). Silica and  $\text{Al}_2\text{O}_3$  show no obvious patterns related to bedrock and the high values of  $\text{Al}_2\text{O}_3$  reflect the bauxitic nature of the area. The CaO, MgO, and  $\text{Na}_2\text{O}$  concentrations are very low, a common feature of lateritic materials. The mean abundances of  $\text{K}_2\text{O}$  are 0.07% with a range commonly from 0.02 to 0.41%. The mean concentration of  $\text{TiO}_2$  is 2% with values ranging from 1.4 to 3.8%.

Some of the analytical data related to Au mineralisation for pisolitic and nodular lag from Pit A and Pit D areas are shown in Figs. 5.8 to 5.11, that show both the analytical values and manually drawn contours. Many trace elements show a close relationship to bedrock type: W, Mo, Sn, Bi being related to mineralised andesite, Cu related to dolerite. In Pit D, these patterns are complementary.

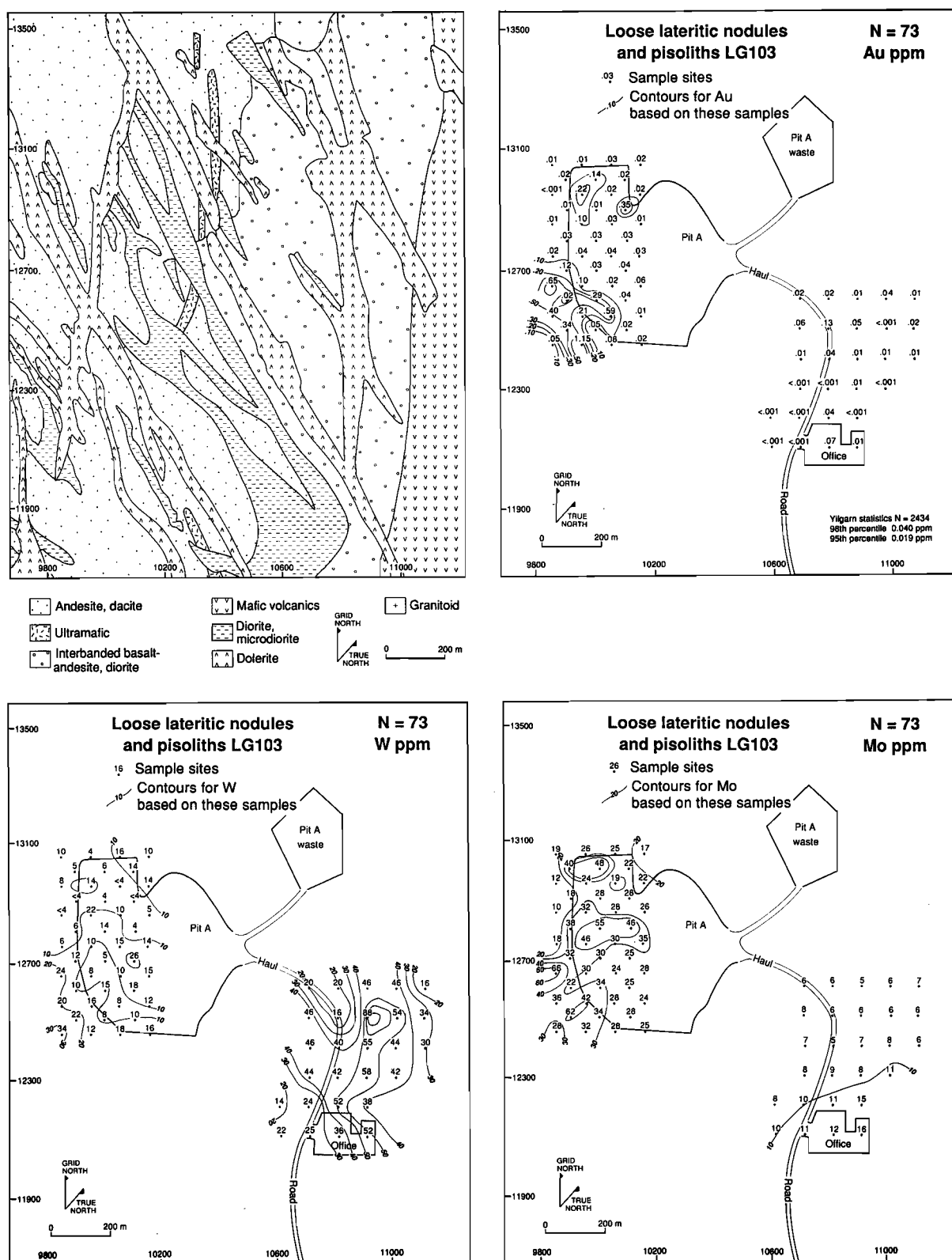
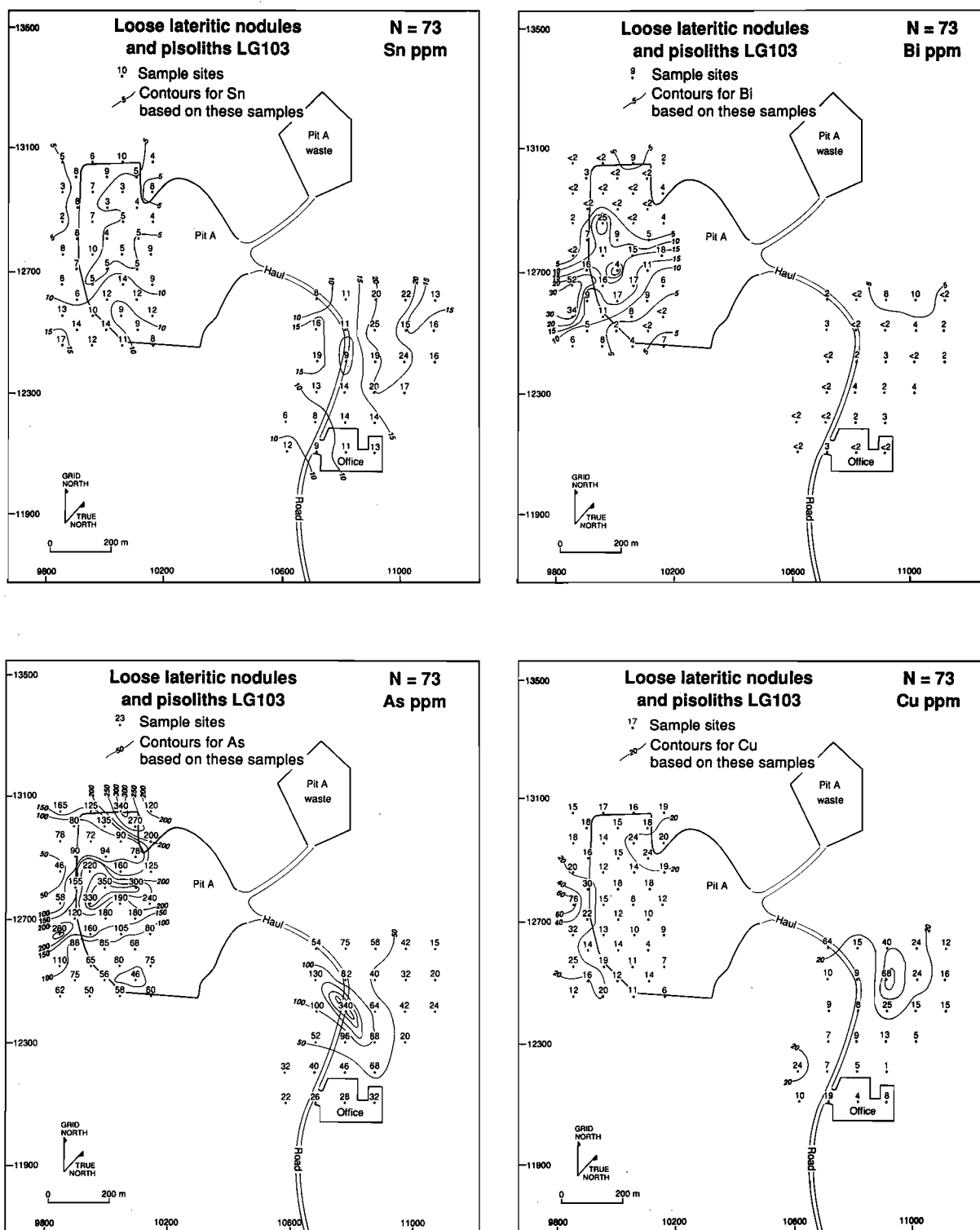


Fig. 5.8 Map showing the bedrock geology of Pit A and its surroundings (modified after Symons *et al.*, 1990) and the distribution of Au, W and Mo in lateritic nodules and pisoliths from Pit A, Boddington.



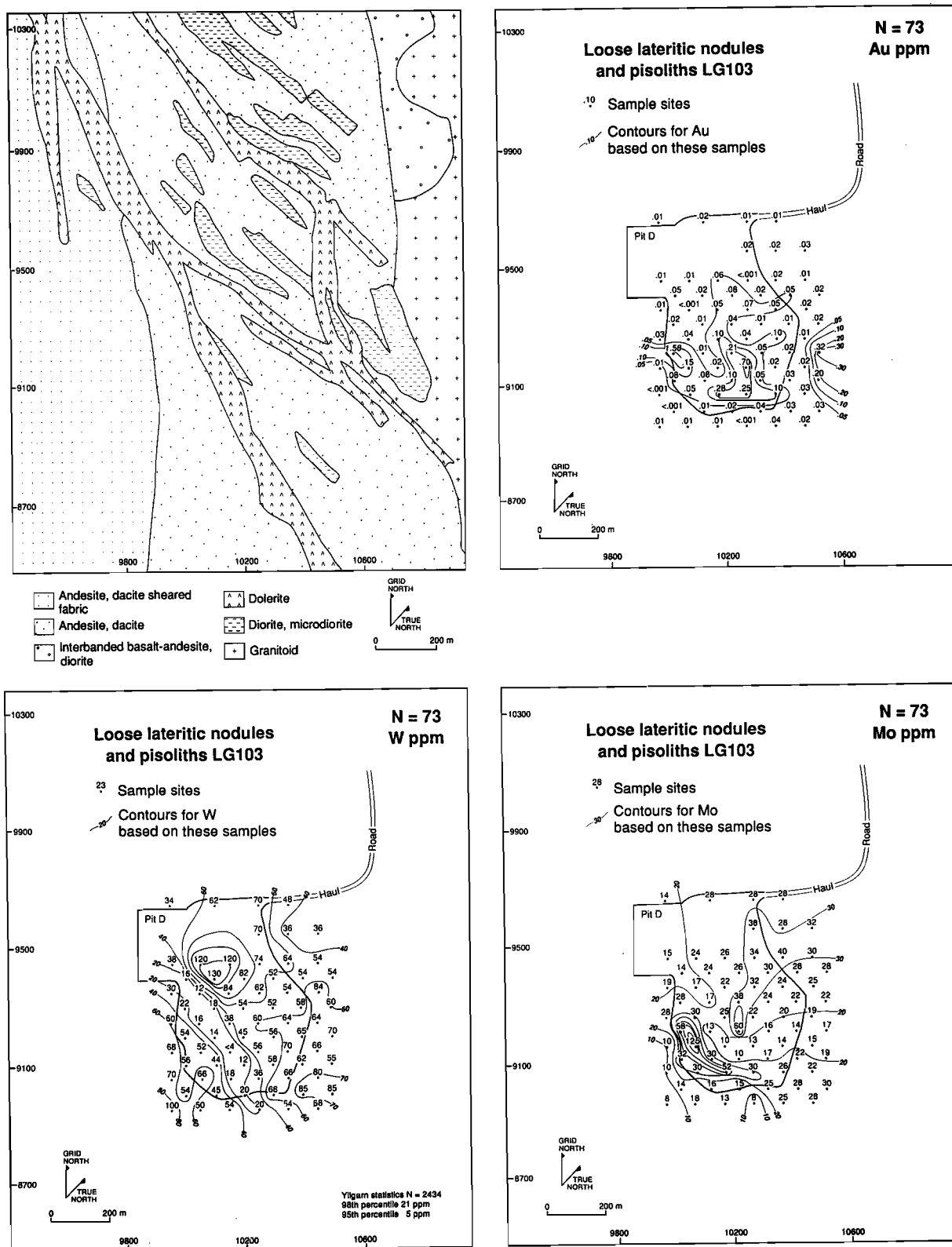


Fig. 5.10 Maps showing the bedrock geology of Pit D and its surroundings (modified after Symons *et al.*, 1990) and the distribution of Au, W and Mo in lateritic nodules and pisoliths from Pit D, Boddington.



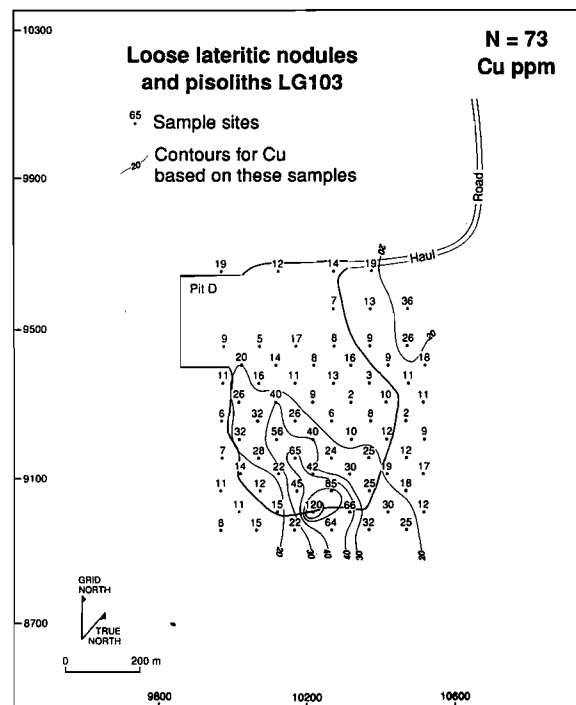
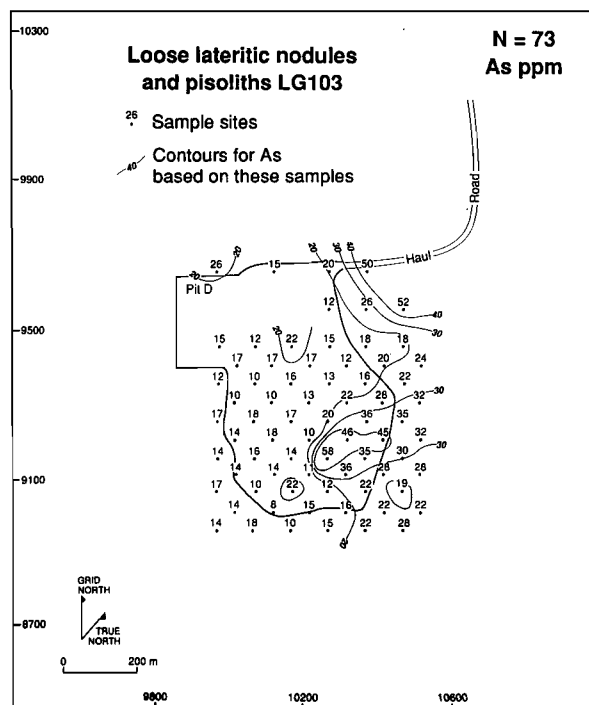
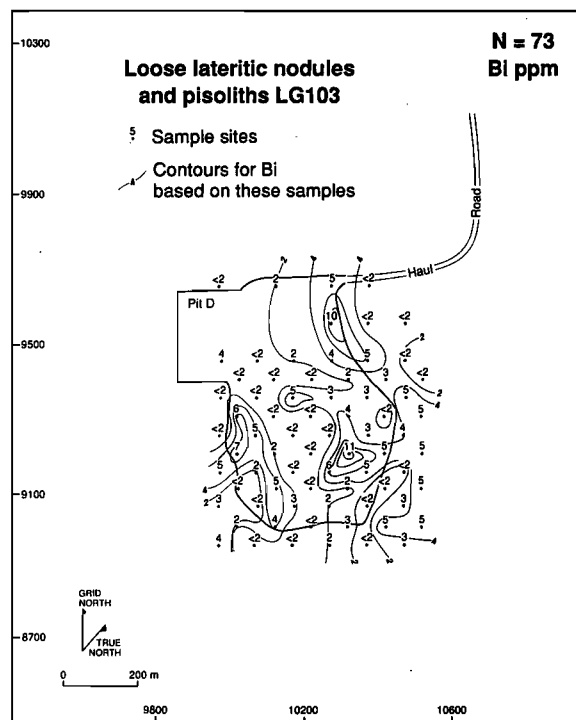
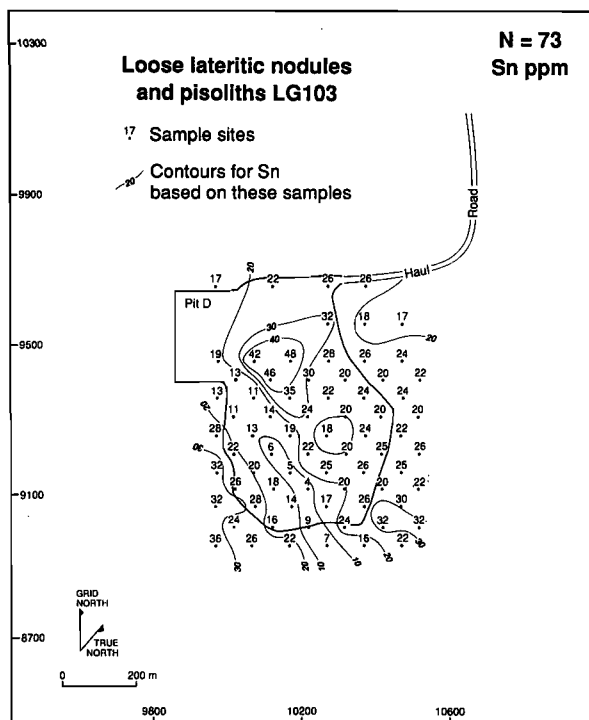


Fig. 5.11 Maps showing the distribution of Sn, Bi, As and Cu in lateritic nodules and pisoliths from Pit D, Boddington.

*Au*

The geochemical pattern for Au in lateritic nodules and pisoliths at surface (Figs. 5.8 and 5.10) shows small abundances and an erratic distribution over the Pit A and Pit D areas with the exception of some higher concentrations (to 1150 ppb) at the southern end of Pit A. Gold abundances, particularly southeast of Pit A are very small. A threshold of 30 ppb would be appropriate in reconnaissance exploration for such an anomaly, based upon experience from elsewhere in the Yilgarn Craton. Gold distribution shows that, in general, there is a limited surface expression of the bedrock abundances. However, as discussed earlier, Au is relatively more abundant in the underlying fragmental duricrusts and the bauxite zone. The highest and most continuous Au abundances in the lateritic profile are over mineralised bedrock (Symons *et al.*, 1988, 1990). In contrast, Davy and El-Ansary (1986) suggest that Au may have dispersed in lateritic residuum more than 500 m from the source.

*As*

The As pattern is strong and extensive over Pit A (reaching 350 ppm) but is relatively weaker (to 58 ppm) over Pit D (Figs 5.9 and 5.11). It measures some 400 m long and 300 m wide over Pit A and shows a more consistent and widespread distribution than Au. The most marked feature of the As pattern is that it is very strong (reaching 350 ppm) at the north-western end of Pit A. There are also local highs in the south-east of Pit A, which may be related to the nature of the bedrock mineralisation. High concentrations of As in Pit A reflect arsenopyrite mineralisation of the bedrock. These results are consistent with the profile data.

*W*

Tungsten shows a more consistent and widespread distribution, being strongest and most widespread in the south-east of Pit A and in Pit D (Figs. 5.8 and 5.10). Tungsten is low in abundance in Pit A (reaching 34 ppm) and is consistently, strongly anomalous over the office and plant area. The W pattern measures some 500 m wide and 400 m long and shows a close relationship to bedrock type. The maximum concentrations of W in lateritic nodules and pisoliths are 130 ppm.

*Sn*

The Sn distribution is similar to W in the strike continuity and breadth of its dispersion patterns, although the anomalies are rather subdued with a peak maximum at 48 ppm (Figs. 5.9 and 5.11). Tin is relatively more abundant in Pit D and is related to scheelite in bedrock.

*Cu, Zn*

Copper and Zn are depleted in loose nodules and pisoliths (Figs. 5.9 and 5.11). Their patterns are weak and do not appear to be particularly useful in defining patterns related to mineralisation. However, local highs (to 120 ppm) of Cu at the southern end of Pit D may be attributed to bedrock mineralisation.

*Mo*

The surface patterns of Mo are anomalous, both over Pit A and Pit D, reaching a maximum of 125 ppm (Figs. 5.8 and 5.10). However, it is low in abundance in the south-east of Pit A and at the office and plant sites.

*Bi*

Bismuth is not uniformly distributed within the overall multi-element anomaly, being strongest and most widespread in the south-western corner of Pit A (Figs. 5.9 and 5.11). Bismuth reaches a maximum concentration of 52 ppm; the high concentrations are related to bedrock mineralisation.

*Other elements*

The pattern for Sb (not shown) in loose nodules and pisoliths is weak with values ranging from 2 to 10 ppm. Silver was detected in all the samples with values ranging from 0.3 to 0.8 ppm. Lead, Ni, and Co have generally flat surface patterns which do not reflect the bedrock. Cobalt shows a particularly restricted pattern with most analyses below the detection limit of 4 ppm.

*Distribution of minerals and elements - all samples*

Two hundred and eighty four samples were grouped according to the nature of the regolith type. These include pisolitic and nodular lag, loose pisoliths (sub-surface), pisolitic duricrust, fragmental duricrust, bauxite zone, clay zone, and saprolite.

### Ternary diagrams

Aluminium,  $\text{Fe}_2\text{O}_3$  and  $\text{SiO}_2$  are the major components of the samples analysed (Fig. 5.12). As expected,  $\text{SiO}_2$  is present in greater amounts in the clay zone and saprolite, whereas  $\text{Fe}_2\text{O}_3$  and  $\text{Al}_2\text{O}_3$  dominate in the various categories of laterite (loose pisoliths, pisolitic duricrust, fragmental duricrust) and the bauxite zone. However, there is a wide range of  $\text{SiO}_2$  and  $\text{Al}_2\text{O}_3$  values in the clay zone and saprolite reflecting variable contents of kaolinite and quartz. The duricrusts and loose pisoliths are characterised by greater amounts of  $\text{Fe}_2\text{O}_3$  and  $\text{Al}_2\text{O}_3$  and low contents of  $\text{SiO}_2$ .

### Lithological discrimination

The identification of bedrock types from their weathering products using geochemistry largely depends upon the presence of diagnostic immobile elements or elements immobilised in resistant minerals. Davy (1979) provided a review of the topic in his study of lateritic profiles and bedrock compositions in the Darling Range. Ratios and plots of Ti and Zr contents have been reported to be commonly effective in discriminating between the major lithological groups (Hallberg, 1984), whether fresh or moderately weathered, but have been found to be less reliable for the lateritic residuum and mottled zone. In the present study, Ti/Zr ratios, originally proposed by Hallberg, were found to be a reliable discriminator of rock type for highly-weathered materials (lateritic duricrust and loose pisoliths), Fig. 5.13A. Samples of lateritic duricrust and loose pisoliths of known lithologies (andesite and dolerite) can be related to particular bedrock lithologies (Fig. 5.13B,C). However, a sample of loose pisoliths derived from a known dolerite lithology lies in the andesite field. The results are not surprising because the fabric of the rock is easily recognisable in the majority of samples suggesting *in situ* formation with little modification. The majority of samples studied occupy the andesitic field which is consistent with the geology of the mine area.

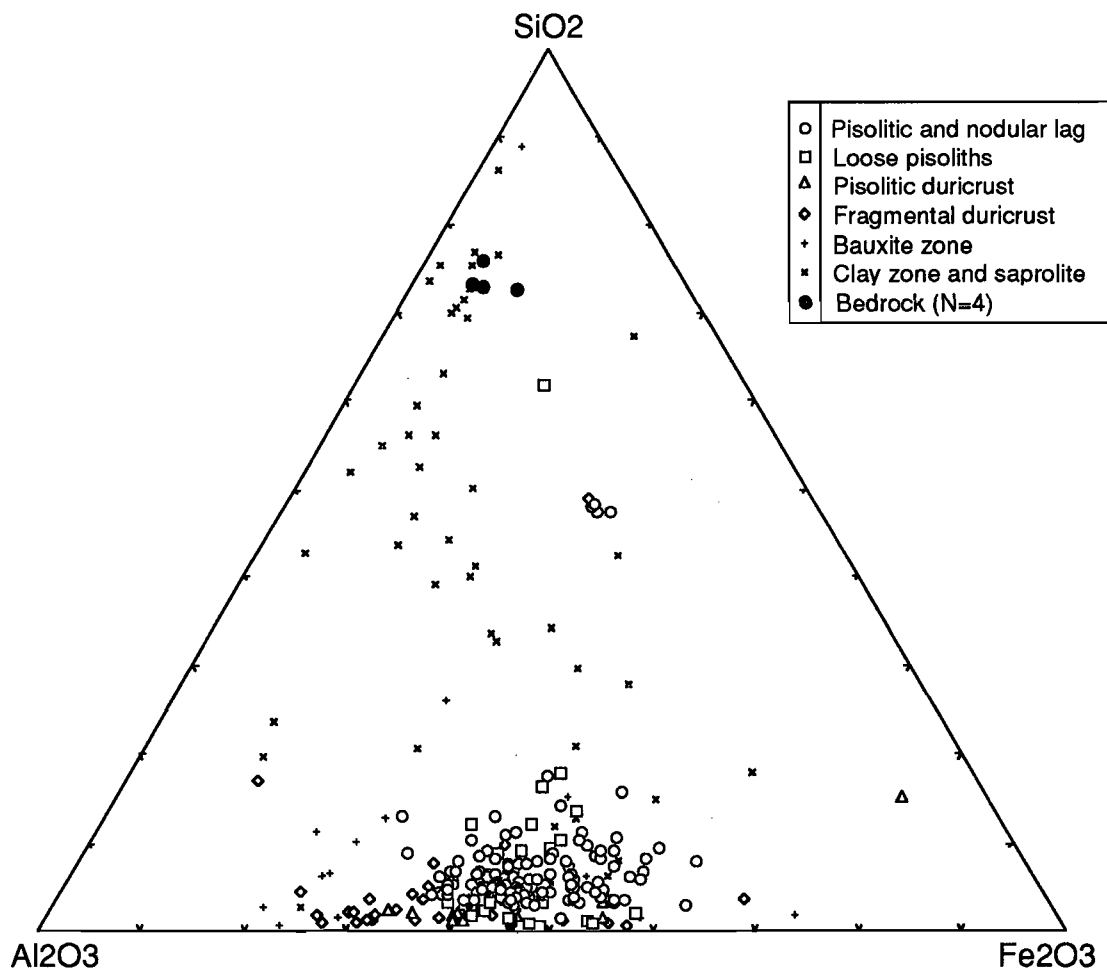


Fig. 5.12 Ternary diagram of the major oxides of the regolith units of the lateritic profile. Bedrock samples are included for comparison, Boddington orientation samples.

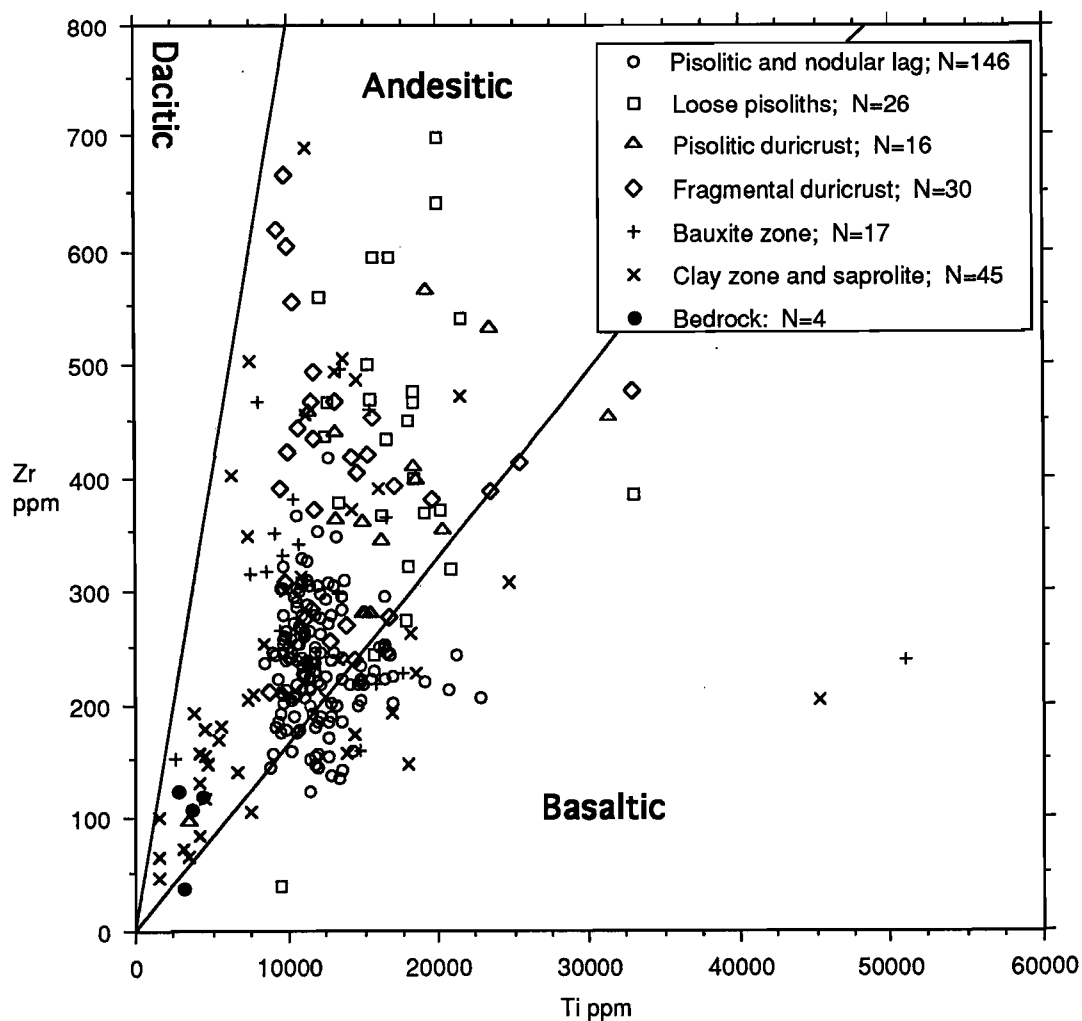
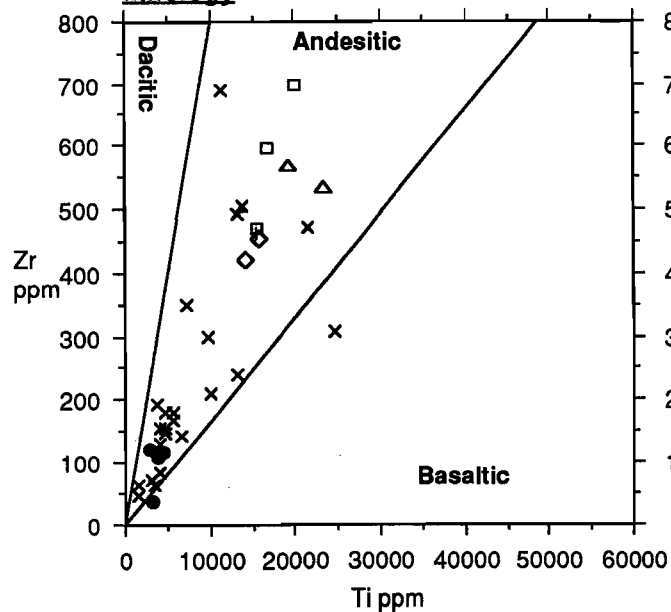
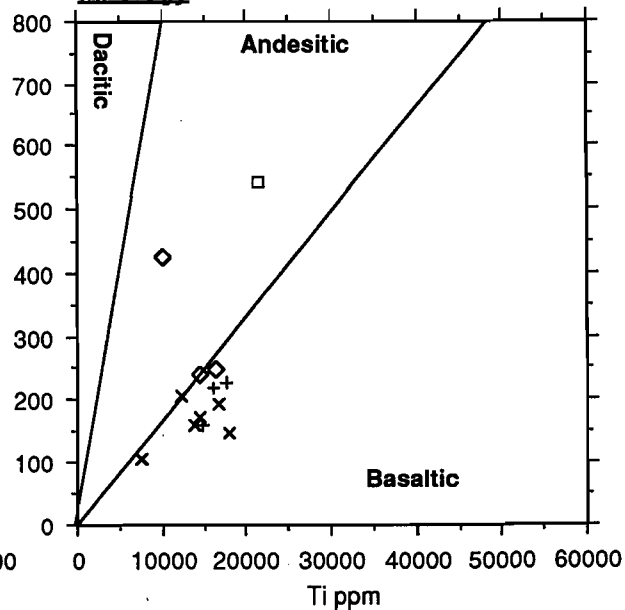
**A - All Samples****B - Samples of known (andesitic) lithology****C - Samples of known (doleritic) lithology**

Fig. 5.13 Ti-Zr plots for weathered materials and bedrocks, Boddington. Lithological fields from Hallberg (1984).

### *Geochemistry*

Summary statistics for the six sample groups are given in Tables 5.2 - 5.7. Box plots for the elements used are given in Figs. 5.14 to 5.17 and display the 10th, 25th, 50th, 75th, and 90th percentiles for each element. Each figure comprises six box plots; pisolitic and nodular lag, loose pisoliths, pisolitic duricrust, fragmental duricrust, bauxite zone, clay zone and saprolite, and bedrock. Box plots summarise the distribution of elements in a lateritic weathering profile developed from andesite, dolerite and dacite bedrocks.

The box plots for  $\text{SiO}_2$ ,  $\text{Al}_2\text{O}_3$  and  $\text{Fe}_2\text{O}_3$  (Fig. 5.14) illustrate the evolution of bedrock to lateritic pisoliths in terms of these three major components. Iron and  $\text{Al}_2\text{O}_3$  are the most abundant components of the lateritic duricrust and pisolitic lag. Aluminium is a residual element and, in comparison with bedrock, is enriched in the lateritic profile. There is an abrupt rise in total  $\text{Al}_2\text{O}_3$  at the bedrock-clay interface. Above the bauxite zone, the total  $\text{Al}_2\text{O}_3$  content varies little, with only a slight increase towards the surface.

Other elements examined include Ti, Cr, V, Ga, Nb, and Zr, all of which have higher concentrations in the lateritic duricrust and loose nodules and pisoliths, and progressively increase from the bedrock to the surface. However, Ti, Nb and Zr contents in nodular and pisolitic lag are lower than in the underlying loose pisoliths and pisolitic duricrust (see Tables 5.2 to 5.7).

Manganese, Zn, Ni, Cu, Ag, Ba and, to a lesser extent, Co, decrease in abundances upwards throughout the profile, although there is a general near-surface increase in these components in the pisolitic lag gravels. In contrast, As, Bi, Mo, Sn, and W are concentrated up the profile but decrease appreciably in pisolitic and nodular lag. The mean Ag concentrations are much higher in the pisolitic lag (0.60 ppm) than in the pisolitic duricrust (0.03 ppm), bauxite zone (0.17 ppm) and saprolite (0.03 ppm) Tables 5.2 to 5.7.

It is interesting to note that the Au concentrations (Fig. 5.17) are greatest in the bauxite zone, being slightly higher than concentrations for the fragmental duricrust and saprolite clay zone. Pisolitic and nodular lag contain the lowest concentrations of Au. Analyses of black (magnetic) and red fragments/pisoliths (non-magnetic) separated from bulk specimens show that red pisoliths in general, are higher in Au than are black pisoliths. No relationship was observed between the Au abundances in fragmental duricrust and the overlying pisolitic duricrust (Fig. 5.18). In contrast, a strong relationship exists between the Au abundances in the bauxite zone and the overlying fragmental duricrust. This suggests precipitation of Au at the bauxite zone, and subsequent gradual leaching/modification during the formation of pisoliths.

### *Element associations and gold morphology*

The major conclusion is that the associations between the elements are not consistent throughout the weathered profile, suggesting that differences in the behaviour of the elements are due to a changing chemical or mineral environment.

A strong negative correlation exists between  $\text{SiO}_2$  and  $\text{Fe}_2\text{O}_3$  in saprolite and remains stronger throughout the whole profile except in pisolitic and nodular lag. In contrast,  $\text{Al}_2\text{O}_3$  and  $\text{Fe}_2\text{O}_3$  show a very strong negative relationship for the upper part of the weathering profile and a weak or no correlation in saprolite.

Iron, V, Al and Ga and Ti and Nb, K, and Ba are positively correlated throughout the whole profile. However, the strengths of these associations vary between the regolith type. Some associations are not evident in the lateritic residuum and pisolitic and nodular lag. For example, Mg and Zn, Mg and Mn, Cu and Ag, which were strongly associated in saprolite, are almost independent in the bauxite zone, lateritic duricrust, and pisolitic and nodular lag. The relationships between Ga - Zr, Ga - Nb, and Ti - V become weaker towards the upper part of the weathering profile. Manganese and Co are strongly correlated throughout the whole profile, except in pisolitic and nodular lag.

Arsenic and Sb, Sn - Bi, and W - Sn are moderately to strongly associated with each other, being more strongly associated in saprolite. Gold is more closely correlated with Bi, Mo and Sn in saprolite and pisolitic duricrust than in the bauxite zone and fragmental duricrust.

The variations in association between elements reflect mineralogical transformations and leaching of elements. The largest change in relationships occurs between the saprolite and the lateritic residuum, implying that many elements were dissolved/leached and reprecipitated in the lateritic horizons. The dispersion of the elements into lateritic residuum tends to homogenise the trace element contents in these horizons.

Table 5.2 Summary statistics for pisolitic and nodular lag LG103.

Element		Method	ltd #values	25th	50th	75th	90th	95th	98th	99th	Min	Max	Mean	S.D.	
SiO2	wt%	icp	0.1	146	3.84	4.58	6.18	8.128	9.25	11.136	13.302	1.2	14.59	5.288	2.214
Al2O3	wt%	icp	0.01	146	40.795	44.97	47.71	50.45	51.496	52.16	52.415	28.53	54.23	44.016	5.267
Fe2O3	wt%	icp	0.01	146	36.58	39.55	42.75	46.668	49.994	50.843	53.091	23.7	55.33	40.078	5.233
MgO	wt%	icp	0.003	146	0.02	0.031	0.042	0.053	0.071	0.082	0.093	0.001	0.125	0.033	0.02
CaO	wt%	icp	0.007	146	0.055	0.064	0.078	0.091	0.101	0.112	0.115	0.038	0.167	0.068	0.018
Na2O	wt%	icp	0.007	146	0.012	0.016	0.019	0.022	0.024	0.027	0.03	0.009	0.036	0.016	0.005
K2O	wt%	icp	0.06	146	0.02	0.06	0.1	0.15	0.194	0.262	0.291	0.02	0.41	0.07	0.066
TiO2	wt%	icp	0.002	146	1.76	1.92	2.15	2.478	2.74	3.173	3.472	1.42	3.79	2.014	0.396
LOI	wt%		0.01	146	5.315	6.2	8.12	10.156	11.255	12.887	14.665	3.65	16.81	6.901	2.359
Mn	ppm	xrf	15	146	69	91	127	182.6	237.8	351.12	432.68	28	626	112.47	79.294
Cr	ppm	icp	20	146	399.5	492	589.5	687	762.8	860	867.02	84	879	502.41	152.55
V	ppm	icp	5	146	622.5	721	860	988.2	1097.5	1216.8	1244.6	84	1430	749.96	190.77
Cu	ppm	aas	2	146	10	15	23	33.6	61.6	68.64	80.86	0.66	120	19.532	16.945
Pb	ppm	xrf	2	146	14	18	22	26.8	30	32	35.24	0.66	80	18.735	8.284
Zn	ppm	aas	2	146	15	18	20	24	25	30.64	38	10	58	18.5	5.523
Ni	ppm	aas	4	146	25	30	34	42	63	80.16	87.4	16	125	32.527	14.828
Co	ppm	aas	4	146	1.33	1.33	4	4	5	6	6	1.33	6	2.395	1.46
As	ppm	xrf	2	146	17	32	79	160	234	330.8	340	8	350	64.288	74.335
Sb	ppm	xrf	2	146	0.66	3	4.5	6	6	7.08	8	0.66	10	3.046	2.069
Bi	ppm	xrf	2	146	0.66	2	5	9.4	15.7	18.56	29.86	0.66	52	4.287	6.304
Mo	ppm	xrf	1	146	13.5	24	29	38	47.4	60.16	64.16	5	125	23.705	14.962
Ag	ppm	aas	0.1	146	0.5	0.6	0.6	0.7	0.7	0.7	0.754	0.3	0.8	0.571	0.09
Sn	ppm	xrf	2	146	9	15	22	26.8	32	36.48	44.16	2	48	16.384	9.213
Ge	ppm	xrf	2	146	0.66	0.66	2	2	3	3.08	4	0.66	5	1.15	0.883
Ga	ppm	xrf	4	146	86	96	105	110	115	120	122.7	58	130	95.055	13.997
W	ppm	xrf	4	146	14	36	56	70	84	101.6	120	133	130	38.593	27.309
Ba	ppm	icp	5	146	34	45	58.5	75.4	85.8	120.52	138	23	149	50.096	21.958
Zr	ppm	icp	5	146	206.5	238	266	303	310.7	348.48	361.56	124	419	238.03	49.977
Nb	ppm	xrf	2	146	13	15	16	18.4	19	20	21.08	8	24	14.658	2.803
Se	ppm	xrf	2	146	0.667	0.667	2	4	5	6.08	7	0.667	8	1.594	1.576
Be	ppm	icp	1	146	1	1	1	2	2	2	2	1	2	1.144	0.352
Au	ppm	gf-aas	0.001	146	0.01	0.02	0.05	0.204	0.334	0.654	0.943	0.001	1.58	0.081	0.191

Table 5.3 Summary statistics for loose pisoliths LT102

Element		Method	ltd	#values	25th	50th	75th	90th	95th	98th	99th	Min	Max	Mean	S.D.
SiO2	wt%	icp	0.1	26	1.08	2.57	8.77	12.836	15.016	31.418	40.094	0.64	48.77	6.88	9.686
Al2O3	wt%	icp	0.01	26	36.33	40.6	42.945	45.868	46.688	48.222	49.046	15.43	49.87	39.566	6.46
Fe2O3	wt%	icp	0.01	26	34.155	36.04	38.755	40.798	41.892	43.951	44.976	14.59	46	36.019	5.604
MgO	wt%	icp	0.003	26	0.02	0.04	0.05	0.07	0.126	1.796	2.688	0.01	3.58	0.175	0.695
CaO	wt%	icp	0.007	26	0.03	0.05	0.08	0.208	0.22	4.962	7.531	0.03	10.1	0.456	1.968
Na2O	wt%	icp	0.007	26	0.01	0.02	0.03	0.04	0.047	0.972	1.471	0.003	1.97	0.095	0.383
K2O	wt%	icp	0.06	26	0.02	0.02	0.12	0.182	0.221	0.249	0.26	0.02	0.27	0.079	0.074
TiO2	wt%	icp	0.002	26	2.395	2.77	3.1	3.392	3.54	4.492	4.991	1.57	5.49	2.852	0.749
LOI	wt%		0.01	26	10.7	14.2	16.4	17.68	18.99	21.468	22.534	1.67	23.6	13.712	4.34
Mn	ppm	xrf	15	26	60	85	126	184.8	452.1	1021.8	1271.4	5	1521	165.15	294.42
Cr	ppm	icp	20	26	349	399	450.5	518.8	561.7	596.8	612.4	68	628	402.92	108.08
V	ppm	icp	5	26	578	669	692.5	768.6	788	926.48	998.24	356	1070	655.39	131.25
Cu	ppm	aas	2	26	7	11	18.5	41	67.9	123.4	150.7	2	178	21.885	35.678
Pb	ppm	xrf	2	26	6	14	19.5	20.8	22	22.48	22.74	0.67	23	12.768	7.371
Zn	ppm	aas	2	26	9	12	13.5	36	46	96.52	122.26	7	148	20.231	28.18
Ni	ppm	aas	4	26	6.665	18	23	27.4	40.6	86.8	108.9	1.33	131	20.615	24.869
Co	ppm	aas	4	26	1.33	1.33	1.33	3.198	6.7	33.88	48.44	1.33	63	4.1	12.096
As	ppm	xrf	2	26	20	75	182	280.4	327	421.68	471.34	6	521	120.81	128.51
Sb	ppm	xrf	2	26	0.67	2	3.5	6	8.1	9.48	9.74	0.67	10	2.741	2.694
Bi	ppm	xrf	2	26	2	4	5	7.4	10.1	11.48	11.74	0.67	12	4.088	2.984
Mo	ppm	xrf	1	26	28	36	43	55.8	61.4	62	62	0.33	62	35.743	14.772
Ag	ppm	aas	0.1	26	0.03	0.03	0.03	0.03	0.03	0.03	0.03	0.03	0.03	0.03	0
Sn	ppm	xrf	2	26	10.5	13	23	54.8	56	58.88	60.44	3	62	21.808	18.284
Ge	ppm	xrf	2	26	0.67	0.67	0.67	0.67	2.298	3.96	4.48	0.67	5	0.917	0.951
Ga	ppm	xrf	4	26	74	87	102.5	110	124	137.2	141.1	14	145	87.885	25.475
W	ppm	xrf	4	26	16	24	48	189	195	197.4	198.7	1.33	200	53.551	63.856
Ba	ppm	icp	5	26	16	25	40	47	53.7	58.8	61.4	8	64	28.923	15.352
Zr	ppm	icp	5	26	344.5	435	489.5	596	628.9	670.36	685.18	40	700	428.08	138.68
Nb	ppm	xrf	2	26	19.5	22	24.5	28.4	29.7	30.96	31.48	0.67	32	21.718	6.259
Se	ppm	xrf	2	26	0.67	0.67	3	4.4	5	5.48	5.74	0.67	6	1.821	1.736
Be	ppm	icp	1	26	0.33	0.33	2	2.4	3	3	3	0.33	3	0.987	0.991
Au	ppm	gf-aas	0.001	26	0.02	0.08	0.14	0.314	0.576	0.785	0.852	0.01	0.92	0.152	0.212



Table 5.4 Summary statistics for pisolitic duricrust LT202.

Element		Method	ltd	#values	25th	50th	75th	90th	95th	98th	99th	Min	Max	Mean	S.D.
SiO <sub>2</sub>	wt%	icp	0.1	16	1.07	1.7	2.78	3.17	5.552	10.621	12.31	0.64	14	2.593	3.159
Al <sub>2</sub> O <sub>3</sub>	wt%	icp	0.01	16	39.29	42.3	44.5	45.78	46.556	47.41	47.695	7.38	47.98	39.991	9.491
Fe <sub>2</sub> O <sub>3</sub>	wt%	icp	0.01	16	30.46	31.1	35.4	42.648	48.676	61.17	65.335	24.31	69.5	34.766	10.612
MgO	wt%	icp	0.003	16	0.01	0.02	0.02	0.03	0.064	0.146	0.173	0.01	0.2	0.029	0.046
CaO	wt%	icp	0.007	16	0.03	0.04	0.04	0.05	0.072	0.125	0.142	0.03	0.16	0.047	0.031
Na <sub>2</sub> O	wt%	icp	0.007	16	0.003	0.01	0.02	0.03	0.032	0.037	0.038	0.003	0.04	0.014	0.011
K <sub>2</sub> O	wt%	icp	0.06	16	0.02	0.02	0.02	0.02	0.054	0.136	0.163	0.02	0.19	0.031	0.043
TiO <sub>2</sub>	wt%	icp	0.002	16	2.2	2.52	3.07	3.582	4.16	4.784	4.992	0.6	5.2	2.749	0.977
LOI	wt%		0.01	16	17.6	19.3	22.2	23.92	24.5	24.74	24.82	7.6	24.9	19.625	4.248
Mn	ppm	xrf	15	16	42	56	68	348.2	758.8	1293.52	1471.76	5	1650	191	409.407
Cr	ppm	icp	20	16	352	402	453	510.6	571.2	574.08	575.04	243	576	404.625	91.939
V	ppm	icp	5	16	490	584	648	708.6	721.6	747.04	755.52	405	764	579.5	105.806
Cu	ppm	aas	2	16	10	18	33	95.8	113.2	123.28	126.64	3	130	33.938	38.853
Pb	ppm	xrf	2	16	4	7	9	11.6	23.2	45.28	52.64	0.66	60	9.729	13.864
Zn	ppm	aas	2	16	6	9	11	13.8	82.4	236.96	288.48	3	340	29.438	82.887
Ni	ppm	aas	4	16	1.33	14	18	21.6	32.4	52.56	59.28	1.33	66	15.103	15.698
Co	ppm	aas	4	16	1.33	1.33	1.33	2.398	6.4	12.16	14.08	1.33	16	2.414	3.684
As	ppm	xrf	2	16	19	47	125	410	420	444	452	13	460	131.812	159.283
Sb	ppm	xrf	2	16	0.66	2	4	5	5.4	6.36	6.68	0.66	7	2.831	1.999
Bi	ppm	xrf	2	16	2	3	5	8.4	14.2	26.68	30.84	0.66	35	5.749	8.224
Mo	ppm	xrf	1	16	26	36	50	66.4	70.8	72.72	73.36	6	74	40.062	19.716
Ag	ppm	aas	0.1	16	0.03	0.03	0.03	0.03	0.03	0.03	0.03	0.03	0.03	0.108	0.16
Sn	ppm	xrf	2	16	12	17	54	62	73.6	79.84	81.92	2	84	33.25	25.629
Ge	ppm	xrf	2	16	0.66	0.66	0.66	0.66	0.66	0.66	0.66	0.66	0.66	0.66	0
Ga	ppm	xrf	4	16	72	76	100	107	114.6	125.64	129.32	38	133	85.562	23.085
W	ppm	xrf	4	16	22	31	154	188	206	220.4	225.2	16	230	92.688	78.407
Ba	ppm	icp	5	16	11	15	23	26.4	78	200.4	241.2	9	282	33	66.697
Zr	ppm	icp	5	16	279	361	440	488.2	538.4	553.76	558.88	97	564	373.125	111.505
Nb	ppm	xrf	2	16	15	19	22	24.8	26.8	28.72	29.36	3	30	18.625	6.206
Se	ppm	xrf	2	16	0.667	0.667	3	3	3	3	3	0.667	3	1.479	1.109
Be	ppm	icp	1	16	0.333	2	2	2	2.2	2.68	2.84	0.333	3	1.375	0.91
Au	ppm	gf-aas	0.001	16	0.03	0.07	0.13	0.204	0.308	0.399	0.43	0.001	0.46	0.109	0.116

Table 5.5 Summary statistics for fragmental duricrust LT205.

Element		Method	ltd	#values	25th	50th	75th	90th	95th	98th	99th	Min	Max	Mean	S.D.
SiO <sub>2</sub>	wt%	icp	0.1	30	0.9	1.51	2.995	5.63	10.005	24.42	33.66	0.41	42.9	3.741	7.788
Al <sub>2</sub> O <sub>3</sub>	wt%	icp	0.01	30	39.25	43.7	47.05	49.2	49.4	49.892	50.261	19.1	50.63	42.196	7.466
Fe <sub>2</sub> O <sub>3</sub>	wt%	icp	0.01	30	21.38	25.32	31.865	41.59	43.045	47.422	50.596	8.87	53.77	27.592	9.422
MgO	wt%	icp	0.003	30	0.01	0.02	0.02	0.03	0.05	0.072	0.081	0.01	0.09	0.022	0.017
CaO	wt%	icp	0.007	30	0.02	0.03	0.04	0.04	0.045	0.078	0.099	0.02	0.12	0.033	0.018
Na <sub>2</sub> O	wt%	icp	0.007	30	0.003	0.003	0.01	0.03	0.03	0.038	0.044	0.003	0.05	0.01	0.012
K <sub>2</sub> O	wt%	icp	0.06	30	0.02	0.02	0.055	0.13	0.185	0.274	0.337	0.02	0.4	0.059	0.082
TiO <sub>2</sub>	wt%	icp	0.002	30	1.7	1.97	2.585	3.24	4.055	4.72	5.095	1.47	5.47	2.352	0.887
LOI	wt%		0.01	30	21.45	25.3	27.35	28	28.75	29.04	29.07	10.5	29.1	23.91	4.828
Mn	ppm	xrf	15	30	22	36	75.5	113	177	522.6	769.801	5	1017	85.467	181.358
Cr	ppm	icp	20	30	287.5	349	396	420	440.5	452.8	457.9	113	463	337	79.741
V	ppm	icp	5	30	372	431	585	791	915.5	1113.6	1191.3	169	1269	510.433	235.242
Cu	ppm	aas	2	30	21	30	43.5	90	188.5	290.6	299.3	8	308	50.833	69.395
Pb	ppm	xrf	2	30	1.33	5	7	14	15.5	41.4	59.7	0.66	78	7.587	13.947
Zn	ppm	aas	2	30	7	9	11.5	14	14.5	18.6	21.3	4	24	9.833	3.983
Ni	ppm	aas	4	30	1.33	12	16	16	20	24	27	1.33	30	10.454	7.856
Co	ppm	aas	4	30	1.33	1.33	1.33	7	7.5	8	8	1.33	8	2.486	2.268
As	ppm	xrf	2	30	15.5	26	97.5	280	319.5	352	361	7	370	83.3	105.402
Sb	ppm	xrf	2	30	0.66	2	3	4	5.5	6.8	7.4	0.66	8	2.175	1.877
Bi	ppm	xrf	2	30	3	4	5.5	7	9	11.6	12.8	0.66	14	4.577	2.923
Mo	ppm	xrf	1	30	24	38	54	58	74	104.8	117.4	3	130	40.667	25.289
Ag	ppm	aas	0.1	30	0.03	0.03	0.03	0.2	0.45	0.5	0.5	0.03	0.5	0.09	0.136
Sn	ppm	xrf	2	30	12	25	46	48	54	56.8	57.4	2	58	28.367	17.934
Ge	ppm	xrf	2	30	0.66	0.66	0.66	0.66	2	2	2	0.66	2	0.794	0.409
Ga	ppm	xrf	4	30	60.5	70	78	80	85	88.4	90.2	42	92	69.4	12.602
W	ppm	xrf	4	30	16.5	57	147.5	175	190	192	193.5	1.33	195	80.889	68.582
Ba	ppm	icp	5	30	12	20	32.5	53	86.5	307.8	456.9	1.66	606	44.466	108.285
Zr	ppm	icp	5	30	281	405	461	556	611.5	637.2	651.6	212	666	402.3	116.128
Nb	ppm	xrf	2	30	12	14	20	24	24.5	26.2	27.1	8	28	16.167	5.18
Se	ppm	xrf	2	30	0.667	0.667	3	5	7	8.4	8.7	0.667	9	2.178	2.314
Be	ppm	icp	1	30	0.333	1	1.5	2	2	2	2	0.333	2	1	0.678
Au	ppm	gf-aas	0.001	30	0.11	0.25	0.555	1.45	2.03	3.394	4.207	0.001	5.02	0.612	0.991

Table 5.6 Summary statistics for bauxite zone samples bz.

Element		Method	ltd	#values	25th	50th	75th	90th	95th	98th	99th	Min	Max	Mean	S.D.
SiO <sub>2</sub>	wt%	icp	0.1	17	1.433	4.275	7.903	14.717	29.88	63.132	74.216	0.43	85.3	10.026	20.041
Al <sub>2</sub> O <sub>3</sub>	wt%	icp	0.01	17	30.93	40.05	47.362	50.938	52.106	52.126	52.133	7.85	52.14	38.637	12.221
Fe <sub>2</sub> O <sub>3</sub>	wt%	icp	0.01	17	16.122	20.08	35.82	42.91	45.318	51.127	53.064	2.93	55	25.856	13.633
MgO	wt%	icp	0.003	17	0.01	0.02	0.037	0.135	0.182	0.223	0.236	0.01	0.25	0.049	0.067
CaO	wt%	icp	0.007	17	0.02	0.02	0.03	0.043	0.063	0.109	0.125	0.003	0.14	0.03	0.031
Na <sub>2</sub> O	wt%	icp	0.007	17	0.01	0.02	0.03	0.04	0.041	0.047	0.048	0.003	0.05	0.022	0.014
K <sub>2</sub> O	wt%	icp	0.06	17	0.02	0.052	0.165	0.323	0.645	1.002	1.121	0.02	1.24	0.172	0.305
TiO <sub>2</sub>	wt%	icp	0.002	17	1.467	1.755	2.56	2.801	3.752	6.583	7.526	0.43	8.47	2.299	1.718
LOI	wt%		0.01	17	21.525	22.95	26.55	28.34	29.705	30.062	30.181	2.01	30.3	22.771	6.69
Mn	ppm	xrf	15	17	9.5	23	81.25	108.4	415.599	1417.24	1751.12	2	2085	160.294	497.491
Cr	ppm	icp	20	17	220.25	323	377.25	485.1	494.95	511.78	517.39	75	523	317.176	120.487
V	ppm	icp	5	17	277.75	359.5	771.25	913.5	929	969.8	983.4	51	997	510.647	298.276
Cu	ppm	aas	2	17	36	61	98.75	124.3	126.35	130.94	132.47	17	134	69.235	39.487
Pb	ppm	xrf	2	15	1	3	6.5	13.5	18.5	26.6	29.3	1	32	6.133	8.34
Zn	ppm	aas	2	17	7	9.5	11.75	13.6	18.75	31.5	35.75	5	40	11.412	7.882
Ni	ppm	aas	4	17	3	3	11	18.9	21.75	24.3	25.15	3	26	7.824	7.544
Co	ppm	aas	4	17	1.333	2	2	2	2.6	4.64	5.32	1.333	6	2.039	1.066
As	ppm	xrf	2	17	10.25	34	69.75	169.7	296.35	300.94	302.47	5	304	69.882	92.992
Sb	ppm	xrf	2	12	1	2	4	4	4.8	5.52	5.76	1	6	2.75	1.658
Bi	ppm	xrf	2	13	4	5.5	11.5	21.6	24.35	24.74	24.87	2	25	9.154	7.872
Mo	ppm	xrf	1	17	7.5	14.5	23.75	56	65.6	98.24	109.12	1	120	26.059	29.805
Ag	ppm	aas	0.1	17	0.03	0.167	0.167	0.167	0.167	0.167	0.167	0.03	0.167	0.123	0.064
Sn	ppm	xrf	2	17	6	16.5	31.25	53.8	73.05	76.62	77.81	1	79	23.176	23.458
Ge	ppm	xrf	2	10	1.333	1.333	2	2	3	3.6	3.8	1	4	1.767	0.861
Ga	ppm	xrf	4	17	47.25	57	60.75	69.5	80	80	80	22	80	55.647	13.729
W	ppm	xrf	4	17	7	25	99.5	155	171.4	179.56	182.28	4	185	61.118	63.414
Ba	ppm	icp	5	17	16.5	38.5	56	95.7	164.4	233.76	256.88	2	280	54.529	67.458
Zr	ppm	icp	5	17	231	316.5	361.5	464.1	473.2	487.48	492.24	153	497	317.471	100.837
Nb	ppm	xrf	2	17	10	13	14.75	21.3	23.8	29.92	31.96	4	34	14.294	6.989
Se	ppm	xrf	2	17	1	1	3.75	7.3	8.45	9.98	10.49	1	11	3.059	2.989
Be	ppm	icp	1	17	0.333	0.333	1	2	2.15	2.66	2.83	0.333	3	0.863	0.85
Au	ppm	gf-aas	0.001	17	0.333	0.605	2.062	6.246	6.686	8.134	8.617	0.05	9.1	1.954	2.66

Table 5.7 Summary statistics for saprolite samples sap.

Element		Method	ltd	#values	25th	50th	75th	90th	95th	98th	99th	Min	Max	Mean	S.D.
SiO <sub>2</sub>	wt%	icp	0.1	45	16.895	36.9	60.48	67.165	69.625	71.38	72.055	1.93	72.73	38.686	21.918
Al <sub>2</sub> O <sub>3</sub>	wt%	icp	0.01	45	21.815	29.755	33.528	39.29	46.47	50.591	51.271	8.05	51.95	29.109	9.604
Fe <sub>2</sub> O <sub>3</sub>	wt%	icp	0.01	45	5.295	11.29	27.315	38.25	41.115	44.285	47.952	1.36	51.62	17.235	13.818
MgO	wt%	icp	0.003	45	0.03	0.05	0.125	0.805	1.128	1.151	1.155	0.01	1.16	0.209	0.347
CaO	wt%	icp	0.007	45	0.02	0.035	0.04	0.165	0.273	0.55	0.73	0.01	0.91	0.08	0.155
Na <sub>2</sub> O	wt%	icp	0.007	45	0.032	0.07	0.11	0.26	0.315	0.434	0.452	0.01	0.47	0.108	0.107
K <sub>2</sub> O	wt%	icp	0.06	45	0.082	0.195	0.707	1.07	1.283	1.717	2.918	0.02	4.12	0.488	0.69
TiO <sub>2</sub>	wt%	icp	0.002	45	0.77	1.34	2.312	3.01	3.45	4.435	5.987	0.25	7.54	1.74	1.29
LOI	wt%		0.01	45	7.967	12.4	15.475	20.75	24.075	25.43	26.915	5.03	28.4	13.048	5.742
Mn	ppm	xrf	15	45	5	34.5	145.25	278	322.5	524.398	1156.2	5	1788	128.689	274.524
Cr	ppm	icp	20	45	86.25	128	261.75	420	476.25	529.7	631.85	6.66	734	193.851	160.65
V	ppm	icp	5	45	103.75	220	483.5	736	790.5	836.4	838.2	71	840	317.4	249.034
Cu	ppm	aas	2	45	104.5	199	383.25	3735	5615	7066	8533	10	10000	1069.84	2120.48
Pb	ppm	xrf	2	45	0.66	3.5	6	9.5	14	20.2	21.1	0.66	22	4.857	4.913
Zn	ppm	aas	2	45	13	18.5	35.75	101	115.25	118.1	118.55	2	119	35.444	34.772
Ni	ppm	aas	4	45	19	36	49.5	61.5	84.5	116.5	127.75	1.33	139	38.807	27.534
Co	ppm	aas	4	45	1.33	6	8.75	14	14.75	29.8	78.4	1.33	127	8.754	18.648
As	ppm	xrf	2	45	7.25	19	55.5	128.5	186	371.4	467.7	0.66	564	55.088	101.202
Sb	ppm	xrf	2	45	0.66	0.66	1.665	2.5	4.75	6	6	0.66	6	1.328	1.39
Bi	ppm	xrf	2	45	0.66	2	5	15	19.25	23.3	24.65	0.66	26	4.841	6.506
Mo	ppm	xrf	1	45	5	11	21	41.5	55.25	89.6	101.3	0.33	113	18.555	22.358
Ag	ppm	aas	0.1	45	0.03	0.03	0.03	0.03	2	4.05	6.525	0.03	9	0.372	1.458
Sn	ppm	xrf	2	45	4	14.5	24.75	47	55	65.5	67.75	0.66	70	19.407	18.366
Ge	ppm	xrf	2	45	0.66	0.66	2	3.5	4	4.1	4.55	0.66	5	1.693	1.244
Ga	ppm	xrf	4	45	24	35.5	45	58	70.75	82.1	82.55	1.33	83	37.03	18.029
W	ppm	xrf	4	45	6.25	15	27	60	77.75	171.7	246.85	1.33	322	30.429	52.648
Ba	ppm	icp	5	45	23.25	98	218.5	631	690.5	759.9	889.95	1.66	1020	185.496	239.657
Zr	ppm	icp	5	45	148.25	204.5	312.75	480	500.75	524.3	606.65	48	689	246.511	146.733
Nb	ppm	xrf	2	45	6	11	14	19.5	21.75	25.9	34.45	0.66	43	11.177	7.625
Se	ppm	xrf	2	45	0.667	0.667	2	4	4	21.4	50.2	0.667	79	3.4	11.761
Be	ppm	icp	1	45	0.333	0.333	0.333	0.333	0.333	1.1	1.55	0.333	2	0.385	0.265
Au	ppb	gf-aas	0.001	45	0.155	0.505	1.683	4.055	5.142	7.527	9.763	0.01	12	1.519	2.305

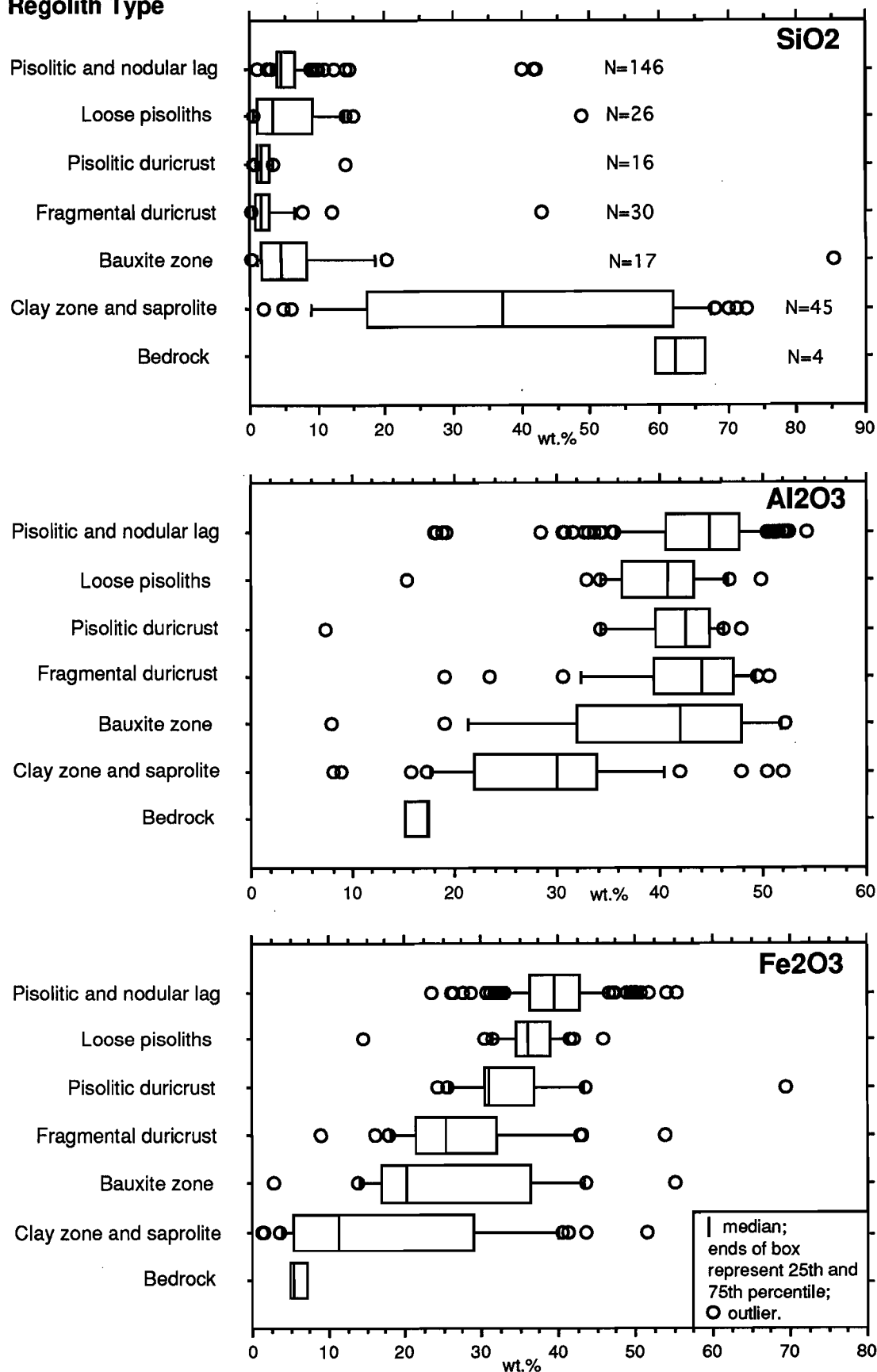
**Regolith Type**

Fig. 5.14 Box plots showing the distribution of SiO<sub>2</sub>, Al<sub>2</sub>O<sub>3</sub> and Fe<sub>2</sub>O<sub>3</sub> in several regolith materials and bedrock arranged vertically in order of the regolith stratigraphy, Boddington.

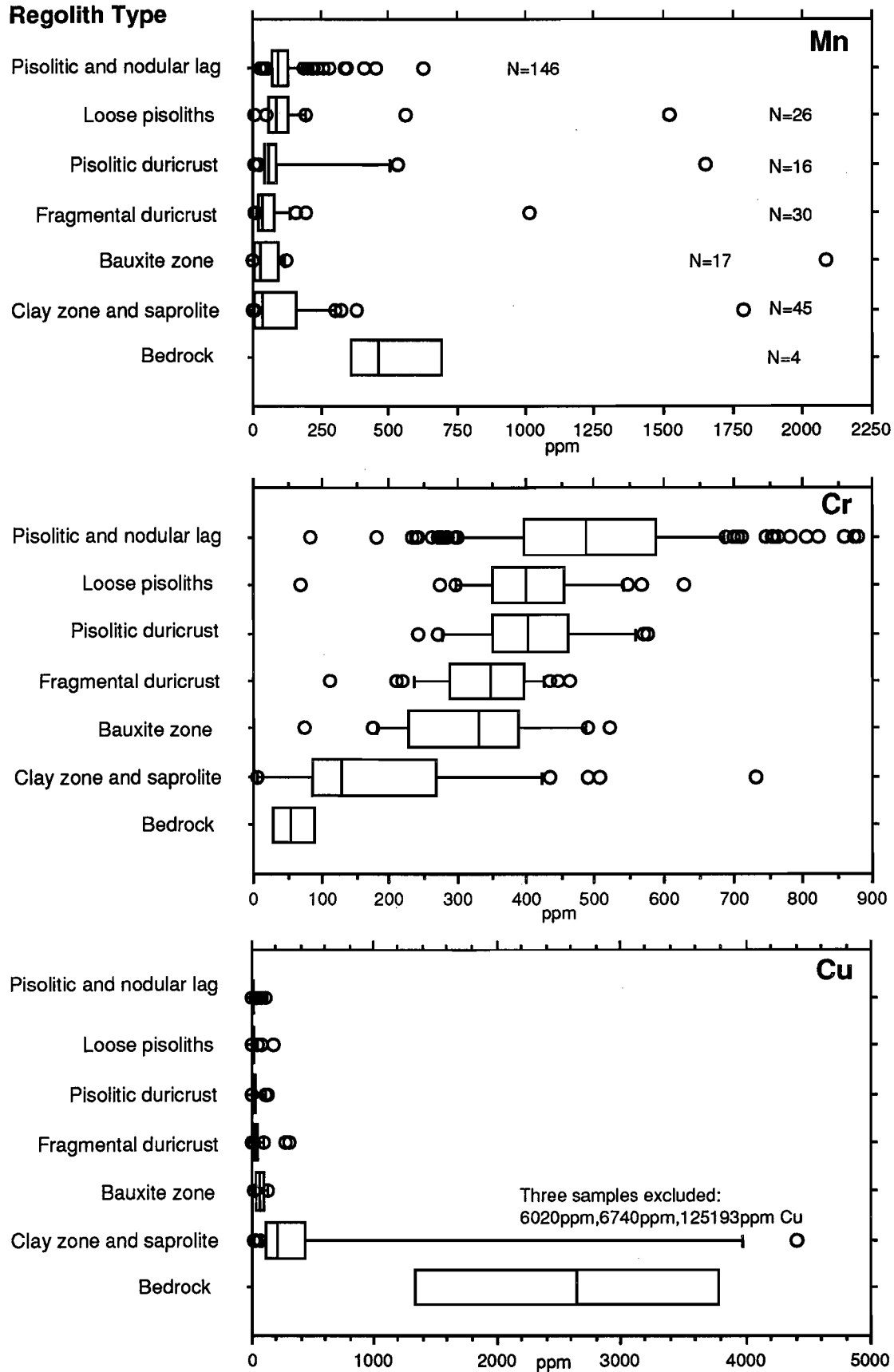
**Regolith Type**

Fig. 5.15 Box plots showing the distribution of Mn, Cr and Cu in several regolith materials and bedrock arranged vertically in order of the regolith stratigraphy, Boddington.

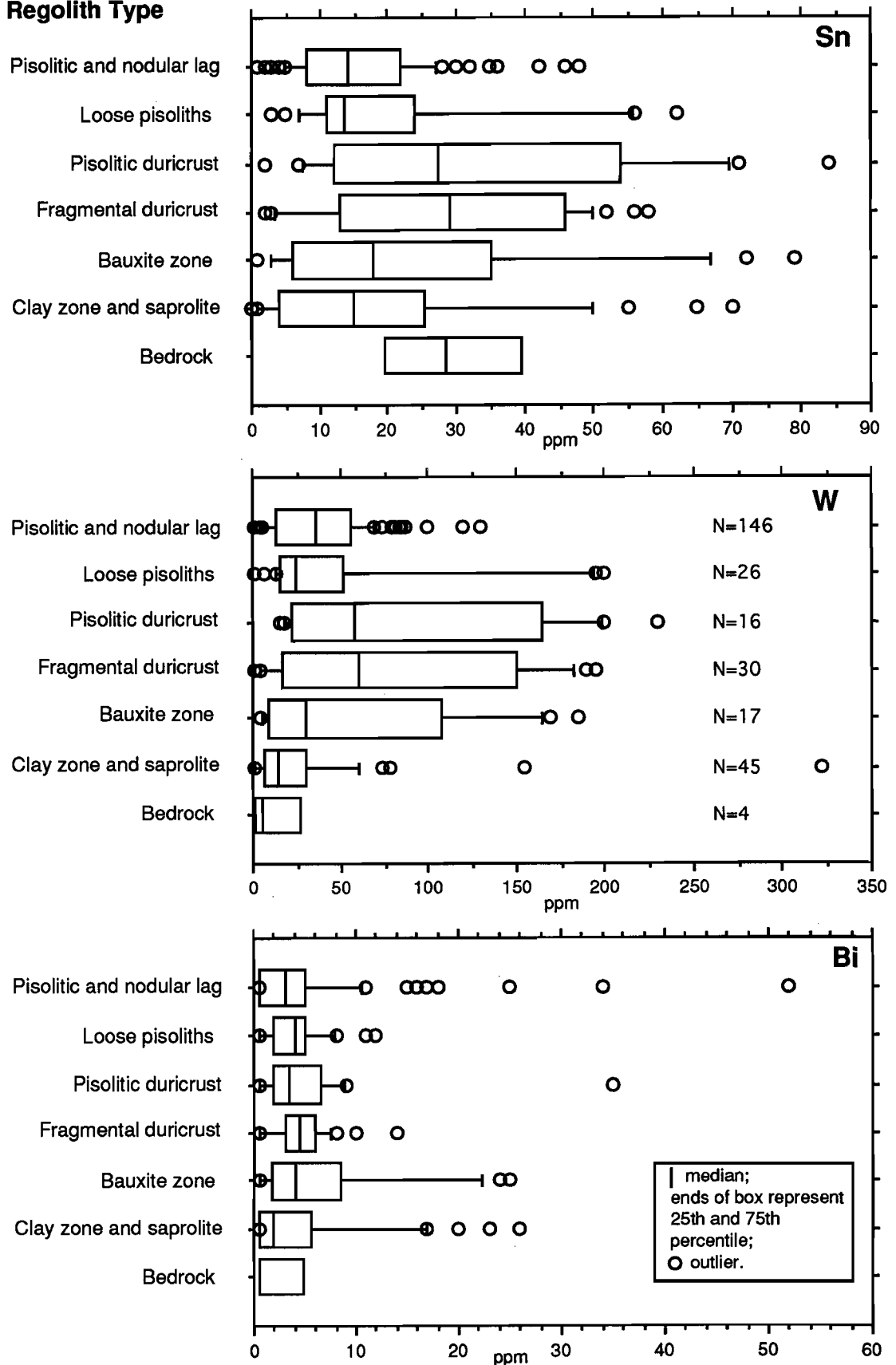
**Regolith Type**

Fig. 5.16 Box plots showing the distribution of Sn, W and Bi in several regolith materials and bedrock arranged vertically in order of the regolith stratigraphy, Boddington.

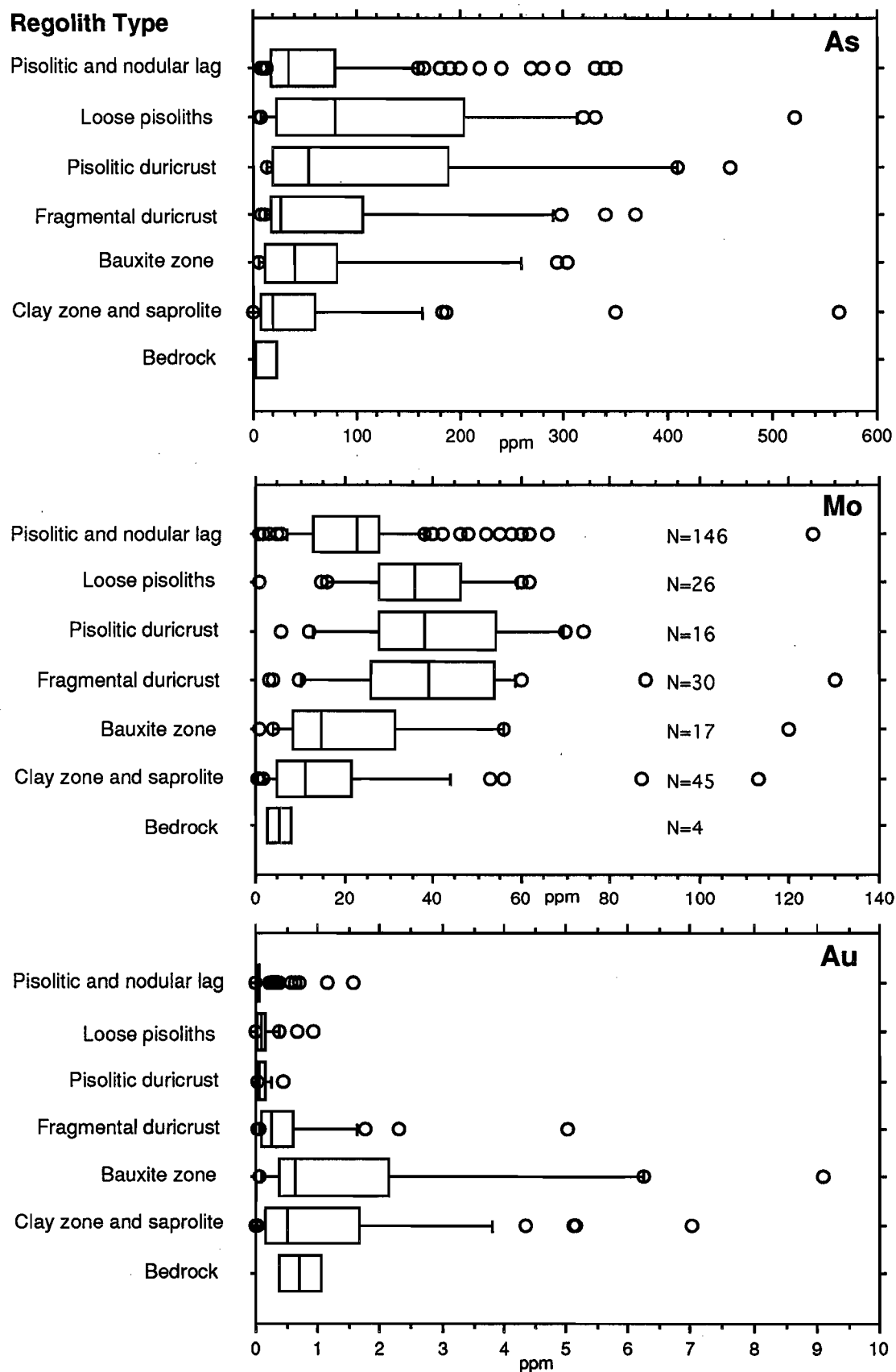


Fig. 5.17 Box plots showing the distribution of As, Mo and Au in several regolith materials and bedrock arranged vertically in order of the regolith stratigraphy, Boddington.



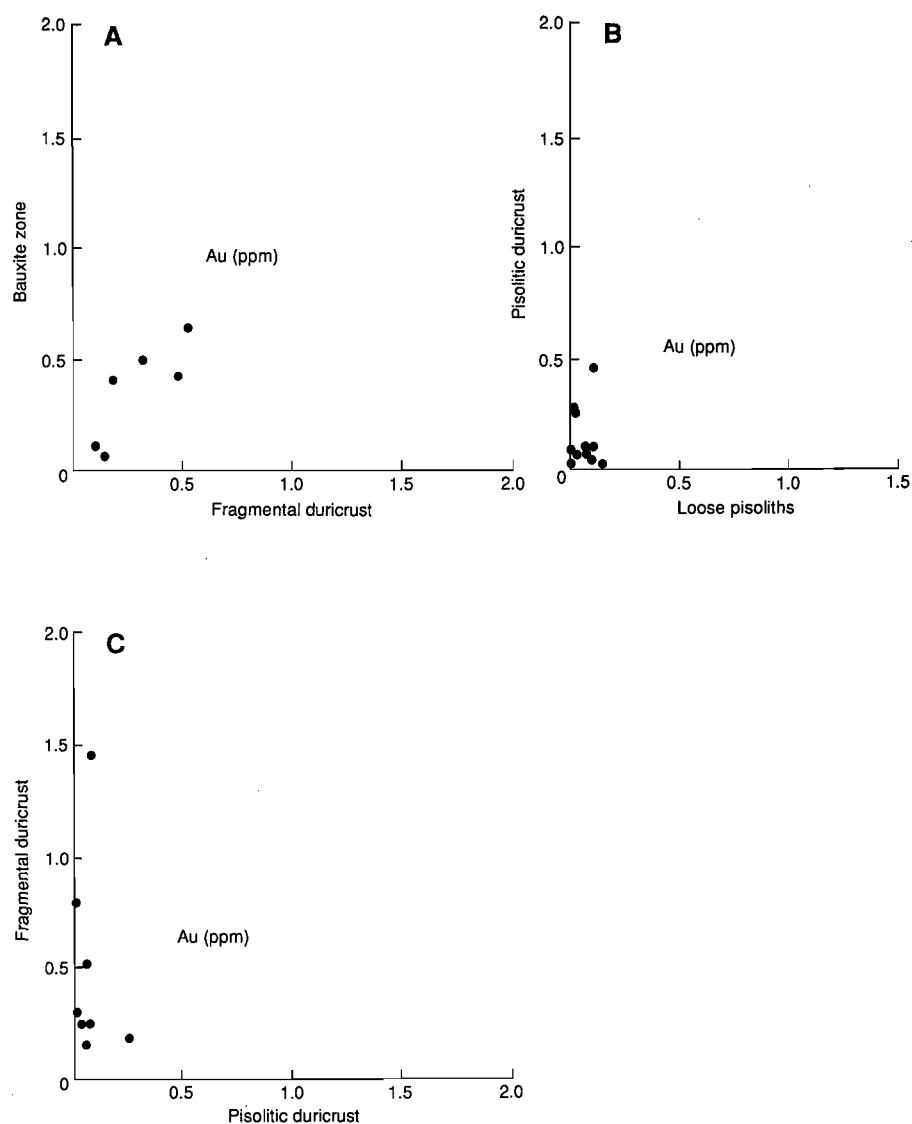


Fig. 5.18 Relationship between the Au abundances in (A) bauxite zone and loose pisoliths, (B) pisolithic duricrust and loose pisoliths, and (C) fragmental duricrust and pisolithic duricrust, Boddington orientation study.

Examination of Au-rich material from the different parts of the profile revealed only three small ( $<5 \mu$ ) droplet-like Au grains in the clay and bauxite zones. No Au visible under the microscope was found in lateritic duricrust nor in loose pisoliths, suggesting that it is in a sub-microscopic form or is chemically combined, or that the surfaces examined contained no Au.

Scanning electron microscope studies of polished sections of lateritic nodules and pisoliths show that much of the Sn occurs as irregularly-shaped cassiterite. This suggests that most Sn is dispersed mechanically during laterite formation. Some W occurs as scheelite, only two grains of scheelite were identified in samples of the bauxite zone and lateritic duricrust.

Some As occurs as arsenopyrite. Two grains of arsenopyrite were recognised in the cores of pisoliths. Because of susceptibility to weathering, their presence in loose pisoliths was surprising. However, it appears that some arsenopyrite grains may have been protected by Fe-oxide coatings that surround them.

### 5.2.5 Discussion and conclusions

A model is presented for the regolith evolution and geochemical dispersion, including mobilisation and deposition of Au and the distribution of ore-associated elements within the regolith of Boddington. Implications of these findings in exploration are discussed and listed in Table 5.8.

#### *Regolith evolution*

The regolith at Boddington developed over a long period, which is inferred to have taken place sequentially under the three major climatic episodes:

- (i) under a seasonally-warm, humid climate with high water tables, deep weathering of andesite and dolerite resulted in the development of a lateritic profile. Weathering profiles are thicker on andesite than on dolerite;
- (ii) under a subsequent arid climate, the profile dried and the watertable declined, resulting in the deposition of Fe-oxides in the profile, with reduced weathering at depth and hardening to form a lateritic duricrust at the surface. Vegetation changed with climate, resulting in slope instability. With decreased vegetation and channelling of surface drainages, the regolith on upper slopes and valley floors in particular was truncated by erosion.
- (iii) development of gibbsite during the recent climate. Several workers (*e.g.* Tomich, 1964; Loughnan and Sadleir, 1984; Anand *et al.*, 1991) observed that the better quality bauxite appeared to correspond with areas of high rainfall (*i.e.* 1000 mm). They took this to indicate that either recent rainfall was a factor in bauxite development or that the present rainfall distribution patterns were similar to those in existence when the bauxite was formed. Bauxitisation requires effective internal drainage to minimise the residence time of silica-laden solutions and assure a high level of leaching intensity, and hence Si removal and bauxite development. The extensive development of bauxite on mid-slopes, as opposed to hill crests or valley floors, illustrates the role of good drainage and large volumes of water moving through depositional sites. Bauxite deposits formed preferentially in areas of moderate relief where drainage was good, but not rapid, nor dominated by surface runoff; very steep slopes tend to be areas of 'physical' erosion rather than 'chemical' weathering.

The profile at Boddington contains components of the regolith stratigraphy seen elsewhere in the Yilgarn. However, at Boddington, the bauxite zone is present, whereas, hardpan and calcrete that are extensive in the arid terrains of the Yilgarn, are absent.

Lateritic residuum forms a blanket over some 30% of the landscape; however, the thickness and facies of lateritic residuum vary with topographic position. Laterite is either more developed or better preserved on midslopes than on crests or lower slopes. In the valley floors the laterite is absent, possibly because of truncation. Soil materials derived by erosion of the lateritic duricrust on crest- and upslope-positions have been transported as colluvium to lower slopes, a process presently continuing. As a result, the sandy gravels are shallow on crests and upper slopes and increase in thickness downslope. The gravels, consisting mostly of lateritic nodules and pisoliths, have been deposited on the slopes and the fine earth fraction has been transported further downslope to the valley floor by fluvial action. The processes active in transporting these materials result from gravity and water movement, including surface wash.

Lateral variations in duricrust morphologies occur in the Boddington area. Some relate to their location in the landscape while others reflect differences in the nature of the parent rock. The duricrust is more ferruginous than the underlying bauxite zone and may be fragmental, nodular, pisolitic, or vermiform. The midslope positions are dominated by pisolitic duricrust which is typically underlain by fragmental duricrust. By contrast, pisolitic and nodular duricrust and loose pisoliths and nodules are generally absent in crest- and upslope-positions where only fragmental duricrust occurs. The absence of pisolitic duricrust suggests removal by erosion and the detrital components (the gravel as well as the fine fractions) have been deposited on the lower slopes and valley floors. However, the possibility that pisolitic duricrust may never have existed on some of the crests cannot be excluded.

Fragmental duricrusts are commonly not developed on the lower slopes. Lower slope positions are occupied by packed pisolitic gravels which can, in places, reach a thickness of 5 m. Packed gravels may develop with the destruction of the matrix of lateritic duricrust in the upper slopes, followed by colluviation of the nodules and pisoliths, their subsequent deposition, and later recementation by secondary enrichment with Fe and Al minerals (Pullan, 1967). However, *in situ* breakdown of the duricrust, due to dissolution of the components of the matrix can also result in packed gravels. Indeed, evidence for both mechanisms of formation (*i.e.* lateral transportation and breakdown of the duricrust) have been observed in Pits A and D.

#### *Development of lateritic residuum*

Field relationships and laboratory data suggest that the lateritic duricrust and associated lateritic pisoliths and nodules at Boddington are largely residual, with transported nodules and pisoliths on the lower slopes. Relict textures after andesite are visible through some of the profiles to the level of the fragmental duricrust and correlate with bedrock relationships which have been established through drilling. Feldspars, in fabrics similar to those of the bedrock, have been pseudomorphed by gibbsite, showing that the fragmental duricrust is essentially residual. Relict fabrics derived from dolerite are also present as residual ilmenite in the bauxite zone and the fragmental duricrust. The dolerite results in a redder fragmental duricrust and bauxite zone than in those horizons derived from the felsic andesite, the dolerite having a higher Fe content.

Comparisons between the respective chemical and mineralogical compositions of bauxitic laterite and their parent rocks (chiefly either felsic andesite or dolerite) reveal a relatively simple relationship. Parent rock mineralogy and chemistry strongly influence the composition of laterite. Lateritisation and bauxitisation have involved the residual enrichment of Al and Fe (with addition of H<sub>2</sub>O) in proportion to the combined effect of Si depletion and the almost total loss of Mg, Ca, Na, and K. Intense leaching occurred in the bauxite and laterite zones, where Fe, precipitated as Fe-oxides, and most of the kaolinite is desilicified to form gibbsite. Iron is generally enriched towards the surface by solution, transport, and precipitation in the form of Fe-oxides and oxyhydroxides as a result of ferrolysis, and then by residual accumulation.

Brimhall *et al.* (1988) suggested that Al and Fe enrichment in the lateritic weathering profile were due partly to the addition of aeolian material transported westwards from the Yilgarn Craton. However, the close relationship between laterite composition and bedrock type suggests that aeolian-derived constituents are generally minor. The upper section (soils, loose pisoliths, and pisolitic duricrust) of the laterite profiles include variable amounts of transported material but the source of this material is uncertain. It is difficult to distinguish exotic aeolian constituents from more, locally-derived alluvial or colluvial material.

Magnetic nodules and pisoliths are more ferruginous than co-existing, non-magnetic nodules and pisoliths. Their magnetism is due to the presence of maghemite. In this study, amorphous Al-oxide has also been identified as an important Al-bearing mineral in magnetic pisoliths. Maghemite and corundum formation by surface heating of goethite during bush fires is the most likely process responsible for the magnetic character of surface pisoliths and nodules, as there is no evidence of maghemite below the lateritic residuum (Anand and Gilkes, 1987). Amorphous Al-oxide can also form from heating of gibbsite. The high temperatures in forest fires can adequately explain the observed transformations.

Near the surface, the duricrust displays numerous voids, cracks and fissures, which develop laterally and vertically, that break the duricrust into fragments, nodules, and pisoliths. In the upper part of the pits, the duricrust was crumbly and forming essentially *in situ* a gravelly horizon composed of fragments, nodules, and pisoliths. The duricrust matrix breaks down by dissolution of gibbsite and Fe-oxides. This allows the separation of nodules and pisoliths to produce a highly porous horizon of nodules and pisoliths dispersed in a clayey sand matrix. Colluviation leads to the deposition of these gravels on the mid- and lower-slopes.

#### *Geochemical dispersion in regolith*

During the oxidation of sulphides (pyrite, chalcopyrite, pyrrhotite and arsenopyrite) at the base of the profile and the destruction of primary minerals, the following trends in the distribution of the major elements during lateritic weathering are evident:

##### *Major elements*

- Silica contents decrease progressively from the base of the profile to the top of the pisolitic duricrust. In overlying loose pisoliths, the SiO<sub>2</sub> contents increase.

- Iron and Ti concentrations increase towards the top of the profile, with a strong enrichment in the pisolitic duricrust and loose pisoliths.
- Aluminium concentrations increase progressively from the saprolite to the bauxite zone and fragmental duricrust, and then decrease slightly in the pisolitic duricrust and loose pisoliths.

#### Trace elements

Weathering and secondary dispersion processes have disturbed primary trace element associations and created some new ones. Some associations, which occur in saprolite, are not present in laterite, suggesting differences in the behaviour of the elements due to changing chemical or mineral environments. Thus trace-element correlations from the surface samples are not representative of primary associations. The following trends were recognised:

- The distribution patterns of Mn, Cu, Zn, Ni and Co have a number of similarities. These elements are dissolved at the early stages of weathering and are leached from the upper horizons of the profile. However, there are some near-surface concentrations of Mn, Zn, Ni, and Co suggesting that they are accumulated by pedogenetic processes. Similarities between the distributions of Zn, Co, Ni and Mn, deep in the profile, imply that these elements are hosted by the same primary minerals, *i.e.* ferromagnesian minerals, and are released together on weathering. These elements are present mostly in octahedral sites in biotite and amphiboles, where they substitute for Mg and  $\text{Fe}^{2+}$ . Major losses of these elements from these minerals, indicate that they were lost during weathering, and thus behave similarly to Mg.
- Silver is the most mobile element. It is dissolved at the early stages of weathering and is strongly leached in the pisolitic duricrust and bauxite zone.
- Elements such as V, Cr, As, Bi, Sn, Ga, W, Zr, Nb, Mo and Pb are essentially retained or enriched throughout the whole profile. These elements tend to increase progressively from the bedrock to the surface and have higher abundances in the pisolitic duricrust than in the bedrock. They are either associated with Fe-oxides or occur as resistant primary minerals such as zircon, cassiterite and scheelite.
- A comparison between the laterite profile above andesite and dolerite rocks shows that the behaviour of the elements is similar. Most of the leaching in the dolerite profile has taken place in the lower part of the saprolite.

A geochemical dispersion model for the Boddington area is shown in Fig. 5.19. The dispersion mostly results from a combination of hydromorphic (H), residual (R), and mechanical (M) processes, both past and present, related to the formation or modification of the lateritic profile. In the kaolinitic saprolite, Cu, Mo, W, Bi and Sn are mostly residual with some hydromorphic dispersion of Cu and Mo. The dispersion halo widens in the bauxite zone, but reaches its greatest in the pisolitic duricrust and loose pisoliths but Au is more leached in the loose pisoliths. The protore mineralisation is depicted by a multi-element geochemical halo in the lateritic residuum, both in the duricrust and loose pisoliths. Compared to the bedrock, the concentrations observed in this halo are enriched in As, Mo, Bi, Sn and W and depleted in Cu and Au. Tungsten, As, Mo and, to some degree, Sn show a more widespread and homogeneous distribution than Cu and Bi. Copper, Mo and As exhibit different dispersion characteristics in the various horizons of the lateritic weathering profile. Molybdenum has a strong affinity for the Fe-oxides and is therefore abundant in the loose pisoliths and pisolitic duricrust; possibly after some hydromorphic migration, an enlarged dispersion halo has resulted. Conversely, Cu is less stable in the Fe-rich environment, and is relatively depleted in the ferruginous horizon (Zeegers *et al.*, 1981). Bismuth is little remobilised and disperses very slightly, whereas Ag is completely leached and can only be detected near the source. In the samples studied, most of the As is associated with goethite and hematite, but some As is there as arsenopyrite; Sn is held in cassiterite, some Cu in goethite, and most of the W is in the Fe oxides and gibbsite but some is held in scheelite. These observations indicate residual and hydromorphic dispersion. However, in the undulating landscape of Boddington, mechanical dispersion has enlarged the halo, particularly on the slopes, although simultaneously causing dilution of element concentrations. There, loose pisoliths and nodules are semi-residual. The formation of pisoliths and nodules involves intense chemical alteration and it is probable that at least part of the Fe accumulated in them has been transported for some distance; some trace elements (As, Mo) may have behaved similarly, resulting in a large dispersion halo.

## A-type models, seasonally humid terrains

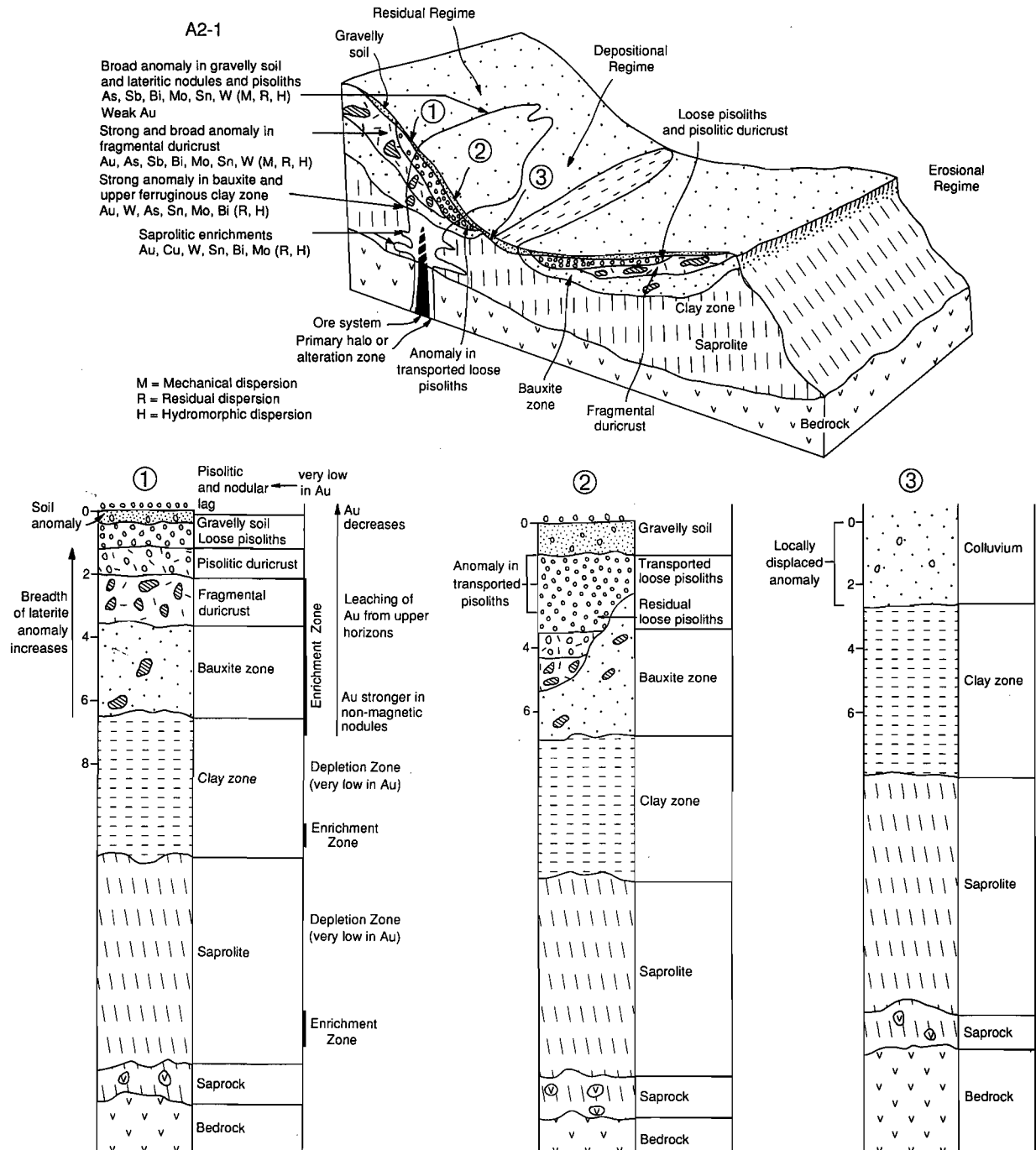


Fig. 5.19 Geochemical dispersion model for the Boddington gold deposit.

### Gold distribution

There is a wide anomalous zone of Au close to the surface, within the fragmental duricrust and bauxite zones. In these parts of the profile, Au was precipitated, in association with Fe-oxides, at a redox front at or near the Tertiary water table. The mobility of Au during deep lateritic weathering in a humid environment is best explained by the ferrolysis model of Mann (1983). This model involves the oxidation of sulphides in the saprolite zone of the weathering profile, to produce acidic ferrous solutions. These circulate upward in the ground water, oxidise at the redox interface (the water table) and precipitate goethite and hematite to form the laterite. In this acidic oxidising environment, any Au in the system may be mobilised as either organic, thiosulphate or chloride complexes, and dispersed laterally in the redox front, i.e. in the zone of laterite formation. As a result of ground water flow, Au solutions may travel for some distance and re-enter the reduction field, where they precipitate as elemental particles. This process is a co-precipitation along with Fe as Fe-oxides and oxyhydroxides, a process which traps the micron scale Au in the laterite.

The changes to a drier climate, perhaps with some epirogenic uplift, caused a lowering of the water table. As a result, upper horizons of the profile are unsaturated and the pre-existing profile is subjected to decreased leaching with alkalis and alkaline earths being retained in the profile. Evaporation exceeds precipitation so that sodium chloride and other salts, derived largely from rainfall, concentrates both in the unsaturated zone and in the ground water. In the Darling Range, reversal to a humid climate has restored conditions conducive to deep weathering (Bowler, 1982). Accordingly, the lowering of the water table would have been punctuated by still stands or temporary rises. The increased rainfall leaches precipitated salts and recreates redox conditions suitable for ferrolysis and thus produces an acidic, saline and oxidising groundwater capable of dissolving Au (Mann, 1984 a). This results in Au depletion in the middle part of the clay zone, and enrichment in the lower horizons. During these humid periods, therefore, Au may be dissolved and mobilised, to be re-precipitated with Fe-oxides by reduction by  $\text{Fe}^{2+}$  at the water table. Successive humid periods during the general lowering of the water table can account for the presence of two subhorizontal enrichments within the saprolite. However, this view is not shared by Symons *et al.* (1988) who reported that the disposition of Au within the clay zone reflects a primary Au distribution.

Gold gradually decreases towards the surface, i.e. from the bauxite zone through the lateritic duricrust (fragmental, pisolitic) to the loose pisoliths. Loose pisoliths and the pisolitic duricrust commonly contain Au below 0.1 ppm. In contrast, there is enrichment of Au in the fragmental duricrust and the bauxite zone. Gold depletion in loose pisoliths and nodules suggests that it is being leached from loose pisoliths and concentrating in the fragmental duricrust and bauxite zone. Gold has probably been mobilised as organic complexes as described by Bowell *et al.* (1993).

Table 5.8 The implications in exploration listed against the research findings, Boddington orientation study.

Research Findings	Implications in Exploration
<ul style="list-style-type: none"> <li>Regolith-landform relationships mapped on a district scale; residual regimes on undulating uplands, with erosional regimes on gentle to moderate slopes.</li> </ul>	<ul style="list-style-type: none"> <li>- Appropriate exploration medium chosen to suit regolith-landform regime.</li> </ul>
<ul style="list-style-type: none"> <li>Lateritic duricrust and associated lateritic nodules and pisoliths are largely residual, with transported nodules and pisoliths on the lower slopes.</li> </ul>	<ul style="list-style-type: none"> <li>- Establishes framework for the interpretation of geochemical data.</li> </ul>
<ul style="list-style-type: none"> <li>Ti/Zr ratios were found to be a reliable discriminator of rock type for lateritic duricrust.</li> </ul>	
<ul style="list-style-type: none"> <li>Strong multi-element geochemical anomalies occur both in the lateritic duricrust and the lateritic nodules and pisoliths. The element association is As, Mo, Sn, W, Bi with more erratic Cu and Au.</li> </ul>	<ul style="list-style-type: none"> <li>- This type of orebody has a strong multi-element signature.</li> </ul>
<ul style="list-style-type: none"> <li>The concentration of Au decreased from the bauxite zone through the lateritic duricrust to loose pisoliths. Gold in pisolitic gravel at surface is relatively weak. Tin, W, Mo and As are strongly anomalous at surface.</li> </ul>	<ul style="list-style-type: none"> <li>- Gold maybe depleted from surface materials (pisolitic lag, gravelly soil) due to leaching. Unwise to expect Au to always dominate the dispersion anomaly in lateritic residuum. Chalcophile anomalies, with or without Au, seems to be the best and most reliable indicator of a Au deposit.</li> <li>- Samples of fragmental duricrust instead of loose pisoliths should be collected, particularly at the anomaly delineation stage.</li> </ul>
<ul style="list-style-type: none"> <li>Geochemical data sets were established for several sample media.</li> </ul>	<ul style="list-style-type: none"> <li>- Provides well controlled 'target' reference data sets for use in multivariate analyses.</li> </ul>



### 5.3 Mount McClure district

#### 5.3.1 Introduction

##### *Location*

The Mt. McClure Gold Mine is located some 700 km northeast of Perth and 65 km northeast of Leinster (Fig. 5.20). Access to the mine is gained via the recently constructed road which links the mine and the Leinster township. The study area is centred around an extensive alluvial and colluvial plain in which the two largest deposits (Calista and Lotus) of the Mt. McClure Gold Mine are situated. The Mt. McClure district studied here is an area of some 185 km<sup>2</sup> and was chosen to establish the setting for the Mt. McClure gold deposits. The district contains truncated, lateritic profiles on uplands and lateritic residuum buried under thick and extensive colluvial and alluvial plains.

##### *Climate and vegetation*

The area has a hot, arid climate with an erratic median annual rainfall of approximately 200 mm. Rain may fall in both summer and winter, mostly in late summer from cyclonic rain-bearing depressions. The area is characterised by sparse, low acacia woodlands, with mulga dominant (*Acacia* spp.). The shrub layer is dominated by poverty bush, turpentine and rattle bush.

##### *Geology and mineralisation*

The Mt. McClure district lies on the western margin of the Yandal greenstone belt. This belt is bounded to the east by the Celia Lineament, and to the west by two major shear zones in gneissic and granitic rocks (Fig. 5.21). The presence of these shear zones is suggested by the development of a schistose fabric in the felsic volcanic rocks.

The Ockerburry Fault is proposed to explain the offset and juxtaposition of folded strata in the central area of the belt (Bunting *et al.*, 1979). This fault trends north-north-east and diagonally crosscuts the belt linking the Celia Lineament to the Keith Kilkenny Lineament of the adjacent Agnew-Wiluna belt, further to the south. Bunting *et al.* (1979) recognised a thick stratigraphic succession in which a mafic intrusive and extrusive sequence is overlain by a felsic volcanic complex, interbedded with minor mafic extrusive and intrusive rocks.

The Calista deposit is the largest deposit of the six comprising the Mt. McClure Gold Mine. The mineralisation here is hosted in an overturned, steep, westerly dipping sequence of rocks. The oldest unit intersected by drilling in this sequence is a greenish tremolite-chlorite-talc-carbonate schist after peridotitic komatiite. The contact between this meta-komatiite and an overlying brecciated chert-massive sulphide horizon is generally sharp. The unoxidised sulphide assemblage is dominated by pyrrhotite, with lesser pyrite, minor chalcopyrite and traces of sphalerite. The primary mineralisation is characterised by Au, Bi, Cu, Zn, Sn, W, As, and Ag.

##### *Thesis produced*

This orientation study included an Honours thesis by A. Williamson (1992, University of WA) on the regolith-landform setting and geochemical dispersion from the Au deposits into the regolith.

#### 5.3.2 Objectives

The overall objectives of the Mt. McClure study were to provide a regolith-stratigraphic framework for the district and within this, to complete multi-element, orientation geochemical dispersion studies about the concealed Calista Au deposit.

Specific objectives were:

1. To establish the regolith-stratigraphic relationships around the Calista Au deposit at local and district scales.
2. To find methods to reliably distinguish transported clays from the residual saprolitic clays and thus to establish regolith stratigraphy from drill spoil.
3. To establish regolith-bedrock relationships.
4. To carry out a concise orientation study of geochemical dispersion at the concealed Calista Au deposit.

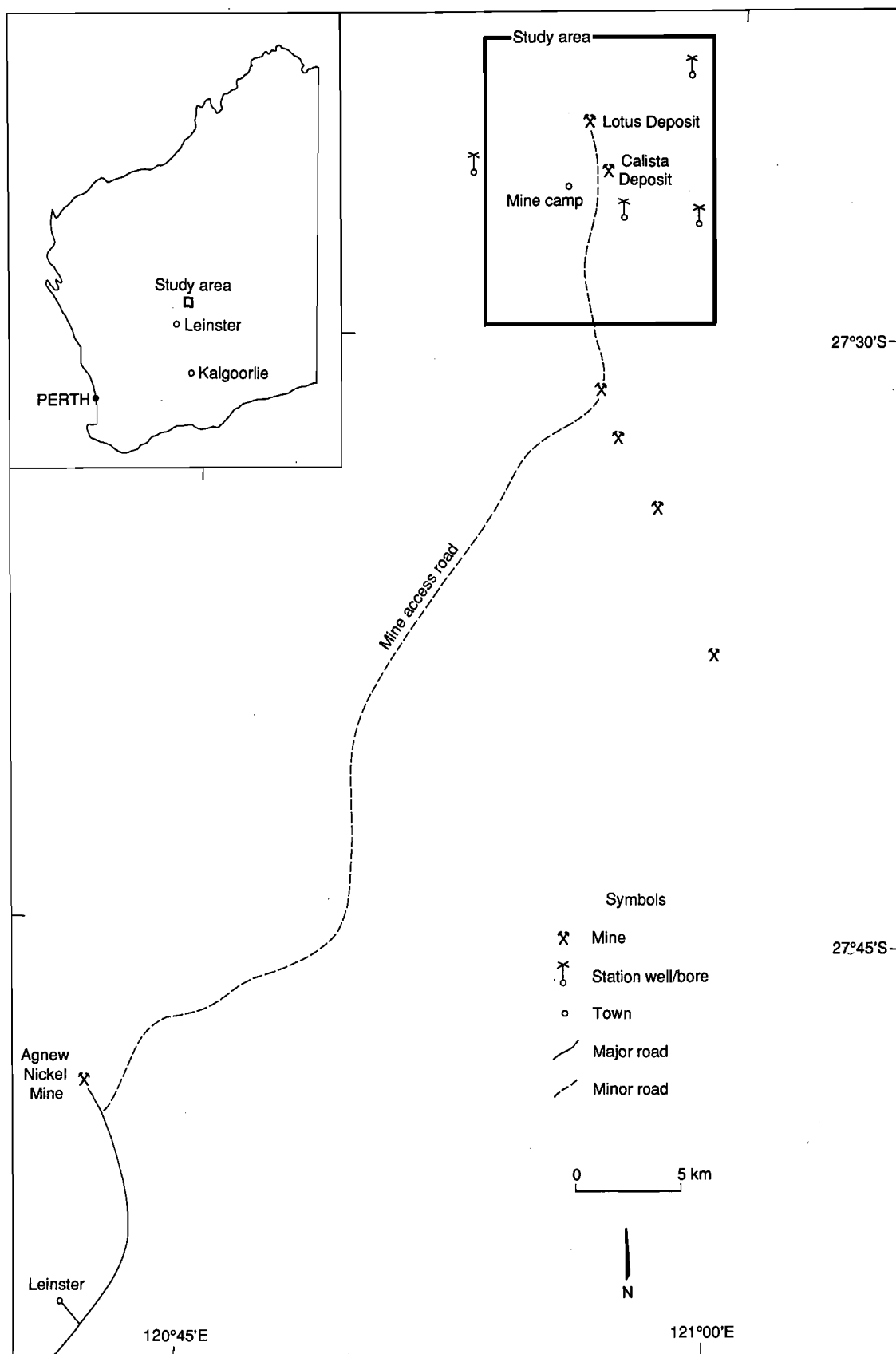
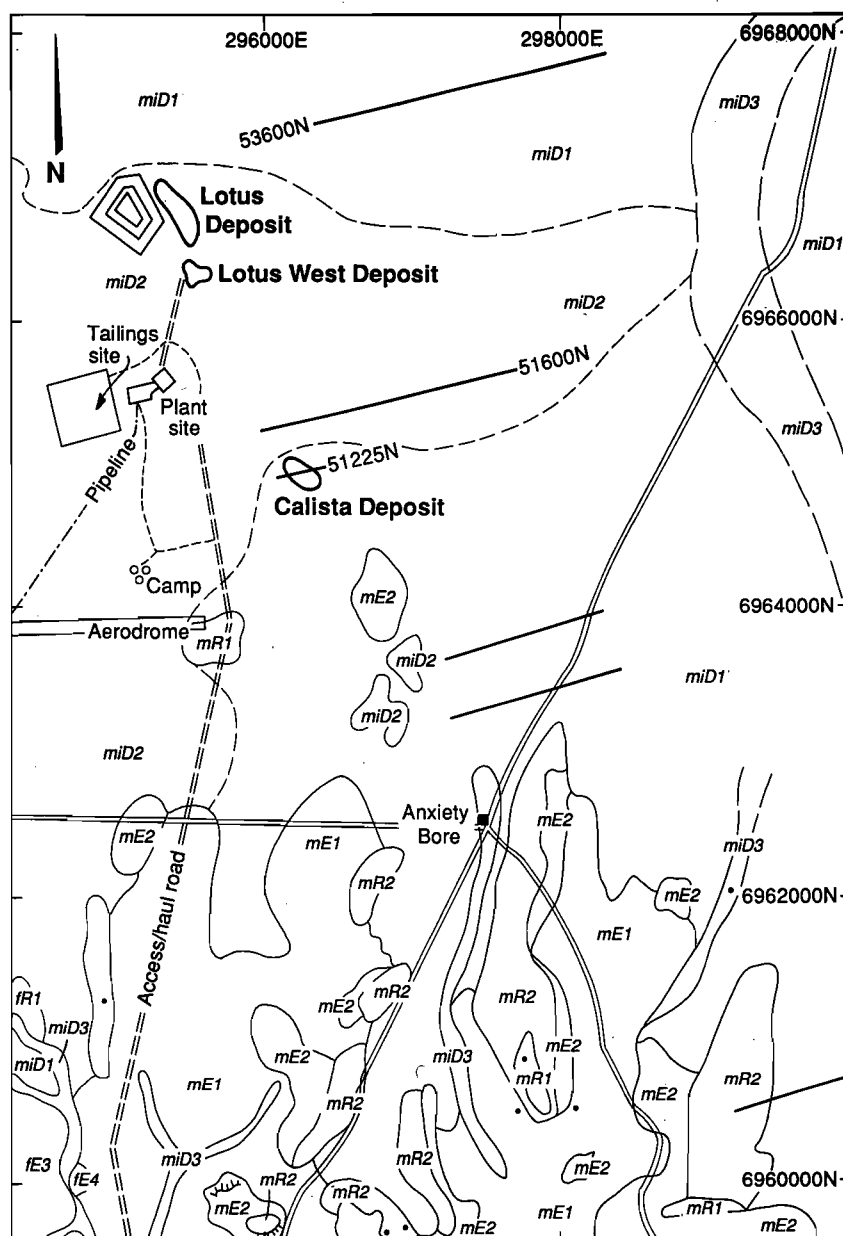


Fig. 5.20 Map of Mt. McClure district showing the location of the Mt. McClure gold deposits.



Fig. 5.21 Regional geology of the Yandal Greenstone Belt (after Bunting *et al.*, 1979), showing the location of the Mt. McClure district.



RESIDUAL REGIME		
Regolith units on mafic bedrock	mR1	Black, Fe-rich duricrust
	mR2	Lateritic nodules and pisoliths
Regolith units on felsic bedrock	fR1	Nodular duricrust
EROSIONAL REGIME		
Regolith units on mafic bedrock	mE1	Iron segregations
	mE2	Ferruginous saprolite
Regolith units on felsic bedrock	fE3	Quartz fragments
	fE4	Ferruginous saprolite
DEPOSITIONAL REGIME		
miD1	Polymictic lag, lateritic residuum beneath 20 m of transported overburden	
miD2	Polymictic lag, saprolite beneath 20-30 m of transported overburden	
miD3	Polymictic lag, saprolite beneath 10-20 m of transported overburden	

mi = mixed in origin

/ Inferred mapping unit boundaries

/ RAB line used for stratigraphic purposes

• Sample and/or photographic locality

Fig. 5.22 Detailed map of regolith-landform units in the Mt. McClure district.

### 5.3.3 Regolith-stratigraphic relationships

#### Regolith distribution

A map of the regolith-landform relationships at 1:25,000 scale was produced for the Mt. McClure district (Fig. 5.22, Appendix IX). The landscape of the Mt. McClure district was divided into three major regimes, namely *residual*, *erosional* and *depositional*, as recommended in this project, where the focus is on the degree of preservation or truncation of the lateritic residuum. These three primary groups of regolith-landform units have been further subdivided according to the provenance of the associated regolith. The regolith of one group is related to felsic rocks, that of the second group to mafic rocks, and a third has a regolith of mixed origin. Several well-defined regolith types were mapped within these groups.

Three regolith-landform units were mapped within the residual regimes. They were subdivided according to the source of regolith, *i.e.* mafic vs. felsic. Residual areas on mafic rocks are mantled by brown, nodular duricrust and reddish brown, lateritic nodules and pisoliths. Pockets of black, Fe-rich duricrusts also occur. Black, Fe-rich duricrusts are characterised by higher concentrations of  $\text{Fe}_2\text{O}_3$  (65-80%) and low concentrations of  $\text{Al}_2\text{O}_3$  (4-6%) and  $\text{SiO}_2$  (3-12%). The dominant minerals are hematite and goethite with smaller amounts of maghemite, kaolinite and quartz. In contrast, brown nodular duricrusts are lower in  $\text{Fe}_2\text{O}_3$  (26-50%) and higher in  $\text{Al}_2\text{O}_3$  (25-55%) and  $\text{SiO}_2$  (20-35%), relative to the Fe-rich duricrust. These brown, nodular duricrusts are dominated by goethite and kaolinite, with smaller amounts of hematite and maghemite. The occurrence of goethite and kaolinite-rich cutans is typical of residual nodules and pisoliths.

Residual areas on felsic rocks are characterised by gravelly, sandy soils with yellowish brown, nodular duricrust at a shallow depth (*e.g.* 0.3 m). The duricrusts over the felsic rocks are less indurated and less ferruginous relative to the duricrusts formed from the weathering of mafic rocks.

In the erosional regimes, the deeper units of a lateritic profile, as well as fresh bedrock, are exposed. Twelve units were mapped within the erosional regimes. The regolith is dominated by ferruginous saprolite, iron segregations and saprolite which are either exposed or mantled by shallow soil. Ferruginous saprolite is yellowish brown and is dominated by kaolinite and goethite whereas iron segregations are black and largely consist of goethite and hematite. Iron segregations are characterised by higher concentrations of  $\text{Fe}_2\text{O}_3$  (>80%), Mn (2310-4150 ppm), Zn (350-858 ppm), and Co (146-394 ppm). Some samples of iron segregations show goethite pseudomorphs after pyrite and pyrrhotite. These findings are consistent with the previous findings in the Lawlers district (Section 4.4 in Report 236R).

Partially indurated saprolite characterises regolith units in erosional regimes, where bedrock types are felsic. Pale, grey-brown, gritty, loamy, sandy soils are common.

Depositional regimes comprise the lower slopes as well as the colluvial and alluvial plains. Depositional regimes account for about half of the 185 km<sup>2</sup> mapped area. Five units were mapped within the depositional regimes. They were subdivided according to the presence or absence of lateritic residuum beneath the sediments. This was established by logging the regolith stratigraphy from drill spoil. For example, in unit MiD1, extensive sheets of pisolitic-nodular lateritic residuum form the principal substrate to the 15-20 m thick, hardpanised colluvium. These sheets of lateritic residuum are from 2 to 5 m thick. In places, the sediments reach 30 m in thickness. Exploration drilling shows that buried residual laterite profiles are widespread beneath the sediments of the alluvial plains.

#### Regolith stratigraphy and profile development on komatiite bedrock - Calista Deposit

##### Line 51225 mN

Here a complete lateritic profile is buried beneath 15-20 m of transported overburden (Figs 5.22 and 5.23). The transported overburden consists of sandy soil, sandy, hardpanised colluvium and gravelly hardpanised colluvium. The gravel components in the gravelly hardpanised colluvium consist of transported pisoliths and nodules (lacking cutans), and increase towards the base of the unit. Silica and  $\text{Al}_2\text{O}_3$  are the major constituents of the transported overburden and principally occur as quartz and kaolinite. The upper, sandy, hardpanised colluvium and soil appear to have been derived from the stripping of the granitic and gneissic weathered profiles to the west. Hardpan is strongly developed in the colluvium and alluvium to a depth of 15 m.

The lateritic profile, formed from the weathering of komatiites, is about 60-70 m thick. The saprolite is 20-30 m thick and the transition from unweathered to weathered rock occurs below 60 m depth. The rock fabrics are preserved in the saprolite. The saprolite becomes softer and clay-rich towards the surface and, as a result of settling and consolidation, the rock fabrics are destroyed and saprolite merges with clay zone. Locally, however, recognisable fabrics are preserved. Kaolinite, talc, chlorite,

and interstratified chlorite-vermiculite are the major minerals in clay zone and saprolite. Gossan from the sulphide horizon persists through the saprolite into the clay zone. The gossan is dominated by hematite with lesser goethite and quartz.

The mottled zone is transitional between the clay zone and the lateritic residuum. It consists of irregularly shaped, brown mottles, set in yellowish brown clays. Mottles are comprised of goethite and kaolinite.

Lateritic residuum forms the uppermost unit of a residual, lateritic profile and was present as an almost continuous unit over the deposit. It varied in thickness from 2 to 6 m. The lateritic residuum is pisolitic or nodular and is dominated by hematite, goethite, maghemite and kaolinite. The lateritic pisoliths and nodules range in diameter from 5 to 30 mm and have a characteristic 1-2 mm thick, yellowish brown cutan. The pisoliths and nodules contain pseudomorphs after primary minerals and gossan fragments within their cores.

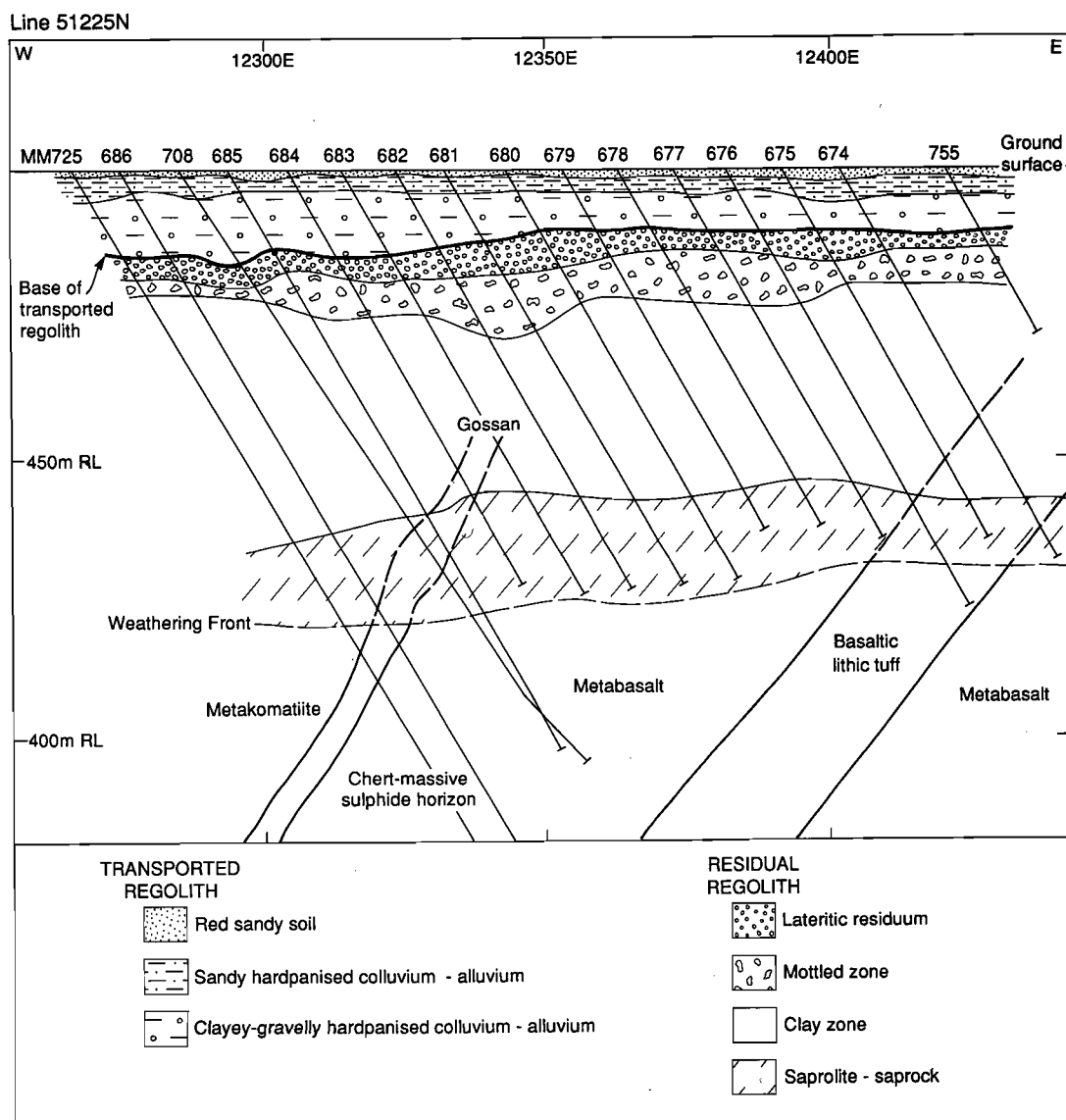


Fig. 5.23 Cross section showing the regolith stratigraphy for Line 51225 mN, Mt. McClure district, from Williamson (1992).

*Line 51600 mN*

Transported overburden reaches 30 m in thickness along this line and directly overlies the mottled zone or, in places, saprolite (Figs 5.22 and 5.24). Here, lateritic residuum is absent beneath the sediments. Transported overburden comprises soil, sandy hardpan, gravelly hardpan, lenses of transported laterite and white bleached clays. There is also prominent development of a smectite-rich unit at about 30 m depth which overprints both the transported and residual regolith. This unit contains high concentrations of Mn-nodules (5 to 15 mm in diameter) which are dominated by pyrolusite and lithiophorite. Electron microprobe analyses of the Mn-nodules show them to consist of MnO (65%), BaO (12%), SiO<sub>2</sub> (5%), Al<sub>2</sub>O<sub>3</sub> (2%), K<sub>2</sub>O (1%), Cu (400 ppm) and Zn (300 ppm).

*Line 53600 mN*

This section illustrates the topographic variability of the former lateritic weathering surface (Figs 5.22 and 5.25). The gravelly facies of the hardpanised colluvium is absent in the eastern parts of this cross section, where the clay and the saprolite zones lie 1 and 4 m, respectively, below the present surface. This former topographic high probably represents an old drainage divide where deposition was lacking until more recent times. Lateritic debris forms a scree on lateritic residuum, adjacent to this former high. This lateritic residuum is preserved beneath 10-15 m of transported overburden on the western end of the section.

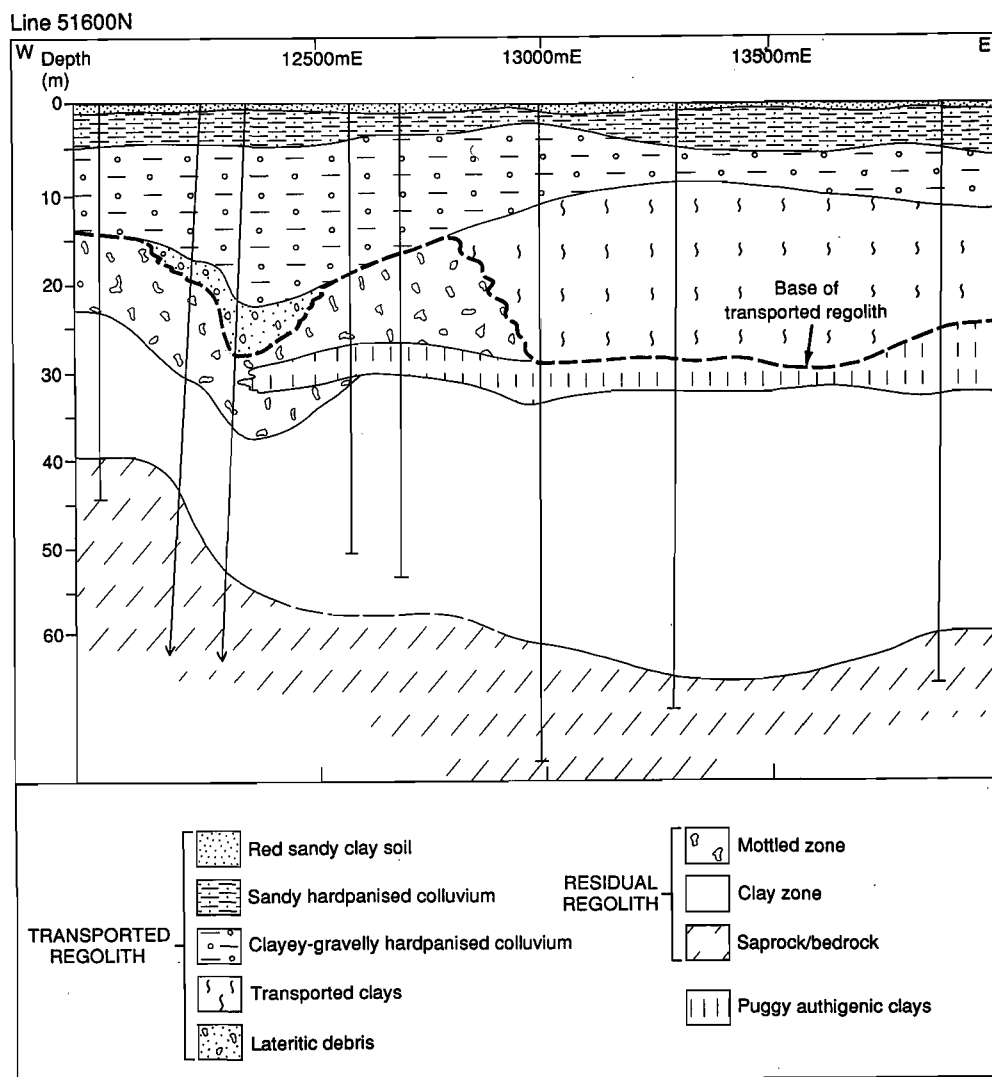


Fig. 5.24 Cross section showing the regolith stratigraphy for Line 51600 mN, Mt. McClure district, from Williamson (1992).



#### 5.3.4 Regolith-landform model

A generalised regolith-landform model summarising the regolith stratigraphy for the three dominant regimes developed from the weathering of mafic, ultramafic and granite rocks is shown in Fig. 5.26. The development of the regolith can be related to processes of deep lateritic weathering, subsequent erosion, deposition and modification through leaching and cementation.

The lateritic duricrust is strongly developed over mafic and ultramafic bedrocks. As a consequence, an almost complete profile, 40-70m thick, is present on crests and backslopes of breakaways. Over granitic lithologies, the weathering profile is generally truncated, commonly to the level of saprolite. Generally, red clayey soils and cobbles of iron segregations, quartz and ferruginous saprolite are deposited here from the upland mafic terrain.

Buried residual laterite profiles are widespread beneath the colluvium and alluvium. Their distribution is, however, erratic and difficult to predict because of partial stripping of the old surface.

The transported overburden is derived from erosion of the granitic and mafic profiles in upland areas. The upper sandy facies of the hardpanised colluvium and the white clays are limited to the central and western parts of the colluvial plain, where they are proximal to their likely source, the sandy soils and saprolite formed over the granitic and gneissic country to the west of the study area. Closely associated with the transported white clays is an authigenic horizon dominated by smectite and Mn-oxides. The formation of Mn-rich nodules is possibly related to the redox front associated with the present day water table.

Ferruginous saprolite is commonly exposed beneath the breakaways and is formed by the infusion of Fe into clay-rich saprolite. Some iron segregations are gossan fragments which exhibit boxwork fabrics, while others are formed by the ferruginisation of the wall rocks and redeposition of Fe in the saprolite, forming stringers, pods and tabular bodies. These bodies of iron segregations breakdown at the surface, producing a cobbly, ferruginous lag. Both ferruginous saprolite and iron segregations are useful sampling media in situations where the lateritic residuum is truncated (Anand *et al.*, 1991).

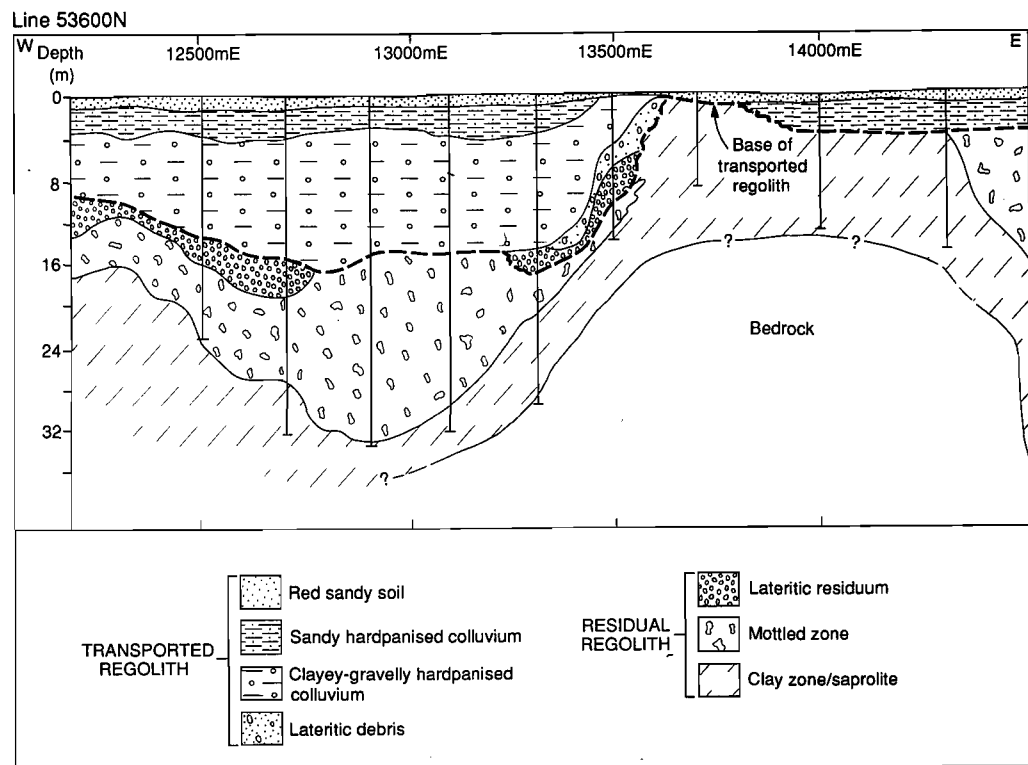


Fig. 5.25 Cross section showing the regolith stratigraphy for Line 53600 mN, Mt. McClure district, from Williamson (1992).

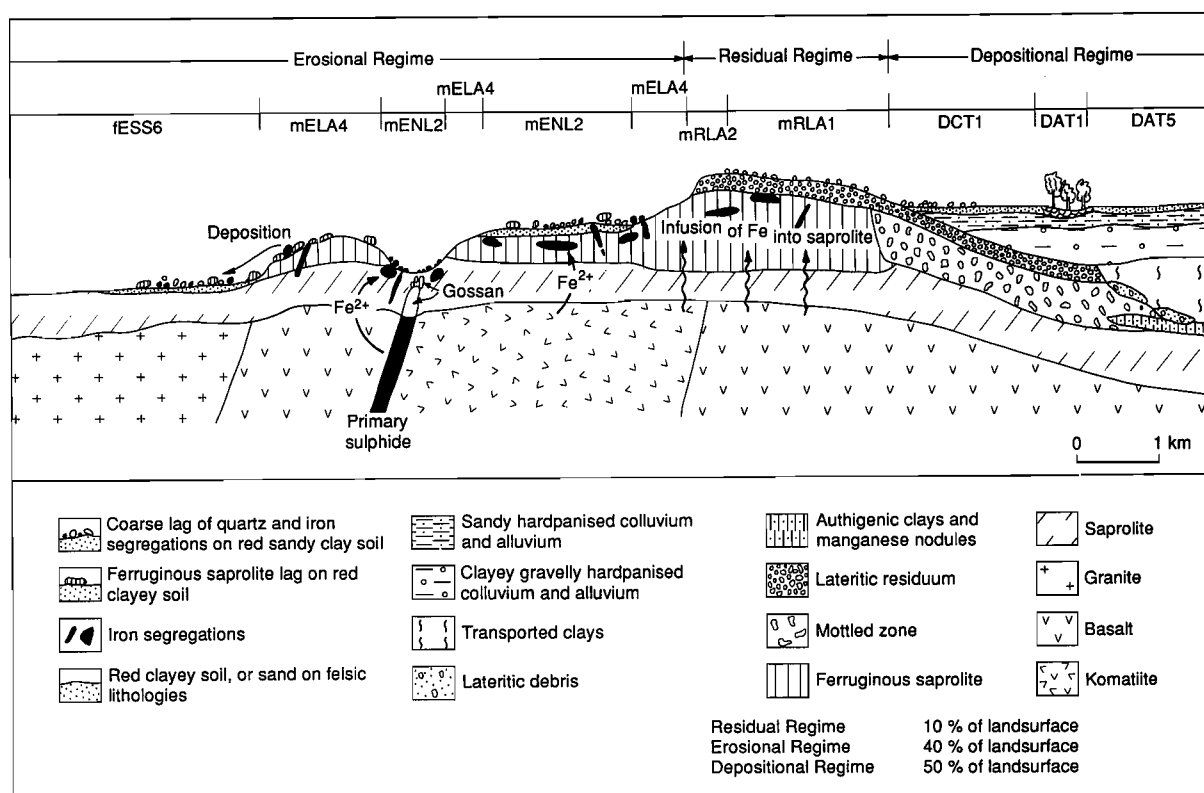


Fig. 5.26 Regolith-landform model for the Mt. McClure district showing regolith stratigraphy and landforms, from Williamson (1992).

### 5.3.5 Geochemical dispersion in lateritic residuum and transported overburden

#### Sampling

Here the multi-element geochemical dispersion patterns in the regolith (particularly the lateritic residuum and transported overburden) overlying the Calista deposit were studied. Much of the findings have been presented in the Honours thesis by A. Williamson (1992). It was established from the examination of RC drill spoil over the Calista deposit, that a horizon of residual laterite is overlain unconformably by colluvium of varying thickness (5-20 m). The colluvium contains components derived by the partial or complete stripping of the lateritic residuum and saprolite elsewhere. A total of 77 samples were collected from one traverse (51225 mN) and their location is shown in Fig. 5.27. The regolith stratigraphy of this traverse was discussed in detail above. The number of samples collected from each unit are as follows:

Soil samples	8
Sandy, hardpanised colluvium and alluvium	15
Gravelly, clayey, hardpanised colluvium and alluvium	15
Upper lateritic residuum	15
Lower lateritic residuum, near the mottled zone interface	13
Saprolite, clay zone	5
Mineralised zones	6

The upper, lateritic residuum consists of loose pisoliths and nodules whereas the lower lateritic residuum is dominantly a pisolitic or nodular duricrust. However, it was generally not possible to establish the exact nature of the lateritic residuum from drill spoil and lateritic residuum was therefore only subdivided into an upper and lower unit, not into two textural types.

Summary statistics for the geochemistry of these sample groups are given in Tables 5.9 and 5.10 and the results are summarised below. The results are fully tabulated and plotted in Appendix X. Histograms of the elements for the lateritic residuum, soils, sandy hardpan and gravelly hardpan are also shown in the Appendix.

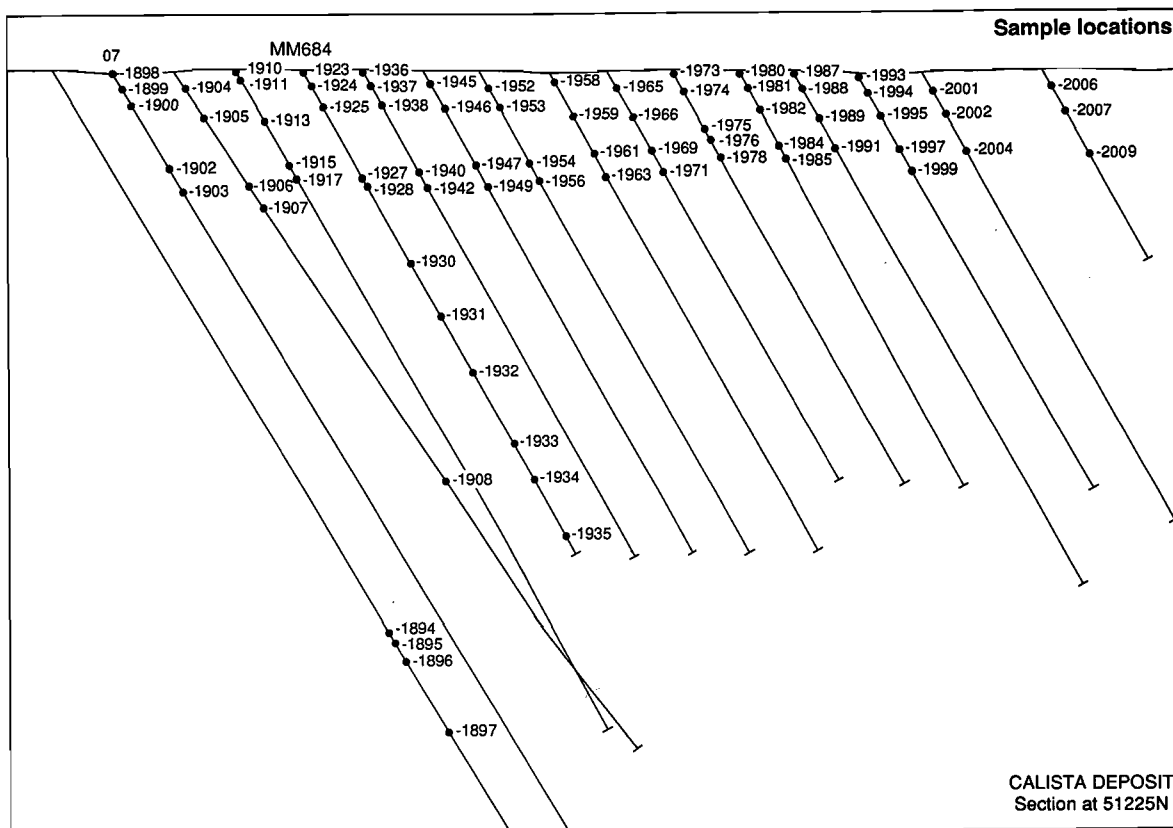


Fig. 5.27 Cross section at 51225 mN showing location of samples from the Calista Au deposit, Mt. McClure district, from Williamson (1992).

#### *Si-Al-Fe relationships*

The chemical compositions of bulk samples of the main regolith units (transported overburden and lateritic residuum) have been plotted on a ternary  $\text{SiO}_2\text{-Al}_2\text{O}_3\text{-Fe}_2\text{O}_3$  diagram (Fig. 5.28). As expected, sandy soils and sandy hardpanised colluvium are relatively enriched in  $\text{SiO}_2$  due to high contents of quartz and amorphous silica. On the other hand, gravelly hardpanised colluvium is relatively enriched in Fe due to its high detrital content of lateritic nodules and pisoliths, which themselves are rich in Fe. Samples of the lateritic residuum have high contents of  $\text{Fe}_2\text{O}_3$  and lesser contents of  $\text{Al}_2\text{O}_3$  and  $\text{SiO}_2$  relative to the mottled zone and saprolite. Among the lateritic residuum categories, lower lateritic residuum is enriched in Fe relative to the upper lateritic residuum.

#### *Element behaviour in the lateritic weathering profile*

This section addresses the geochemistry of the weathering profile sampled from hole MM684 (Figs 5.27 and 5.29) in the context of a section along line 51225 mN through the Calista deposit (Figs 5.30 to 5.35).

Silica,  $\text{Al}_2\text{O}_3$  and  $\text{Fe}_2\text{O}_3$  are the principal weathering products of deep chemical weathering, occurring as the Fe-oxides and clay minerals. Iron is strongly enriched towards the top of the profile, being concentrated in the lateritic residuum. The silica content of the lateritic residuum is much lower than in the underlying clay zone and saprolite. The higher  $\text{SiO}_2$  content in the saprolite and clay zone is due to the presence of quartz and kaolinite. The minor oxides  $\text{Na}_2\text{O}$ ,  $\text{K}_2\text{O}$ ,  $\text{CaO}$  and  $\text{MgO}$  are strongly depleted in the clay zone and in the overlying horizons.

The ore-associated elements W, Sn, Bi, As and Se are markedly enriched in the lateritic residuum, relative to the saprolite and clay zone (Figs 5.29 to 5.34). Tungsten and Sn occur as scheelite and cassiterite respectively. These minerals were identified by using a scanning electron microscope. Bedrock lithology related elements, including Cr, V, Ga, Zr, Nb and Ti, are also enriched in the lateritic residuum. Arsenic, Se, Cr and Ga are associated with goethite and hematite. Some of the elements are retained in the primary minerals, which are resistant to weathering, such as zircon (Zr, Nb).

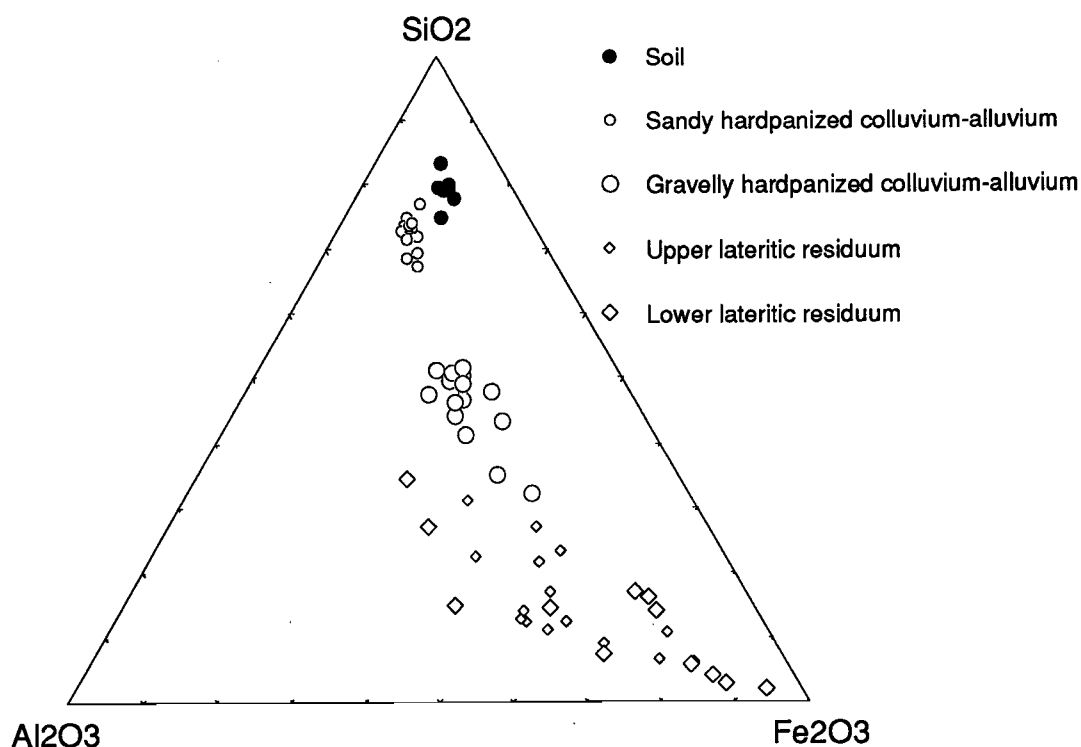


Fig. 5.28 Triangular diagram showing compositions of transported and residual regoliths in terms of SiO<sub>2</sub>, Al<sub>2</sub>O<sub>3</sub> and Fe<sub>2</sub>O<sub>3</sub>, Calista deposit, Mt. McClure district.

The Cr contents of the lateritic residuum is strongly influenced by the parent lithology (Fig. 5.30). Lateritic residuum, derived from the weathering of komatiite is Cr-rich and this may be used to establish parentage.

The elements Mn, Cu, Ni, Co and Zn have many similarities in chemical behaviour in the weathering environment. These elements are strongly leached both from both the clay zone and the lateritic residuum. Cobalt however, is enriched in the clay zone, but is leached from the lateritic residuum.

#### *Dispersion of ore-related elements in the lateritic residuum*

The results showed that the Calista Au deposit is overlain by the high-grade part of a chalcophile multi-element (Au, Bi, Cu, W, Sn, As, Se) geochemical anomaly (Figs. 5.31 to 5.36). The anomaly appears to be widest for As, Bi and Au. The lower lateritic residuum shows a more consistent and stronger geochemical anomaly than the upper lateritic residuum. When compared with the upper lateritic residuum, the lower lateritic residuum, comprising duricrust, has experienced very little or no transportation and is closer in geochemical characteristics to the mineralisation. The extent of dispersion however, varies between the ore-related elements.

The distribution of Au in the regolith is characteristic of many deposits in the Yilgarn Craton. There is a widespread zone of Au enrichment in both the upper and lower lateritic residuum (Fig. 5.31). However, the distribution of Au is erratic (11-6860 ppb). This presumably reflects inhomogeneities in the occurrence of Au, as well as the variable presence of particulate Au.

A leached and depleted zone, 30-40 m thick is present just beneath the lateritic residuum and mottled zone. This corresponds to the clay-rich zone. Supergene enrichment, 5-10 m thick, is present in the lower saprolite. The Au is secondary, having been reprecipitated in a clayey matrix representing the weathered bedrock (Arimco, unpublished data).

Copper appears to be leached from the lateritic residuum, except at the extrapolated intersection of the main mineralisation (12345 mE-12355 mE), where a strong anomaly (1100 ppm), limited to two samples over 10 m, indicates the presence of the main mineralised horizon. Similarly, Ag is leached from the lateritic residuum, although its abundance does show a weakly anomalous, broad rise towards the mineralisation, which is again marked by a sharp Ag anomaly in one sample. This sample is from the

Table 5.9. Some summary statistics for residual regolith, Mt. McClure district.

Element	Upper lateritic residuum n=15					Lower lateritic residuum n=12				
	Mean	Std. Dev.	Min	Max	Median	Mean	Std. Dev.	Min	Max	Median
SiO <sub>2</sub> %	13.6	6.2	5.6	25.9	11.2	10.9	7.8	1.9	27.4	11.4
Al <sub>2</sub> O <sub>3</sub> %	21.7	5.6	10.9	27.9	23.0	16.7	9.2	4.4	30.4	12.3
Fe <sub>2</sub> O <sub>3</sub> %	50.7	11.3	32.1	72.5	48.5	55.9	20.1	22.8	84.1	58.4
MgO %	0.17	0.06	0.08	0.30	0.15	0.17	0.07	0.07	0.25	0.20
CaO %	0.13	0.04	0.08	0.21	0.13	0.10	0.02	0.06	0.11	0.11
Na <sub>2</sub> O %	0.09	0.02	0.05	0.13	0.09	0.07	0.03	0.03	0.15	0.06
K <sub>2</sub> O %	0.02	0.00	0.02	0.02	0.02	0.02	0.00	0.02	0.02	0.02
TiO <sub>2</sub> %	1.66	0.87	0.54	3.47	1.30	1.60	0.78	0.63	3.04	1.41
LOI %	10.5	2.9	5.4	15.6	10.0	12.6	5.4	4.6	20.5	13.2
TOTAL	98.48	0.55	97.50	99.30	98.70	97.93	0.78	96.60	99.40	97.90
Mn ppm	188	75	96	342	154	177	109	43	440	159
Cr ppm	3202	1982	670	6880	2970	4130	3054	421	9610	3840
V ppm	789	234	396	1230	742	830	525	232	1730	787
Cu ppm	58	21	36	99	51	183	301	18	1100	94
Pb ppm	29	11	13	45	27	7	9	0	26	4
Zn ppm	34	12	15	58	37	49	26	23	117	41
Ni ppm	150	78	93	404	123	113	62	25	207	112
Co ppm	25	18	8	77	23	26	17	6	58	20
As ppm	76	29	40	146	66	111	106	13	351	72
Sb ppm	2.5	1.7	0.7	5.0	3.0	2.5	1.7	0.7	6.0	2.5
Bi ppm	10.4	4.1	0.7	18.0	10.0	17.5	13.2	4.0	43.0	13.5
Mo ppm	2.8	1.7	0.7	5.0	3.0	4.3	2.3	0.7	8.0	5.0
Ag ppm	0.5	0.2	0.2	0.9	0.5	0.5	0.4	0.1	1.5	0.4
Sn ppm	6.0	2.6	2.0	10.0	6.0	8.3	6.7	2.0	26.0	6.5
Ge ppm	2.8	1.2	0.7	4.0	3.0	2.7	2.2	0.7	8.0	2.5
Ga ppm	60.9	24.9	24.0	105.0	66.0	50.8	29.6	14.0	102.0	40.0
W ppm	10.9	5.2	1.0	20.0	11.0	12.5	6.5	1.0	21.0	12.5
Ba ppm	117	75	25	266	101	54	55	15	188	25
Zr ppm	169	39	111	246	162	145	42	40	205	149
Nb ppm	7.8	4.1	4.0	18.0	6.0	6.6	3.3	1.0	12.0	6.0
Se ppm	3.7	3.2	1.0	12.0	3.0	7.3	8.0	1.0	31.0	4.0
Be ppm	1.1	0.4	1.0	2.0	1.0	0.9	0.2	0.7	1.0	1.0
Au ppb	1735	2091	11	6860	1060	1092	1891	16	6600	400

Table 5.10. Some summary statistics for transported overburden, Mt. McClure district.

Element	Soil n=8					Sandy hardpan n=15					Clayey-gravelly hardpan n=15				
	Mean	Std. Dev.	Min	Max	Median	Mean	Std. Dev.	Min	Max	Median	Mean	Std. Dev.	Min	Max	Median
SiO <sub>2</sub> %	73.3	2.9	67.4	77.7	73.9	63.4	2.9	58.7	69.2	63.9	39.5	5.0	28.3	45.3	40.7
Al <sub>2</sub> O <sub>3</sub> %	8.7	1.1	7.3	10.7	8.3	15.4	1.2	12.6	17.3	15.3	19.8	1.9	16.4	23.5	20.3
Fe <sub>2</sub> O <sub>3</sub> %	10.6	1.4	8.3	12.3	10.6	8.7	1.3	7.3	11.6	8.2	26.5	5.6	20.4	40.9	24.3
MgO %	0.10	0.07	0.07	0.27	0.08	0.44	0.07	0.35	0.60	0.45	0.47	0.13	0.30	0.73	0.45
CaO %	0.06	0.06	0.03	0.21	0.04	0.29	0.18	0.14	0.71	0.22	0.26	0.17	0.13	0.81	0.21
Na <sub>2</sub> O %	0.04	0.01	0.03	0.07	0.04	0.17	0.03	0.11	0.22	0.16	0.21	0.03	0.16	0.24	0.20
K <sub>2</sub> O %	0.62	0.06	0.52	0.69	0.63	0.84	0.06	0.73	0.93	0.86	0.26	0.09	0.08	0.43	0.26
TiO <sub>2</sub> %	0.48	0.02	0.45	0.52	0.48	0.68	0.07	0.59	0.78	0.69	1.19	0.27	0.85	1.81	1.14
LOI %	4.6	0.8	3.8	6.5	4.5	8.7	1.0	7.2	11.0	8.4	10.6	1.3	8.4	13.2	10.5
TOTAL	98.46	0.40	97.80	99.00	98.45	98.65	0.38	98.10	99.30	98.60	98.74	0.63	97.10	99.60	98.70
Mn ppm	405	478	139	1580	250	387	133	197	684	383	361	172	148	731	317
Cr ppm	281	45	198	338	297	193	40	155	304	182	876	594	396	2390	610
V ppm	184	24	146	225	181	153	25	119	203	143	554	158	378	956	485
Cu ppm	36	20	20	76	29	35	5	27	43	35	85	15	67	122	83
Pb ppm	18	11	11	42	14	15	2	12	20	14	12	4	7	20	12
Zn ppm	23	5	17	34	22	39	4	32	45	40	51	13	27	70	49
Ni ppm	29	11	21	55	26	41	5	34	55	41	71	8	61	90	70
Co ppm	11	10	5	34	8	14	3	10	18	13	17	5	10	24	16
As ppm	6	3	2	10	7	4	2	0	7	4	27	10	14	51	25
Sb ppm	1.3	0.7	0.7	2.0	1.3	0.8	0.5	0.7	2.0	0.7	1.7	1.1	0.7	4.0	2.0
Bi ppm	0.7	0.0	0.7	0.7	0.7	0.7	0.3	0.7	2.0	0.7	0.7	0.3	0.7	2.0	0.7
Mo ppm	2.1	0.7	0.7	3.0	2.0	2.1	1.1	0.7	4.0	2.0	1.1	0.8	0.7	3.0	0.7
Ag ppm	0.3	0.1	0.2	0.4	0.3	0.3	0.2	0.2	0.7	0.3	0.3	0.2	0.1	0.8	0.3
Sn ppm	2.8	1.2	0.7	4.0	3.0	3.3	1.4	2.0	7.0	3.0	3.0	1.3	0.7	5.0	3.0
Ge ppm	0.7	0.0	0.7	0.7	0.7	0.7	0.0	0.7	0.7	0.7	1.2	0.7	0.7	2.0	0.7
Ga ppm	13.9	1.2	13.0	16.0	13.0	23.4	1.9	20.0	27.0	23.0	36.6	11.9	1.0	55.0	36.0
W ppm	3.0	1.9	1.0	6.0	3.5	4.3	1.5	1.0	7.0	5.0	2.3	1.8	1.0	6.0	1.0
Ba ppm	276	341	145	1120	159	364	160	191	824	317	266	166	95	678	186
Zr ppm	173	9	157	183	173	208	19	171	230	213	161	53	5	210	169
Nb ppm	8.1	1.4	6.0	10.0	8.5	12.5	1.4	10.0	15.0	12.0	8.9	2.9	1.0	13.0	9.0
Se ppm	1.3	0.7	1.0	3.0	1.0	1.0	0.0	1.0	1.0	1.0	1.4	0.8	1.0	3.0	1.0
Be ppm	1.1	0.4	1.0	2.0	1.0	1.1	0.3	1.0	2.0	1.0	1.0	0.0	1.0	1.0	1.0
Au ppb	16	17	5	55	8	10	6	4	28	8	126	183	9	580	31

lower lateritic residuum and is not only highly anomalous in Cu (1100 ppm), and Ag (1.5 ppm) but also Se (31 ppm), Bi (43 ppm), W (21 ppm), and Sn (26 ppm). This is attributed to the presence of gossan fragments within the cores of pisoliths and nodules from the lateritic residuum.

Tin (2-26 ppm) and Se (1-31 ppm) are a little more widely dispersed, over 80 m around the mineralised zone. Lead, although not considered anomalous in the mineralisation, also shows a response to mineralisation.

Bismuth (1-43 ppm) and W (1-21 ppm) are widely dispersed with broad anomalies along the entire line in the lower and upper lateritic residuum. Both show peaks in abundances where the mineralisation intersects the residuum and on the down dip side of the mineralisation to the west.

An important feature of the W, Sn and Bi distribution is their retention in both the Fe-oxides and in resistant primary minerals such as scheelite and cassiterite. These elements thus give a widespread anomaly, broadly coincident with that of gold.

#### *Dispersion of ore-related elements in the transported overburden*

Gold levels in the surface soil are consistently around 10-20 ppb except for one sample containing 60 ppb (Fig. 5.35). Gold and Ag are both anomalously high in the gravelly hardpanised colluvium. Gold reaches a maximum concentration of 600 ppb (Fig. 5.35).

In the gravelly facies of the hardpanised colluvium, Cu occurs in concentrations reaching a maximum value of 120 ppm. Copper is, however, much lower in sandy hardpan. Although no background or threshold concentrations have been established for this unit, these concentrations are considered anomalous. The anomaly covers a wide area (150 m across), but its size was not precisely defined. Bismuth, W, Se, As, Zn and Sn occur in very low concentrations in all the units of the transported overburden.

It is not known if Au, Cu and Ag levels in the gravelly, hardpanised colluvium are related to the underlying Au mineralisation. The Au-enrichment in the hardpan may reflect the original levels of Au in the materials derived from the erosion of the upper part of the weathering profile. Introduction of Au into the hardpan at a much later stage is also a possibility. At the Calista deposit, the gravelly hardpanised colluvium has a high proportion of lateritic nodules and pisoliths derived from the dismantling of lateritic residuum elsewhere and includes detritus derived by erosion of saprolite. These gravels represent relatively proximal lateritic debris, which in part may have been derived from the now-truncated profile overlying the Lotus deposit, 1.5 km to the north-northwest. Only two of the 15 samples of gravelly hardpan were taken from near its base (9-11 m depth), and both these contain >0.5 ppm Au, whereas samples from 5-7 m depth contain 0.01-0.02 ppm. Mine data show that these Au concentrations persist in the bottom 5-6 m of this unit for at least 150 m across the strike of mineralisation.

#### *5.3.6 Implications in exploration*

Extensive areas of complete laterite profiles are common beneath the widespread transported colluvium and alluvium. The extent of buried lateritic residuum is in marked contrast with the restricted area of lateritic residuum exposed at the surface, the latter being about 10% of the mapped area. Broad Au anomalies and anomalous concentrations of W, Sn, Bi, Cu and As in the buried lateritic residuum and ferruginous saprolite at the Calista deposit are effective indicators of primary and supergene mineralisation. The lower lateritic residuum shows a more consistent and stronger geochemical anomaly than the upper lateritic residuum. The extent of dispersion, however, varies between the ore-related elements. In drilling to sample buried laterite, it is important to distinguish between the transported lateritic debris and residual laterite.

The occurrence of anomalous concentrations of Au, Cu, As and Ag in the transported hardpanised colluvium over the Calista deposit suggests considerable exploration significance. The Au enrichment in the hardpan unit may reflect the original levels of Au in the materials derived from the erosion of the upper part of the weathering profile. Introduction of Au into the hardpan at a much later stage is also possibility. Further orientation studies are needed to assess the significance.

Some of the more important implications of the Mt. McClure research in exploration are listed in Table 5.11 and a geochemical dispersion model for the Calista deposit is shown in Fig. 5.36.

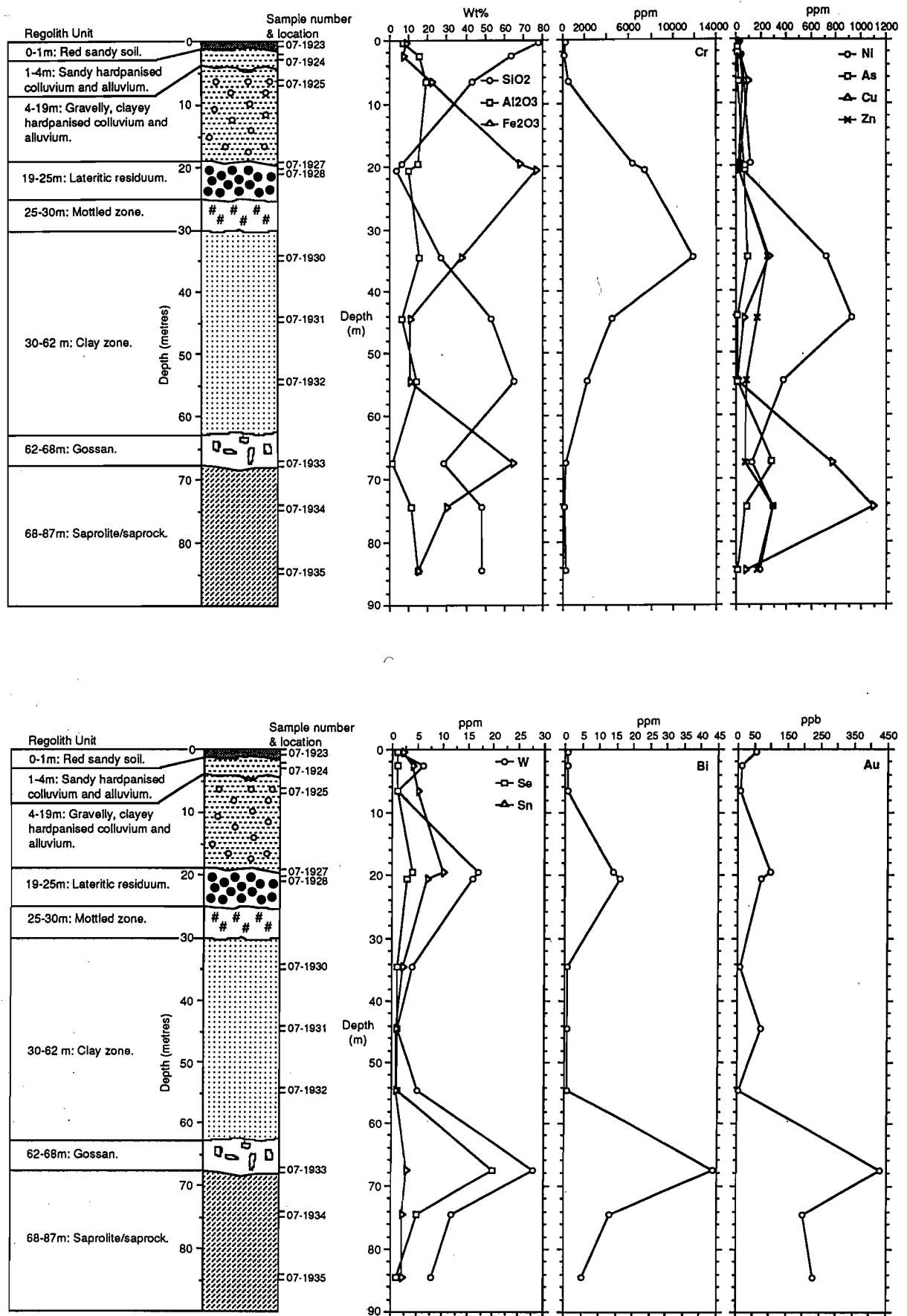


Fig. 5.29 Vertical distribution of some major, minor and trace elements in the ultramafic profile over the mineralisation, drill hole MM684, Calista deposit, Mt. McClure district, from Williamson (1992).



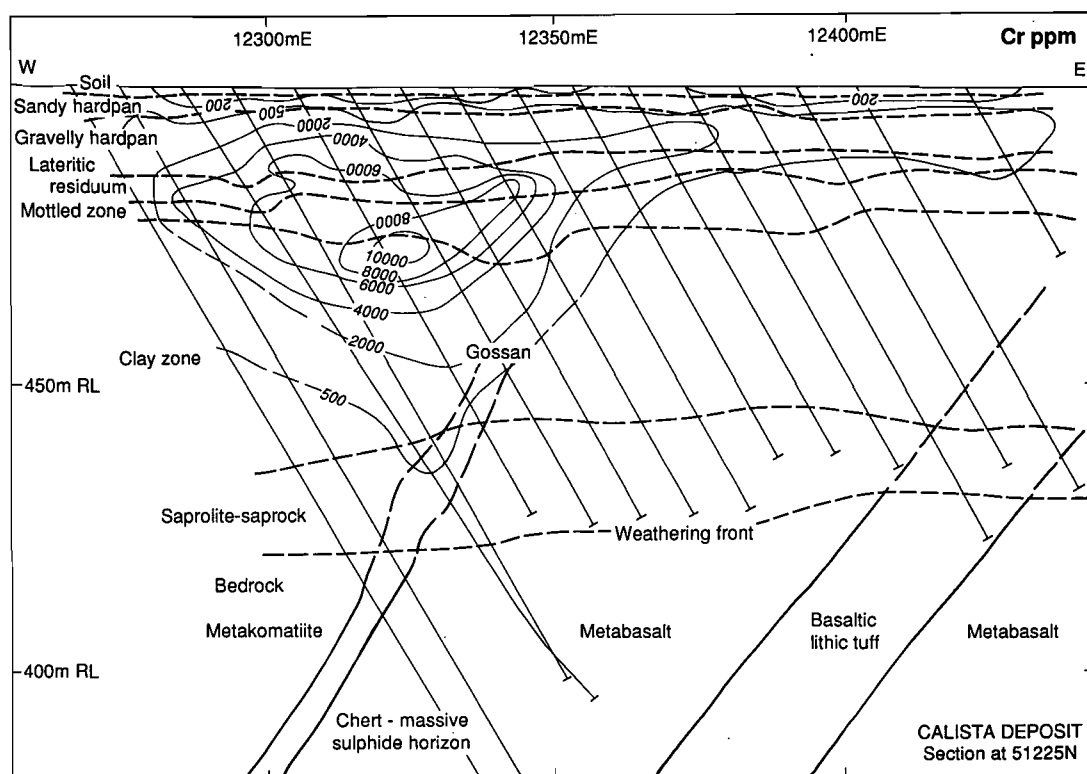


Fig. 5.30 Cross section at 51225 mN showing contoured Cr abundances for the Calista deposit, from Williamson (1992).

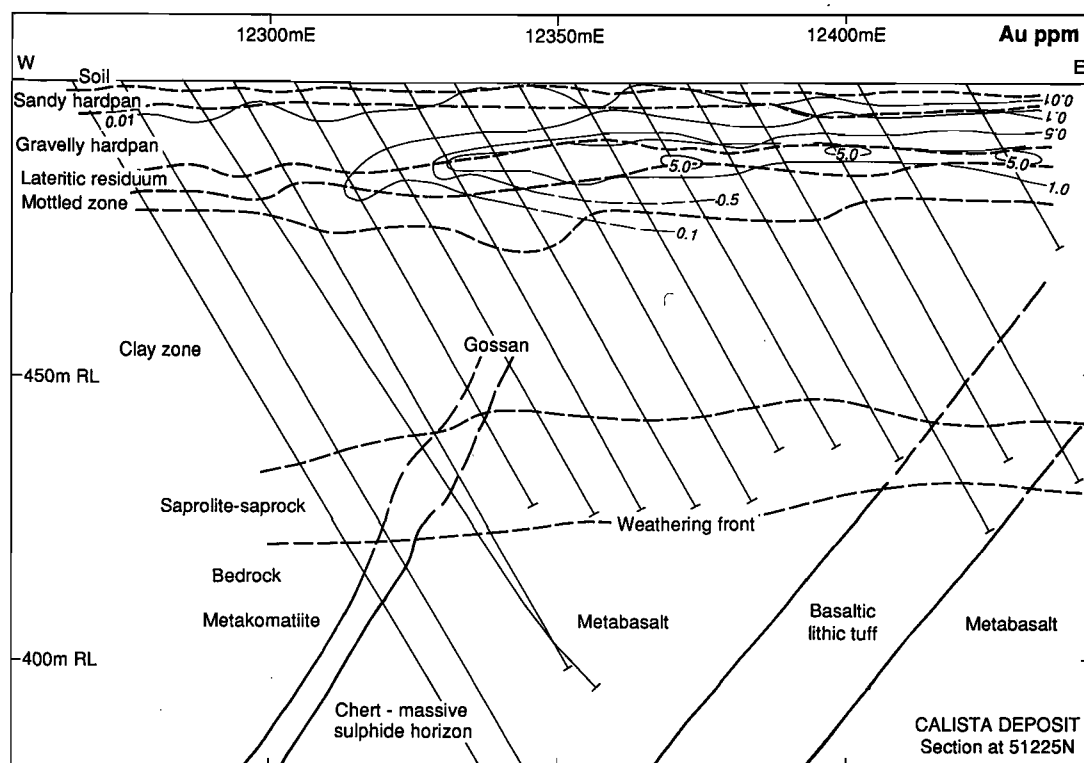


Fig. 5.31 Cross section at 51225 mN showing contoured Au abundances for the Calista deposit, from Williamson (1992).

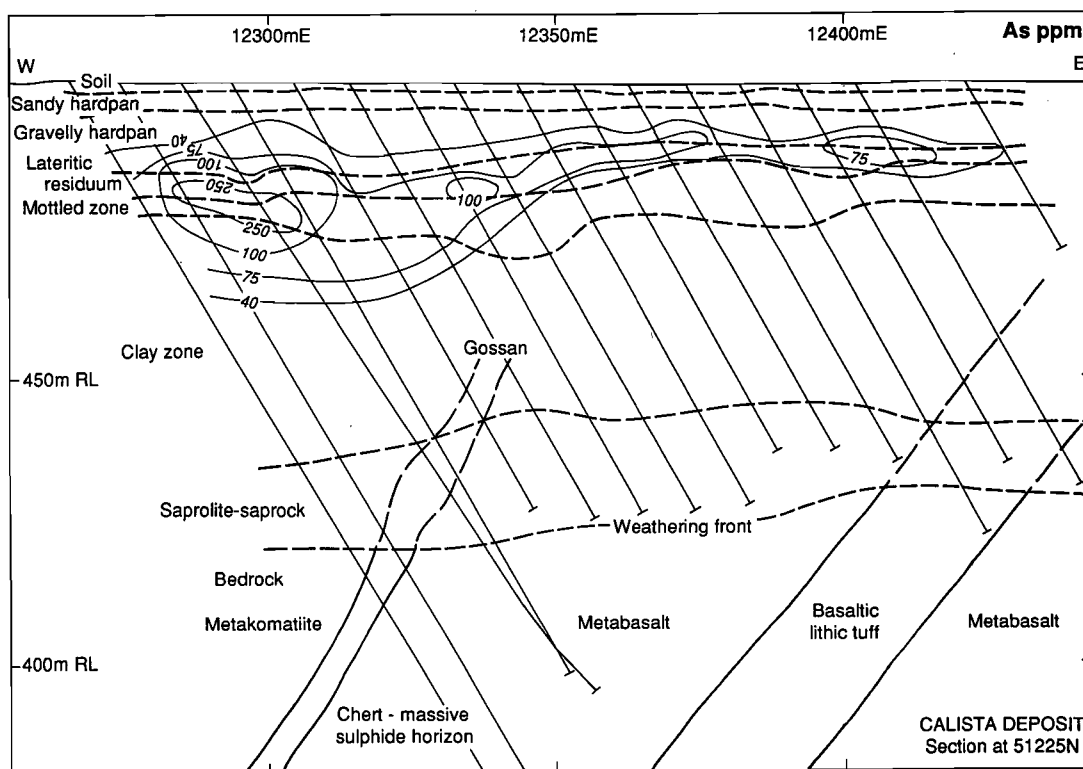


Fig. 5.32 Cross section at 51225 mN showing contoured As abundances for the Calista deposit, Mt. McClure district, from Williamson (1992).

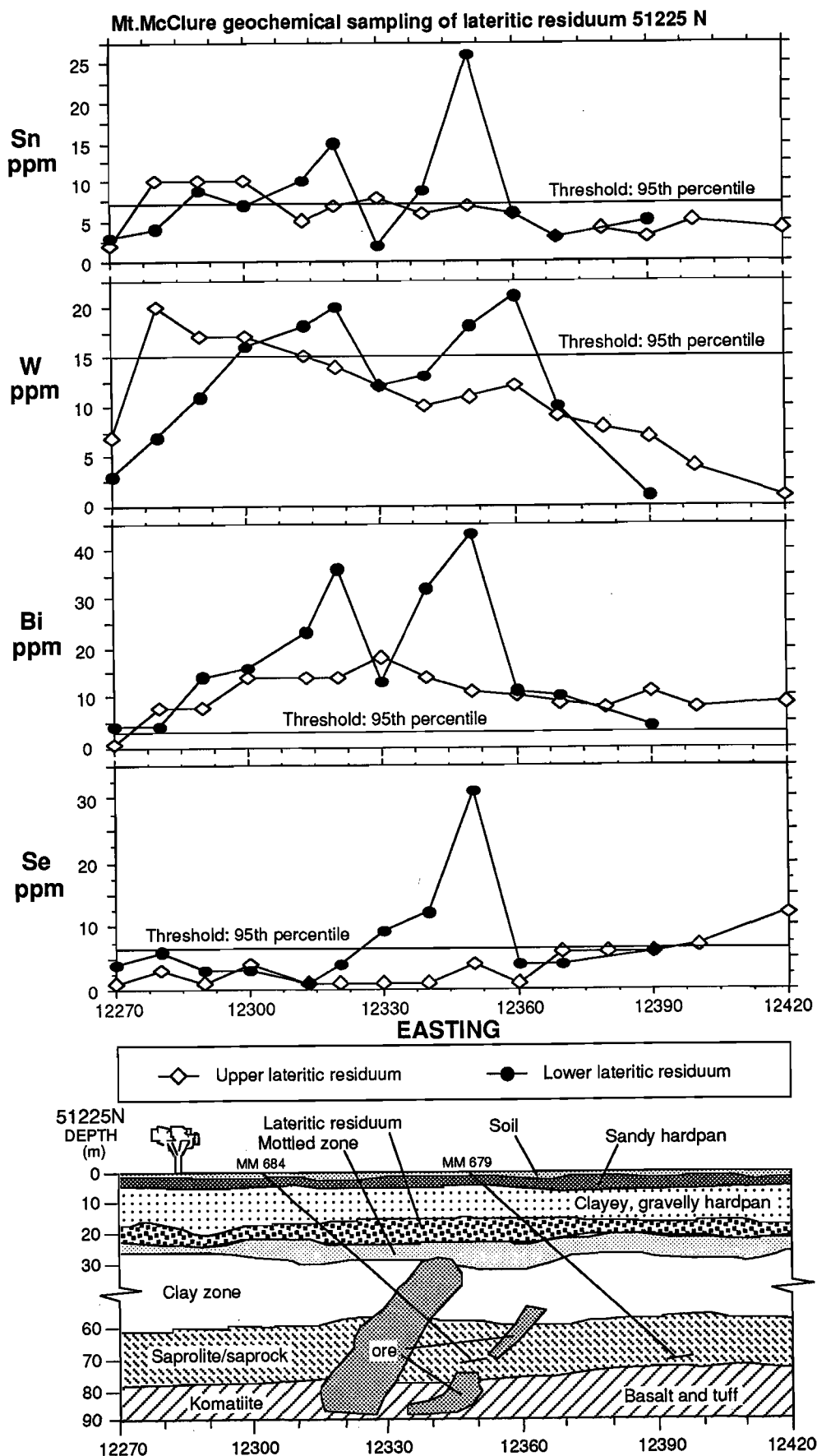


Fig. 5.33 Traverse along line 51225 mN showing the distribution of Sn, W, Bi and Se in upper and lower lateritic residuum, Calista deposit, Mt. McClure district. Modified after Williamson (1992).

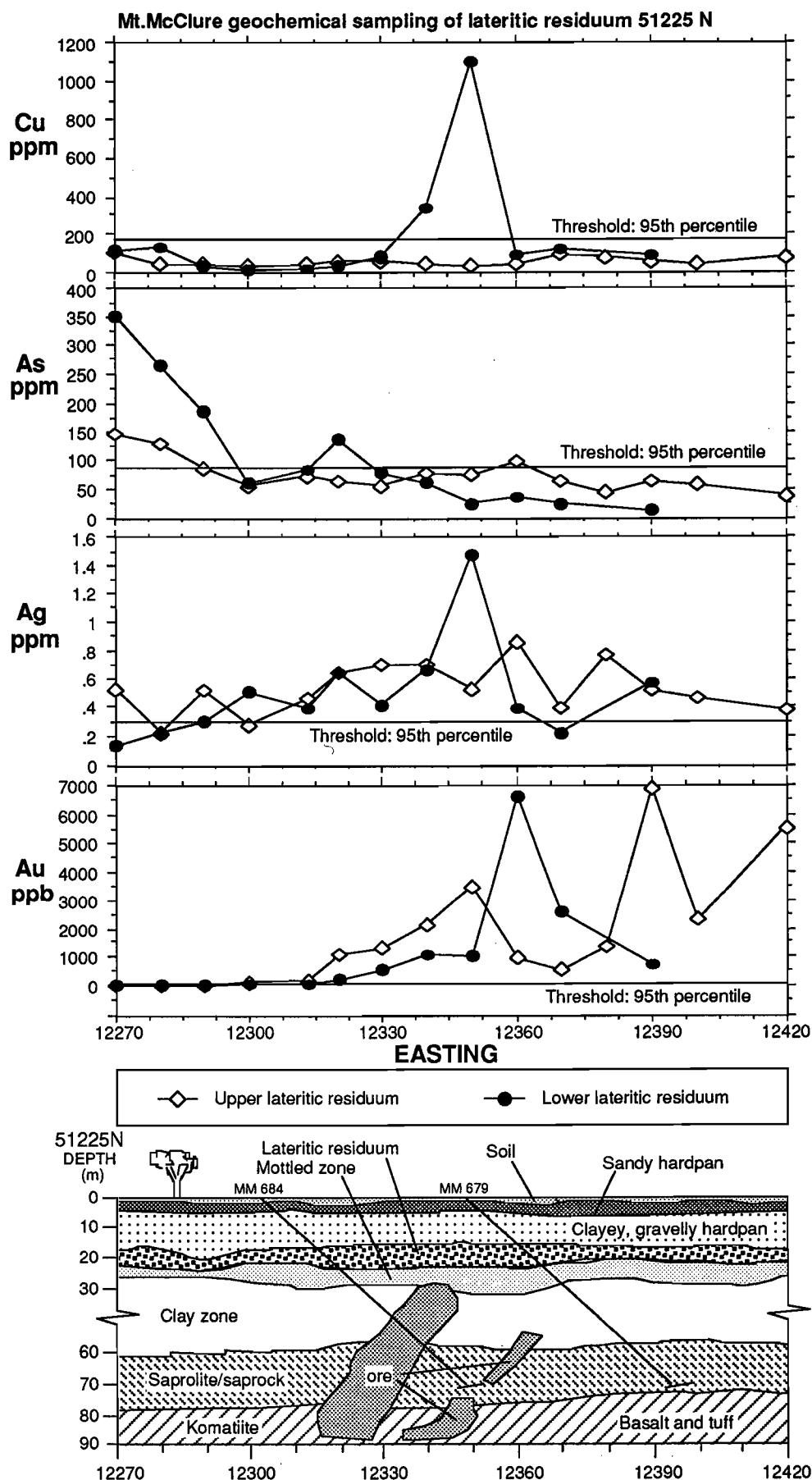


Figure 5.34 Traverse along line 51225 mN showing the distribution of Cu, As, Ag and Au in upper and lower lateritic residuum, Calista deposit, Mt. McClure district. Modified after Williamson (1992).

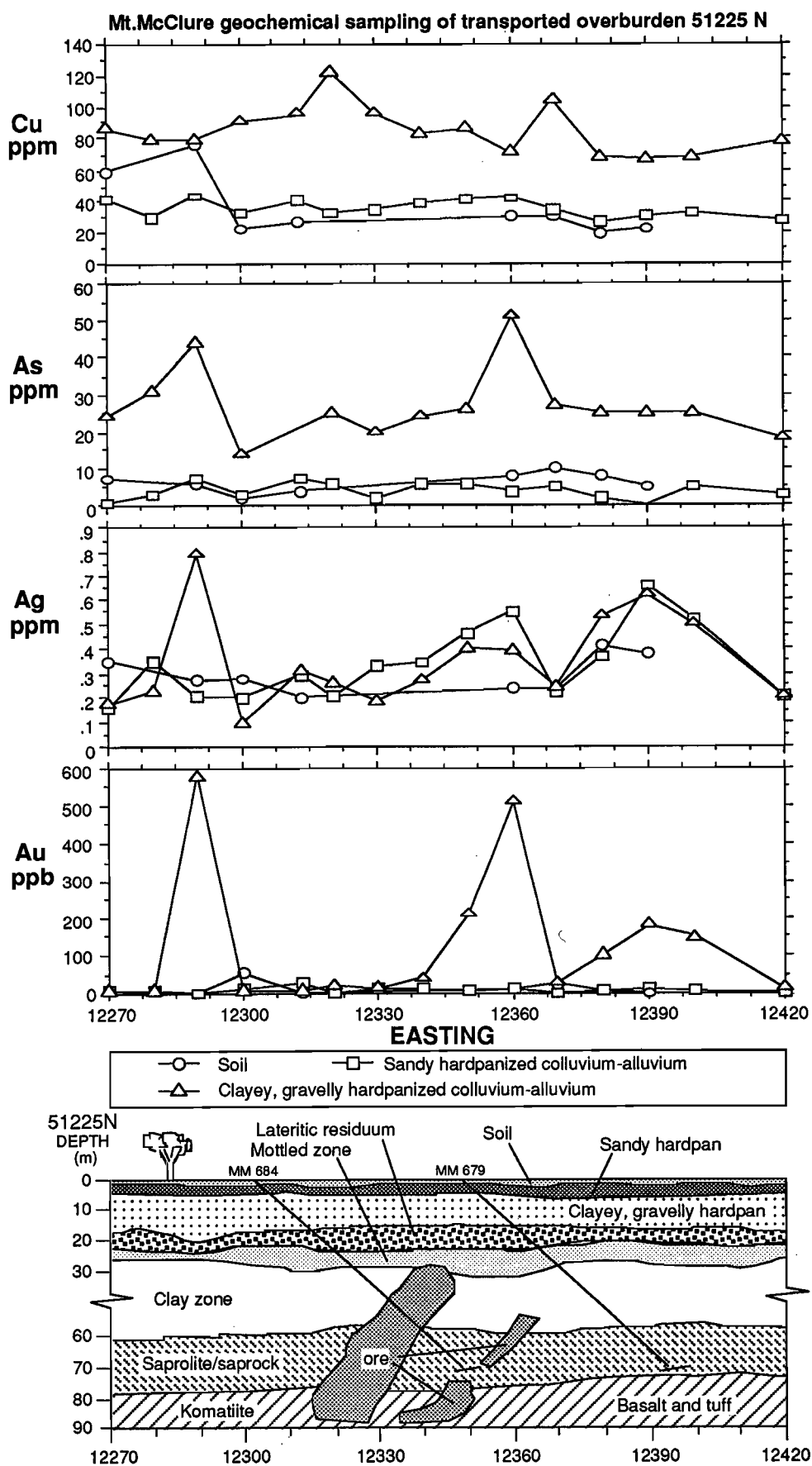


Fig. 5.35 Traverse along line 51225 mN showing the distribution of Cu, As, Ag and Au in transported regolith, Calista deposit, Mt. McClure district. Modified after Williamson (1992).

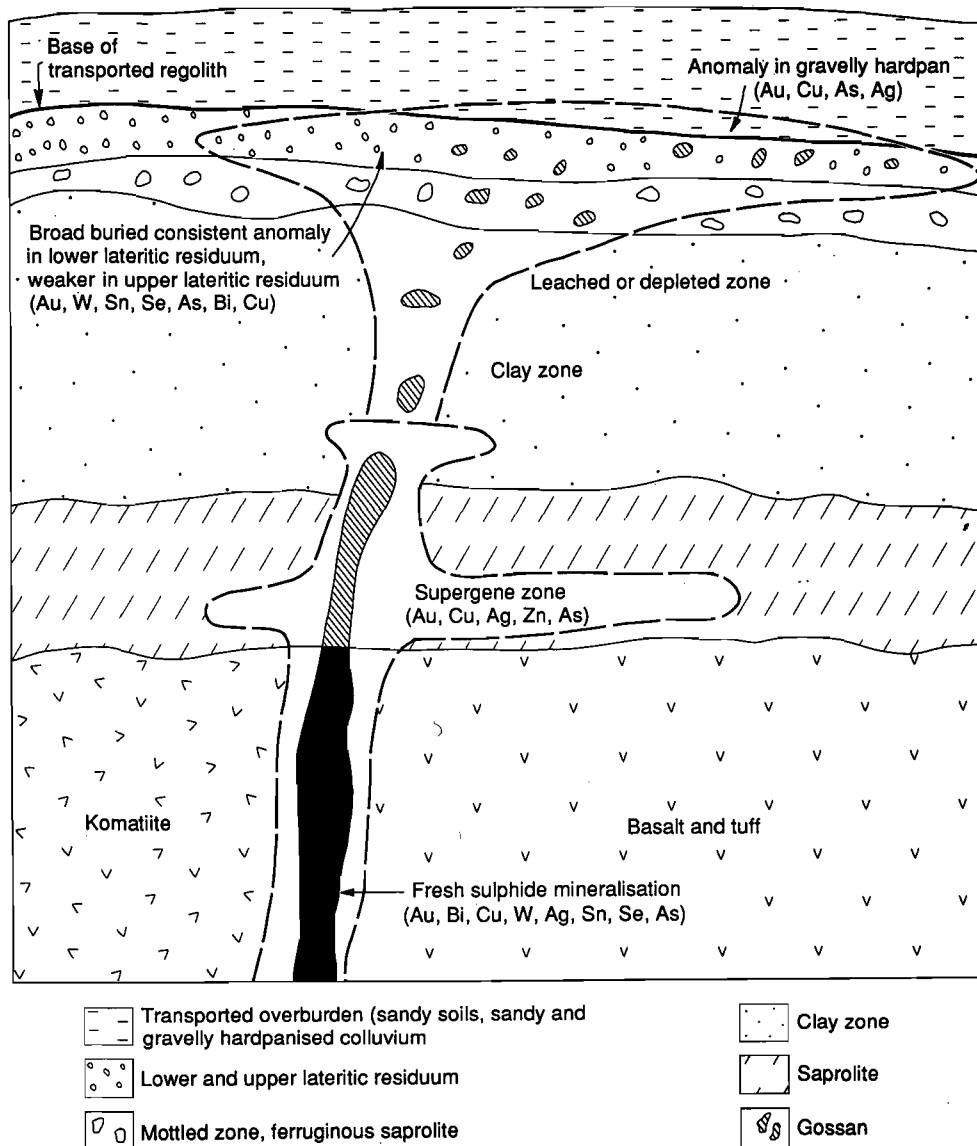


Fig. 5.36 Geochemical dispersion model for the Calista deposit, Mt. McClure district.

Table 5.11 The implications in exploration listed against the research findings, Mt. McClure district study and orientation at the Calista Au deposit.

Research Findings and Outcomes	Implications in Exploration
<ul style="list-style-type: none"> <li>Regolith landform evolution is explained by polyphase dismantling of lateritic profiles and consequent burial. Mapping and understanding of regolith stratigraphy revealed that a complete lateritic weathering profile, including lateritic residuum and ferruginous saprolite, is preserved over half the 185 km<sup>2</sup> area, either at surface or beneath the sediments.</li> <li>District scale regolith-landform relationships were established.</li> <li>Regolith models were established.</li> <li>A large geochemical anomaly (Au, W, Sn, Bi, Cu, Se, As) is present in lateritic residuum. Gold, W, Sn and Bi are the best indicators of mineralisation.</li> <li>In detail, the multi-element dispersion anomaly is more consistent and stronger in the lower lateritic residuum (nodular duricrust) than in the upper lateritic residuum (loose pisoliths and nodules). Anomalous element assemblages are similar in both media.</li> <li>Au, Cu and Ag anomaly is also present in gravelly hardpanised colluvium.</li> <li>Well-documented project material has been generated.</li> </ul>	<ul style="list-style-type: none"> <li>Exploration can be directed at buried geochemical haloes in laterite and ferruginous saprolite to locate concealed mineral deposits beneath alluvial and colluvial plains. Both these media enlarge target size and cut exploration costs.</li> <li>Establishes framework for exploration geochemistry.</li> <li>Provides control for interpretation of satellite imagery for regolith mapping.</li> <li>Enables prediction in appropriate terrain elsewhere.</li> <li>A wide strong multi-element signature provides an enlarged exploration target. Zoning allows delineation of drilling targets.</li> <li>Loose pisoliths should be used for reconnaissance exploration (broader anomalies), lateritic duricrust for follow-up and for defining drilling targets.</li> <li>Suggests that geochemical dispersion has taken place within hardpanised colluvium.</li> <li>Provides material for educational training of explorationists.</li> </ul>



#### 5.4 Waroonga and Genesis Au deposits, Lawlers district

(Section 5.4 is largely condensed from the B.Sc. Honours Thesis by Richard F. Twomey, University of WA, 1992)

##### 5.4.1 Introduction

The study area of 100 km<sup>2</sup>, Figs 1.1 and 5.37, is located in the north-west part of the Lawlers orientation district. It extends to the west and north the Agnew-McCaffery detailed area previously studied (Figs 4.27 and 4.28 in Report 236R). The study area includes the old Agnew Hotel and post office site and is referred to here as the Agnew area.

The study area includes the contact between the Agnew supracrustal belt and the Waroonga Gneiss terrain to the west (Fig. 5.37). The greenstone sequence, comprising an association of differentiated tholeiitic sills and lavas with some komatiites, is overlain by feldspathic sediments and conglomerate, which grade upwards into fine-grained pelitic sediments. The western limb of the Lawlers anticline is overlain by the 1500 m thick Scotty Creek metasedimentary sequence, a west-facing mainly quartzo-feldspathic sandstone sequence.

The Genesis Au deposit differs from other Au deposits at Lawlers. It is hosted in a quartzite unit of the Scotty Creek clastic sequence and consists of thin, mineralised quartz vein sets. Although arsenopyrite is disseminated throughout the orebody, Au is only rarely associated with it, and is mainly free-milling and within quartz veins.

Reconnaissance drilling of the regolith profile in the Lawlers district in 1989, seeking geochemical haloes in buried lateritic residuum, detected several anomalies. Follow up drilling of one of these, a Au, As anomaly, resulted in discovery of the Waroonga Au deposit. Open-cut mining commenced during 1990. The Waroonga deposit comprises a lateritic, duricrust-hosted, Au deposit, which was overlain by barren, hardpanised, transported sediments. Gold also occurs within a Permian glaciofluvial, conglomeratic deep-lead at Waroonga, which unconformably overlies saprolite derived from the Archaean Scotty Creek clastic sequence. The total ore mined at Waroonga exceeded 300,000 tonnes, at an average grade of 1.9 g/t. Exploration drilling about the Waroonga deposit resulted in discovery of the Genesis Au deposit, adjacent to the west.

The climate is arid, with an average annual rainfall of 200 mm. The mean daily maximum temperature for January is 36°C and 18°C for July. The area is subject to both drought and short-term flooding and has a relief ranging from 475 to 557 m above sea level.

Broad colluvial outwash plains and braided stream tracts in the area are characterised by a sparse cover of low shrubs and mulga (*Acacia* spp.). Areas of low hills have a similar assemblage, although growth is somewhat denser. *Eucalyptus* sp. occurs in well-defined creeks and seepages along breakaway faces are characterised by shrubby eucalypts and native pines.

##### 5.4.2 Objectives

The main objectives were:

1. to establish the detailed regolith-landform relationships in the area; and
2. to conduct a multi-element geochemical orientation study of dispersion in the regolith profile over the Genesis and Waroonga Au deposits.

##### 5.4.3 Research components

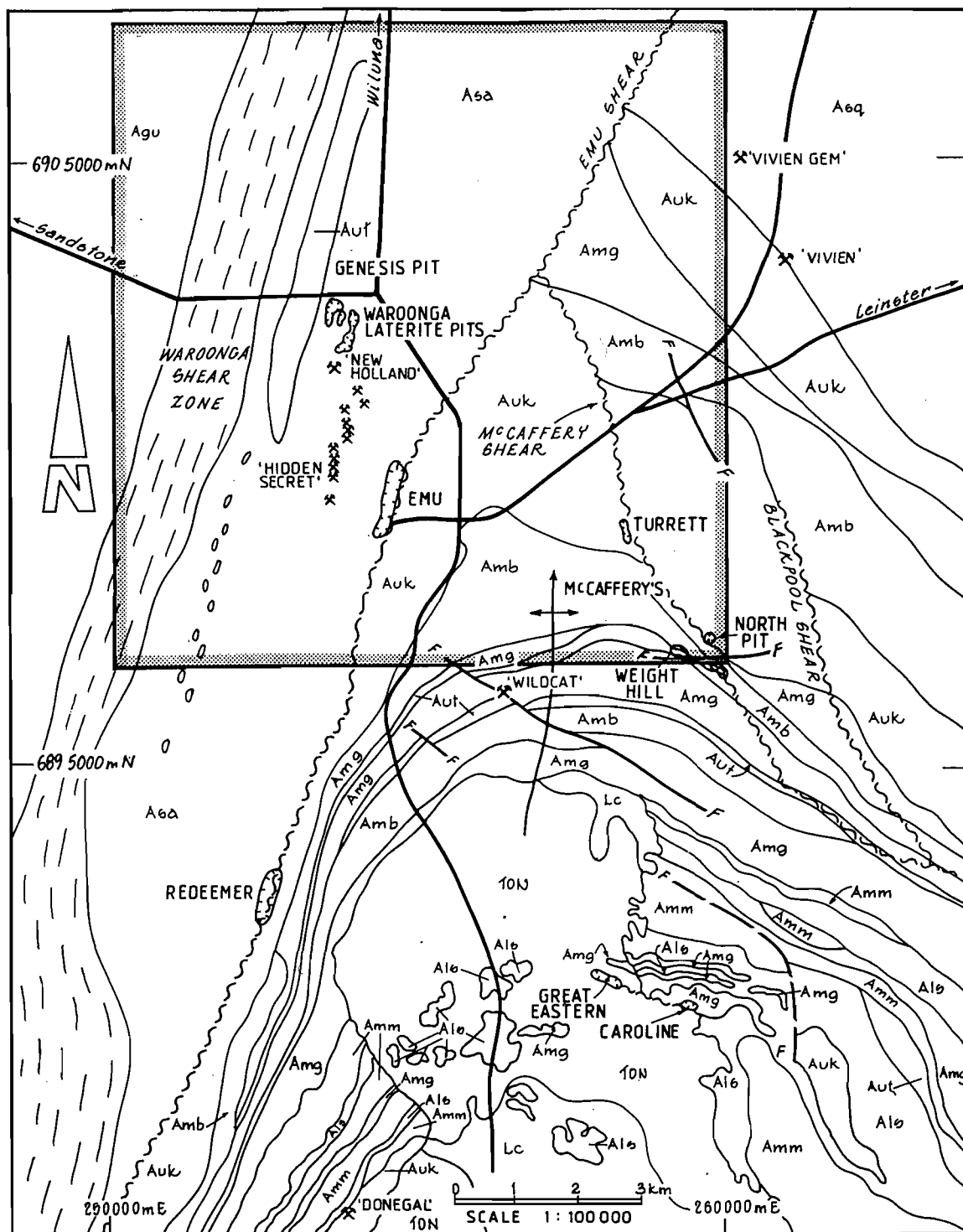
The scope of the study included the following:

- Regolith-landform mapping over the 100 km<sup>2</sup> area;
- establishing the regolith stratigraphy;
- Orientation geochemical dispersion studies about the Waroonga and Genesis Au deposits;
- Duricrust composition and bedrock relationships;
- Synthesis and implications in exploration.

##### 5.4.4 Regolith-landform relationships

The study area was mapped at 1:25,000 scale using colour airphotos as a base for field traverses. The distribution and stratigraphy of the regolith units are interpreted in terms of the dynamics of formation, preservation and dismantling of the complete weathering profile.

Large tracts of the Agnew area are characterised by colluvium and alluvium, with approximately 65% being occupied by outwash plains and braided stream systems. About 10% of the area is characterised by bedrock outcrop and subcrop. The broad-scale distribution of the regolith units, developed in the Agnew area, is largely controlled by two distinct geomorphic regimes. Areas south of



## LEGEND

Lc	Leucogranite	Alb	Layered gills (with ultramafic/mafic cumulative zone)	—	Graded road
10N	tonalite	Amg	Differentiated gabbroic gills	⋈	North plunging anticline
Agu	Undifferentiated granitoids	Amb	Basalt	~	Shear zone
///	Gneiss in Waroonga Shear Zone	Amm	High-mg basalt	-f-	Fault
Aga	Scotty Creek sequence	Aut	Ultramafic rocks	○	Open cut mine
Aeq	Vivien sequence	Auk	Komatiite	*	Old workings

Fig. 5.37 Geological map of the northwest part of the Lawlers district. From Twomey (1992).

the regional drainage divide have been subject to protracted erosion and, with the exception of local areas of sandy colluvium on felsic bedrock, the regolith weathering profile has been removed. North of the divide, the characteristic regolith distribution pattern comprises the dissected remnants of lateritic weathering profiles, variably exposed higher in the landscape, which occur marginal to extensive alluvial and colluvial plains. Complete laterite profiles are commonly preserved beneath the depositional units (Section 4.4 in Report 236R).

The land-surface was classified into residual, erosional and depositional regimes, as discussed in Section 3.3. The geochemistry of lateritic residuum (lateritic duricrusts, pisoliths, nodules and oolites) is related to the primary associations in the bedrock ( $\pm$  mineralisation). The geochemical response of erosional materials (hardened mottles, ferruginous saprolite, lithic fragments) can reflect the geochemistry of the underlying bedrock and mineralisation. However, dislocation, inherent in pedogenic processes on slopes and the downslope transport of lag materials such as iron-segregations or gossan fragments, may obscure the original relationship. The intrinsic geochemistry of the depositional regimes shows no direct relationship to the substrate, although hydromorphic dispersion of ore-associated elements can result in anomalous concentrations in the colluvial sediments over primary and secondary mineralisation.

The mineralogy of the regolith materials is dominated by a simple assemblage of kaolinite, hematite, goethite and quartz, with minor amounts of maghemite and resistant primary minerals variably occurring. The type and relative proportions of these secondary minerals are documented in the residual profiles and in the overlying colluvial sediments, because effects such as co-precipitation or adsorption of trace elements by Fe- and Mn-oxides have a significant impact on the geochemical response of the sample. Regolith stratigraphy and effects such as the preferential development of a deep regolith profile over the primary mineralisation in the Genesis deposit were also documented, because of their significance in geochemical exploration.

These regolith-landform regimes comprise the mapping units shown in Fig. 5.38.

#### 5.4.5 Regolith stratigraphy

Table 5.12 summarises the regolith stratigraphy in terms of the residual, erosional and depositional regimes of the area. Colluvium forms the most extensive unit in the area. The variable nature and provenance of the colluvial sediments and their topographic setting reflects their derivation by erosional dismantling of the weathering profile.

The sequence of colluvial units in the vicinity of the Genesis and Waroonga deposits are generally less than 5 m in thickness. An unconsolidated veneer of red, sandy, clay soils with an associated lag of mixed origin overlies a polymictic gravelly unit, which has a maximum thickness of 2 m. The unit consists of rare pisoliths, lithorelics and abundant reddish-black to dusky red, hematitic saprolite fragments and quartz clasts in a brownish-yellow matrix, which contains numerous voids of probably biogenic origin. The voids are continuous through the unit and are arranged in a dendritic, enteric or vermiform manner, suggestive of tree-root patterns. The matrix in the void infills is red and is quartz- and kaolinite-rich. The unit outcrops along a series of subdued breakaways and is shown as regolith-landform mapping unit 6b.

The underlying unit represents a change to a finer, more clay-rich facies. A maximum thickness of 2 m of fine, weakly hardpanised, gravelly clays is exposed beneath the more coarsely clastic unit. Both colluvial units show the effects of further weathering, subsequent to deposition, in the development of goethitic spots and mottles and in the secondary goethite associated with the void-infill material.

Lenses and pipe-like bodies of transported pisolitic and nodular lateritic debris occur towards the base of the colluvial sequence.

The colluvial sedimentary cover thins and ultimately is absent on the flanks of elevated areas, where either lateritic residuum (duricrusts) or the upper zone of the saprolite profile is exposed. Lateritic duricrusts also occur discontinuously throughout the area buried beneath variable thicknesses of colluvium. A pisolitic-nodular duricrust represents the top of the residual weathering profile developed over the Waroonga gneiss terrain in the west of the area, Fig. 5.47B.

Iron-rich duricrusts are exposed, overlying an elongate, ultramafic dunite/peridotite body approximately one kilometre west of the Genesis Pit. Maximum thickness is approximately 3 m and the duricrusts show a relatively sharp transition to pervasively ferruginous saprolite, Figs 5.39, 5.46B and 5.47A.

Weathering of the felsic rocks results in a relatively homogeneous, pale, kaolinitic, saprolite profile. In the lower saprolite, weathering is essentially isovolumetric. The top of the saprolite profile, however, is characterised by intense leaching, resulting in volume loss and local collapse, obliterating any

trace of primary fabric. Resistant bodies, such as quartz veins, persist in the lower saprolite profile but become dismembered in the upper zone, where collapse breccias occur, Fig. 5.46A.

In contrast to the felsic rocks, weathering of the mafic and ultramafic rocks produces iron-rich secondary minerals such as smectite, vermiculite and chlorite and only minor kaolinite in the lower saprolite profile (Lawrance, 1992). The upper, more evolved saprolite has a higher kaolinite content and is characterised by the occurrence of discrete iron segregations in a ferruginous, yellow to reddish brown clay matrix. The dominantly hematitic and goethitic segregations occur as small pods to large bodies, some 10 to 25 m across (Anand *et al.*, 1991), as well as anastomosing vein-like arrays, controlled by relict structural surfaces such as schistosity or joint sets. The uppermost horizon comprises pervasively ferruginised saprolite and consists of yellowish-brown to dark brown saprolite which has been replaced mainly by goethite. The major stratigraphic units of the weathering profile are shown in Fig. 5.39.

**Waroonga Pit.** The Waroonga Pit adjoins the south-eastern wall of Phase 4 of Genesis and extends a further 700 m to the south. Mining of the lateritic Au ore is now complete and has exposed the upper 15 m of the profile. A complete residual regolith profile is preserved over the bedrock metasediments and is, in turn, unconformably overlain by transported colluvial sediments, Fig. 5.40.

The lateritic duricrust horizon and an underlying Permian channel deposit formed the Waroonga orebody. The upper surface of the duricrust is planar and, at the southern end of the pit, it intersects the current landsurface. It dips very gently northwards, over the length of the pit, to the point where it has been truncated by a former erosion surface, in the eastern wall of Phase 4 of the Genesis Pit.

**Genesis Pit.** The stratigraphy of the weathering profile of the Genesis deposit comprises two distinct units, of contrasting origin. The lower unit consists of variably developed saprock, saprolite and mottled saprolite horizons. The profile has been eroded and, with the exception of the eastern wall of Phase 4 of the pit, the lateritic duricrust horizon has been removed. This partly truncated profile is unconformably overlain by a diverse, transported regolith sequence, Fig. 5.41.

The unconformity separating the residual profile and the transported overburden represents a palaeo-landsurface which has been progressively buried by clastic debris, distally derived by erosion of the surrounding lateritic uplands. Although it occurs at a similar stratigraphic level over the pit area, the unconformity is a variable, essentially planar, sub-horizontal surface to the north and a variable surface, locally steeply incised into the underlying saprolite to the south. The stratigraphic thickness of the overburden generally ranges between 6 and 8 m, locally attaining a maximum of 10 m in the incised areas.

#### 5.4.6 Duricrust composition and bedrock type

A west to east traverse across the bedrock stratigraphy, giving the levels of some of the lithology-related elements is shown in Figs 5.42 and 5.43. The traverses show the relatively high levels of Si and Al in duricrusts over the granitic gneisses and metasediments in comparison with those over ultramafic bedrock. The latter are characterised by relatively high abundances of Cr, V, Fe, Ti and Nb, compatible with project findings elsewhere.

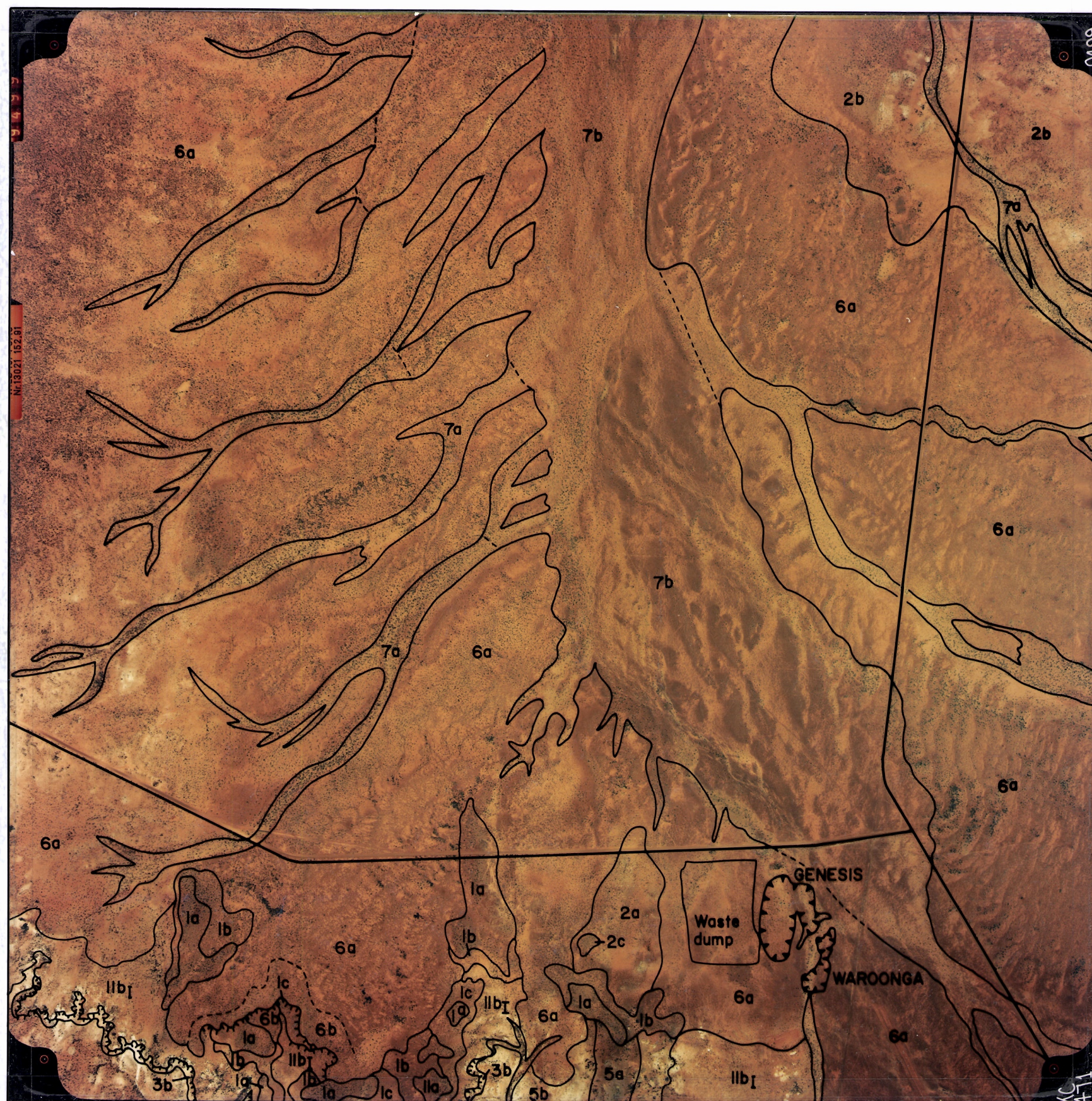
#### 5.4.7 Dispersion of Au and ore-associated elements

Weathering of primary Au mineralisation can result in supergene Au deposits and also gives rise to other secondary dispersion haloes in the regolith profile (such as in lateritic residuum) which involve Au and ore-associated elements. These dispersion haloes are particularly important because they can provide larger targets in exploration for primary deposits and thus cut exploration costs.

The multi-element dispersion study in the regolith profile over the Genesis deposit indicates that factors such as the occurrence of the Au and the primary geochemical associations of the orebody largely control the resulting dispersion patterns. Primary Au in the Genesis pit characteristically occurs in a relatively pure native form, armoured within quartz veins, which resist dissolution and mobilisation processes in the weathering profile. The characteristically low primary concentrations of the ore-associated suite of elements also result in limited dispersion patterns in the overlying regolith.

At Genesis and Waroonga, As is dispersed at anomalous concentrations in the residual profile and is less, but still anomalous (153 ppm max.), in the transported overburden. Lead and W show a certain immobility and occur at higher concentrations in the saprolitic profile, reflecting limited dispersion of the primary accessory phases, galena and scheelite. Copper and Zn are present at higher concentrations in the transported overburden, which probably relates more to the geochemistry of the clastic components than to the underlying mineralisation. Antimony and Mo occur at very low concentrations throughout the profile.





## EROSIONAL REGIME

- 2a Soil, lag on mafic/ultramafic saprolite; pedogenic calcrete variably developed
- 2b Soil, lag on felsic saprolite
- 3b Mottled felsic saprolite
- 5a Outcrop of mafic/ultramafic bedrock
- 5b Outcrop of felsic bedrock
- 11b1 Outcrop of indurated, Fe-stained saprolite caprock after felsic bedrock

## RESIDUAL REGIME

- 1a Pisolithic-nodular duricrust
- 1b Lateritic gravel
- 1c Basal zone of duricrust, also includes transition to mottled saprolite and saprolite breccias

## DEPOSITIONAL REGIME

- 6a Colluvium as sheetwash
- 6b Hardpanized colluvium
- 7a Alluvium in tributaries
- 7b Alluvium in braided systems

1 km

N

Fig 5.38 The mapped distribution of regolith units as an overlay to a colour aerial photograph by Kevron Aerial Surveys 9497-9512 Run 3, 6/12/88, published with permission of Homestake Gold of Australia Limited. Northwest part of the Agnew thesis area of Twomey (1992), Lawlers District.





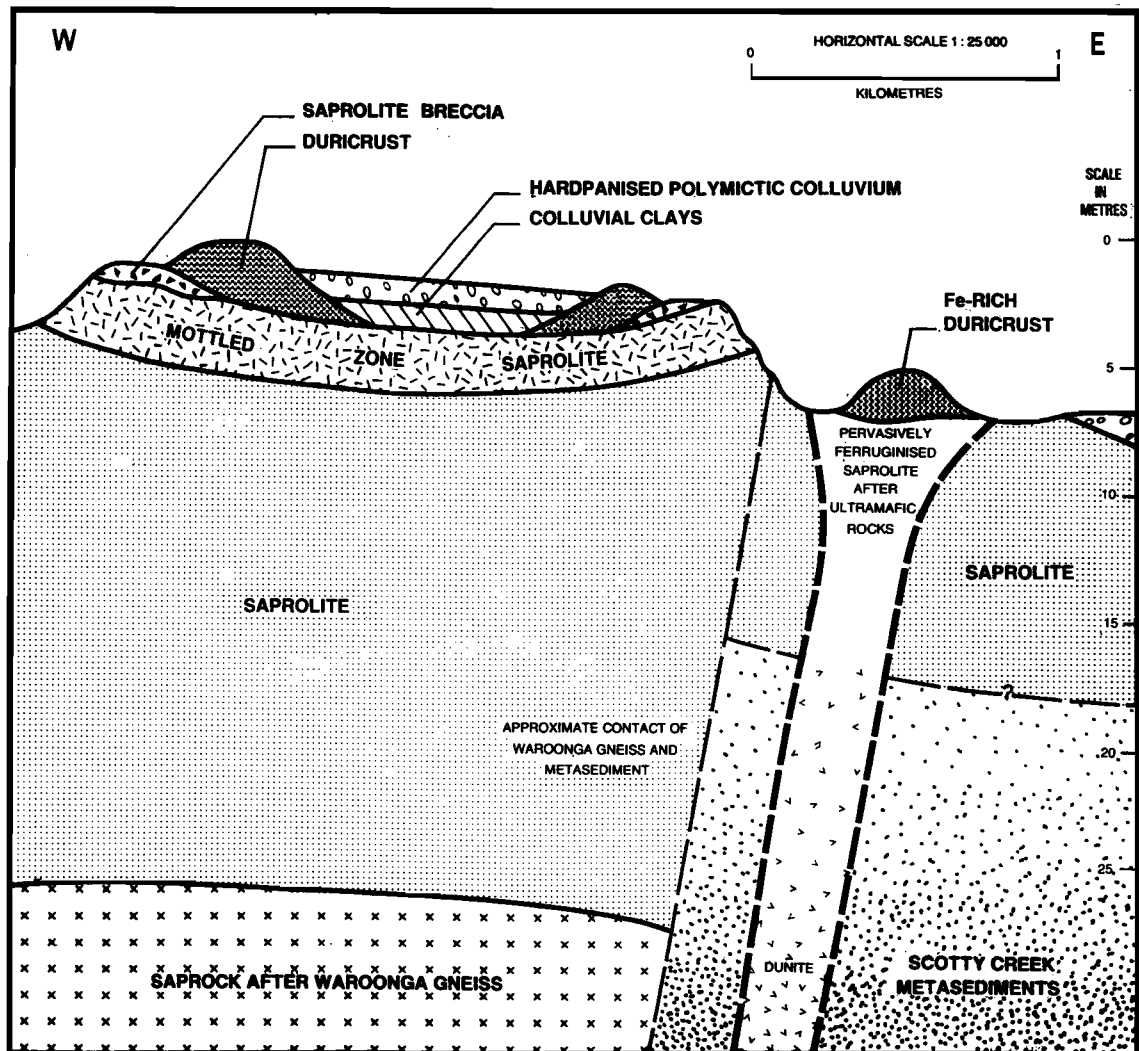


Fig. 5.39 Schematic west to east section for the western part of the Agnew area, from Twomey (1992).



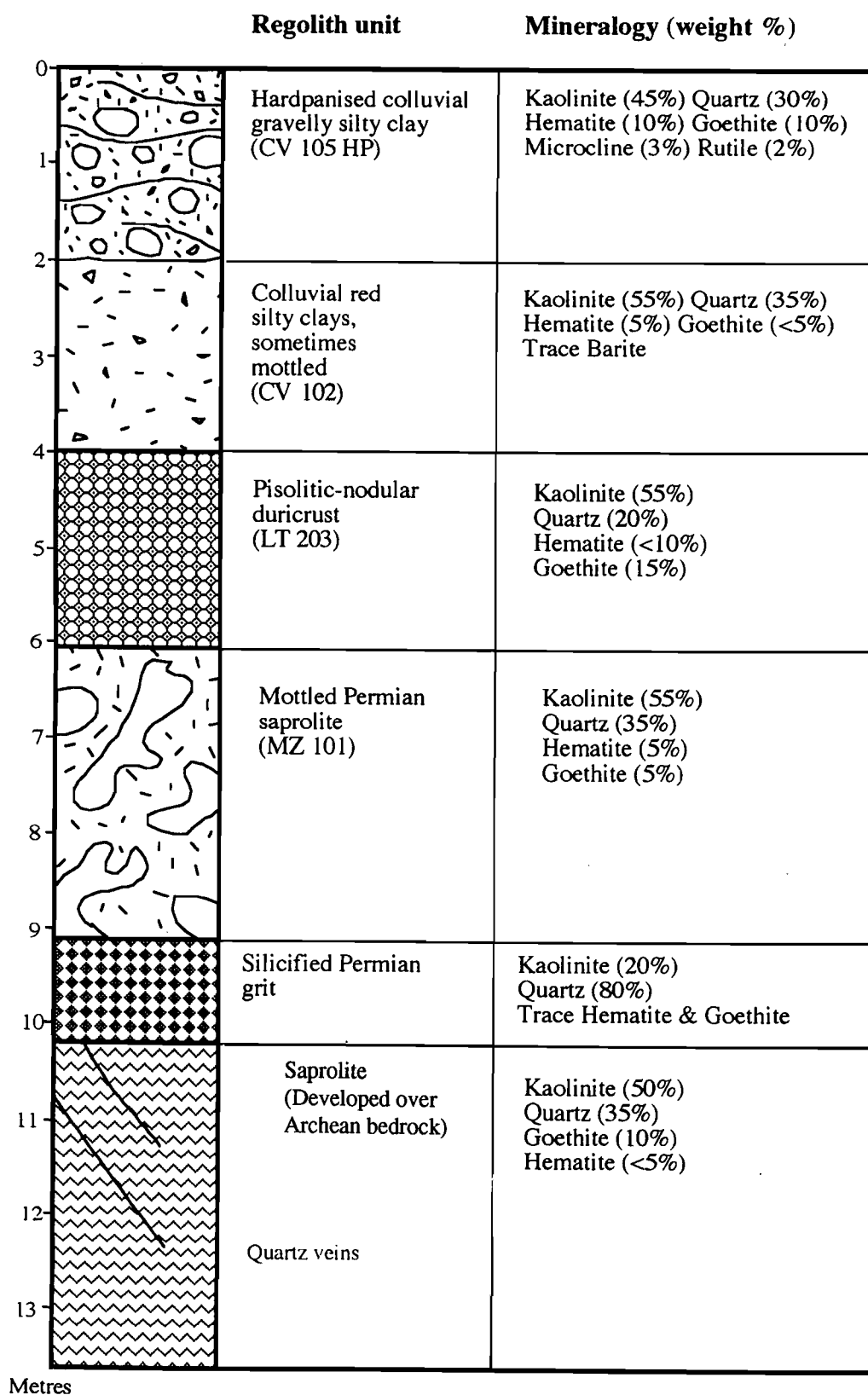


Fig. 5.40 Schematic stratigraphic profile for the Waroonga Pit, Lawlers district. From Twomey (1992).

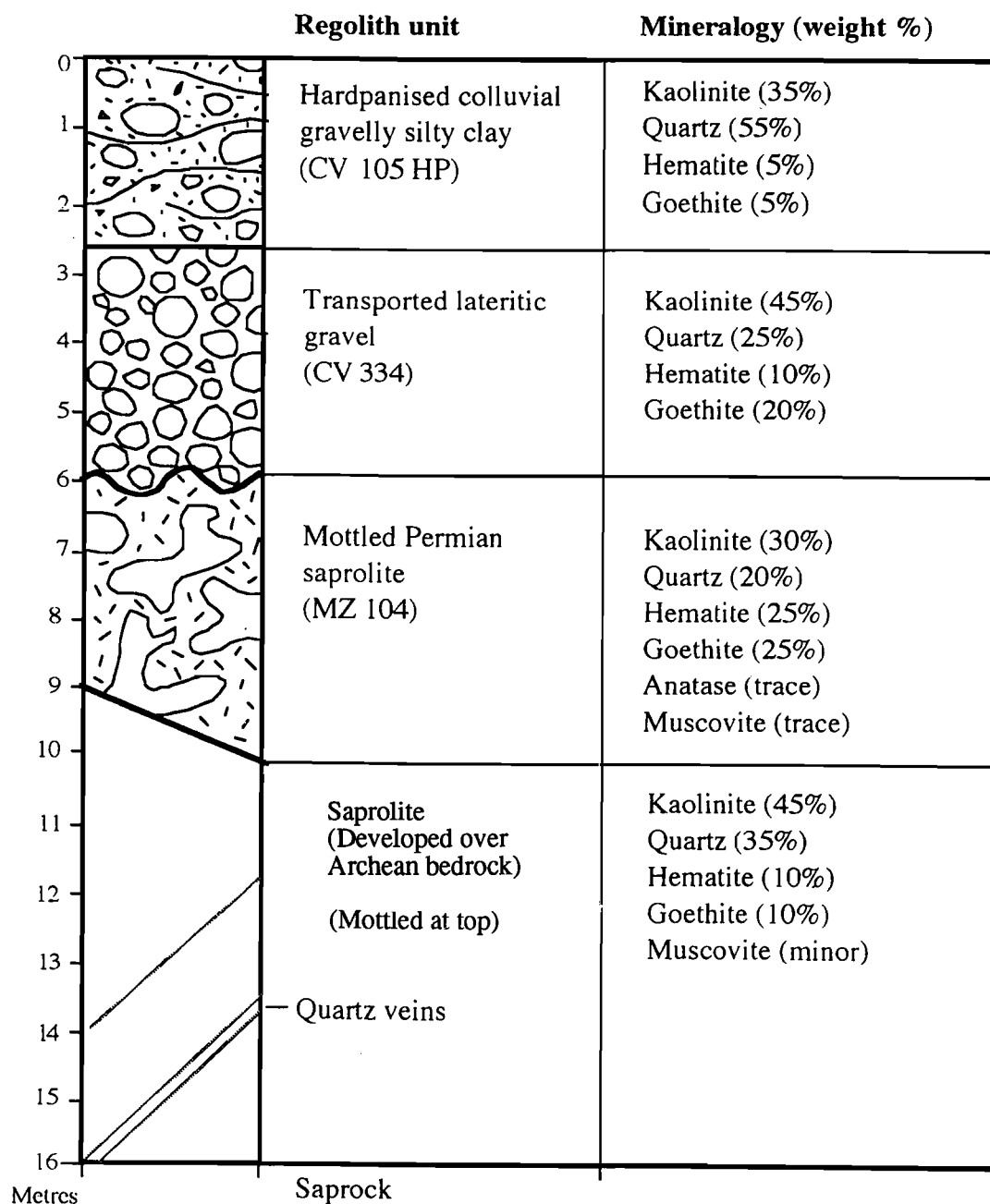


Fig. 5.41 Profile 6, through the regolith stratigraphy from the south end of the Genesis Pit, Lawlers district. From Twomey (1992).

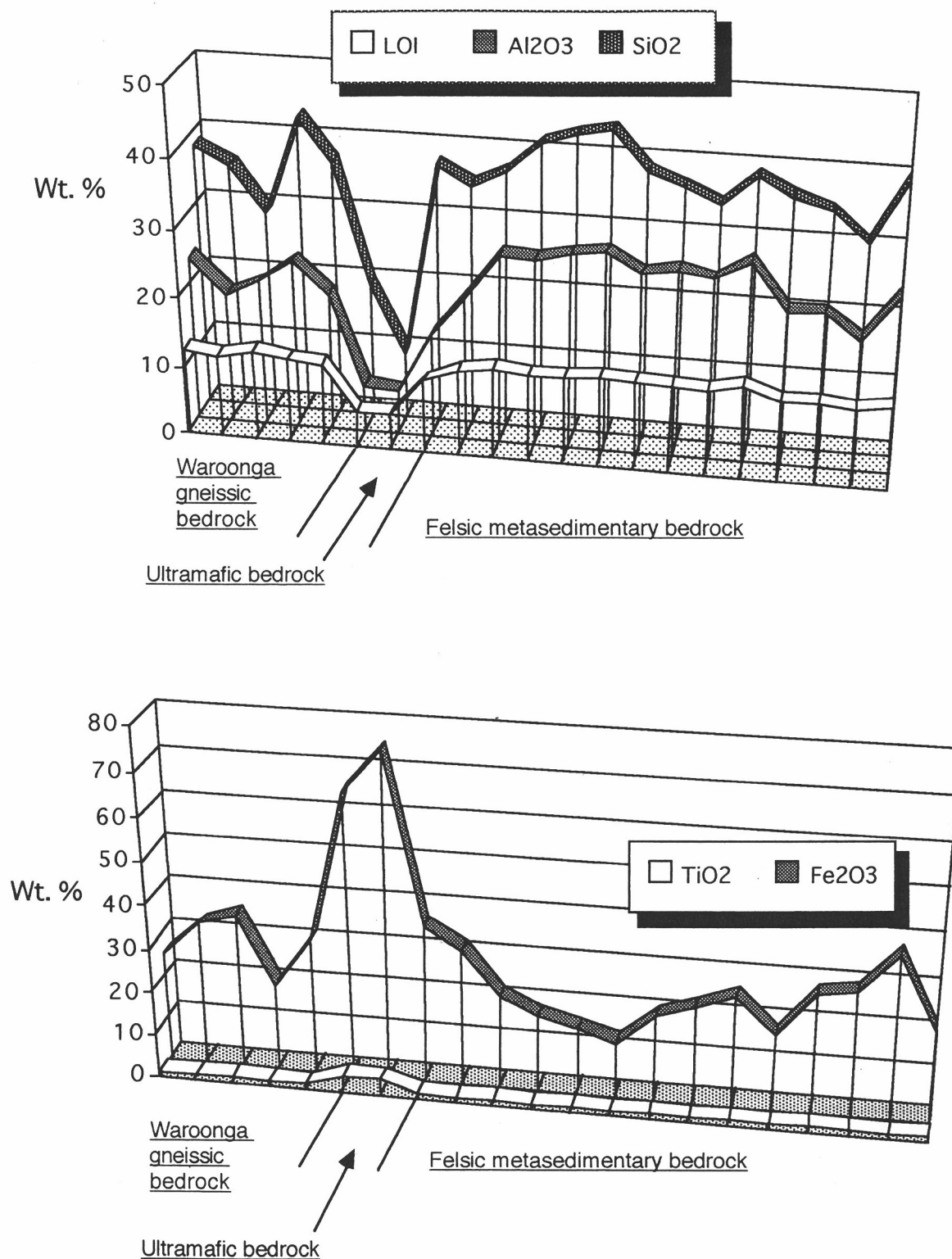


Fig. 5.42 Compiled west to east traverse across the western part of the Agnew area showing the relationship of lateritic duricrust composition to bedrock type. Samples taken at intervals along 6902000 mN between 250500 mE and 254000 mE. From Twomey (1992).

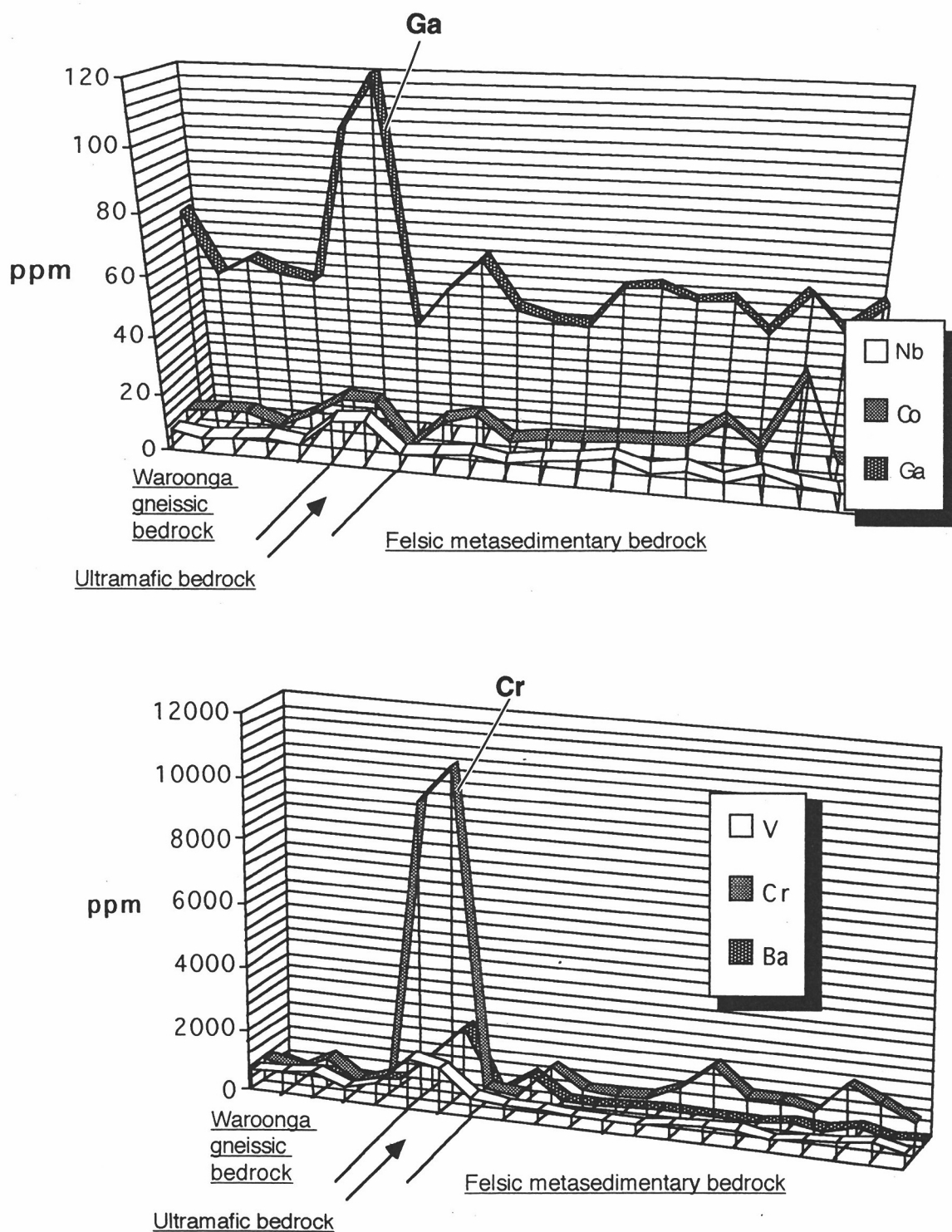


Fig. 5.43 Lithophile trace element variation in lateritic duricrusts related to bedrock type, samples as in Fig. 5.42. From Twomey (1992).

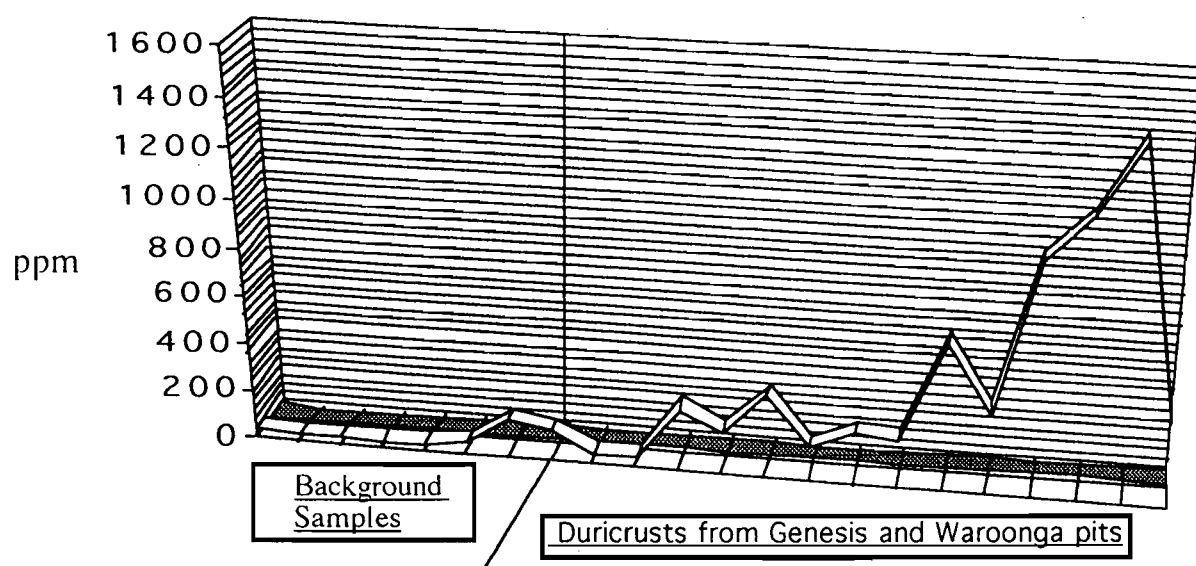


Fig. 5.44 Compilation of As variation in lateritic duricrust samples from regolith profiles at the Genesis and Waroonga deposits, compared with background values 1 to 3 km west of the Genesis Pit. From Twomey (1992).

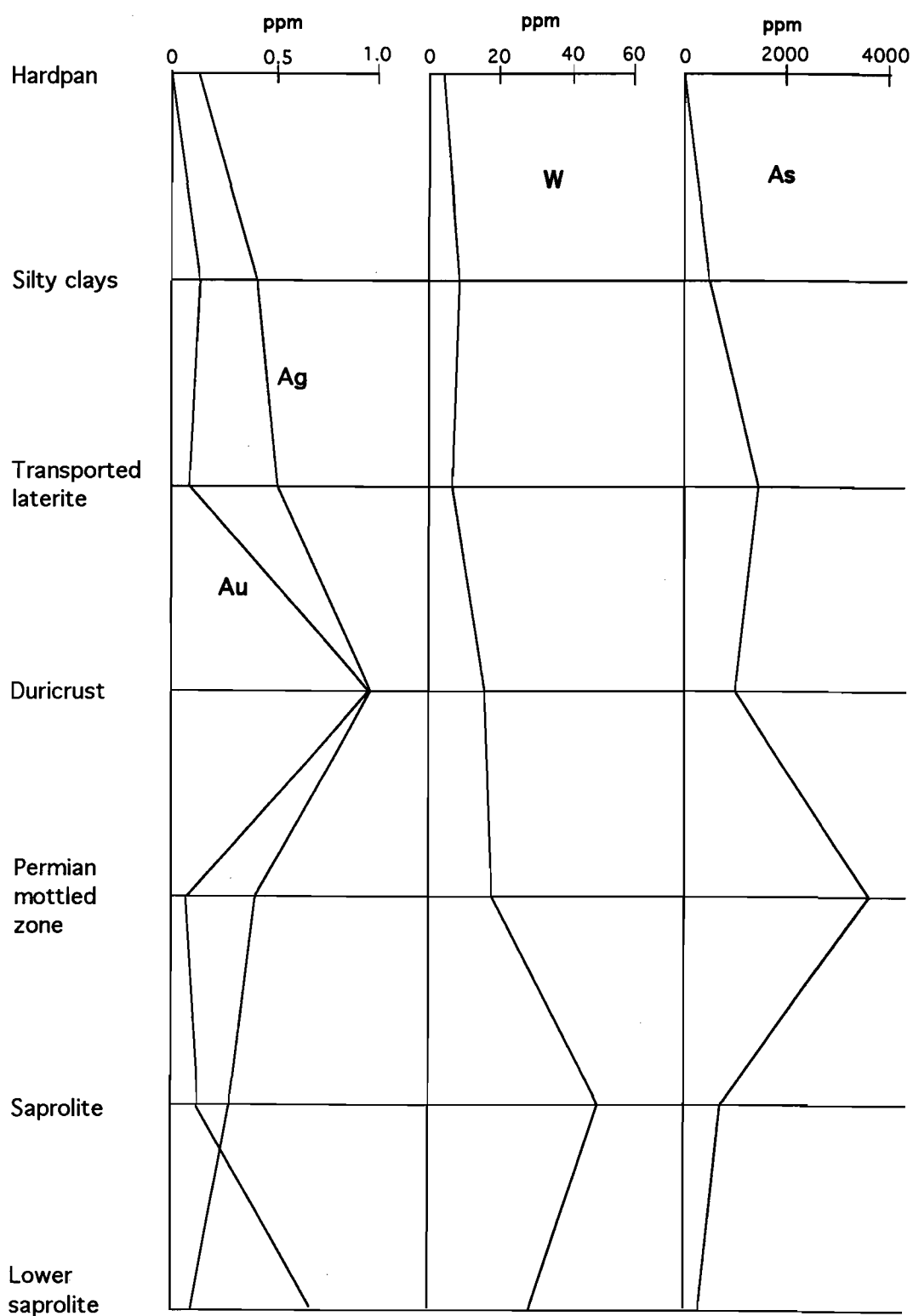


Fig. 5.45 The variation of the ore-associated elements Au, Ag, W and As within units of the regolith stratigraphy from Profile 4, between the Genesis Phase 4 and Waroonga Pits. From Twomey (1992).





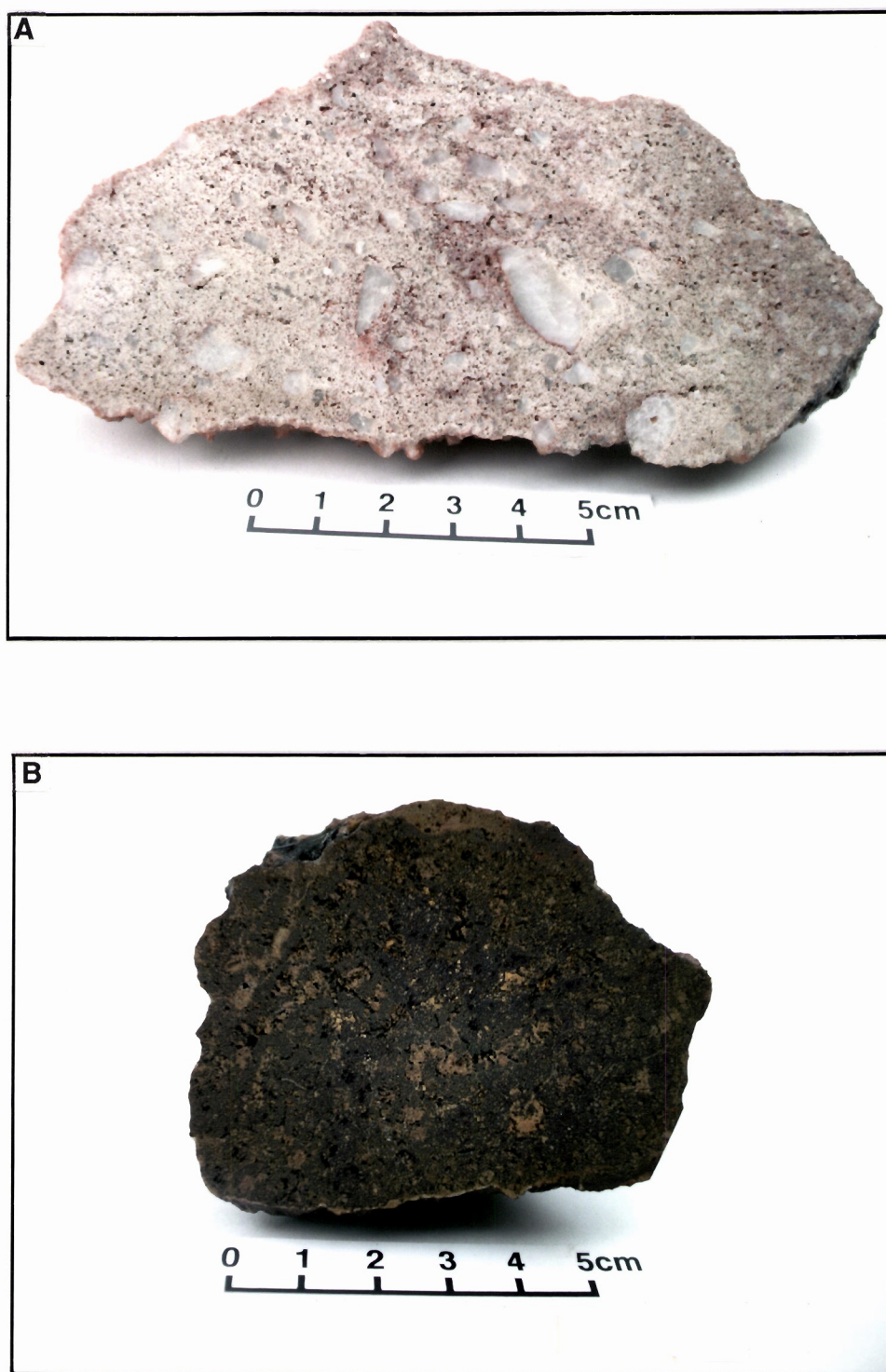


Fig. 5.46 A. Collapse saprolite breccia derived from the Waroonga granitic gneiss, sample location 250200 mE, 6901800 mN, Lawlers district.  
B. Pervasively ferruginised saprolite, sample location 258100 mE, 6904500 mN, Lawlers district.  
A and B both from Twomey (1992).



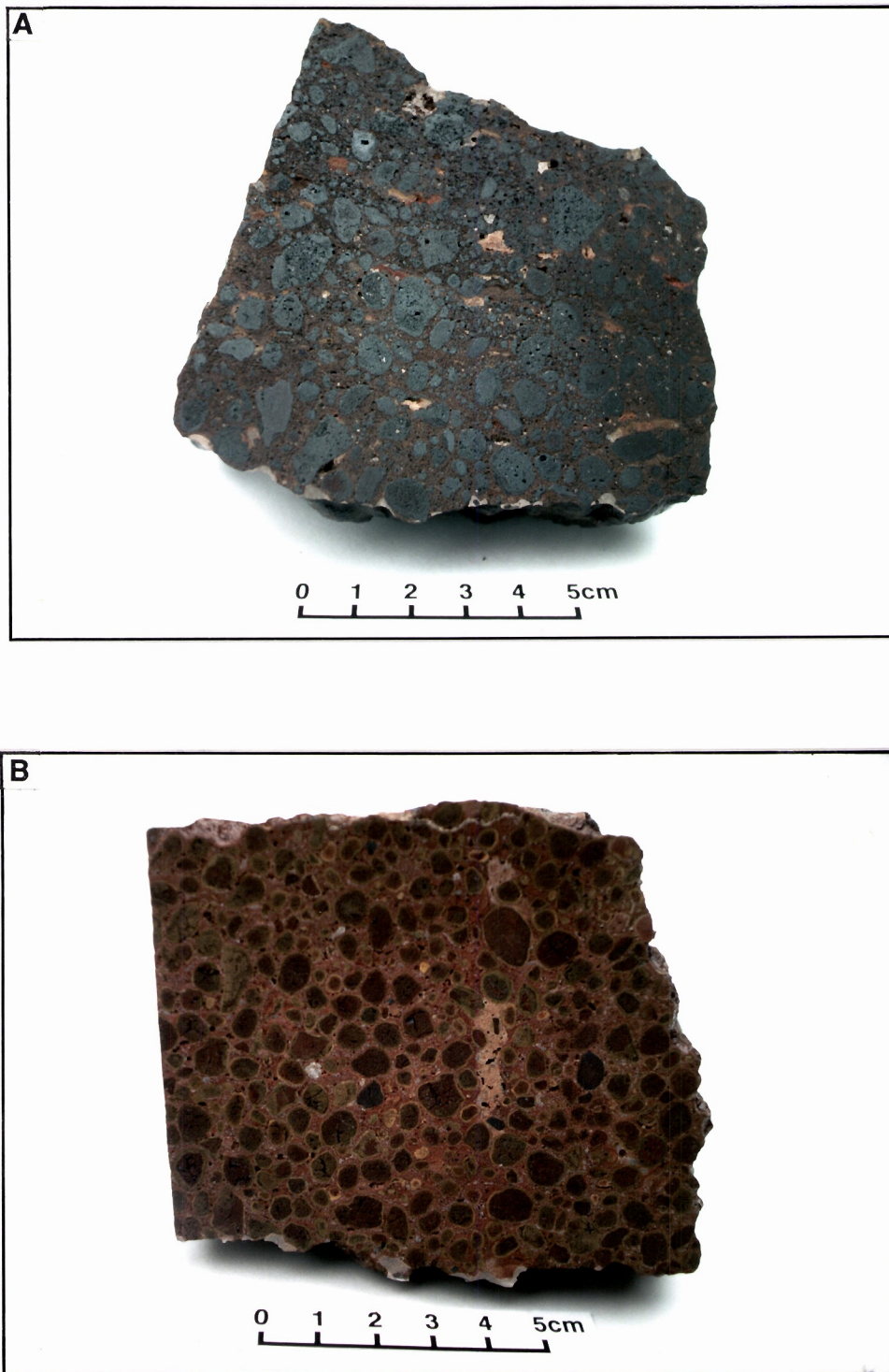


Fig. 5.47 A. Iron-rich lateritic duricrust developed over ultramafic rocks (Pisolitic-nodular duricrust, code LT223). Sample location 258150 mE, 6904800 mN, Lawlers district.  
B. Lateritic duricrust developed over felsic metasedimentary rocks (Pisolitic duricrust, code LT202). Sample location 254000 mE 6902250 mN, Lawlers district.  
A and B both from Twomey (1992).



The distribution of As in lateritic duricrust in a compiled traverse across the Genesis and Waroonga Pits and their environs is shown in Fig. 5.44. Vertical profiles for Au, Ag, W and As, linked to regolith stratigraphy, are shown in Fig. 5.45. Geochemical relationships have been summarised and incorporated into the dispersion models in Section 9.

#### 5.4.8 Implications in exploration

Historically, mineral exploration in deeply weathered terrain, characterised by extensive non-outcropping areas with a variable regolith cover, has been difficult. Consequently, large areas of prospective terrain have not been systematically explored. The approach used in this project, classifying the landsurface into residual, erosional and depositional regimes, each with its characteristic geochemical response, overcomes many of these problems. Regolith-landform control is essential to allow correct decisions on appropriate sampling media, sampling methods and to provide an interpretive framework for the data. In association with current work on imaging the regolith environment by remote means (Landsat TM, Airborne Radiometrics, Airborne EM systems), multi-element regolith geochemistry, properly constrained by landform control, provides an effective and economic exploration tool.

The occurrence of low, but anomalous, concentrations of Au and As in the transported colluvial horizons over the Waroonga and Genesis deposits has considerable exploration significance. Accordingly, it is important to establish a database of the characteristic background geochemical associations in the hardpanised colluvial sediments. Research into the detailed sedimentology of the colluvial sediments, including the type and provenance of the clastic components as well as diagenesis is needed.

The main implications in exploration for the Waroonga-Genesis study at Lawlers are listed in Table 5.13.

Table 5.13 The implications in exploration listed against the research findings, Waroonga and Genesis Au deposits, Lawlers district.

Research Findings	Implications in Exploration
<ul style="list-style-type: none"> <li>Discovery of the Waroonga deposit (Geochemex, Forsayth and CSIRO) was a demonstration of the research concept of drilling for buried geochemical haloes in laterite beneath areas of sedimentary cover.</li> </ul>	<ul style="list-style-type: none"> <li>- Emphasised the importance of recognising regolith stratigraphy.</li> <li>- Shows the importance of As haloes with associated Au in lateritic residuum.</li> </ul>
<ul style="list-style-type: none"> <li>Regolith-landform relationships were mapped over the area, regolith stratigraphy established.</li> </ul>	<ul style="list-style-type: none"> <li>- Provides a well-documented example of areas of transported cover and associated regolith stratigraphy; important for training explorationists.</li> </ul>
<ul style="list-style-type: none"> <li>Low yet anomalous levels of Au and As occur in hardpanised colluvium over the Genesis and Waroonga deposits.</li> </ul>	<ul style="list-style-type: none"> <li>- Suggests that geochemical dispersion has taken place into the hardpanised cover sequence. (More research is required.)</li> </ul>



## 5.5 Bottle Creek deposits

### 5.5.1 Introduction

Research at the Bottle Creek Au deposit, which was discussed, in part, in Report 236R (Smith *et al.*, 1992), has been completed. It was a 'greenfield' discovery (Legge *et al.*, 1990) and was found by open-spaced (1 km triangular grid) magnetic lag geochemistry, which revealed a distinctive multi-element (As, Sb, Au) anomaly at the Emu deposit. The VB and Boags deposits were not detected by this method but were subsequently discovered by drilling along strike. Prior to mining, the areas surrounding the mineralised zones were sampled in detail by CSIRO. Mining has left two large pits, at VB and Boags, and a test pit, at Emu, providing good exposure of the regolith in both depositional and residual regimes.

#### *Location, access, climate and vegetation*

The Bottle Creek Gold deposits, held by Norgold Limited, are located 210 km northwest of Kalgoorlie (Fig. 1.1). The area has an arid climate with an average annual rainfall of 180-190 mm, mainly between January and April. The vegetation is dominated by mulga and by various types of poverty bush and turpentine. On the major depositional surfaces there is *mulga* with tall shrubs on the steeper slopes and breakaways. Thickets of eucalypts grow on erosional tracts. Isolated kurrajong trees occur on a variety of land surfaces (Churchward *et al.*, 1992). The area is located very close to, but just north of, the Menzies Line.

#### *Geology*

The Bottle Creek Au deposits are located at the northwestern tip of the Mt. Ida Greenstone Belt comprising a north-northwest striking, eastward dipping succession, surrounded by variably deformed adamellitic rocks (Kriewaldt, 1970). The western part of the belt is marked by a laterally extensive sequence of banded iron formations, interspersed with coarse-grained mafic rocks. The remainder of the belt is dominated by high-magnesian basalts and intercalated interflow metasediments (black shales and cherts). To the north, a prominent meta-tholeiite unit in the centre of the belt changes along strike to intensely sheared and brecciated black shales and felsic porphyries to the south (Emu Complex) which hosts the mineralisation.

In the immediate environs of the deposit, mafic volcanics, with interflow sediments, are locally intruded by quartz-eye porphyries. The host to the mineralisation is said to be a steeply-dipping, sheared, sulphidic rock. The surrounding rocks show extensive potassic alteration, silicification and carbonation. Weathering penetrates to 100 m. The micro-fine nature of the Au and extensive alluvial cover over the gossans had precluded previous discovery by panning and loaming.

Mining commenced in October 1987 and a total of 908,273 tonnes of ore was mined at VB and Boags to November 1989. Although outlining of the pit at Emu was commenced, operations there were subsequently suspended.

### 5.5.2 CSIRO work program

Research by CSIRO at Bottle Creek comprises studies of the unweathered rocks of the ore environment (Binns, 1988), the mineralogy and geochemistry of gossans (Taylor, 1989), preliminary regolith studies (van der Heyde, 1988), petrography of ferruginous nodules and lags (Davy, unpublished), regolith landform relationships (Churchward *et al.*, 1992) and some ground waters (Gray, 1992). Additional geochemical investigations were by R. Wills in 1992, as part of an Honours project with Curtin University of Technology (Wills, 1992); the surficial geochemical investigation was completed by Robertson and Wills (1993).

Work by Binns (1988) on fresh drill core from the Emu deposit, indicated a complex alteration history about narrow zones of deformation. Alteration of tholeiites has produced a biotite-garnet schist and a banded, mafic rock of hornblende and biotite. These were subsequently pervasively altered (phyllic carbonate) prior to or during ductile deformation, together with sulphide introduction. Argillic and silicic alteration of porphyry was followed by brittle deformation and quartz-pyrite veining, which formed an horizon of massive pyrite. Graphitic horizons here could have been interflow, carbonaceous sediments or a product of this alteration. Static, prograde metamorphism to amphibolite facies was followed by retrograde alteration along fractures and shears.

Investigation of surface and subsurface gossans from Emu, Boags and VB by Taylor (1989) indicated that they are composed largely of quartz, muscovite, kaolinite, goethite and hematite with minor talc, rutile, tourmaline and Mn oxides. Secondary As- and Pb-rich minerals, of the jarosite and alunite groups, are common in gossans and wall rocks respectively. The gossans were derived from a protore of pyrite with minor tetrahedrite, sphalerite, arsenopyrite, marcasite and magnetite in a gangue of kaolinite,



muscovite, quartz, chlorite, siderite, dolomite and calcite. The gossans are anomalous in Ag, As, Au, Cu, Pb, Sb and Zn, although there is a marked depletion at the surface. Gold distribution in the gossan was patchy. The groundwaters at Boags are rich in As, Cd, Sb, I, Au, Ca and  $\text{SO}_4^-$  but not in Pb (Gray, 1992).

#### 5.5.3. Regolith-landforms

A framework of landforms and regolith stratigraphy was established by Churchward *et al.*, (1992). The nature of the regolith stratigraphy is related to landform, so a framework of landform regimes provides a useful guide to the regolith and an essential guide to exploration strategy. Several well-defined regolith units are related to a deeply weathered mantle, progressively modified by landform processes. These regolith units were either horizons of a deep profile, developed by *in situ* weathering of basement rock, or of transported debris, derived from this profile by erosion.

Relatively stable, deeply weathered tracts form relics of a once more extensive land surface that has been fragmented by fluvial action and replaced by erosional and depositional regimes. At Bottle Creek, the ancient, deeply weathered land surfaces are expressed by varieties of the upper, ferruginous horizon of the regolith (the residual regimes), along with the mottled zone, saprolite and saprock, where erosion has been more severe. Several transported regolith types, of colluvial and alluvial origin, occur in both erosional and depositional regimes.

The ferruginous horizon comprises various types of lateritic residuum, the more common being duricrusts with abundant pisoliths. At depth, this material merges with mottled clays. Large, irregular to lenticular, Fe-rich duricrust bodies occur in the upper part of the regolith, which contrast with the surrounding lateritic residuum. There is also ferruginous saprolite, vermiform duricrust and fragmentary duricrust. Goethite-rich pods occur in the upper regolith. These gossan-like bodies occur close to a carbonaceous, previously pyritic zone in the underlying greenstones.

#### Residual regimes

The residual regimes form extensive, gently undulating tracts. Most crests are slightly stripped, exposing an array of ferruginous materials. These contribute to the colluvial mantle that extends down slope from the crest, covering the lateritic residuum; the latter forms the most extensive substratum of the residual regimes. The lag varies with position in the landscape. Fragments of ferruginous saprolite dominate the crests; pisoliths occur over subcropping lateritic residuum. Down slope, the dominant lag is dark granules, with little quartz or lithic material. Hardpans are common at depths below 1 m.

#### Erosional regimes

These landforms, and their regoliths reflect previous and active geomorphic processes. Deeper units of the weathered mantle and country rock are exposed. The regolith is covered by a lag of lithic fragments; there are outcrops of vein quartz and goethitic segregations. Pediments below low breakaways are blanketed by a coarse lag of ferruginous saprolite, lithic fragments and quartz.

#### Depositional regimes

Extensive depositional tracts are covered with acidic red earths on alluvial clay. The lag is of dark granules of mixed origin; lithic, ferruginous saprolite fragments and minor quartz. The alluvium overlies saprolite and saprock at 1.0-1.5 m but, in places, it mantles pockets of lateritic residuum and fluvial palaeochannel deposits. Such a palaeochannel runs between VB and Boags.

#### Regolith evolution and a framework for geochemical dispersion

The topographic relationships and regolith stratigraphies reveal a complex history (Churchward *et al.*, 1992). The relatively stable residual regimes are dominated by intense, *in situ* weathering although some of this regolith has been transported and deposited by local colluviation. The depositional regimes contain diverse, fluvial detritus of distant origin, in places mixed with material of local origin. Prior to deposition, some areas have been subjected to widespread, though incomplete, regolith stripping. The regolith in erosional regimes is, in detail, complex, with exposure of a variety of variably weathered lithologies.

VB-Boags and Emu lie in depositional and residual-erosional regimes respectively (Figs 5.48 and 5.50). However, VB-Boags was formerly in an erosional regime and, later, in a depositional regime. It lies on the edge of an alluvial plain, where the cover is largely thin. Unlike elsewhere, erosion at VB-Boags was less severe, so that remnants of the ferruginous saprolite, mottled zone and basal laterite are preserved. These have been subsequently buried by alluvium. At Emu, the regolith is thick and well-

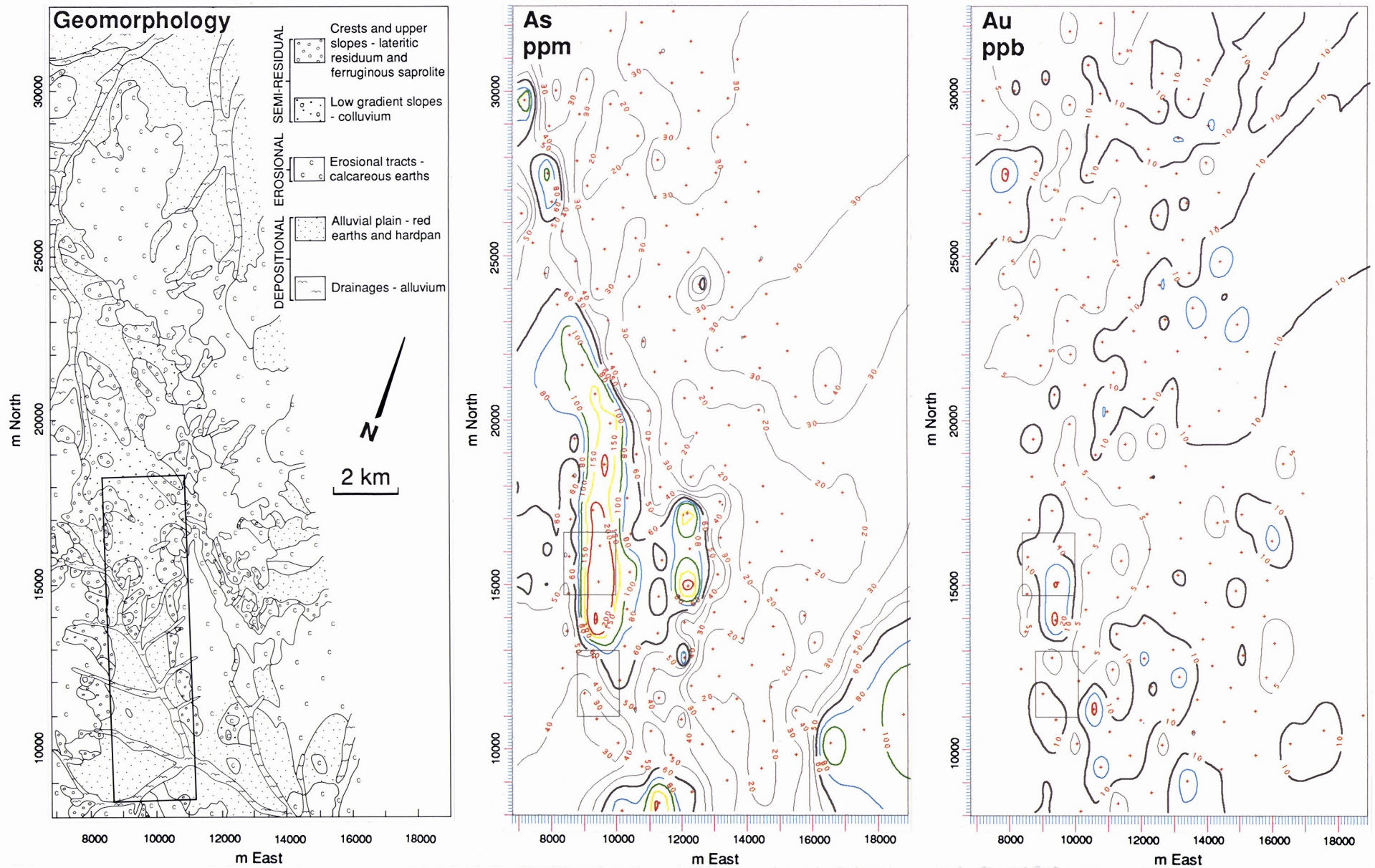


Fig. 5.48 Regional geomorphology (from Report 247R) and initial As and Au geochemistry for magnetic lag (Electrolytic Zinc Co.) for the Bottle Creek district. Emu and VB-Boags locations are shown by the two rectangles on the geochemical map.



developed to the south but, to the north, it thins, where the relief is greater, and the profile has been stripped to expose porphyry saprock and gossan. Understanding this geomorphic framework is essential to appreciate geochemical dispersion and it provides a basis for sampling strategies in this complex terrain of weathered residual and transported materials.

#### *Thickness of overburden*

The veneer of hardpanned alluvium and soil in the depositional regime around VB-Boags is quite thin, in places (at Boags 0.1-0.5 m). Photo-interpretation revealed a low rise of greenstone saprock or saprolite in what is now the centre of the Boags pit. Colluvial-alluvial cover was thicker in the area now occupied by the VB pit. It seems that sporadic silicification, associated with mineralisation, has indurated the ore horizon and nearby rocks in places, making them more resistant to weathering and erosion. They seem to have formed a positive palaeotopography during the erosive phase and were blanketed by a very thin cover of unconsolidated soil during subsequent sheet alluvial deposition. The thickness of cover in the depositional areas is very variable, ranging from a few metres to nil. A surface geochemical response to underlying mineralisation in covered areas is very dependant on the existence of places where the cover is locally very thin.

#### 5.5.4 Gossan

Gossan sampling (see also Taylor, 1989) showed anomalous  $Au > As > Pb, K, Na > Sb, Ba > Bi, Cu, Se, W > Mo$  with much inhomogeneity. There was a range of anomaly strengths in relation to background;  $Au$  (x 3000),  $As$  (x 700),  $Pb, K, Na$  (x 300),  $Sb, Ba$  (x 100),  $Bi$  (x 20),  $Cu, Se, W$  (x 10) and  $Mo$  (x 4). Gossans provide a source of enriched material that becomes incorporated and dispersed in the soil and lag. The process of dispersion improves the anomaly homogeneity but reduces its contrast. On passing from gossan to lag, most elements showed a decrease in geochemical abundance (x 0.5-0.3), although  $As$  was significantly depleted (x 0.1) suggesting some hydromorphic dispersion of  $As$  (Fig. 5.49).

None of the gossans examined had a detectable magnetic (maghemite) component, so use of magnetic soil and lag fractions might discard the small, though important, gossanous component and would rely on secondary hydromorphic dispersion of target and pathfinder elements within the laterite. Analysis of all the material (magnetic and non-magnetic) is advisable.

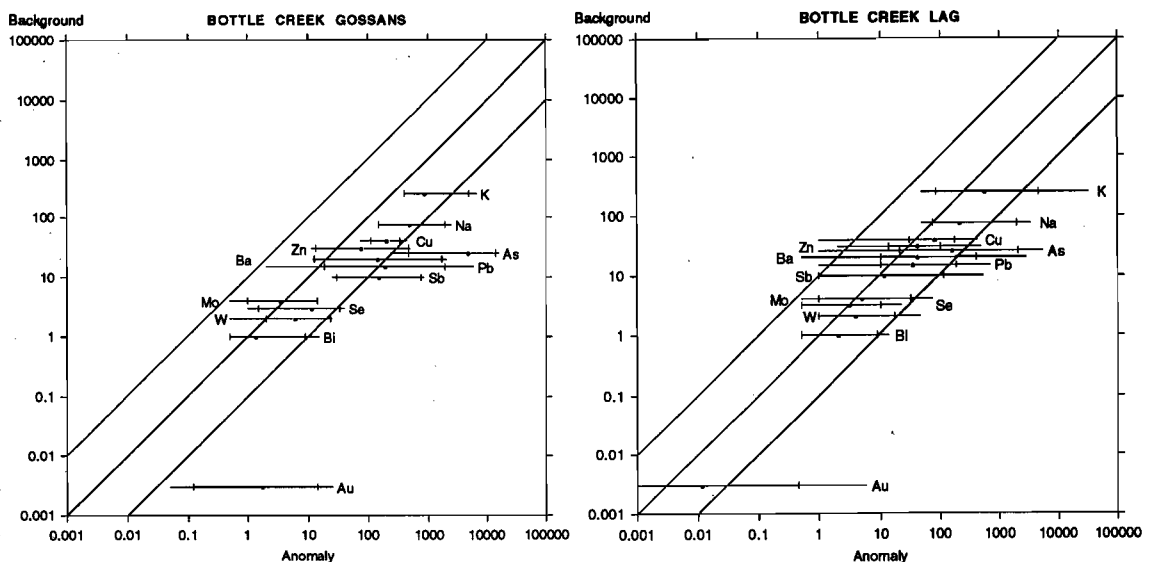


Fig. 5.49 Log-log anomaly characterisation diagram for gossans and lag from the Bottle Creek orientation study.

#### 5.5.5 Lag Sampling (Electrolytic Zinc Co.)

After initial stream sediment sampling, 172 magnetic lag samples were collected over about 190 km<sup>2</sup>, on a 1 km triangular grid. Only about 10% of the ferruginous lag is magnetic. The samples were analysed for Au, As, Pt, Cr, Fe and W.

A later, more detailed sampling of 134 magnetic lag samples, also on a triangular grid (0.5 km) was completed covering the smaller but highly anomalous south-east part of the first exploration area. A fairly full chalcophile and lithophile multi-element suite (Au, As, Sb, Zn, Pb, Cu, W, Ni, Mo, Cr, V, Fe) was determined. These data have been assessed.

#### Initial geochemistry

Backgrounds and thresholds for As (25, 60 ppm) and Au (5, 20 ppb) respectively were established. A 17 km long, slightly curved zone of anomalous As is apparent in the eastern part of the area. The As anomaly (Fig. 5.48) is restricted to areas covered by lateritic residuum and low gradient colluvial slopes and is truncated by the hardpan-underlain alluvial plains and alluvium-filled drainages. There is a small, parallel anomaly to the east, largely in an erosional area. Gold anomalies (Fig. 5.48) are patchy and are only coincident with As at Emu, where the regolith is residual. Arsenic is a better indicator element in this environment. Neither Au nor As anomalies project into the depositional area occupied by VB-Boags.

#### Follow-up geochemistry

Backgrounds and thresholds were established for Au (2, 10 ppb), As (60, 150 ppm), Sb (8, 15 ppm), Pb (35, 50 ppm), Zn (55, 100 ppm), Cu (35, 45 ppm), Mo (4, 6 ppm) and W (1, 3 ppm) respectively. The known strong As anomaly was confirmed by the follow-up geochemistry, with additional anomalies in Sb and, to a limited extent, in Pb and Au. The first three elements accurately locate the mineralised horizon at Emu but not at VB-Boags. Distributions in Cu, Mo and W were unhelpful. There was only a marginal improvement in resolution and similar results were produced, although the additional pathfinders (Sb and Pb) serve to confirm the anomalies. Follow-up work of this kind requires a change in resolution of an order of magnitude (to 0.1 km) to successfully define drill targets and to take advantage of locally thin alluvial/colluvial cover in the depositional areas (see below).

#### 5.5.6 Lag sampling by CSIRO

##### Mineralogy and petrography

The mineralogy of the lag, from a traverse each across Boags and Emu, was investigated by X-ray diffraction. The lag of depositional tracts (VB-Boags) contains more quartz and less kaolinite than that of residual or erosional areas (Emu). Although hematite dominates the Fe oxide mineralogy at Emu, goethite is slightly more abundant over mineralisation, displacing some kaolinite. The increased Fe oxide content probably reflects the Fe-rich (sulphidic) nature of the mineralised zone. Although there is a muscovite anomaly in the lag of both areas, the anomaly at Emu is greater by an order of magnitude. Binns (1988) reported 4-15% K<sub>2</sub>O in the porphyry from Emu and suggested that major alteration had occurred after porphyry intrusion. This included the introduction of potassium, possibly as muscovite (phyllic alteration). Muscovite was not sufficiently abundant to be detected in the lag by infra-red spectroradiometry carried out in the laboratory (Wills, 1992).

The ferruginous lag preserves fabrics not readily visible in other near-surface materials. Samples, from close to the Emu pit, contained particularly well-formed K mica (which is visible by hand-lens examination). Linear mica flakes and equant, subhedral hematite pseudomorphs after magnetite and/or sulphide are set in massive to spongy goethite. Traces of As were found in the hematite pseudomorphs and in the surrounding goethite. Lag samples collected more distant from the pit show pseudomorphic fingerprint fabrics, typical of saprolitic clays derived from mafic rocks. In places, these clays (largely kaolinite) have been recrystallised into accordion structures prior to pseudomorphic replacement and encasement in goethite. Later recrystallisation of goethite to hematite has left dehydration cracks and 'cauliflower' structures. Dissolution of goethite has left numerous channelways and irregular voids, some of which have been infilled or lined by later goethite, some with a cusped form.

##### Geochemistry

The outcropping gossans are anomalous in Au, As, Ba, Bi, Cu, Pb, Sb and Zn; Ag is also anomalous in subsurface gossans (Taylor, 1992). The geochemistry of the lag from lateritic and colluvial material has been investigated to determine if these pathfinder elements persist in more widespread media. Geochemical backgrounds and thresholds were determined empirically.

Most of the residual regime and some of the colluvium at Emu is occupied by a broad As anomaly, with peaks exceeding 2000 ppm, centred over the pit (Fig. 5.50). The As anomaly is more restricted at VB-Boags for reasons given above. The As anomaly clearly marks the locations of the Boags Pit, where the cover is known to be thin, and the southern end of the VB Pit. The As anomaly, between the VB and Boags pits, is completely obscured by the palaeochannel. Lead and Sb anomalies have similar characteristics to As. Although Pb and Sb maxima at both sites are similar (300-500 ppm), the anomaly is more restricted at Emu. The Zn peaks are not quite co-incident with As, Pb and Sb but similarly mark the targets. Boags is not depicted by Zn but there is a distinct Zn anomaly at VB. The Cu anomaly is weak, in few places exceeding threshold, although slightly elevated Cu abundances appear to mark the general strike of the mineralised zone. The Se anomaly is indistinct and weak.

Gold anomalies of 300-400 ppb in a background of <10 ppb, about 300-400 m across, clearly indicate the mineralisation at both sites (Fig. 5.51); the anomalies are broader at Emu, due to greater dispersion in the lateritic duricrust. The smaller and more patchy nature of the Au anomalies at VB-Boags is probably due to paucity of lateritic duricrust and variations in thickness of the colluvium-alluvium, which was probably most thin over the centre of the Boags Pit.

The phyllic halo is shown clearly by lag geochemistry at Emu, where a wide, bull's-eye K anomaly marks the north end of the pit. At VB-Boags, both pits are similarly indicated but the anomaly is more restricted and of lesser magnitude (Fig. 5.52). Similar anomalies result from Na but the peaks are only in part co-located with K. Although Rb was determined only in a small number of the samples, its high correlation with K suggests that it would similarly indicate phyllic alteration. The distribution of Ba may be related to the phyllic alteration halo although Ba may also reflect weathered feldspars of the porphyries.

#### Comparisons

**Emu:** The best pathfinder elements at Emu are  $As > Sb > Au > Pb$ . The width of the As anomaly is 1200 m, that of Sb approximately 1000 m, Au 500 m and Pb 400 m. All these anomalies overlie the mineralised horizon and are relatively regular and linear. However, As, Pb and Sb only approximately locate the best Au mineralisation. These four elements could be used effectively in a regional lag exploration program with a sample spacing of 1000 m on a triangular grid, to identify targets for follow up exploration because they directly reflect the mineralisation. The phyllic halo around the mineralisation is shown by anomalies in  $K > Na > Ba$ . The K (and Rb) anomaly accurately locates the mineralisation; those of Na and Ba locate only parts. Although porphyries are associated with the mineralisation, intense weathering would destroy the K-feldspar and remove the K as K-micas are rare. Generally, K survives only in K-micas in the upper saprolite, mottled zone and duricrust. Thus, medium to high resolution, possibly airborne, radiometric surveys may have some potential for locating an exposed phyllic halo. The K abundance in the regolith is not very great so, where it is diluted by other regolith materials, its use may be significantly reduced; where it is concealed by overburden, it would be ineffective.

**VB-Boags:** Arsenic, Au, Pb and Sb are less effective at VB-Boags. Only one sample is consistently anomalous at VB and only samples from the central-east portion of Boags are anomalous. These anomalous samples occur where very thin, loose, sheet flood detritus directly overlies the mottled zone, with no intervening hardpanised alluvium. Anomalous clasts were probably dispersed mechanically into the largely exogenous surficial layers by bioturbation (root plucking, insect activity) and illuviation. All remaining laterite is covered by hardpanised alluvium, restricting the anomaly, despite abundant, underlying, ferruginous material. At the northern end of Boags, the anomaly has been truncated by a drainage channel, filled with fluvial sediments derived from the west.

The contrasting nature of the geochemical anomalies and the regolith-landforms over Emu and VB-Boags highlight the importance of regolith-landform mapping in planning a geochemical program and in subsequent interpretation. Stable, exposed, lateritic regions must be differentiated from depositional regimes such as alluvial plains for cost effective sampling. In the former (e.g., Emu), wide spaced lag sampling (up to 1 km) on a triangular grid, using As, Au, Ba, Pb, Rb and Sb as indicator elements, will delineate mineralisation and its phyllic halo. In depositional regimes, where the hardpanised colluvial substrate is known to be thin, lag can also be used but sample spacing should be reduced to 400 m, or much less, to detect zones of thin cover. Such a strategy would include an appreciable risk of non-detection. It is suspected that success is very dependant on induration of the mineralised zones, their greater resistance to erosion and consequent thin cover. However, deepening of the cover and its hardpanised substrate may well frustrate surface geochemical prospecting. Drilling through this substrate,



into the lateritic residuum or ferruginised saprolite with fairly open spacing (e.g. 400 m) would then be necessary. Alternatively, systematic drilling into saprolite with closer spacings may be required.

#### *Soil and soil geochemistry*

A small suite of samples of the carbonate-free, red, stony soil were collected immediately south of the Boags pit. They consist of a major proportion (>80%) of ferruginous nodules and lithorelics, typical of soils over mafic rocks, north of the Menzies Line. The ferruginous clasts consist of black, glossy, goethite nodules, dark brown goethite nodules and angular fragments, some of which are magnetic, and brown to yellow-brown, non-magnetic, ferruginous, clay nodules and fragments. Included with these are very minor *non-magnetic*, cellular, gossan fragments. The fine, sandy fraction consists of hematite-coated, angular, quartz grains with about 5% aeolian grains. This soil is very similar to that of Beasley Creek (Robertson, 1990). The distribution of samples did not extend into background. The abundance and distribution of Ba, Au, Sb, Bi, Mo and W reflect those shown by the lag survey.

There are insufficient data to determine the relative efficacy of soil sampling and lag sampling at Bottle Creek. However, since the soil consists largely of ferruginous nodules and lithorelics, which are the source of the lag, analysis of the coarse soil fraction would be as effective as lag, the choice being more of cost and convenience. The soil may show slightly less dispersion and so may require a slightly closer sampling grid. Use of a magnetic coarse soil fraction is not recommended as it would probably exclude gossanous material.

#### *5.5.7 Implications in exploration*

Lag geochemistry is effective in erosional-residual areas, particularly where the lateritic duricrust subcrops beneath a thin soil. In contrast, the effectiveness of lag geochemistry is severely limited, in depositional areas, by the thickness of the transported cover and the ability of bioturbation to bring material from the residual substrate to the surface. This is made more difficult where the layer of colluvial-alluvial sheet-flood debris has been hardpanised. Sporadically, where this layer is thin, the lag shows a few indications. Where saprolite is overlain by narrow, gravel-filled channels, geochemical signals are prevented from becoming incorporated in the lag.

The best elements, as shown by the orientation study at Bottle Creek, are  $As > Sb > Au > Pb$  and show anomaly widths at Emu of 1200, 1000, 500 and 400 m respectively. The phyllic alteration is reflected by  $K > Na > Ba$ . As for Au, these anomalies are small and patchy at VB-Boags.

Almost 60% of the study area lies in residual-erosional regimes, in which surficial geochemistry is likely to be successful (Fig. 5.48). Only 10% of this is covered by exposed lateritic residuum, in which anomaly sizes would be enhanced by lateritic dispersion, allowing wide-spaced sampling. The remaining 50% lies in erosional regimes, in which the laterite has been partly or largely stripped and anomaly sizes are likely to be smaller, requiring a closer-spaced sampling.

Over 40% of the area is underlain by depositional regimes, in which surficial geochemistry is unlikely to be reliable and drilling through the cover would be necessary. Although surficial geochemistry could be used along the margins of these areas, relying on bioturbation of thin cover to carry anomalous material to the surface, this would be risky. Discovery of mineralisation in thinly covered depositional areas, such as at VB-Boags, is very dependant on chance thinning of the cover and/or on discovery of geochemical anomalies in adjacent residual-erosional areas, with subsequent follow-up by drilling. North of the Menzies Line, a consistent strategy of restricting surficial geochemistry to residual-erosional areas and drilling the covered areas is regarded as highly advisable; south of the Menzies Line, sampling of soil carbonates in covered areas may be used for auriferous deposits but not for non-auriferous polymetallic mineralisation.



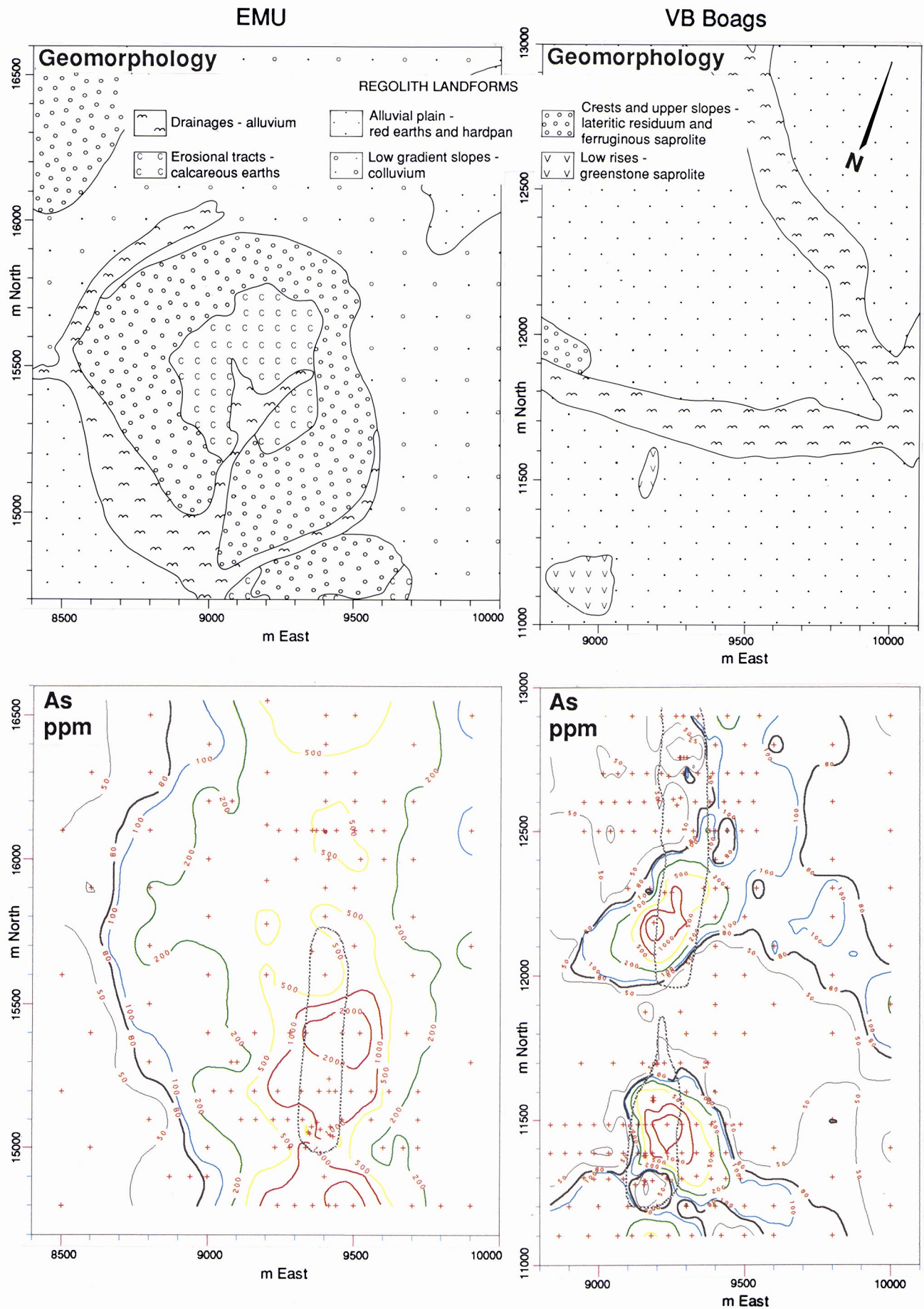


Fig. 5.50 Geomorphology and detailed surficial As geochemistry of the Emu and VB-Boags areas at Bottle Creek.



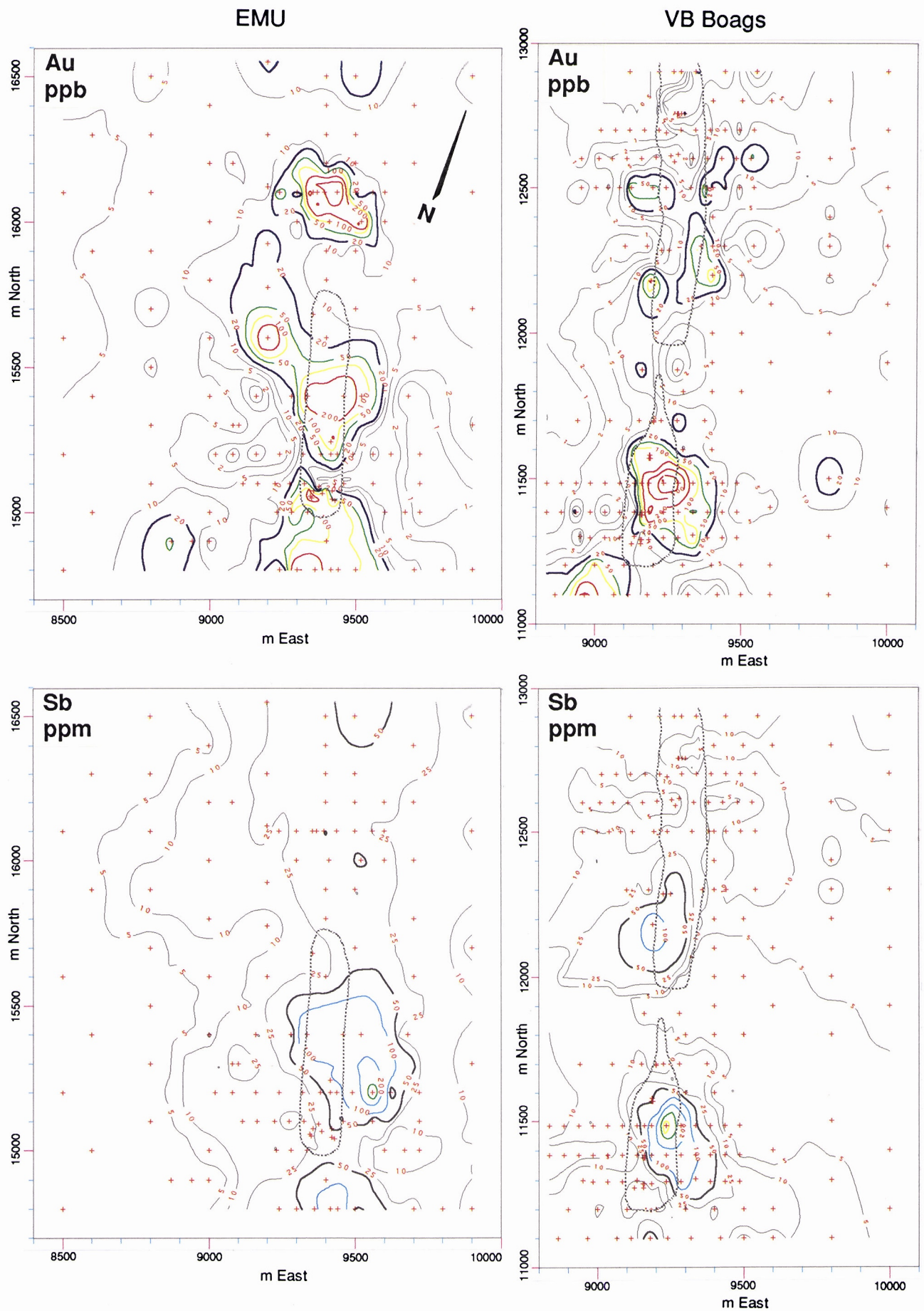


Fig. 5.51 Detailed surficial Au and Sb geochemistry of the Emu and VB-Boags areas of Bottle Creek.





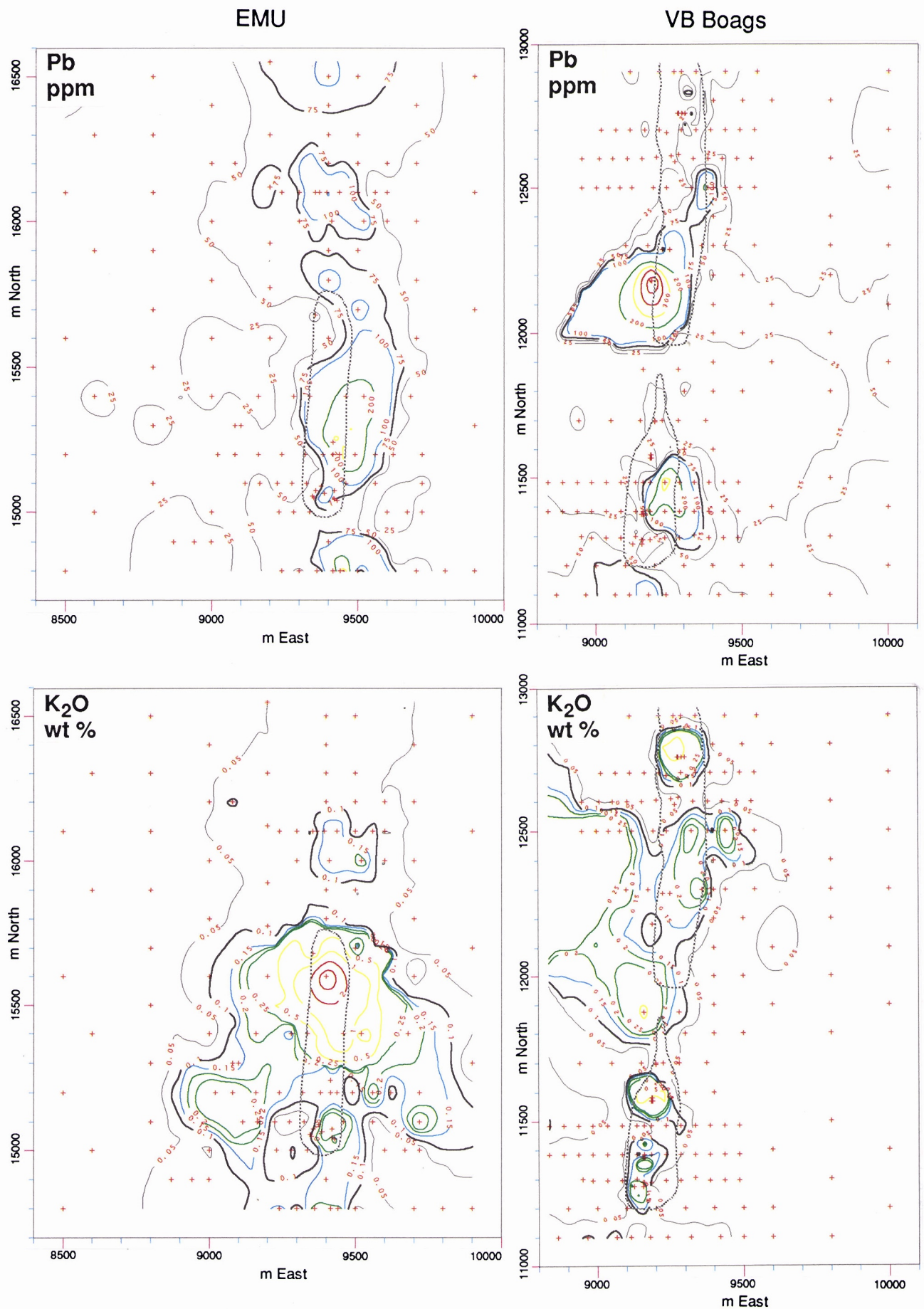


Fig. 5.52 Detailed surficial Pb and K geochemistry of the Emu and VB-Boags areas at Bottle Creek.



Table 5.14. The implications in exploration listed against the research findings, Bottle Creek Au deposits.

Research Findings	Implications in Exploration
<ul style="list-style-type: none"> <li>• The Emu Deposit lies in a residual-erosional regime; the VB-Boags deposits are in a depositional regime. Initial exploration magnetic lag geochemistry outlined the Emu Deposit but not VB-Boags.</li> </ul>	<ul style="list-style-type: none"> <li>- Careful regolith-landform mapping is essential for proper planning of geochemical surveys.</li> </ul>
<ul style="list-style-type: none"> <li>• Substantial lag anomalies in As &gt; Sb &gt; Au &gt; Pb reveal the Emu deposit.</li> </ul>	<ul style="list-style-type: none"> <li>- This is a particularly pathfinder-element rich Au deposit.</li> </ul>
<ul style="list-style-type: none"> <li>• Close-spaced lag sampling showed restricted anomalies in Au and chalcophile elements at VB-Boags.</li> </ul>	<ul style="list-style-type: none"> <li>- Lag sampling of the margins of depositional regimes may give indications but this is very dependent on thin cover and adequate bioturbation. Drilling below the cover is advisable.</li> </ul>
<ul style="list-style-type: none"> <li>• Lag petrography reveals relics of micas, magnetite and sulphide pseudomorphs.</li> </ul>	<ul style="list-style-type: none"> <li>- Some potential for petrography of coarse lag to assist in rock type identification.</li> </ul>
<ul style="list-style-type: none"> <li>• Soil composed of ferruginous granules, quartz-rich sand-silt and clay, with some minor, non-magnetic gossan fragments.</li> </ul>	<ul style="list-style-type: none"> <li>- Coarse soil fraction probably as good a geochemical medium as lag. Selective analysis of magnetic soil and lag fractions not recommended.</li> </ul>
<ul style="list-style-type: none"> <li>• Anomalies in K, Rb and in muscovite depict the Emu deposit and, to a much lesser extent, VB-Boags.</li> </ul>	<ul style="list-style-type: none"> <li>- A phyllic halo about the mineralisation may be detectable by high-resolution gamma-spectrometry.</li> </ul>
<ul style="list-style-type: none"> <li>• Geochemical lag data sets established over contrasting regolith regimes.</li> </ul>	<ul style="list-style-type: none"> <li>- Provides well controlled reference data for use in multivariate interpretation.</li> </ul>



## 5.6 Golden Grove Cu-Zn-Au VHMS Deposits

### 5.6.1 Introduction

The Golden Grove volcanic-hosted massive sulphide deposits, Scuddles and Gossan Hill, lie approximately 380 km north-northeast of Perth on the Yalgoo (SH50-2) 1:250,000 scale map.

The climate is semi-arid, with an erratic rainfall averaging 260 mm per annum. Vegetation consists of a thick low scrub cover of drought-resistant mulga (*Acacia* spp.) with an incomplete ground cover of shrubs and grasses. The regolith setting has been described by Smith and Perdrix (1983). The relief is generally low to gently undulating with preservation of a full laterite profile characterising much of the plains except where active erosion has cut into upper saprolite. The area lies north of, but close to, the interpreted position of the Menzies line (Butt *et al.*, 1977).

The geology of the Scuddles deposit and the Golden Grove general setting has been described by Mill *et al.* (1990) from which the following is summarised: The Golden Grove deposits are located in the Warriedar Fold Belt (Baxter and Lipple, 1979) which is bounded largely by intrusive granitoids (Myer and Watkins, 1985). The two known massive sulphide deposits occur in the Gossan Hill Group at the base of the fold belt (Baxter, 1982) in a sequence dominated by felsic and intermediate volcanoclastic sediments, lavas and associated autoclastic breccias, on the east limit of a regional syncline. Many gabbro and dolerite dykes have infilled fractures during a later extensional tectonic event. The sequences show greenschist facies metamorphism.

The area has been subjected to lateritic weathering, with lateritic residuum forming an undulating blanket over much of the landscape. Typically the plains and broad valleys are characterised by loamy soil overlying pisolitic and nodular laterite, lateritic duricrust and, in turn, some 50 m of a deeply weathered, pale, saprolite or clay zone. Lateritic residuum, typically 1-3 m thick, blankets about 75% of the landscape in the 25 km of strike length in the Golden Grove valley. Lateritic residuum also occurs on the flanks of some of the ridges, in places covered by colluvium. At Gossan Hill, lateritic residuum occurs on the shoulders of the hill, and in saddle areas. However, erosional windows have exposed bedrock, gossans and ironstones by removal of lateritic residuum at the top of the hill, the original discovery area. Sulphides are oxidised to 60 m depth, in places to 100 m (Mill *et al.*, 1990).

At Golden Grove, the two base metal sulphide deposits occur along 5 km of strike length of the host sequence. The Gossan Hill deposit sporadically outcrops as gossans over some 800 m of strike. Recognition that these were base metal gossans, partly based on their Cu values exceeding 1000 ppm (8 samples out of the original 36 taken), some with supporting Pb and Zn, resulted in the original discovery (J.N. Pitt, personal communication, 1979). The Scuddles deposit (now in production) was both blind (within bedrock and saprolite) and concealed beneath soil and a thin, discontinuous layer of lateritic residuum. Discovery of the Scuddles deposit was largely based upon investigation of a subsidiary airborne magnetic anomaly which coincided with the detailed stratigraphy of the prospective sequence, which was being followed northwards from Gossan Hill by rotary air blast drilling. The settings of the ore deposits are described by Frater (1978, 1983) and Mill *et al.* (1990).

Gossan Hill was the test area for initial CSIRO research on geochemical dispersion into lateritic residuum, which commenced in 1978. That research followed a study of the outcropping gossan and ironstones in 1977, which showed that they were characterised by anomalous ore-associated minor and trace elements (As, Sb, Bi, Sn and Se), as well as some being anomalous in Cu, Pb and Zn, as mentioned above. Following recognition of a 1 km wide geochemical halo in lateritic residuum about Gossan Hill, the laterite research was extended, in 1979, to cover some 20 km of strike length of the prospective sequence in the Golden Grove district. More detailed sampling of lateritic pisoliths was later carried out, including a traverse across the surface projection of the Scuddles deposits. A stage of research into the use of multivariate statistics for laterite geochemistry was also undertaken, with focus on the area from Gossan Hill to Scuddles (Smith *et al.*, 1984).

The research presented here includes re-analysis of archived CSIRO samples from the original orientation studies, concentrating on the area from Gossan Hill to Scuddles, shown in Fig. 5.53. Sample locations at Gossan Hill are shown in Fig. 5.54.

In order to improve the quality of the original data and standardise the suite of elements analysed, ANALABS were consulted and agreed to be involved in updating the Golden Grove dataset. ANALABS became a sponsor in kind, for this extension project, by providing analytical expertise and analyses at a reduced rate. Senior ANALABS staff involved included Mr G. Moore, Mr J. Cooper, Mr C. Scully and Mr D. Hall. The analysis report was received in June 1993 and the data have been included in Appendix X.

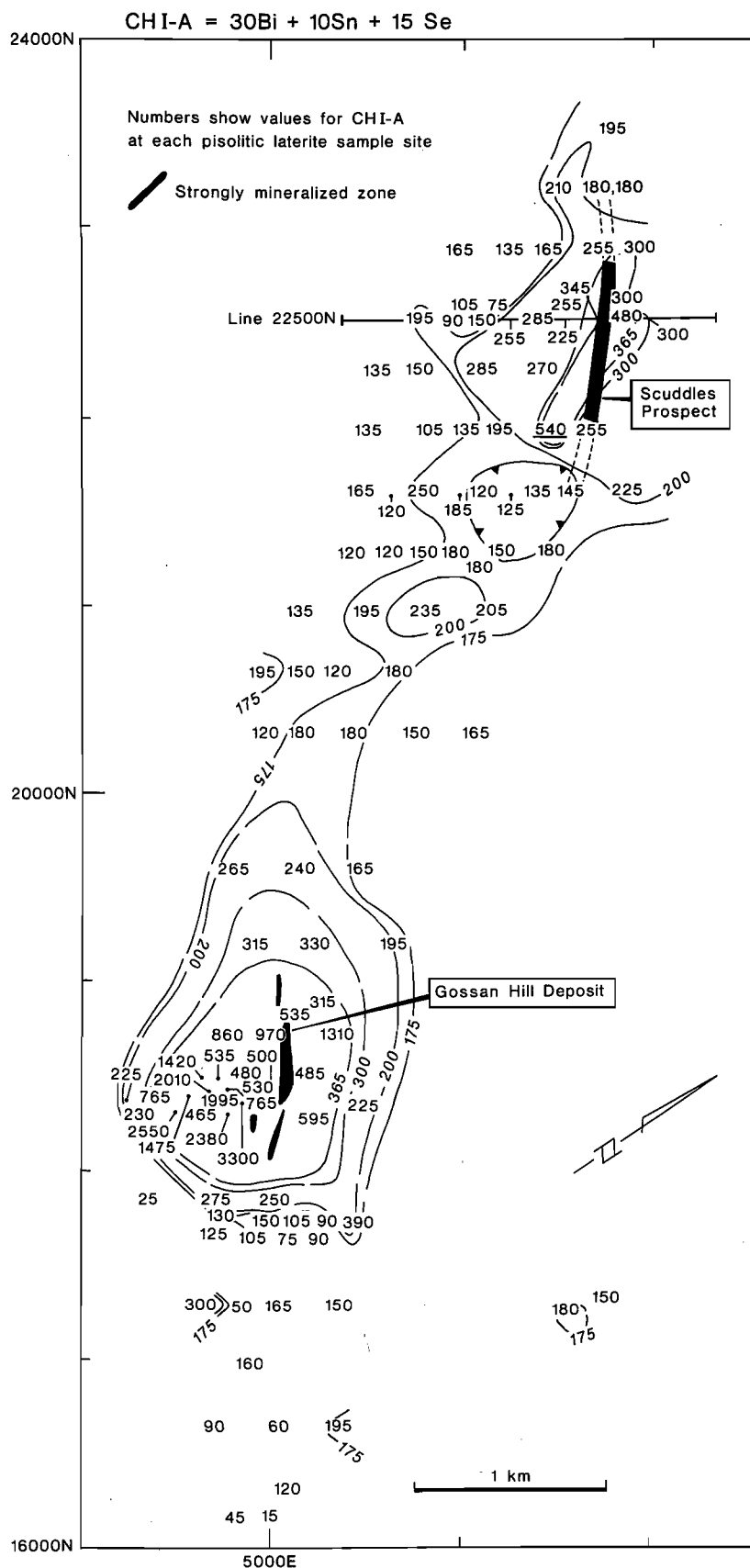


Fig. 5.53 Map of part of the Golden Grove massive sulphide district showing the area studied in this report. The distribution of samples of lateritic residuum are shown by the numbers which refer to values for the chalcophile index CHI-A. From Smith and Perdris (1983). Northings and eastings are for the mine grid.

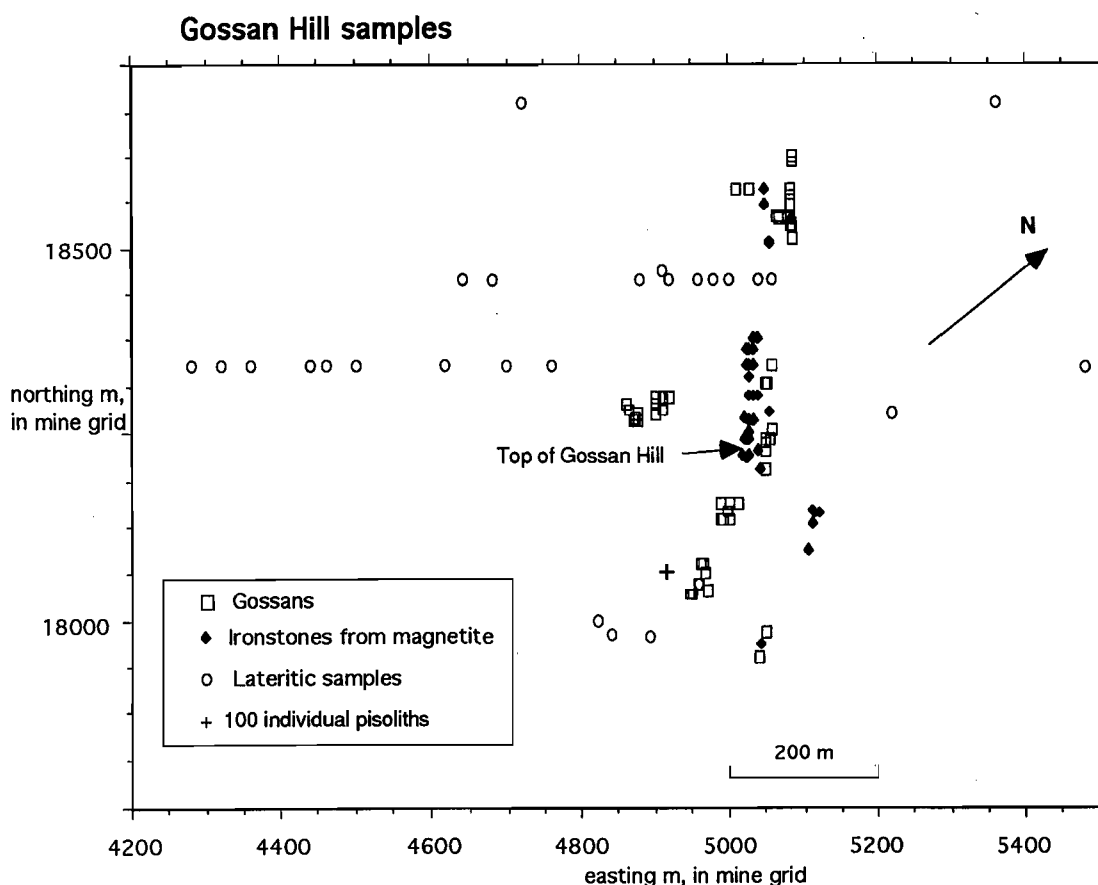


Fig. 5.54 Map showing the distribution of samples at Gossan Hill, on which the research for this section is based, coordinates are for the mine grid.

### 5.6.2 Objectives

The objectives of this follow-up study were:

1. To assess improvements in methods of chemical analyses, which provide greater analytical sensitivity, particularly for Au, Sb, and Bi over those which were available to the study by Smith and Perdrix (1983); and
2. To review the orientation research in the light of geochemical knowledge of Yilgarn Fe-rich materials generated over the last decade.

### 5.6.3 Gossan geochemistry

All of the original gossan samples were analysed for Au as part of this extension project and data were also extended to complete the major and minor elements. Originally, Au was analysed on only three of the samples because of the relatively high cost of Au analyses (screened fire assay) at that time. These new data allow comparisons of these gossans to be made with data from the nearby lateritic residuum. Results are summarised in Table 5.15, which shows samples grouped into base metal gossans, pyrrhotite-pyrite gossans, and ironstones lenses after massive magnetite.

Based upon their dominant geochemical characteristics, the gossans and ironstones, overall, are characterised by anomalous As, Sb, Bi, Sn and Se, with Cu and Au anomalous in some. They stand out with their high chalcophile and related element associations when compared with ironstones not related to mineralisation, such as the non-lateritic ironstones within the AGE database (Table 7.2 in Report 236R).

The Fe-rich bodies at Gossan Hill fall into two broad classes, the gossans (after base metal sulphides, pyrrhotite and pyrite) and the ironstones (after massive magnetite). The term gossan is not used for the latter: gossan *sensu stricto* refers to an iron cap after a sulphide body, whereas the ironstones are after massive magnetite.

At this stage of investigation, considerable overlap in chemical characteristics exists between the base metal (Cu), base metal (Pb-Zn) and iron sulphide gossans. Presumably this is in part because the iron sulphide gossans proximal to the mineral deposit would be carrying minor base metals and ore-associated trace elements. The gossans representing disseminated base metal sulphides do, however, have

Table 5.15 Golden Grove summary statistics for gossan types.

	Combined data.						Gossan from base metal sulphide					
	Mean	Std. Dev.	Count	Min	Max	Median	Mean	Std. Dev.	Count	Min	Max	Median
SiO2%	28	22.9	103	2.4	89	18.6	28.1	24.4	30	2.4	89.0	14.6
Al2O3%	2.6	2.2	103	0.4	14.2	2	2.6	1.4	30	0.4	5.5	2.1
Fe2O3%	61.4	22.3	103	4.1	93.5	70.3	60.8	22.7	30	6.0	85.9	71.5
MgO%	0.05	0.05	103	0	0.231	0.033	0.04	0.03	30	0.00	0.10	0.03
CaO%	0.09	0.07	103	0.01	0.336	0.084	0.11	0.06	30	0.02	0.25	0.11
Na2O%	0.03	0.07	103	0	0.445	0.004	0.01	0.01	30	0.00	0.05	0.01
K2O%	0.15	0.47	103	0.02	2.795	0.033	0.05	0.06	30	0.02	0.25	0.03
TiO2%	0.13	0.13	103	0	0.71	0.08	0.14	0.14	30	0.02	0.63	0.09
LOI%	5.32	3.23	103	0.9	14.3	4.6	6.2	2.6	30	1.0	10.4	6.2
TOT%	100.1	3.3	103	90.6	111.1	99.8	97.9	2.5	30	93.3	103.2	97.7
Mn ppm	37	66	103	3	353	15	39	58	30	3	266	20
Cr ppm	25	29	103	2	157	15	33	38	30	6	157	22
V ppm	26	49	103	3	372	3	39	73	30	3	372	22
Cu ppm	926	1350	103	3	10253	416	1006	746	30	47	2414	912
Pb ppm	60	173	103	2	1698	28	121	311	30	5	1698	44
Zn ppm	139	254	103	2	1424	35	251	411	30	7	1424	54
Ni ppm	4	2	103	3	15	3	5	3	30	3	15	3
Co ppm	16	15	103	5	101	11	13	12	30	1	44	8
As ppm	220	522	103	4	3840	60	420	818	30	6	3840	188
Sb ppm	27.4	95.7	103	0.7	816.0	11.1	61.1	173.9	30	0.9	816.0	11.1
Bi ppm	47.9	78.5	103	0.3	300.0	3	89.1	108.2	30	0.3	300.0	25.0
Mo ppm	9	32.1	103	0.7	292.0	0.7	13.6	25.2	30	0.7	107.0	0.7
Ag ppm	1.2	2.4	103	0	15.0	0.4	2.1	3.7	30	0.0	15.0	0.5
Sn ppm	85	381	103	0	3811	23	60	100	30	5	518	28
Ge ppm	2	4	103	1	30	1	3	6	30	1	30	1
Ga ppm	10	9	103	1	50	7	12	9	30	1	30	9
W ppm	47	43	103	5	280	30	50	59	30	8	280	25
Ba ppm	132	164	103	10	836	68	119	152	30	10	629	45
Zr ppm	62	61	103	0	377	49	76	76	30	3	377	54
Nb ppm	3	5	103	0	47	1	3	4	30	0	18	1
Se ppm	20	41	103	1	300	9	40	67	30	1	300	13
Au ppb	406	901	103	2	5130	39	752	1372	30	2	5130	216

Iron sulphide gossans							Ironstones after massive magnetite.						
	Mean	Std. Dev.	Count	Min	Max	Median	Mean	Std. Dev.	Count	Min	Max	Median	
SiO2%	22.6	17.3	18	4.7	64	19.2	20.3	14.2	38	3.2	57.5	15.9	
Al2O3%	1.7	0.8	18	0.6	3.4	1.6	2.0	1.4	38	0.4	7.4	1.8	
Fe2O3%	63.6	14.5	18	28.7	80.3	64	71.7	13.8	38	36.9	93.5	75.2	
MgO%	0.03	0.02	18	0.00	0.10	0.02	0.08	0.07	38	0.00	0.23	0.07	
CaO%	0.11	0.08	18	0.02	0.31	0.11	0.08	0.07	38	0.01	0.25	0.08	
Na2O%	0.01	0.01	18	0.00	0.04	0.01	0.01	0.01	38	0.00	0.03	0.00	
K2O%	0.04	0.04	18	0.02	0.15	0.03	0.06	0.06	38	0.02	0.28	0.03	
TiO2%	0.13	0.17	18	0.00	0.71	0.06	0.08	0.06	38	0.00	0.25	0.06	
LOI%	9.03	2.34	18	4.5	14.3	9.2	2.9	1.5	38	0.9	8.1	2.5	
TOT%	102	3.9	18	96.4	111.1	101.4	98.1	2.8	38	90.6	104.3	98.2	
Mn ppm	101	117	18	3	353	53	16	21	38	3	76	3	
Cr ppm	24	20	18	2	77	19	13	17	38	2	105	9	
V ppm	18	20	18	3	65	7	10	14	38	3	58	3	
Cu ppm	1569	705	18	460	3060	1628	218	442	38	3	2266	79	
Pb ppm	71	33	18	23	149	62	21	19	38	2	122	17	
Zn ppm	194	118	18	16	578	172	70	131	38	2	595	15	
Ni ppm	4	2	18	3	10	3	4	2	38	3	15	3	
Co ppm	8	5	18	2	21	7	23	19	38	0	101	20	
As ppm	304	446	18	33	1810	133	43	77	38	4	407	17	
Sb ppm	9.8	6.6	18	2.4	24.7	7.2	18.7	11.7	38	3.7	63.5	16.7	
Bi ppm	65.9	70.9	18	0.3	300.0	60	12.6	30.7	38	0.3	100.0	0.3	
Mo ppm	1.6	2.4	18	0.7	10.0	0.7	11.7	47.5	38	0.7	292.0	0.7	
Ag ppm	1.6	2.3	18	0.2	10.0	0.7	0.4	0.5	38	0.0	3.0	0.3	
Sn ppm	272	896	18	0	3811.0	16	49	50	38	7	210	27	
Ge ppm	1	0	18	1	2	1	3	2	38	1	10	3	
Ga ppm	5	5	18	1	20	2	12	8	38	1	30	10	
W ppm	33	32	18	5	134	22	38	20	38	12	103	33	
Ba ppm	72	44	18	23	168	62	126	145	38	12	788	70	
Zr ppm	36	43	18	0	156	15	44	24	38	0	132	43	
Nb ppm	5	11	18	0	47	2	2	3	38	0	9	1	
Se ppm	21	14	18	5	65	20	9	22	38	1	140	3	
Au ppb	821	865	18	85	2950	464	22	55	38	2	233	2	

lower Cu (all less than 1400 ppm) and lower Fe (all less than 52 wt%  $\text{Fe}_2\text{O}_3$ ) than most of the other gossans and ironstones.

Some 52% of the Fe-rich bodies which were sampled (gossans plus ironstones after magnetite) at Gossan Hill are anomalous in Au, using a threshold of 23 ppb (95th percentile of the 500 non-lateritic family in the AGE database). A statistical summary of the gossan geochemistry is given in Table 5.15 and their multi-element characteristics shown in Fig. 5.55. For the base metal gossans, only a minority are anomalous in Zn, whereas the majority are anomalous in Cu, Pb, As, Sb, Bi, Mo, Sn, W, Se and Au. For Au, Table 5.15 shows that whereas each of the gossan or ironstone categories at Gossan Hill is anomalous, the base metal and iron sulphide gossans (arithmetic mean 752 ppb Au) have, on average, 30 times more Au than the ironstones after magnetite (arithmetic mean 22 ppb Au).

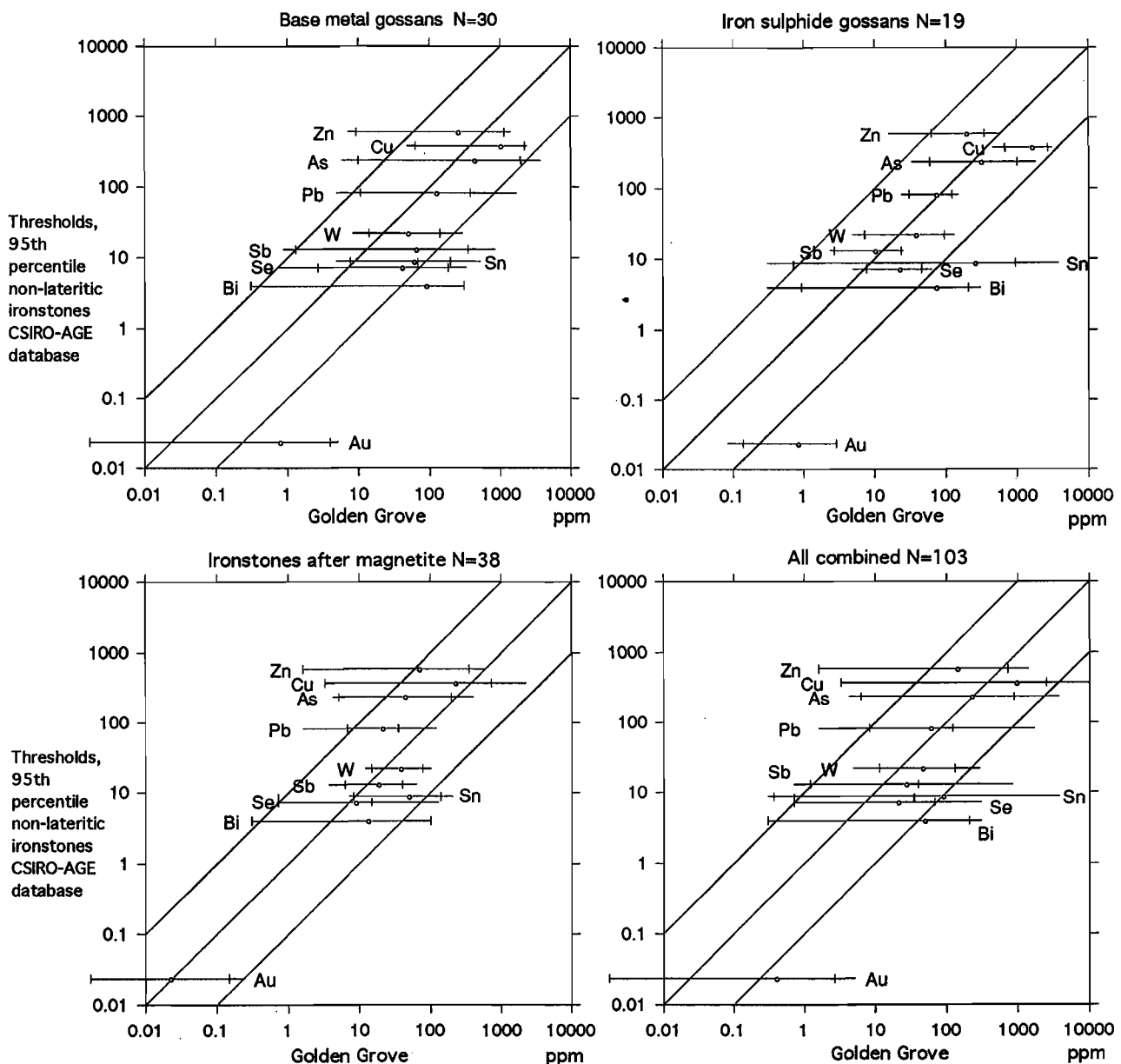


Fig. 5.55 Log-log anomaly characterisation diagrams for gossans from Gossan Hill, Golden Grove district. Thresholds used are the 95th percentiles of non-lateritic ironstones in the CSIRO-AGE geochemical database, Table 7.2 in Report 236R.

#### 5.6.4 Lateritic residuum at Gossan Hill

The geochemical anomaly in lateritic residuum at Gossan Hill measures some 1 km across strike and 2 km along strike, based upon individual elements. The strike length can be further enhanced with data treatment using chalcophile indices, *e.g.* Fig. 5.53 (from Smith and Perdrix, 1983). The distributions of selected target-associated elements (Cu, As, Sb, Au, Bi and Sn) across this anomaly are shown in Figs. 5.56 and 5.57. Gossan fragments are known to have contributed to the dispersion anomaly in lateritic residuum by mechanical dispersion (Smith and Perdrix, 1983), together with hydromorphic dispersion of elements released during oxidation of the ore system and/or its gossans. The positions of base metal gossans and ironstones after magnetite, in relationship to the anomaly in lateritic residuum, are shown on the sections, Figs. 5.56 and 5.57.

The anomaly in the lateritic residuum is asymmetric, with the strongest multi-element association on the southwest side of the hill. The Au anomaly is localised in comparison with the other elements. Thus, the use of Au did not enlarge the anomaly size but closely indicated the locality where Au was most strongly anomalous in the base metal gossans. This would be of use in delineating drilling targets in anomaly follow up.

At Gossan Hill, maghemite-bearing ironstones, after the massive magnetite bodies, are abundant but they are not the exploration targets. The sought after targets are the base metal gossans which are generally non-magnetic and carry a very strong chalcophile and associated element signature, as discussed above. Some are also strongly anomalous in Au. In contrast, the magnetic ironstones have a weaker multi-element signature and tend to be barren of Au. In exploration for VHMS deposits, gossans and ironstones are likely sources for ferruginous lag. Therefore, preferentially sampling magnetic lag could be misleading and certainly it would not be the best sample medium. A total, representative lag sample is recommended. Further information is provided in Section 5.6.6.

#### 5.6.5 Traverse across Scuddles

Samples of the thin layer of lateritic residuum collected in the original orientation traverse over Scuddles were re-analysed to see whether improvements in analytical methods would better delineate the dispersion anomaly. Relevant methods were ICPMS for Bi which gives a lower limit of detection (LLD) of 0.1 ppm (compared with 1 ppm for extended count XRF, as used by Smith and Perdrix, 1983). Instrumental neutron activation analysis (INAA) was used to provide Au analyses (LLD of 5 ppb) and 0.2 ppm for Sb (compared with 2 ppm for the original extended count XRF). Gold had not been analysed in the original data.

For Au, results showed that almost all samples (except two at 10 and 26 ppb) were less than 5 ppb; no anomaly was delineated. Results for Bi by three analytical methods (the original XRF and optical emission spectroscopy, together with new ICPMS data) are shown in Fig. 5.58. The distribution of As is also shown for comparison. Results show an incremental improvement for Bi through lowering of analytical noise at low abundances. The results also indicate that the mixed acid digestion for ICPMS (which includes hydrofluoric acid) is dissolving Bi reliably. The ICPMS results for Bi show the same features as the XRF and optical emission spectroscopy analyses (the classical method using photographic plates) which both measure the total amount of the element present.

The new, more sensitive Sb analyses (ICPMS, LLD 0.05 ppm and INAA, LLD 0.2 ppm) showed excellent correlation with each other and with the original XRF analyses. In the tests on Sb (not shown) the traverse across Scuddles did not change significantly from the patterns established from the original XRF data. However, the improved LLD for Sb seems to be significant in allowing the data for lateritic residuum, from Scuddles to Gossan Hill, to be contoured at levels as low as 2.0 ppm. This results in a wider Sb anomaly (1500 m compared with 500 m for the XRF data). The Sb anomalies at Gossan Hill and Scuddles appear to link and the Sb pattern (using either ICPMS or INAA data). The improved LLDs for Sb by ICPMS and INAA should be significantly advantageous in routine exploration when dealing with weak anomalies.

A comparison of the multi-element characteristics of the anomalies in lateritic residuum at Gossan Hill and at Scuddles are shown in Fig. 5.59, using thresholds for felsic bedrock in the Yilgarn Craton from the AGE database (page 32 in Report 161R). Both locations are distinctly anomalous and the element associations are different. Gossan Hill is strongly anomalous in Bi and Sn, and is anomalous in As and Sb. Lateritic residuum at Scuddles is anomalous in Bi, As and Sb, but Sn is at background level. Differences are partly interpreted to result from interrelationships between the geometry of the ore deposits and the erosional surface. These features are discussed further in Section 9, Dispersion Models, subsection 9.3.3.

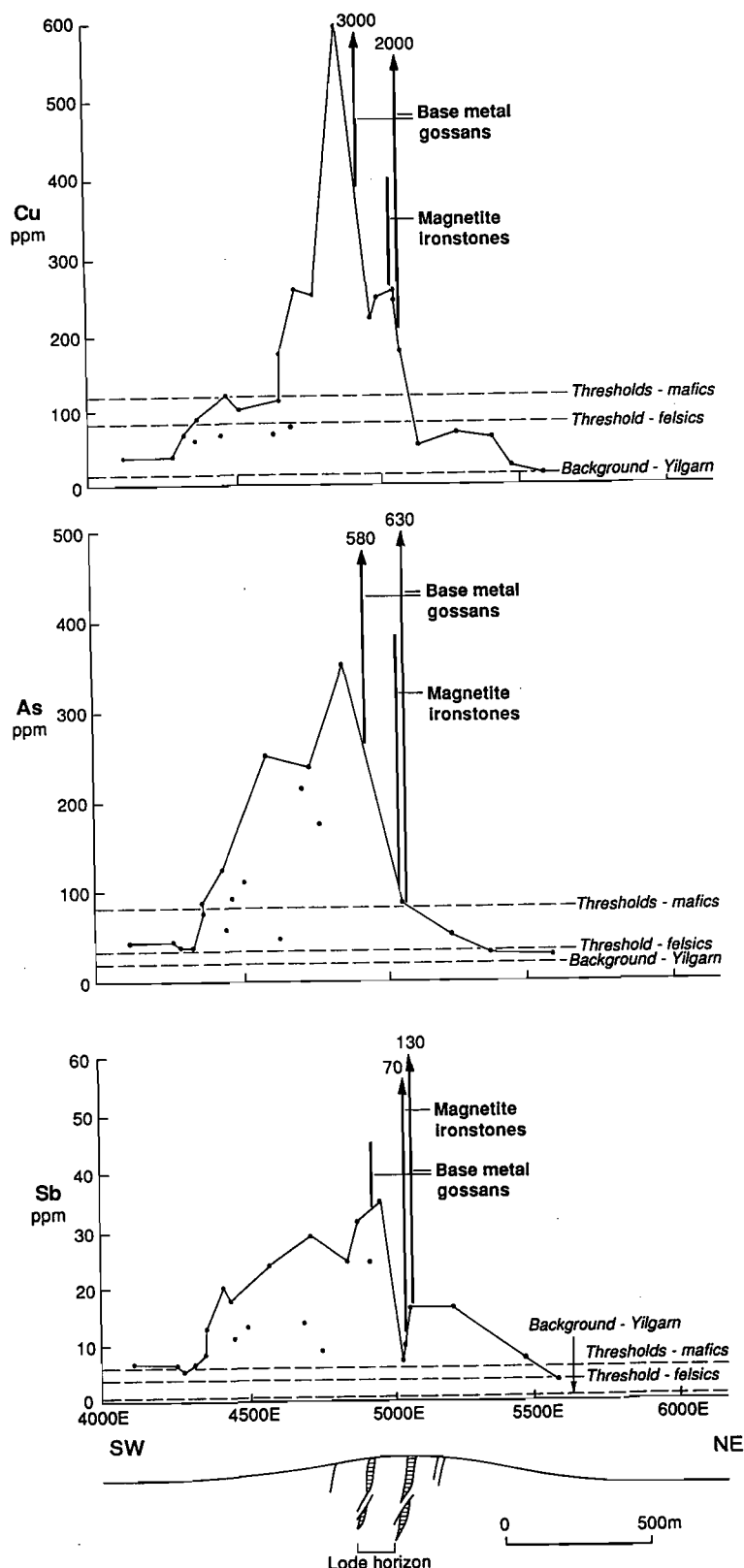


Fig. 5.56 Traverse across the Gossan Hill geochemical anomaly showing the distribution of Cu, As and Sb in lateritic residuum. The anomaly for each element is shown by an envelope enclosing samples with high values. Individual points within the envelope indicate some of the variability to be expected. Also shown are the positions of gossans and ironstones after massive magnetite with their corresponding elemental abundances. Data have been compiled between 18250 and 18500 mN.



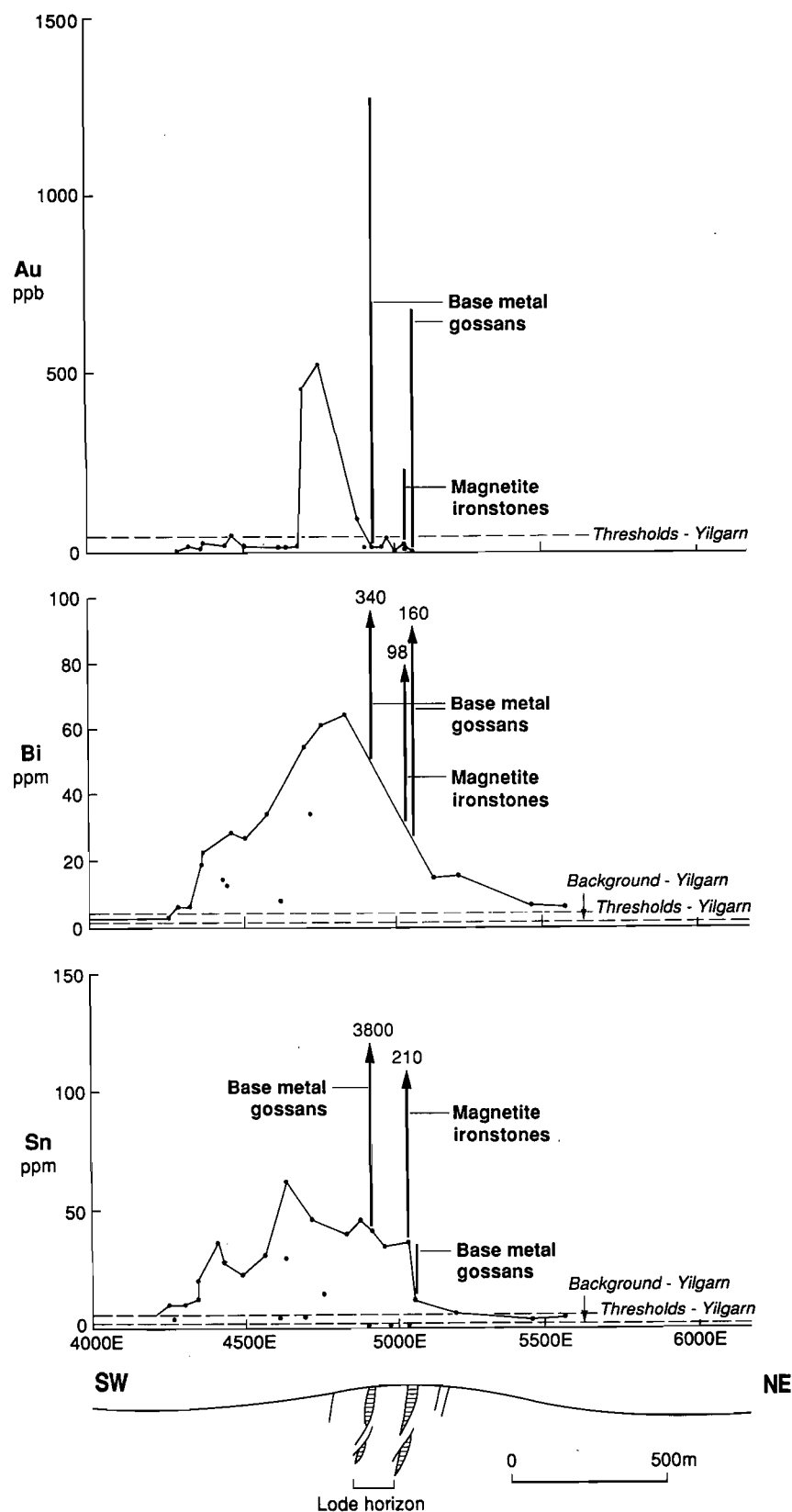


Fig. 5.57 Traverse across the Gossan Hill geochemical anomaly showing the distribution of Au, Bi and Sn. The anomaly for each element is shown by an envelope enclosing samples with high values. Individual points within the envelope indicate some of the variability to be expected. Also shown are the positions of gossans and ironstones after massive magnetite with their corresponding elemental abundances. Data have been compiled between 18250 and 18500 mN.

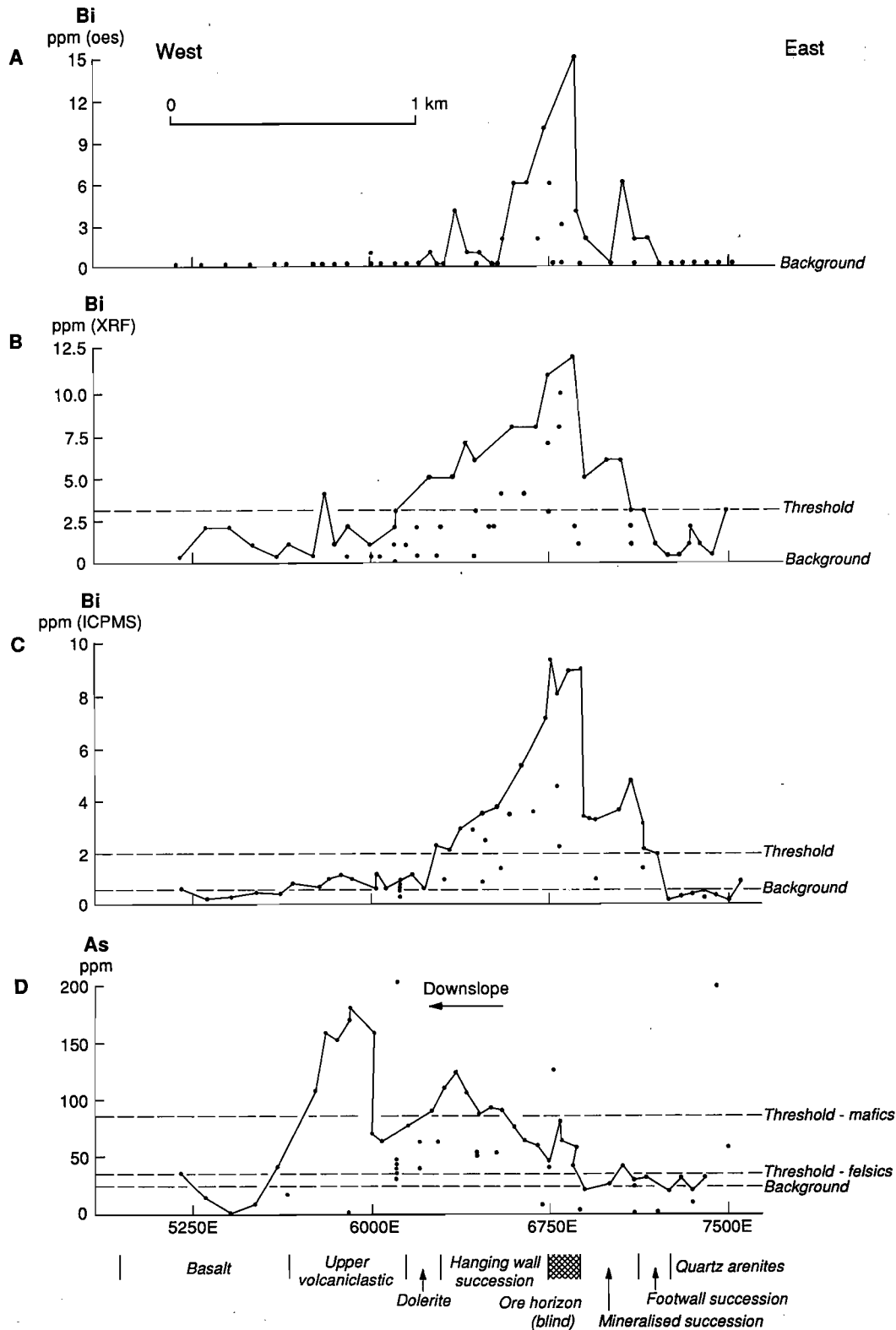


Fig. 5.58 Traverse across the Scuddles deposit showing the distribution of Bi and As in lateritic residuum. A and B show original data (optical emission spectroscopy and x-ray fluorescence) for Bi from Smith and Perdrix (1983) as well as some additional samples. C shows the ICPMS data generated during this project. D shows the As anomaly for comparison. Lateritic residuum was thin to vestigial over the eastern 500 m of the traverse. Individual points within the envelope indicate some of the variability to be expected.

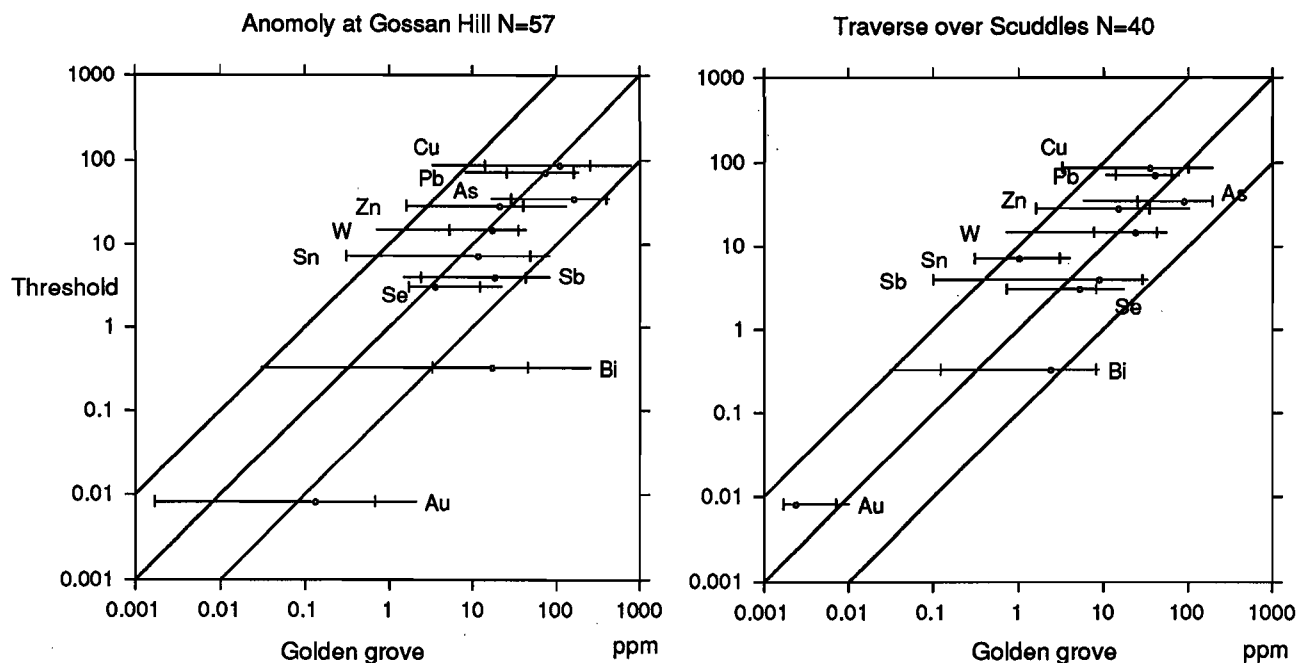


Fig. 5.59 Log-log anomaly characterisation diagram for the geochemical anomalies in lateritic residuum at Gossan Hill and Scuddles, Golden Grove district. Thresholds used are those for terrain characterised by felsic bedrock, being the 95th percentiles of lateritic samples from the Albany Fraser area in the CSIRO-AGE geochemical database (Table 3a, page 32 in Report 161R).

#### 5.6.6 Analysis of individual lateritic pisoliths at Gossan Hill

As part of an investigation of dispersion processes at Gossan Hill, 100 individual lateritic pisoliths or nodules were collected by R.E. Smith and J.L. Perdrix in 1981. Each pisolith was sawn in half to provide material for petrography and chemical analysis. The samples were collected at random over a 10 m radius from a site at the edge of the lateritic blanket, being some 50 m from gossan outcrops, Fig. 5.54.

Results show that all of the lateritic pisoliths are strongly anomalous in the elements which characterise the Gossan Hill ore deposit (Cu, As, Sb, Bi, In, Mo, Sn, W and Au). The histogram for Bi (Fig. 5.60) illustrates that each and every one of the lateritic pisoliths is anomalous. All are greater than or equal to 30 ppm Bi compared with a threshold of 3 ppm using the 95th percentile of lateritic samples in the CSIRO-AGE database (Table 7.1 in Report 236R which is based on routine 1 kg samples). Results also show that there are two types of clasts represented in the sampling, seen as two clusters in the plot of Si versus Fe (Fig. 5.61). Investigations by A.A. Levinson show that these correspond to magnetic and non-magnetic pisoliths.

The two categories of lateritic pisoliths are further illustrated by histograms for some of the elements which are bimodal, Fig. 5.60. It seems that the magnetic group of pisoliths have been derived by weathering (during lateritisation) of the ironstones after massive magnetite. The non-magnetic pisoliths, with their strongly anomalous levels of Au, As, Sb, In, and Cu, are derived from base metal sulphide gossans. Bismuth is more evenly distributed between these two categories of lateritic pisoliths.

The results clarify some of the processes of formation of dispersion anomalies in lateritic residuum. Smith and Perdrix (1983) showed, petrographically, that gossan fragments had been incorporated in lateritic residuum. That study also showed that Cu, Zn and As had dispersed hydromorphically in forming the anomaly in lateritic residuum. The observation that all 100 of the individual lateritic pisoliths studies are anomalous in Bi is interesting. Either the source gossans and ironstones after magnetite were consistently anomalous in Bi (which is not borne out by gossan and ironstone analyses) or Bi has been dispersed hydromorphically, with the Fe-oxyhydroxides of the pisoliths acquiring anomalous Bi from the local environment, presumably during lateritisation.

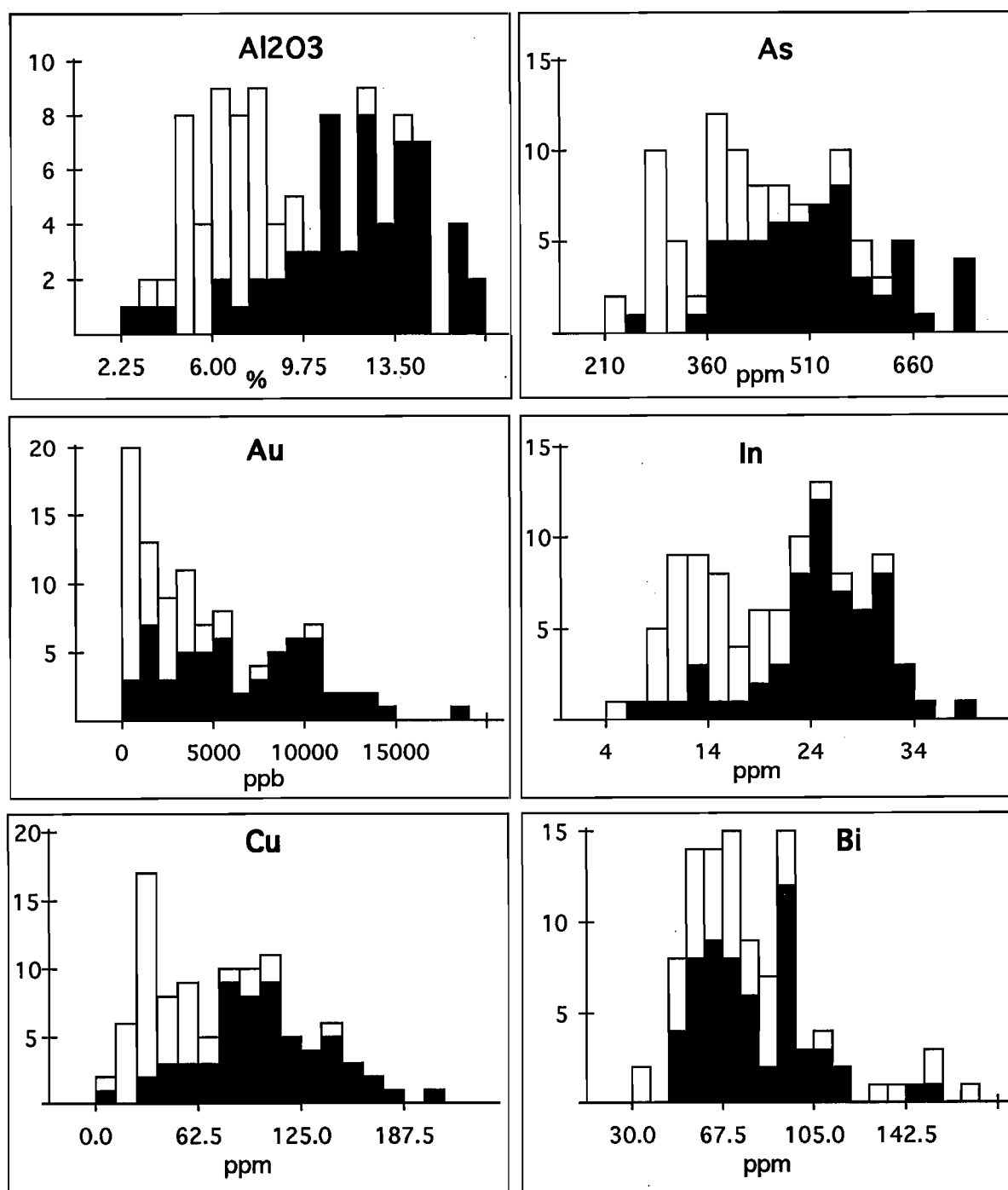


Fig. 5.60 Histograms for elemental abundances in 100 individual lateritic pisoliths collected from the strongest part of the Gossan Hill laterite geochemical anomaly. Both magnetic (unshaded) and non-magnetic pisoliths (shown in black) are present.

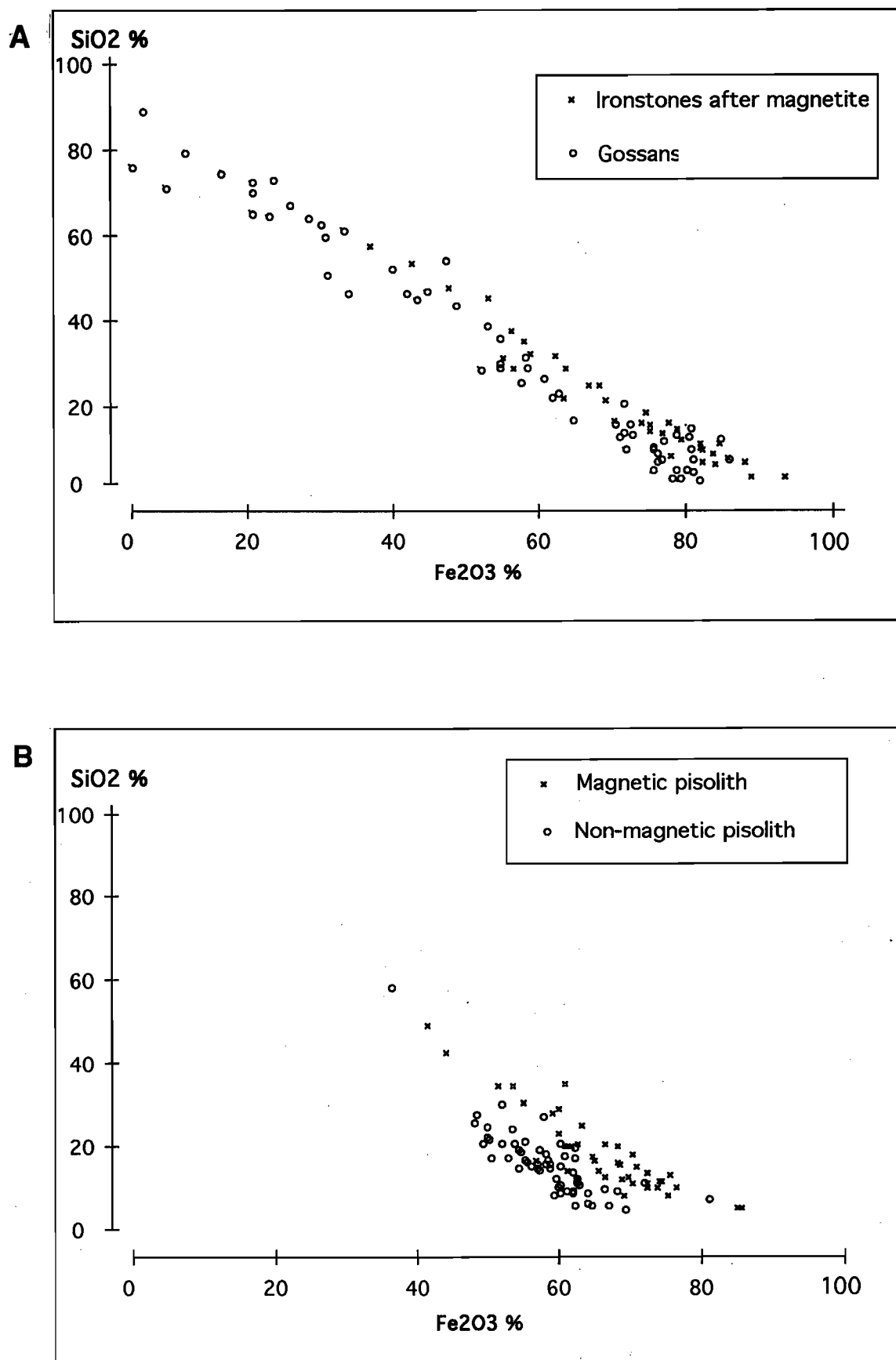


Fig. 5.61 Scatter plots showing the distribution of Si and Fe, A, in ironstones and gossans from Gossan Hill, and B, in 100 individual lateritic nodules from Gossan Hill. The plots suggest that the non-magnetic lateritic pisoliths are derived by lateritisation of gossan, whereas the magnetic pisoliths are derived from the ironstone lenses after massive magnetite.

### 5.6.7 Implications in exploration

This study shows that care must be taken in seeking and interpreting dispersion haloes arising from base metal sulphide deposits. Whereas substantial Au anomalies in lateritic residuum will always be important in exploration, a Au-bearing VHMS deposit, for example, does not necessarily generate a prominent Au anomaly. Rather, the anomaly characteristics depend upon the inter-relationships of the geometry of the weathering surface and the ore deposit, its primary halo (or alteration zone) or the ore horizon. For these reasons it is important that a suite of chalcophile and associated elements be used in base metal exploration. It is also important to have a clear conceptual model of each ore deposit type being sought and to translate these models to the terrain types being explored.

The study of individual lateritic pisoliths shows that the magnetic pisoliths do not represent the target sought. Rather, the pisoliths derived from the base metal gossans are non-magnetic. The implication is clear: it is inadvisable to collect preferentially magnetic, lateritic pisoliths, or magnetic lag. A representative 'whole' sample should be collected instead. The data on the 100 individual lateritic pisoliths, each individual of which is anomalous, confirm that a 1 kg mass of such material would provide a representative sample.

The traverse across Scuddles showed that analysis by ICPMS, with its lower limit of detection of 0.1 ppm for Bi, is an advantage in laterite geochemistry and should result in clearer backgrounds with better identification of anomalies. Likewise, the LLDs for Sb by ICPMS (0.05 ppm) and INAA (0.2 ppm) should be advantageous in delineating weak anomalies.

The main implications in exploration are listed in Table 5.16 and a dispersion model based upon the Golden Grove orientation study is given in Section 9.3.

Table 5.16 The implications in exploration listed against the research findings, Golden Grove orientation study.

Research Findings	Implications in Exploration
<ul style="list-style-type: none"> <li>The Au dispersion anomaly in lateritic residuum highlights areas of gossans which are anomalous in Au.</li> </ul>	<ul style="list-style-type: none"> <li>- Confirms that Au geochemistry is important in exploration for VHMS deposits.</li> </ul>
<ul style="list-style-type: none"> <li>The target-element suite in the laterite anomaly varies with element zoning in the ore deposit and with its inter-relationship with the weathering surface.</li> </ul>	<ul style="list-style-type: none"> <li>- Be aware of ore deposit zonation and geometric relationships.</li> <li>- Use a suite of target-associated elements and be flexible in interpretation.</li> </ul>
<ul style="list-style-type: none"> <li>Within the centre of the laterite geochemical anomaly, magnetic, lateritic pisoliths are derived from barren massive ironstones after magnetite. Non-magnetic pisoliths are derived from the base metal sulphide gossans.</li> </ul>	<ul style="list-style-type: none"> <li>- Take representative 'whole' samples (not magnetic fractions) when sampling lateritic pisoliths or lag.</li> </ul>
<ul style="list-style-type: none"> <li>Analyses by ICPMS, with a lower limit of detection of 0.1 ppm for Bi, provides better delineation of the Bi anomaly in lateritic residuum across the blind Scuddles VHMS deposit. Likewise, for Sb by ICPMS (0.05 ppm) and INAA (0.2 ppm)</li> </ul>	<ul style="list-style-type: none"> <li>- Should result in clearer backgrounds and better delineation of Bi and Sb anomalies. This is important in both base metal and Au exploration.</li> </ul>
<ul style="list-style-type: none"> <li>Each of the 100 individual lateritic pisoliths from the strongest part of the Gossan Hill anomaly was anomalous in target-associated elements.</li> </ul>	<ul style="list-style-type: none"> <li>- Confirms that bulk samples of pisolitic laterite (e.g. of 1 kg) should be representative for identifying and delineating anomalies.</li> </ul>

## 5.7 Beasley Creek and Lights of Israel - a comparison of soil geochemistry north and south of the Menzies Line.

### 5.7.1 Introduction

The two orientation studies discussed here, some 150 km apart and lying on either side of the Menzies line (Butt *et al.*, 1977), provide useful comparisons in the response of soil geochemistry from two contrasting settings in the Yilgarn Craton.

Separate reports have been produced on each of these studies: Beasley Creek, Report 26R (Geomorphology and surface geology); Report 27R (Geochemistry, petrography and mineralogy of ferruginous lag); Report 105R (Soil mineralogy and geochemistry); Lights of Israel, Report 232R (Soil and lag geochemistry).

The salient findings from the two studies are now discussed and a synthesis of comparisons and contrasts presented.

### 5.7.2 Regional settings

The Beasley Creek Au mine is 12 km west-northwest of Laverton (Fig. 1.1) with an average annual rainfall of approximately 200 mm. It is north of the Menzies line, in an environment having relatively fresh groundwater, soils that are mostly carbonate-poor and underlain by hardpan, and with vegetation dominated by acacia. The site occupied a low hill, flanked by wash plains, situated between broad drainage floors. The regolith has been partly stripped and lateritic duricrust was present only over the eastern flank of the hill, closely following the upper surface of the host rock. There are sporadic outcrops of ironstone and calcrete near the top of the hill, where the soil is thin and alkaline.

The Lights of Israel Au mine is 2 km northeast of Davyhurst (Fig. 1.1), south of the Menzies line, in an area of saline groundwater, calcareous soils and eucalypt-dominated vegetation. Average annual rainfall for the area is approximately 260 mm. Erosion at the Lights of Israel site has been more severe than at Beasley Creek and the presumed pre-existing lateritic profile has been truncated to the saprolite. The soil is largely residual and has a calcareous upper horizon underlain by a discontinuous gypsiferous layer, and by carbonate-free, red-brown clays and saprolite.

Mineralisation at Beasley Creek is enclosed in a presumed sulphidic black shale, relatively rich in pathfinder elements. Saprolites of Permian sediments overlap mafic and ultramafic saprolites in the eastern margin of the pit. The mineralised zone at Lights of Israel is a plagioclase-biotite-amphibole schist, poor in sulphides (1-3%; pyrite and trace chalcopyrite) and having low abundances of pathfinder elements. The wall-rocks at both sites are mafic amphibolites, intruded by felsic dykes, and the weathering front is at about 40-50 m depth. However, the depth of oxidation of the Au-rich sulphidic shale at Beasley Creek exceeds 200 m. Despite the great depth of weathering of the primary mineralisation, the regolith at Beasley Creek is far richer in pathfinder elements than that at Lights of Israel. Background abundances of the pathfinder elements (except for Sb) in fresh rock and saprolite are similar, but the As and Sb anomalies are much stronger (1-1.5 orders of magnitude) at Beasley Creek (Fig. 5.62). Zinc and Cu, which are depleted in the near surface, are slightly anomalous (<1 order of magnitude) at Lights of Israel.

### 5.7.3 Size fractions and mineralogy of soils

The soils at each site were sieved to three contrasting fractions. At Beasley Creek, these are:

1. Coarse (>710  $\mu\text{m}$ ): dense, black, goethitic saprolite-derived granules, some of which are magnetic; red to yellow, less dense ferruginous, duricrust-derived clay granules and relatively rare, non-magnetic gossan fragments. The goethitic granules contain pseudomorphs after mica and kaolinitic lithorelics, set in a variety of massive, spongy, vesicular and colloform secondary goethite.
2. Sandy-silty fraction (75-710  $\mu\text{m}$ ): hematite-coated wind-blown quartz sand, with minor grains of feldspar. This is a dynamic, largely wind-blown fraction that dilutes the soil.
3. Fine fraction (<75  $\mu\text{m}$ ): quartz and small, locally-derived kaolinite and Fe oxide particles (mostly <4  $\mu\text{m}$ ).



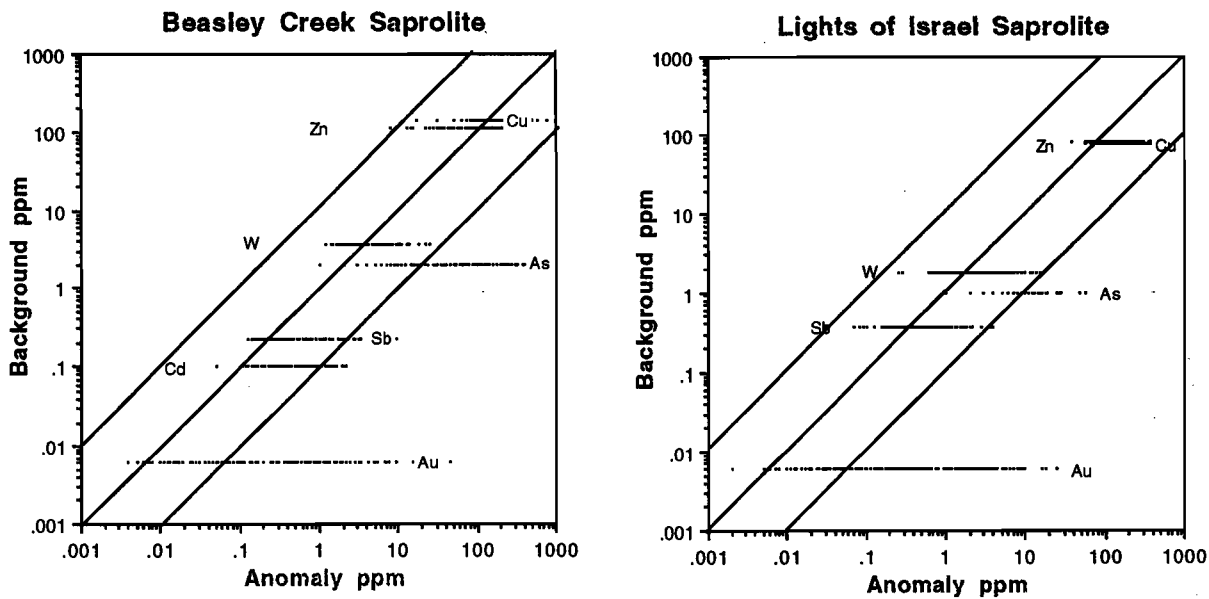


Fig. 5.62 Comparisons of abundances of Au and potential pathfinder elements in saprolite from background sites and mineralisation at the Beasley Creek and Lights of Israel orientation areas. Elements with similar abundances to the backgrounds plot on the diagonal; lines parallel to diagonal represent 10x backgrounds (right side of diagonal) 0.1x background (left).

Erosion by deflation and sheetwash has left a discontinuous desert armour of lag similar to the coarse soil fraction that also includes minor calcrete fragments and unevenly distributed coarse (>15 mm), black, ferruginous fragments. Bedrock lithology can, in places, be identified by pseudomorphed and relict fabrics preserved in goethite and hematite that represent saprolites of mafic and ultramafic rocks, phyllites and Permian glacial sediments. Gossan fragments in the lag probably contain most of the geochemical signal.

The mineralogy of equivalent fractions at Lights of Israel is more complex:

1. Coarse fraction (>600  $\mu\text{m}$ ): dense, black, goethite- and hematite-rich nodules, some of which are magnetic, slightly less dense, red to yellow, ferruginous clay granules, quartz fragments and scarce, fresh, crystals of tourmaline and, near mineralisation, gossan fragments. The Fe-rich fragments have lithorelics, containing microscopic relicts of smectites and kaolinite set in, and largely replaced by, massive, spongy, vesicular or colloform goethite. The minor gossan fragments show pyrite pseudomorphs. The clay-rich granules consist largely of hematite- or goethite-stained kaolinite and some include goethite-rich lithorelics. Some upper soil horizons are rich in carbonates and contain crystals of pedogenic gypsum and halite.
2. Intermediate fraction (75-600  $\mu\text{m}$ ): sand and silt of bright, clear, angular, drusy quartz, with minor grains of feldspar, small ferruginous granules and fine pedogenic calcite. This is largely of local derivation, with very little aeolian input, although the aeolian content increases slightly in its finer parts.
3. Fine fraction (<75  $\mu\text{m}$ ): quartz grains and smaller kaolinite and Fe oxide particles (<4  $\mu\text{m}$ ), with minor sericite in the <4  $\mu\text{m}$  fraction. Pedogenic calcite occurs as very fine-grained particles.

Tourmaline in the coarse and intermediate fractions has a composition indistinguishable from that in veinlets in the saprolite in the mine, suggesting that the soil at Lights of Israel is largely residual. As at Beasley Creek, the coarse and fine surface lag is identical to ferruginous material found within the soil and has accumulated on the surface due to loss of the fine fractions of the upper horizons by deflation and sheetwash. There is a much greater aeolian component in the silty fraction at Beasley Creek. At both sites, bioturbation and illuviation have mixed the aeolian material with the residual substrate.

#### 5.7.4 Soil geochemistry

The lag, the complete soil and its coarse ( $>600\ \mu\text{m}$ ), intermediate ( $<75\ \mu\text{m}$ ) and fine ( $<4\ \mu\text{m}$ ) fractions were separately assessed. The quartz-rich 75-710  $\mu\text{m}$  fraction (largely wind blown) was discarded. The lag was split into a coarse ( $>15\ \text{mm}$ ) and a fine component ( $<4\ \text{mm}$ ). The fine lag was further split into magnetic (maghemite-rich) and non-magnetic sub-components.

**Gold:** Gold is one of the best indicators of Au mineralisation in lag and soil at both sites. At Beasley Creek, Au is slightly enriched (200-400 ppb) in the ferruginous, coarse fraction (710-4000  $\mu\text{m}$ ), relative to the complete soil, due to dilution by the sandy fraction (Fig. 5.63). Enrichment in the coarse lag is locally much greater (1300 ppm) but is very erratic. In contrast, at Lights of Israel, Au is largely associated with soil carbonates, here present particularly in the  $<75$  and  $<4\ \mu\text{m}$  fractions, with the soil anomaly reaching 230-750 ppb Au. Gold anomalies at Lights of Israel are small and lack an extensive dispersion halo. Anomalies in lag (80-72 ppb) are narrow (75 m) and erratic, particularly in the coarse materials, and not well-defined. In soil, the anomaly is about 125 m wide, little greater than the projection (40-60 m) of the relatively shallow-dipping primary and secondary mineralisation that it directly overlies. At Beasley Creek, anomalies are broader (800 m), in part due to chemical dispersion of Au in the soil parent material, particularly the lateritic duricrust.

**Pathfinder elements:** Abundances of pathfinder elements in the soils and their size fractions are compared in Fig. 5.64, relative to local backgrounds established from samples collected up to 800 m from the subcrop of mineralisation. The multi-element signature is weak and subtle in all sampling media at Lights of Israel and is likely to be overlooked by exploration unless there is very careful control of the analytical process and geochemical background is properly established. Although some pathfinder elements (As, Sb, Cu and Cd) did not give a recognisable peak in the traverse, their general abundance is above the regional background. The only distinctive anomaly is given by Au, shown by the lag and, particularly, by the fine soil fractions. This contrasts with Beasley Creek, where there is a strong multi-element signature (Cu, As, Cd, W, and Au), particularly in the coarse, ferruginous sampling media. This difference in multi-element signature in lag is related to the higher primary abundances, and to the lesser degree of erosion. Only Au is enriched in the carbonate-rich fraction at Lights of Israel.

Because of its residual nature, lag is a convenient means of sampling the coarse, generally highly ferruginous soil fraction. Dispersion of the finer lag, by sheetwash, is generally greater than that of the residual soils and gives a larger target. The less-widely dispersed coarse lag ( $>15\ \text{mm}$ ) may have some advantages for follow-up, although the time-consuming collection and preparation required to obtain a sample large enough (several kg, to avoid erratic results) may outweigh its advantages. Comparison of the magnetic and the non-magnetic fine components of lag at both sites showed that the non-magnetic material, which contains the gossan fragments, displayed better pathfinder element anomaly contrasts although not necessarily enhanced abundances. Although magnetic samples provide a consistent, Fe-rich matrix, selective use of this material is not recommended. Conversely, its removal presents no significant exploration advantage either, as the proportion of magnetic material is relatively low (10-35%). Representative sampling of fine lag is therefore recommended.

**Sulphur:** There are S anomalies in the soil over mineralisation at both sites. At Lights of Israel, there is a layer of gypsum in the soil and at Beasley Creek, coarse gypsum occurs in the upper saprolite and minor barite is enclosed in the lag. Gypsum is generally common and widespread in the landscape and it is probable that the anomalies are coincidental. Nevertheless, at Lights of Israel, the isotopic composition of S is slightly heavier (1.2 per mil) than that expected if the S were derived from meteoric sources alone, thus there could be some bedrock S component - although the mineralisation is sulphide-poor. At Beasley Creek, which is more sulphide-rich but more deeply weathered, the S isotopic composition is typically meteoric ( $15.2 \pm 0.47$  per mil) for that location (A.S. Andrew, written communication, 1992).

**Ti-Zr ratio and origin of soil fractions:** The coarse (Fe-rich) soil fractions from both sites have similar and relatively constant Ti/Zr ratios, reflecting an homogeneous material of mafic origin (Figure 5.65); similar linear trends, with lower Ti/Zr ratios, are apparent in the  $<4\ \mu\text{m}$  fractions. The silty ( $<75\ \mu\text{m}$ ) soil fractions at each site have contrasting Ti-Zr geochemistry; the wide scatter, with a generally low Ti/Zr ratio, at Beasley Creek reflects considerable input from transported zircon-rich granitic material whereas the slight scatter at Lights of Israel, superimposed on a trend more related to the coarse soil fraction, indicates little input from transported material, despite close proximity to the granite.

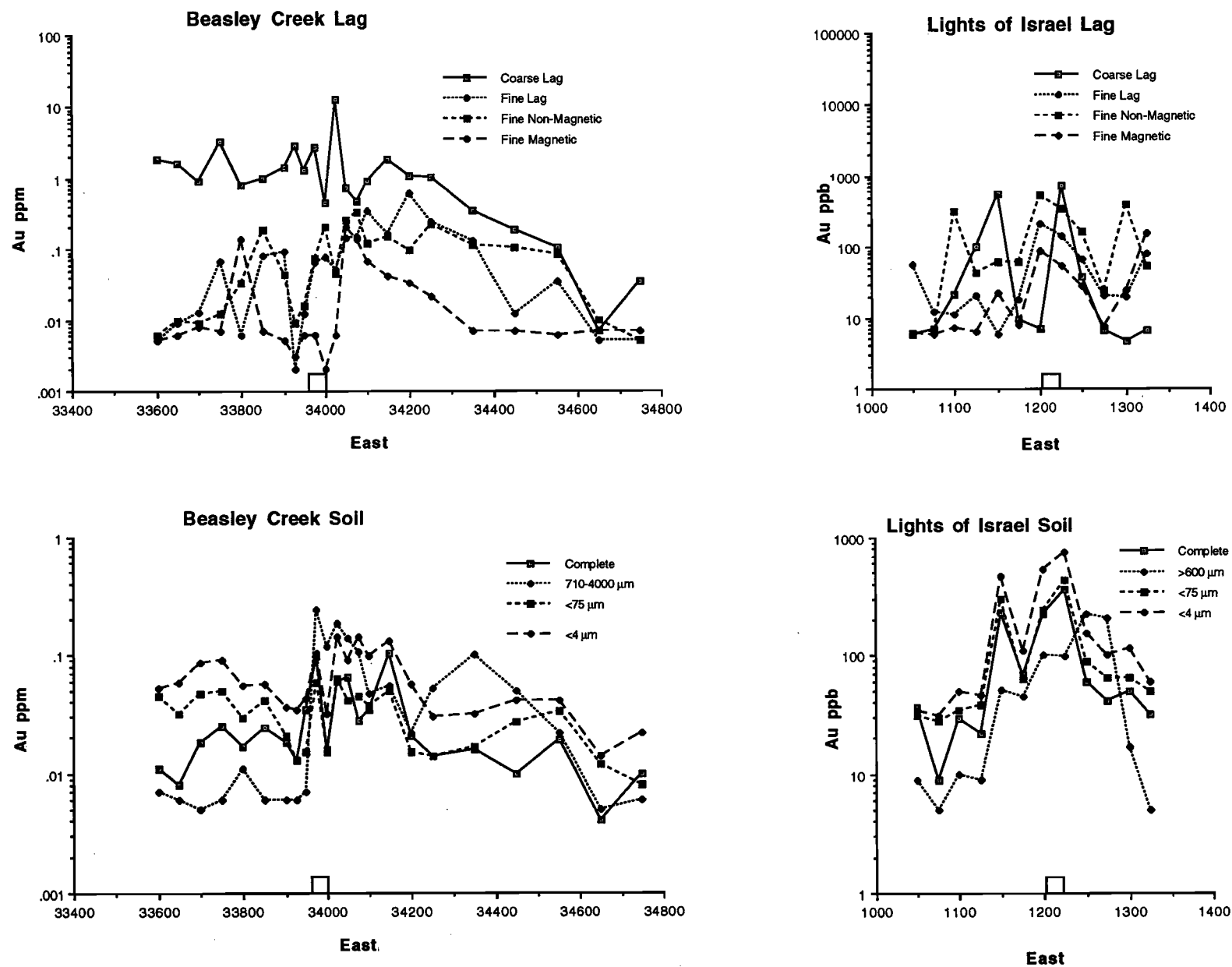


Fig. 5.63 Traverses across mineralisation at Beasley Creek and Lights of Israel, illustrating the distribution of gold shown by different soil fractions and lag.

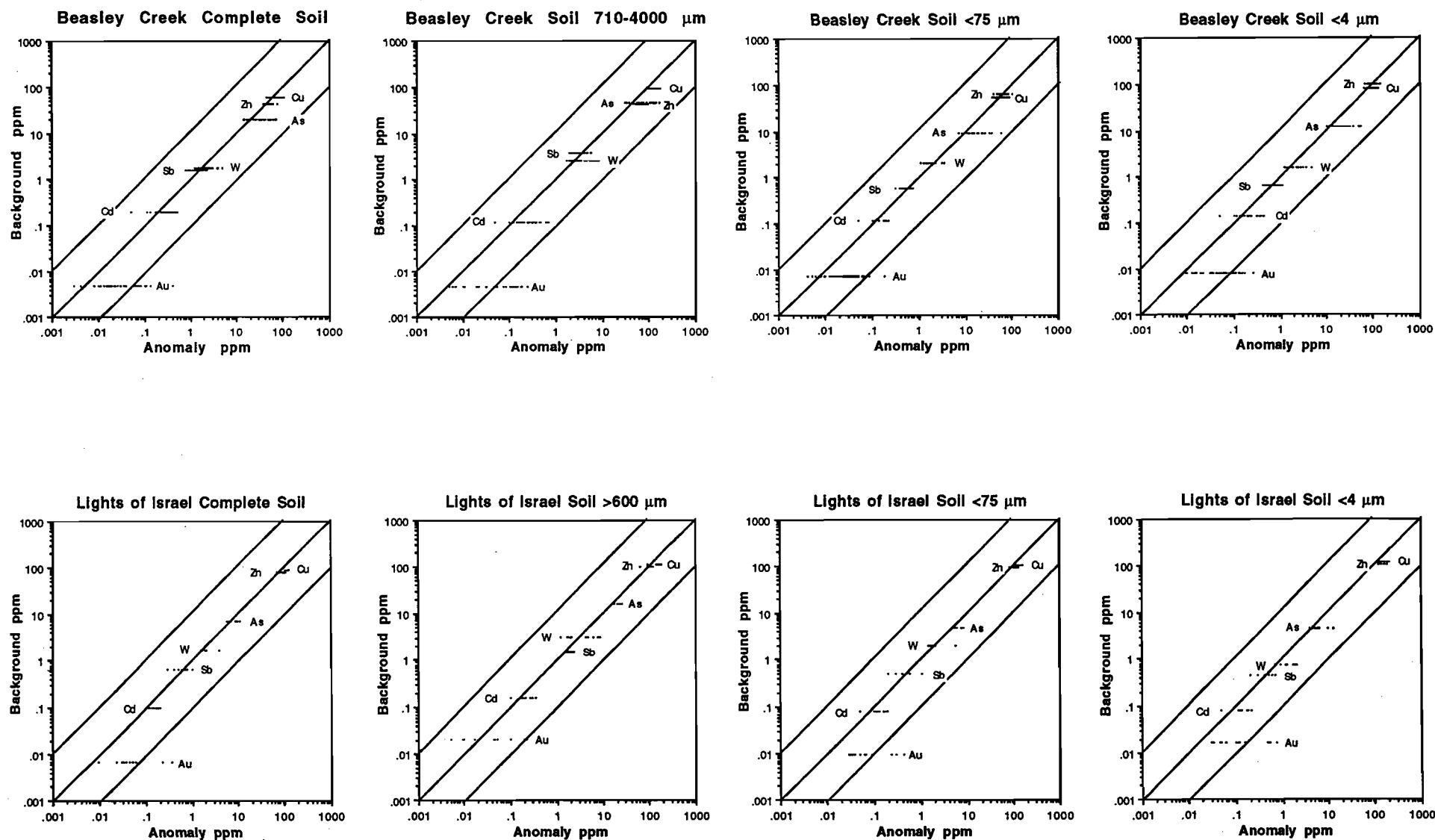


Fig. 5.64 Comparison of abundances of Au and potential pathfinder elements in soil from background sites and mineralisation at Beasley Creek & Lights of Israel. Elements with similar abundances plot on the diagonal; lines parallel to diagonal represent 10x background (right) 0.1x background (left).

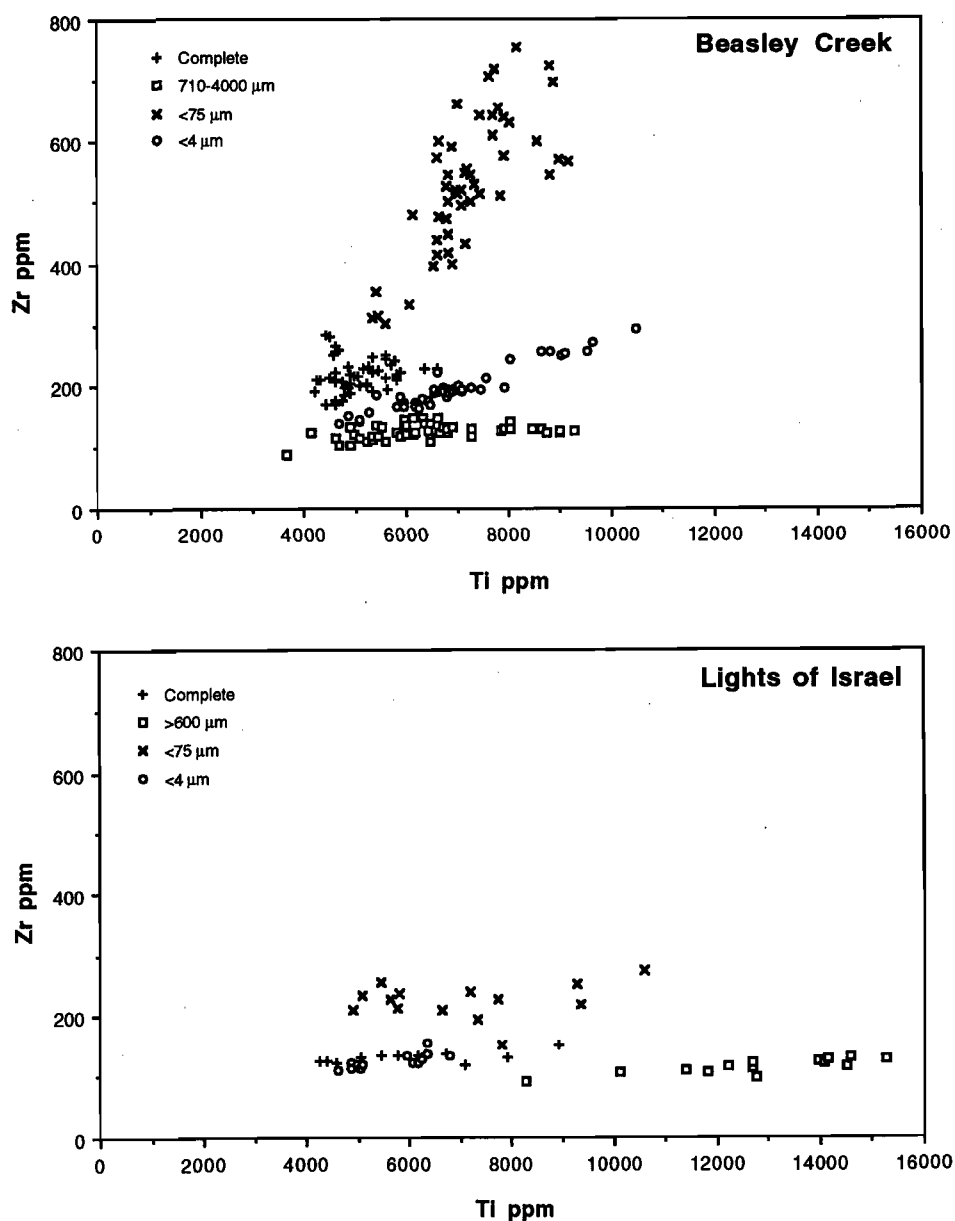


Fig. 5.65 Plot illustrating differences in the Ti-Zr ratio in various soil fractions at Beasley Creek and Lights of Israel.

#### 5.7.5 Implications in exploration

The results of these two detailed studies confirm the important regional difference in the occurrence of Au in soils, which has significant implications in Au exploration. North of the Menzies Line, Au is associated dominantly with the ferruginous, usually coarse, components in the soil, including lag, whereas, to the south, it is associated with pedogenic carbonates, which may either be dominantly in the fine fraction (as at Lights of Israel, Mt. Hope) or in all fractions, including very coarse nodules (*e.g.* Mulline, Mt. Percy). Of the ore-associated elements, only Au is enriched with the carbonates and, indeed, carbonate is a diluent for other elements. Despite the close associations of Au with the ferruginous and carbonate fractions, marked variations in background abundances, thresholds and anomaly dimensions can be anticipated in different parts of the landscape. Regolith-landform mapping, therefore, integrated with orientation studies or appropriate published case studies, should be used to design soil surveys and to control data interpretation.

Table 5.17. The implications in exploration listed against the research findings, Beasley Creek and Lights of Israel orientation studies

Research Findings	Implications in Exploration
<ul style="list-style-type: none"> <li>• North of the Menzies Line, Au occurs largely in the coarse, ferruginous soil fraction; to the south it is also contained in shallow, pedogenic carbonates, where they occur.</li> <li>• The geochemical haloes are much larger where the duricrust and mottled zone occur; where the profile has been stripped to the saprolite, the geochemical haloes are small.</li> <li>• The target at Beasley Creek is very rich in pathfinder elements (As, Cu, Cd, W) and so gives a strong, multi-element geochemical signature; that at Lights of Israel is poor in pathfinder elements where Au is the only effective element.</li> <li>• Gossan fragments in the ferruginous, coarse soil fraction are non-magnetic at both sites. The pathfinder geochemistry of the magnetic fraction at both sites is the least effective.</li> </ul>	<ul style="list-style-type: none"> <li>- In planning soil surveys it is essential to take into account the climatic and vegetation setting and to complete, or have available, an orientation survey where necessary to determine the optimum soil medium.</li> <li>- Regolith-landform mapping must be used to determine sampling strategy and sampling intervals in particular.</li> <li>- Account should be taken of the geochemical signature of the target sought. Targets, such as Lights of Israel, with additional difficulties such as a Au depletion in the near surface and located north of the Menzies Line, could present a significant exploration conundrum.</li> <li>- Use of magnetic lag or the coarse soil fraction, although yielding a very consistent medium, is not recommended; rather the complete lag or coarse, ferruginous soil fraction should be used.</li> </ul>





## 5.8 Madoonga

### 5.8.1 Introduction

This section summarises some of the results from research carried out on the Madoonga 1:50,000 map sheet (2444-III), which straddles the Weld Range, approximately 700 km north-northeast of Perth and some 50 km north of Cue (see Fig. 1.2). In particular, it presents the regolith-landform mapping component of the study. The Madoonga district has proved to be an excellent case study for illustrating how regolith-landform relationships can be determined from the interpretation of air-photos and multispectral satellite remote sensing data, namely Landsat TM imagery. Some of the dynamic processes involved in regolith-landform evolution are very apparent in both a black and white air-photo mosaic and enhanced Landsat TM data. In the latter case, spectrally enhanced images have proved particularly useful for detailing regolith stratigraphic relationships and delineating important regolith units at the district scale, e.g. 1:50,000.

The work has highlighted the considerable potential of Landsat TM data, when suitably processed, for providing valuable and unique information on the spatial and compositional attributes of regolith materials in the semi-arid and arid interior. When combined with selected field traverses and the use of higher spatial resolution air-photos, this study has indicated that the various attributes of Landsat TM imagery, including their spatial comprehensiveness, flexibility of aggregation and synoptic coverage, can combine to substantially improve the efficiency and effectiveness of regolith-landform mapping for mineral exploration in complex lateritic environments such as those that characterise the Madoonga district.

The research described here formed the basis for a Bachelor of Applied Science Honours Thesis, through the School of Applied Geology at Curtin University of Technology, W.A., by David Von Perger. The study, started in 1991 and concluded in late 1992, was linked to investigations on regolith-landform and laterite geochemistry through the *Laterite Geochemistry Project* and this extension project. The work is described in full in Report 238R (Von Perger, 1991).

### 5.8.2 Climate, geology and physical setting

#### *Climate and vegetation*

A semi-arid climate prevails in the Madoonga district with annual rainfall averaging approximately 200 mm. Mulga (*Acacia* spp.) is nearly ubiquitous, forming a sparse cover over the area. This has significant implications for the application of satellite remote sensing techniques for mapping surface materials as the observed variations in the imagery are largely controlled by the regolith and bedrock rather than the vegetation.

#### *Geological setting and geomorphology*

The Madoonga area is characterised by gently sloping plains and pediments, broken by the strike ridges of the Weld Range, low hills and breakaways. The region lies within the Murchison granite-greenstone Province and comprises rocks of the Weld Range Greenstone Belt in the south, adjoining younger granitic terrain to the north (Watkins and Hickman 1990).

#### *Regolith-landform associations*

The regolith-landform associations in the central and northern parts of the Madoonga district show similarities with those described for the Mt. Gibson Au mining district (Anand *et al.* 1989). The northern part of the study area is represented by a partially dismantled, gently undulating laterite surface, ascribed to the early Tertiary. Deep saprolitic weathering profiles, breakaways and preserved lateritic residuum, coupled with sand plains, are a typical association. This contrasts with the those found on the flanks of the Weld Range which trends from southwest to the northeast, starting in the lower left corner of the study area. The flanks of the range are characterised by polymictic colluvial and alluvial gravels forming extensive, gentle slopes and plains. These tracts are underlain in places by buried lateritic profiles. In many respects this is analogous to the regolith-landform associations observed in the Lawlers district (see Anand *et al.* 1991, and Section 4.4 in Report 236R). The SE corner of the study area is typified by truncated lateritic profiles, with saprolite, saprock and subcropping greenstones and metasediments.

### 5.8.3 Background

The work at Madoonga arose, in part, out of activity with the CSIRO-AGE sponsored research of 1983-86 (Section 7 in Report 236R), which had recognised a regionally significant As-Sb anomaly along the southern flank of the Weld Range during a trial application of laterite geochemistry for mineral exploration. Follow-up exploration had identified anomalous As-Sb-(Au) in saprolite underlying the

anomalous laterites. The Honours project (Von Perger, 1991) was designed to investigate the regolith setting of this geochemical anomaly and to study the regolith evolution of the surrounding district. To that end, a major component of the work involved mapping regolith-landform relationships over a 680 km<sup>2</sup> area. For completeness and convenience, an area covering the Madoonga 1:50,000 airphoto mosaic, sheet 2444-III, was selected. This mosaic forms part of the Belele 1:250,000 map sheet (SG 50-11).

#### 5.8.4 *Regolith-landform (mapping) units*

##### *Definition of regolith-landform units*

Spectral (tonal/colour) variations, patterns and textures in remote sensing images and air-photos generally formed the basis of regolith-landform mapping (Report 338R). They are largely related to the interactions of bedrock, surficial geology, soil, vegetation, and landform. Regolith-landform units are defined as areas (usually delineated from remote sensing data interpretation), within which a particular association of regolith materials and landforms occur which can be distinguished by mapping, at the scale chosen, from adjacent areas which have been differently defined, using similar principles. An area is thus mapped by delineating regolith-landform units from the interpretation of stereo aerial photographs, satellite imagery (such as Landsat TM) and/or airborne multispectral scanner imagery and airborne radiometrics. A crucial component to the work is a reconciliation of observed relationships with carefully selected, detailed, field traverses. There is no substitute for field work. A choice of mapping scales is also important. The scale of airphotos or other imagery will influence the choice and definitions of regolith-landform units because of the practicalities of representing heterogeneous assemblages at these scales. The more detailed the scale becomes, the more the mapping units become regolith rather than landform-based (Anand and Smith 1990).

From an exploration perspective, different geochemical thresholds may apply to different sampling media and to different regolith-landform mapping units. One purpose of producing a regolith-landform map is to delineate areas or units within which data may be treated uniformly. If the variation in sample characteristics is too great, true geochemical dispersion anomalies will be lost among the natural variation in sample characteristics, related to changes in regolith-landform situations (Anand and Smith 1990). Regolith-landform maps also identify and delineate areas characterised by complex surficial relationships which may require specialised exploration approaches in contrast with areas which require, for example, straight-forward soil sampling.

##### *Regolith mapping technologies - satellite multispectral remote sensing data*

Aerial photographs (black/white and/or colour) are a standard regolith-landform mapping tool. In the context of the Madoonga study, mapping was accomplished through the interpretation of stereoscopic black and white aerial photos at 1:50,000 scale, closely coupled with field traverses. A final compilation was generated by transferring detail from individual air-photos onto the 1:50,000 photo mosaic (sheet 2444-III). Whilst the stereo photos enabled the limited interpretation of surface types in relation to landform, some problems were encountered in the reliable correlation of regolith materials and regolith-landform associations across the whole study area.

These problems were offset through the use of spectrally enhanced Landsat TM data covering the area. The Landsat scene was for path/row:112/79, acquired on 28 October 1986. Recent research (e.g. Gozzard and Tapley, 1992; Gozzard *et al.* 1992) has also indicated that satellite multispectral remote sensing data can provide new and unique information on the spatial and compositional attributes of the regolith in environments that characterise the Yilgarn Craton. Landsat TM data, when spectrally enhanced, exhibits considerable variation which can be related to the nature of regolith materials. Given their synoptic coverage these data have the potential to permit the comparison and contrast of regolith-landform units from one area to another. However, a key to the successful extrapolation of information in this manner is the careful choice of image enhancement/processing techniques to be used.

##### *Image enhancement - band ratios*

Appropriate processing methods are those that are scene independent. A very effective enhancement technique which meets this requirement is Band Ratioing (the division of one spectral band by another). Ratios suppress variations in images that relate to surface brightness, topographically controlled modulations in irradiance and the effects of atmospheric transmittance. In doing this, the method enhances the more subtle variations that relate to the composition of surface materials. The computational simplicity, combined with the effectiveness in enhancing differences between materials and the ease by

which ratio values can be related to mineralogical controls resulted in the use of the method for the Madoonga study.

The choice of particular band ratios to discriminate between regolith materials is largely driven by the spectral features that influence broad-band spectral data. The coarse spectral resolution of Landsat TM limits the system to detecting the presence of Fe (in its ferric or ferrous state), phyllosilicates (Al-OH/Mg-OH), and/or sulphates and carbonates. In the Yilgarn, extensive lateritic weathering has resulted in a preponderance of Fe oxides, kaolinite and quartz at the surface. Where the weathered profile is truncated other minerals such as the smectites, amphiboles, chlorite and talc may also occur. All these minerals are characterised by distinctive spectral features in the 0.4 - 2.5  $\mu\text{m}$  wavelength region and their presence can influence the response measured by Landsat TM.

An additional factor to consider when discussing the spectral response characteristics of regolith materials is the presence of minerals that have a low, flat response in the region covered by Landsat TM. These include magnetite and ilmenite. Although widely present in very small amounts, these minerals significantly reduce the spectral contrast and hence the ability to discriminate between regolith materials where they occur.

Whilst a range of options are available to determine the particular band ratio to be used for discriminating between regolith materials, final choice for the Madoonga study was determined by the interactive comparison of various band ratio combinations. Selection was also constrained by an understanding of the dominant mineralogical controls that regolith materials were likely to exert on spectral response. The particular ratio combination that provided a good range of hues (colours) for the Madoonga area was TM bands 5/7, 4/7 and 4/2. These were combined on red, green and blue respectively and yielded the image shown in Fig. 5.66. This particular enhancement, when used as a basis for mapping regolith materials, is referred henceforth as CSIROREG. An alternative to using ratio 5/7 is to use the CSIRO DEM Least Squares Fit algorithm and calculate a residual of TM Band 7 (Green and Berman, 1990). This has the effect of suppressing the influence of vegetation whilst enhancing mineralogical variations that are observed in TM band 7. However, the technique was not applied at Madoonga, largely because of the sparse nature of the vegetation cover over the study area.

#### *Image interpretation - regolith-landform associations*

A thorough interpretation of the Landsat TM CSIROREG colour composite was beyond the scope of the project. However, correlating the image colours with information collated from the interpretation of air-photos and selected ground traverses indicated that this particular image enhancement was a very valuable aid for mapping regolith-landform associations in the Madoonga area. In particular, specific colours in image linked to particular landform settings proved to be a reliable means for predicting the nature and distribution of regolith materials, hence regolith stratigraphy. This was particularly true for relatively iron-enriched areas, including outcrops of lateritic residuum. Given the importance of being able to identify the location of lateritic materials from an exploration geochemistry perspective, this observation alone suggests that, suitably enhanced, Landsat TM data have the potential to serve as a valuable aid when planning and conducting exploration oriented geochemical surveys in lateritic terrains.

It is particularly important to be able to compare and contrast regolith-landform units from one exploration area with those of another. This is pertinent when examining or defining geochemical thresholds for different regions and establishing the relative importance of geochemical anomalies. It is also fundamental to the selection of geochemical exploration methods for a given area. Results from the Madoonga district have suggested that given the synoptic coverage of Landsat TM data coupled with their availability across the whole of the Yilgarn, the potential exists for their use in extrapolating regolith models outwards from one exploration area or to new districts. However, it is important to note that this goal can only be achieved through the use of scene independent enhancement techniques, such as band ratioing, that work effectively across the varying climatic gradient and contrasting regolith and vegetation settings that characterise the Yilgarn Craton. Further studies are required to assess the true value of the CSIROREG enhancement for such purposes.

The combined use of air-photo interpretation, analysis of the Landsat TM ratio colour composite (Fig. 5.66) and selected field traverses enabled the production of a detailed regolith-landform map at 1:50,000 scale for the whole of the Madoonga map sheet in a relatively short period of time. The ability to extrapolate regolith-landform associations using the colours portrayed in the Landsat image substantially improved the efficiency of the mapping process, making it possible to map a large area in relatively short time (approximately three weeks field work). A simplified regolith-landform map of the district is reproduced in Fig. 5.67.

Enhanced TM data can be used for mapping regolith-landform relationships at regional (e.g. 1:100,000) and district (1:50,000) scales. Mapping at more detailed scales with TM becomes problematic because of the coarse spatial resolution (30 m) of the instrument. Significant improvements in the spatial information content of such images can be gained by merging the data with suitably enhanced SPOT Pan images or B/W airphotos. Recent research (e.g. Gozzard *et al.*, 1992) has indicated that combined SPOT Pan, and spectrally enhanced Landsat TM imagery (e.g. CSIROREG) have the potential to be used as a mapping base at scales more detailed than 1:50,000, such as 1:25,000. These detailed scales are more relevant to exploration geochemistry activities in the Yilgarn Craton. As indicated here, when combined with a field and photo-interpretation based mapping strategy, Landsat TM can be used as an effective regolith mapping aid.

Scrutiny of the simplified regolith-landform map for the Madoonga area (Fig. 5.67), coupled with the CSIROREG image (Fig. 5.66), indicates that the study area can be divided into essentially two regions. The Weld Range, running from bottom left to middle right, effectively divides the area. To the north of the range, regolith units associated with granitic terrain have been defined. On the flanks and immediately to the southwest of the range regolith units associated with the Weld Range Greenstone Belt have been delimited. Regolith-landform associations from these two regions have a distinctive appearance in the Landsat TM image.

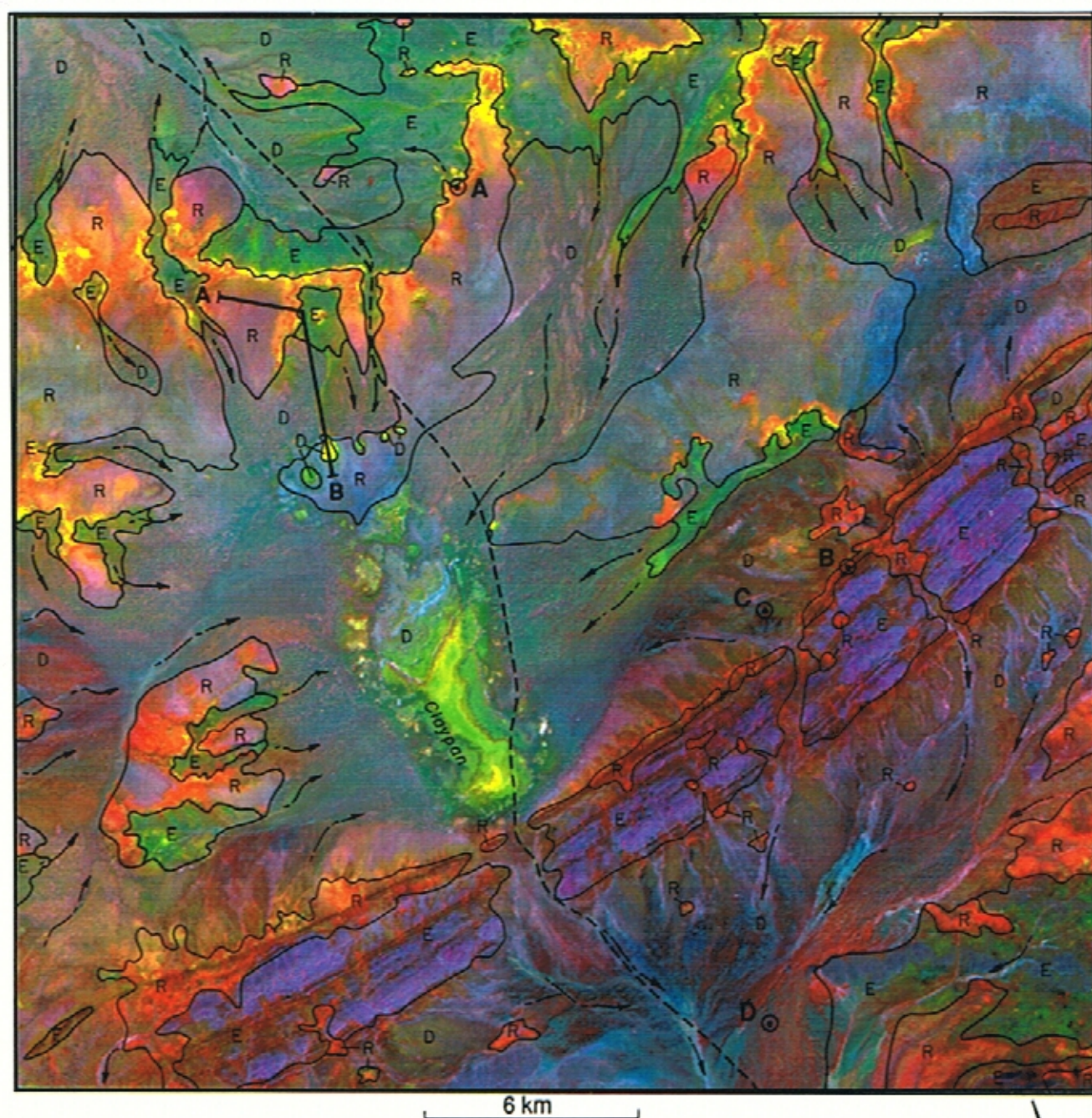
In the granitic terrain country, the breakaways have a most striking appearance on the image. Of particular interest are the regolith stratigraphic relationships which are clearly depicted. Breakaways over the granites are marked by a yellow line which has been interpreted to correspond to Unit GB1 - consisting of pale silcrete and/or hardened granite saprolite having a thin veneer of iron staining as a capping (see Fig. 5.68A). Regolith Unit GB2, mapped as occurring on the lower breakaway slopes and adjoining pediments, appears green in the image. It comprises mainly of kaolinised granite saprolite. Lateritic residuum has been mapped as occurring behind the breakaways, marginal to the silcrete cappings (Unit GB1), on the crests and upper slopes of low rises. These areas appear as orange in the Landsat colour composite. This unit gives way to GD1 - gently undulating sand-plain country which appears as pale magentas through pale blues in the image. A view across this transitional zone from the silcrete capped granite saprolite (foreground) to the sand-plain country (background) is shown in Fig. 5.68B. A locality characteristic of the regolith-landform associations depicted in Fig. 5.68 is shown on the overlay to the Landsat image (marked A).

Extensive tracts of colluvial and alluvial materials occupying outwash plains (Units GD1 and GD2) have been mapped over the granites. These units have a distinctive texture and pattern in both the air-photos and the CSIROREG Landsat image. In the latter case they are not characterised by a particularly distinctive colour. Claypans and associated deposits (Units GD3 and GD4) are also well defined in the imagery and air-photos. However, it is apparent that when mapping these units using the Landsat TM image, their colour alone is not sufficient for discrimination from other materials, notably granite saprolite (Unit GB2). Rather, a combination of colour, shape, texture and pattern is required for their delineation.

The stratigraphic relationships of the abovementioned units is shown in a schematic cross section (Fig. 5.69). A representative traverse which roughly correlates with this section is shown on the overlay to the Landsat image (Fig. 5.66).

In common with those regolith units mapped over the granite terrains, regolith-landform units associated with the Weld Range Greenstone Belt are characterised by distinctive spectral response characteristics as depicted in the CSIROREG colour ratio composite. Areas of lateritic residuum are preserved along the flanks and within the range itself. Lateritic residuum marginal to the strike ridges are best preserved on the northern flanks of the range. They are closely associated with areas of ferruginous saprolite and in the image these materials appear as reds and oranges. Figure 5.70 illustrates the regolith-landform associations associated by these flanking residual units - mapped as WL1 (see locality B on overlay to Fig. 5.66 for an indication of the appearance of this unit in the image). On the southern flanks of the Weld Range, this unit is partially or wholly truncated, or buried beneath colluvial/alluvial sediments. However, small 'windows' where the residuum pokes through these sediments are apparent in the Landsat image. Residuum associated with low hills (Unit WL2) away from the range are also depicted in reds and orange in the image. Iron-rich duricrusts (Unit WS2) show up as patches of red within the Weld Range. These units cap the tops of low hills or mesas. Other residual units (not shown in Fig. 5.67, but mapped at 1:50,000 scale) occur as low mesas adjacent to the creeks that dissect the Weld Range.



**Key:****Colours**

Red-orange  
Yellow  
Lime green-yellow  
Green  
Purple-blue  
Black-brown  
Cyan-white  
Magenta-blue

**Regolith Materials**

Lateritic residuum, lateritic lags, iron-rich clays.  
Iron stained silcrete capping breakaways.  
Clays (sepiolite?) in claypans.  
Koalinetic clays and felsic saprolite.  
Mafic bedrock.  
BIF strike ridges, colluvial/alluvial outwash plains.  
Dense vegetation.  
Sand plains.

**Geomorphic Regimes**

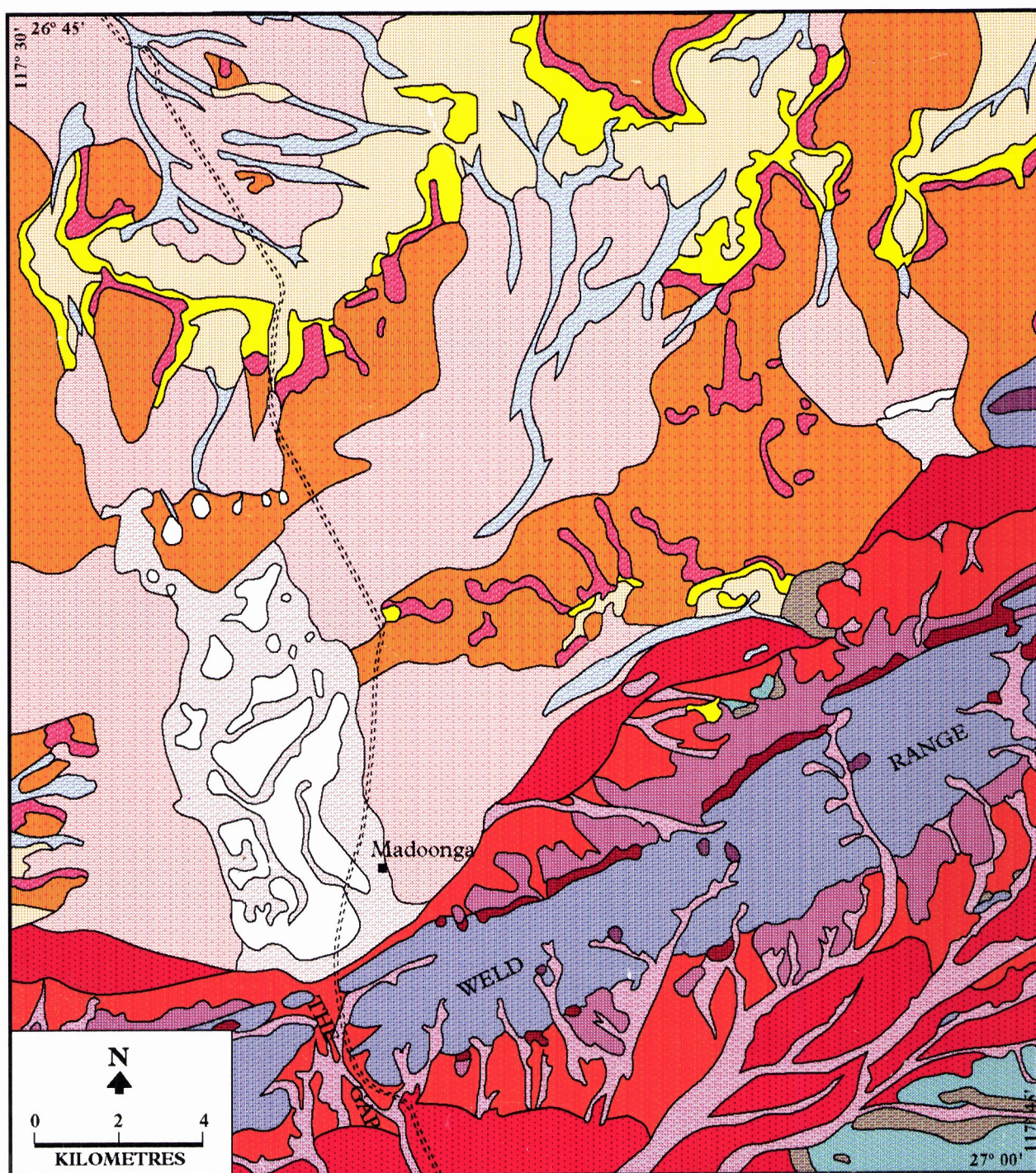
R Residual regime  
E Erosional regime  
D Depositional regime

Flow direction  
A ⊙ Type locality for a regolith-landform association  
A — B Representative section line (Figure 5.69)

Figure 5.66: Landsat TM CSIROREG colour ratio composite of the Madoonga district, with an overlay showing type localities for regolith-landform associations, and a representative section line linked to Figure 5.69. The overlay also shows the regolith-landform regimes that characterise the district. The image comprises Landsat TM band ratios 5/7 (red), 4/7 (green) and 4/2 (blue). Image acquired for path/row 112/79 on 28<sup>th</sup> Oct 1986.





**Residual Regimes**

- GL - Lateritic residuum
- GB1 - Silcrete forming capping of breakaways
- GD1 - Sandplain
- WL1 - Lateritic residuum marginal to strike ridges
- WL2 - Lateritic residuum on gentle rises
- WS2 - Iron-rich duricrusts

**Erosional Regimes**

- GB2 - Granite saprolite and outcrop on pediments
- WB1 - Mafic saprolite and outcrop
- WB2 - Felsic metasedimentary saprolite and outcrop

**Depositional Regimes**

- GD2 - Alluvial tracts over granitoid
- GD3 - Colluvial/Alluvial plains
- GD4 - Claypans
- GD4a - Sandy deposit marginal to claypans
- WS1 - Old colluvial/alluvial deposits
- WD1 - Alluvial tracts
- WD2 - Colluvial/alluvial deposits on gentle slopes
- WD3 - Alluvial/colluvial deposits on plains

Prefix: G: regolith unit in granitic terrain; W: regolith unit in Weld Range Greenstone Belt

Fig. 5.67 Simplified regolith-landform map of the Madoonga district. Modified from Von Perger (1993).





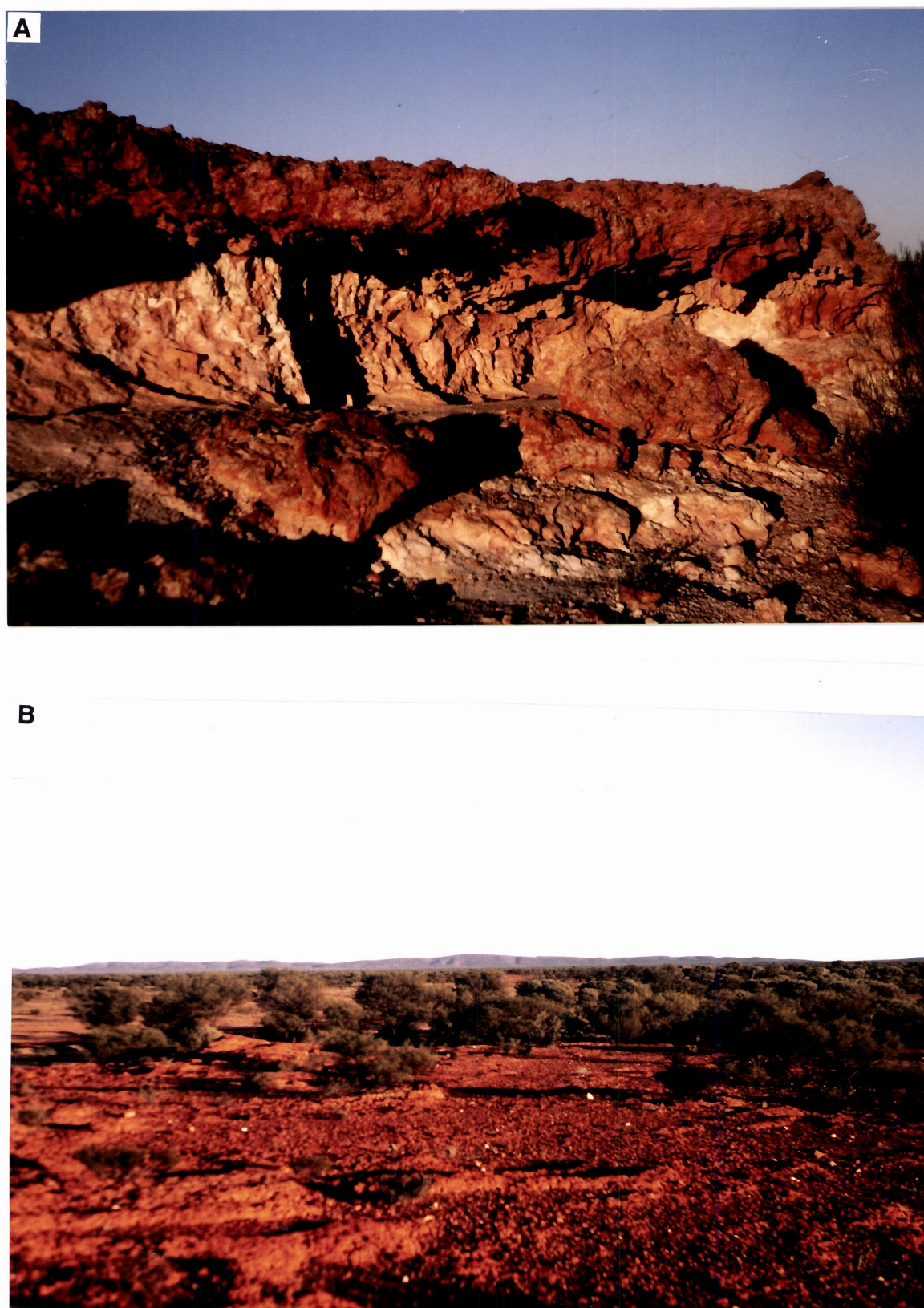


Fig. 5.68 Regolith and landform relationships in the Madoonga district:  
A. Silcrete-capped breakaway from Unit GB1, granitic terrain.  
B. View towards the Weld Range across sand-plain terrain from outcropping silcrete-capped granitic saprolite in foreground.



As mentioned above, extensive tracts of depositional materials flank the Weld Range. These have been depicted as unit WS1 on the regolith-landform map. This unit comprises older colluvial/alluvial materials characterised by a coarse polymictic lag (see Fig. 5.71 - representative of locality C on overlay to Fig. 5.66). The appearance of this and other depositional units (WD2 and WD3) shown in the Landsat image is nondescript, they appear as browns tinged with blues and reds. The gradational nature of their boundaries is very apparent however. Figure 5.72 illustrates the characteristics of Unit WD3 - alluvial/colluvial deposits on outwash plains. This is representative of locality D on the overlay to Fig. 5.66.

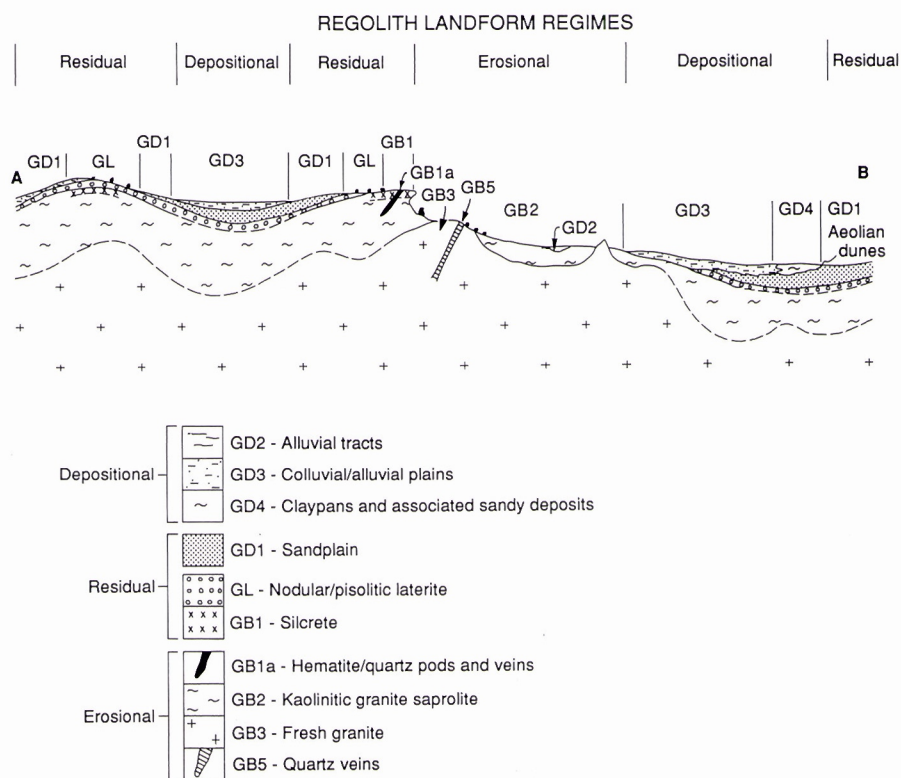


Fig. 5.69 Schematic regolith stratigraphy for the granitic terrain in the Madoonga district, interpreted from surface relationships. Modified from Von Perger (1991). The regolith-landform regimes are those as used by Anand *et al.* (1989, 1991) and summarised in Section 3.3.



#### 5.8.5 *Regolith-landform regimes*

The transparent overlay on the image (Fig. 5.66) shows an interpretation of the regolith-landform regimes that characterise the Madoonga district, using terminology explained in Section 3.3. The interpretation is based on the combined analysis of the Madoonga air-photo mosaic and the enhanced Landsat TM image.

Mapping the broad regolith-landform regimes in an area helps define which geochemical sampling media to use when conducting a geochemical sampling program. For example, in the erosional regimes, soil geochemistry, either conventional soil geochemistry, or bulk-leach cyanide-extractable gold (BLEG), is commonly very effective. However, in the residual regimes, laterite geochemistry is superior to soil geochemistry, because laterite geochemical anomalies are relatively large and consistent. Moreover, soil sampling on a lateritic substrate may result in weaker contrast anomalies, erratic Au patterns, and imposes an extra weathering process to be understood. Much, however, depends on the size fraction used.

#### 5.8.6 *Summary and implications in mineral exploration*

A regional picture of the nature and distribution of regolith-landform associations was established in the Madoonga district through mapping regolith materials at 1:50,000 scale. Spectrally enhanced Landsat TM data, when combined as band ratios in a colour composite of TM bands 5/7 (red), TM bands 4/7 (green) and TM bands 4/2 (blue), proved to be of particular value in mapping regolith materials when used in conjunction with photo-interpretation and field traversing.

These results showed that, when used as part of an integrated exploration strategy, suitably processed Landsat TM data have the potential to assist in the comparison and contrast of regolith-landform units from one exploration area with those of another. This is particularly pertinent when examining or defining geochemical thresholds for different regions, predicting the applicability of geochemical dispersion models and establishing the relative importance of geochemical anomalies.

In addition, being able to predict, with some reliability, the nature of regolith materials using Landsat TM imagery improves the efficiency and effectiveness of mapping the regolith-landform units and regimes in an area. This in turn can help define which geochemical sampling media to use when conducting a geochemical sampling program. Having a regolith-landform framework helps in the design and execution of a geochemical sampling programme properly and enables the appropriate presentation and interpretation of the resultant data.

Table 5.18 summarises the implications in exploration of the research findings.





Fig. 5.70 Regolith and landform relationships in the Madoonga district.

- A. Unit WL1, lateritic residuum marginal to strike ridges of the Weld Range. Incised convex slopes expose mafic saprolite in breakaways and gullies.
- B. Close-up view of lateritic residuum and ferruginous saprolite associated with Unit WL1.







Fig. 5.71 Regolith and landform relationships in the Madoonga district.

- A. Colluvial/alluvial deposits on the flanks of the Weld Range, representative of Unit WS1.
- B. Close up of the coarse polymictic lag of Unit WS1. Fragments of banded iron formation and quartz dominate the lag.







Fig. 5.72 Regolith and landform relationships in the Madoonga district.

- A. Colluvial/alluvial deposits forming outwash plains, representative of Unit WD3. Looking northwards towards the Weld Range.
- B Close up of the fine, polymictic lag lying on fine sandy loams of Unit WD3.



Table 5.18. The implications in exploration listed against the research findings, Madoonga orientation study.

Research Findings	Implications in Exploration
<ul style="list-style-type: none"> <li>• Customised processing of Landsat TM was developed to enhance systematic colour variation and patterns associated with different units of the regolith stratigraphy. Referred to as CSIROREG, is a ratio colour composite (bands 5/7 - Red, 4/7-Green and 4/2 - Blue).</li> <li>• Landsat TM data, when combined with airphoto interpretation and field traverses, provides the basis for regolith-landform mapping at regional and district scales (1:25,000-1:50,000).</li> <li>• Spectrally processed Landsat TM imagery serves as a reliable indicator of regolith material, providing information on regolith stratigraphy, in lateritic environments.</li> <li>• Well documented project material has been generated to assist in processing and interpretation of Landsat TM data.</li> </ul>	<ul style="list-style-type: none"> <li>- Indicates nature and distribution of regolith materials.</li> <li>- Substantially reduces time taken in regolith-landform mapping.</li> <li>- These data are in routine use by some sponsors.</li> <li>- Provides a framework for choice of exploration methods, including the design and execution of a geochemical sampling, data interpretation and use of geophysical methods.</li> <li>- Assists in the comparison and contrast of regolith materials and regolith-landform units from one exploration area to another.</li> <li>- Provides material for training of explorationists.</li> </ul>



## 6.0 CLASSIFICATION OF REGOLITH-LANDFORM MAPPING UNITS

### 6.1 Introduction

It is useful, in exploration, to be able to make comparisons between the regolith-landform mapping units of widely disparate areas. This is particularly relevant when considering geochemical thresholds for different areas and in establishing the relative importance of geochemical anomalies. It is also particularly relevant in deciding the applicability of regolith models in geochemical and geophysical interpretation.

Reasons, including these, led to the topic being set as a priority by sponsors at the first project meeting in September 1991. An expandable, loose-leaf volume entitled *Classification and atlas of regolith-landform mapping units - exploration perspectives for the Yilgarn Craton* (Report 440R) by Anand *et al.* (1993) was produced in November 1993.

This classification scheme and atlas has been designed from an exploration perspective, especially in relation to exploration geochemistry in the Yilgarn Craton. Its objective was to provide standardisation for the description and classification of the diverse range of regolith-landform associations that are mappable on the Yilgarn Craton. Such a standardised mode of description should allow mapping units from one region of the Yilgarn Craton to be compared with those from another. Furthermore, the scheme and atlas should assist in the mapping of regolith-landform associations and subsequent selection of sampling media in geochemical exploration.

The scheme is simple, factual, hierarchical and expandable, to allow incorporation of findings from other areas. The scheme has been tested in the project orientation areas before release to sponsors.

Report 440R (a) classifies regolith-landform relationships in terms of four tables, each having landforms as the horizontal axis and subdivisions of the regolith stratigraphy as the vertical; (b) describes the approach used; (c) sets out instructions for use; and (d) provides examples of maps and corresponding tables for orientation areas selected from the project.

The report should be of interest to exploration geologists, geochemists and geophysicists working in regolith terrains. It is intended to be used in the field at the project geologist level. Codes are provided for entry into digital databases and geographic information systems.

Classification of regolith-landform *mapping units* is a considerably more complex topic than classification of regolith *materials*, for example, as covered in Report 60R. Report 440R is a companion volume to Report 60R and the two are compatible.

### 6.2 Regolith-landform mapping

Recommended procedures for regolith-landform mapping are described in Report 440R. In lateritic terrain it is important to establish the presence or absence of lateritic residuum, and to delineate areas where there is substantial sedimentary cover. Two boundaries are, therefore, very important and need to be clearly delineated in regolith-landform mapping where possible. These are the boundaries which mark the base of the lateritic residuum and those which enclose areas of sedimentary cover. By identifying and delineating these two boundaries, the regolith-landform relationships can be mapped in terms of residual, erosional and depositional regimes, where the focus is on evidence of preservation versus truncation of the lateritic residuum. Where these broad regolith-landform regimes are mapped in an area, it usually becomes clear which media should be sampled in geochemical exploration.

### 6.3 Guide for use

The detailed procedures for use of the classification scheme are outlined in the Report 440R, together with a large body of information in the classification tables. To facilitate the more effective day-to-day use of these classification tables, priorities are set up. In the case of the residual and erosional regimes, priority should be given to ferruginous lag for the basis of the mapping unit nomenclature. Where ferruginous materials are rare, *e.g.* in many areas of erosional regimes, soils, sub-crop and outcrop of bedrock or saprolite should be used instead. In the depositional regimes, the substrate to the transported overburden is preferred for classification and nomenclature, although this is not always possible. Classification of the depositional units is best carried out using shallow drilling to establish the regolith stratigraphy.

The symbols allocated to the mapping units comprise regolith-landform regime, and regolith material (*e.g.* RLA1, where R is for residual regime, LA for lateritic family, 1 for lateritic nodules, pisoliths). The information on the bedrock, from which the regolith has been derived, can be added as a prefix (*e.g.* mRLA1, where m indicates a mafic bedrock sequence). Examples of coded maps from several orientation districts in the Yilgarn Craton are presented in Report 440R. Figure 6.1 and Tables 6.1 and 6.2 reproduced here provide examples.



#### **6.4 Classification tables**

Two versions of classification tables are given. These include (a) classification tables with condensed codes (excluding landforms) and (b) classification tables with extended codes (including landforms).

The classification tables contain information about regolith-landform regimes, landforms and regolith materials, the latter are arranged vertically in the order of the regolith stratigraphy. The system seeks to establish a hierarchical framework for identifying regolith-landform mapping units; that is, units which are defined in terms of various regolith and landform characteristics. The first level is the regime, that is residual, erosional or depositional - where the focus is on preservation and truncation of the lateritic residuum. The second level relates to specific landforms, for example, hills, crest, back slopes, etc. The third level is concerned with the regolith materials themselves, for example, lag or soils.

Alpha-numeric codes are given for all the classifications described. An attempt is made to show the likely occurrence of various regolith types within each regolith-landform regimes and the constituent landform categories. The relationships between the landforms and regolith materials are also presented.

#### **6.5 Atlas of regolith-landform mapping units**

The atlas comprises a collection of representative photographs and accompanying descriptions of regolith-landform mapping units that, with time, can be expanded (Fig. 6.2 provides an example). They are arranged in the same order as those of the classification tables. The classification codes are shown on the right hand side of the photos. The user may then match the appearance and descriptions of these mapping units with those from the area being studied.

The alpha-numeric codes provide links between the photographs, descriptions, classification tables, example maps and models.

#### **6.6 Glossary**

The main terms used in the regolith-landform mapping process are listed alphabetically in the Glossary with standardised notes.

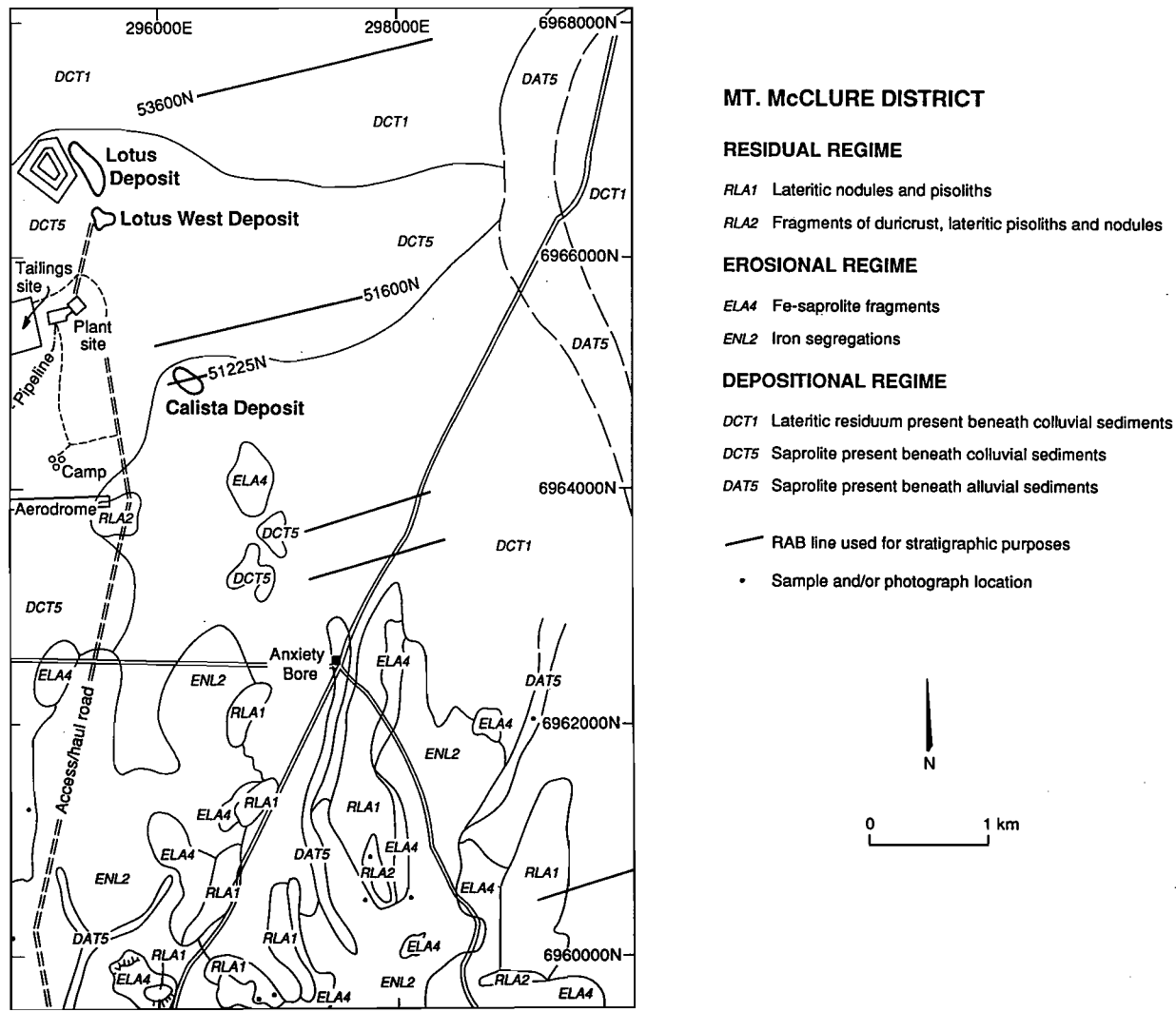


Fig. 6.1 Example of a coded map using the classification scheme for the Mt. McClure district, refer to Tables 6.1 and 6.2.

Table 6.1: Example, classification table for the coded map in Fig. 6.1.

## Mt. McCLURE DISTRICT-LAGS

			Residual regimes(R)		Erosional regimes (E)									Depositional regimes (D)							
			Back slopes	Crests	Back slopes	Crests	Break away	Ridges	High hills	Low hills	Stripped Slopes	Pedl-ments	Undulat-ing plain	Colluvial plains	Alluvial plains	Major drainage floors	Small drainage floors	Valley floors	Playas	Dunes hills plain	
	<i>Clasts</i>	<i>Code</i>	<i>BS</i>	<i>CR</i>	<i>BS</i>	<i>CR</i>	<i>BK</i>	<i>RG</i>	<i>HH</i>	<i>LH</i>	<i>SS</i>	<i>PD</i>	<i>UP</i>	<i>CP</i>	<i>AP</i>	<i>MD</i>	<i>SD</i>	<i>VF</i>	<i>PY</i>	<i>DU</i>	
FERRUGINOUS	LATERITIC FAMILY  <b>LA</b>	Lateritic nodules, pisoliths	LA1	RLA1	RLA1																
		Lateritic nodules, pisoliths, fragments of lateritic duricrust, Fe-saprolite, mottles	LA2		RLA2																
		Lateritic nodules, pisoliths, mottles, Fe-saprolite	LA3	RLA3	RLA3																
		Mottled, Fe-saprolite fragments	LA4			ELA4	ELA4	ELA4			ELA4		ELA4							ELA4	
		Lateritic nodules, pisoliths, fragments of black Fe-rich duricrust, Fe-saprolite	LA5		RLA5																
		Black lateritic nodules, pisoliths, Fe-saprolite	LA6	RLA6	RLA6																
	NON-LATERITIC FAMILY  <b>NL</b>	Gossan fragments	NL1				ENL1			ENL1	ENL1										ENL1
		Iron segregations	NL2								ENL2		ENL2								ENL2
		Fe-lithic fragments	NL3				ENL3	ENL3		ENL3	ENL3		ENL3	ENL3							ENL3
Iron segregations, Fe-lithic fragments		NL4				ENL4				ENL4		ENL4	ENL4							ENL4	
Ferruginous granules		NL5									ENL5		ENL5							ENL5	
NON-FERRUGINOUS	LITHIC FAMILY  <b>LI</b>	Saprolite fragments	LI1				ELI1			ELI1		ELI1	ELI1							ELI1	
		Saprock fragments	LI2				ELI2			ELI2	ELI2	ELI2	ELI2	ELI2						ELI2	
		Bedrock fragments	LI3							ELI3	ELI3	ELI3								ELI3	
		Quartz fragments	LI4						ELI4		ELI4				See following table for codes of depositional regimes						
		Bedrock, saprock, quartz fragments	LI5				ELI5					ELI5								ELI5	
(Lateritic + Non-lateritic + Lithic)  <b>MI</b>	MIXED	Brown ferruginous granules, quartz	MI1											DMI1	DMI1					DMI1	
		Black ferruginous granules, quartz	MI2											DMI2	DMI2					DMI2	
		Iron segregations, lithic fragments, lateritic nodules, pisoliths, quartz	MI3											DMI3	DMI3	DMI3	DMI3	DMI3		DMI3	
		Lateritic nodules, pisoliths, fragments of Fe-saprolite, iron segregations, quartz	MI4											DMI4	DMI4	DMI4	DMI4	DMI4		DMI4	
		Quartz, lateritic nodules, pisoliths	MI5											DMI5	DMI5	DMI5	DMI5	DMI5		DMI5	

Fe=Ferruginous

Prefix: m=mafic; um=ultramafic; f=felsic in greenstone; g=granite; s=sedimentary rocks

Table 6.2: Example, classification table for the coded map in Fig. 6.1.

**Mt. McCLURE DISTRICT-  
SUBSTRATE TO TRANSPORTED OVERBURDEN**

			Residual regimes(R)		Erosional regimes (E)									Depositional regimes (D)						
			Back slopes	Crests	Back slopes	Crests	Break away	Ridges	High hills	Low hills	Stripped Slopes	Pediments	Undulating plain	Colluvial plains	Alluvial plains	Major drainage floors	Small drainage floors	Valley floors	Playas	Dunes
		Code	BS	CR	BS	CR	BK	RG	HH	LH	SS	PD	UP	CP	AP	MD	SD	VF	PY	DU
COLLUVIAL SEDIMENTS	Lateritic residuum present beneath colluvial sediments	CT1												DCT1				DCT1		
	Mottled zone present beneath colluvial sediments	CT2												DCT2				DCT2		
	Ferruginous saprolite present beneath colluvial sediments	CT3												DCT3				DCT3		
	Clay zone present beneath colluvial sediments	CT4												DCT4				DCT4		
	Saprolite present beneath colluvial sediments	CT5												DCT5				DCT5		
	Bedrock present beneath colluvial sediments	CT6												DCT6				DCT6		
	Not known	CT7												DCT7				DCT7		
ALLUVIAL SEDIMENTS	Lateritic residuum present beneath alluvial sediments	AT1													DAT1	DAT1	DAT1	DAT1		
	Mottled zone present beneath alluvial sediments	AT2													DAT2	DAT2	DAT2	DAT2		
	Ferruginous saprolite present beneath alluvial sediments	AT3													DAT3	DAT3	DAT3	DAT3		
	Clay zone present beneath alluvial sediments	AT4													DAT4	DAT4	DAT4	DAT4		
	Saprolite present beneath alluvial sediments	AT5													DAT5	DAT5	DAT5	DAT5		
	Bedrock present beneath alluvial sediments	AT6													DAT6	DAT6	DAT6	DAT6		
	Not known	AT7													DAT7	DAT7	DAT7	DAT7		
EOLIAN SEDIMENTS	Lateritic residuum present beneath eolian sediments	ET1																		DET1
	Mottled zone present beneath eolian sediments	ET2																		DET2
	Ferruginous saprolite present beneath eolian sediments	ET3																		DET3
	Clay zone present beneath eolian sediments	ET4																		DET4
	Saprolite present beneath eolian sediments	ET5																		DET5
	Bedrock present beneath eolian sediments	ET6																		DET6
	Not known	ET7																		DET7

Prefix: m=mafic; um=ultramafic; f=felsic in greenstone; g=granite; s=sedimentary rocks

**mRLA2- FRAGMENTS OF LATERITIC DURICRUST, LATERITIC NODULES, PISOLITHS  
AND FERRUGINOUS SAPROLITE FRAGMENTS- BARDOC QUARRY, KALGOORLIE  
REGION**

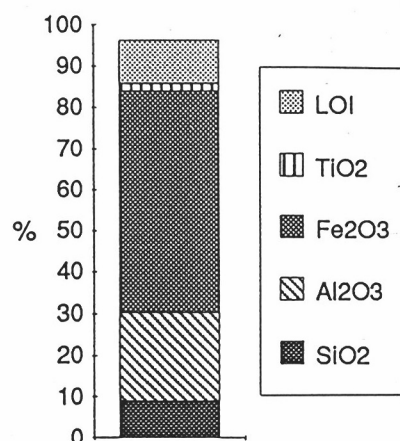
Lateritic nodules and pisoliths, along with some scattered fragments of nodular duricrust occur on a broad, smooth convex crest. This lag is derived from the weathering of gabbro and is dominated by fine to medium (generally <10 mm, with some reaching 20 mm), reddish brown pisoliths and nodules. Goethite, kaolinite and hematite are the major minerals comprising the nodules and pisoliths.

The soil is red, calcareous, gravelly, friable, fine sand clay loam, with moderate, fine pisoliths and nodules. This nodular and pisolitic material relates closely to the underlying calcified lateritic residuum.

Lateritic nodules and pisoliths developed from the weathering of gabbro have the mean chemical composition (N=2) :

<i>SiO<sub>2</sub></i>	<i>Al<sub>2</sub>O<sub>3</sub></i>	<i>Fe<sub>2</sub>O<sub>3</sub></i>	<i>MgO</i>	<i>CaO</i>
9.0%	21.3%	53.5%	0.10%	0.12%
<i>Na<sub>2</sub>O</i>	<i>K<sub>2</sub>O</i>	<i>TiO<sub>2</sub></i>	<i>LOI</i>	
0.01%	<0.06%	1.85%	10.6%	

<i>Mn</i>	<i>Cr</i>	<i>V</i>	<i>Cu</i>	<i>Pb</i>
195ppm	1080ppm	875ppm	114ppm	2ppm
<i>Zn</i>	<i>Ni</i>	<i>Co</i>	<i>As</i>	<i>Sb</i>
24ppm	82ppm	12ppm	15ppm	2ppm
<i>Bi</i>	<i>Mo</i>	<i>Sn</i>	<i>Ga</i>	<i>W</i>
<2ppm	2ppm	3ppm	46ppm	<4ppm
<i>Ba</i>	<i>Zr</i>	<i>Nb</i>	<i>Au</i>	
60ppm	160ppm	4ppm	13ppb	



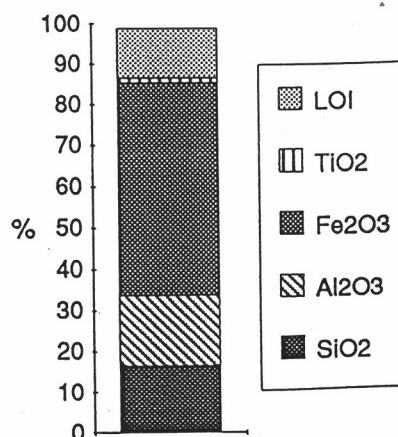
**umELA4 - MOTTLED AND FERRUGINOUS SAPROLITE FRAGMENTS-  
LADY EVELYN AREA, KALGOORLIE REGION**

This example of fragments of mottled and ferruginous saprolite occurs on a broad crest. Fragments of all these materials form a coarse lag (to < 40 mm) and are developed from the weathering of talc-chlorite-schist. The lag is underlain by a shallow, light brown, friable, calcareous sandy clay loam soil, containing like fragments. It overlies 1m thick, calcified ferruginous saprolite. Yellowish brown ferruginous saprolite fragments are goethite-kaolinite-rich, whereas reddish brown fragments are hematite-rich. Small amounts of talc are also present.

Mottled and ferruginous saprolite fragments derived from the weathering of talc-chlorite-schist have the chemical composition:

<i>SiO<sub>2</sub></i>	<i>Al<sub>2</sub>O<sub>3</sub></i>	<i>Fe<sub>2</sub>O<sub>3</sub></i>	<i>MgO</i>	<i>CaO</i>
16.5%	17.2%	51.5%	0.21%	0.12%
<i>Na<sub>2</sub>O</i>	<i>K<sub>2</sub>O</i>	<i>TiO<sub>2</sub></i>	<i>LOI</i>	
0.02%	<0.06%	1.20%	12.45%	

<i>Mn</i>	<i>Cr</i>	<i>V</i>	<i>Cu</i>	<i>Pb</i>
302ppm	11050ppm	692ppm	180ppm	2ppm
<i>Zn</i>	<i>Ni</i>	<i>Co</i>	<i>As</i>	<i>Sb</i>
44ppm	930ppm	72ppm	19ppm	2ppm
<i>Bi</i>	<i>Mo</i>	<i>Sn</i>	<i>Ga</i>	<i>W</i>
<2ppm	<2ppm	2ppm	26ppm	<4ppm
<i>Ba</i>	<i>Zr</i>	<i>Nb</i>	<i>Au</i>	
75ppm	58ppm	2ppm	3ppb	





LAGS

mRLA2



umELA4



Fig. 6.2 An example from the atlas of regolith-landform mapping units showing the alpha-numeric codes for the mapping units and descriptions (opposite).





## 7.0 COMPARATIVE STUDIES OF REGOLITH EVOLUTION AND GEOCHEMICAL DISPERSION

### 7.1 Introduction

Weathering under prolonged humid, stable conditions has resulted in widespread, deep weathering profiles over the Yilgarn Craton. Subsequent differential erosion and chemical modification has added to the complexity. Consequently, there is a great variety of regolith materials exposed on the land surface forming intricate regolith-stratigraphic relationships with the landforms. For geochemical exploration, regolith materials form the dominant sampling media in the initial stages of most programs. Some of these are more appropriate for sampling than others. Thus, an understanding of the regolith-stratigraphic relationships and knowledge of the geochemical and mineralogical characteristics of regolith are key ingredients in effective exploration in lateritic terrains. These factors govern the nature of the geochemical and geophysical expressions of weathered or otherwise concealed ore deposits in these terrains. An understanding of regolith-stratigraphic relationships allows: choice of appropriate exploration methods; design and execution of optimal geochemical programmes; sensible data interpretation; and soundly-based integration of exploration findings.

Three major contrasting geographical regions (the Darling Range, Leonora-Wiluna and Kalgoorlie regions) have been identified based on their regolith-landform characteristics (Table 7.1). This is based on the findings in this project and its precursor. For selected districts within these regions, regolith-landform relationships were mapped, the regolith stratigraphy established, regolith units characterised, models erected, and the regolith evolution interpreted. These aspects are briefly discussed below.

Research findings have been further synthesised in Section 9 where generalised dispersion models and exploration procedures are drawn together.

### 7.2 Regolith Evolution - Darling Range, Leonora-Wiluna and Kalgoorlie regions

#### 7.2.1 Weathering

The Yilgarn Craton has been exposed to long periods of lateritic weathering, involving leaching of alkali and alkaline earth elements and silica, leading to deep kaolinisation of bedrock. During lateritic weathering, much of the ferrous iron, released into the groundwaters by breakdown of the primary minerals can, particularly where the water table is near the ground surface, be oxidised and precipitated. As a result, a ferruginous horizon (lateritic residuum and ferruginous saprolite) typically develops in the upper part of the deeply weathered profile (Fig. 7.1). The left hand side of the figure shows a profile commonly developed through lateritic weathering of mafic and ultramafic rocks, with a characteristic ferruginous saprolite. Lateritic residuum, in such cases, is formed by the fragmentation of ferruginous saprolite. In contrast, a profile with a strongly developed mottled zone commonly formed on felsic bedrocks, is shown on the right.

Rocks rich in Fe, however, may weather directly to Fe-rich duricrusts without forming deep saprolites. Furthermore, under some circumstances, it seems that thick, widespread, red, clay soils may form instead of well developed laterite. Such is the case in the Kalgoorlie region, where red soils probably once blanketed much of the land surface.

The chemical composition (major, minor and trace elements) of lateritic residuum is largely lithodependent at a landscape scale. However, there is evidence to suggest that some Fe-rich black duricrusts may have been produced by the absolute accumulation of Fe in valley floors, followed by relief inversion in response to drainage incision (Sections 3.4.1 and 3.5.1). Detailed work has shown that lateritic nodules and pisoliths in lateritic residuum are formed by a combination of several processes, including ferruginisation, fragmentation, residual accumulation and multiple phases of leaching, migration and deposition of Fe-oxides. Biological processes also contribute to this re-organisation. Thus, formation of lateritic residuum is complex, consisting of numerous stages expressed by different facies. Most residual lateritic pisoliths and nodules have thin (1-2 mm) goethite-kaolinite-rich cutans and were formed by the deposition of Fe and Al around a nucleus.

In the Darling Range, the lateritic residuum is very highly weathered and markedly aluminous. Here, in the upper part of the profile, kaolinite is weathered to gibbsite. The major secondary minerals are gibbsite, hematite, and goethite. Inland, the lateritic residuum from similar parent rock types tends to be less aluminous, more ferruginous and the major minerals are kaolinite, hematite, and goethite together with relict quartz. Black, lateritic pisoliths, both in the Darling Range and inland, are generally magnetic and are more abundant near the surface. The non-magnetic pisoliths contain greater amounts of goethite and kaolinite relative to the magnetic pisoliths, whereas maghemite is present only in magnetic pisoliths.

Table 7.1 Salient regolith, landform and vegetation features in the Darling Range, Kalgoorlie and Leonora-Wiluna Regions.

Regolith	Darling Range	Kalgoorlie Region	Leonora-Wiluna Region*
Annual rainfall	1000 mm	230-250 mm	approx. 200 mm
Vegetation	Eucalyptus (Jarrah)	Eucalyptus (Salmon gum)	Acacia (Mulga)
Landform	Undulating lateritic plateau, high relief	Gently undulating terrain, low relief	Gently undulating terrain, low relief
Depth of weathering	Variable	Highly variable	Variable
Thickness of <i>in situ</i> profiles	Shallow (upper slopes) to deep (midslopes)	Very shallow (uplands) to deep (plains)	Deep
Calcareous clays	Absent	Abundant	Trace
Pedogenic carbonates	Absent	Abundant	Trace
Plastic red clays	Absent	Abundant	Absent
Ferruginous granules** in soils	Absent	Common	Trace
Aeolian quartz in top 1m	Absent	Abundant	?
Colluvium/alluvium	Shallow	Shallow to deep	Deep
Hardpan in colluvium/alluvium	Absent	Shallow, mild	Deep
Lateritic residuum	Extensive, discontinuous (bauxitic)	Patchy (ferruginous)	* Extensive, discontinuous (ferruginous)
Fe-rich duricrust	Absent	Patchy	Patchy
Hardpan in lateritic residuum	Absent	Absent	Common
Silicified/calcified lateritic residuum	Absent	Common	Common
Mottled zone	Extensive (bauxitic)	Common	Common
Mega-mottles in palaeochannel profiles	Absent	Common	Absent
Ferruginous saprock/saprolite	Absent	Common	Extensive
Fe-segregations in saprolite	Absent	Rare	Abundant
Geochemical sampling media favoured for reconnaissance, area evaluation and initial target definition	Lateritic residuum particularly fragmental duricrust	Ferruginous granules in soils, mottles in ferruginous saprolite, calcareous soils	Lateritic residuum, ferruginous saprolite, iron-segregations

\* Buried complete laterite profiles occur.

\*\* Ferruginous granules occur in soils or as lag. They are black, sub to well-rounded and vary in size from 0.5 to 10 mm.

Various other forms of Fe-enrichment (such as iron segregations) also occur within the saprolite and ferruginous saprolite. Iron segregations, representing zones of intense ferruginisation, occur as pods, lenses and large slabs. Its members are not confined to a single unit of the regolith stratigraphy. Their Fe is derived from a variety of sources including weathering of Fe-rich lithologies, gossans, leaching from upper horizons and upland areas. Iron segregations are black and are dominated by goethite, with variable amounts of hematite and quartz. It is significant that the iron segregations do not have cutans. The members of the iron segregation family can also be distinguished chemically from members of the lateritic family. Iron segregations have generally more Fe, Mn, Zn, Co, Cu and Ba and less  $\text{Al}_2\text{O}_3$ ,  $\text{TiO}_2$ , Cr, V, Ga and Zr contents than the laterite family. Different thresholds have, therefore, to be used in geochemical exploration based on samples of iron segregations, or a lag derived from them, than those used in laterite geochemistry.

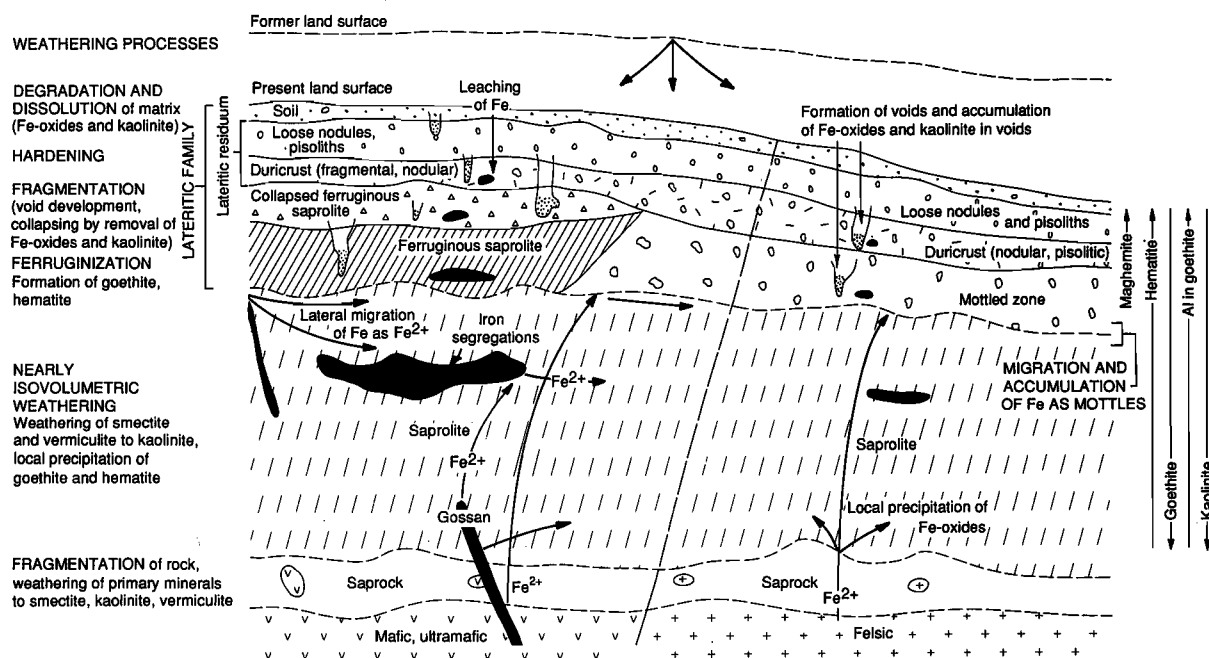


**Fig. 7.1** Diagram showing the differences in the characteristics of the weathering mantle developed from mafic, ultramafic and felsic bedrocks. This diagram is based on findings in the Darling Range and the Mt. Gibson, Lawlers, Mt. McClure and Bottle Creek districts.

Several well-defined regolith types occur in all three regions and relate, directly or indirectly, to a deeply weathered mantle and to its modification by regolith-landform processes. As used in this report, regolith materials include horizons of deep profiles developed by in situ weathering of bedrock and units of transported debris, derived from local weathering profiles by erosion. Many of the regolith types, resulting from these complex processes, occur in distinctive patterns. These are described in terms of the distribution of (a) residual regimes, where the near-complete lateritic profile is preserved; (b) erosional regimes, where the lateritic profile has been truncated to the level of saprolite or bedrock; (c) depositional regimes, characterised by sedimentary units largely derived by the erosion of the lateritic profile (Section 3.3; Anand *et al.*, 1989; Anand *et al.*, 1991).

Erosion has occurred in each of the geographical regions discussed, however, the extent of the stripping varies. In the Leonora-Wiluna region, (e.g. in the Mt. McClure and Lawlers districts, Sections 5.3 and 5.4 in this report; and Section 4.4, Lawlers, in Report 236R), residual regimes vary considerably in area, depending on erosional stripping, which can be extensive, exposing various levels of the saprolite. The detritus from this process has commonly accumulated in low-lying areas, forming alluvial and colluvial plains. The depositional regimes represent areas that are dominated by a regolith generally of diverse origin. Research and extensive exploration drilling have shown that complete laterite profiles can occur buried beneath the sediments, which can reach 30 m or more in thickness, particularly in the extensive alluvial plains (Fig. 7.2). In some districts (e.g. Lawlers, Mt. McClure) buried complete lateritic profiles are common.

In the Kalgoorlie region, residual regimes, as defined above, are localised, patchy and are dominated by black, Fe-rich duricrusts. In depositional regimes, calcareous clays (with a thickness of 0.2-1 m) are common at the surface. Their immediate substrate is acid, red clay, rather than lateritic residuum as seen in many of the depositional regimes at Lawlers and Mt. McClure (Fig. 7.3). These soils may contain significant amounts of aeolian quartz. Red clays are uniformly Fe-stained and commonly contain ferruginous granules. Presence of the ferruginous granules in the red clays is a notable feature in the Kalgoorlie region. Red clays are generally underlain by a thick saprolite. The landscape is characterised by extensive stripping of upland areas, very shallow to deep weathering, patchy development of laterite and extensive occurrence of red soils. In contrast, lateritic residuum is widely preserved in the Darling Range. Depositional regimes are restricted in the Darling Range possibly because of high relief coupled with high rainfall, which, together, cause sediments to be mostly removed.

Calcareous earths and pedogenic carbonates are extensive in the Kalgoorlie region. In contrast, in the Leonora-Wiluna region, there is little development of pedogenic carbonate, but valley calcretes are common along stream channels. Hardpan is extensive, both in the residual and transported materials, in the Leonora-Wiluna region. *Hardpanisation* commonly occurs within the top few metres of the regolith, particularly in wide, past or present depressions. The maximum penetration of hardpanisation seems to be about 15 m. Widespread hardpanisation of many regolith units indicates mobilisation and deposition of silica in the upper regolith. Hardpanisation appears to have resulted from periodic waterlogging of the sediments and the underlying regolith, followed by desiccation under semi-arid to arid conditions. Some of the carbonate has developed subsequent to the hardpan, forming stringers of soft carbonate along subhorizontal partings. Calcrete is most extensive on the more stripped land surface. Erosion and stripping of the upper, more weathered, parts of the regolith, appear to be important factors influencing the gross distribution of carbonates coupled with the distribution of mafic and ultramafic rocks.

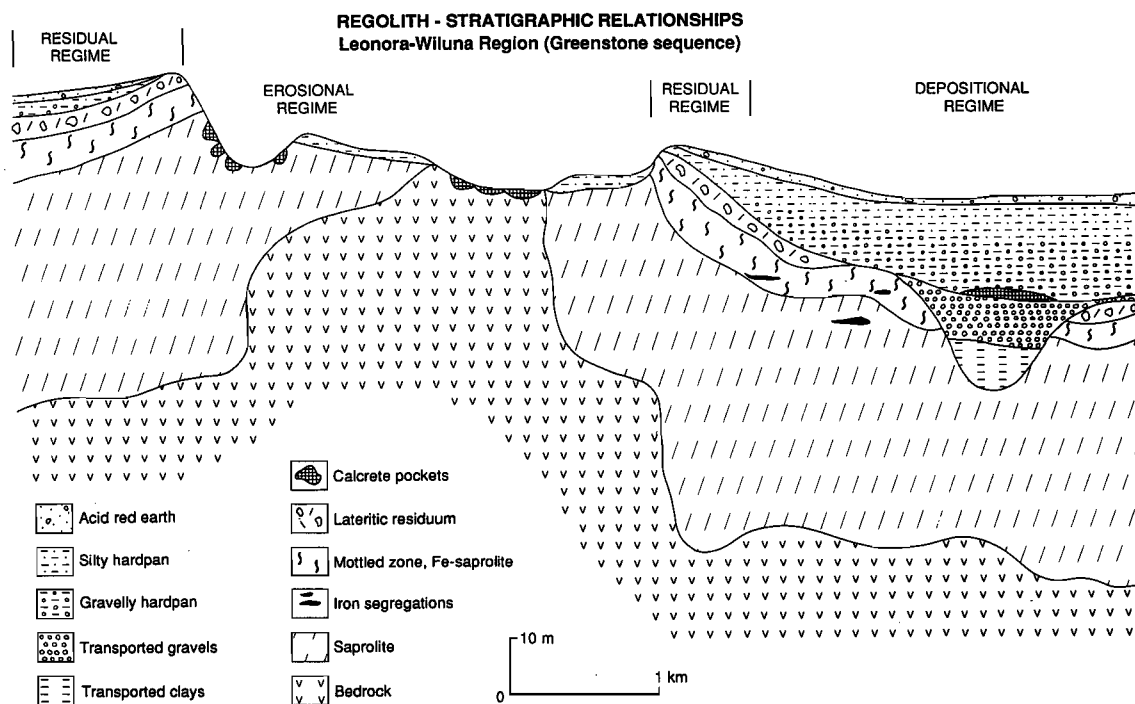


Fig. 7.2 Generalised regolith-stratigraphic relationships for the Leonora-Wiluna region.

Hardpan and calcrete do not occur in the regolith of the Darling Range. However, strong leaching of the upper horizons, under a thick vegetative cover, has given rise to a bauxitic horizon (Fig. 7.4).

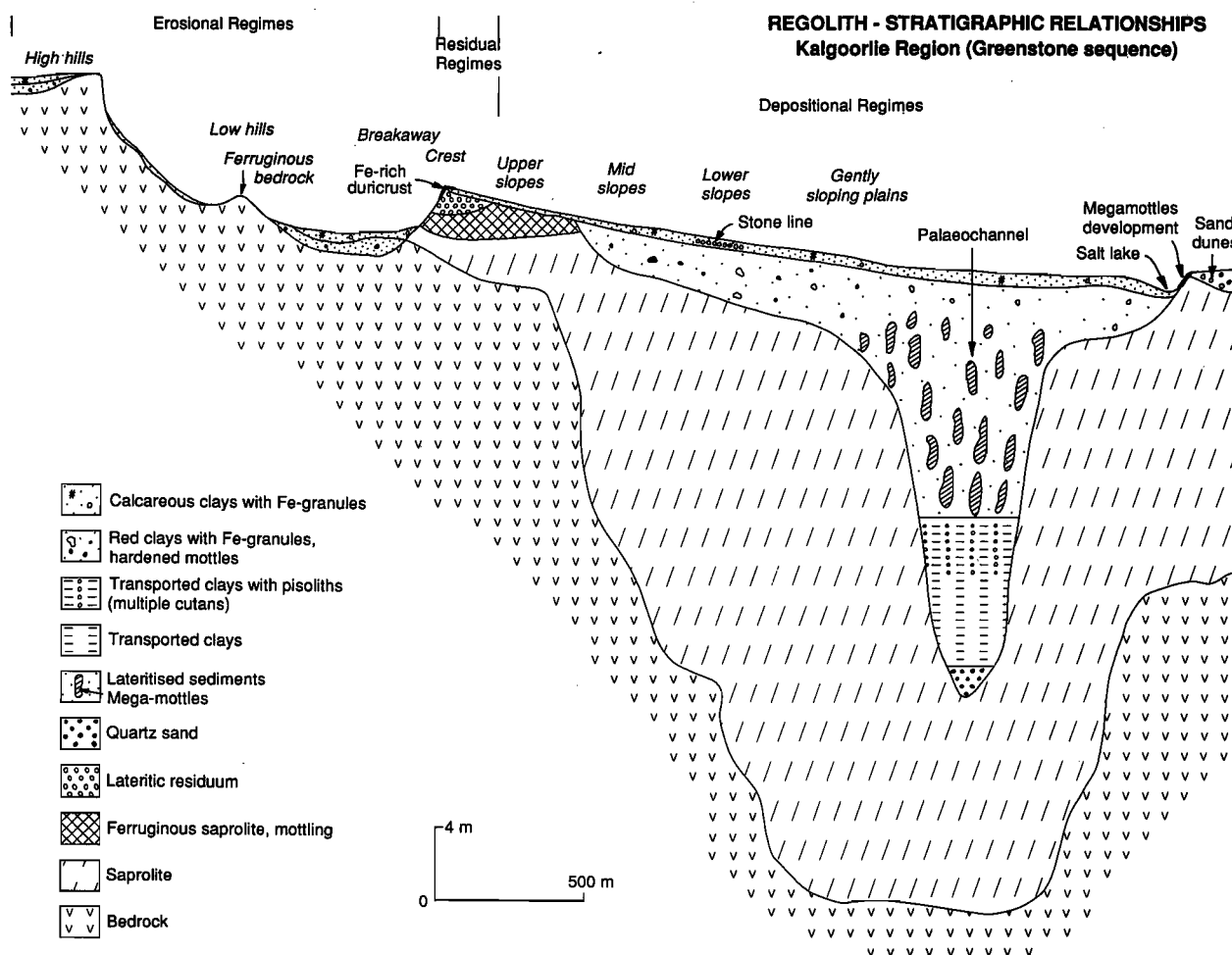


Fig. 7.3 Generalised regolith-stratigraphic relationships for the Kalgoorlie region.

### 7.3 Geochemical dispersion - Darling Range, Leonora-Wiluna and Kalgoorlie regions

In geochemical exploration, regolith materials form the dominant sampling media in the initial stages of most programmes in those areas where bedrock has very restricted outcrop or is completely concealed beneath surficial regolith units. Understanding the regolith-landform framework for a region assists an appreciation of geochemical dispersion and thus provides a basis for developing sampling strategies in weathered terrain. As discussed above, the Darling Range, Leonora-Wiluna, and Kalgoorlie regions are characterised by different arrays of regolith types and each requires a different geochemical exploration approach, particularly in terms of choice of sampling media.

In the Darling Ranges and in the Leonora-Wiluna region, the lateritic residuum and ferruginous saprolite form ideal sampling media for use in reconnaissance down to target definition. Here it is necessary to seek widespread dispersion haloes for Au, base metals and target associated elements. Ferruginous saprolite is commonly formed where the bedrock sequences are mafic and ultramafic. Compared with lateritic residuum, the ferruginous saprolite is less weathered and is closer in geochemical characteristics to the mineralisation. Samples may be collected from the surface (although Au may be depleted at surface in high rainfall areas) or near surface in residual and erosional regimes.



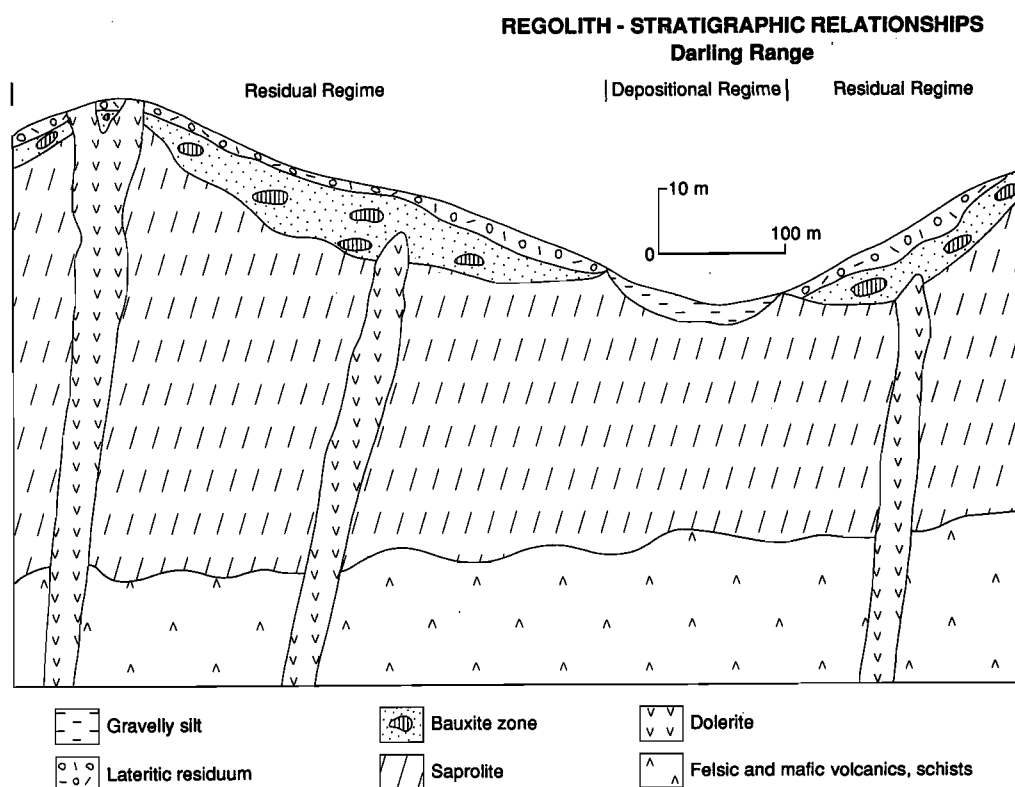


Fig. 7.4 Generalised regolith-stratigraphic relationships for the Darling Range.

In depositional areas, broad Au anomalies and anomalous concentrations of ore-related elements in buried lateritic residuum and ferruginous saprolite can be effective indicators of primary and supergene Au mineralisation (Fig. 7.5). This requires accurate, sub-surface sampling of the lateritic materials and knowledge of the regolith stratigraphy (Anand *et al.*, 1991; Smith *et al.*, 1992). In drilling to sample buried laterite, it is important to recognise and distinguish between the hardpanised colluvium containing lateritic debris and residual laterite and ferruginous saprolite. Iron segregations are suitable sampling media in partly truncated areas (*e.g.* Lawlers district), in lieu of lateritic residuum and ferruginous saprolite (Anand *et al.*, 1991; Smith *et al.*, 1992).

Enrichment in Au and ore-related elements can occur towards the base of hardpan (particularly gravelly hardpan), overlying lateritic residuum. Such is the case in the Lawlers, Mt. McClure and Mt. Gibson Au deposit orientation studies. The occurrence of Au and anomalous concentrations of ore-related elements in the transported overburden has considerable exploration significance. The Au-enrichment in the hardpan may reflect the original levels of Au in the materials derived from the erosion of the upper parts of the weathering profiles nearby. Introduction of Au into the hardpan at a much later stage is also a possibility.

In the Kalgoorlie region where the occurrence of lateritic residuum is patchy, alternative sampling media are required. Ferruginous granules and mottles in soils and sediments and ferruginous saprolite and calcareous soil are the preferred sampling media, even in areas of transported cover, and give superjacent anomalies to concealed mineralisation (Fig. 7.6). Ferruginous granules commonly occur in red soils and the multi-element anomaly, defined by these ferruginous granules, seems to be much broader and stronger than in the soils, considerably enlarging target size.

There are differences in the distribution of Au in the ferruginous saprolite and lateritic residuum as revealed by the Boddington orientation study, in comparison with the distributions of Au seen in the Mt. Gibson, Lawlers and Bottle Creek orientations (Table 7.2). Lateritic Au deposits were formed at each, possibly during the same lateritisation period, when climatic conditions were similar over most of the Yilgarn Craton. However, differences in the present climate and geomorphology are probably responsible for the differences in the nature of the lateritic residuum and the distribution of Au in the profile. The current climatic conditions experienced at Mt. Gibson and Lawlers (semi-arid and arid) are

different from those at Boddington (moderately high, seasonal rainfall). Thus, the non-bauxitic nature of the laterite at Mt. Gibson, Lawlers and Bottle Creek, compared with the bauxitic laterite at Boddington, is probably a function of the difference in present rainfall, vegetation and drainage characteristics (intensity of leaching) at these deposits. Bauxite formation has been shown to be related to the present-day topography and required an adequate, seasonal rainfall to remove Si from the clay zone. The surface lateritic pisoliths and nodules in the Boddington area differ in mineralogy and chemical composition from those at Mt. Gibson and other parts of the Yilgarn Craton. An explanation for the abundant maghemite and amorphous Al-oxide in surface lateritic pisoliths and nodules at Boddington may be the high temperatures reached in bush fires which are comparatively common due to thick vegetation at Boddington.

The trend in the distribution of Au in the ferruginous part of the profile at Boddington is opposite to those of the Mt. Gibson, Bottle Creek and Lawlers Au deposits (Fig. 7.7). At Boddington, Au decreases in abundance upwards from the bauxite zone through lateritic duricrust to loose nodules and pisoliths, but Au increases in abundance from the mottled zone and ferruginous saprolite to loose nodules and pisoliths at Mt. Gibson and Lawlers. Gold is low to almost absent in the surficial lateritic pisoliths and nodules at Boddington. The differences in abundance and position of Au within the ferruginous part of the profile may be a function of the differences in leaching. At Boddington, high rainfall and water, rich in organic materials produced from the abundant vegetation, may result in the leaching of Au from the loose pisoliths. The leached Au is dissolved by organic acids and reprecipitated at the base of the bauxite zone. Such processes have been discussed for Au mobility in tropical rain forest soils of Ghana by Bowell *et al.* (1993).

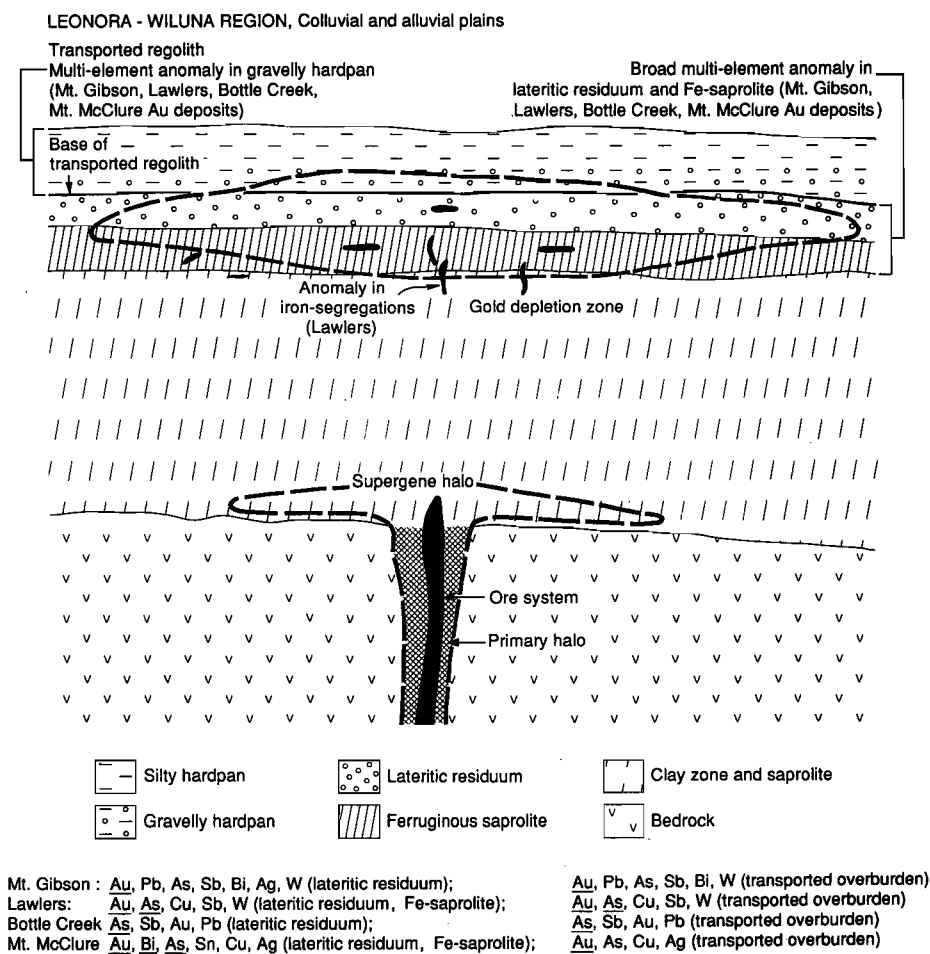


Fig. 7.5 Generalised geochemical dispersion model for the colluvial and alluvial plains of the Leonora-Wiluna region.

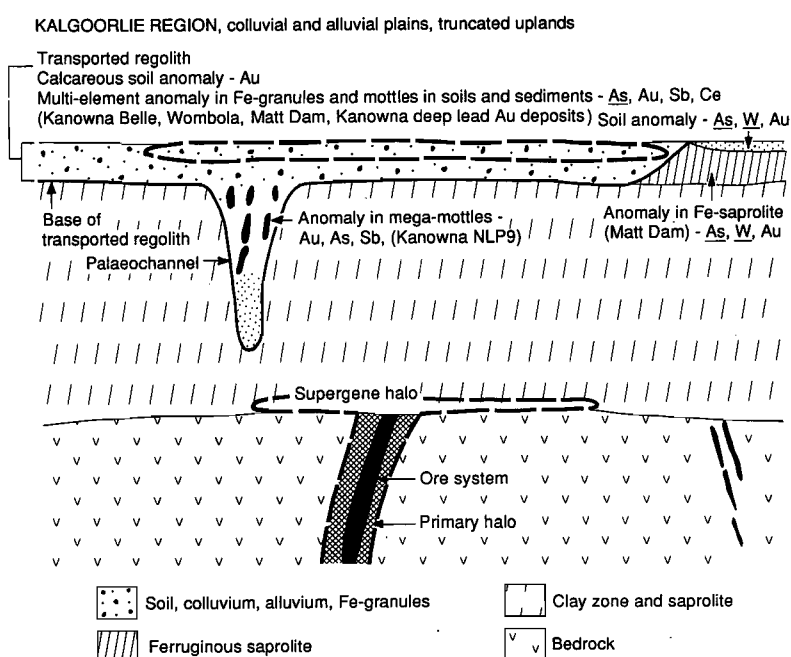


Fig. 7.6 Generalised geochemical dispersion model for the Kalgoorlie region.

Table 7.2 Comparison of the Boddington and Mt. Gibson Gold Deposits

	Boddington	Mt. Gibson
Average annual rainfall	810 mm	250 mm to 280 mm
Landform	Gently undulating terrain, low relief	Undulating lateritic plateau, high relief
Lateritic deposit	Gold occurs in lateritic residuum	Gold occurs in lateritic residuum
Lateritic residuum	Bauxitic	Non-bauxitic
Carbonates, Silcrete	Not present	Calcified/silicified duricrust
Kaolinite in lateritic residuum	Minor	Abundant
Gibbsite in lateritic residuum	Abundant	Traces
Maghemite in loose pisoliths	Abundant	Minor
Au in loose pisoliths	Little or no (0.08 ppm*)	Abundant (2.51 ppm)
Au in lateritic duricrust	Minor (0.11 ppm pisolitic duricrust, 0.6 ppm fragmental duricrust)	Abundant (1.83 ppm)
Au in mottled/bauxite zone	Abundant (1.96 ppm)	Moderate (0.80 ppm)
Size of Au particles	Fine grained <5µm	Fine grained 15-100µm
Depletion zone	Occurs in clay zone and saprolite	Occurs in clay zone and saprolite
Primary Au	Occurs in quartz veins	Occurs in quartz veins
Lateritic enrichment	Evident in saprolite	No trend
Dispersion of Au	More than 500 m (Davy and El-Ansary, 1986)	50-100 m
Multi-element dispersion	As, W, Sn, Mo, Bi	Cu, Bi, As, Pb

\* Mean abundance

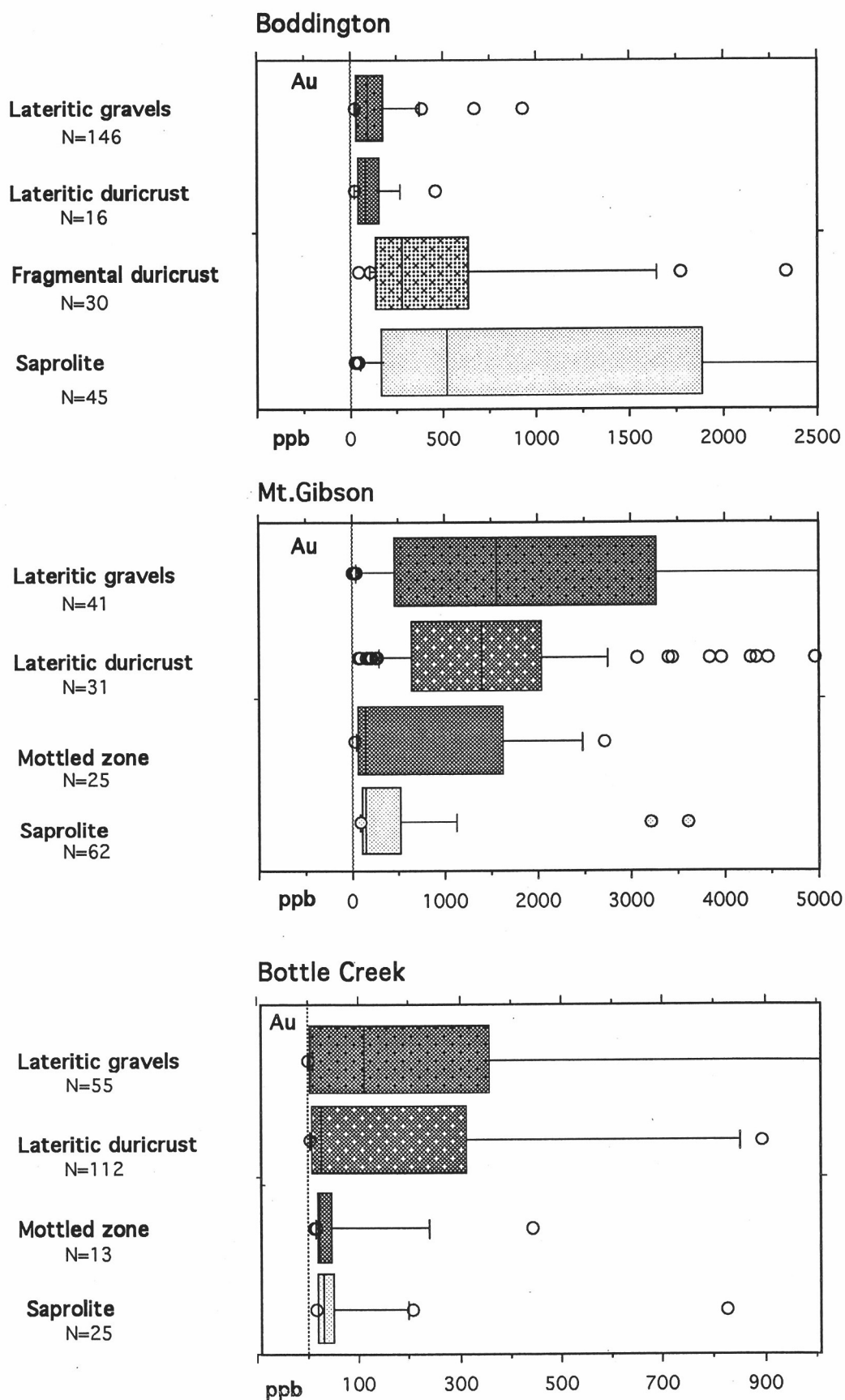


Fig. 7.7 Box plots showing the distribution of Au in selected units of the regolith stratigraphy for the Boddington, Mt. Gibson and Bottle Creek orientation areas.

#### 7.4 Implications in exploration

In the Leonora-Wiluna region, Au and ore-related elements are associated with the lateritic residuum, ferruginous saprolite and iron segregations. However, in the Kalgoorlie region, lateritic residuum is scarce, and emphasis can be placed on Au and target-associated elements in ferruginous granules, mottles, ferruginous saprolite and calcareous soils. Ferruginous granules (Table 7.3) and mottles commonly occur in soils and sediments and give broad multi-element anomalies related to the underlying mineralisation. Different geochemical thresholds generally apply to different sampling media.

Gold may accumulate in some units of the hardpan (*e.g.* Mt. Gibson, Lawlers, Mt. McClure Au deposits). In these cases, sampling the gravelly hardpan can delineate a multi-element geochemical dispersion halo. However, these findings cannot be extrapolated to all the areas where hardpan is present. Furthermore, mechanisms of Au enrichment in hardpan are not yet understood and hardpan therefore cannot be used as a reliable sampling medium.

Table 7.3 Comparison of the recommended geochemical sampling media in exploration for Au deposits in the Darling Range, Leonora-Wiluna, and Kalgoorlie regions.

Darling Range (Boddington Au deposit)	Leonora-Wiluna Region (Mt. Gibson, Bottle Creek, Lawlers, Mt. McClure Au deposits)	Kalgoorlie Region (Kanowna Belle, Matt Dam, Wombola deposits)
<ul style="list-style-type: none"> <li>• Lateritic pisoliths and nodules</li> <li>• Lateritic duricrust</li> <li>• Fragmental duricrust (has most reliable Au geochemical patterns)</li> </ul> <p>The above sample media are exposed at the surface or concealed beneath shallow soil (&lt;1m).</p>	<ul style="list-style-type: none"> <li>• Lateritic pisoliths and nodules</li> <li>• Pisolitic-nodular duricrust</li> <li>• Ferruginous saprolite</li> <li>• Iron segregations</li> </ul> <p>The above sample media are exposed at the surface in the residual and erosional regimes or buried beneath the sediments (3-30m).</p>	<ul style="list-style-type: none"> <li>• Ferruginous granules and mottles in soils and sediments</li> <li>• Ferruginous saprolite</li> <li>• Soils</li> </ul> <p>These materials occur near the surface (&lt;3m).</p>

## 8.0 DATA INTERPRETATIONAL METHODS

### 8.1 Introduction

Following the usefulness of multi-element geochemistry in the precursor project, well-characterised regolith samples have continued to be analysed and the resultant data investigated by several methods during this extension. Multi-element geochemistry has shown that a variety of useful sample types accumulate different indicator elements over mineralisation, but that interpretation of the surface anomalies is dependent on understanding the regolith-landform situation of both the mineralisation and the sample medium. Interpretation of geochemical data in parallel with field studies is therefore an essential component of data interpretation.

Interpretation of complex multi-element data is facilitated by graphical procedures. Line plots of geochemical data along traverses over mineralisation can be used to compare variation of elemental concentrations in different sample types. As Garrett (1993) states, even with sophisticated multivariate tools at our disposal, there is a need for thorough preliminary exploratory data analysis (EDA). For example, normal probability plots illustrate the frequency distribution of the data and compare them to a normal distribution, highlighting outliers and revealing whether they are polymodal (Garrett, 1993). Graphical procedures that help visualise the relationship between data and expression of mineralisation in the regolith will particularly assist exploration. The procedures used below in the interpretation of geochemical data sets are taken, in part, from Grunsky (1991). Progress has been aided by significant improvements in commercially available, interactive, graphical software which was used in the EDA stage. Demonstrations of the use of this software have been given to individual sponsors during the term of the project.

Those data used for the comparisons are taken from project orientation areas widely distributed across the Yilgarn Craton. Areas from the Kalgoorlie region are not represented because of the general abundance of erosional and depositional regimes there, and the consequent scarcity of lateritic residuum.

### 8.2 Some comparisons between data sets

#### 8.2.1 *Major elements*

Combining the data sets from Boddington, Bottle Creek, Mt. Gibson and Lawlers in a triangular plot of  $\text{SiO}_2$ ,  $\text{Al}_2\text{O}_3$  and  $\text{Fe}_2\text{O}_3$  (Fig. 8.1) indicates the range of regolith compositions sampled in the project and its precursor. The mineralogy of these regolith samples can be described largely in terms of kaolinite, gibbsite/boehmite, hematite/goethite, and quartz. Bedrock type, location in the landform and the degree of post-lateritisation leaching influence the major, minor and trace element geochemistry.

The well-leached, acid environment of Boddington, which is within a world-class bauxite province, produces a  $\text{SiO}_2$ -poor and  $\text{Al}_2\text{O}_3$ -rich, lateritic residuum (Fig. 8.2A). This is in marked contrast with the arid environment of Bottle Creek which is characterised by an  $\text{Fe}_2\text{O}_3$ -rich,  $\text{Al}_2\text{O}_3$ -poor, lateritic residuum (Fig. 8.2B). The lateritisation processes at Lawlers, where mafic to ultramafic bedrock dominates, have produced a lateritic duricrust of cemented fragments of ferruginous saprolite. A restricted range of compositions for the three sample types at Lawlers is shown in Fig. 8.2C. Ternary plots have a severe limitation in that they plot ratios. They only approximate true proportions where the three components plotted make up the majority of the sample material (as here for Si, Al, Fe in regolith).

Stacked box and whisker plots can be useful in comparisons of different materials from several study areas. Box plots show medians, the 25th and 75th percentiles at the ends of the boxes. The 10th and 90th percentiles are represented by the whiskers. Major elements in lateritic residuum from four of the orientation areas are compared in Fig. 8.3. This shows that  $\text{Al}_2\text{O}_3$  has a small range in each of the study areas, relative to the ranges of  $\text{Fe}_2\text{O}_3$  and  $\text{SiO}_2$ . The lateritic residuum from Boddington has little  $\text{SiO}_2$  and this has a very restricted range, despite being derived from felsic, intermediate and mafic rock types. This reflects the bauxitic tendency of the regolith at Boddington.

The use of interactive data manipulation software has the capacity to rotate these components plotted on three mutually perpendicular axes and separate sample groups that would otherwise overlap on a binary plot (Fig. 8.4). The two sample groups used to illustrate this are calcretes and calcified lateritic residua from Mt. Gibson (where the Si-Al-Fe-rich compositions of the lateritic samples are diluted by calcite), and bauxitic, lateritic residuum from Boddington (where samples have more  $\text{Al}_2\text{O}_3$  than can be accommodated in kaolinite). However, the majority of samples lie within the Si-Al-Fe plane at right angles to the page (Fig. 8.4).



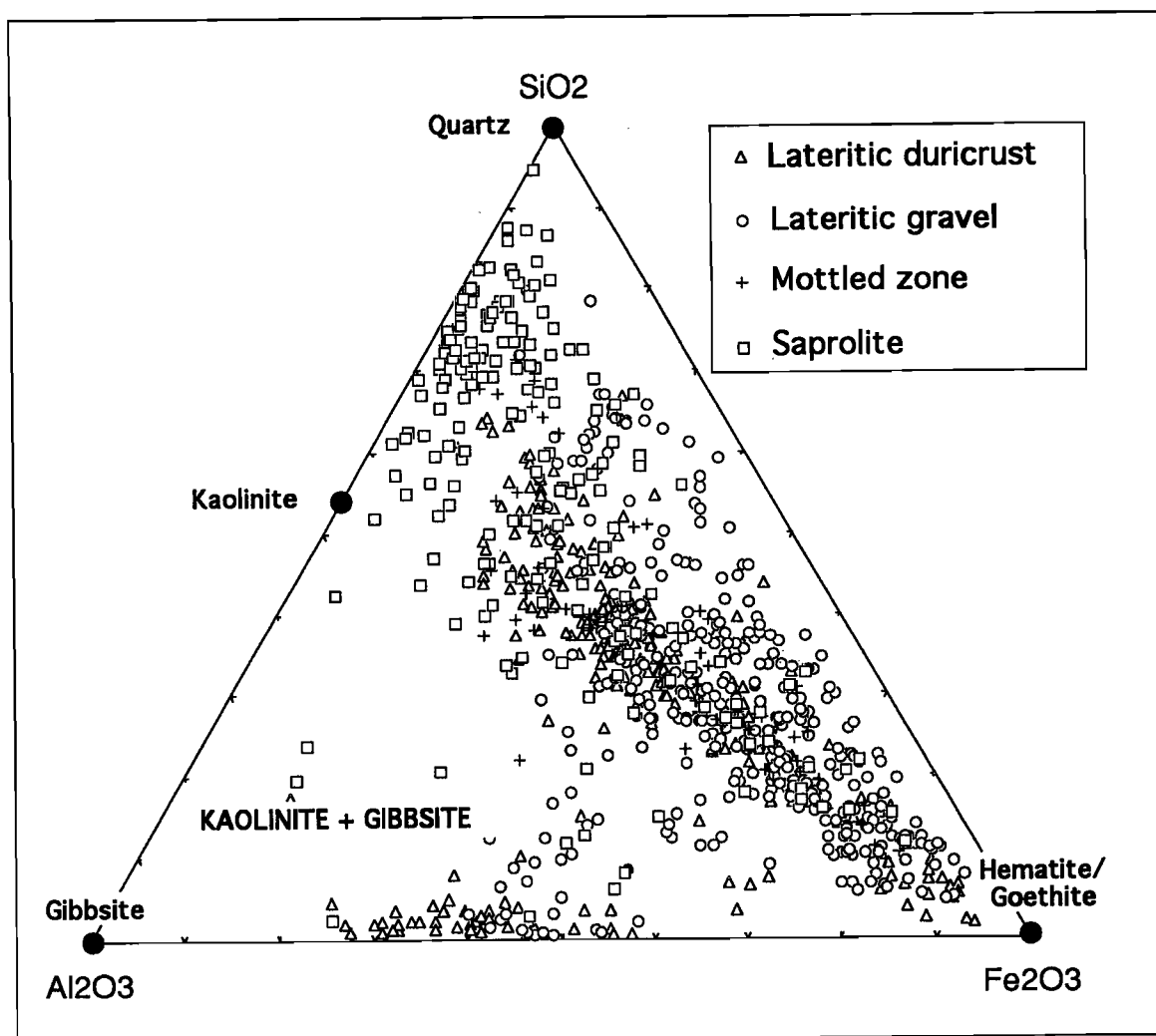


Fig. 8.1. A ternary diagram of  $\text{SiO}_2$  -  $\text{Al}_2\text{O}_3$  -  $\text{Fe}_2\text{O}_3$  showing the spread of sample compositions for four samples types from Boddington, Bottle Creek, Mt. Gibson and Lawlers orientation areas.

Bauxitic, lateritic residua, shown in Fig. 8.5A, form the majority of the samples, having more than 30%  $\text{Al}_2\text{O}_3$  relative to the trend of the kaolinitic group of samples. Some samples from Mt. Gibson, containing gibbsite, are included in the bauxitic group, which are mainly from Boddington. The bimodal distribution of the data is also demonstrated in the  $\text{Al}_2\text{O}_3$  histogram, Fig. 8.5B, which shows less detail because the data are allocated into intervals (in this example into 24 intervals of 2 wt %  $\text{Al}_2\text{O}_3$ ).

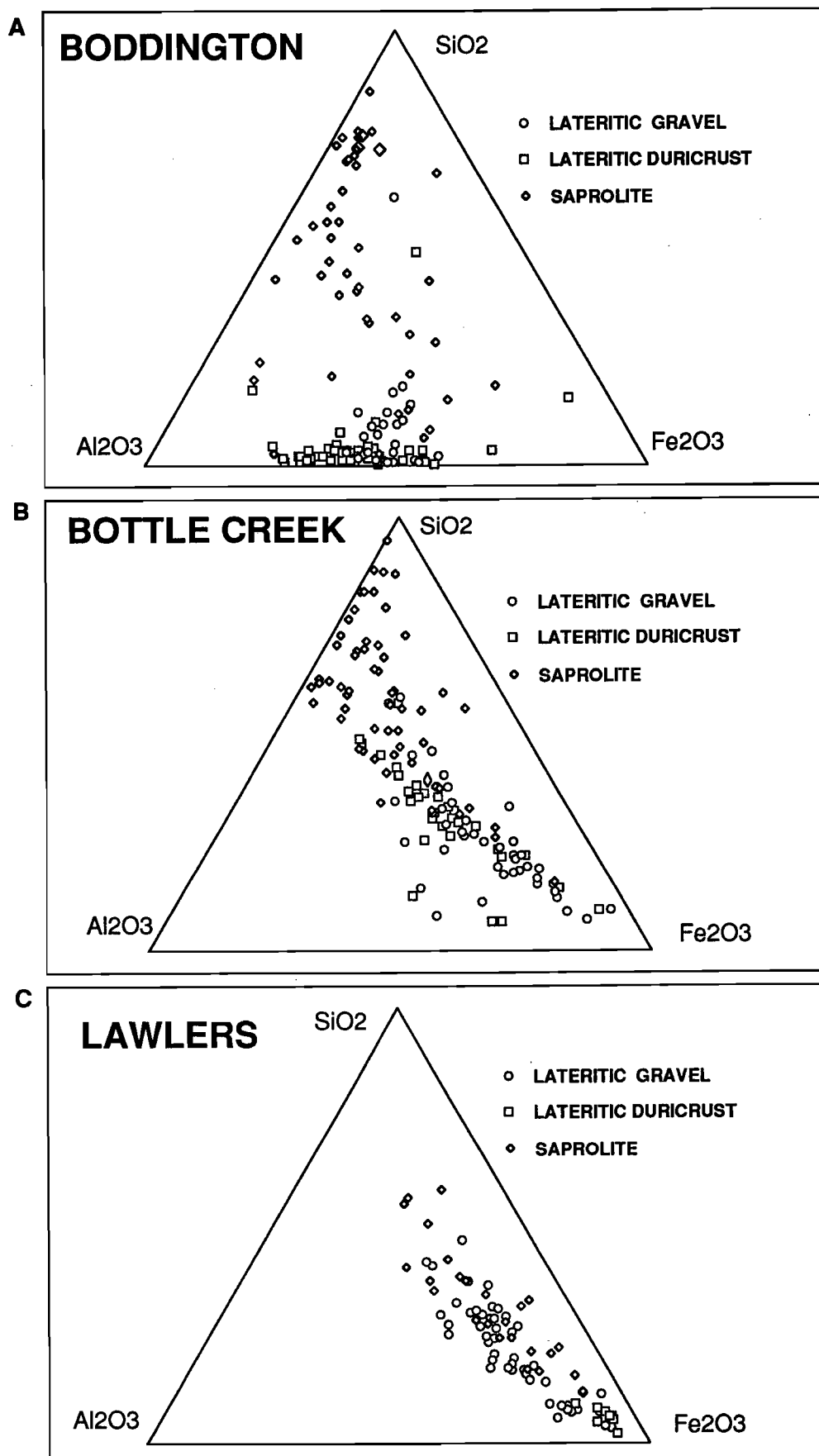


Fig. 8.2. Ternary plots for SiO<sub>2</sub> - Al<sub>2</sub>O<sub>3</sub> - Fe<sub>2</sub>O<sub>3</sub> with data on three sample types separated into three orientation areas: Boddington, Bottle Creek and Lawlers.

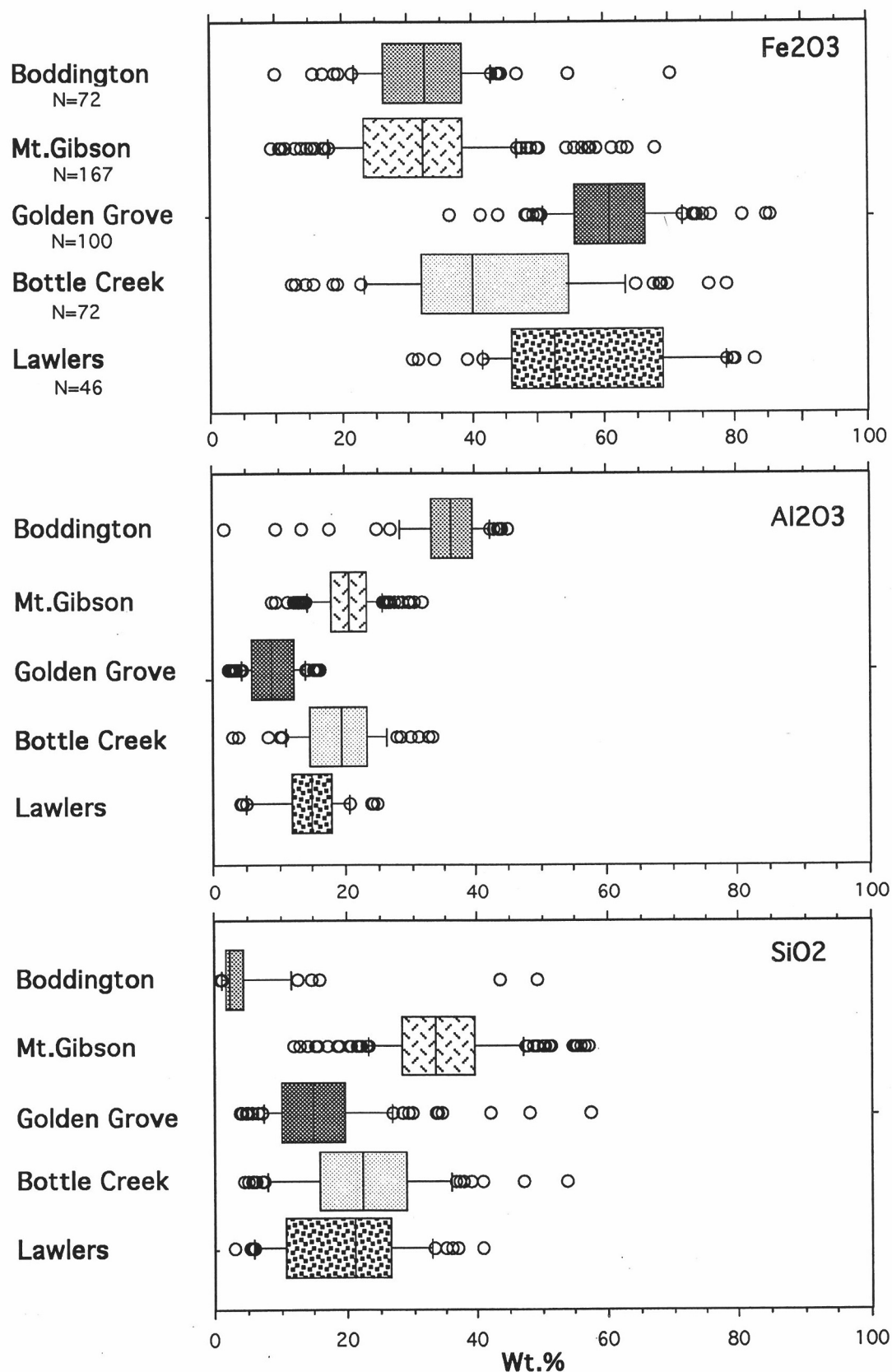


Fig. 8.3 Box plots comparing Fe<sub>2</sub>O<sub>3</sub>, Al<sub>2</sub>O<sub>3</sub> and SiO<sub>2</sub> in lateritic residuum from five orientation areas, as indicated.

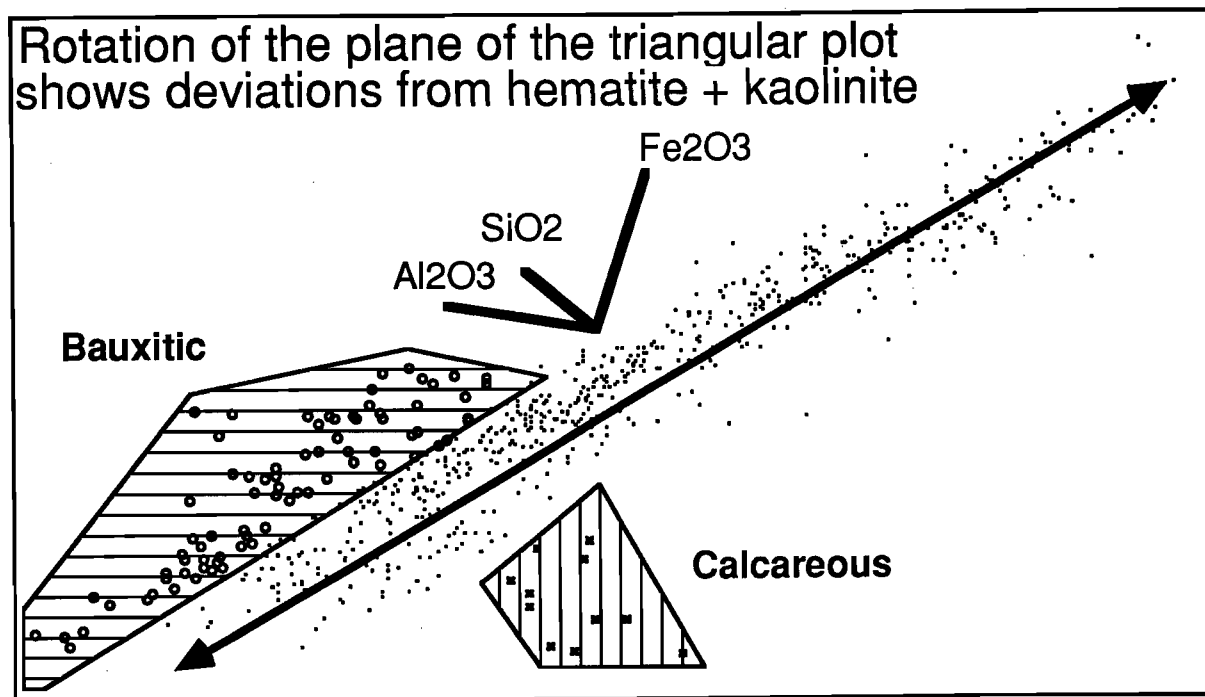


Fig. 8.4. Plot showing the distribution of lateritic residua in  $\text{SiO}_2$  -  $\text{Al}_2\text{O}_3$  -  $\text{Fe}_2\text{O}_3$  space, rotated such that the  $\text{SiO}_2$  -  $\text{Al}_2\text{O}_3$  -  $\text{Fe}_2\text{O}_3$  plane which contains the majority of the sample types is perpendicular to the page. Bauxitic and calcareous samples are highlighted as two groups of outliers above and below the plane of kaolinitic samples.

### 8.2.2 Minor and trace elements

The relative variation for As and Au in different orientation areas is highlighted by the box and whisker plots of Fig. 8.6. At Boddington, Au has moved down the lateritic profile to the bauxite zone and upper saprolite whereas Au at Bottle Creek and Mt. Gibson is more abundant in the surface gravels and in the lateritic duricrust. At Boddington, As is associated with  $\text{Fe}_2\text{O}_3$  in the surface lateritic gravels, as well as the duricrusts, making it useful for exploration where the Au anomaly is weak in the surface or near-surface units. At Mt. Gibson, Au and As behave similarly, increasing upwards in the profile. However, because the surface Au values are consistently high, As is of less importance in exploration at Mt. Gibson. Lateritic residuum at Bottle Creek is rich in As and poor in Au compared with Mt. Gibson, but has greater Au abundances in surface lateritic gravel than at Boddington.

Systematic relationships between the composition of lateritic residua and bedrock type were recognised early in the evolution of the laterite geochemistry project (circa 1978). These relationships continue to be clarified as the laterite geochemical databases have developed and through research such as that by Davy (1979). In the CSIRO-AGE database bedrock type was recorded if available (e.g. page 30 in Volume 1 of Report 161R). During the AGE Project, various elements, individually or in suites using indices, had been used routinely, to identify and delineate concealed greenstone belts in poorly outcropping gneissic terrain. Elements in lateritic residuum, which are increased by underlying mafic and ultramafic bedrocks include: Fe, Mn, Ti, Cr, V, Cu, Zn, Ni and Co. Titanium, however, can show complexities related to differentiation trends of intermediate to mafic igneous rocks. Granitic and other felsic bedrocks show corresponding increases in Si, Zr and, in places, Nb in lateritic residuum.

Based upon dominant bedrock types, the orientation areas progress from ultramafic and mafic, to felsic rocks, as follows: Lawlers (differentiated mafic and ultramafic rocks); Bottle Creek (high Mg metabasalts, quartz-feldspar-porphyry and localised sulphidic schists); Mt. Gibson (sheared metavolcanic, mafic and felsic rocks); Boddington (felsic andesite, mafic andesite, diorite, with some mafic dykes); and Golden Grove (felsic and intermediate volcanoclastic sediments, lavas and breccias).

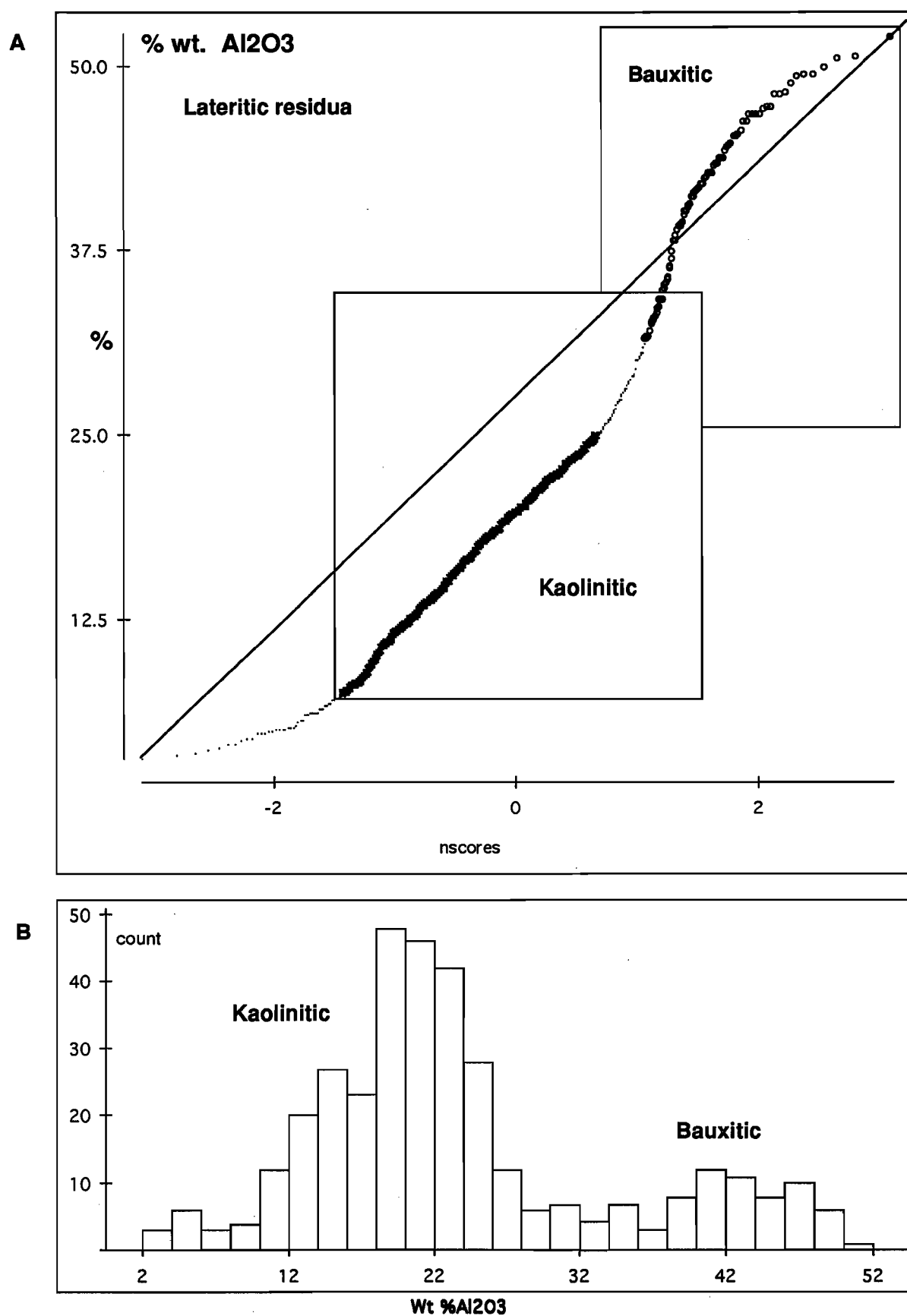


Fig. 8.5. A comparison of  $\text{Al}_2\text{O}_3$  data for lateritic residua described in a normal probability plot (A) and a histogram (B).

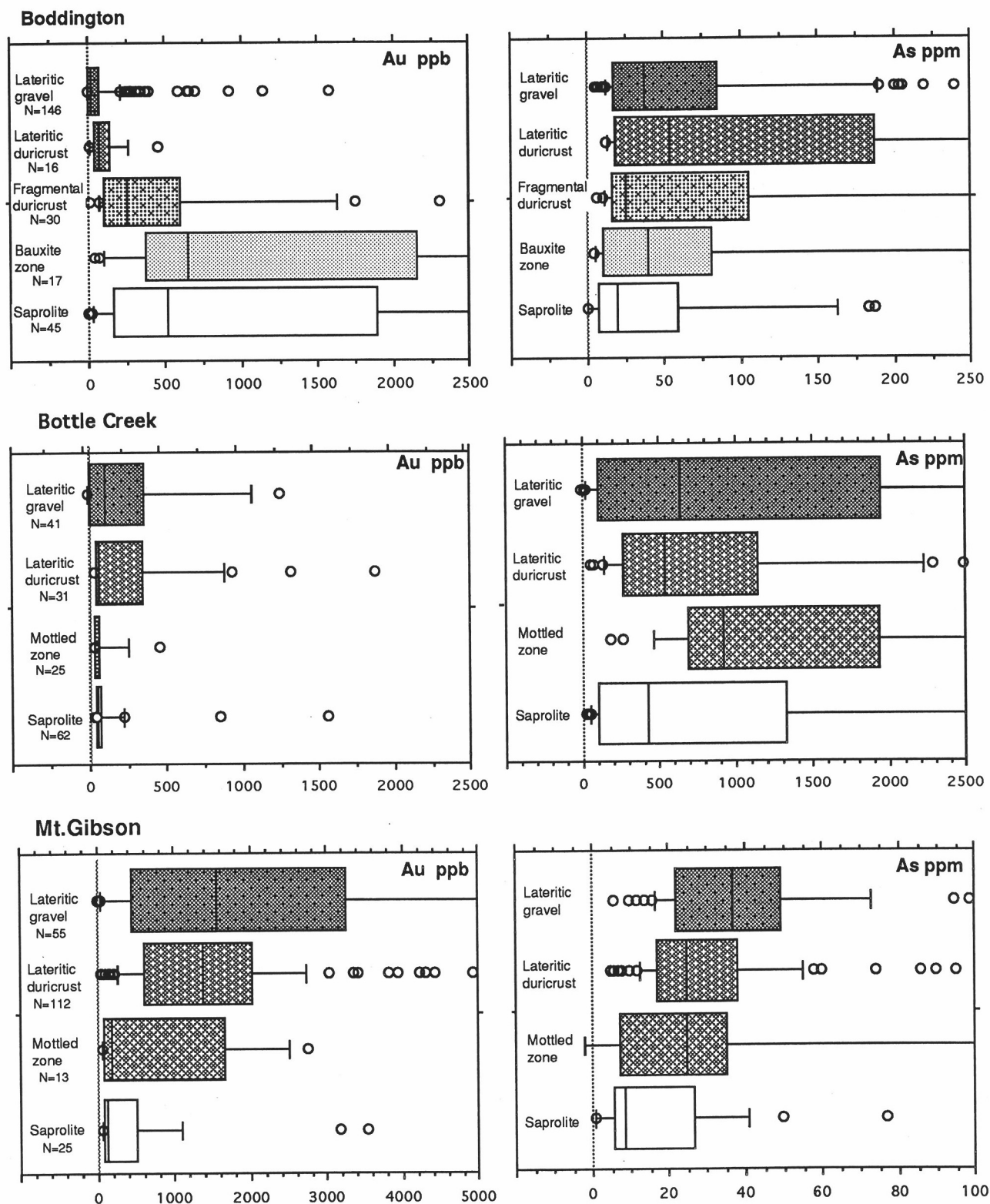


Fig. 8.6 The variation in Au and As through the lateritic profile is compared using box plots for three study areas.

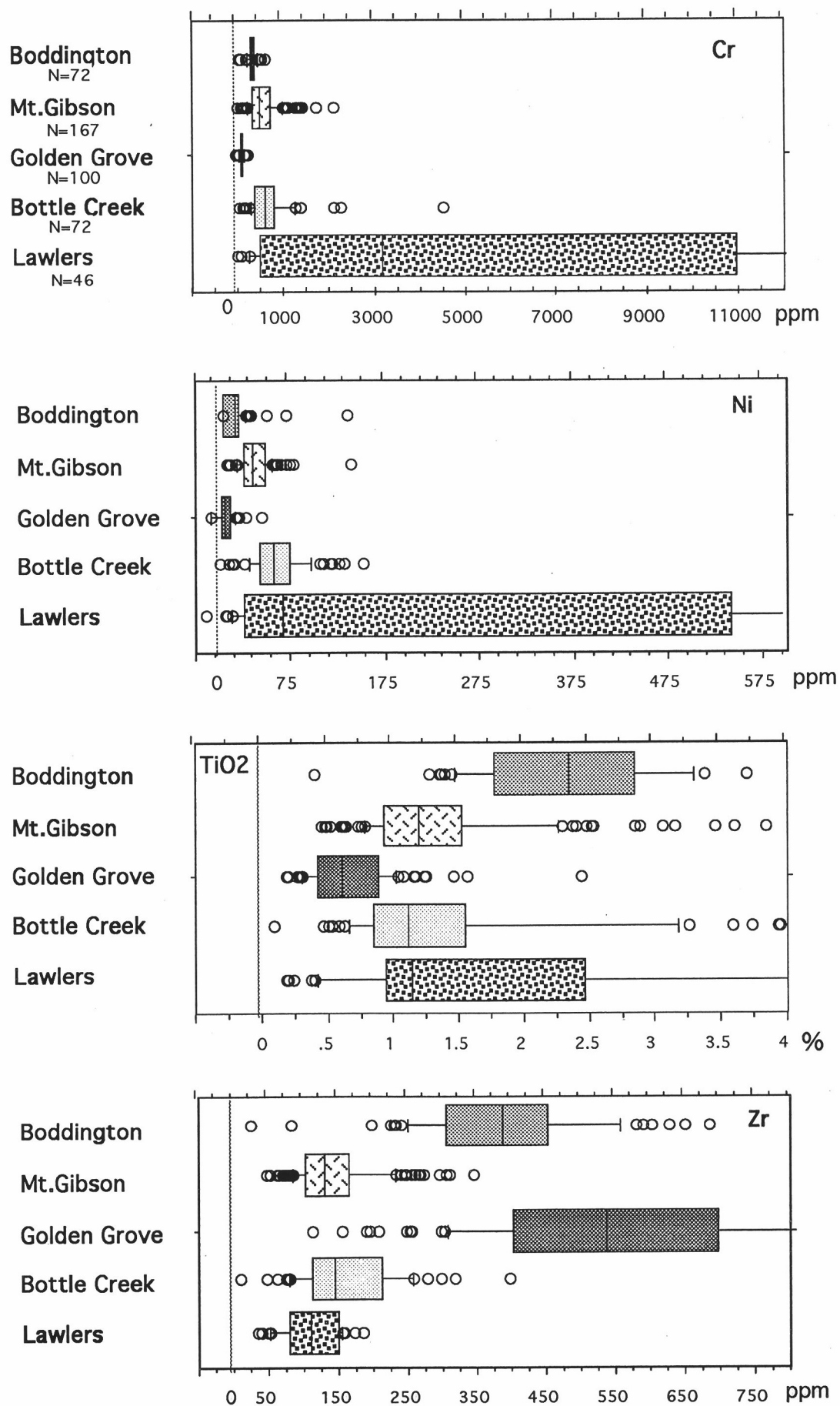


Fig. 8.7 Elements indicative of bedrock geochemistry plotted for lateritic residuum from five study areas.



Some of the elements (Cr, Ni, Ti and Zr), which relate to bedrock type, are shown in Fig. 8.7, for samples of lateritic residuum from five of the orientation areas. The distribution of Cr and Ni emphasises the mafic-ultramafic characteristics of the sequence at Lawlers. The relationships between composition of lateritic residuum and dominant bedrock types are well shown by data from the other orientation areas.

### 8.3 Data interpretation practical

A practical laboratory session for the interpretation of multi-element geochemical data has been established. It is based upon interactive graphical methods for exploratory data analysis. The practical currently uses Apple Macintosh® computers and Data Desk 4.0® software, specifically the demonstration Data Desk Test Flight program provided by Data Description, Ithaca, NY.

Three exercises are incorporated in the practical at this stage. All use data arising from the project orientation areas and include sample codes from the projects classification scheme (Report 60R). The first exercise covered x-y plots, histograms, normal probability plots, three-dimensional rotating plots and contouring by colouring ranges of gold values. All these plots can be viewed on the screen simultaneously, with interaction between the windows to highlight chosen data or to colour-code sample types. Figure 8.4 is modified from one of the rotating plots used for this exercise.

The second exercise relates laterite geochemistry to bedrock type using bedrock-related elements. Rotating plots of major elements and normal probability plots of Cr, Ni and Zr are used to separate the areas into those dominated by felsic, intermediate, mafic and ultramafic bedrocks. The third exercise compares target-associated elements from the Mt. Gibson, Bottle Creek, Lawlers and Boddington areas.

The ease of use of modern software, such as Data Desk, makes the best use of multi-element data and shows that EDA is a useful tool for evaluating multi-element data which can otherwise be an almost inscrutable mass of numbers. The above practical is available to sponsors of the project in CSIRO laboratories by appointment.



## 9.0 GEOCHEMICAL DISPERSION MODELS AND EXPLORATION PROCEDURES

### 9.1 Introduction

#### 9.1.1 Purpose of geochemical dispersion models

Although the weathering of each ore deposit and its host bedrock sequence is unique, weathering products and dispersion characteristics of ore deposits can be generalised within regions of similar weathering history. Idealised dispersion models are, therefore, developed for use in exploration. These models summarise geochemical dispersion from ore deposits in terms of the local regolith, landform, bedrock, and environmental relationships.

This section brings research findings together in the form of such models, drawing largely from the project orientation studies. It extends the models which had been developed in Report 236R and links with Section 7 of this report: Comparative studies - regolith evolution and geochemical dispersion. This section then translates this information into recommended exploration procedures. The intent is that the dispersion models which result (a) will allow ease of reference to generalised patterns of dispersion, and (b) can be used predictively in areas with comparable regolith, landform, and environmental characteristics.

Originally, the project focussed on geochemical dispersion patterns within lateritic residuum at surface, near-surface, or buried beneath transported cover. As the project progressed, emphasis spread with the recognition that geochemical dispersion patterns occur in upper-most ferruginous saprolite as well as in iron segregations (*e.g.* Lawlers, Section 4.4.6 in Report 236R) and ferruginous mottles of the mottled zone. Each of these materials can preserve geochemical dispersion haloes which enlarge target size. Ferruginous saprolite, iron segregations and ferruginous mottles, thus become important sample media particularly where lateritic residuum is missing. In the Kalgoorlie region, where lateritic residuum is commonly missing, ferruginous granules and mottles developed in soils and sediments are preferred sampling media, even in areas of transported cover, and give superjacent anomalies to concealed mineralisation. The models discussed below bring these additional media into perspective. Some emphasis is also placed on the use of detailed stratigraphic relationships, including subdivision of lateritic residuum.

#### 9.1.2 Classification of dispersion models

The models are grouped and discussed in terms of broad subdivisions of terrain types: whether the full lateritic profile is present or is partly truncated; high rainfall versus semi-arid or arid climates; and the presence or absence of transported cover. Use of the information in this section should be facilitated by reference to the terrain headings. The essential characteristics of the models, appropriate to each terrain, are presented and pertinent exploration methods are discussed. Emphasis is placed on using regolith-forming processes to advantage in exploration.

The classification scheme used, Fig. 9.1, is that of Butt and Zeegers (1992) which is primarily based upon the extent of preservation of the original weathering profile. Further subdivision takes into account the continuity of recent modification and weathering of the profile and finally (right hand side of the figure) the nature of any overburden.

### 9.2 Full lateritic profile, high seasonal rainfall, no surficial cover

#### 9.2.1 Dispersion model

Model: A2-1

Examples: Boddington Au deposit (Section 5.2), and Greenbushes rare metal (Ta, Sn, Nb, Li) pegmatite deposit (Smith *et al.*, 1987).

Regolith-stratigraphic relationships are drawn from studies in the Darling Range and generally throughout the southwest of Western Australia (see Section 7.2, Fig. 7.4). Geochemical dispersion information is drawn from orientation studies at the Boddington gold deposits, the surrounding Saddleback greenstone belt (Section 4.6.4 in Report 236R), and from studies about the Greenbushes rare metal pegmatite system (Smith *et al.*, 1987). Figure 9.2 shows the main A-type models for Au and base metal exploration in this high rainfall climate.

It is recognised that a similar, wide range of target-associated elements characterise the Boddington Au-Cu porphyry mineralisation and the Golden Grove VHMS deposits in the semi-arid interior (Section 9.3). The suite of ore and associated elements includes Cu, Au, As, Sb, Bi, In, Mo, Sn and W, with Pb, Zn, Cd and Ag being added for Golden Grove. Because of this similarity, orientation at Boddington should give indications of what to expect for Golden Grove-type VHMS deposits in this high rainfall region.

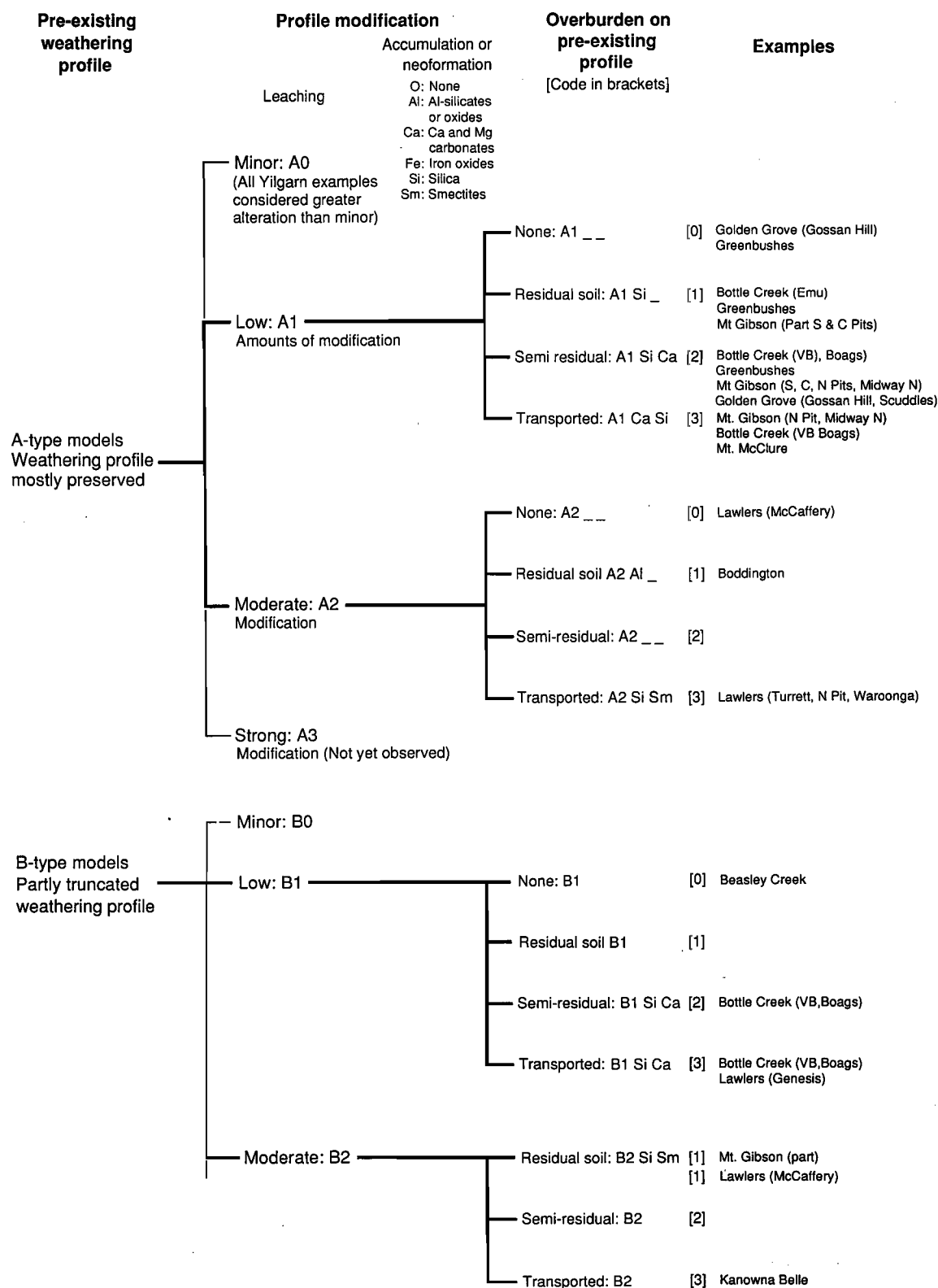


Fig. 9.1 Part of the classification scheme for geochemical dispersion models from Butt and Zeegers (1992), with examples of orientation studies referred to in this report and Report 236R.

## A-type models, seasonally humid terrains

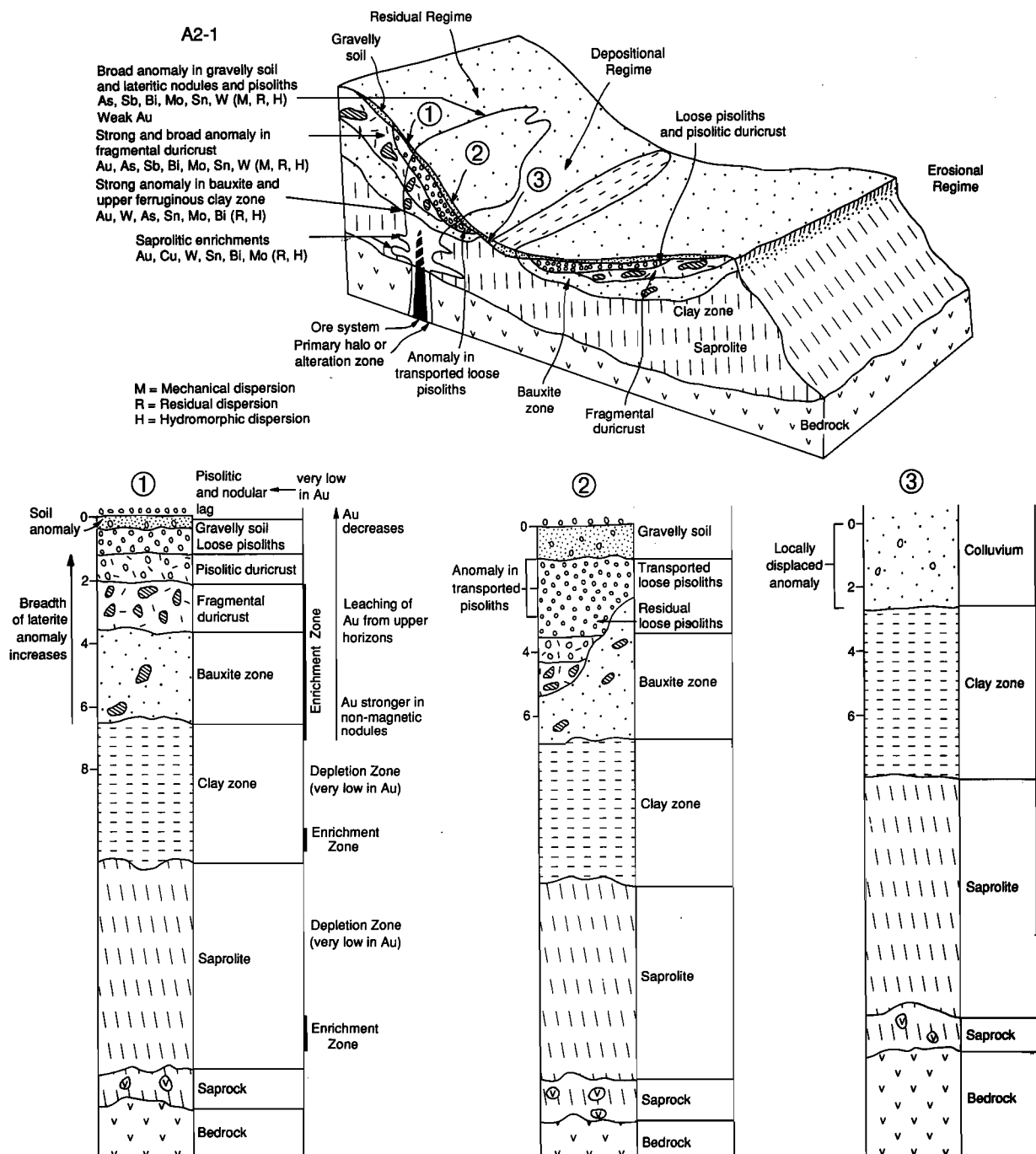


Fig. 9.2 Block diagram with columns for regolith stratigraphy showing an A2-1 dispersion model, full lateritic profile, high seasonal rainfall. Based largely on the Boddington orientation study (Section 5.2).

A striking feature at the Boddington Au deposit is the distribution of Au within the lateritic weathering profile. Published sections (Davy and El-Ansary, 1986; Monti, 1987; Symons *et al.*, 1990) and research in this project indicate vertical mobility which is an important factor in the cause of the 'lateritic' gold reserves. Rather than being in the overlying lateritic residuum, much of the ore, however, formed in the bauxite, saprolite and saprock zones. A deleterious characteristic of Au mobility, however, has been the strong leaching of Au from the immediate surface materials. It is particularly important, therefore, to appreciate where anomalous Au is distributed in the regolith stratigraphy and where Au geochemical patterns give a reliable indication that there is an underlying Au-mineralised system. Table 9.1 (page 276) summarises the distribution of target associated elements, including Au, in units of the regolith stratigraphy.

In the absence of other orientation information on Au deposits in this high rainfall region, the geochemical relationships at Boddington are assumed to apply elsewhere in the lateritic bauxite regions of the Darling Range and, generally, in the southwest.

### 9.2.2 Exploration procedures

It is particularly important, in exploration, to appreciate that a characteristic, broad, multi-element, dispersion imprint is preserved in surface lateritic residuum and gravelly soils above the Boddington deposits, even though Au may be leached to almost background levels in these materials. Gold becomes markedly anomalous in gravelly surface soils only at a local scale directly over the anomaly centres (Section 5.2.4).

Orientation at Boddington and Greenbushes shows that both As and Sb are retained in lateritic residuum and lag gravels at surface in this high rainfall region. Both elements provide broad, regular and reliable dispersion haloes, as they also do in the semi-arid and arid interiors.

At Boddington, the best 'imprint' showing a clear Au association (and this is supported by a wide range of target associated elements) comes from the fragmental duricrust, rather than the stratigraphically higher units of the regolith stratigraphy. Thus, for target definition in particular, fragmental duricrust is the most appropriate unit to sample of the subdivisions of lateritic residuum.

In the Darling Range, lateritic duricrust and loose nodules and pisoliths occur in upland areas (upper to lower slopes) where the pre-existing weathering profile has neither been truncated nor degraded during later climatic episodes. However, in the undulating landscape of the Darling Range, loose pisoliths and nodules have experienced some local transport and are therefore semi-residual. The distribution of these materials can be established by mapping the regolith and determining the regolith stratigraphy. Where the duricrust or loose pisoliths and nodules are covered by soil, it is better to sample the duricrust by augering rather than collect surface soil, because higher elemental abundances and contrasts will be obtained. Similarly, loose lateritic gravel is preferable to the associated soil as a sample medium and fine material should be discarded prior to analysis. Lag gravels may be swept up for sampling from the surface and are best sieved (plus 2 mm or plus 5 mm) to reject fine, transported material.

The broad dispersion haloes permit very wide sample spacings to be used, as discussed in Section 10 of Report 236R. Sampling on 1 km to 3 km centres may be adequate for the detection of regional patterns, closing progressively to 100-200 m for detailed follow up. Sampling for regional surveys should be directed at the loose pisoliths and nodules whereas, for target evaluation, sampling should be directed at the deeper fragmental duricrust horizon.

## 9.3 Full lateritic profile, semi-arid to arid climate, little or no surficial cover

### 9.3.1 Models and terrain types

Models: A1-1 for gently undulating areas;

B1-0 on hills rising above lateritic uplands, or in erosional catchments

Examples: Gossan Hill and Scuddles VHMS deposits at Golden Grove; partly Mt. Gibson Au deposit (S and C Pits); partly Bottle Creek Au deposit (Emu); and, partly Beasley Creek Au deposit.

Terrains for which these models apply are very widespread in the Yilgarn Craton as well as in other lateritic regions of Australia. The terrains are commonly characterised by pisolitic or nodular lateritic gravels at surface, sometimes associated with yellow, white or red soils or sand plains. Widespread areas of lateritic duricrust are exposed where the topsoil and loose lateritic gravels are missing.

The geochemical dispersion model is shown in Fig. 9.3. The most important characteristic with regards to mineral exploration is the large dispersion halo that is typically present in lateritic residuum overlying a concealed mineral deposit.

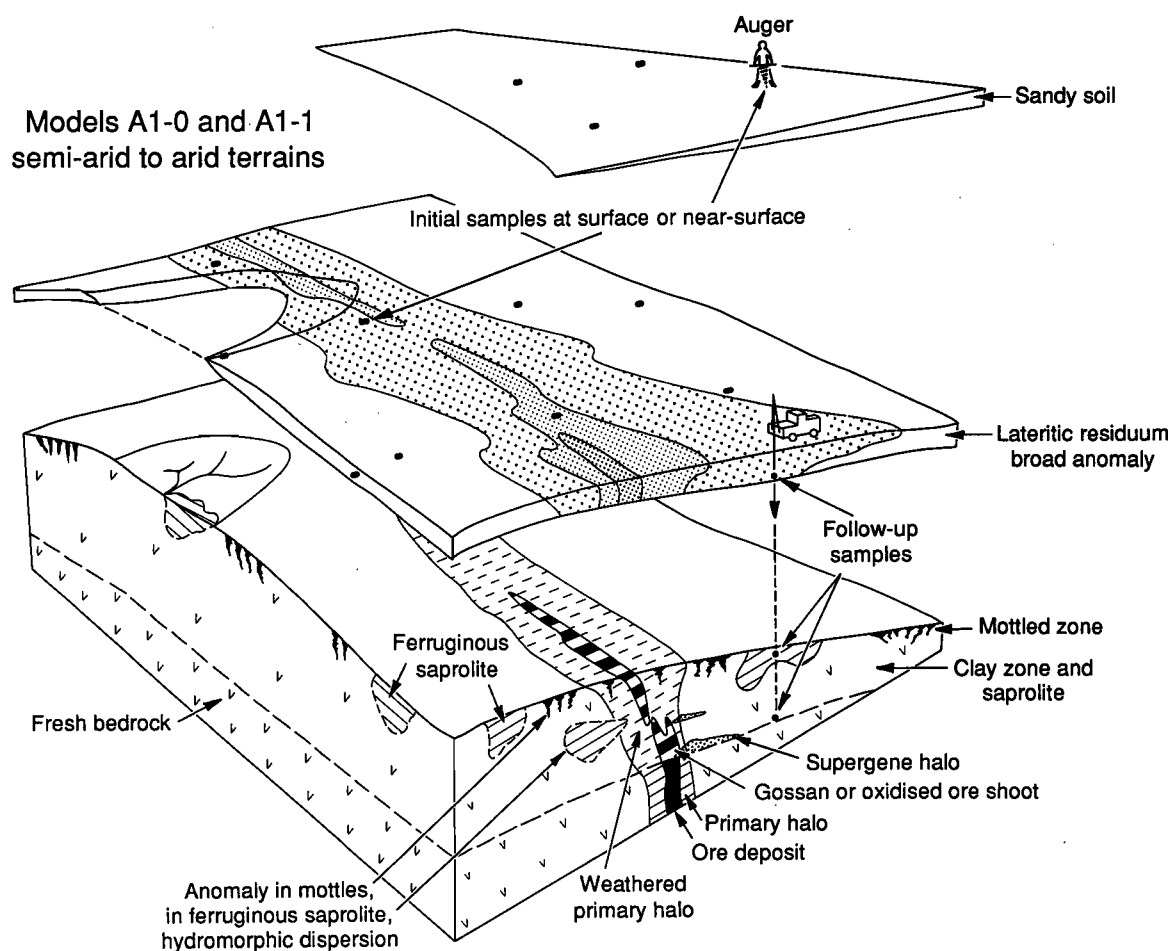


Fig. 9.3 Block diagram showing A1-0 and A1-1 dispersion models, full lateritic profile, semi-arid and arid terrains. In some situations ferruginous saprolite can form an almost continuous horizon in the regolith stratigraphy.

Terrain characterised by a full laterite profile with only soil, thin sand cover or no cover can be readily explored using laterite geochemistry. The concepts and methods involved have reached a substantial level of maturity over the last eight years. Such terrains are now viewed as classic cases of using regolith-forming processes to advantage in exploration. Geochemical dispersion inherent in lateritisation processes has resulted in greatly increased sizes of targets (commonly 100 to 400 times greater in area, Report 236R) compared with the size of the corresponding ore deposits. Multi-element haloes indicate target type; their strength and the superimposition for haloes of different elements provide vectoring for target definition. Furthermore, lithophile elements can be used to crudely map bedrock type, where this is required. Bedrock information can also be provided through petrography and mineralogy of lateritic residuum. Properly carried out, areas with full lateritic cover can now be explored at relatively low cost, much lower, for example, than areas of mixed outcrop and variable soil cover.

Exploration methods for these regolith situations were extensively covered in Report 236R. Those findings are updated here (Fig. 9.3), using information from Mt. Gibson, Bottle Creek, Beasley Creek and the revisited study of Golden Grove. It is also useful to translate some of the characteristics shown in the Boddington orientation study for application in the semi-arid and arid terrains.



### 9.3.2 Sample media, their use, and precautions

#### *Gossans in the search for VHMS deposits:*

In lateritic terrain gossans may, in places, protrude through lateritic residuum or be exposed in local windows (as at Gossan Hill, Section 5.6, and Smith and Perdrix 1983), in either case, providing opportunities for gossan sampling in outcrop. Gossans high in the laterite profile will be partly lateritised and 'mature' (strongly leached, thus tending to be depleted in Cu, Pb, Zn compared with those exposed by deep levels of truncation through erosion or encountered in deep drilling).

Multi-element geochemistry of leached gossans provides a powerful approach to exploration. Broad suites of target-associated trace elements can be more useful than simply using base metals which tend to be leached. Useful data interpretational methods are given by Taylor and Scott (1982), Smith *et al.* (1983) and Eggo (1991).

Gossan fragments contribute to laterite geochemical anomalies through mechanical and residual incorporation to the lateritic blanket. Hydromorphic dispersion can also be involved through elements released during the weathering of the sulphide bodies (*i.e.* during gossan formation) or during the weathering of gossans.

Gossan sampling is very specific: it is likely to provide an answer to what was actually sampled not what occurs nearby. In comparison, laterite geochemistry gives information on the local environment, which may be several tens of square metres in area for basal duricrust to perhaps a square km for the upper pisolitic, gravelly, lateritic residuum.

#### *Lag*

Lag sampling needs to be tied to regolith mapping since lag type, its characteristics and its dispersal will vary widely with regolith substrate and landform position (*e.g.* Section 5.5, Bottle Creek).

Research in the project has shown that selection of the magnetic fraction of lag is not recommended. It is likely to result in sampling less useful material, as at Golden Grove (Section 5.6). Based on the findings of several orientation studies (Golden Grove, Beasley Creek, Lights of Israel, Mt. Gibson and Bottle Creek), it is recommended that representative samples of lag be taken in lag surveys.

It is generally more reliable, however, to sample lateritic residuum itself where this can be done easily, rather than, for example, to take a lag sample from topsoils which, in turn, may overlie lateritic residuum. In such a case it would be far better to dig into and sample pisolitic or nodular lateritic residuum, see Section 9.4.4.

For base metal sulphide deposits, Au, though present in some, is not an essential ingredient of the ore or its immediate environs. A suite of elements is therefore required, commonly some combination of Cu, Pb, Zn, As, Sb, Bi, Cd, In, Mo, Sn, W, Ge, as well as Au.

For some Au deposits, certain of the target associated elements can form larger and more consistent anomalies than Au. Gold generally will still be important, yet may not appear significant until the centres or strongest parts of the anomalies are being delineated. This is the case at Bottle Creek (Section 5.5) where As and Sb form anomalies up to 1.5 km wide and several km long, centred on the ore horizon. Anomalies for Au and Pb are more localised (about 200 m wide) and give sporadic patterns distributed along strike, again centred on the ore horizon.

Commonly, superimposition of dispersion haloes for individual elements identifies the most important part of the concealed mineralising system by coincidence of the strongest parts of individual element anomalies. (This is emphasised when using indices of the NUMCHI type, Section 8.3 of Report 236R).

### 9.3.3 Exploration comments: VHMS deposits

VHMS deposits are typically zoned in terms of the sulphide mineralogy and hence their geochemistry (ore elements, minor and trace elements, Fig. 9.4). The gossan geochemistry, not surprisingly, inherits this variability, although modified by weathering processes.

It is important to recognise that the geochemical signature of lateritic residuum (or other regolith units) will depend upon where the deposit is intersected by the weathering surface relative to the original three-dimensional geometry of the deposit. In some cases only a primary halo or an alteration zone will be intersected, in other cases it might be the Cu-rich feeder zone or the exhalite horizon. Examples are shown by the hypothetical traverses in Fig. 9.5.

It is generally wise to cast a fairly broad net in terms of the element suite used and to be flexible in terms of expectations at the interpretational stage. Besides depending on the type of ore deposit sought, the suite of elements that proves to be useful in an area will depend upon the sequence of bedrock lithologies. These are a far greater contributor to the overall geochemistry of lateritic residuum than the

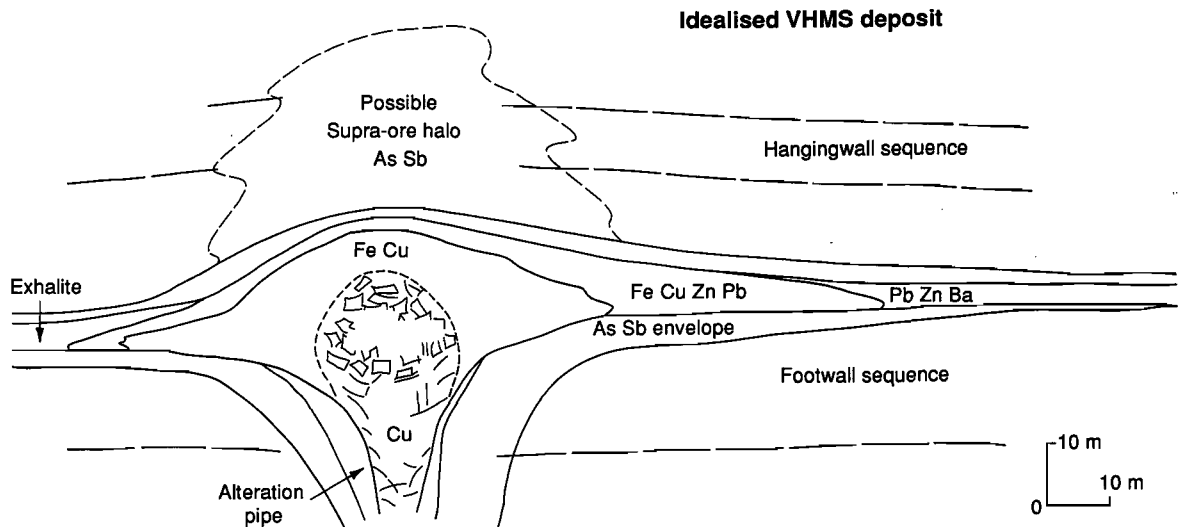


Fig. 9.4 A section through an idealised volcanic-hosted massive sulphide deposit (VHMS) showing element zonation of ore types.

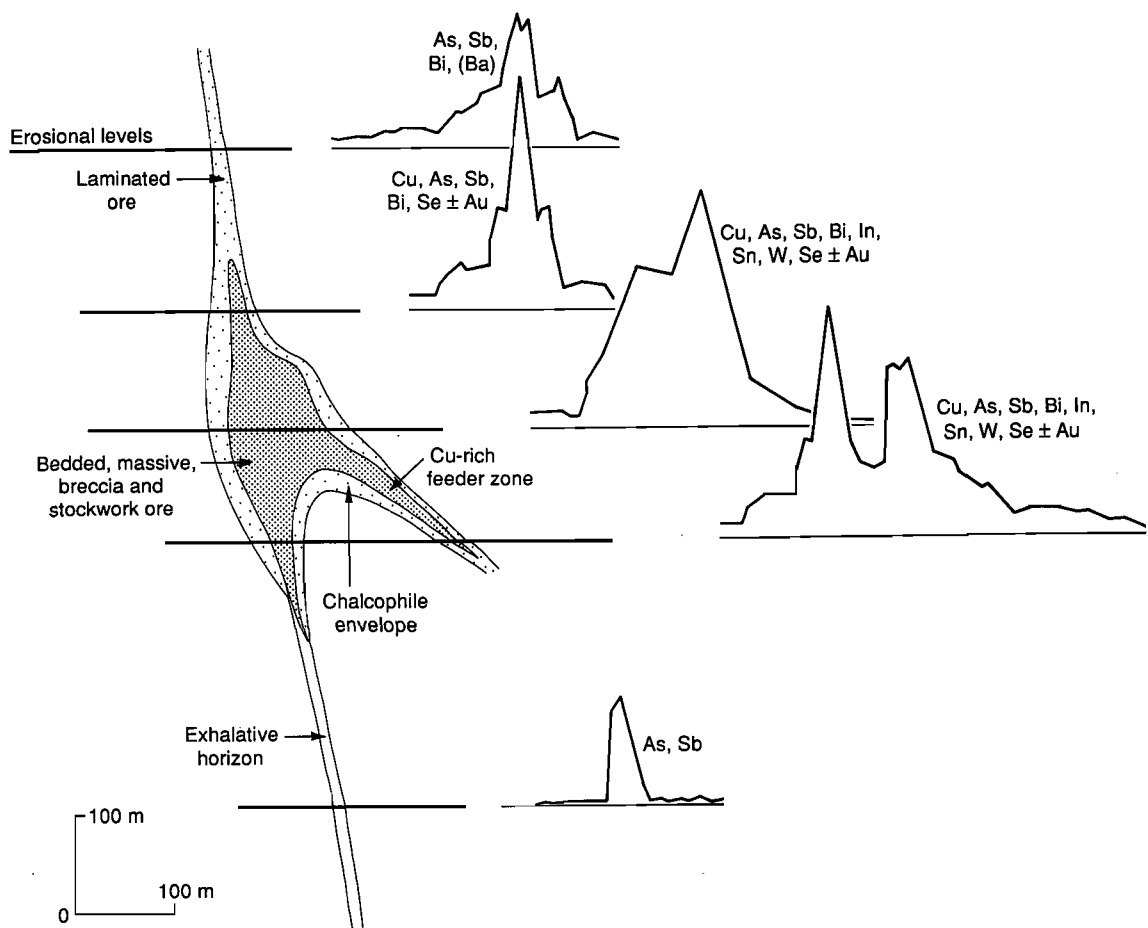


Fig. 9.5 Diagrammatic cross-section through an idealised VHMS deposit showing examples of the different element associations that can result from a series of erosional levels. Based upon the Golden Grove orientation study, Section 5.6. Schematic geochemical traverses for lateritic residuum are shown.

very sporadic occurrences of mineralisation or an even more rare concealed ore deposit. An important factor in recognition, therefore, is the contrast of an ore system against its host bedrock.

Thus at Mt. Gibson (Section 4.2 in Report 236R) and Golden Grove (Section 5.6 in this report), one can meaningfully contour As anomalies in lateritic residuum at low abundances of 30 ppm because the As background is also low. This is not usually the case where BIFs are present in the bedrock sequence. The commonly high As levels in BIFs then tend to dominate the As geochemical patterns in lateritic residuum and As anomalies, as seen at Mt. Gibson or Golden Grove, may not be identifiable.

#### 9.3.4 Exploration comments: Archaean porphyry Au-Cu deposits in the arid interior.

Results of the Boddington orientation study can be translated to the semi-arid and arid interior with the following expectations.

The targets are large in volume and, depending on the geometry of how the weathering surface intersects the ore system, can have large areal extent. This being the case, a large, distinctive anomaly in lateritic residuum can be expected with some combination of Au, As, Sb, Bi, In, Mo, Sn and W. In contrast to the high rainfall areas, a reliable Au anomaly is likely in the upper lateritic residuum and not just in the basal fragmental duricrust as at Boddington.

As with any deposit type, the level of truncation of the ore system by the weathering surface will govern the element suite acquired by the lateritic residuum. A broad envelope of As, Sb and Bi, with enclosed geochemical 'hot spots' of Au, Mo, Sn, W and perhaps Cu, may be expected.

### 9.4 Full lateritic profile, semi-arid to arid climate, transported cover

#### 9.4.1 Models and terrain types

Model: A1-3 and A2-3

Examples: Turrett and Waroonga deposits at Lawlers, Calista deposit at Mt. McClure also Midway North deposit at Mt. Gibson, all being Au deposits.

Models of this type (Figs 9.6, 9.7 and 9.8) are now recognised as having widespread application in the alluvial and colluvial plains of the inland Yilgarn Craton.

Research at Lawlers (in Section 4.4, Report 236R) and Mt. McClure (Section 5.3 of this report) showed that extensive areas of full lateritic profiles can occur beneath alluvial and colluvial cover, even where lateritic residuum may only comprise a minor proportion of the surface landscape. For the Lawlers district lateritic residuum comprises only some 15% of the landsurface yet can be a substrate to more than 60% of the colluvial and alluvial plains, Section 5.4. At Mt. McClure, mapping over a 185 km<sup>2</sup> area has suggested that the lateritic residuum is preserved beneath the sediments over approximately half of the study area (Section 5.3).

Concepts and relationships shown by the models in Figs. 9.6 and 9.8 had application in the Bronzewing Au discoveries by Great Central Mines (*pers. communication*, E. Eshuys and J. Wright, Great Central Mines N.L., November 1993).

These models can also apply along the flanks of ridges and ranges which may or may not show preservation of a blanket of lateritic residuum at surface. Examples include the flanks north and south of the Weld Range in the Madoonga district (Section 5.8), the ridge marking the southwest margin of the broad valley at Golden Grove and the hills west of Bottle Creek.

#### 9.4.2 Drilling for regolith stratigraphy

Preservation of a complete laterite profile beneath cover sequences can greatly reduce the cost of exploration through cover when compared with conventional methods, because the target size, by aiming for geochemical haloes in lateritic residuum, is commonly and substantially enlarged. Research in this project shows that halo sizes range from some 100 to 400 times the area of the corresponding ore deposit target (Table 5.1 in Report 236R). Whereas target size is enlarged, a further characteristic is the ability to 'home-in' on a concealed ore deposit source using the increasing strength of anomalous geochemistry and the superposition of haloes of several target-associated elements.

Probing for regolith stratigraphy is an important early step in exploring areas of transported cover. Air-core drilling for this purpose can provide valuable and cost-effective information because it provides samples of the subsurface units, commonly from cm-sized pieces up to cores that may be 10 cm or so in length. The fabric of the sediments or lateritic units can be preserved, for example. This can include sedimentary structures, siliceous cementation along bedding, Mn staining, concretions, pisoliths, nodules, etc.

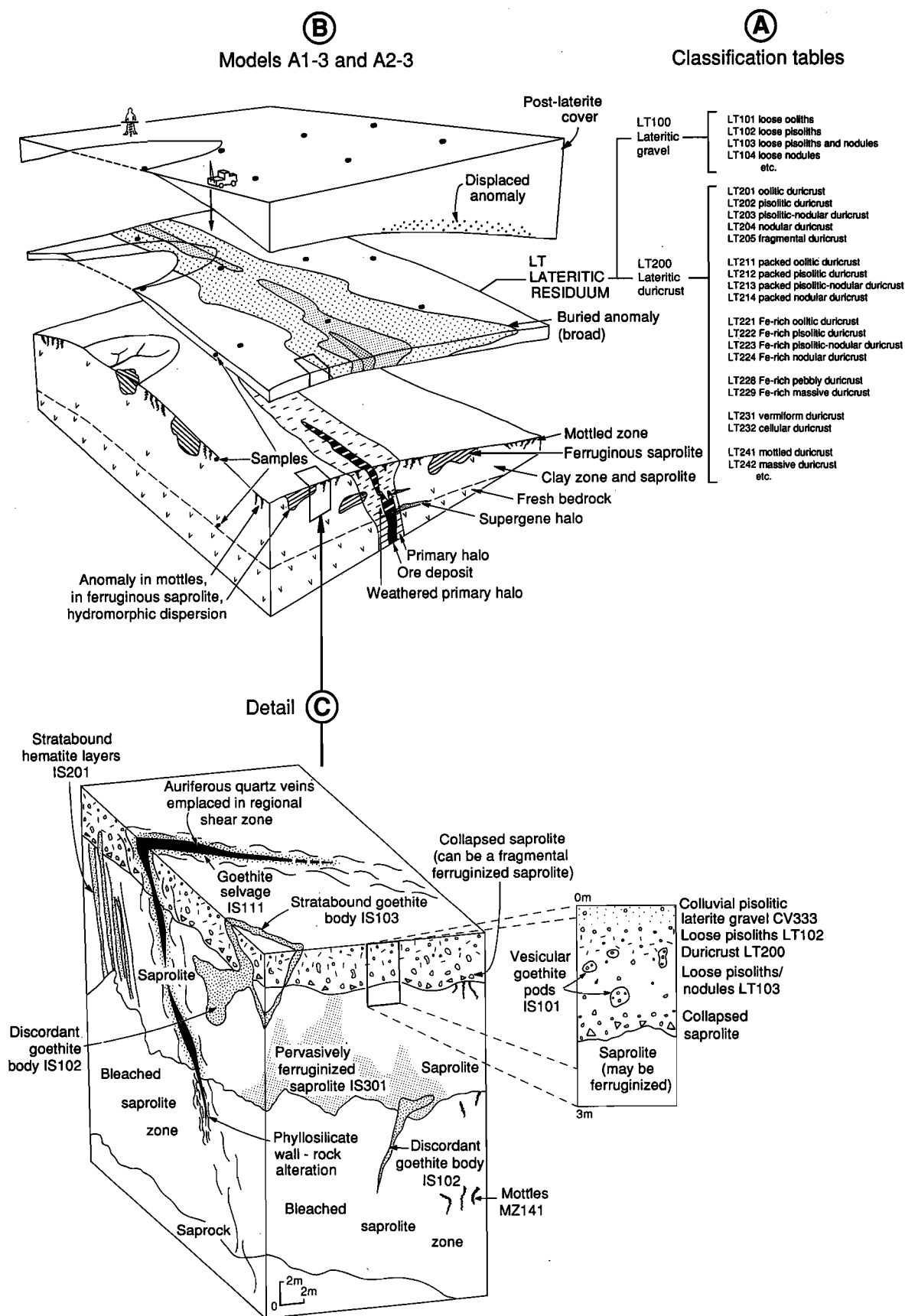


Fig. 9.6 Block diagram showing A1-3 and A2-3 dispersion models, full lateritic profile, semi-arid to arid, transported cover. Based largely on the Lawlers and Mt. McClure orientation studies, Section 4.4 of Report 236R and Sections 5.3 and 5.4, this report: A, Classification codes for lateritic residuum from the project's *Terminology, Classification, and Atlas*, Report 60R. B, Dispersion model. C, Detail showing several types of ferruginous materials with their classification codes.

## Models A1-3 and A2-3

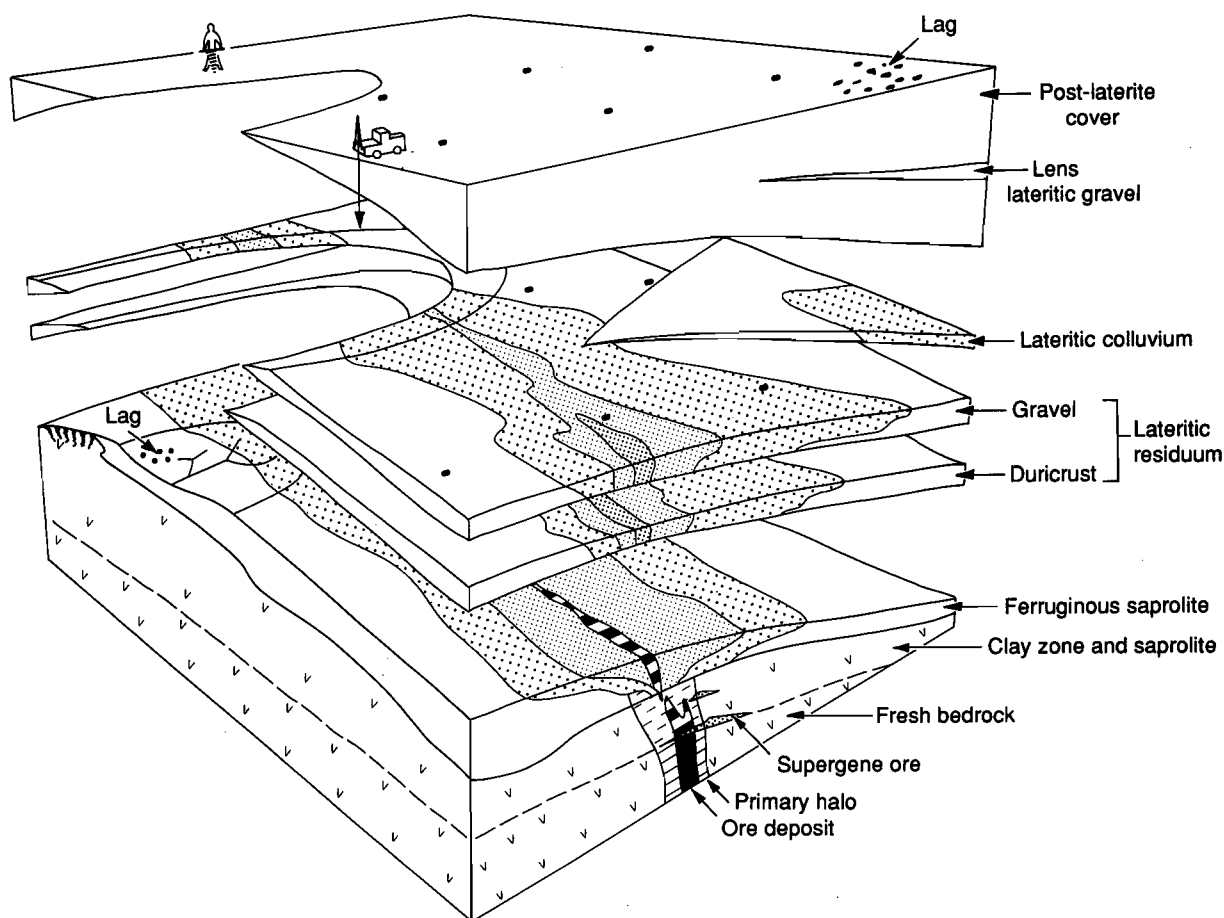


Fig. 9.7 Block diagram showing A1-3 and A2-3 dispersion models, full lateritic profile, semi-arid and arid terrains, transported cover, with subdivision of lateritic residuum accompanied by an underlying layer of ferruginous saprolite.

Establishing the regolith stratigraphy, facies variations, presence of unconformities and the characteristics of buried erosional surfaces are fundamental to understanding the sequences and in deciding which units to sample. Such work requires more care and time than is possible when a geologist has to keep pace with an efficiently operating, rotary air blast (RAB) drilling rig. Once the regolith stratigraphy has been established, routine logging can be carried out effectively and quickly. However, selected holes are likely to need revisiting for careful logging, including examination of the drill spoil by binocular microscope.

An important early step in exploration in areas of transported cover is to try to first detect, and then determine the extent of areas where the full laterite profile is preserved. Conversely, areas where the weathering profile is partly or extensively truncated are also delineated. In the latter cases, models from Section 9.5 may apply.

In logging drill spoil, where there is transported cover, it is good practice to work upwards from recognisable saprolite. This may require, every so often, some regolith stratigraphic holes being drilled deeper than needed for routine exploration. Working upwards is a guarantee against mistaking shallow weathering profiles developed in cover sequences, which may include mottles and pisoliths, for a deeper weathering profile developed from basement. The latter generally (but not in every case) is the one sought for geochemical dispersion patterns.

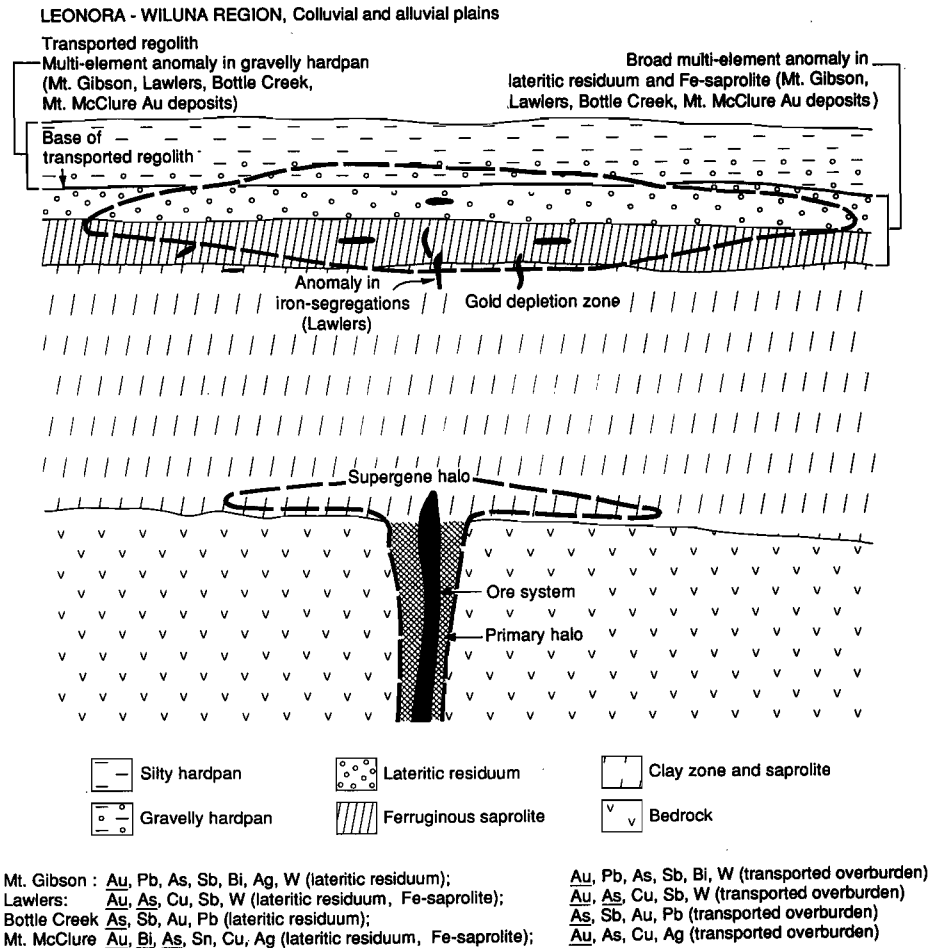


Fig. 9.8 Cross section through an A2-3 dispersion model (of Fig. 9.6), showing the element associations from some of the project orientation areas.

#### 9.4.3 Ground geophysical methods for delineating regolith stratigraphy

Ground geophysical methods, particularly electromagnetics (EM) but also detailed magnetics, have been shown to provide cost-effective information on regolith stratigraphy, including the detection and delineation of buried laterite profiles. This research has been carried out through collaboration with V.C. Wilson of Curtin University's Department of Exploration Geophysics, facilitated by CRCAMET funding. Using a Geonics Protem 47, buried lateritic residuum has been detected and delineated at depths of up to 10 m, the base of saprolite at 50 m or more, as well as stratigraphic information in hardpanised colluvium. In some cases the erosional unconformity between the buried, partly truncated lateritic weathering profile and the cover sequence can be delineated in cross sections. Modelling of ground EM is most accurate when constrained by geological information on the stratigraphy provided by sporadic drill holes. Seismic reflection and ground probing radar will be tested in future research.

#### 9.4.4 Stratigraphic subdivision of lateritic residuum

Logging and subdividing lateritic residuum and related units in drill spoil can be both workable and worthwhile in exploration, based on the concepts shown in Fig. 9.7.

Sampling lateritic colluvium, where it directly overlies lateritic residuum can broaden the ability to detect a geochemical halo in a near-miss situation. Sampling takes advantage of enlargement of anomaly size by mechanical transportation in proximal colluvium. If transport is too extensive, the anomaly will be indistinguishable from background and/or the source will be untraceable. This technique is, in part, reliant on bioturbation carrying mineralised particles to the near-surface; if the colluvium is thick, this may be prevented.

Commonly, the uppermost part of lateritic residuum is a lateritic gravel. A typical characteristic is mechanical dispersion, which took place during, or after, lateritisation. Furthermore, because this unit generally has the highest permeability in the weathering profile, hydromorphic dispersion tends to be widespread. For these reasons, geochemical dispersion haloes in lateritic gravel tend to be broadest of the lateritic units and therefore best suited to reconnaissance exploration. Pisolitic gravels generally give broader patterns than underlying nodular gravels. Sampling the uppermost lateritic residuum is best for the broad-spaced stage of reconnaissance drilling, *e.g.* 400 m to 800 m spacing (possibly wider) of drill holes in reconnaissance Au exploration.

As exploration progresses to anomaly delineation and then to defining the strongest parts of these anomalies for testing by drilling, sampling should move progressively from lateritic gravel to duricrust, then to basal duricrust. Sampling basal duricrust, using shallow drill holes, can be particularly effective at the target definition stage. The main difference being broader geometry of anomalies in the upper units.

The suites of elements recommended are essentially the same for each of the subdivisions of lateritic residuum. The data can usually be grouped together for broad-scale interpretation. Choice of elements will depend on target type(s), knowledge of the mineralised system, the stage of exploration, and whether predictions of bedrock type are to be made. For Au exploration, Au alone may be sufficient as a geochemical indicator. Many examples can be quoted where a broad, regular Au halo (which can be readily contoured) in laterite is adequate for locating a concealed saprolitic and bedrock Au deposit. These include the Mt. Gibson, Plutonic, Mt. McClure, Lawlers (several deposits) and Bronzewing deposits. The use of geochemical haloes preserved in ferruginous saprolite is described in Section 9.5.

#### 9.4.5 Geochemical dispersion patterns in buried lateritic residuum

As far as is known from this research, element suites to be expected in buried geochemical haloes in lateritic residuum are the same as those in lateritic residuum at or near the surface, as described in Section 9.3. Whilst possibilities exist for Au to be mobile, no orientation studies showing depletion of Au from lateritic residuum in the semi-arid to arid interior are yet known. A useful example would be where a geochemical halo is immersed in saline groundwaters. Does the Au remain or become depleted in such a situation?

In sampling, one needs to be alert for lenses of lateritic gravel in the colluvial or alluvial units as these can be mistaken for lateritic residuum. They should generally be avoided in sampling. An exception can be basal lateritic colluvium, mentioned above, which can enlarge halo size through translation of an anomaly and be useful in near-miss situations.

Tungsten carbide bits are commonly used in drilling so care is needed in interpreting W (and Co) geochemical anomalies. Tungsten anomalies can still be recognised and be useful, however, interpretation needs to rely on the association of W with a suite of target-associated elements.

In exploring by drilling for buried geochemical haloes in laterite, gaps in the data coverage should be expected due to lateritic residuum being absent, commonly through erosion, but perhaps also through lateritic residuum not having been developed everywhere. It is important, therefore, to be prepared to merge interpretations based upon alternative sample media. Thus model A1-3 (Fig. 9.7) will merge with B1-3 (Fig. 9.9) from Section 9.5. In merging the data, account must be taken of differing thresholds for different sample media.



Models A1-3 and B1-3

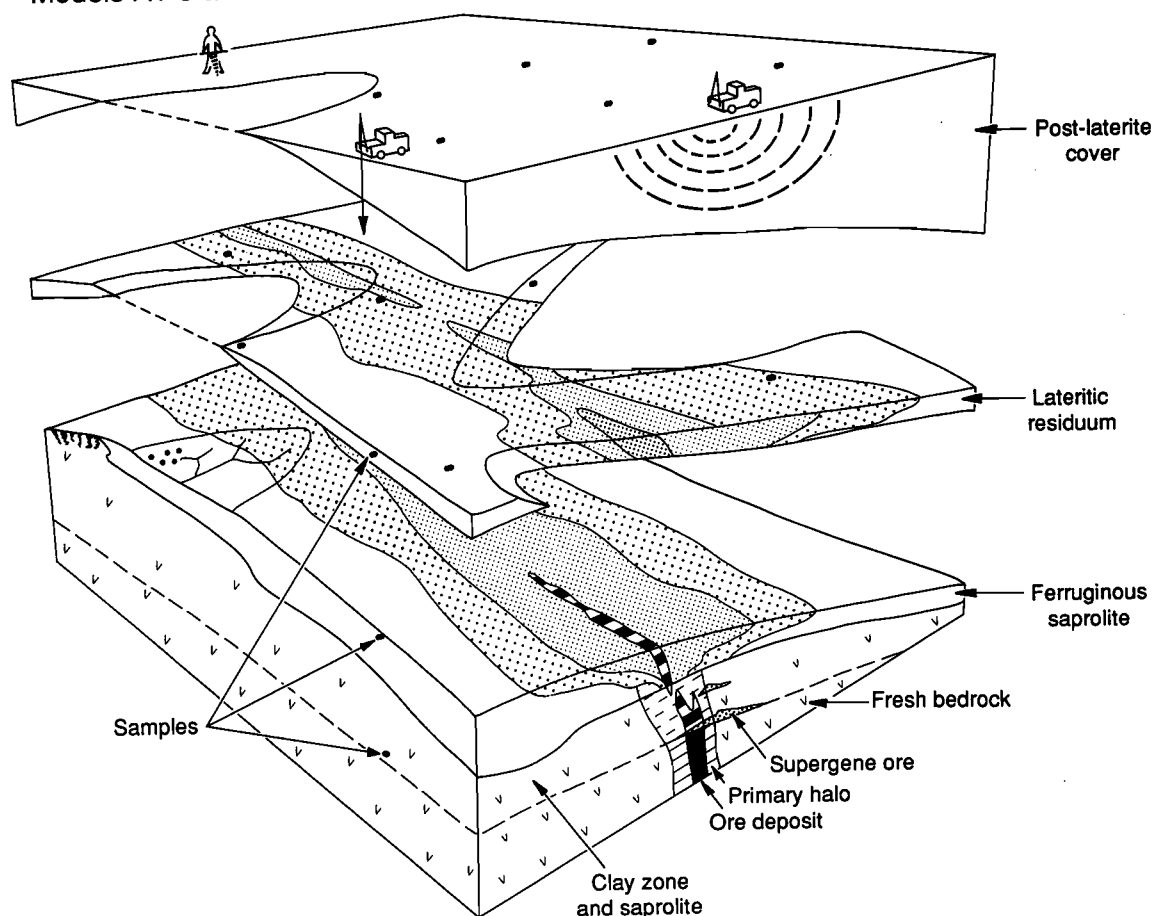


Fig. 9.9 Block diagram showing A1-3 and B1-3 dispersion models, partly truncated profiles, semi-arid and arid terrains, transported cover. Where lateritic residuum is missing, sampling can be directed at ferruginous saprolite. Based on Waroonga (Section 5.4) and Mt. McClure (Section 5.3) orientation studies.

#### 9.4.6 Depleted upper saprolite

It is common (but not universal) in the Yilgarn interior to encounter Au depletion from the upper saprolite over a zone 10 to 15 m thick, immediately below lateritic residuum. The reasons and controls are not yet adequately understood. However, where Au depletion occurs in upper saprolite, lateritic residuum still provides a reliable multi-element geochemical dispersion halo, Figs 9.6 and 9.8. As well, target-associated elements can carry through the Au depletion zone in saprolite. These elements include As, Sb, Bi, Sn and W. Ferruginous mottles, which can occur close to the interface with lateritic residuum, can carry anomalous suites of As, Sb, Bi, Sn, W and Au. Ferruginous mottles can, in this way, form useable geochemical dispersion haloes in the search for concealed Au or base metal deposits.

Clearly, it is important to recognise if a model characterised by a Au depletion zone applies to an area being explored. Where it does, sampling lateritic residuum, or where this medium is absent, ferruginous mottles, can obviate the problem. However, in testing targets defined as geochemical anomalies in these media, it is important to drill to sufficient depth to penetrate beneath the Au depletion zone. Furthermore, a supergene halo in Au (and possibly Cu) may usefully enlarge target size near the saprolite (or saprock) interface with bedrock (as at Kanowna Belle, Section 4.3 and Fig. 9.10).

## 9.5 Partly truncated profile, semi-arid to arid, transported cover

### 9.5.1 Models and terrain types

Model: Part A1-3, B1-2, B1-3

Examples: Kanowna Belle; Matt Dam; Kanowna deep leads; Mt. McClure; Bronzewing; VB and Boags at Bottle Creek; Genesis and Waroonga at Lawlers - all being Au deposits

The situations of partly truncated, buried laterite profiles, as exemplified in Figs 9.9 to 9.11, are also widespread in the alluvial and colluvial plains of the Yilgarn Craton. Initially they are indistinguishable from the situation shown in Section 9.6. Subsurface information is required, particularly from drilling. However, research shows that ground geophysical methods (Section 9.4.3, particularly EM) can provide information on regolith stratigraphy including the presence, distribution and absence of buried lateritic residuum (Mayes, 1992; Anning, 1993; Dauth, 1993).

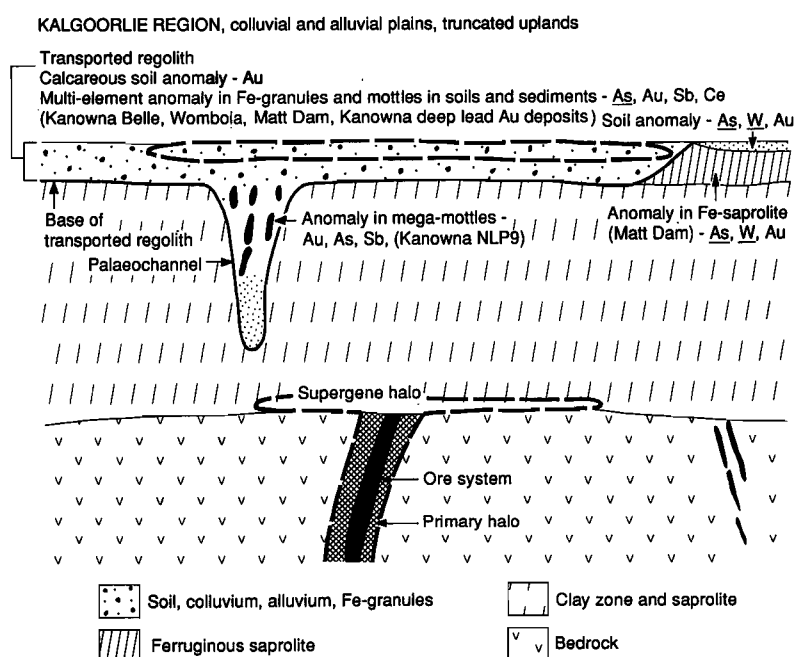


Fig. 9.10 Cross section through a B2-2 dispersion model, showing the element associations from orientation studies in the Kalgoorlie region.

### 9.5.2 Sampling and exploration procedures, lateritic residuum, ferruginous saprolite, ferruginous granules and mottles

When it is recognised that the model in Fig. 9.9 applies, clearly it is advantageous to be able to position drill holes so that they will sample preserved lateritic residuum. This is one of the main reasons behind the testing of geophysical methods for delineating regolith stratigraphy.

Where lateritic residuum is missing, however, sampling should be directed at ferruginous saprolite because geochemical haloes in the upper ferruginous saprolite can also enlarge target size in a similar fashion to those in lateritic residuum (Section 4.4.6 in Report 236R). Ferruginous saprolite is commonly formed where the bedrock sequences are mafic. Ferruginous mottles also form a useful sampling medium.

Of the media which enlarge target size, no one sample medium is likely to provide continuous coverage in areas where this model applies. Consequently, at the data interpretational stage it becomes important to use valid methods for merging geochemical data arising from the different sample media.

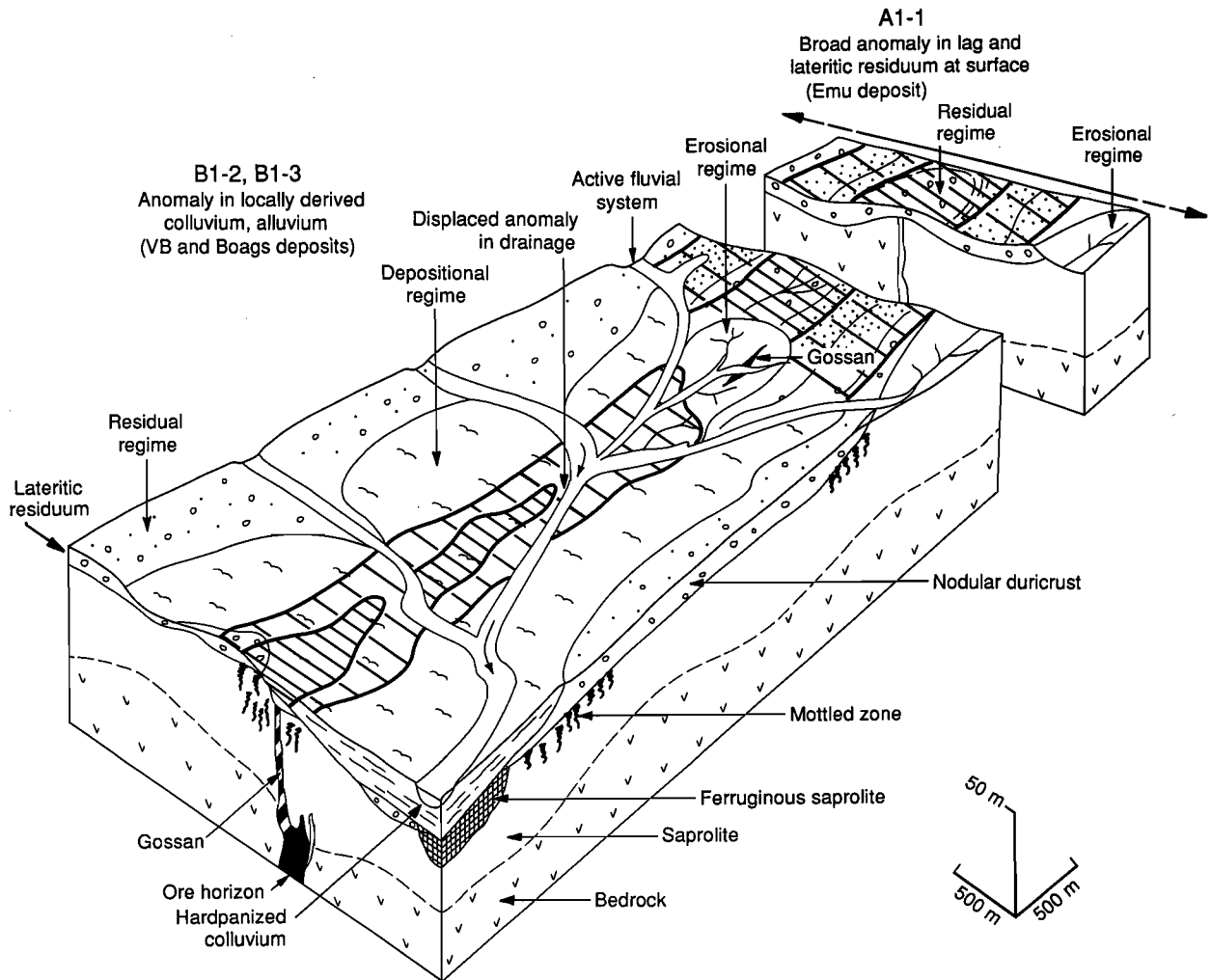


Fig. 9.11 Block diagram showing A1-1 (full lateritic profile); B1-2 and B1-3 (partly truncated profile) dispersion models, semi-arid to arid terrain, based largely on the Bottle Creek orientation study (Section 5.5).

Different thresholds will generally apply when comparing anomalous levels of an element between sample media. It is likely that the geometry of dispersion patterns will be somewhat more localised and irregular when based upon sampling of ferruginous saprolite or ferruginous mottles compared with lateritic residuum.

Because of the general lack of lateritic residuum in the Kalgoorlie region, sampling should be directed at the priority alternatives, namely ferruginous saprolite, ferruginous granules, mottles developed in sediments and calcareous soils (Fig. 9.10). Ferruginous granules and mottles commonly occur in red soils. The multi-element anomaly is defined by these ferruginous granules and mottles and it seems to be much broader and stronger than those based on soil geochemistry, considerably enlarging the target size. Confirming the findings reported by Butt *et al.* (1991), the results from the Kalgoorlie region show that Au can be associated with pedogenic carbonates and that the carbonate horizon should therefore be identified and sampled during exploration. Such Au-carbonate anomalies are however, restricted in lateral extent.

### 9.5.3 Using basal colluvium and basal alluvium

Figure 9.11 shows a geochemical dispersion model based on orientation studies at Bottle Creek (Section 4.3 in Report 236R; Section 5.5 of this report). At and about the VB and Boags deposits, a broad depositional regime is characterised by this colluvium and alluvium, in which there has been some mechanical incorporation and mixing of locally derived material from the upper part of the weathering profile. Clasts are seen to be derived from lateritic residuum, mottled zone, ferruginous saprolite and gossans from the ore zone. Similar regolith relationships and enrichment of Au and ore-related elements was observed at the Calista deposit (Mt. McClure, see Fig. 9.8).

In such cases, sampling the basal colluvium/alluvium can delineate a useful multi-element geochemical dispersion halo. Where encountered in systematic drilling of such areas, relics of lateritic residuum can provide the opportunity of more reliable geochemical haloes and should also be sampled.

Table 9.1 Summary of element associations linked to regolith stratigraphy for dispersion model A2-1, full lateritic profile, high seasonal rainfall, Au and base metal deposits. Based on the Boddington orientation study.

Regolith stratigraphic unit						
Broad term	Intermediate term	Working term	Code*	Target-associated elements	Lithological indicator elements (high for mafics)	Comments
Lag	Lateritic lag	Pisoliths and nodules	LG102 LG103	As Sb Bi Mo Sn W (Au)	Fe Ti Mn Cr V Cu Ni	
Soil, undifferentiated		Yellow brown sandy gravel	SU102	As Sb Bi Mo Sn W (Au)		
Lateritic residuum	Lateritic gravel	Loose lateritic pisoliths, nodules	LT102 LT103 LT104	As Sb Bi Mo Sn W (Au)	Fe Ti Mn Zr V Cu Ni	Zr (Nb) for felsic and granitic bedrocks
	Lateritic duricrust	Pisolitic duricrust	LT202	As Sb Bi Mo Sn W Au	Fe Ti Mn Cr V Cu Ni	As above
		Fragmental duricrust	LT205	As Sb Bi Mo Sn W Au	Fe Ti Mn Cr V Cu Ni	As above
Bauxite zone				As Bi (Mo) Sn W Au		
Clay zone				As (Bi) (Mo) Sn W Au		
Saprolite				As (Bi) (Mo) Sn W Au		
Saprock						

\* See classification tables for regolith materials in Report 60R.

## 10.0 OUTLOOK

### 10.1 General

Research, which commenced in the *Laterite Geochemistry Project* and was extended during this *Yilgarn Lateritic Environments* project, will continue to evolve. Currently, there are many practical procedures, that have arisen from these projects, which are being used effectively, widely and successfully throughout the exploration industry. The initial focus on laterite geochemistry has broadened into a comprehensive approach to exploration of lateritic environments in the Yilgarn. This incorporates regolith-landform mapping and establishing regolith stratigraphy. Multi-element geochemical methods for exploration have been extended to a substantial range of ferruginous materials. Some of the main evolutionary activities are discussed below.

### 10.2 Yilgarn transported overburden, AMIRA P409

The CSIRO Laterite Geochemistry and Weathering Processes Groups have joined forces to focus on the strategic issue of exploring in areas of transported overburden in the Yilgarn Craton. The project commenced June 1993, with substantial industry sponsorship, and runs initially for three years. Research achievements of both of these groups will be extended in the joint research and new environments will be investigated.

### 10.3 Teaching and training

A wealth of project materials have arisen during the six years of sponsored research of the *Laterite Geochemistry* and *Lateritic Environments Projects*. These include air photography, airphoto enlargements, satellite imagery, field mapping, reference samples and quality, multi-element geochemical data. Participating companies are thanked for their provision of project material. As project components come out of confidentiality these materials become particularly valuable in teaching and training. The well-documented orientation districts become the focus of field workshops as well as of further research.

Incorporation of Bachelors degree Honours students into the research projects has been an important method of experience transfer. Some nine students (spanning geology, geochemistry and geophysics) now have completed their studies and are working in industry, carrying with them the ethos, as well as the skills, they acquired by working with the researchers. Most have joined sponsoring companies and we expect their influence will be an additional mechanism for experience transfer within the teams they join.

### 10.4 Developments in regolith mapping technologies

Developments in the use of satellite imagery, which began in the AMIRA Project P243, *Remote Sensing for Gold, WA* and were further developed in this *Yilgarn Lateritic Environments Project*, have had a substantial impact on exploration by dramatically reducing the time required for regolith mapping in sparsely vegetated semi-arid and arid terrains. We see considerable potential for growth in the use of satellite and aircraft scanner imagery, particularly as knowledge of the reflective spectral properties of minerals increases and reconciliation of imagery with field studies continues to grow.

### 10.5 Regolith characterisation and the CRCAMET

Research activities, in collaboration with the Co-operative Research Centre for Australian Mineral Exploration Technologies, continue to develop. This research focuses on regolith characterisation for the use of exploration geophysics in regolith-dominated terrain. Systematic coverage, by airborne electromagnetics, of some of the orientation districts of this project, as well as of some outside the Yilgarn, will add new dimensions to regolith mapping and interpretation. The knowledge gained will then be used for modelling to remove regolith effects in interpretation of bedrock relationships and ore deposit delineation.

### 10.6 Developments in GIS and 3D visualisation

Development and application of systems for 3D visualisation should have a major impact on the ease and quality of interpretation of regolith relationships. These developments will also encourage the interplay of geology, geochemistry and geophysics, as well as the translation of selected ore deposit models into varying regolith settings. Already Geographic Information Systems (GIS) are taking much of the drudgery out of data input and presentation in regolith mapping. Increasingly, we will see map output and information on regolith stratigraphy available to users in machine readable form.

**10.7 North Queensland regolith, AMIRA Project P417**

The Yilgarn regolith geochemistry groups, joining with colleagues in Sydney, Canberra, Brisbane and Townsville (again in collaboration with the CRCAMET) will be commencing research on regolith environments in Queensland. These environments, which include multiple weathering surfaces and lateritised sediments, are more complex than those in the Yilgarn. The Queensland activities should provide important comparisons and contrasts with current research findings in the Yilgarn.

## 11.0 CONCLUSIONS

### 11.1 Reconciling project outcomes with objectives and expected benefits

The findings of this extension project are listed below with the objectives stated in the Project Proposal, April 1991 and are in accordance with priorities established at the first meeting of sponsors, 10 September 1991.

#### *Overall objective:*

*The overall objective of the Yilgarn Lateritic Environments Project has been to continue to develop and improve methods for finding mineral deposits (particularly gold and base metals) in complex lateritic environments of the Yilgarn Craton, using geochemistry, integrated within a sound regolith-landform framework.*

#### **Broad Outcomes:**

- A regolith-landform framework for the Kalgoorlie region (an area of 10,000 km<sup>2</sup>) was established, compared and contrasted with relationships for orientation districts of the precursor project and this extension. As a result, our understanding of regolith evolution of the Yilgarn Craton, and the use of geochemical exploration, have both advanced substantially.

The landscape in the Kalgoorlie region is characterised by extensive stripping of upland areas, very shallow to deep weathering, patchy development of lateritic residuum and extensive occurrence of calcareous and acid, red clay soils. In depositional areas, the immediate substrate to the calcareous clays is acid, red clay, rather than lateritic residuum, as seen in many of the depositional areas at Bottle Creek, Lawlers and Mt. McClure. Red clay soils commonly contain ferruginous granules. Erosional stripping of the upper, more weathered, parts of the regolith, appear to be important factors influencing the gross distribution of carbonates coupled with the distribution of mafic and ultramafic rocks.

- Eight additional orientation studies were completed, new geochemical dispersion models were established, and existing models updated.

#### *Additional orientation studies*

Boddington Au  
Kanowna Belle Au  
Lawlers - Waroonga, Genesis Au  
Lights of Israel Au  
Madoonga (Au prospect)  
Mt. McClure Au  
Ora Banda - Matt Dam Au  
Wombola (Au prospect)

#### *Updated orientation studies*

Bottle Creek Au  
Golden Grove Cu Zn Au

#### *Other orientation studies (precursor project)*

Mt. Gibson Au  
Beasley Creek  
Lawlers - McCaffery, Turrett Au

- Several new sample media were demonstrated to have specific application in exploration. These provide additional capabilities to those already established in the precursor project, particularly for application where lateritic residuum is missing.

In the 'effective' category are ferruginous saprolite, iron segregations, ferruginous mottles developed in the upper saprolite and ferruginous granules develop in soils (including soils on transported overburden). In the 'promising' category are ferruginous mottles developed in cover sequences. Sampling procedures are given in Section 9.

- Regolith stratigraphies in several important settings (*e.g.* in the eight additional orientation areas) were documented, and criteria were established for distinguishing transported overburden from *in situ* weathering of basement in three of these orientation areas.
- Methods of enhancement of Landsat TM imagery for regolith mapping in lateritic environments were developed to an operational stage, made available to sponsors and transferred through regolith mapping workshops.



- Regolith and dispersion models have been established which incorporate orientation findings in the Kalgoorlie region at Ora Banda, Matt Dam, Kanowna Belle and Wombola. Outside the Kalgoorlie region, models were established which incorporate findings at Mt. McClure, Waroonga-Genesis (at Lawlers), Boddington and Golden Grove. All are Au orientation studies except for Golden Grove (Cu-Zn-Au).

#### Specific Objectives:

The overall objective would be achieved through the following specific objectives:

*Specific Objective (i): To expand the knowledge base of the physical and chemical processes and patterns of dispersion from concealed mineral deposits within complex lateritic environments.*

#### Outcomes:

- The knowledge base of potential sample media for exploration geochemistry was widened to include (a) near-surface ferruginous granules which occur in soils and in thin alluvium over deeply leached saprolite; (b) ferruginous saprolite which occurs near surface or buried beneath the sediments; and (c) ferruginous mottles in cover sediments.

**Ferruginous granules in soil.** It was shown, at Kanowna Belle and supported by data at Matt Dam, that near-surface ferruginous granules hold trace element indicators (As, Sb, Au) forming a broad (>400 m wide) anomaly in the thin, transported cover over the deeply leached but partly truncated profile. These ferruginous granules are a distinctive sample medium. They are quite separate from lateritic nodules which are generally absent from the environs. It is expected (although not yet tested) that broad, strong anomalies, defined by using these ferruginous granules, will be indicative of large concealed deposits, potentially being a method for distinguishing such locations from otherwise misleading occurrences of minor mineralisation. The use of these ferruginous granules thus holds considerable promise in exploration for Au and base metal deposits in areas of deeply leached and partly truncated profiles, with or without the presence of transported cover. Such situations are common in the Kalgoorlie region.

**Ferruginous saprolite.** At Matt Dam, ferruginous saprolite gave a strong multi-element anomaly (Au, As, W) over the deeply leached, partly truncated profile. These findings are similar to those observed at Lawlers, where broad Au anomalies and anomalous concentrations of target-related elements in ferruginous saprolite are effective indicators of primary and supergene Au mineralisation. Ferruginous saprolite is common, both in the Kalgoorlie and Leonora-Wiluna regions, and forms an ideal sampling medium which can be used at scales ranging from reconnaissance to target definition. Samples may be collected from the surface or by drilling in areas of sedimentary cover.

**Ferruginous mottles in cover sediments.** It was shown by the research at Kanowna (Kanowna Deep leads) and Matt Dam that such ferruginous mottles in the vicinity of concealed Au deposits can carry anomalous As, Sb, W and Au. Both the mottles and their anomalous signatures were apparently generated through hydromorphic dispersion (As, Sb, and Au) during continued weathering after sediment deposition.

**Soils.** At Matt Dam and Kanowna Belle, the calcareous soils show anomalous concentrations of Au related to the underlying mineralisation. Below this surface expression, there is a depleted or leached zone to depths of 30 m.

- There are systematic differences in the distribution of Au between the high and low rainfall areas as revealed by the Boddington orientation study, in comparison with the distribution of Au seen in the Mt. McClure and Lawlers Au orientations. The trend in the distribution of Au, in the ferruginous part of the profile at Boddington, is opposite to those of the Mt. McClure and Lawlers Au deposits. At Boddington, Au decreases in abundance upwards from the bauxite zone, through lateritic duricrust, to loose nodules and pisoliths, whereas Au increases in abundance upwards from the mottled zone and ferruginous saprolite to loose

nodules and pisoliths at Mt. McClure and Lawlers. Gold has a very low abundance in the surficial lateritic pisoliths and nodules at Boddington. However, Sn, W, Mo, and As are strongly anomalous at surface. The differences in abundance and position of Au within the ferruginous part of the profile may be a function of the differences in leaching. At Boddington, high rainfall and water rich in organic materials produced from the abundant vegetation, may result in leaching of Au from loose pisoliths and reprecipitation at the base of the bauxite zone.

*Specific Objective (ii): To establish a framework of reference for classification of Yilgarn regolith-landform mapping units for the purposes of exploration geochemistry.*

**Outcome:**

- A framework of reference was established by deriving four simplified matrices using landforms as the horizontal axis and regolith stratigraphy as the vertical. These tabular matrices allow most regolith-landform mapping units so far encountered in the orientation districts in the Yilgarn, to be classified. We believe that this classification will now allow, for the Yilgarn Craton, mapping units of one region to be compared with those of another. An atlas was also prepared which should help exploration geologists, geochemists and geophysicists to recognise the nature of the regolith materials being mapped or sampled. The classification, framework and atlas, together with guidelines for its use in exploration, are given in Report 440R.

*Specific Objective (iii): To provide examples of comparative testing alternative methods for interpretation of multivariate geochemical data using the well-controlled data sets from the orientation studies.*

**Outcome:**

- Training exercises in exploratory data analysis (EDA) have been set up using a dynamic graphical package (Data Desk 4.0® used with Apple Macintosh® computers) to provide a contrast with modelled approaches, using discriminant analysis as presented in the precursor project. These exercises use data sets from project orientation areas. They show variations of target-associated elements between the orientation areas, use of lithological indicator elements, and variations of elements with sample types. Practical interpretational sessions in the CSIRO Floreat Park laboratories are available to sponsors by appointment.

*Specific Objective (iv): To provide some well-controlled data sets from partly truncated, buried weathering profiles in carefully chosen orientation situations, with emphasis on ferruginous material, saprolite and soils.*

**Outcome:**

- Multi-element data sets, with stringent regolith stratigraphic control from such settings have been generated for the Mt. McClure, Waroonga, Genesis, Bottle Creek (VB, Boags), and Kanowna Belle orientation areas, all being Au deposits.

*Specific Objective (v): To continue to integrate the research findings into progressively more effective exploration methods and to carry out feasibility tests of promising procedures.*

**Outcomes:**

- The findings have been integrated into new geochemical dispersion models: A2-1, Full lateritic profile, high seasonal rainfall, no surficial cover (based on Boddington Au); A1-1, Full lateritic profile, semi-arid to arid climate, little or no cover (Golden Grove, VHMS Cu-Zn; Mt. Gibson, Bottle Creek and Beasley Creek Au). Updated models were also generated: A1-3 and A2-3 Buried, complete profile, arid terrain (based on Kanowna Belle, Matt Dam, Kanowna deep leads, Boags, Mt. McClure, Waroonga, Au), B1-2, B1-3 Buried, partly truncated profile, arid terrain (based on Kanowna Belle, Matt Dam, Kanowna deep leads, Boags, Mt. McClure, Waroonga and Genesis, Au).

- Early application of the principles established by the research group directly assisted Great Central Mines NL, as a sponsor of the research, with the discovery of the major Bronzewing Au deposits. This included exploring areas of thick transported cover, by drilling for buried geochemical haloes in laterite (where profiles were complete) or ferruginous saprolite (where profiles were partly truncated) coupled with drilling into saprolite and saprock.
- Sampling pebbly clasts of ferruginous saprolite at surface was a practical useful addition to sampling clasts of lateritic residuum in the discovery of the Plutonic Au deposits by Great Central Mines.
- The feasibility of using ferruginous granules in soil, based on the model for Kanowna Belle and Matt Dam, remains to be tested in application trials.

*Objective (vi): To improve the criteria for identification of regolith units in drill spoil and for distinguishing between residual and transported regolith materials.*

**Outcome:**

- Such criteria were extended by studies of regolith stratigraphy in orientation studies at Kanowna Belle, the Kanowna deep leads, Mt. McClure, Waroonga and Genesis.

*Specific Objective (vii): To characterise iron oxides in surficial materials so as to establish their surficial environments of formation and the nature of the underlying bedrock.*

**Outcomes:**

- Certain Fe-rich duricrusts were demonstrated to have formed from lateritic weathering of mafic and ultramafic bedrocks (Lawlers, Ora Banda). The mineralogical and chemical compositions of these duricrust generally reflect the underlying lithologies.
- Other, localised types of Fe-rich duricrust are developed in sediments (Ora Banda). They are remnants of what was an ancient, lower surface or depression, in which sediments accumulated. Iron impregnated the sediments in these original depressions. They now occur as hills or ridges in the present landscape because of inversion of relief.
- Ferruginous granules in soil and in zones of mega-mottles have largely developed in place, being formed by a combination of pathways. These include mobilisation and segregation of Fe in the soils and sediments, and ferruginisation of bedrock or saprolite fragments.
- The extent of aluminium substitution in goethite and hematite is a sensitive indicator of the weathering environment of Fe-oxide formation and is dependent on the accompanying minerals. The Al substitution in goethite appears to have potential for the identification of the diverse types of ferruginous samples used in exploration. The differences in Al substitution in goethite between the regolith types suggests different environments and/or mechanisms of formation. Goethites (and hematites), with high levels of Al-substitution (15 to 35 mole%), are shown to be restricted to the Al-rich (kaolinite, gibbsite) lateritic weathering environments. Conversely, those Fe-oxides with low levels of Al-substitution (< 10 mole%) are confined to environments almost free of soluble Al.

## 11.2 Transfer of research findings to sponsors

Considerable importance was placed on the transfer of research findings to sponsors through comprehensive research reports, review meetings, workshops and a field trip, Appendices I to IV.

**Outcomes:**

- A one-day workshop for sponsors on regolith mapping methods has been held five times, through demand, during the project extension. In total, some 75 explorationists from sponsoring companies have participated.
- Four project review meetings.

- A four-day field trip was held, visiting parts of the Kalgoorlie region, the Bottle Creek and Lawlers orientation districts.
- Comprehensive project reports have been produced for the Bottle Creek (394R) and Boddington (246R) orientation studies, a discussion paper on regolith-landform mapping (338R), and the subsequent full report on the classification and terminology for regolith-landform mapping (440R).
- This final report is a synthesis of the project outcomes. It includes pertinent findings from the nine Honours theses carried out within the project.

### **11.3 Final comment**

The level of expertise in exploration of Yilgarn lateritic environments has increased substantially during the term of this extension project. This has been made possible by the continued high level of industry sponsorship, matching funding from CSIRO and collaborators, AGSO and GSWA, the last two through the CRCAMET. Other contributing factors have been collaboration with those universities which have participated through Honours studies, namely Curtin University of Technology, the University of WA and the University of Tasmania. Together with collaborators, project staff have continued to play a key role in lifting the level of expertise and in developing applications based on the research findings.

It is also pleasing to note substantial exploration successes where the concepts and knowledge generated during the project have been implemented and have contributed to discoveries of ore deposits. Most prominent are the Bronzewing discoveries of Great Central Mines, during this extension project, and the earlier Plutonic discoveries by the same team. Both of these (each in excess of 2 million ounces of Au) are world-class discoveries. In addition, there have been smaller, yet particularly significant, discoveries made by other sponsors using the concepts or knowledge arising from the project or its extension, at times in concert with other methods. Discovery of the Turrett and Waroonga Au deposits at Lawlers were significant because they emphasised, early in the course of the project, that research findings could be translated into exploration practice and for this reason these areas have been an important focus for field trips.



## 12.0 ACKNOWLEDGEMENTS

We wish to thank the sponsoring companies and their exploration personnel for providing financial support and encouragement during the two-year project extension. Important building blocks for the project continued to be the orientation studies. Access to the mining areas and their surroundings, as well as discussions with the mine site geologists and hospitality of the company management over the several years duration of the precursor project and this extension are gratefully acknowledge. Specifically we wish to thank: The Mt. Gibson Gold Project (Forsayth NL and Reynolds Australia Mines), Bottle Creek Gold Mine (Norgold, now Geopeko), Forsayth Lawlers-Plutonic Resources, Boddington Gold Mines, Western Mining Corporation (Beasley Creek Gold mine), Newcrest Mining (Matt Dam prospect), Croesus (Wombola prospect), Arimco (Mt. McClure) and Aberfoyle Resources (Lights of Israel).

Word processing of a challenging manuscript was carried out by Ms Jenny Porter, with assistance from Mrs Vivienne Baker and Mrs Beverley Hall. Besides being an author of the report, Mr John Wildman managed its production including, with Ms Porter, the compositing. Most diagrams were drafted by Mr Angelo Vartesi under the supervision of Mr Colin Steel. Samples were prepared by Ms Jenny Wilson and Mr Wayne Maxwell, the latter providing much of the research support during the final year which included report production. Thin sections were prepared by Mr Ray Bilz. Assistance on the scanning electron microprobe and Cameca microprobe was given by Mr Bruce Robinson. The in-house x-ray fluorescence analyses were performed by Mr Michael Hart and Mr Michael Cheeseman. Other chemical analyses were carried out by ANALABS (for x-ray fluorescence, ICP and ICPMS analyses) and Becquerel Laboratories (for instrumental neutron activation analyses).

Collaborative support of the Co-operative Research Centre for Australian Mineral Exploration Technologies is gratefully acknowledged, as is collaboration with Honours students and their supervisors from Curtin University of Technology, The University of Western Australia and The University of Tasmania.





### 13.0 REFERENCES

- Ahmat, T., Gole, M., Goleby, B., Morris, P., Swager, C. and Wyche, S., 1993. Greenstone terranes and the eastern goldfields seismic traverse. In: Williams, P.R. and Haldane, J.A., *An international conference on crustal evolution, metallogeny and exploration of the Eastern Goldfields*. Excursion Guidebook, Australian Geological Survey Record 1993/53, 144 pp.
- Anand, R.R. and Gilkes, R.J., 1984. Mineralogical and chemical properties of weathered magnetite grains from lateritic saprolite. *Journal of Soil Science*, **35**: 559-567.
- Anand, R.R. and Gilkes, R.J., 1987. The occurrence of maghemite and corundum in Darling Range laterites, Western Australia. *Aust. J. Soil Res.* **25** (3): 303-311.
- Anand, R.R. and Smith, R.E., 1990. Geochemical exploration. In: S.E. Ho, D.I. Groves and J.M. Bennett (Editors), *Gold deposits of the Archaean Yilgarn Block, Western Australia: Nature, genesis and exploration guides*. Geology Department and University Extension, UWA, Publication No.20: 331-336.
- Anand, R.R., Churchward, H.M., Smith, R.E. and Grunsky, E.C., 1991. *Regolith-landform development and consequences on the characteristics of regolith units, Lawlers district, Western Australia*. CSIRO Division of Exploration Geoscience Restricted Report 166R, 160 pp.
- Anand, R.R., Churchward, H.M., Smith, R.E., Smith, K., Gozzard, J.R., Craig, M.A. and Munday, T.J., 1993. *Classification and Atlas of Regolith-Landform Mapping Units*. CSIRO Restricted Report 440R, 87 pp.
- Anand, R.R., Smith R.E., Innes J., Churchward, H.M., Perdrix, J.L. and Grunsky, E.C., 1989. *Laterite types and associated ferruginous materials, Yilgarn Block, WA. Terminology, Classification and Atlas*. CSIRO Division of Exploration Geoscience Restricted Report 60R, 90 pp.
- Anand, R.R., Smith, R.E., Innes, J. and Churchward, H.M., 1989. *Exploration geochemistry about the Mt. Gibson gold deposits, Western Australia*. CSIRO Division of Exploration Geoscience Restricted Report 20R, 93 pp.
- Barnes, J.F.H. 1985. Unpublished Electrolytic Zinc Company Progress Report.
- Baxter, J.L., 1982. Stratigraphy and structural setting of the Warriedar Fold Belt, In: J.L. Baxter (ed.), *Archaean Geology of the Southern Murchison, Excursion Guide*, pp.31-36 (Geological Society of Australia, Western Australian Division: Perth).
- Baxter, J.L. and Lipple, S.L., (Comps.), 1985. Perenjori, Western Australia - 1:250 000 Geological Series, Geological Survey of Western Australia Explanatory notes. SH 50.56.
- Binns, R.A., 1988. *Preliminary report on petrological and geochemical studies at Bottle Creek, Western Australia*. CSIRO Division of Exploration Geoscience Restricted Report 1767R.
- Bowell, R.J., Foster, R.P. and Gize, A.P., 1993. The mobility of gold in tropical rain forest soils. *Economic Geology*, **88**: 999-1016.
- Bowler, J.M., 1982. Aridity in the late Tertiary and Quaternary of Australia. In: W.R. Parker and P.J.M. Greenslade (eds.), *Evolution of flora and fauna of arid Australia*. Peacock Publications, Adelaide, S.A., 35-45.
- Brimhall, G.H., Lewis, C.J., Ague, J.J., Deitrich, W.E., Hampel, J., Teague, T. and Rix, P., 1988. Metal enrichment in bauxites by deposition of chemically mature aeolian dust. *Nature*, **333**: 819-824.
- Bunting, J.A. and Williams, S.J., 1979. Explanatory notes on the Sir Samuel geological sheet. 1:250,000 Geological Series: Explanatory notes, Geological Survey of Western Australia, Perth, 40 pp.
- Butt, C.R.M. and Zeegers, H., 1992. Regolith exploration geochemistry in tropical and subtropical terrains. In: G.J.S. Govett (ed.) *Handbook of Exploration Geochemistry*, Volume 4. Elsevier Science Publishers B.V. Amsterdam, 607 pp.
- Butt, C.R.M., Horwitz, R.C.H. and Mann, A.W., 1977. *Uranium occurrences in calcretes and associated sediments in Western Australia*, Report FP16. CSIRO Australia, Division of Mineralogy, Perth, 67 pp.

- Butt, C.R.M., Gray, D.J., Lintern, M.J. and Robertson, I.D.M., 1993. *Gold and associated elements in the regolith-dispersion processes and implications for exploration*. Final Report, Project P241A. Exploration Geoscience Restricted Report 396R, 64 pp.
- Butt, C.R.M., Gray, D.J., Lintern, M.J., Robertson, I.D.M., Taylor, G.F. and Scott, K.M., 1991. *Gold and associated elements in the regolith - dispersion processes and implications for exploration*. Final Report, CSIRO/AMIRA Weathering Processes Project P241. CSIRO Division of Exploration Geoscience Restricted Report 167R, 114 pp.
- Butt, C.R.M., Williams, P.A., Gray, D.J., Robertson, I.D.M., Schorin, K.H., Churchward, H.M., McAndrew, J., Barnes, S.J. and Tenhaeff, M.F.J., 1992. *Geochemical exploration for platinum group elements in weathered terrain*. Final Report, Volume IIA, CSIRO/AMIRA Project P252. Exploration Geoscience Restricted Report 332R, 80pp.
- Churchward, H.M., Butler, I.K. and Smith, R.E., 1992. *Regolith-landform relationships in the Bottle Creek orientation study, Western Australia*. CSIRO Division of Exploration Geoscience Restricted Report 247R, 65 pp.
- Commander, D.P., Kern, A.M. and Smith R.A., 1992. *Hydrogeology of the tertiary palaeochannels in the Kalgoorlie Region. (Roe Palaeodrainage)*. Western Australian Geological Survey, Record 1991/10.
- Craig, M.A. and Anand, R.R., 1993. (Comps). Map, Kalgoorlie-Kurnalpi Regolith Landforms, 1:250 000 Special Edition, Australian Geological Survey Organisation.
- Davy, R. and El-Ansary, M., 1986. Geochemical patterns in the laterite profile at the Boddington gold deposit, Western Australia. *Journal of Geochemical Exploration*, 26: 119-144.
- Davy, R., 1979. A study of laterite profiles in relation to bedrock in the Darling Range, near Perth, WA. Western Australian Geological Survey, Report Series, 8, 87 pp.
- Dell, M.R., 1992. *Regolith-landform relationships and geochemical dispersion about the Kanowna-Belle Au Deposit, W.A.* Honours Thesis, Dept. of Geology, University of Tasmania, Hobart, Tasmania, 89pp plus appendices.
- Didier, P., Nahon, D., Fritz, B. and Tardy, Y., 1983. Activity of water as a chemical controlling factor in ferricretes; a thermodynamic model in the system; kaolinite, Fe-oxyhydroxides, Fe-Al. *Petrologie des alterations et des sols*; colloque internationale du CRNS. Volume 71: 35-44.
- Eggo, A.J. 1991. Data processing and interpretation procedures for geochemical exploration. Advanced exploration geochemistry. Australian Mineral Foundation, Adelaide, 88pp.
- El-Ansary, M., 1980. Exploration for commodities other than bauxite in the Worsley Project area. Reynolds Australia Mines Pty. Ltd., unpublished report.
- Fortescue, J.A.C., 1975. The use of landscape geochemistry to process exploration geochemical data. *Journal of Geochemical Exploration*, 4: 3-13.
- Fortescue, J.A.C., 1992. Landscape geochemistry: retrospect and prospect - 1990. *Applied Geochemistry*, 7: 1-53.
- Frater, K.M., 1978. *The Golden Grove copper-zinc deposit, Western Australia - an Archaean exhalative, volcanogenic occurrence*. PhD thesis (unpublished), The University of Newcastle, New South Wales.
- Frater, K.M., 1983a. Geology of the Golden Grove prospect, Western Australia: a volcanogenic massive sulfide-magnetite deposit. *Economic Geology*, 78: 875-919.
- Garrett, R.G., 1993. Another cry from the heart. *Explore*, No.81, p.9-15.
- Goudie, A., 1973. *Duricrust in tropical and subtropical landscapes*. Oxford Research studies in Geography, Oxford University Press, London, 174 pp.
- Gozzard, J.R. and Tapley, I.J., 1992. *Landform and regolith mapping in the Lawlers district: Terrain classification mapping*. CSIRO Division of Exploration Geoscience Restricted Report 240R.

- Gozzard, J.R., Munday, T.J., Hunter, W.M. and Gabell, A.R., 1992. *An evaluation of SPOT Panchromatic imagery as an aid to regolith-landform mapping in the Ora Banda area, Eastern Goldfields Province, WA*. CSIRO Division of Exploration Geoscience Restricted Report 233R.
- Gray, D.J., 1992. *Hydrogeochemistry of sulphide weathering at Boags Pit, Bottle Creek, Western Australia*. CSIRO Division of Exploration Geoscience Restricted Report 237R, 13 pp.
- Green, A.A. and Berman, M., 1990. Detecting concealed alteration with remote sensing. *Exploration Research News*, Vol.4: 6-7.
- Grunsky, E.C., 1991. Strategies and methods for the interpretation of geochemical data. Discussion paper applied to laterite geochemistry. CSIRO Division of Exploration Geoscience Discussion paper, 74 pp.
- Hallberg, J.A., 1984. A geochemical aid to igneous rock type identification in deeply weathered terrain. *Journal of Geochemical Exploration*, 20: 1-8.
- Harrison, N., Bailey, A., Shaw, J.D., Petersen G.N. and Allen, C.A., 1990. Ora Banda gold deposits. In: F.E. Hughes (ed.), *Geology of the Mineral Deposits of Australia and Papua New Guinea*, Volume 1. *The Australasian Institute of Mining and Metallurgy*, 389-394.
- Hickman, A. and Keats, W., 1990. Gold. In: *Geology and mineral resources of Western Australia*. Western Australia Geological Survey, Memoir 3: 645-669.
- Jutson, J.T., 1950. The physiography (geomorphology) of Western Australia. *Geological Survey of Western Australia Bulletin*, 95, (3rd Ed.), 366 pp.
- Kriewaldt, M., 1970. 1:250,000 Geological Series - Explanatory Notes, Menzies. Bureau of Mineral Resources, Geology and Geophysics.
- Lawrance, L.M., 1991. *Distribution of Gold and Associated Elements Within Lateritic Weathering Profiles of the Yilgarn Block, Western Australia*. Ph.D. Thesis, University of Western Australia.
- Legge, P.J., Mill, J.H.A., Ringrose, C.R. and McDonald, I.R., 1990. The Bottle Creek gold deposit. In: Hughes F.E. (ed.), *Geology of the Mineral Deposits of Australia and Papua New Guinea*, Volume 1. *The Australasian Institute of Mining and Metallurgy*, 357-361.
- Lintern, M.J. and Butt, C.R.M., 1993. Pedogenic Carbonate: An important sampling medium for gold exploration in semi-arid areas. *Exploration Research News*, 7, pages 7, 10 & 11.
- Loughnan, F.C. and Sadlier, S.B., 1984. Geology of established bauxite producing areas in Australia. In: L. Jacob (ed.), *Bauxite Proceedings. 1984 Bauxite Symposium*, Los Angeles, California. The Society of Mining Engineers of American Institute of Mining, Metallurgical and Petroleum Engineers: 435-461.
- Mabbutt, J.A., 1980. Weathering history and landform development. In: C.R.M. Butt and R.E. Smith (eds.), *Conceptual Models in Exploration Geochemistry - Australia*. *Journal of Geochemical Exploration*, 12: 96-116.
- Mann, A.W., 1983. Hydrogeochemistry and weathering on the Yilgarn Block, Western Australia - ferrolysis and heavy metals in continental brines. *Geochimica Cosmochimica Acta*, 47: 181-190.
- Mann, A.W., 1984. Mobility of gold and silver in laterite weathering profiles: some observations from Western Australia. *Economic Geology*, 79: 38-49.
- Mayes, K.A., 1992. *Applications of geophysical electrical and magnetic methods to regolith mapping at Lawlers, Western Australia*. Honours thesis, Geophysics Department, Curtin University of Technology, Perth.
- Mill, J.H.A., Clifford, B.A., Dudley, R.J. and Ruxton, P.A., 1990. Scuddles zinc-copper deposit at Golden Grove. In: F.E. Hughes (Editor), *Geology of the mineral deposits of Australia and Papua New Guinea*. Australasian Institute of Mining and Metallurgy, Melbourne: 583-590.

- Monti, R., 1987. The Boddington laterite gold deposit, Western Australia: a product of supergene enrichment processes. In: S.E. Ho and D.I. Groves (eds.), *Recent advances on understanding Precambrian gold deposits*. Geology Department and University Extension, University of WA. Publication 11: 355-368.
- Myers, J.S. and Watkins, K.P., 1985. Origin of granite-greenstone patterns, Yilgarn Block, Western Australia, *Geology*, **13**: 778-780.
- Nelson, M.J., 1992. *Mapping the regolith and basement using airborne magnetic and radiometric data, Lawlers area, Western Australia*, Honours thesis, Department of Exploration Geophysics, Curtin University of Technology.
- Ollier, C.D., Chan, R.A., Craig, M.A. and Gibson, D.L., 1988. Aspects of landscape history and regolith in the Kalgoorlie region, Western Australia. *BMR Journal of Australian Geology and Geophysics*, **10**: 309-321.
- Peachey, T.R., 1991. The Kanowna Belle Gold Deposit Geological Report. Delta Gold Limited (Unpublished).
- Perel'man, A.I., 1972. Landscape Geochemistry, Vysshaya skhola, Moscow (1966), translation from the Russian. (Geological Survey of Canada Translation No.676, Pt. I and II).
- Pullan, R.A., 1967. A morphological classification of lateritic ironstones and ferruginized rocks in Northern Nigeria. *Nigerian Journal of Science*, **1**: 161-174.
- Ramanaidou, E.R., Horwitz, R.C. and Morris, R.C., 1991. *Channel iron deposits - Progress Report No.2*, CSIRO Division of Exploration Geoscience Restricted Report 162R, 63pp.
- Robertson, I.D.M. 1990. *Mineralogy and geochemistry of soils overlying the Beasley Creek Gold Mine - Laverton, W.A.* CSIRO Division of Exploration Geoscience Restricted Report 105R, 158 pp.
- Robertson, I.D.M., and Wills, R., 1993. *Petrology and geochemistry of surface materials overlying the Bottle Creek Gold Mine, WA.* CSIRO Division of Exploration Geoscience Restricted Report 394R, 44pp., plus Appendices.
- Ross, A., 1993. Archaean lode gold deposits of the Kanowna Region. In: Williams, P.R. and Haldane, J.A., *An international conference on crustal evolution, metallogeny and exploration of the Eastern Goldfields*. Excursion Guidebook, Australian Geological Survey Organisation Record 1993/53, 122-126.
- Roth, E. and Symons, P., 1990. Boddington Gold Mine. In: S.E. Ho, D.I. Groves and J.M. Bennett (Editors), *Gold deposits of the Archaean Yilgarn Block, Western Australia: Native genesis and exploration guidelines*. Section 1.8.4.1: 185-186, Geology Department (Key Centre) and University Extension, University of Western Australia Publication No 20, 407 pp.
- Smith, R.E. and Perdrix, R.L., 1983. Pisolitic laterite geochemistry in the Golden Grove massive sulphide district, Western Australia. *Journal of Geochemical Exploration*, **18**: 131-164.
- Smith, R.E., 1989. Using lateritic surfaces to advantage in exploration. In: G.D. Garland (Editor), *Proceedings of Exploration 1987. Third Decennial International Conference on Geophysical and Geochemical Exploration for Minerals and Groundwater*. Special Volume 3. Ontario Geological Survey, Toronto: 312-322.
- Smith, R.E., Anand, R.R., Churchward, H.M., Robertson, I.D.M., Grunsky, E.C., Gray, D.J., Wildman, J.E. and Perdrix, J.L., 1992. *Laterite geochemistry for detecting concealed mineral deposits*. CSIRO Division of Exploration Geoscience Restricted Report 236R, 171 pp.
- Smith, R.E., and Perdrix, J.L., 1983. Pisolitic laterite geochemistry in the Golden Grove massive sulphide district, Western Australia. *Journal of Geochemical Exploration*, **18**(2): 131-164.
- Smith, R.E., Campbell, N.A. and Litchfield, R., 1984. Multivariate statistical techniques applied to pisolite laterite geochemistry at Golden Grove, Western Australia. *Journal of Geochemical Exploration*, **22**: 193-216.

- Smith, R.E., Campbell, N.A. and Perdrix, J.L., 1983. Identification of some Western Australian gossans by multi-element geochemistry. In: R.E. Smith (Editor), *Geochemical exploration in deeply weathered terrain*. CSIRO Australia, Division of Mineralogy, Floreat Park, Western Australia: 75-90.
- Smith, R.E., Perdrix, J.L. and Davis, J.M., 1987. Dispersion into pisolitic laterite from the Greenbushes mineralised Sn-Ta pegmatite system, Western Australia. In: R.G. Garrett (Editor), *Geochemical Exploration 1985, Part I. Journal of Geochemical Exploration*, 28: 251-265.
- Smith, R.E., Wildman, J.E., Anand, R.R. and Perdrix, J.L., 1992. *Reference data sets from the Mt. Gibson orientation study, Western Australia*. CSIRO/AMIRA Laterite Geochemistry Project P240. CSIRO Division of Exploration Geoscience Restricted Report 157R, 105 pp.
- Swager, C.P., Griffin, T.J., Witt, W.K., Wyche, S., Ahmat, A.L., Hunter, W.M. and McGoldrick, P.J., 1990. Geology of the Kalgoorlie Terrane - an explanatory note. Geological Survey of Western Australia, Record 1990/12.
- Symons, P.M., Anderson, G., Beard, T.J., Hamilton, L.M., Reynolds, G.D., Robinson, J.M. and Staley, R.W., 1988. The Boddington gold deposit. The Second International Conference on Prospecting in Arid Terrain, Perth. Excursion Guidebook: 77-84.
- Symons, P.M., Anderson, G., Beard, T.J., Hamilton, L.M., Reynolds, G.D., Robinson, J.M., Staley, R.W. and Thomson, C.M., 1990. Boddington gold deposit, In: Hughes F.E. (ed.), *Geology of the Mineral Deposits of Australia and Papua New Guinea, Volume 1*. The Australasian Institute of Mining and Metallurgy: 165-169.
- Taylor, G.F. 1992. *Gossan geochemistry at Bottle Creek*. In: Eastern Goldfields Trip 6-9 May 1992. CSIRO Division of Exploration Geoscience, 2pp.
- Taylor, G.F. and Scott, K.M., 1982. Evaluation of gossans in relation to lead-zinc mineralisation in the Mt. Isa Inlier, Queensland. *BMR Journal of Australian Geology and Geophysics*, 7: 159-180.
- Taylor, G.F., 1989. *Mineralogical and geochemical studies of gossan and wall rocks, Bottle Creek, Western Australia*. CSIRO Division of Exploration Geoscience Restricted Report 36R, 36pp.
- Taylor, R.M. and Schwertmann, U., 1974. Maghemite in soils and its origins. I. Properties and observations in soil maghemites. *Clay Mineralogy*, 10: 289-298.
- Thomson, R.M. and Peachey, T.R., 1993. The Kanowna Belle case study - the discovery of a concealed orebody. In: Williams, P.R. and Haldane, J.A. *An international conference on crustal evolution, metallogeny and exploration of the Eastern Goldfields*. Excursion Guidebook, Australian Geological Survey Record 1993/53, 144 pp.
- Tomich, S.A., 1964. Bauxite in the Darling Range, Western Australia. *Australian Institute of Meteorology Proceedings*, 212: 125-35.
- Twidale, C.R., 1983. Australian laterites and silcretes; ages and significance. *Revue de Geologie Dynamique et de Geographie Physique*, 1: 35-45.
- Twomey, R.F., 1992. *Regolith-landform relationships in the Agnew area and multi-element dispersion in to the weathering profiles of the Genesis and Waroonga gold deposits, Lawlers district*. Honours thesis, Geology Department, University of Western Australia.
- van der Heyde, H.A., 1988. Geochemical sampling of surface nodular lateritic material at Bottle Creek: Report to Norgold. CSIRO Laterite Geochemistry Project (Unpublished).
- Von Perger, A.D., 1991. *Regolith development and geochemistry of the Madoonga Area, Western Australia*. Honours thesis, School of Applied Geology, Curtin University of Technology, Perth. CSIRO Exploration Geoscience Restricted Report 238R, 144pp.
- Von Perger, A.D., 1993. Regolith map of the Madoonga Area, 1:150,000 scale. Unpublished.
- Watkins, K.P., and Hickman, A.H., 1990. Geological evolution and mineralisation of the Murchison Province, Western Australia. Geological Survey of Western Australia, Bull. 137, 267pp.

- Wilde, S.A. and Pidgeon, R.T., 1986. Geology and geochronology of the Saddleback Greenstone Belt in the Archaean Yilgarn Block, southwestern Australia. *Australian Journal of Earth Science*, 33: 491-501.
- Wilde, S.A., 1976. The Saddleback Group - a newly discovered Archaean greenstone belt in the southwest Yilgarn Block. Western Australian Geological Survey, Annual Report: 92-95.
- Wilde, S.A., 1980. The Jimperding Metamorphic Belt in the Toodyay Area and the Balingup Metamorphic Belt and Associated Granitic rocks of the Southwestern Yilgarn Block. 2nd International Archaean Symposium, Perth 1980, Excursion Guide. Geological Society of Australia, Perth, 41pp.
- Wilde, S.A. and Low, G.H., 1980. Pinjarra, Western Australia: Western Australia Geological Survey, 1:250 000 Geological Series Explanatory Notes, 31 pp.
- Williams, I.R., 1970. Kurnalpi Western Australia, 1:250,000 Geological Series - Explanatory Notes, Geological Survey of Western Australia, 37 pp.
- Williamson, A., 1992. *Regolith-landform evolution and geochemical dispersion from the Calista gold deposit, Mount McClure district*, Western Australia. Honours thesis, Geology Department, University of Western Australia, 99pp.
- Wills, R.J., 1992. *Regolith-landforms and geochemical dispersion about the Bottle Creek gold deposits, Western Australia*. B.Sc. (Hons) Thesis, School of Applied Geology, Curtin University, Perth, Western Australia, 101pp.
- Zeegers, H., Goni, J. and Wilhelm, E., 1981. Geochemistry of laterite profiles over a disseminated Cu-Mo mineralization in Upper Volta, (West Africa). Preliminary results. In: *Lateritisation Processes*. Balkema Publishers, Rotterdam, 359-368.

## 14.0 APPENDICES

## APPENDIX Ia

**REPORTS ISSUED BY THE LATERITE GEOCHEMISTRY PROJECT P240**  
**(The precursor project)**

<i>Report No.</i>	<i>Title, Author(s), etc.</i>
Un-numbered	Laterite geochemistry in the Moora, Perth, Pinjarra, Collie and Pemberton sheets. J. Innes, R.E. Smith, and J.L. Perdrix, April 1988. 21 pages with data on diskette.
2R	Laterite geochemistry in the CSIRO-AGE database, South Murchison Region (Yalgoo, Kirkalocka, Perenjori, Ninghan Sheets). E.C. Grunsky, J. Innes, R.E. Smith, J.L. Perdrix, December 1988. 92 pages with data on diskette.
4R	The aqueous geochemistry of gold in the weathering environment. D.J. Gray, December 1988, (jointly with Project P241).
20R	Exploration geochemistry about the Mt. Gibson gold deposits, Western Australia. R.R. Anand, R.E. Smith, J. Innes and H.M. Churchward, March 1989, 93 pages.
26R	Geomorphology and surface geology, Beasley Creek orientation study. I.D.M. Robertson and H.M. Churchward, July 1989, 39 pages.
60R	Laterite types and associated ferruginous materials - <i>Terminology, Classification, and Atlas</i> . R.R. Anand, R.E. Smith, J. Innes, H.M. Churchward, J.L. Perdrix and E.C. Grunsky, August 1989. Expandable, loose-leaf format.
68R	Laterite geochemistry in the CSIRO-AGE database for the Northern Murchison region (Cue, Belele, Glengarry, Sandstone Sheets). E.C. Grunsky, R.E. Smith, J.L. Perdrix, November 1989. 148 pages, with data on diskette.
27R	Beasley Creek Orientation Study: Geochemistry, petrography and mineralogy of ferruginous lag overlying the Beasley Creek Gold Mine - Laverton W.A. I.D.M. Robertson, November 1989. Vol. I, 75 pages; Vol. II, 98 pages; with data on diskette.
121R	Laterite geochemistry in the CSIRO-AGE database for the Central Yilgarn Region (Barlee, Bencubbin, Corrigin, Hyden, Jackson, Kalgoorlie, Kellerberrin, Southern Cross Sheets). E.C. Grunsky, July 1990. Vol. I, 114 pages; Vol. II, 162 pages with data on diskette.
Un-numbered	Eastern Goldfields Trip: Introduction and Bottle Creek orientation study, field guide, October, 1990, 24 pages.
Un-numbered	Eastern Goldfields Trip: Lawlers orientation study, field guide. R.R. Anand, R.E. Smith, H.M. Churchward, and J.L. Perdrix, compilers, October 1990, 30 pages.
154R	Laterite geochemistry in the CSIRO-AGE database for the Wiluna region (Duketon, Kingston, Sir Samuel, Wiluna) E.C. Grunsky, December 1990, 161 pages with data on diskette.



- 105R      Beasley Creek Orientation Study: Mineralogy and Geochemistry of soils overlying the Beasley Creek gold mine - Laverton, W.A.  
I.D.M. Robertson, December 1990. Vol. I, 53 pages; Vol. II, 99 pages.
- 161R      Laterite geochemistry in the CSIRO-AGE database for the Albany-Fraser region (Collie, Dumbleyung, Mount Barker, Pemberton sheets)  
E.C. Grunsky, April 1991. Vol. 1, 61 pages with data on diskette; Vol. 2, 145 pages.
- 120R      Hydrogeochemistry in the Mount Gibson gold district.  
D.J. Gray, April 1991, 80 pages.
- Un-numbered      Strategies and Methodologies for the Interpretation of Geochemical Data - Discussion Paper Applied to Laterite Geochemistry.  
E.C. Grunsky, August 1991, 77p.
- 166R      Regolith-landform relationships and consequences on the characteristics of regolith units, Lawlers District, Western Australia.  
R.R. Anand, H.M. Churchward, R.E. Smith and E.C. Grunsky, August 1991, 160p, data on diskette.
- 165R      Regolith-landform development and siting and bonding of elements in regolith units, Mt. Gibson district, Western Australia.  
R.R. Anand, H.M. Churchward and R.E. Smith, September 1991, 95p, data on diskette.
- 157R      Reference geochemical data sets from the Mt. Gibson orientation study, Western Australia.  
R.E. Smith, J.E. Wildman, R.R. Anand and J.L. Perdrix, March 1992, 105p, data and animated demonstrations on diskettes.
- 247R      Regolith-landform relationships in the Bottle Creek orientation study, Western Australia, November 1992, 65 pages.  
H.M. Churchward, I.K. Butler and R.E. Smith.
- 236R      Laterite geochemistry for detecting concealed mineral deposits, Yilgarn Craton, Western Australia.  
R.E. Smith, R.R. Anand, H.M. Churchward, I.D.M. Robertson, E.C. Grunsky, J.E. Wildman and J.L. Perdrix, November 1992. Summary Report for the CSIRO-AMIRA Project P240, 171pp.

## APPENDIX Ib

**REPORTS ISSUED BY THE YILGARN LATERITIC ENVIRONMENTS PROJECT P240A**  
(The extension project)

<i>Report No.</i>	<i>Title, Author(s), etc.</i>
338R	Regolith-landform mapping in the Yilgarn Craton, Western Australia: Towards a Standardised Approach. Discussion Paper, M.A. Craig, R.R. Anand, H.M. Churchward, J.R. Gozzard, R.E. Smith and K. Smith, January 1993, 43 pages.
246R	Regolith-landform evolution and geochemical dispersion from the Boddington Gold deposits, Western Australia. R.R. Anand, November 1992, 149 pages, scheduled for release to sponsors March 1994.
394R	Petrology and geochemistry of surface materials overlying the Bottle Creek Gold deposits, W.A. I.D.M. Robertson and R. Wills. December 1993, 44 pages. (Report issued jointly with Project P241A, Dispersion Processes.)
232R	Petrography, mineralogy and geochemistry of soil and lag overlying the Lights of Israel Gold Mine, Davyhurst, Western Australia. I.D.M. Robertson and M.F.J. Tenhaeff, October 1992, Volume I, 52 pages, Volume II, 21 Appendices with data on diskette. (Report issued jointly with Project P241A, Dispersion Processes.)
440R	Classification and atlas of regolith-landform mapping units - Exploration perspectives for the Yilgarn Craton. R.R. Anand, H.M. Churchward, R.E. Smith, K. Smith, J.R. Gozzard, M.A. Craig and T.J. Munday, November 1993. Expandable, loose-leaf format.
442R	Geochemical exploration in complex lateritic environments of the Yilgarn Craton, Western Australia. Final Report for AMIRA Project P240A. R.R. Anand, R.E. Smith, C. Phang, J.E. Wildman, I.D.M. Robertson and T.J. Munday, December 1993. Volume I, 297 pages; Volume II, 116pp and III, 141pp, Appendices with data on diskettes.

## APPENDIX II

**REPORTS ISSUED TO TENEMENT HOLDERS PROJECT 240A**

246R	Regolith-landform evolution and geochemical dispersion from the Boddington Gold deposits, Western Australia. R.R. Anand, November 1992, 149 pages.
394R	Petrology and geochemistry of surface materials overlying the Bottle Creek gold mine, W.A. I.D.M. Robertson and R. Wills, October 1993, Volume I, 44 pages, Volume II Appendices.

**APPENDIX III****MEETINGS HELD WITH SPONSORS PROJECT 240A**

10 September 1991	Project planning meeting on objectives, scope, priorities
12 December 1991	Hands-on training workshop, regolith mapping for exploration geochemistry
3 May 1992	Regolith mapping workshop repeated (Kalgoorlie)
4 May	Regolith mapping workshop repeated (Kalgoorlie)
5 May 1992	Project review meeting (Kalgoorlie)
6-9 May 1992	Joint field trip (with AMIRA P241A, Dispersion Processes) Kalgoorlie, Bottle Creek and Lawlers
14 December 1992	Project review meeting
15 December 1992	Regolith mapping workshop repeated
26, 27 August 1993	Catch-up workshop for BHP geologists (who joined sponsorship during extension period with appropriate subscription for earlier stage)
Scheduled for 25 February 1994	Final meeting

## APPENDIX IV

**BACHELOR OF SCIENCE HONOURS THESES  
CARRIED OUT IN COLLABORATION WITH PROJECT P240A***1991 Academic Year*

- Cant, G.P. Geophysical investigations to delineate laterite within regolith stratigraphy at Lawlers WA. Department of Exploration Geophysics, Curtin University of Technology, 35 pages.
- King, J.D. Relation of bedrock geology to regolith-landform and geochemistry in the Gindalbie area, Western Australia. School of Applied Geology, Curtin University of Technology, 187 pages.
- Von Perger, A.D. Regolith development and geochemistry of the Madoonga area, Western Australia. School of Applied Geology, Curtin University of Technology, 144 pages, CSIRO Division of Exploration Geosciences, Report 238R.

*1992 Academic Year*

- Dell, M.R. Regolith-landform relationships and geochemical dispersion about the Kanowna Belle gold deposit, Western Australia. Geology Department, University of Tasmania, 89 pages plus appendices.
- Mayes, K.A. Applications of geophysical electrical and magnetic methods to regolith mapping at Lawlers Western Australia. Department of Exploration Geophysics, Curtin University of Technology, 64 pages.
- Nelson, M.J. Mapping the regolith and basement using airborne magnetic and radiometric data, Lawlers area, Western Australia. Department of Exploration Geophysics, Curtin University of Technology.
- Twomey, R.F. Regolith-landform relationships in the Agnew area and multi-element dispersion into the weathering profiles of the Genesis and Waroonga gold deposits, Lawlers district. Geology Department, University of Western Australia, 98 pages.
- Williamson, A. Regolith-landform evolution and geochemical dispersion from the Calista gold deposit, Mount McClure district, Western Australia. Geology Department, University of Western Australia, 99 pages.
- Wills, R. Regolith-landforms and geochemical dispersion about the Bottle Creek Au-Ag deposits, Western Australia. School of Applied Geology, Curtin University of Technology, 101 pages.